Rhodium/Ruthenium-Catalyzed Strategies for the Synthesis of Fused and Functionalized *N*-Aryl-2,3-dihydrophthalazine-1,4-diones

THESIS

Submitted in partial fulfillment

of the requirements for the degree of

DOCTOR OF PHILOSOPHY

by

PIDIYARA KARISHMA

ID. NO. 2016PHXF0404P

Under the supervision of

Dr. RAJEEV SAKHUJA

DEPARTMENT OF CHEMISTRY
BIRLA INSTITUTE OF TECHNOLOGY AND SCIENCE
PILANI (RAJASTHAN) INDIA
2022

BIRLA INSTITUTE OF TECHNOLOGY AND SCIENCE
PILANI (RAJASTHAN)

CERTIFICATE

This is to certify that the thesis entitled "**Rhodium/Ruthenium-Catalyzed Strategies for the Synthesis of Fused and Functionalized *N*-Aryl-2,3-dihydrophthalazine-1,4-diones**" submitted by **Ms. PIDIYARA KARISHMA**, ID No. **2016PHXF0404P** for the award of Ph.D. Degree of the Institute embodies the original work done by her under my supervision.

Signature in full of the Supervisor

Name in capital block letters: **Dr. RAJEEV SAKHUJA**
Designation: Associate Professor, Birla Institute of Technology and Science Pilani, Pilani Campus, Rajasthan India.

Date:

Dedicated to

My Parents,

Sisters and Brother

ACKNOWLEDGEMENTS

First and foremost, I would like to devote myself to the supreme power, who graced me to identify a righteous path and to accomplish this task. The journey to a Ph.D. is an entirely new world with lots of ups and downs, support and criticisms. However, my thesis is the result of many experiences I have encountered at BITS Pilani and from the support I received from remarkable individuals. I would like to express my sincere gratitude to all of them. I owe a high debt to my beloved family for their continuous love, affection and support. I am blessed to have such amazingly caring family members, Without their emotional and tangible support, I would not have come this far. It gives me immense pleasure to dedicate my thesis to my family.

Firstly, I would like to express my deep sense of gratitude to my Ph.D. supervisor Dr. Rajeev Sakhuja, for his valuable suggestions, continuous supervision and encouragement throughout my doctoral research.

I would also take this opportunity to express my whole-hearted gratitude to Prof. Souvik Bhattacharyya (Vice-Chancellor, BITS Pilani), Prof. Sudhirkumar Barai (Director, BITS Pilani, Pilani Campus), Prof. Ashoke K. Sarkar (Ex-Director, BITS Pilani, Pilani Campus), Prof. S. K. Verma (Dean, Administration) and Prof. Jitendra Panwar (Associate Dean, AGSRD) for allowing me to pursue my doctoral studies by providing necessary facilities and financial support.

I am very much grateful to my Doctoral Advisory Committee members, Prof. Dalip Kumar and Prof. Indresh Kumar. Their insightful suggestions and comments always broaden the perspectives related to research.

I want to extend my sincere thanks to Prof. Madhushree Sarkar (Convener, Departmental Research Committee, Department of Chemistry, BITS Pilani, Pilani Campus) and Prof. Ram Kinkar Roy (Head, Department of Chemistry, BITS Pilani, Pilani Campus) for their kind support.

I am immensely thankful for all the cooperation and affection I received from the faculty members of the Department of Chemistry, BITS Pilani, which has made my stay here very productive. My sincere regards to Prof. S. C. Sivasubramanian, Prof. Anil Kumar, Prof. Bharti Khungar, Prof. Inamur Rahaman Laskar, Prof. Saumi Ray, Prof. Ajay Kumar Sah, Prof. Shamik Chakraborty, Prof. Prashant Uday Manohar, Prof. Surojit Pande, Dr. Bibhas Ranjan Sarkar and Prof. Paritosh Shukla. I am highly thankful to Dr. Kiran Bajaj for her valuable discussions and suggestions. In addition, The central Instrumentation Facility and DST-FIST are also deeply acknowledged for providing instrumentation facilities. My sincere thanks to

Dr. Ranjan Sinha Thakur, Librarian, BITS Pilani and other staff of the library for their support and help rendered in utilizing the library services.

"If you want to master something, teach it", I understood the spirit of this beautiful quote by Richard Feynman when I got the privilege to teach the lab practicals to graduate and undergraduate students. Interactions with them always helped me in refining my ideas.

I would like to acknowledge my seniors and fellow labmates Dr. Abdul Shakoor, Dr. Santosh Kumari, Dr. Devesh S Agarwal, Mr. Mahesha, Ms. Sushma, and Mr. Narendra who always helped me in need. My special thanks to all the research scholars of Department of Chemistry, BITS Pilani, Pilani campus. I am extremely thankful to the office staff and lab staff (Department of Chemistry) especially Ms. Pushpa, Mr. Suresh and Mr. Nandalal for allowing me to access the general lab equipments and providing general chemicals. I would like to extend my gratitude to my research collaborator Prof. Sanjay K. Mandal, IISER Mohali for providing single crystal X-ray analysis.

I feel fortunate to have a great company of research scholars from the Department of Pharmacy. It was a great opportunity to share ideas and receive their support in need. Earnest thanks to my friends Dr. Vidhi Vyas, and Ms. Soumya Kar for their moral support and friendly gesture. I cannot forget to acknowledge Ms. Shreya Das for the fun time spent together and for making the pandemic time a memorable one.

Words cannot express my gratitude towards my family and teachers (Chandra teacher and Mary teacher) and cannot be counted on these pages. I would like to thank My parents Mr. Narendra Kumar and Ms. Lalitha for giving me the strength and encouraging me to pursue my research with enthusiasm and confidence. My Sisters Ms. Dharani Deepika, Ms. Pooja, Ms. Kathyaeni Vidmahe and my brother Eshaan for always cheering me up.

Finally, my sincere thanks to all my relatives and well-wishers whose faith, encouragement, and constant moral support have contributed in a big way to the completion of this work. I express my sincere and special thanks to all of them.

Date: **PIDIYARA KARISHMA**

ABSTRACT

Transition metal catalysis has played a center-stage role in designing an ample range of complex heterocyclic architectures. In this realm, diazaheterocycles have been considered as the most valuable targets in synthetic organic chemistry because of their wide range of applications in medicinal and material chemistry. The work disclosed in the present thesis entitled "**Rhodium/Ruthenium-Catalyzed Strategies for the Synthesis of Fused and Functionalized *N*-Aryl-2,3-dihydrophthalazine-1,4-diones**" deals with the functionalization and annulation of *N*-aryl-2,3-dihydrophthalazine-1,4-dione scaffold with different coupling partners *via* metal-catalyzed oxidative strategies. The thesis is divided into six chapters.

The first chapter of the thesis presents a brief background on directing group-assisted transition metal-catalyzed C-H bond activation approaches, especially in light of the catalytic role played by rhodium and ruthenium in such strategies. Further, the chapter describes two efficient Rh(III)-catalyzed additive-modulated protocols for the synthesis of unprecedented hydroxy-dihydroindazolo[1,2-*b*]phthalazines and phthalazino[2,3-*a*]cinnolines by the reaction of *N*-aryl-2,3-dihydrophthalazine-1,4-diones with α-diazo carbonyl compounds in good-to-excellent yields. The developed strategies relies on the role of additives, CsOAc and $AgSbF_6$ in commencing [4+1] and [4+2] annulative cyclizations, respectively.

The second chapter of the thesis presents a brief overview on the significance of fused and functionalized cinnolines, especially phthazino-fused cinnolines. Following this, the chapter documents a Rh(III)-catalyzed methodology for the synthesis of hydroxyimino functionalized phthalazino[2,3-*a*]cinnolines by reductive [4+2] annulation between *N*-aryl-2,3-dihydrophthalazine-1,4-diones with varied nitroolefins. The targeted oxime decorated tetracyclic fused-cinnolines were synthesized *via* sequential C-H activation/olefin insertion/reduction under reducing-agent free conditions.

The third chapter of the thesis describes a one-pot protocol for the spirocyclization of *N*-aryl-2,3-dihydrophthalazine-1,4-diones with maleimides *via* Rh(III)-catalyzed sequential *ortho*-alkenylation followed by intramolecular aza-Michael-type addition/protonation process. The featured strategy furnishes a series of thirty-one diversely decorated spiro[indazolo[1,2-*b*]phthalazine-13,3'-pyrrolidine]-2′,5′,6,11-tetraones in high yields from substituted *N*-aryl-2,3-dihydrophthalazine-1,4-diones and *N*-aryl/alkyl maleimides. Isolation and characterization of a

maleimide-coordinated five-membered rhodacyclic intermediate provides a strong evidence for the proposed mechanism of the reaction.

The fourth chapter of the thesis presents a brief background on the reactivity of *α*-carbonyl sulfoxonium ylides as a coupling partner in metal-catalyzed C-H activation processes. After this, the chapter discloses a detailed synthetic protocol for the synthesis of *ortho*-C(sp^2)-H acylmethylation of *N*-aryl-2,3-dihydrophthalazine-1,4-diones with *α*-carbonyl sulfoxonium ylides to furnish 2-(*o*-acylmethylaryl)-2,3-dihydrophthalazine-1,4-diones under Ru(II)-catalyzed condition. Furthermore, independent series of 6-arylphthalazino[2,3-*a*]cinnoline-8,13-diones and 5-acyl-5,6-dihydrophthalazino[2,3-*a*]cinnoline-8,13-diones were synthesized by the cyclization of 2-(*o*-acylmethylaryl)-2,3-dihydrophthalazine-1,4-diones with Lawesson's reagent and $BF_3{\cdot}OEt_2$, respectively. Of these, the $BF_3{\cdot}OEt_2$-mediated cyclization proceeded in DMSO that acted as a solvent and a methylene source as well in the cyclization.

The fifth chapter of the thesis describes efficient Ru(II)-catalyzed strategies towards direct carbocyclization of diversely substituted *N*-aryl-2,3-dihydrophthalazine-1,4-diones using isocyanates as carbonyl source. This methodology proceeded *via* sequential *ortho*-amidation followed by intramolecular nucleophilic substitution, delivering substituted indazolo[1,2-*b*]phthalazine-triones in good-to-excellent yields. By modifying the reaction parameters, a series of *ortho*-amidated products were also isolated in excellent yields.

Finally, in **the sixth chapter** of the thesis, a summary of the thesis work is presented along with the future scope of the research work.

LIST OF TABLES

LIST OF FIGURES

LIST OF ABBREVIATIONS / SYMBOLS

Abbreviation/Symbol	Description
α	Alpha
β	Beta
γ	Gamma
λ	Lambda
δ	Chemical shift in parts per million
η	Eta
°C	Degree centigrade
σ	Sigma
π	Pi
Å	Angstrom
%	Percentage
Z	Zusammen
S	Sinister
ACN	Acetonitrile
Ar	Aryl
Aq	Aqueous
$AgNTf_2$	Silver triflimide
AgOAc	Silver acetate
AdCOOH	1-Adamantane carboxylic acid
ADA	Adenosine deaminase
atm	Atmosphere
Bn	Benzyl

B_2Pin_2	Bis(pinacolato)diboron
$BF_3{\cdot}OEt_2$	Boron trifluoride etherate
t-BuOH	*tert*-Butyl alcohol
^{13}C	Carbon-13
$CDCl_3$	Deuterated Chloroform
CD_3COOD	Deuterated Acetic Acid
Cy_2NMe	*N*,*N*-Dicyclohexylmethylamine
COSY	Correlation Spectroscopy
CsOPiv	Cesium pivalate
$Cu(OAc)_2$	Copper acetate
Calc.	Calculated
COD	Cyclooctadiene
CCDC	Cambridge Crystallographic Data Center
m-CPBA	*meta*-Chloroperoxybenzoic acid
d	Doublet
dd	Doublet of doublet
DG	Directing Group
DCE	1,2-Dichloroethane
DEAD	Diethyl azodicarboxylate
DCM	Dichloromethane
DIAD	Diisopropyl azodicarboxylate
DIPA	Diisopropylamine
DIPEA	Diisopropyl ethyl amine
DMF	*N*,*N*-Dimethylformamide
DMSO-d_6	Deuterated dimethylsulfoxide

DMA	Dimethylacetamide
DMSO	Dimethylsulfoxide
ESI-MS	Electron Spray Ionization-Mass Spectrometry
Et_2O	Diethyl ether
EtOAc	Ethyl acetate
EtOH	Ethanol
EWG	Electron Withdrawing Group
EDG	Electron Donating Group
equiv.	Equivalent
g	Gram
h	Hours
HFIP	Hexafluoroisopropanol
HRMS	High Resolution Mass Spectrometry
HSQC	Heteronuclear Single Quantum Correlation
HMBC	Heteronuclear Multiple bond Correlation
Hz	Hertz
^{i}Pr	Isopropyl
J	Coupling constant
KOAc	Potassium acetate
KIE	Kinetic Isotopic Effect
k_H	Protonated rate constant
k_D	Deuterated rate constant
P_H	Protonated product constant
P_D	Deuterated product constant
LiO^tBu	Lithium tertiary butoxide

LiOAc	Lithium acetate
LAH	Lithium Aluminium Hydride
LC/MS	Liquid Chromatography/Mass Spectrometry
mp	Melting point
m	Meta
m	Multiplet
mL	Millilitre
mg	Milligram
MHz	Megahertz
min	Minutes
mmol	Millimole
mol %	Mole percent
MeOH	Methanol
MeOD	Deuterated Methanol
NaOAc	Sodium acetate
NEt_3	Triethyl amine
NMR	Nuclear Magnetic Resonance
Nu	Nucleophile
o	Ortho
OTf	Triflouromethanesulfonate
ORTEP	Oak Ridge Thermal Ellipsoid Plot
p	Para
Py	Pyridine
PhMe	Toluene
PhCl	Chlorobenzene

Phen	1,10-Phenanthroline
PIDA	Phenyl iodonium diacetate
PivOH	Pivalic acid
$PhCO_2H$	Benzoic acid
ppm	Parts per million
PTFE	Polytetrafluoroethylene
Q-TOF	Quadrupole Time Of Flight
rt	Room temperature
s	Singlet
SET	Single Electron Transfer
S_EAr	Electrophilic Aromatic Substitution
t	Triplet
t-AmOH	*tert*-Amyl alcohol
td	Triplet of doublets
TFA	Trifluoroacetic acid
TEMPO	(2,2,6,6-Tetramethylpiperidin-1-yl)oxyl
TFE	Trifluoroethanol
TBHP	*tert*-Butyl hydroperoxide
THF	Tetrahydrofuran
TLC	Thin layer chromatography
TFBen	Benzene-1,3,5-triyl triformate
XRD	X-Ray diffraction
$Zn(OAc)_2$	Zinc acetate

TABLE OF CONTENTS

CHAPTER 1

Rhodium-Catalyzed [4+1]/[4+2] Annulations of *N*-Aryl-2,3-dihydrophthalazine-1,4-diones with *α*-Diazo Carbonyl Compounds

1.1 Background

Heterocyclic chemistry is one of the important and vast area of research in the field of organic chemistry because of diverse applications of heterocycles as pharmaceuticals, agrochemicals, polymers, sensors, gelators, LEDs, *etc.*[1-3] Fascinating structures of nitrogen-containing natural products and their supremacy in curing deadly diseases has opened inspiring doors for chemists to develop novel methodologies for their synthesis and other related synthetic analogues.[4-6] However, challenges encountered in the total synthesis campaigns of most heterocyclic natural products have provided a rationale for designing efficient synthetic strategies for comparatively simpler functionalized and fused azaheterocycles by conjugating cascade sequences and powerful reactions. Along with the requirements of green chemistry for atom-economy and step-economy transformations for the construction of new chemical bonds, focused efforts have been devoted to develop novel synthetic protocols by directly coupling electron-rich/deficient (hetero)arenes with varied reagents or coupling partners to achieve C-H functionalization and/or subsequent cyclization.[7,8]

With the advent of Pd-dominant Heck,[9] Buchwald-Hartwig[10] and other cross-coupling reactions,[11-13] a hike in the usage of reactive aryl/vinyl halides and unsaturated compounds capable of interacting with transition metals, was observed during their illustrious applications towards fostering C-C/C-N bond formations in the last three decades. However, several steps are necessary for the pre-functionalization of the starting materials, and the production of substantial amount of by-product waste accompanies these reactions, thus, making the overall process cumbersome. Though the development of metal-free strategies were also gearing up, yet the scope and power of transition metal catalysis was unbeatable. Alternatively, transition metal-catalyzed direct carbon–hydrogen activation reactions have opened up an entirely new dimension in synthetic organic chemistry, whereby various transition metal catalysts, including Co, Cu, Pd, Ru, Rh and Ir have played eye-catching roles in constructing complex heterocyclic frameworks, sometimes even by unprecedented and unusual reaction mechanisms.[14,15]

1.1.1 Transition metal-catalyzed direct C-H bond functionalization

Transition metal-catalyzed direct C-H bond functionalization represent a promising class of transformations that converts ubiquitous and generally inert C-H bonds into C-C and C-Het bonds (Het = N, O or X) bonds (Figure 1.1.1.1).[16] This has been accomplished by the use of a transition metal catalyst in combination with appropriate ligand, oxidant and/or additive. Thus, the direct

catalytic cleavage and transformation of the unactivated C-H bonds eradicates the need for the pre-functionalization of the substrates and allows the formation of unlimited library of compounds in fewer steps, and generating lesser by-products.[17]

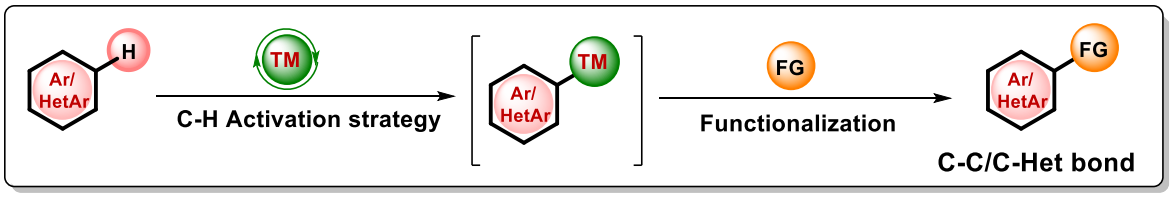

Figure 1.1.1.1 General representation of C-H bond activation and functionalization

The overabundance of C-H bonds in organic molecules with closely similar bond energies has led to the interest of scientists in the C-H bond activation chemistry in the past two decades.[18] Consequently, focused efforts have been made towards elucidating the mechanism of C-H functionalization process *via* metal-catalyzed C-H bond activation.[19,20] In summary, the elementary step of C-H activation has mostly been proposed to occur by one of the four defined processes, *viz* oxidative addition, σ-bond metathesis, electrophilic aromatic substitution and concerted metalation deprotonation pathways. Of these, oxidative addition (OA) commonly occurs when an electron-rich metal center (*i.e.* low oxidation state) strongly interacts with the C-H bond *via* a σ-C-H bond coordination to the metal and a d_π-back donation to the σ^*-C-H orbital, thus lowering the bond order of C-H bond, which results in a cleavage of C-H bond in a homolytic manner and oxidising the metal center by two units (Figure 1.1.1.2a). While, σ-bond metathesis (σ-BM) is commonly exhibited by electron poor metal centers (*i.e.* high oxidation state). Though this pathway, the bond cleavage and the bond forming events take place in a concerted pathway *via* a four-membered metalacycle transition state without changing the oxidation state of the metal center (Figure 1.1.1.2b). On the other hand, the electrophilic aromatic substitution (S_EAr) pathway is based on the interaction between the π-electronic cloud of the substrate and the electrophilic metal centers resulting in a new C(aryl)-M bond without changing the oxidation state of the metal. This enhances the acidity of the vicinal C(aryl)-H bond, which releases the proton easily by re-aromatization or in the presence of a base. The mechanism can also be referred as base-assisted intramolecular electrophilic substitution when the base is in the coordination sphere of the metal center (Figure 1.1.1.2c). Finally, the Concerted Metalation Deprotonation (CMD) mechanism falls out when the C-H bond is in close proximity to the metal center and is usually promoted by a directing donor group. At the same time, the metal center consists of a coordinated base that

promotes the deprotonation of the C-H bond in a concerted fashion (Figure 1.1.1.2d). Often, the mechanistic pathways followed by different organic substrates remains unclear and debatable unless proven by specific experimental results or computational studies.

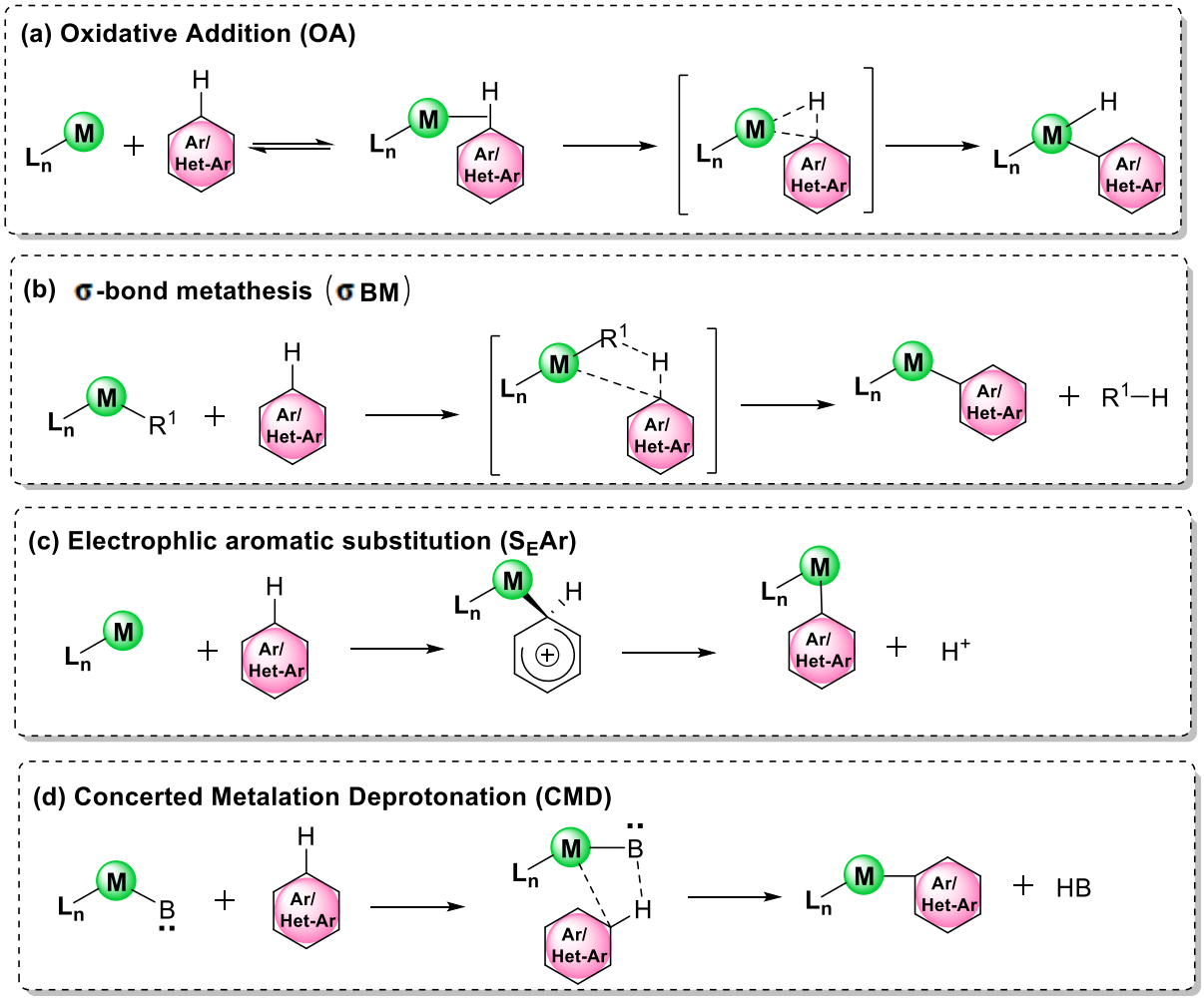

Figure 1.1.1.2 Mechanistic pathways for elementary C-H bond activation step

In spite of great advancements and success, two fundamental issues associated with the C-H activation chemistry remains challenging: (i) the reactivity issues arising due to inertness of C-H bonds,[21,22] and (ii) the regioselective functionalization of any one over the other. The steric or electronic effects in specific substrates and fine tuning of the reaction conditions by correctly choosing the catalyst, ligand, additive and solvent has resolved the above mentioned challenges to a limited extent.[23] The employment of a directing group (DG) in close proximity to the C-H bond to be functionalized has provided an alternate and effective solution to resolve the issue of selectivity in C-H bond activation chemistry.[24]

1.1.2 Directing group (DG)-assisted C-H bond functionalization

The term "directing group (DG)" refers to a heterocyclic moiety or functional group possessing a pair of electrons that can be utilized to coordinate reversibly with a transition metal, thereby bringing the metal to close proximity to the C-H bond to be functionalized.[16,17] This helps in increasing the effective concentration of the metal at that site, thus enhancing the successful insertion of the metal into the desired C-H bond in a regioselective fashion.[25] In heterocyclic compounds, the reactivity of the C-H bond is mainly controlled by the presence of heteroatoms, and the regioselective C-H bond functionalization can be achieved even in absence of a directing group. While, selective functionalization of a non-biased C*(sp²)*-H or C*(sp³)*-H bond in an aromatic or aliphatic compound is inherently difficult, and thus unprecedented reactions can take place. Directing group (DG)-assisted C-H bond functionalization started gaining momentum in the mid-1990s after a landmark contribution by Murai's group.[26] Over the years, chelation-assisted C-H bond activation strategy has not only resolved the selectivity issues, but also offers a unique solution to the rapid synthesis of complex molecules in a convenient and predictable manner.[27,28] In this realm, a plethora of strong and weak directing groups (DGs), including *N*-heterocycles such as pyridine, pyrimidine, triazole, pyrazole, oxadiazole, benzothiazole, 8-aminoquinoline, picolinamide, and functionalities such as amine, amide, imine, carboxylic acid, ester, ketone, nitrile, oxime, hydrazine, hydroxyl, urea, sulfoximine phosphine oxide and urea have been employed as directing groups for C-H bond functionalizations (Figure 1.1.2.1).[29]

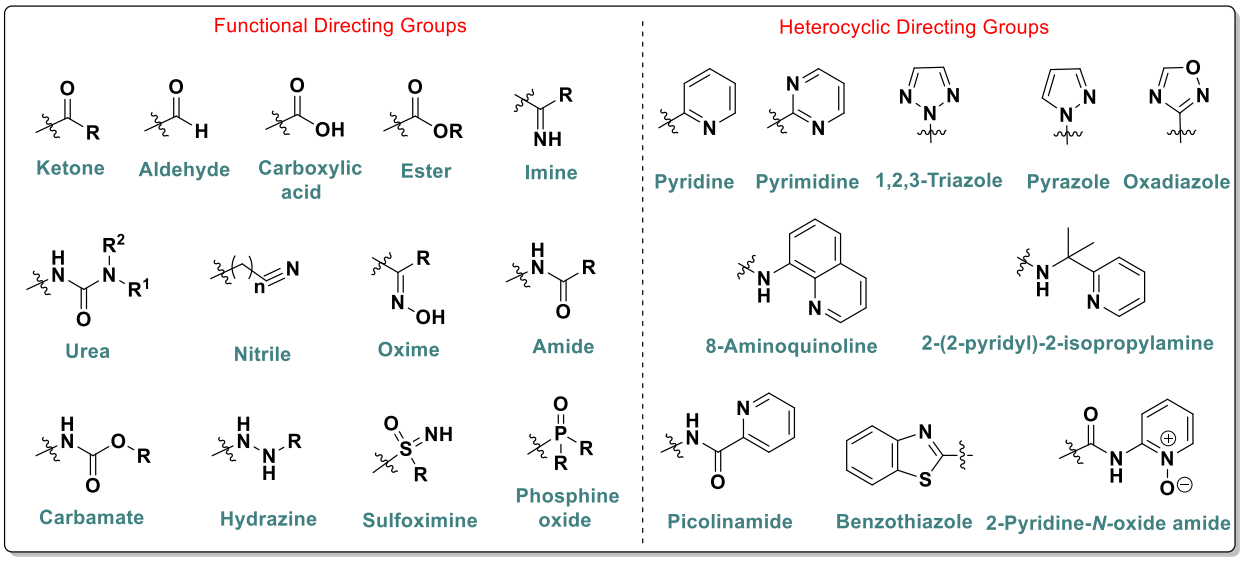

Figure 1.1.2.1 Representative examples of directing group (DGs) explored in C-H activation chemistry

Directing group-assisted C-H bond functionalizations can be broadly classified into two types[27]:

(A) In-built directing group (DG)-assisted C-H bond functionalization, which basically refers to a coordinating functional group that is already present in the molecule (Figure 1.1.2.2A).

(B) Removable directing group (DG)-assisted C-H bond functionalization, in which it is necessary to pre-install the directing group or to install *in-situ* in a molecule *via* functional group transformation to achieve a favored coordination with the metal for certain types of C-H bond functionalizations (Figure 1.1.2.2B).

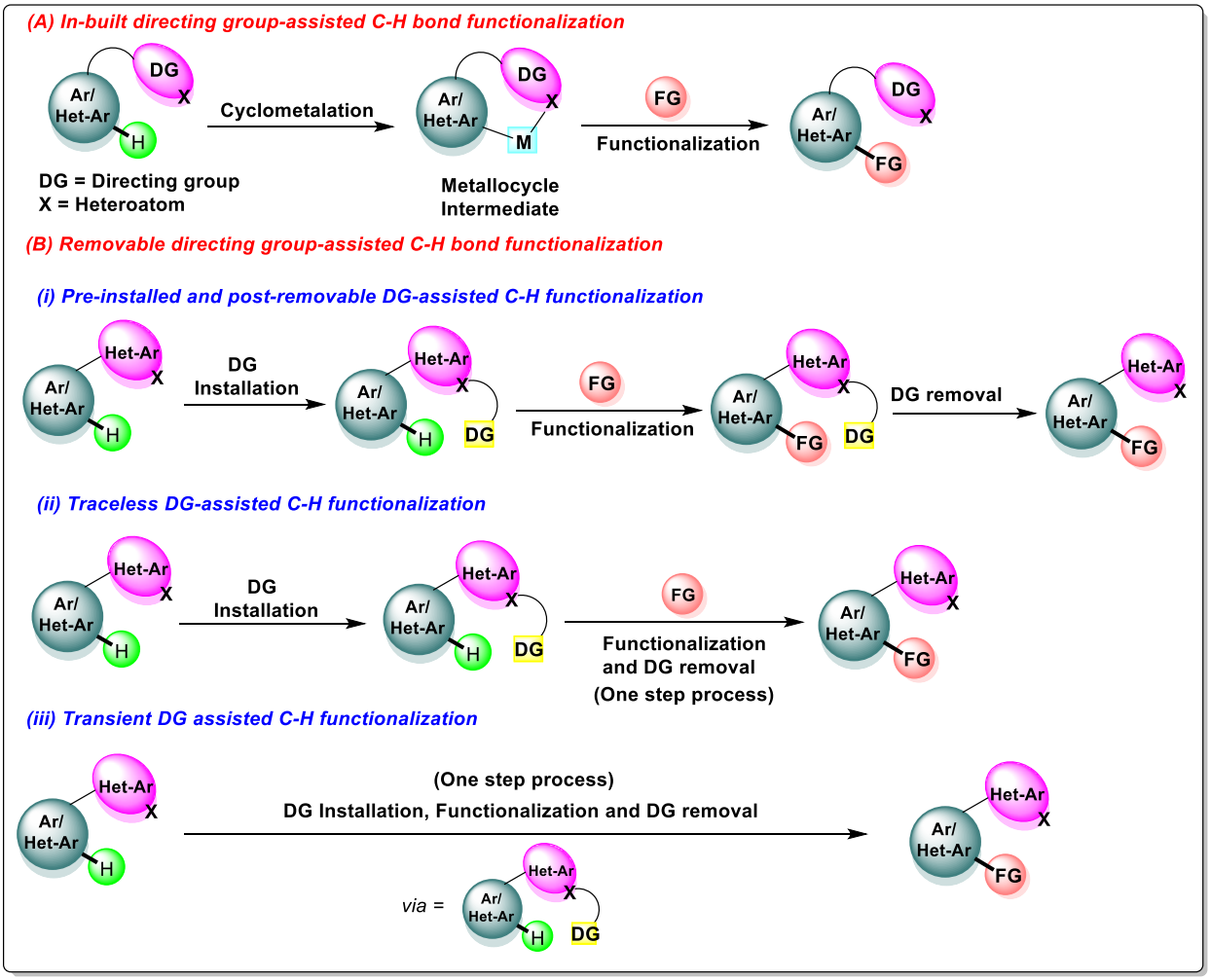

Figure 1.1.2.2 Categories of directing group (DG)-assisted C-H functionalization

The latter is further sub-divided into three categories: (i) pre-installed and post-removal DG-assisted C-H bond functionalization: this process encompasses pre-installation of directing group, C-H functionalization followed by removal of directing group. Although this approach has enjoyed considerable success, yet one of the major concerns is that this strategy is not step-economical and

requires additional steps for the installation and removal of directing group. In this approach the directing group will be a part of the final product (Figure 1.1.2.2Bi). (ii) Traceless directing group (DG)-assisted C-H bond functionalization, wherein insertion of directing group takes place in first step accompanied by C-H functionalization and removal of directing group in next step. This method involves an additional step for the installation of directing group (Figure 1.1.2.2Bii). (iii) Transient directing group (TDG)-assisted C-H bond functionalization, in which *in-situ* installation of the transient directing group, C-H functionalization and removal of directing group takes place in a one-step process (Figure 1.1.2.2Biii).

1.1.3 Rhodium catalysis

Rhodium, a noble metal with an atomic number, Z = 45 and electronic configuration of $[Kr]4d^8 5s^1$, was discovered and isolated by William Hyde Wollaston in 1803. In recent years, remarkable advancements in the rhodium-catalyzed C-H functionalization has been achieved towards the development of numerous C-C, C-N, C-O and C-X bond forming reactions.[30-33] Various commercially available rhodium complexes possessing Rh in variable oxidation states (O.S.) such as, $Rh_4(CO)_{12}$ (O.S. = 0), $RhCl(PPh_3)_3$ (O.S. = +1), $[Rh(OAc)_2]_2$ (O.S. = +2), $[Cp^*RhCl_2]_2$ (O.S. = +3), $Rh_2(oct)_4$ (O.S. = +2), $[RhCl(cod)]_2$ (O.S. = +1), $[RhCl(coe)]_2$ (O.S. = +1) have exemplified interesting catalytic activities for numerous C-H functionalization reactions under additive-driven solvent-modulated experimental conditions (Figure 1.1.3.1).

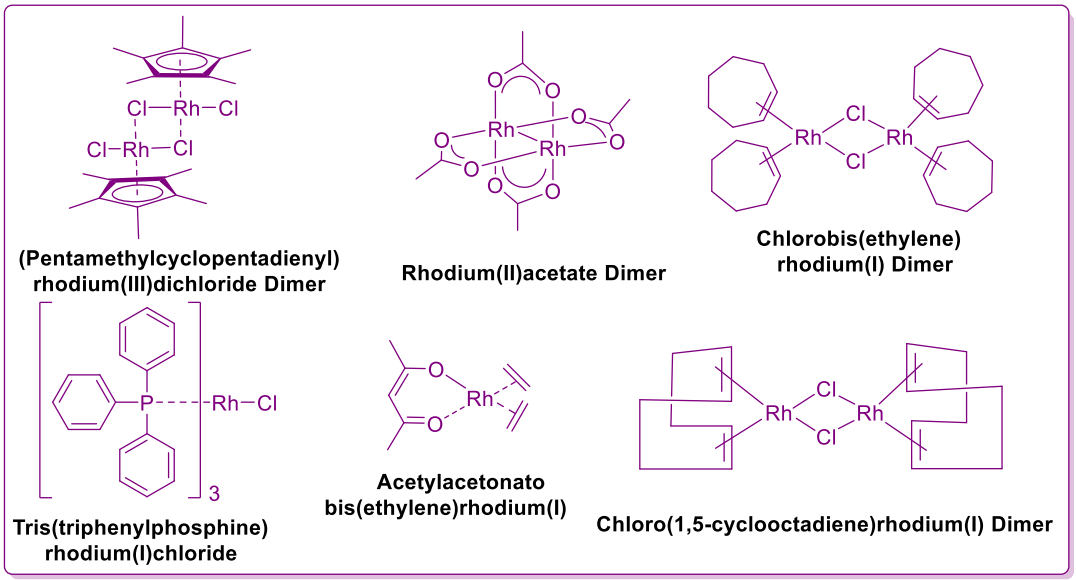

Figure 1.1.3.1 Selective examples of rhodium complexes used in organic synthesis

Compared with other transition metals, rhodium-catalyzed reactions have several advantages, such as (a) good functional group tolerance, (b) high efficiency even with low catalyst loading and (c) broad substrate scope.[34] Rh-catalyzed directed C-H functionalization reactions have been extensively studied in regard to a number of transformations, including allylation,[35] alkylation,[36,37] arylation,[38] halogenations,[39] hydroacylation,[40] alkenylation,[41] amidation[42,43] and annulation[44] (Figure 1.1.3.2). Moreover, rhodium catalysis is mechanistically diverse. As a consequence of its inertness, rhodium is also suitable as an industrial catalyst. In addition, a number of versatile, Rh-catalyzed reactions including hydroformylation,[45] asymmetric hydrogenation,[46,47] diazo compound addition[48] and several new types of cycloadditions have been revealed.[49]

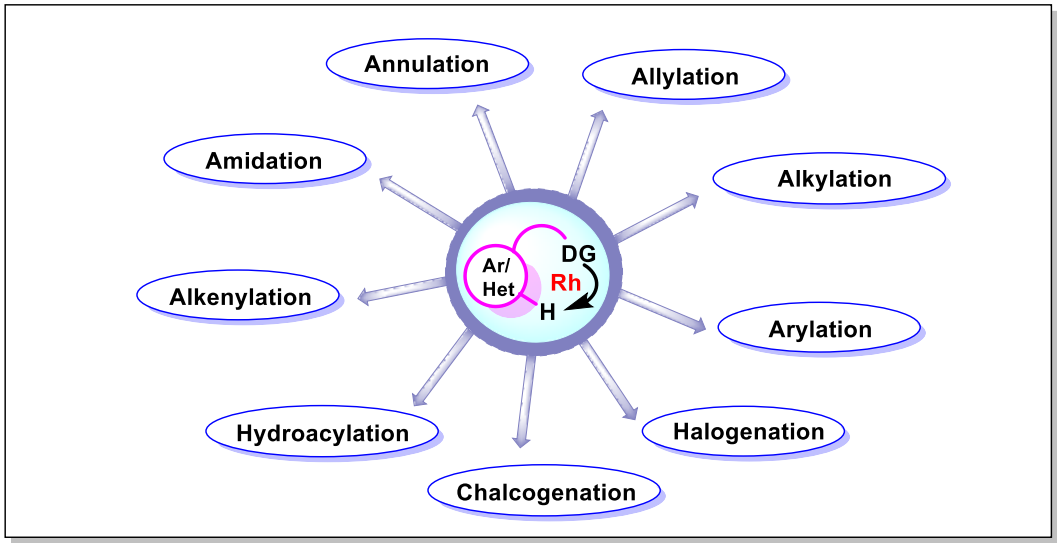

Figure 1.1.3.2 A pictorial representation of reported Rh-catalyzed functionalizations *via* C-H activation

1.1.4 Ruthenium catalysis

Ruthenium (Ru) is the 74th most abundant metal on earth (Z = 44), with an electronic configuration [Kr]4d^{7}5s^1. Ruthenium was discovered and isolated by Karl Ernst Claus in 1844. Ruthenium complexes are powerful and versatile synthetic tools that have been extensively examined in C-H bond functionalization, possibly due to (a) facile formation of cyclometalated species under mild conditions *via* CMD (concerted metalation/deprotonation) process, (b) compatibility with variable oxidants, and (c) ease in handling, and (d) stability to air or moisture.[50] Ruthenium displays a broad range of oxidation states (O.S.) in its various complexes such as [Ru(PPh$_3$)$_3$(MeCN)] (O.S. = 0), [RuCl(dppp)$_2$] (O.S. = +1), [RuCl$_2$(PPh$_3$)$_3$] (O.S. = +2), [Ru(*p*-cymene)Cl$_2$]$_2$ (O.S. = +2), [Cp*Ru(PPh$_3$)$_2$Cl] (O.S. = +2), [RuCl$_3$] (O.S. = +3), Ru(acac)$_3$ (O.S. = +3) (Figure 1.1.4.1).

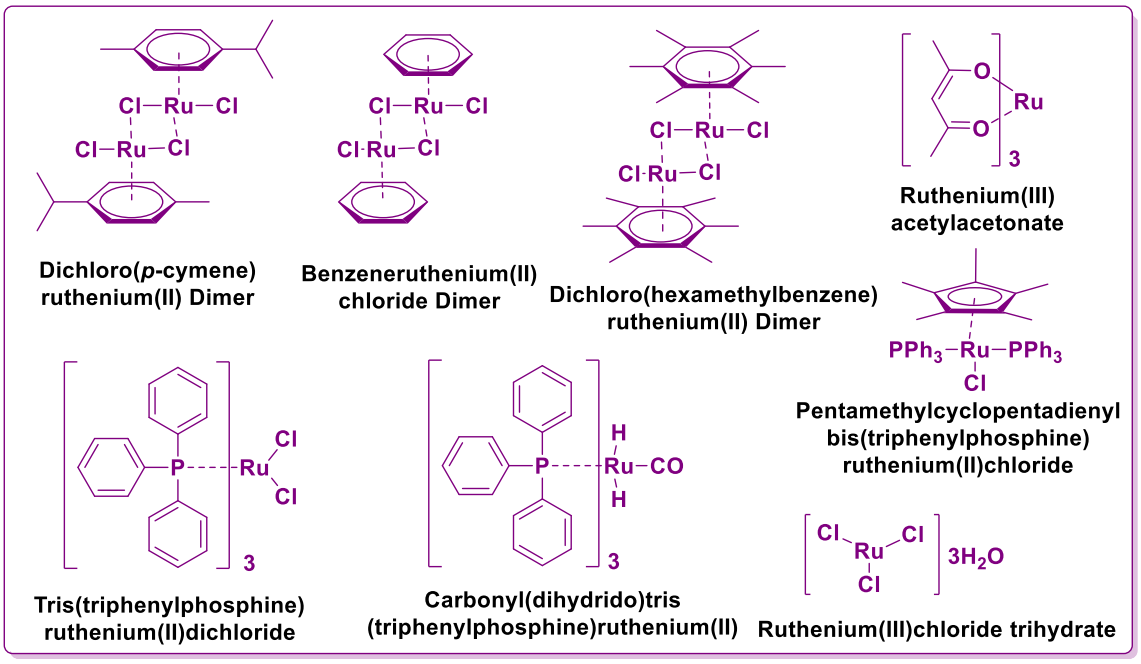

Figure 1.1.4.1 Selective examples of ruthenium complexes used in organic synthesis

Interestingly, in recent years ruthenium complexes has been actively involved in several chelation-assisted functionalization methodologies, such as hydroarylation of alkynes,[51,52] catalytic alkylation of C*(sp²)*–H bonds with alkyl halides,[53] amidation,[54] acylation,[55] hydroxylation of C*(sp²)*–H bonds,[56] carboxylation,[57] and cyanation[58] *etc.* (Figure 1.1.4.2).

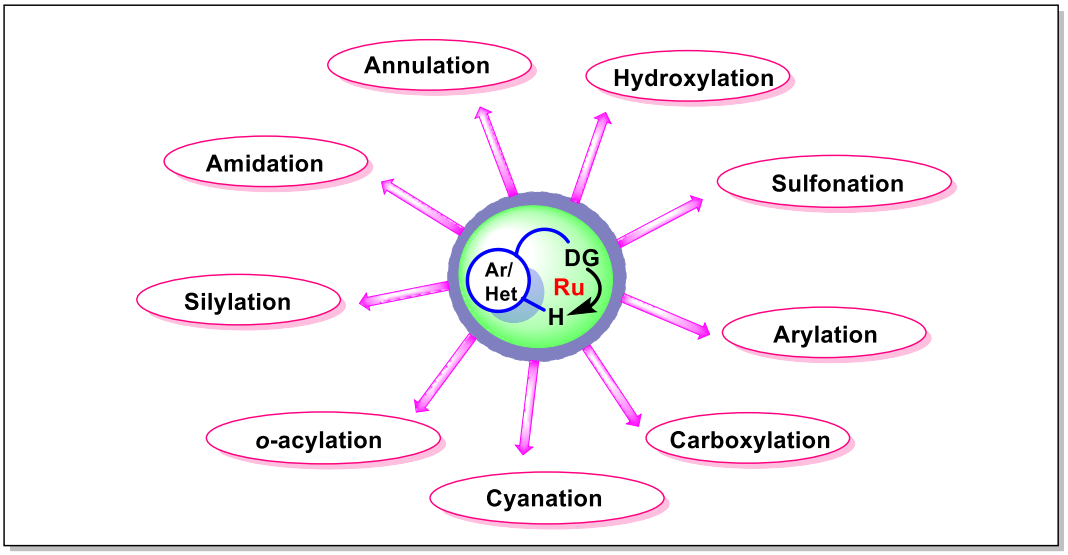

Figure 1.1.4.2 A pictorial representation of reported Ru-catalyzed functionalizations *via* C-H activation

In the backdrop of the above discussion, we undertook the task of systematically performing chelation-assisted C*(sp^2)*-H functionalization and possible cyclizations of *N*-aryl-2,3-dihydrophthalazine-1,4-diones with varied coupling partners under Rh/Ru catalysis, envisioning the directing group influence of intrinsic cyclic amidic moiety in these substrates. The rationale behind selection of specific coupling partners is presented in the introduction section of respective chapters.

1.2 Introduction

Diazaheterocycles have been considered as privileged structures of great interest to the organic chemists due to their natural occurrence and varied applications in medicinal and material chemistry.[59,60] Accordingly, substantial attention has been focused on the development of complementary approaches towards their synthesis in the past.[61] In specific, benzodiazines such as phthalazine (**I**), cinnoline (**II**), quinazoline (**III**) and quinoxaline (**IV**) are ubiquitous moieties forming an integral part of several natural products and established therapeutic drugs and molecules under clinical trials (Figure 1.2.1).[62-68]

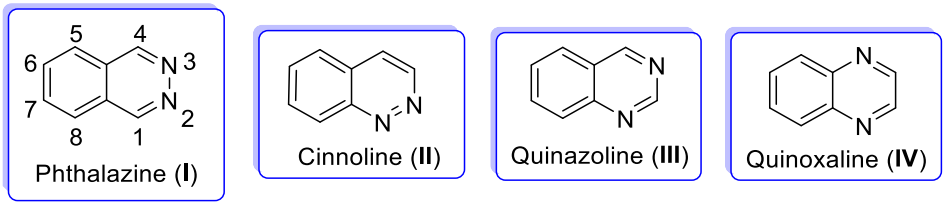

Figure 1.2.1 Chemical structures of benzodiazines

Of these, phthalazine (**I**) is an interesting ubiquitous diazaheterocyclic motif found in numerous marketed drugs[69] and functional materials.[70] Though rarely observed in natural products (*e.g.* Azamerone),[71] phthalazine derivatives exhibit diverse biological activities such as antitumor (*e.g.* Vatalanib),[72-74] anticonvulsant,[75-77] antihypertensive,[78] anti-inflammatory,[79-81] cardiotonic,[82] and antimicrobial,[83-85] activities (Figure 1.2.2).

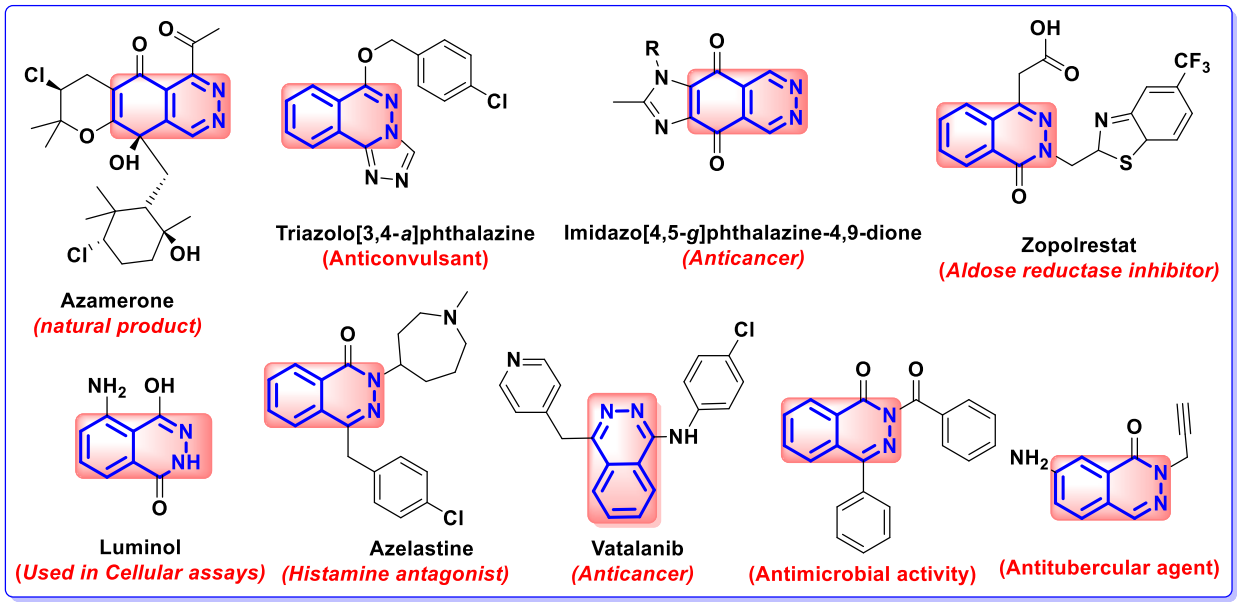

Figure 1.2.2 Selective examples of biologically active fused and functionalized phthalazines

Within this domain, various metal-catalyzed strategies came into the limelight towards the annulation of *N*-aryl-2,3-dihydrophthalazine-1,4-diones with varied coupling partners for the synthesis of indazolo-phthalazines in recent years. For instance, in 2018 Ji *et al.* reported a Rh(III)-catalyzed oxidant-free [4+1] annulation approach for the synthesis of quaternary-center-bearing divergent heterocycles, including indazolo[1,2-*b*]phthalazines (**3**) from the coupling of corresponding *N*-arylphthalazinones (**1**) and propargyl alcohols (**2**) (Scheme 1.2.1).[86]

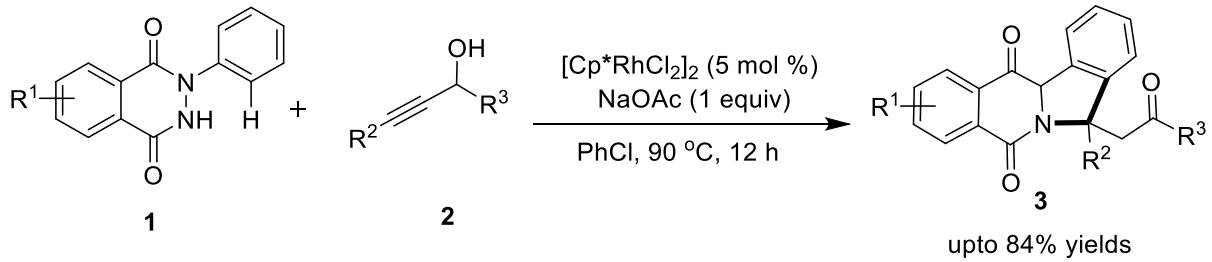

Scheme 1.2.1 Rhodium-catalyzed annulation of *N*-arylphthalazinones (**1**) with propargyl alcohols (**2**)

Likewise, Kianmehr and coworkers disclosed the oxidative C-H bond alkenylation of *N*-aryl-2,3-dihydrophthalazine-1,4-diones (**1**) with acrylates (**4**) *via* intramolecular cyclization under Rh(III)-catalyzed conditions using water as a green solvent, affording a series of indazolo-fused phthalazine derivatives (**5**) in excellent yields (Scheme 1.2.2).[87]

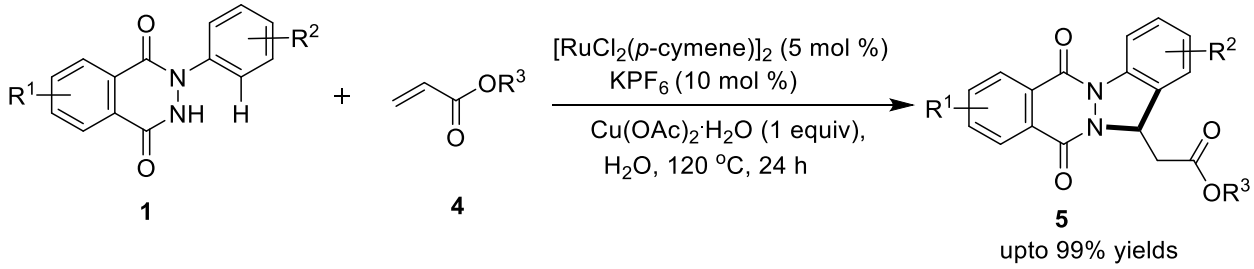

Scheme 1.2.2 Rhodium-catalyzed annulation of *N*-aryl-2,3-dihydrophthalazinones (**1**) with acrylates (**4**)

In 2021, Kim and group reported the Ru(II)-catalyzed C(sp^2)-H activation and hydroxyalkylation of *N*-aryl-2,3-dihydrophthalazine-1,4-diones (**1**) with aldehydes (and activated ketones) (**6**), furnishing an array of hydroxyalkylated phthalazinone substrates (**7**), which undergoes intramolecular Mitsunobu cyclization to produce tetracyclic indazolo-fused phthalazinones (**8**) in good-to-excellent yields (Scheme 1.2.3)[88]

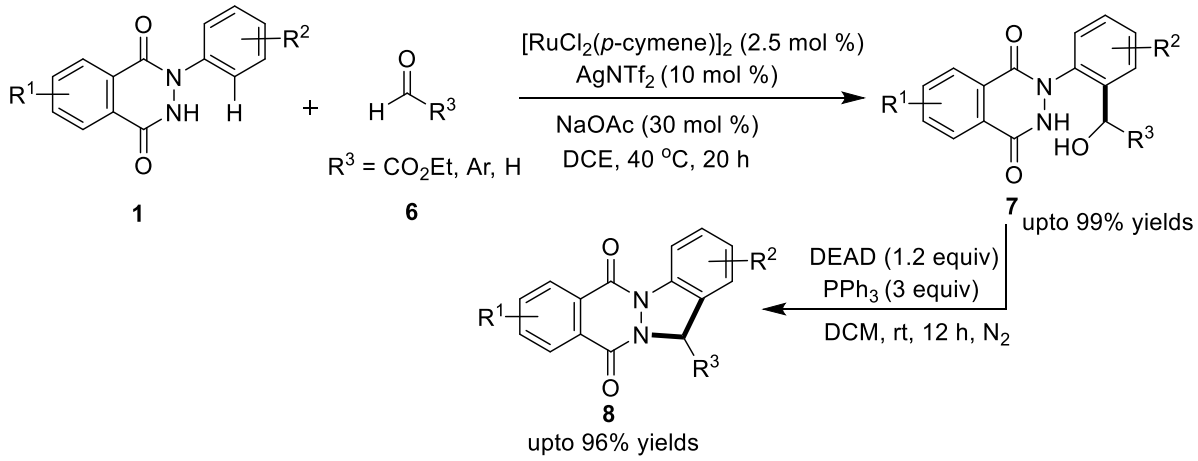

Scheme 1.2.3 Ruthenium-catalyzed hydroxyalkylation and subsequent intramolecular cyclization of *N*-aryl-2,3-dihydrophthalazinones (**1**) with aldehydes (**6**)

Another synthetic protocol towards the construction of indazolo-fused phthalazines (**10**) bearing a quaternary center was successfully developed by Yu and coworkers, coupling *N*-arylphthalazinones (**1**) with allenes (**9**) under $[Cp^{*}RhCl_2]_2$/AgOAc/NaOAC catalytic system in acetonitrile at 120 °C for 12 h. (Scheme 1.2.4).[89]

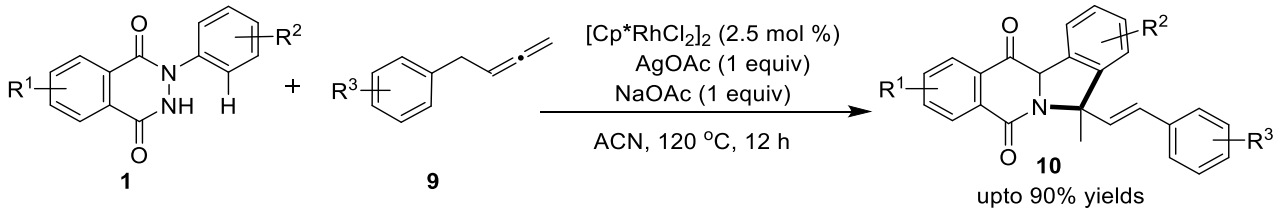

Scheme 1.2.4 Rhodium-catalyzed annulation of *N*-arylphthalazinones (**1**) with allenes (**9**)

The same group reported a Rh(III)-catalyzed spirocyclization of *N*-aryl-2,3-dihydrophthalazine-1,4-diones (**1**) using various substituted cyclic diazo naphthalenones (**11**), resulting in a series of spirocyclic indazolo-fused phthalazinones (**12**) in good yields. The proposed methodology featured broad functional group tolerance and a high atom economy (Scheme 1.2.5).[90]

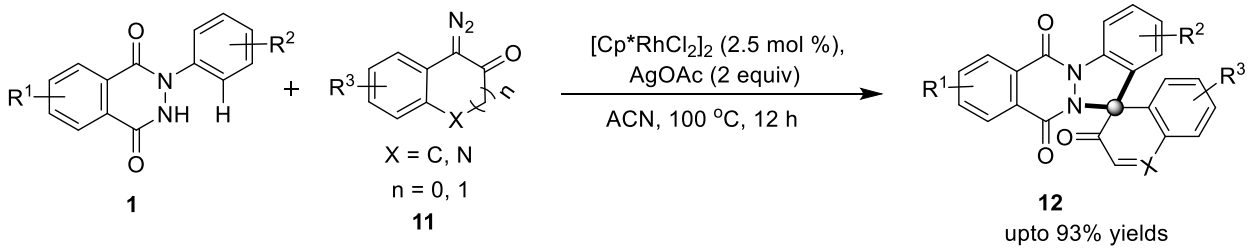

Scheme 1.2.5 Rhodium-catalyzed spirocyclization of *N*-aryl-2,3-dihydrophthalazinones (**1**) with cyclic diazo naphthalenones (**11**)

Strikingly, *α*-diazo carbonyl compounds are valuable one/two-carbon synthons for a carbenoid generation because of their relative "green" character and ease of preparation. Transition-metal stabilized carbenoids generated through the decomposition of such *α*-diazo carbonyl compounds have served as versatile electrophilic intermediates for various alkylation, arylation and [*m*+*n*] annulation reactions,[91-93] thus assisting in the construction of vast domain of heterocycles in an atom-economical and step-economical fashion. Also, the by-product generated in most of the cases is environmentally benign nitrogen gas, thereby dispensing as a greener substitute to multistep-functionalization reactions. Diazo compounds can be classified into three sub-categories based on the nature of the two substitutions attached to them: (i) acceptor/acceptor (ii) acceptor/donor (iii) donor/donor (Figure 1.2.3). The nature of the diazo compounds and their reactivity mainly depends on these substitutions, and their applications in the catalytic reactions can be tuned accordingly.

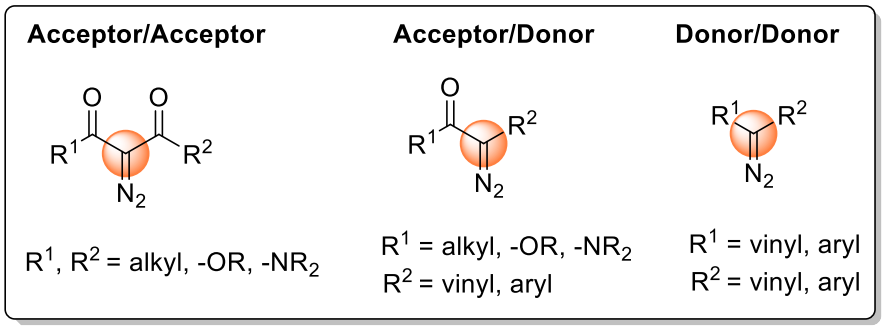

Figure 1.2.3 Classification of diazo compounds

In the last decade, diversely substituted diazo compounds have been successfully employed towards the C*(sp²)*-H functionalization of (hetero)arenes with the aid of varied directing groups. For example, in 2012, the first report on direct aryl C-H bond activation and its subsequent coupling with diazo carbonyls (**14**) under Rh(III)-catalyzed conditions was published by Yu and coworkers. The reaction proceeded smoothly with weakly directing groups (*e.g.* –COOH) to strongly directing groups (*e.g.* pyridyl, secondary amines) (Scheme 1.2.6).[94]

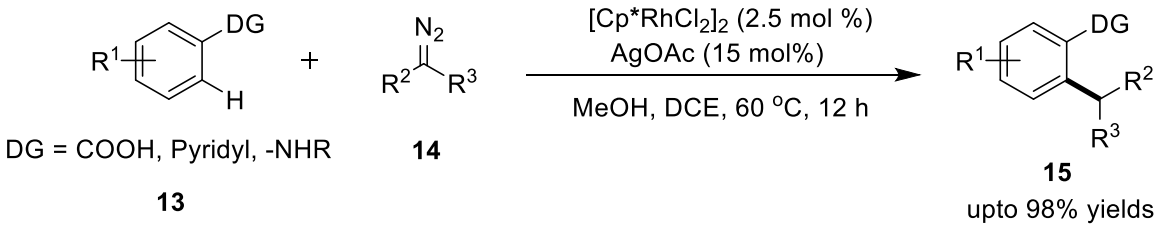

Scheme 1.2.6 Rhodium-catalyzed aryl C-H bond alkylation with diazo compounds (**14**)

Likewise, Xu *et al.* documented a mild condition for the *ortho*-alkylation of aryl sulfonamides (**16**) with *α*-diazo carbonyl compounds (**14**) as coupling partners using Rh(III)-catalyst and silver acetate as an additive in dichloroethane (Scheme 1.2.7).[95] The reaction was proposed to proceed by the formation of a five-membered rhodacyclic intermediate, which upon migratory insertion of the diazo coupling partner followed by protonolysis afforded the desired products (**17**) in appreciable yields.

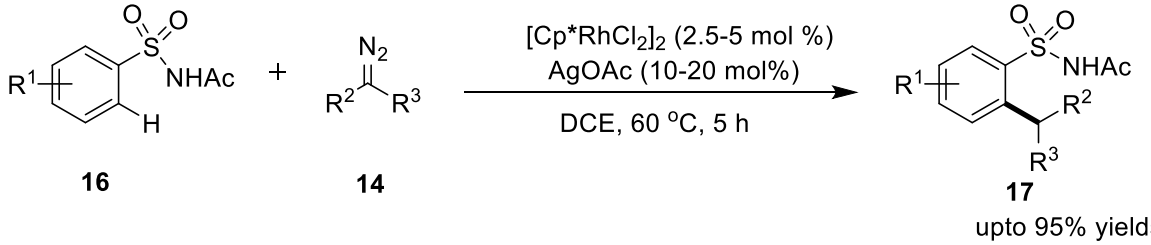

Scheme 1.2.7 Rhodium-catalyzed *ortho*-alkylation of aryl sulfonamides (**16**) with *α*-diazo compounds (**14**)

Similarly, Song and coworkers documented Rh(III)-catalyzed selective synthesis of *α*-aryl ketones (**20**) and esters (**21**) by the C*(sp²)*-H alkyation of 2-arylbenzimidazoles (**18**) with *α*-diazo carbonyl compounds (**19**) under slightly modified conditions in TFE and methanol, respectively. Acidic medium resulted in de-esterification, whereas basic conditions yielded decarbonylated products. (Scheme 1.2.8).[96]

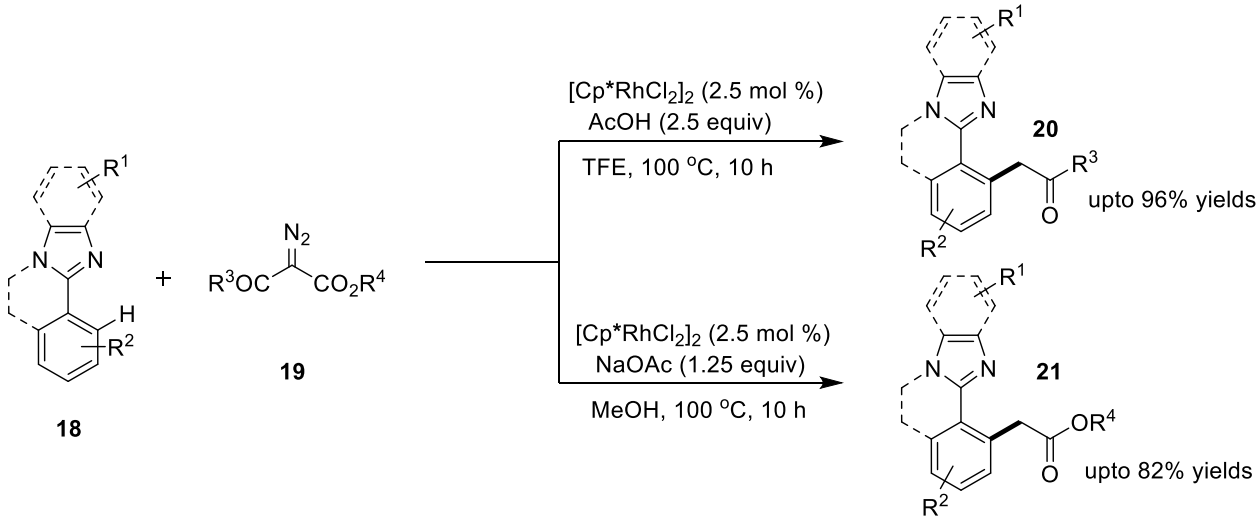

Scheme 1.2.8 Rhodium-catalyzed *ortho*-alkylation of 2-arylbenzimidazoles (**18**) and *α*-diazo carbonyl compounds (**19**)

In the year 2021, a convenient Rh(III)-catalyzed chelation-assisted *ortho*-C-H bond alkylation of *O*-protected phenols (**22**) was recorded by Jiao and coworkers, wherein, an easily accessible *α*-diazomalonates (**23**) have been used as the coupling partner. The protocol offered exclusive regioselectivities, moderate-to-excellent reaction yields and good functional group tolerance (Scheme 1.2.9).[97]

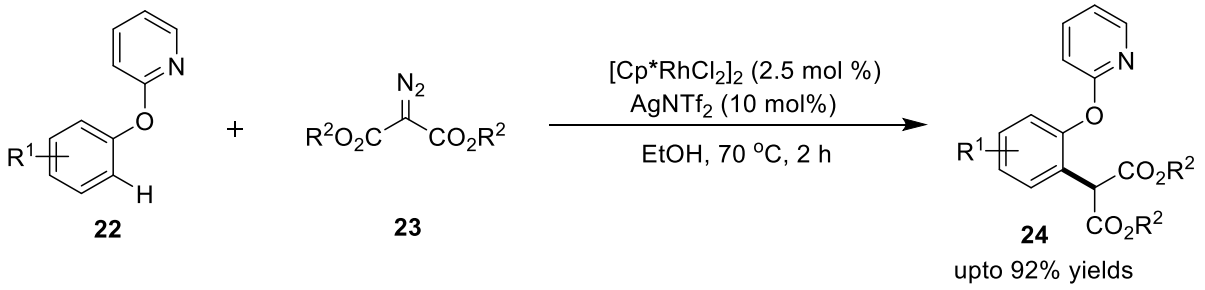

Scheme 1.2.9 Rhodium-catalyzed C-H bond alkylation of *O*-protected phenols (**22**) with diazomalonates (**23**)

Furthermore, Cp*****Rh(III)- and Cp*****Ir(III)-catalyzed arylation of arene C(sp^2)-H bonds with *ortho*- and *para*-benzoquinone diazides (**26**) as efficient coupling partners has been reported by Wang's group, generating wide range of arylated phenol derivatives (**27** & **28**) in excellent yields. This protocol represented the first example of Ir(III)-catalyzed direct C-H arylation, which was proposed to proceed through metallacycle formation, migratory insertion of the carbene and protonolysis using PivOH followed by aromatization. In case of Ir(III)-catalyzed protocol, biarylated products was observed to be major products (Scheme 1.2.10).[98]

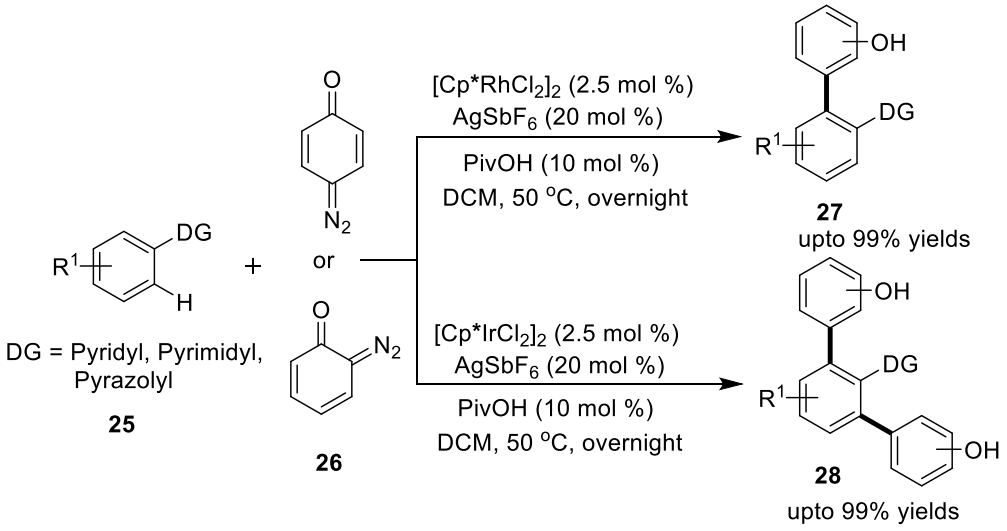

Scheme 1.2.10 Rhodium/Iridium-catalyzed arene C(sp^2)-H bond arylation with quinone diazides (**26**)

Analogously, in the year 2018, Samanta and coworkers disclosed a feasible method for the synthesis of 8-aza-BINOL derivatives (**31**) *via* Rh(III)-catalyzed coupling of quinolone *N*-oxides (**30**) and diazonaphthalene-2(*1H*)-ones (**29)** (Scheme 1.2.11a).[99] Later on, the same group further synthesized biaryl motifs (**33** & **35**) using slightly modified loading of the same Rh(III)/$AgSbF_6$/PivOH catalytic system. Of these, methylene-bridged biaryl naphthol products (**33**) were obtained by C(sp^3)-H bond activation of 8-methylquinoline (**32**) with diazonaphthalene-2(*1H*)-ones/quinone diazides, while benzophenone-type products (**35**) were obtained by arylation of C8-formyl quinolones (**34**) with diazonaphthalene-2(*1H*)-ones (**29)** (Scheme 1.2.11b-c).[100]

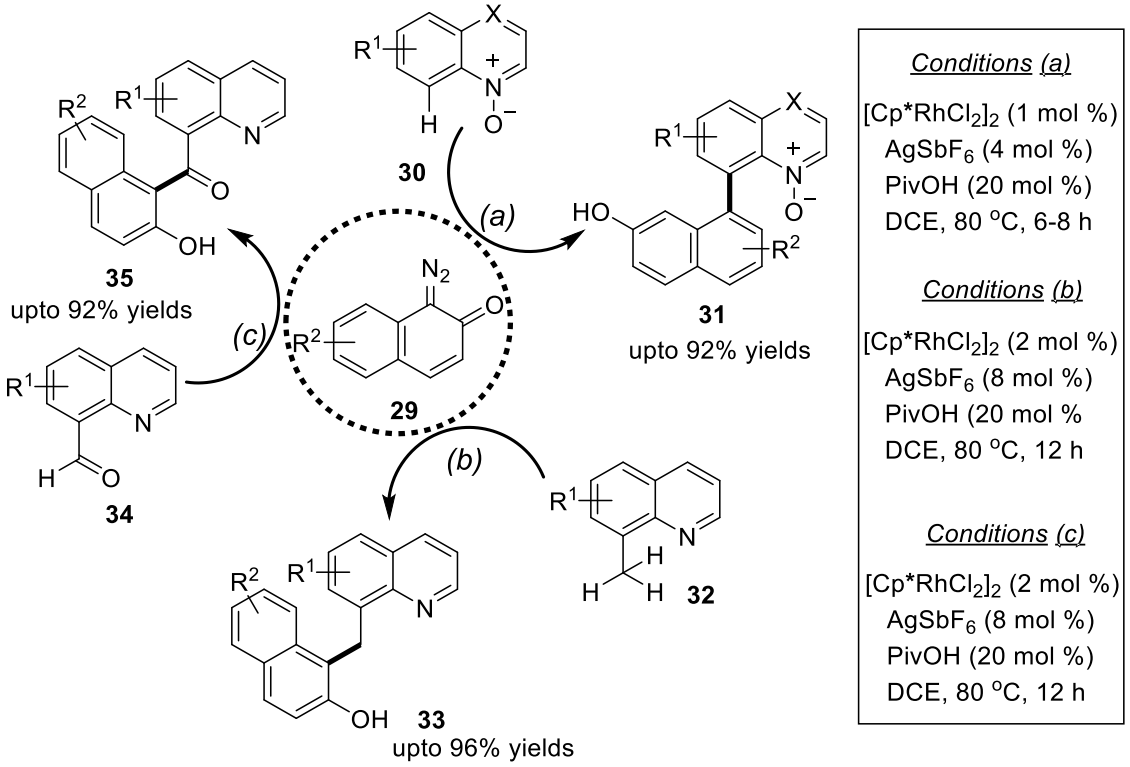

Scheme 1.2.11 Rhodium-catalyzed synthesis of 8-aza-BINOL (**31**) and biaryl derivatives (**33** & **35**) using diazonaphthalene-2(*1H*)-ones (**29)**

Nemoto's group in 2021, documented chelation-assisted Rh(III)-catalyzed annulation of 3-enone tethered indoles (**36**) with α-diazoesters (**23**) to achieve hydrocarbazolones (**37**) in moderate-to-good yields. In this strategy, the enone carbonyl acts as a directing group for C2-H bond alkylation, and assisted in the further cyclization process (Scheme 1.2.12).[101]

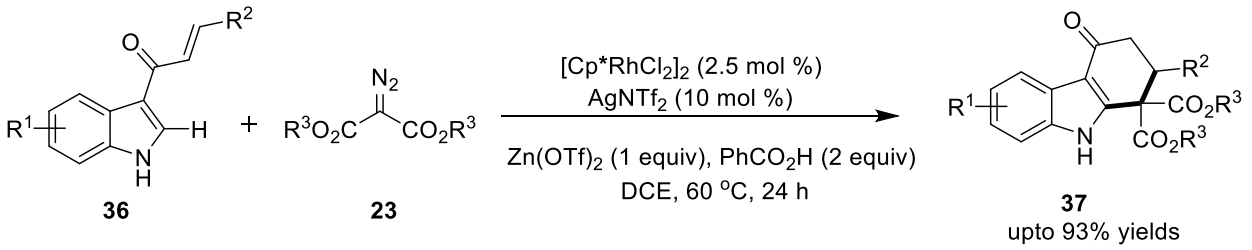

Scheme 1.2.12 Rhodium-catalyzed annulation of 3-enone tethered indoles (**36**) with *α*-diazo esters (**23**)

A one-pot cascade approach for the oxidative annulation of 2-arylindoles (**39** & **41**) with *α*-diazo carbonyl compounds (**14**) has been described by Zhang and Fan group. This method described good generality with respect to both the coupling partners, 2-arylindoles and diazo carbonyls, providing an easy access to diversely decorated benzo[*a*]carbazoles (**38**) and 6-aminobenzo[*a*]carbazoles (**40**) in moderate-to-good yields (Scheme 1.2.13).[102]

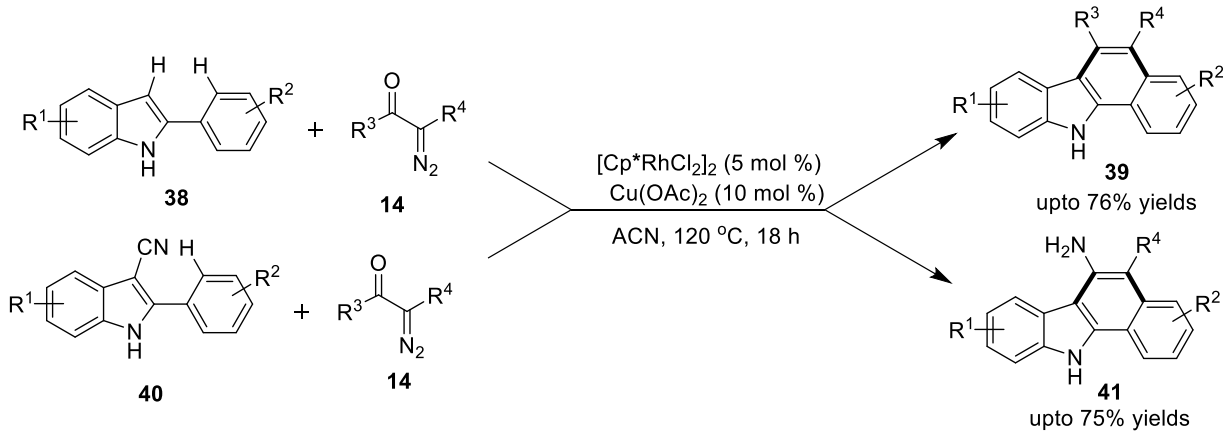

Scheme 1.2.13 Rhodium-catalyzed oxidative annulation of 2-arylindoles (**39** & **41**) with *α*-diazo carbonyl compounds (**14**)

A similar methodology has been reported by Ellman and group for the preparation of azolopyrimidines (**43**) under redox-neutral Rh(III)-catalytic conditions using *N*-azoloimines (**42**) and diazoketones (**14**) (Scheme 1.2.14).[103]

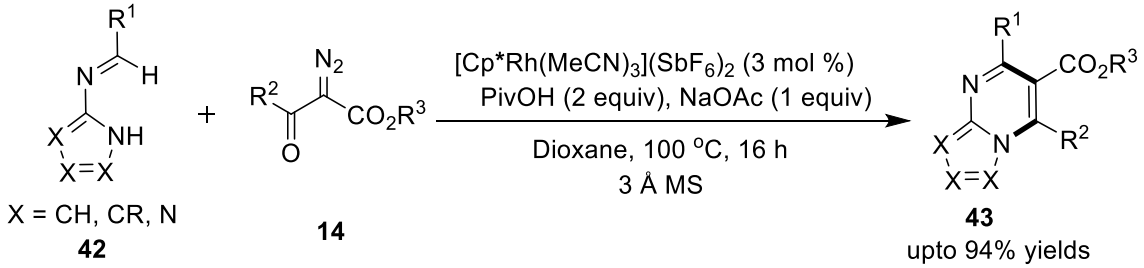

Scheme 1.2.14 Rhodium-catalyzed annulation of *N*-azoloimines (**42**) and diazoketones (**14**)

Shang and coworkers developed an oxidant and additive-free strategy for the synthesis of benzo[*f*]pyrazolo[1,5-*a*][1,3]diazepines (**46**) by the annulation of 1-aryl-1*H*-pyrazol-5-amines (**44**) and cyclic 2-diazo-1,3-diketones (**45**), employing primary amine as a directing group (Scheme 1.2.15).[104]

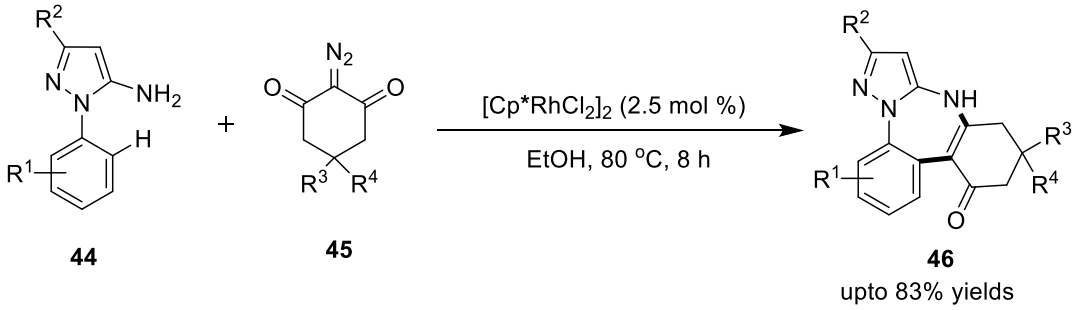

Scheme 1.2.15 Rhodium-catalyzed annulation of 1-aryl-1*H*-pyrazol-5-amines (**44**) with cyclic 2-diazo-1,3-diketones (**45**)

Zhu *et al.* demonstrated an analogous methodology for the synthesis of cinnolines (**48**) *via* Rh(III)-catalyzed annulation of phenylhydrazines (**47)** with diazo carbonyl compounds (**14**). The mechanistic route involved a series of steps involving successive C-H activation, C-C coupling and intramolecular dehydration to achieve substituted cinnoline scaffolds (**48**) in good yields (Scheme 1.2.16).[105]

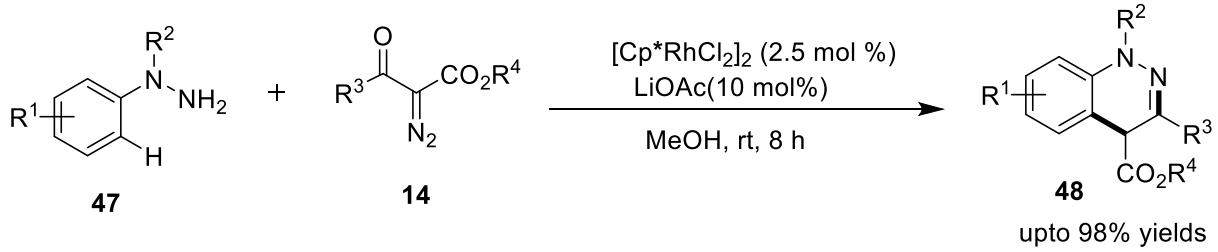

Scheme 1.2.16 Rhodium-catalyzed coupling of phenylhydrazines (**47**) with diazo carbonyl compounds (**14**)

In 2018, our group reported an efficient one-pot Ir(III)-catalyzed method for the synthesis of indazolone-fused cinnolines (**50**) by [4+2] annulation of 1-arylindazolones (**49**) with *α*-diazo carbonyl compounds (**14**) *via* sequential C–H activation/carbene insertion/cyclization in a tandem manner. This method has excellent tolerance towards electron-withdrawing and electron-donating functional groups on 1-arylindazolone and was also found to apply to cyclic *α*-diazo carbonyl compounds (Scheme 1.2.17a).[106] Analogously, Xu *et al.* reported a straightforward and one-pot robust protocol for the construction of cinnoline derivatives (**52**) by the integration of 2-

arylindazolones (**51**) with *α*-diazo compounds (**14**). The developed strategy featured broad substrate scope, and proceeded through a tandem pathway of C-H activation, Ru(II)-carbene formation, migratory insertion and condensation (Scheme 1.2.17b).[107]

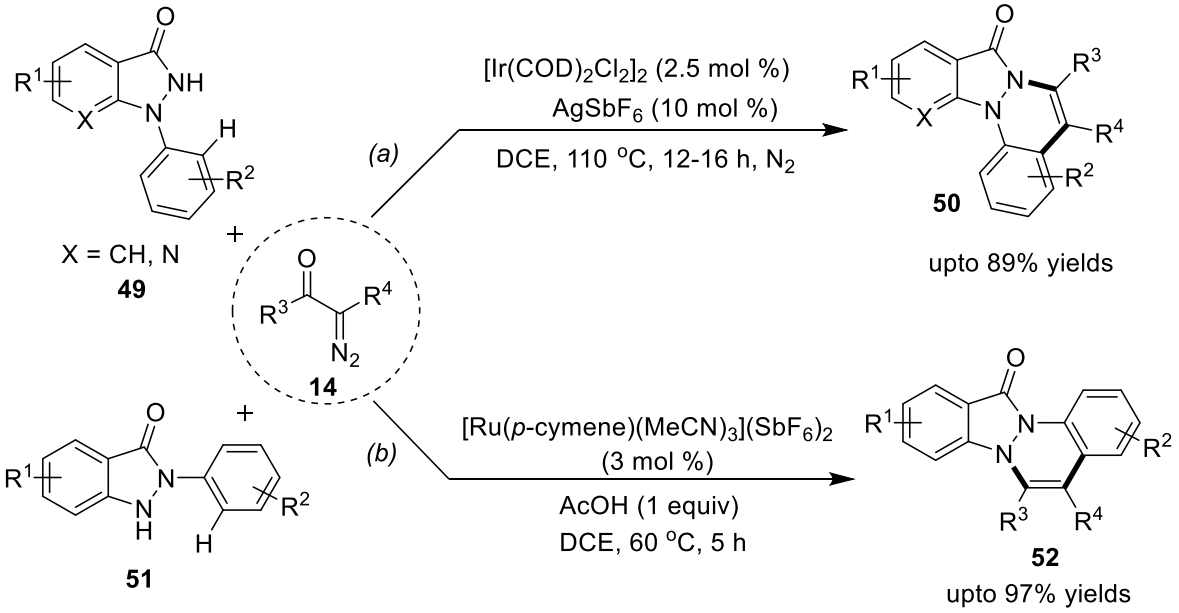

Scheme 1.2.17 Iridium/Ruthenium-catalyzed [4+2] annulation of 1-arylindazolones (**49**)/ 2-arylindazolones (**51**) with *α*-diazo carbonyl compounds (**14**)

Likewise, the construction of potential cinnoline derivatives (**55**) was described in a tandem protocol by Patel's group under mild Ir(III)-catalyzed conditions. The reaction proceeded *via* [4+2] cyclization of azobenzenes (**53**) with *α*-diazotized Meldrum's acid (**54**); whereby electronically different substitutions on aryl rings of azobenzenes successfully transformed into the corresponding cinnolines products in moderate-to-good yields (Scheme 1.2.18).[108]

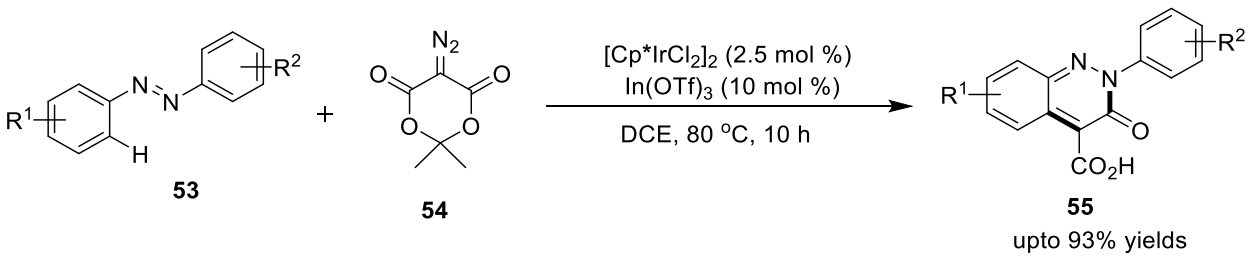

Scheme 1.2.18 Iridium-catalyzed [4+2] cyclization of azobenzenes (**53**) with *α*-diazotized Meldrum's acid (**54**)

Anticipating the in-built directing group ability of cyclic amidic group in *N*-aryl-2,3-dihydrophthalazine-1,4-diones (**1**), in this chapter, we systematically report the synthesis of functionalized phthalazino-fused heterocycles (**56** & **57**) *via* its [4+1]/[4+2] annulation with

diversified α-diazo compounds (**14**) under Rh(III)-catalyzed additive-driven conditions (Scheme 1.2.19).[109]

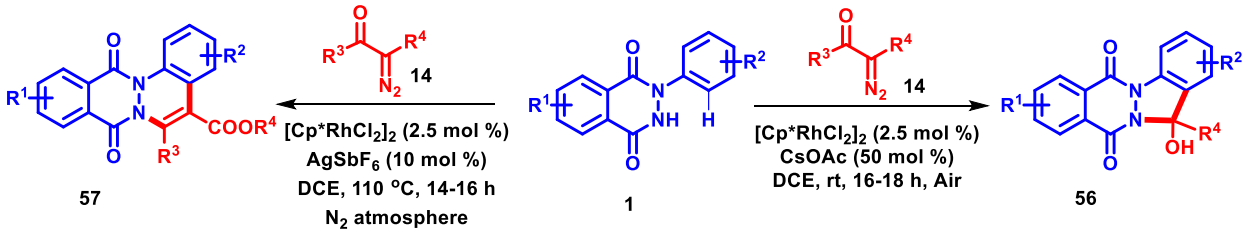

Scheme 1.2.19 Rhodium-catalyzed [4+1]/[4+2] annulation of *N*-aryl-2,3-dihydrophthalazine-1,4-diones (**1**) with α-diazo carbonyl compounds (**14**)

1.3 Results and Discussion

The starting materials, *N*-aryl-2,3-dihydrophthalazine-1,4-diones (**1**) or 1-aryl-1,2-dihydropyridazine-3,6-diones (**61**) required for this work and succeeding works were synthesized by the reaction of substituted phenylhydrazine hydrochlorides (**60**) and substituted phthalic anhydrides (**58**)/maleic anhydride (**59**) in 10% HCl under reflux conditions, following the reported literature procedure (Scheme 1.3.1).[110] The synthesized diversely decorated *N*-aryl-2,3-dihydrophthalazine-1,4-diones (**1**) were characterized on the basis of comparison of their melting point/^{1}H NMR/^{13}C NMR spectra with the reported compounds.

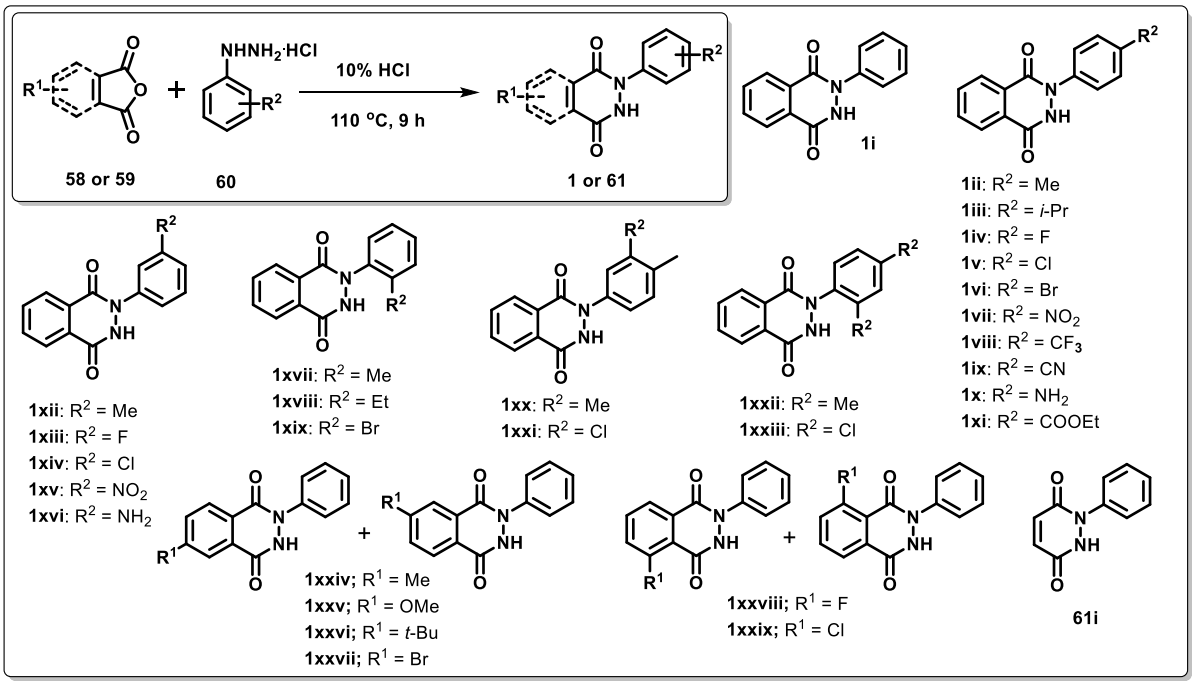

Scheme 1.3.1 Synthesis of *N*-aryl-2,3-dihydrophthalazine-1,4-dione (**1**) or *N*-aryl-1,2-dihydropyridazine-3,6-dione (**61**)

At the onset of our investigation, the reaction between *N*-phenyl-2,3-dihydrophthalazine-1,4-dione (**1a**) and ethyl 2-diazo-3-oxobutanoate (**14a**) using $[Cp^*RhCl_2]_2$ (2.5 mol %) as the catalyst failed to afford a product in the absence of any additive or the presence of $Cu(OAc)_2$ (20 mol %) at room temperature for 18 h (Table 1.3.1, entries 1 and 2). To our delight, an annulated product **56aa** was obtained in 32% yield when NaOAc (20 mol %) was used in combination with $[Cp^*RhCl_2]_2$ (2.5 mol %) in DCE at room temperature for 18 h under air atmosphere (Table 1.3.1, entry 3). Careful analysis of **56aa** confirmed the formation of an unprecedented hydroxy-dihydroindazolo-fused phthalazine, possibly resulting *via* [4+1] annulation of **1a** with **14a**. An increase in the yield of **56aa** to 38% and 49% was observed by replacing NaOAc with KOAc and CsOAc, respectively (Table 1.3.1 entries 4 and 5).

Table 1.3.1 Selected optimization[a] of reaction conditions for the synthesis of **56aa**

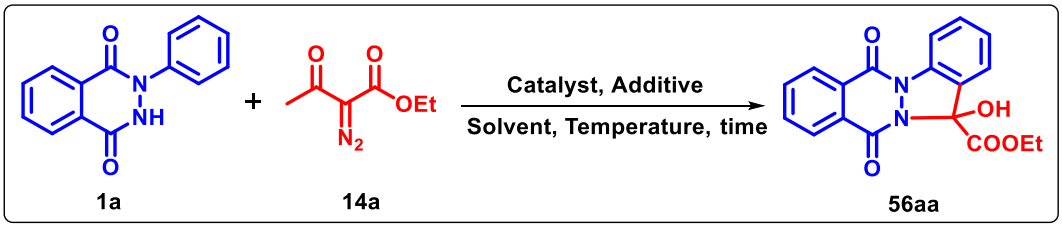

Entry No.	Catalyst (mol %)	Additive (mol %)	Solvent	Temp. (°C)	Yields (%)[b] **56aa**
1.	$[Cp^*RhCl_2]_2$ (2.5)	-	DCE	rt	-
2.	$[Cp^*RhCl_2]_2$ (2.5)	$Cu(OAc)_2$ (20)	DCE	rt	-
3.	$[Cp^*RhCl_2]_2$ (2.5)	NaOAc (20)	DCE	rt	32
4.	$[Cp^*RhCl_2]_2$ (2.5)	KOAc (20)	DCE	rt	38
5.	$[Cp^*RhCl_2]_2$ (2.5)	CsOAc (20)	DCE	rt	49
6.	$[Cp^*RhCl_2]_2$ (2.5)	CsOAc (30)	DCE	rt	56
7.	**$[Cp^*RhCl_2]_2$ (2.5)**	**CsOAc (50)**	**DCE**	**rt**	**86**
8.	$[Cp^*RhCl_2]_2$ (2.5)	CsOAc (100)	DCE	rt	87
9.	$[Cp^*RhCl_2]_2$ (5.0)	CsOAc (50)	DCE	rt	86
10.	$[Cp^*RhCl_2]_2$ (2.5)	CsOAc (50)	Xylene	rt	-
11.	$[Cp^*RhCl_2]_2$ (2.5)	CsOAc (50)	Toluene	rt	-
12.	$[Cp^*RhCl_2]_2$ (2.5)	CsOAc (50)	ACN	rt	60
13.	$[Cp^*RhCl_2]_2$ (2.5)	CsOAc (50)	THF	rt	68
14.	$[Cp^*RhCl_2]_2$ (2.5)	CsOAc (50)	MeOH	rt	40
15.	$[Cp^*RhCl_2]_2$ (2.5)	CsOAc (50)	DMF	rt	20
16.[c]	$[Cp^*RhCl_2]_2$ (2.5)	CsOAc (50)	DCE	rt	<10
17.[d]	$[Cp^*RhCl_2]_2$ (2.5)	CsOAc (50)	DCE	rt	88

[a]Reaction conditions: The reactions were carried out with **1a** (0.20 mmol) and **14a** (0.25 mmol) in the presence of catalyst/additive (as indicated in the table) in 5 mL of solvent for 18 h under air. [b]Isolated yields. [c]In nitrogen atmosphere. [d]In oxygen atmosphere.

Further screening of additive loading revealed that 50 mol % is the optimum CsOAc concentration required to furnish 86% of **56aa** (Table 1.3.1, entries 6 and 7). No further enhancement in the yield was observed either by increasing the catalyst to 5 mol % or additive loading to 100 mol % (Table 1.3.1, entries 8 and 9). Solvent switching to xylene or toluene produced no product; the use of ACN, THF, MeOH, or DMF were found to be detrimental, producing **56aa** in low-to-moderate yields (Table 1.3.1, entries 10-15). It is worth mentioning that only a small amount of **56aa** was observed (along with other overlapping intermediates spots on TLC) when the reaction was performed under the optimized conditions in a nitrogen atmosphere, indicating that aerobic conditions are essential for the desired [4+1] annulation (Table 1.3.1, entry 16). Gratifyingly, under oxygen atmosphere **56aa** was isolated in 88% yield (Table 1.3.1, entry 17).

Using the optimized conditions, we investigated the substrate scope of the two substrates for this Rh-catalyzed [4+1] annulation. As summarized in (Scheme 1.3.2), diversely decorated 2-aryl-2,3-dihydrophthalazine-1,4-diones (subsrates: **1a–i**) with electronically differentiated groups (H, Me, F, Cl, Br) at different positions smoothly undergo [4+1] annulation with acyclic α-diazo ketoester (**14a-b**) or α-diazo diketone (**14c-d**) to give the desired products (**56aa–56ib**) in good-to-excellent yields (68-88%). Notably, during the formation of desired [4+1] annulation product (**53**) from various α-diazo carbonyl compounds, the acyl group is eliminated, while the ester (or the other acyl in the case of α-diazo diketone) functionality is retained. The coupling of 3-diazopentane-2,4-dione (**14c**) and 2-diazo-1-phenylbutane-1,3-dione (**14d**) with **1a** resulted in the formation of the same product (**56ac** or **56ad**), indicating the preferential elimination of benzoyl group over acetyl group during the reaction with **14d**. Similarly, the reaction of ethyl 2-diazo-3-oxobutanoate (**57a**) and ethyl 2-diazo-3-oxo-3-phenylpropanoate (**14e**) with **1a** under Rh-catalyzed optimized conditions afforded the same product (**56aa** or **56ae**). *N*-Aryl-2,3-dihydrophthalazine-1,4-diones bearing electron-withdrawing groups (F, Cl, Br) at the *para* position of phenyl ring (subsrates: **1c–e**) showed comparatively lower reactivity, affording the desired products (**56ca–56eb**) in 68–78% yields. The presence of an electron-donating group (Me) or electron-withdrawing group (Cl) at the *meta* position of phenyl group (subsrates: **1f–h**) furnished the expected products (**56fa–56ha**) in 76–85% yields with **14a-b**. The products (**56ia-56ib**) were obtained as mixtures of two regioisomers in varying ratio, as their starting substrate (substrate: **1i**) was prepared as an inseparable regioisomeric mixture. In striking contrast, other strongly electron-withdrawing groups placed at *meta* or *para* positions (*m*-NO_2, *m*-CF_3, *p*-NO_2, *p*-COOEt, *p*-CN) (subsrates: **1j-**

n) yielded no product at all under described conditions (the starting materials were recovered as such). Furthermore, *ortho*-substituted *N*-aryl,2-3-dihydrophthalazine-1,4-diones (subsrates: **1o**–**p**) bearing Me and Cl substituents failed to react with any α-diazo carbonyl compounds (**1a–d**) under the optimized conditions. As far as α-diazo diester is concerned, diethyl 2-diazomalonate (**1f**) produced *ortho*-functionalized diester product (**56′af**) in 78% yield. The representative ^{1}H NMR and ^{13}C NMR spectrum of **56aa** are depicted in Figure 1.3.1 and Figure 1.3.2, respectively. To further confirm the proposed structure of **56**, single crystals of **56ca** were grown from chloroform for X-ray diffraction (XRD) studies as a representative example. The ORTEP diagram (CCDC No. 1851226) of **56ca** is shown in Scheme 1.3.2.

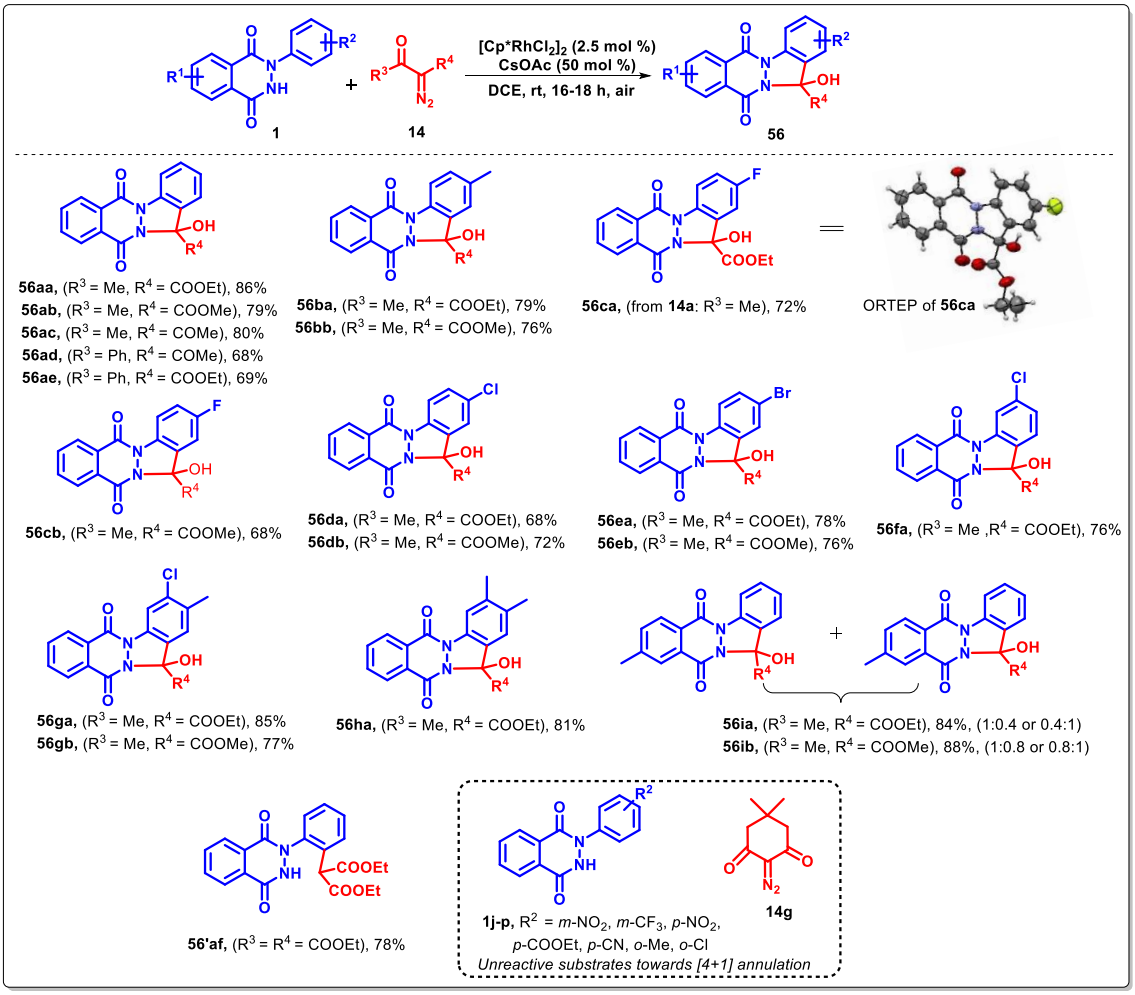

Scheme 1.3.2 Substrate scope of *N*-aryl-2,3-dihydrophthalazine-1,4-diones and α-diazo compounds towards Rh-catalyzed [4+1] annulation

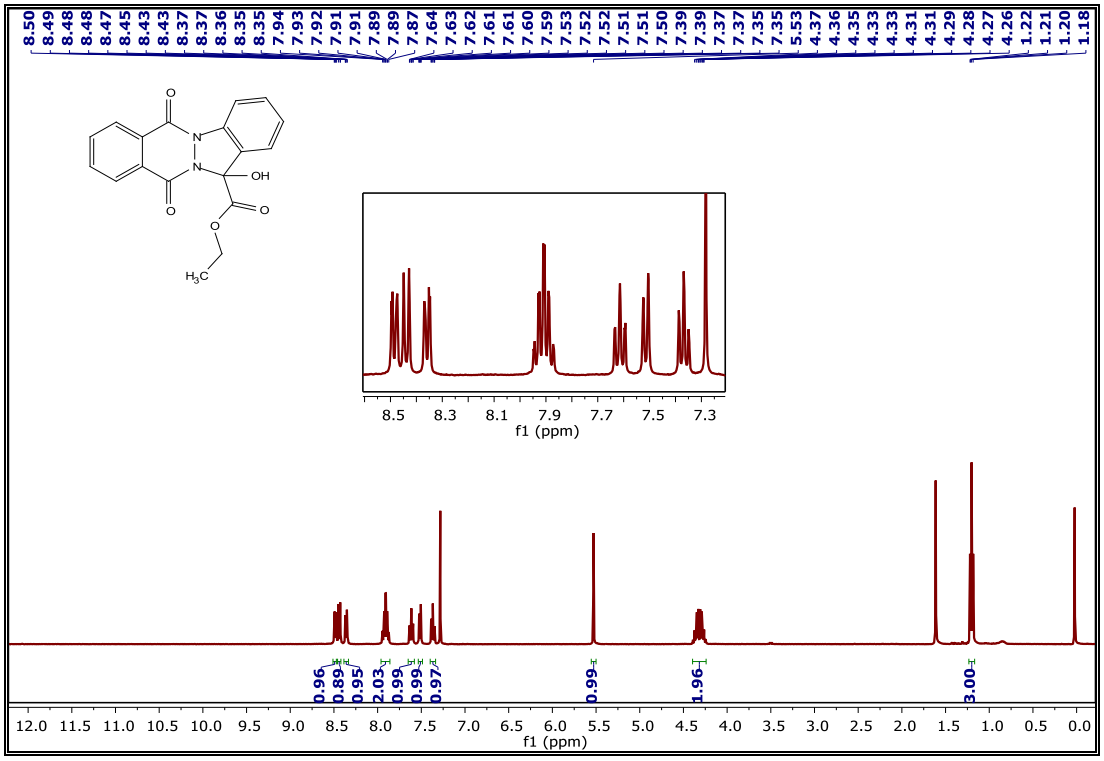

Figure 1.3.1: ^{1}H NMR spectra of **56aa**

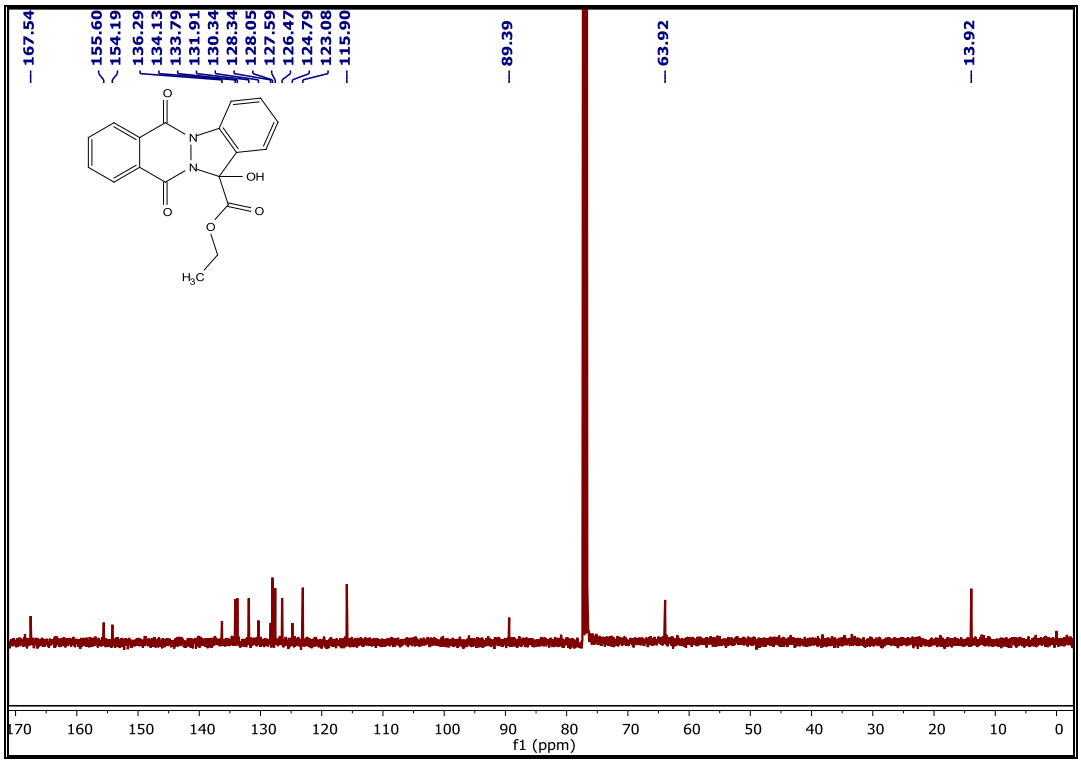

Figure 1.3.2 ^{13}C NMR spectra of **56aa**

Interestingly, during one of the additive-optimization experiment for the reaction between **1a** and **14a**, it was observed that the use of $AgSbF_6$ (5 mol %) as the additive in combination with $[Cp^*RhCl_2]_2$ (2.5 mol %) in DCE at 110 °C resulted in the formation of a new compound (**57aa**) in 58% yield in nitrogen atmosphere after 16 h (Table 1.3.2, entry 1). Purification by column chromatography and subsequent characterization of **57aa** using ^1H and ^{13}C NMR, and HRMS unambiguously confirmed its structure to be ethyl 6-methyl-8,13-dioxo-8,13-dihydrophthalazino[2,3-*a*]cinnoline-5-carboxylate. This prompted us to further optimize this additive-driven [4+2] annulation strategy. Gratifyingly, **57aa** was obtained in 82% yield by increasing the additive loading to 10 mol % (Table 1.3.2, entry 2). However, a further increase in additive loading to 15 mol % or catalyst loading to 5 mol % did not result in an appreciable increase in the yield of **57aa** (Table 2, entries 3 and 4). Surprisingly, the use of KPF_6 in place of $AgSbF_6$ did not furnish any product at all (Table 1.3.2, entry 5).

Table 1.3.2 Selected optimization[a] of reaction conditions for the synthesis of **57aa**

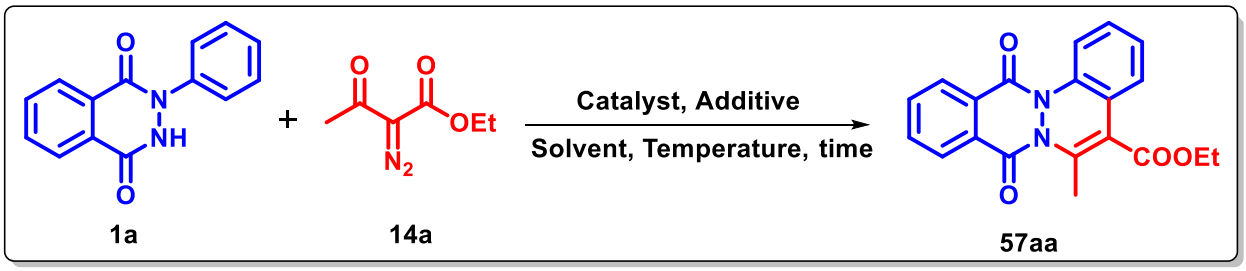

Entry No.	Catalyst (mol%)	Additive (mol%)	Solvent	Temp. (°C)	Yields (%)[b] **57aa**
1.	$[Cp^*RhCl_2]_2$ (2.5)	$AgSbF_6$ (5)	DCE	110	58
2.	**$[Cp^*RhCl_2]_2$ (2.5)**	**$AgSbF_6$ (10)**	**DCE**	**110**	**82**
3.	$[Cp^*RhCl_2]_2$ (2.5)	$AgSbF_6$ (15)	DCE	110	83
4.	$[Cp^*RhCl_2]_2$ (5.0)	$AgSbF_6$ (10)	DCE	110	84
5.	$[Cp^*RhCl_2]_2$ (2.5)	KPF_6 (10)	DCE	110	-
6.	$[Cp^*RhCl_2]_2$ (2.5)	$AgSbF_6$ (10)	Toluene	110	65
7.	$[Cp^*RhCl_2]_2$ (2.5)	$AgSbF_6$ (10)	Xylene	110	62
8.	$[Cp^*RhCl_2]_2$ (2.5)	$AgSbF_6$ (10)	ACN	80	20
9.	$[Cp^*RhCl_2]_2$ (2.5)	$AgSbF_6$ (10)	THF	70	71
10.	$[Cp^*RhCl_2]_2$ (2.5)	Ag_2OTf (10)	DCE	110	20
11.	$[Cp^*RhCl_2]_2$ (2.5)	AgOAc (10)	DCE	110	trace
12.	$[Cp^*RhCl_2]_2$ (2.5)	$AgCO_3$ (10)	DCE	110	-
13.[c]	$[Cp^*RhCl_2]_2$ (2.5)	$AgSbF_6$ (10)	DCE	110	-[d]

[a]Reaction conditions: The reactions were carried out with **1a** (0.20 mmol) and **14a** (0.25 mmol) in the presence of catalyst/additive (as indicated in the table) in 5 mL of solvent for 16 h under nitrogen atmosphere. [b]Isolated yields. [c]In air atmosphere. [d] Charring of the reaction mixture.

Solvent screening studies again showed DCE to be an ideal solvent for the [4+2] annulation, whereas the use of other solvents such as toluene, xylene, ACN, and THF produced comparatively inferior results (Table 1.3.2, entries 6–9). The use of other silver additives such as AgOTf, AgOAc and Ag_2CO_3 were next screened. While AgOTf yielded 20% of the desired product **57aa**, AgOAc afforded **57aa** in trace amounts **(**Table 1.3.2, entries 10–11). Unfortunately, Ag_2CO_3 produced no product at all (Table 1.3.2, entry 12). Notably, charring of reaction mixture was observed when the reaction was performed in DCE at 110 °C in air atmosphere within few hours, and subsequently no product was obtained (Table 1.3.2, entry 13).

After the best conditions were established, we explored the substrate scope and limitation of this [4+2] annulation protocol. Diverse substituents including H, Me, F, Cl, and Br on the phenyl group in *N*-aryl-2,3-dihydrophthalazine-1,4-dione (**s**ubstrates: **1a–1e**) were well tolerated with acyclic *α*-diazo ketoesters (subsrates: **1a–b**), to produce the desired [4+2] annulation products (**57aa–57eb**) in good-to-excellent yields (Scheme 1.3.3). Overall, a small difference was observed in the reactivity of electronically differentiated groups (EDGs or EWGs) on the yield of the corresponding products. The presence of an electron-donating group (Me) or electron-withdrawing group (Cl) at the *meta* position of phenyl group (subsrates: **1f–h**) furnished the expected products (**57fa–57ha**) in 76–85% yields with **14a–b**. Notably, the products **57ia** and **57ib** was obtained as a mixture of two regioisomers, as **1i** itself was prepared as an inseparable 6 & 7-substituted regioisomeric mixture from 5-methylphthalic anhydride and phenylhydrazine. With regard to strong electron-withdrawing groups, *m*eta- and *para*-NO_2 substituted 2-phenyl-2,3-dihydrophthalazine-1,4-diones (subsrates: **1j** & **1l**) delivered the expected [4+2] annulation products (**57ja** & **57la**) in 15% and 8% respectively, while *N*-aryl-2,3-dihydrophthalazine-1,4-diones bearing *m*-CF_3, *p*-COOEt or *p*-CN substitutions (subsrates: **1k, 1m–n**) remain completely unreactive under optimized conditions. Similarly, *ortho*-substituted *N*-aryl-2,3-dihydrophthalazine-1,4-diones (**1o–p**), acyclic *α*-diazo diketone (**1c–d**) and diethyl 2-diazomalonate (**1f**) did not give the expected [4+2] annulation products with their respective coupling partners. Pleasingly, the reaction of 2-diazo-5,5-dimethylcyclohexane-1,3-dione (**1g**) with differently substituted *N*-aryl-2,3-dihydrophthalazine-1,4-diones (subsrates: **1a–c**) furnished the corresponding pentacyclic fused diazaheterocycles in 65–68% yields. The representative ^{1}H NMR and ^{13}C NMR spectra of **57aa** are shown in Figure 1.3.3 and Figure 1.3.4, respectively. The

structure of **54** was finally confirmed by XRD studies on one of the representative examples, **57ba**; the ORTEP diagram (CCDC No. 1851227) of **57ba** is shown in Scheme 1.3.3.

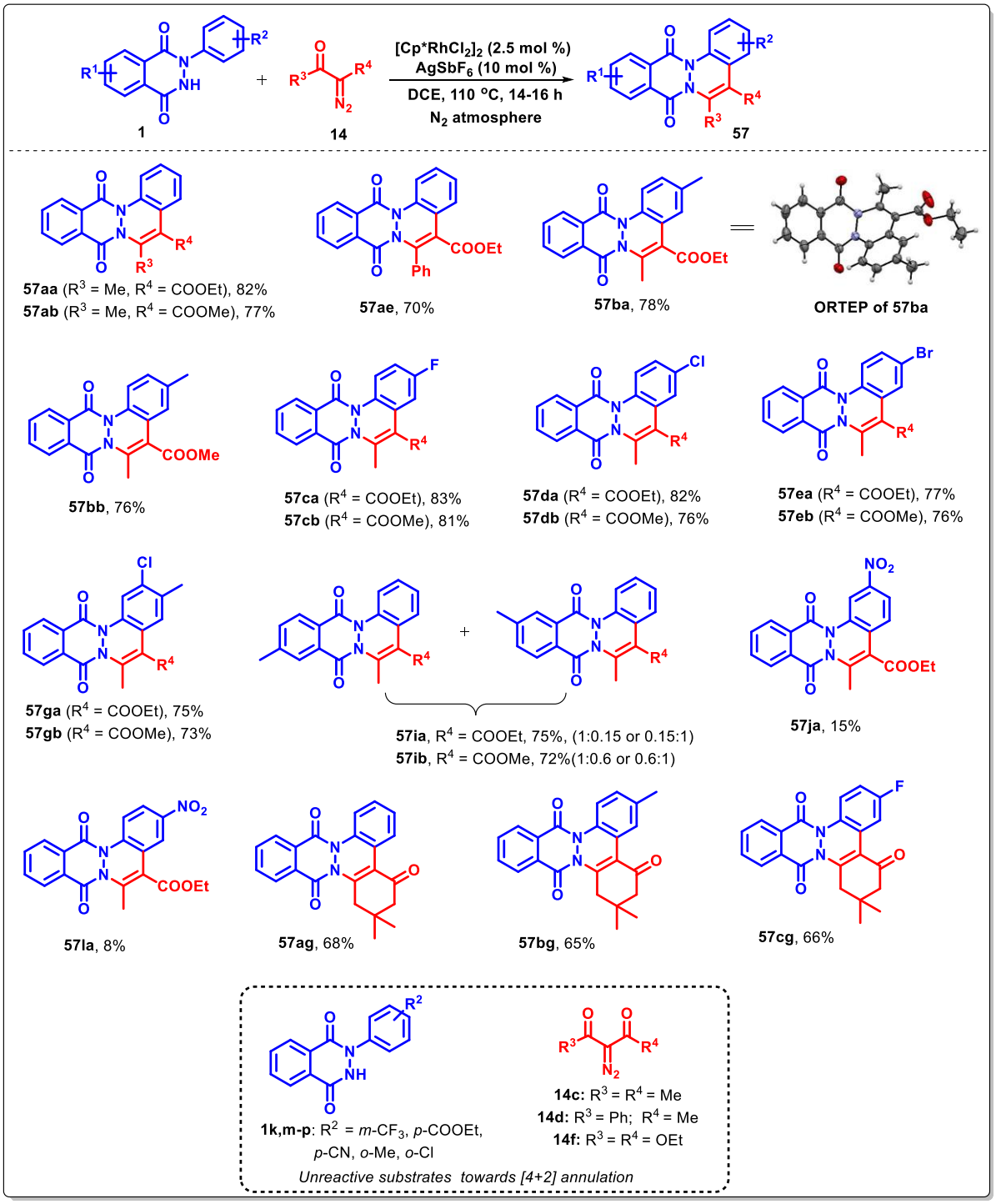

Scheme 1.3.3 Substrate scope of *N*-aryl-2,3-dihydrophthalazine-1,4-diones and *α*-diazo compounds towards Rh-catalyzed [4+2] annulation

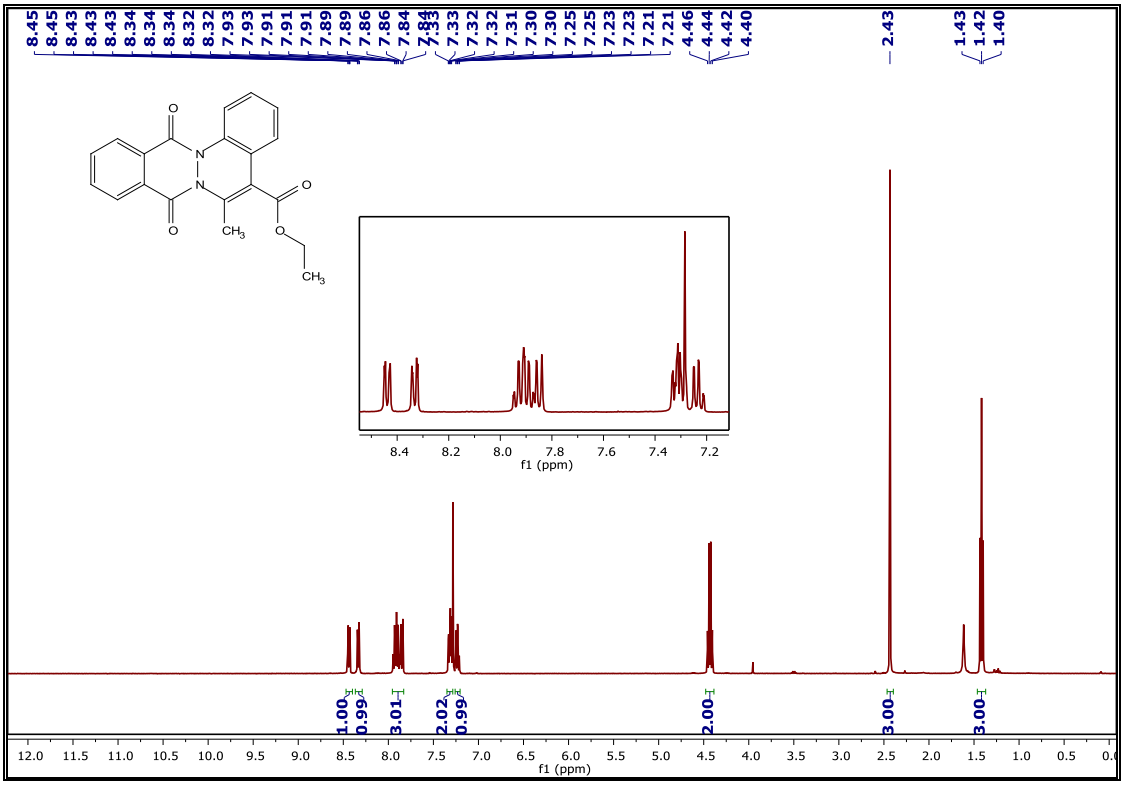

Figure 1.3.3 ^{1}H NMR spectra of **57aa**

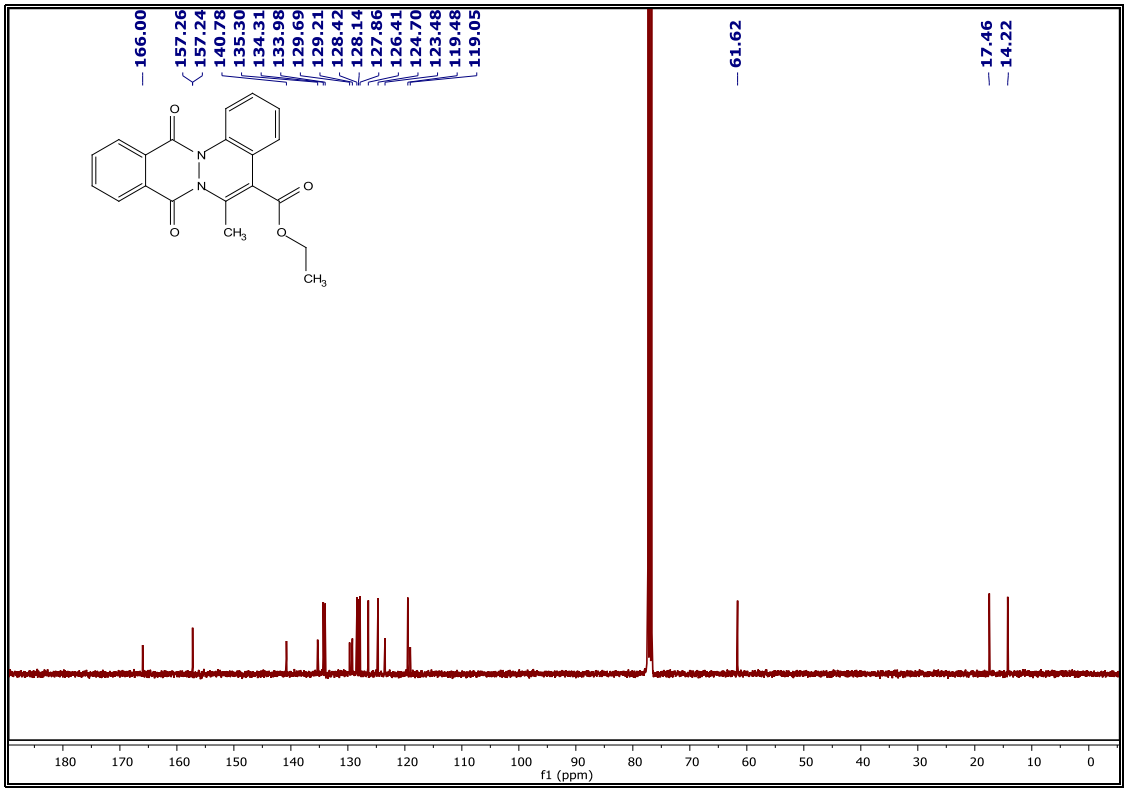

Figure 1.3.4 ^{13}C NMR spectra of **57aa**

To shed some light on the mechanistic pathways of the developed strategies, several preliminary investigations were carried out (Scheme 1.3.4). A set of control experiments concluded that without Rh catalyst the reaction between **1a** and **14a** did not proceed in the presence of $AgSbF_6$ or CsOAc (Scheme 1.3.4i). One-pot intermolecular competitive experiments between electron-rich and electron-deficient *N*-aryl-2,3-dihydrophthalazine-1,4-diones (**1b** and **1c**) with **14a** resulted in the formation of almost equivalent amounts of their corresponding [4+1]/[4+2] annulation products (**56ba:56ca**, 1:1 or **57ba:57ca**, 1:1) under the corresponding conditions (Scheme 1.3.4ii). HRMS analysis of crude mixture for the Rh-catalyzed reaction between **1d** and **14a** under CsOAc conditions after 8 h of stirring at room temperature showed the presence of species **E′** and **H′** (Scheme 1.3.4iii). This inferred the possible formation of an *ortho*-functionalized diacylated product (**E′**) during the reaction, which possibly upon oxidation *via* acyl/acetate ion elimination might have generated species **H′**. Pleasingly, we were able to isolate **E′** by ceasing a part of the reaction mixture after 5 h, which was purified and characterized by ^{1}H NMR and HRMS. **E′** was characterized as a tautomeric mixture (2:1 by ^{1}H NMR) of *ortho*-functionalized diacylated product. Unfortunately, further attempts to isolate any other intermediate (**H′)** failed. This is because overlapping spots on TLC were observed during the transformation of **E′** to the desired product **56da**. Thus, **E′** was subjected to further cyclization under Rh-catalyzed conditions (in absence of **14a),** and the reaction mixture was monitored *via* time-dependent ^{1}H NMR (Scheme 1.3.4iii). These studies indicated the loss of acidic proton (δ 5.00) within 30 min., and thereafter loss of acetyl group (δ 2.13) within 6 h of the course of the reaction (Figure 1.3.5). Similarly, the reaction mixture of **1a** and **14a** under Rh-catalyzed conditions using $AgSbF_6$ was analyzed by mass spectrometry at different intervals of time. Interestingly, five-membered rhodacyclic species (**A**) and Rh(III)-carbene species (**B** or **C**) were detected after 2 h and 3 h of stirring at room temperature, respectively (Scheme 1.3.4iv). Further stirring the reaction mixture for another 3 h led to the formation of an intermediate, which was isolated and characterized (^{1}H NMR and HRMS) as a tautomeric mixture of the *ortho*-functionalized diacylated product (**E**) (Scheme 1.3.4iv). Interestingly, only a trace amount of **57aa** was observed by further stirring the reaction mixture at room temperature, whereas heating at 110 °C in DCE for 10-12 h afforded **57aa** in major amounts (Scheme 1.3.4iv).

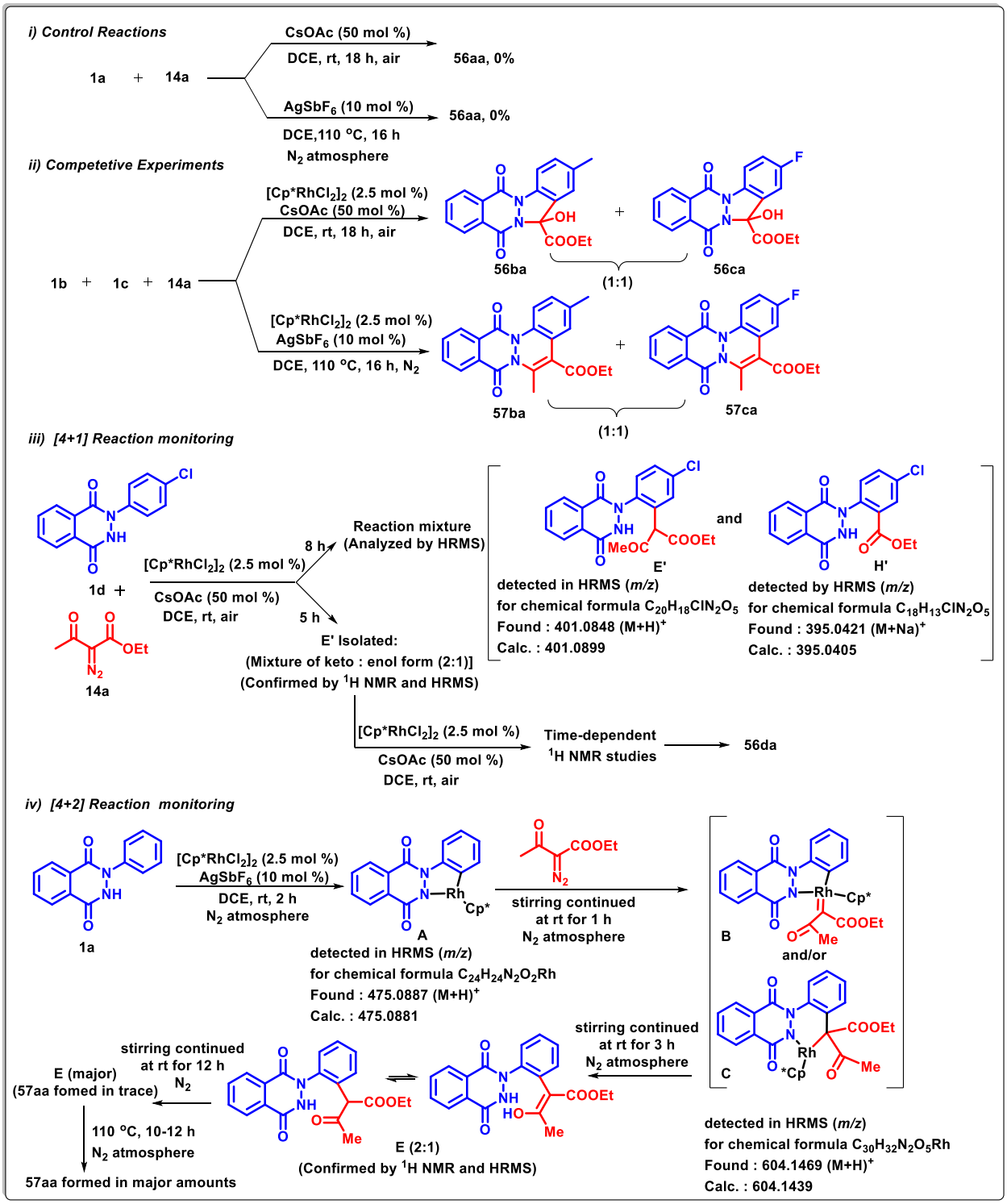

Scheme 1.3.4 Preliminary mechanistic investigations

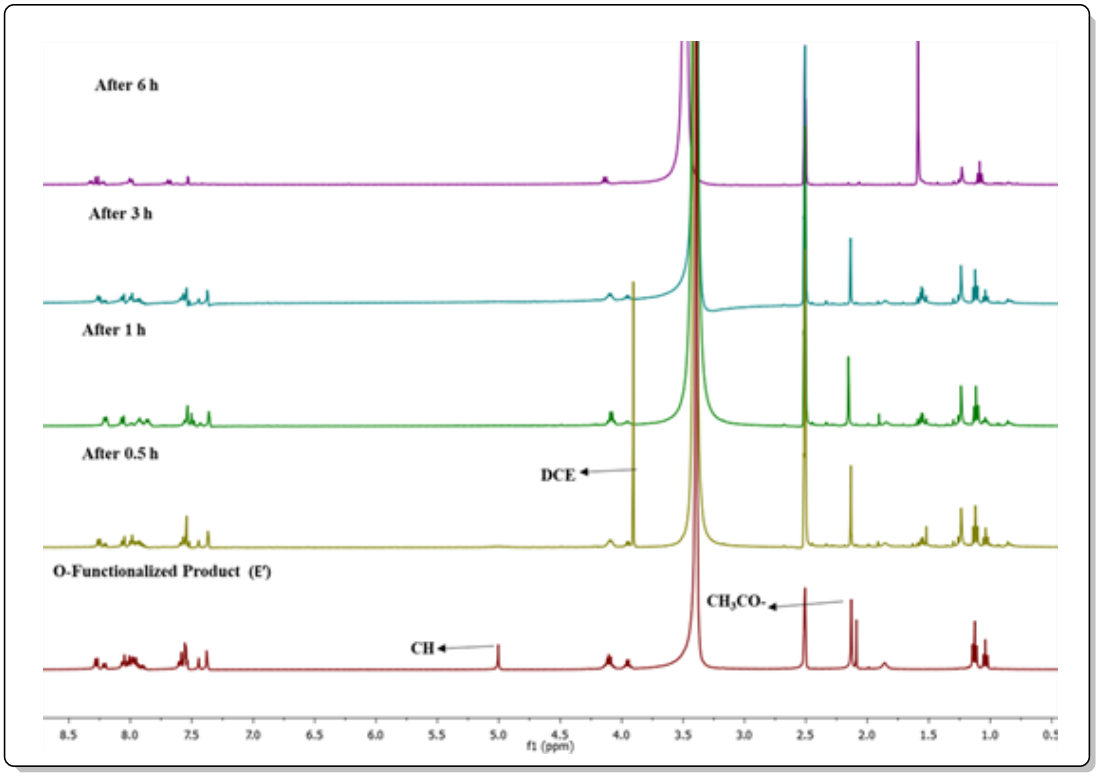

Figure 1.3.5 Time-dependent ^{1}H NMR of reaction mixture of [4+1] annulation

Based on the above-mentioned results and previous reports,[93] a plausible mechanism is proposed (Scheme 1.3.5). For both [4+1]/[4+2] annulations, the reaction is believed to be initiated by the dissociation of dimeric $[Cp^{*}RhCl_2]_2$ with OAc^{-} ion (or SbF_6^{-}) to generate active Rh^{III} species ($[Cp^{*}RhX_2]$; X = OAc or SbF_6), which on cyclometallation with **1a** *via* C–H activation furnishes a rhodacyclic species A. Further, **A** on carbene insertion gives **B**, which upon migratory insertion of diacyl moiety into Rh−Ar bond leads to the formation of **C**. Species **C** on subsequent protonolysis generates **E** *via* **D** along with the regeneration of active Rh^{III} species for the next catalytic cycle. Thereafter, two different pathways are proposed for the [4+1] and [4+2] annulation processes. In the presence of $AgSbF_6$ (Lewis acid), intermediate **E** undergoes an intramolecular nucleophilic addition followed by dehydration to afford the [4+2] annulation product (**57**) (path a). In the presence of CsOAc, it is proposed that oxygen insertion in **F** (formed from **E** via proton abstraction) generates a superoxide ionic species **G**, which on the elimination of R^3COO^{-} gives **H**. Finally, intermediate **H** on intramolecular nucleophilic addition leads to the formation of [4+1] annulation product (**56**) (path b).

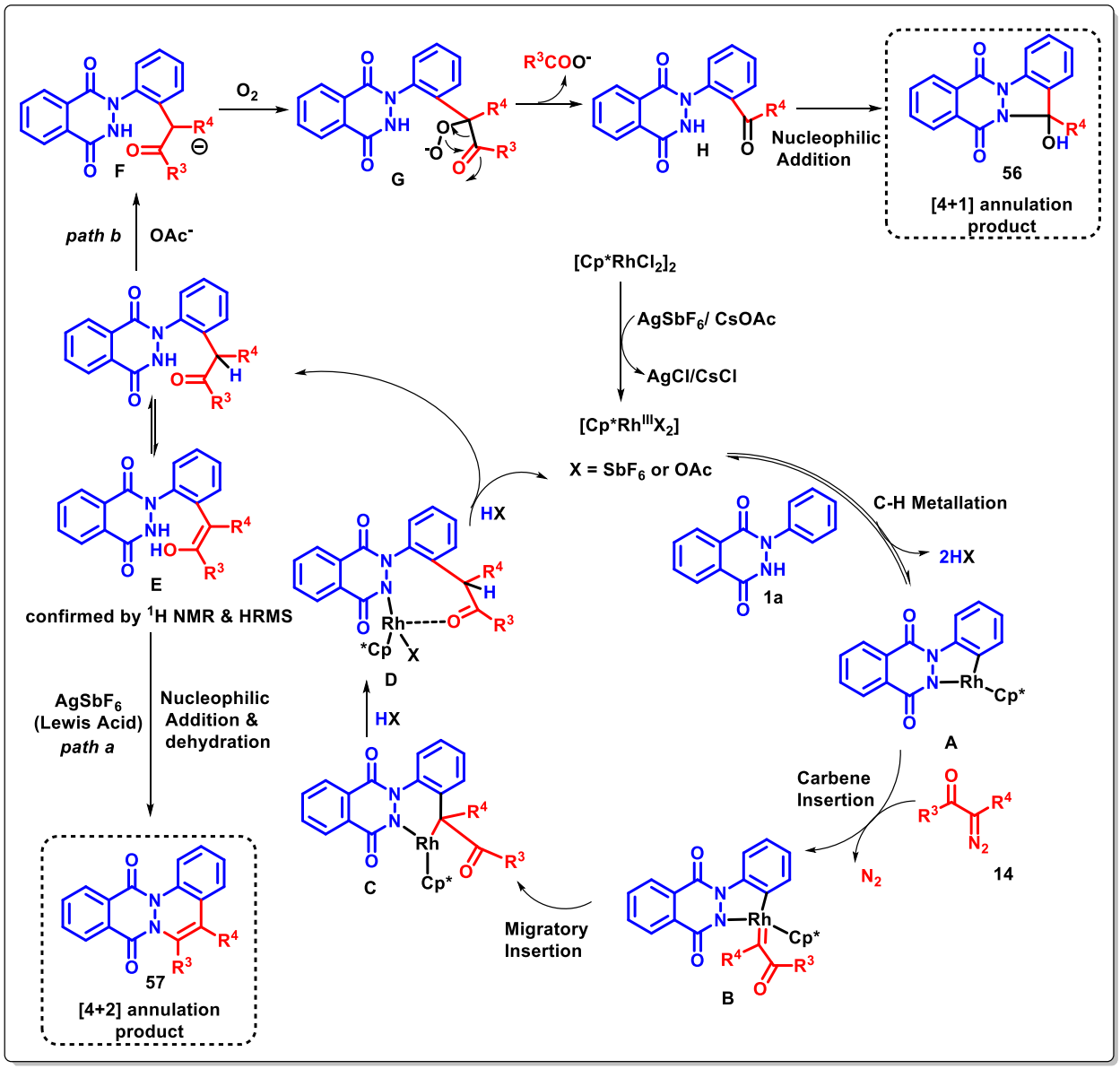

Scheme 1.3.5 Plausible mechanism for [4+1]/[4+2] annulations

In summary, we have developed two efficient Rh(III)-catalyzed additive-modulated strategies for the synthesis of unprecedented hydroxy-dihydroindazolo[1,2-*b*]phthalazines and phthalazino[2,3-*a*]cinnolines *via* [4+1]/[4+2] annulation 2-arylphthalazine-1,4-diones with *α*-diazo carbonyl compounds. Diverse 2-arylphthalazine-1,4-diones and *α*-diazo carbonyl compounds were well tolerated and a total of forty substituted tetra and pentacyclic phthalazine-fused heterocycles were synthesized in good-to-excellent yields.

1.4 Experimental Section

General Considerations

Commercially available reagents were used without purification. Commercially available solvents were dried by standard procedures before use. α-diazo carbonyl compounds[111] were prepared according to the reported procedures. Reactions were monitored by using thin layer chromatography (TLC) on 0.2 mm silica gel F254 plates (Merck). The chemical structures of final products and intermediates were characterized by nuclear magnetic resonance spectra (^{1}H NMR and ^{13}C NMR) were recorded on a 400 MHz spectrometer, and the chemical shifts are reported in δ units, parts per million (ppm), relative to residual chloroform (7.26 ppm) or DMSO (2.5 ppm) in the deuterated solvent. ^{13}C NMR spectra are fully decoupled. The following abbreviations were used to describe peak splitting patterns when appropriate: s = singlet, d = doublet, t = triplet, dd = doublet of doublets, and m = multiplet. Coupling constants *J* are reported in Hz. The ^{13}C NMR spectra are reported in ppm relative to deuterochloroform (77.0 ppm) or [d_6] DMSO (39.5 ppm). Melting points were determined on a capillary point apparatus equipped with a digital thermometer and are uncorrected. High-resolution mass spectra were recorded on Agilent Technologies 6545 Q-TOF LC/MS by using electrospray mode. Column chromatography was performed on silica gel (100-200 mesh) using a varying ratio of ethyl acetate/hexanes as eluent.

General procedure for the synthesis of hydroxy-dihydroindazolo phthalazines (56)

To a stirred solution of *N*-aryl-2,3-dihydrophthalazine-1,4-dione (**1**) (50 mg) in DCE (5 mL), [Cp*****RhCl$_2$]$_2$ (0.0050 mmol), CsOAc (0.10 mmol) was added under ambient conditions. After 15 min., α-diazo carbonyl compound (**14**) (0.25 mmol) in DCE (0.5 mL) was added, and the reaction was stirred at room temperature for 16-18 h. The progress of the reaction was monitored by TLC. After the completion of the reaction, the reaction was quenched by adding water and extracted with DCM (3 x 15 mL). The combined organic layers were separated, dried over anhydrous sodium sulfate, and concentrated under reduced pressure to give a crude mixture. The crude mixture was purified by column chromatography using ethyl acetate/hexanes (3:7) as an eluent system to afford the desired product (**56**).

Detailed procedure for the synthesis of phthalazino-fused cinnolines (57)

To a stirred solution of 2-aryl-2,3-dihydrophthalazine-1,4-dione (**1a-1f, 1g, 1i-1j**, **1l**) (50 mg) in DCE, [Cp*****RhCl$_2$]$_2$ (0.0050 mmol), AgSbF$_6$ (0.020 mmol) was added under a nitrogen atmosphere. After 15 min., α-diazo carbonyl compound (**14**) (0.25 mmol) in DCE (0.5 mL) was added under a

nitrogen atmosphere, and the reaction mixture was stirred at 110 ℃ for 14-16 h. Upon completion, as shown by TLC, the reaction was quenched with water, and extracted with DCM (3 x 15 mL). The organic layers were combined, dried over anhydrous sodium sulfate, filtered, and concentrated under reduced pressure to give a crude mixture. Purification by column chromatography using ethyl acetate/hexanes (1:9) as eluent afforded the desired product (**57**).

Ethyl 13-hydroxy-6,11-dioxo-6,11-dihydro-13*H*-indazolo[1,2-*b*]phthalazine-13-carboxylate (56aa). White solid; yield: 61 mg (86%); mp 178−179 °C; ^{1}H NMR (400 MHz, $CDCl_3$) δ 8.51 – 8.47 (m, 1H), 8.44 (d, J = 8.1 Hz, 1H), 8.36 (dd, J = 7.6, 1.6 Hz, 1H), 7.96 – 7.85 (m, 2H), 7.65 – 7.58 (m, 1H), 7.53 – 7.48 (m, 1H), 7.40 – 7.33 (m, 1H), 5.53 (s, 1H), 4.40 – 4.24 (m, 2H), 1.20 (t, J = 7.1 Hz, 3H); ^{13}C NMR (100 MHz, $CDCl_3$) δ 167.5, 155.6, 154.2, 136.3, 134.1, 133.8, 131.9, 130.3, 128.3, 128.0, 127.6, 126.5, 124.8, 123.1, 115.9, 89.4, 63.9, 13.9; HRMS (ESI-TOF) (*m/z*) calculated $C_{18}H_{15}N_2O_5^+$: 339.0975, found 339.0975 $[M + H]^+$.

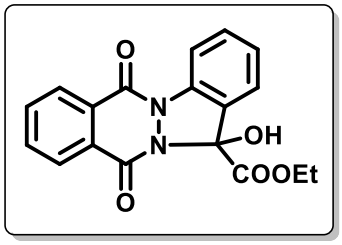

Methyl 13-hydroxy-6,11-dioxo-6,11-dihydro-13*H*-indazolo[1,2-*b*]phthalazine-13-carboxylate (56ab). White solid; yield: 54 mg (79%); mp 190−191 °C; ^{1}H NMR (400 MHz, $CDCl_3$) δ 8.51 – 8.41 (m, 2H), 8.39 – 8.32 (m, 1H), 7.96 – 7.86 (m, 2H), 7.65 – 7.58 (m, 1H), 7.52 (dd, J = 7.7, 1.2 Hz, 1H), 7.40 – 7.34 (m, 1H), 5.64 (s, 1H), 3.83 (s, 3H); ^{13}C NMR (100 MHz, $CDCl_3$) δ 168.1, 155.7, 154.2, 136.3, 134.2, 133.8, 132.0, 130.3, 128.3, 128.1, 127.6, 126.5, 124.6, 123.2, 115.9, 89.3, 54.4; HRMS (ESI-TOF) (*m/z*) calculated $C_{17}H_{13}N_2O_5^+$: 325.0819, found 325.0826 $[M + H]^+$.

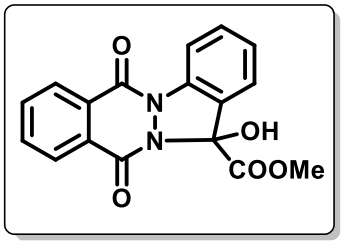

13-Acetyl-13-hydroxy-13*H*-indazolo[1,2-*b*]phthalazine-6,11-dione (56ac) *(obtained from 2c).* White solid; yield: 52 mg (80%); mp 185−186 °C; ^{1}H NMR (400 MHz, $CDCl_3$) δ 8.51 – 8.45 (m, 2H), 8.38 – 8.34 (m, 1H), 7.97 – 7.88 (m, 2H), 7.67 – 7.61 (m, 1H), 7.40 – 7.36 (m, 2H), 5.81 (s, 1H), 2.22 (s, 3H); ^{13}C NMR (100 MHz, $CDCl_3$) δ 198.7, 155.6, 154.3, 136.7, 134.4, 134.0, 132.2, 130.3, 128.2, 128.1, 127.8, 126.8, 124.4, 123.2, 116.2, 92.8, 23.2; HRMS (ESI-TOF) (*m/z*) calculated $C_{17}H_{13}N_2O_4^+$: 309.0870, found 309.0876 $[M + H]^+$.

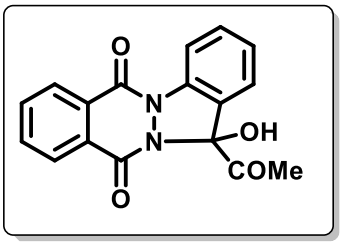

13-Acetyl-13-hydroxy-13*H*-indazolo[1,2-*b*]phthalazine-6,11-dione (56ad) *(obtained from 2d).* White solid; yield: 44 mg (68%); mp 184−186 °C; ^{1}H NMR (400 MHz, $CDCl_3$) δ 8.56 – 8.42 (m, 2H), 8.36 (dd, J = 7.4, 1.7 Hz, 1H), 7.99 – 7.88 (m, 2H), 7.68 – 7.61 (m, 1H), 7.42 – 7.33 (m, 2H), 5.78 (s, 1H), 2.22 (s, 3H); ^{13}C NMR (100 MHz, $CDCl_3$) δ 198.7, 155.6, 154.4, 136.7, 134.4, 134.0, 132.2, 130.3, 128.2, 128.1, 127.8, 126.8, 124.4, 123.2, 116.2, 92.8, 23.3; HRMS (ESI-TOF) (*m/z*) calculated $C_{17}H_{13}N_2O_4^+$: 309.0870, found 309.0873 $[M + H]^+$.

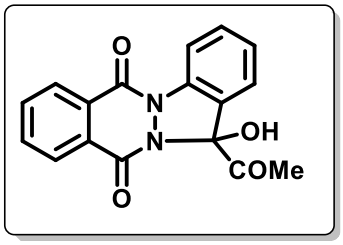

Ethyl 13-hydroxy-6,11-dioxo-6,11-dihydro-13*H*-indazolo[1,2-*b*]phthalazine-13-carboxylate (56ae) *(obtained from 2e)* White solid; yield: 49 mg (69%); mp 178−179 °C; ^{1}H NMR (400 MHz, DMSO-d_6) δ 8. 38 – 8.35 (m, 1H), 8.33 (s, 1H), 8.32 – 8.29 (m, 1H), 8.28 – 8.25 (m, 1H), 8.09 – 8.00 (m, 2H), 7.70 – 7.63 (m, 1H), 7.56 – 7.51 (m, 1H), 7.46 – 7.39 (m, 1H), 4.24 – 4.19 (m, 1H), 4.17 – 4.10 (m, 1H), 1.09 (t, J = 7.1 Hz, 3H); ^{13}C NMR (100 MHz, DMSO-d_6) δ 166.8, 154.6, 154.1, 135.6, 135.0, 132.1, 128.6, 128.1, 127.7, 127.1, 123.6, 115.5, 90.1, 62.9, 14.2.; HRMS (ESI-TOF) (*m/z*) calculated $C_{18}H_{15}N_2O_5^+$ 339.0975, found 339.0981 $[M+H]^+$.

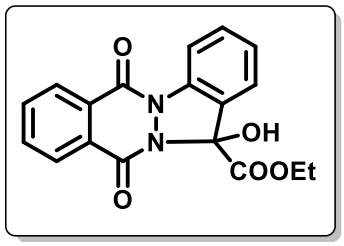

Ethyl 13-hydroxy-2-methyl-6,11-dioxo-6,11-dihydro-13*H*-indazolo[1,2-*b*]phthalazine-13-carboxylate (56ba). White solid; yield: 55 mg (79%); mp 188−190 °C; ^{1}H NMR (400 MHz, $CDCl_3$) δ 8.49 – 8.46 (m, 1H), 8.37 – 8.33 (m, 1H), 8.30 (d, J = 8.3 Hz, 1H), 7.95 – 7.85 (m, 2H), 7.43 – 7.38 (m, 1H), 7.32 – 7.29 (m, 1H), 5.53 (s, 1H), 4.41 – 4.33 (m, 1H), 4.32 – 4.23 (m, 1H), 2.45 (s, 3H), 1.21 (t, J = 7.1 Hz, 3H); ^{13}C NMR (100 MHz, $CDCl_3$) δ 167.6, 155.6, 153.9, 136.9, 134.1, 134.1, 133.7, 132.6, 130.4, 128.3, 128.0, 127.6, 124.8, 123.3, 115.7, 89.4, 63.9, 21.3, 13.9; HRMS (ESI-TOF) (*m/z*) calculated $C_{19}H_{17}N_2O_5^+$: 353.1132, found 353.1122 $[M + H]^+$.

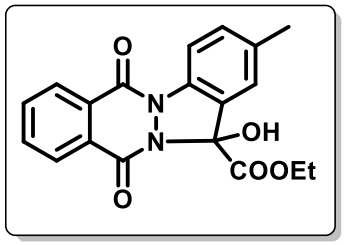

Methyl 13-hydroxy-2-methyl-6,11-dioxo-6,11-dihydro-13*H*-indazolo[1,2-*b*]phthalazine-13-carboxylate (56bb). White solid; yield: 51 mg (76%); mp 200−201 °C; ^{1}H NMR (400 MHz, $CDCl_3$) δ 8.50 – 8.43 (m, 1H), 8.34 (dd, J =7.6, 1.5 Hz, 1H), 8.29 (d, J = 8.3 Hz, 1H), 7.96 – 7.83 (m, 2H), 7.45 – 7.37 (m, 1H), 7.31 (d, J = 1.7 Hz, 1H), 5.62 (s, 1H), 3.83 (s, 3H), 2.44 (s, 3H); ^{13}C NMR (100 MHz, $CDCl_3$) δ 168.1, 155.7, 153.9, 136.9, 134.1, 134.1, 133.7, 132.7, 130.4, 128.2, 128.0, 127.6, 124.7, 123.4, 115.7, 89.3, 54.4, 21.2; HRMS (ESI-TOF) (*m/z*) calculated $C_{18}H_{15}N_2O_5^+$: 339.0975, found 339.0984 $[M + H]^+$.

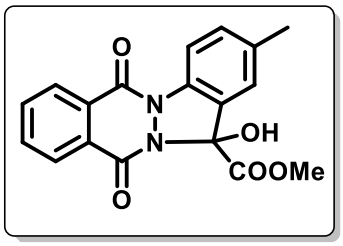

Ethyl 2-fluoro-13-hydroxy-6,11-dioxo-6,11-dihydro-13*H*-indazolo[1,2-*b*]phthalazine-13-carboxylate (56ca). White solid; yield: 50 mg (72%); mp 145−146 °C; ^{1}H NMR (400 MHz, $CDCl_3$) δ 8.47 – 8.39 (m, 2H), 8.34 (dd, J = 7.1, 2.0 Hz, 1H), 7.90 (dd, J = 7.3, 1.6 Hz, 2H), 7.33 – 7.27 (m, 1H), 7.22 (dd, J = 7.2, 2.6 Hz, 1H), 5.81 (s, 1H), 4.40 – 4.25 (m, 2H), 1.21 (t, J = 7.1 Hz, 3H) ; ^{13}C NMR (100 MHz, $CDCl_3$) δ 167.0, 160.6 ($^{1}J_{C\text{-}F}$ = 246 Hz), 155.6, 154.0, 134.2, 133.9, 132.5 ($^{4}J_{C\text{-}F}$ = 2.3 Hz), 130.2, 128.2, 128.0, 127.7, 126.5 ($^{3}J_{C\text{-}F}$ = 8.7 Hz), 119.0 ($^{2}J_{C\text{-}F}$ = 23.6 Hz), 117.4 ($^{3}J_{C\text{-}F}$ = 8.1 Hz), 110.6 ($^{2}J_{C\text{-}F}$ = 25.6 Hz), 89.1 ($^{4}J_{C\text{-}F}$ = 2.5 Hz), 64.2, 13.9; HRMS (ESI-TOF) (*m/z*) calculated $C_{18}H_{14}FN_2O_5^+$ 357.0881, found 357.0905 $[M + H]^+$.

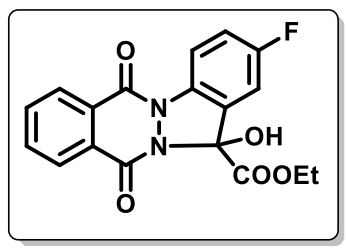

Methyl 2-fluoro-13-hydroxy-6,11-dioxo-6,11-dihydro-13*H*-indazolo[1,2-*b*]phthalazine-13-carboxylate (56cb). White solid; yield: 45 mg (68%); mp 206−207 °C; ^{1}H NMR (400 MHz, $CDCl_3$) δ 8.49 – 8.45 (m, 1H), 8.43 (dd, J = 8.9, 4.4 Hz, 1H), 8.35 (dd, J = 7.5, 1.6 Hz, 1H), 7.96 – 7.87 (m, 2H), 7.35 – 7.30 (m, 1H), 7.22 (dd, J = 7.2, 2.6 Hz, 1H), 5.64 (brs, 1H), 3.85 (s, 3H); ^{13}C NMR (100 MHz, $CDCl_3$) δ 167.6, 160.6 ($^{1}J_{C\text{-}F}$ = 256 Hz), 155.7, 153.9, 134,3, 133.9, 132.5, 130.2, 128.1, 128.0, 127.7, 126.2, 119.1 ($^{2}J_{C\text{-}F}$ = 23.5 Hz), 117.4 ($^{3}J_{C\text{-}F}$ = 8.2 Hz), 110.7 ($^{2}J_{C\text{-}F}$ = 25.6 Hz), 88.9, 54.6; HRMS (ESI-TOF) (*m/z*) calculated $C_{17}H_{12}FN_2O_5^+$: 343.0725, found 343.0729 $[M + H]^+$.

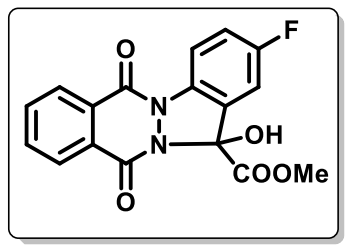

Ethyl 2-chloro-13-hydroxy-6,11-dioxo-6,11-dihydro-13*H*-indazolo[1,2-*b*]phthalazine-13-carboxylate (56da). White solid; yield: 46 mg (68%); mp 150−152 °C; ^{1}H NMR (400 MHz, DMSO-d_6) δ 8.51 (s, 1H), 8.39 – 8.35 (m, 1H), 8.33 – 8.25 (m, 2H), 8.08 – 8.01 (m, 2H), 7.74 (dd, *J* = 8.7, 2.2 Hz, 1H), 7.59 (d, *J* = 2.2 Hz, 1H), 4.26 – 4.22 (m, 1H), 4.18 – 4.13 (m, 1H), 1.11 (t, *J* = 7.1 Hz, 3H); ^{13}C NMR (100 MHz, DMSO-d_6) δ 166.3, 154.5, 154.1, 135.1, 134.5, 132.2, 130.7, 128.6, 128.1, 127.8, 123.6, 117.0, 89.6, 63.1, 14.3; HRMS (ESI-TOF) (*m/z*) calculated $C_{18}H_{13}ClN_2O_5Na^+$: 395.0405, found 395.0421 [M + Na]$^+$.

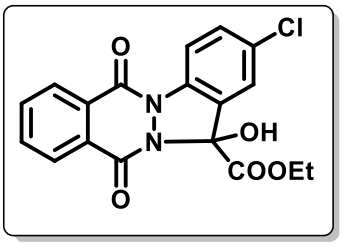

Methyl 2-chloro-13-hydroxy-6,11-dioxo-6,11-dihydro-13*H*-indazolo[1,2-*b*]phthalazine-13-carboxylate (56db). White solid; yield: 47 mg (72%); mp 171−172 °C; ^{1}H NMR (400 MHz, $CDCl_3$ + DMSO-d_6) δ 8.44 – 8.40 (m, 1H), 8.34 (dd, *J* = 8.7, 5.3 Hz, 2H), 7.96 – 7.84 (m, 3H), 7.53 (dd, *J* = 8.6, 2.2 Hz, 1H), 3.81 (s, 3H); ^{13}C NMR (100 MHz, $CDCl_3$ + DMSO-d_6) δ 167.11, 154.9, 154.1, 134.4, 134.0, 133.9, 131.6, 131.3, 129.8, 128.6, 127.8, 127.6, 123.4, 116.8, 89.3, 53.9; HRMS (ESI-TOF) (*m/z*) calculated $C_{17}H_{12}ClN_2O_5^+$: 359.0429, found 359.0438 [M + H]$^+$.

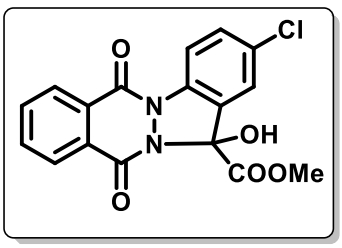

Ethyl 2-bromo-13-hydroxy-6,11-dioxo-6,11-dihydro-13H-indazolo[1,2-*b*]phthalazine-13-carboxylate (56ea). White solid; yield: 52 mg (78%); mp 185−186 °C; ^{1}H NMR (400 MHz, $CDCl_3$) δ 8.49 – 8.43 (m, 1H), 8.37 – 8.28 (m, 2H), 7.95 – 7.88 (m, 2H), 7.71 (dd, *J* = 8.7, 2.0 Hz, 1H), 7.63 (d, *J* = 2.0 Hz, 1H), 5.76 (brs, 1H), 4.42 – 4.35 (m, 1H), 4.32 – 4.25 (m, 1H), 1.22 (t, *J* = 7.1 Hz, 3H); ^{13}C NMR (100 MHz, $CDCl_3$) 167.0, 155.5, 154.2, 135.2, 135.0, 134.3, 134.0, 130.0, 128.3, 128.1, 127.7, 126.7, 126.4, 119.1, 117.3, 88.9, 64.2, 13.9; HRMS (ESI-TOF) (*m/z*) calculated $C_{18}H_{14}BrN_2O_5^+$: 417.0081, found 417.0078 [M + H]$^+$.

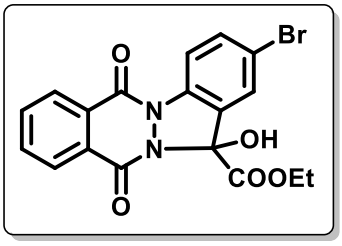

Methyl 2-bromo-13-hydroxy-6,11-dioxo-6,11-dihydro-13*H*-indazolo[1,2-*b*]phthalazine-13-carboxylate (56eb). White solid; yield: 48 mg (76%); mp 207−208 °C; ^{1}H NMR (400 MHz, $CDCl_3$ + DMSO-d_6) δ 8.43 (s, 1H), 8.35 – 8.28 (m, 1H), 8.27 – 8.19 (m, 2H), 7.97 – 7.87 (m, 2H), 7.75 – 7.64 (m, 1H), 7.56 (d, J = 2.1 Hz, 1H), 3.71 (s, 3H); ^{13}C NMR (100 MHz, $CDCl_3$ + DMSO-d_6) δ 166.9, 154.6, 154.1, 134.9, 134.6, 134.4, 134.3, 129.8, 128.9, 128.7, 127.9, 127.7, 126.3, 118.4, 117.2, 89.3, 53.9; HRMS (ESI-TOF) (*m/z*) calculated $C_{17}H_{12}BrN_2O_5^+$: 402.9924, found 402.9913 $[M + H]^+$.

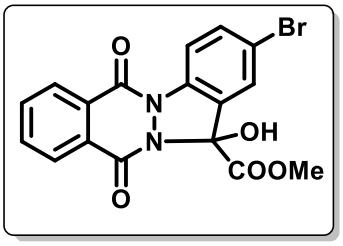

Ethyl 3-chloro-13-hydroxy-6,11-dioxo-6,11-dihydro-13*H*-indazolo[1,2-*b*]phthalazine-13-carboxylate (56fa). White solid; yield: 52 mg (76%); mp 192−193 °C; ^{1}H NMR (400 MHz, $CDCl_3$) δ 8.50 – 8.45 (m, 2H), 8.37 – 8.33 (m, 1H), 7.96 – 7.88 (m, 2H), 7.43 (d, J = 8.2 Hz, 1H), 7.34 (dd, J = 8.2, 1.9 Hz, 1H), 5.60 (s, 1H), 4.39 – 4.32 (m, 1H), 4.31 – 4.24 (m, 1H), 1.20 (t, J = 7.1 Hz, 3H); ^{13}C NMR (100 MHz, $CDCl_3$) δ 167.2, 155.5, 154.3, 137.9, 137.0, 134.3, 134.1, 130.0, 128.3, 128.2, 127.7, 126.7, 124.0, 123.3, 116.2, 89.1, 64.1, 13.2; HRMS (ESI-TOF) (*m/z*) calculated $C_{18}H_{14}ClN_2O_5^+$: 373.0586, found 373.0586 $[M + H]^+$.

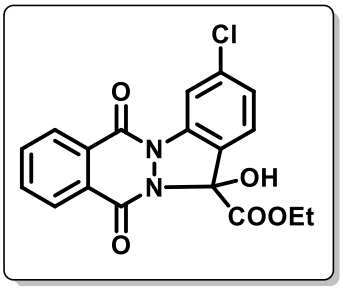

Ethyl 3-chloro-13-hydroxy-2-methyl-6,11-dioxo-6,11-dihydro-13*H*-indazolo[1,2-*b*]phthalazine-13-carboxylate (56ga). White solid; yield: 57 mg (85%); mp 208−209 °C; ^{1}H NMR (400 MHz, $CDCl_3$) δ 8.49 – 8.44 (m, 2H), 8.37 – 8.32 (m, 1H), 7.97 – 7.87 (m, 2H), 7.36 (s, 1H), 5.54 (brs, 1H), 4.42 – 4.32 (m, 1H), 4.31 – 4.22 (m, 1H), 2.45 (s, 3H), 1.21 (t, J = 7.1 Hz, 3H); ^{13}C NMR (100 MHz, $CDCl_3$) δ 167.3, 155.5, 154.0, 137.9, 134.9, 134.3, 133.9, 130.1, 128.3, 128.1, 127.7, 124.8, 123.2, 116.4, 89.1, 64.1, 20.3, 14.0; HRMS (ESI-TOF) (*m/z*) calculated $C_{19}H_{16}ClN_2O_5^+$: 387.0742, found 387.0744 $[M + H]^+$.

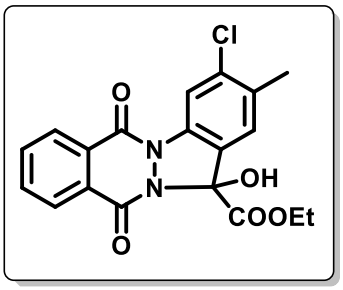

Methyl 3-chloro-13-hydroxy-2-methyl-6,11-dioxo-6,11-dihydro-13*H*-indazolo[1,2-*b*]phthalazine-13-carboxylate (56gb). White solid; yield: 50 mg (77%); mp 216−217 °C; ^{1}H NMR (400 MHz, $CDCl_3$) δ 8.46 (d, J = 9.6 Hz, 2H), 8.34 (dd, J = 7.6, 1.5 Hz, 1H), 7.96 – 7.86 (m, 2H), 7.36 (s, 1H), 3.84 (s, 3H), 2.45 (s, 3H) ; ^{13}C NMR (100 MHz, $CDCl_3$) δ 167.9, 155.6, 154.0, 138.0, 134.9, 134.8, 134.3, 133.9, 130.1, 128.3, 128.1, 127.7, 124.9, 123.0, 116.4, 89.1, 54.5, 20.3; HRMS (ESI-TOF) (*m/z*) calculated $C_{18}H_{14}ClN_2O_5^+$: 373.0586, found 373.0589 $[M + H]^+$.

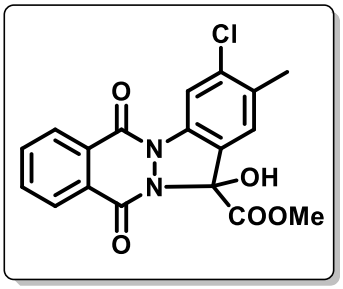

Ethyl 13-hydroxy-2,3-dimethyl-6,11-dioxo-6,11-dihydro-13*H*-indazolo[1,2-*b*]phthalazine-13-carboxylate (56ha). White solid; yield: 56 mg (81%); mp 133−134 °C; ^{1}H NMR (400 MHz, $CDCl_3$ + DMSO-d_6) δ 8.36 – 8.29 (m, 1H), 8.27 – 8.19 (m, 1H), 8.10 (s, 1H), 7.96 – 7.74 (m, 3H), 7.18 (s, 1H), 4.26 – 4.16 (m, 1H), 4.15 – 4.04 (m, 1H), 2.31 (s, 3H), 2.25 (s, 3H), 1.10 (t, J = 7.1 Hz, 3H); ^{13}C NMR (100 MHz, $CDCl_3$ + DMSO-d_6) δ 167.0, 154.7, 153.7, 140.4, 135.2, 134.1, 134.0, 133.8, 130.1, 128.7, 127.7, 127.4, 124.3, 123.6, 116.3, 89.9, 62.7, 20.6, 19.9, 14.1; HRMS (ESI-TOF) (*m/z*) calculated $C_{20}H_{19}N_2O_5^+$: 367.1288, found 367.1285 $[M + H]^+$.

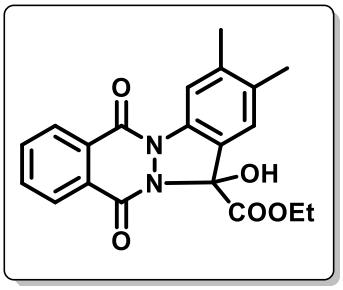

Ethyl 13-hydroxy-8-methyl-6,11-dioxo-6,11-dihydro-13*H*-indazolo[1,2-*b*]phthalazine-13-carboxylate + Ethyl 13-hydroxy-9-methyl-6,11-dioxo-6,11-dihydro-13*H*-indazolo[1,2-*b*]phthalazine-13-carboxylate (56ia) (1:0.4 or 0.4:1). White solid; yield: 59 mg (84%); mp 189−190 °C; ^{1}H NMR (400 MHz, $CDCl_3$) δ 8.46 – 8.40 (m, 1.4H), 8.36 (d, J = 8.0 Hz, 0.4H), 8.27 (s, 1H), 8.23 (d, J = 8.0 Hz, 1H), 8.14 (s, 0.4H), 7.74 – 7.67 (m, 1.4H), 7.64 – 7.58 (m, 1.4H), 7.51 (dd, J = 7.7, 1.3 Hz, 1.4H), 7.40 – 7.33 (m, 1.0 Hz, 1.4H), 5.52 (s, 1.4H), 4.39 – 4.32 (m, 1.4H), 4.31 – 4.24 (m, 1.4H), 2.61 (s, 3H), 2.59 (s, 1H), 1.20 (m, 1.4H); ^{13}C NMR (100 MHz, $CDCl_3$) δ 167.6, 155.8, 154.4, 145.5, 136.3, 134.9, 135.2, 131.9, 130.2, 128.1, 127.6, 126.4, 126.3, 125.8, 124.8, 124.7, 123.1, 115.9, 115.8, 89.3, 63.9, 22.0, 21.9, 13.9; HRMS (ESI-TOF) (*m/z*) calculated $C_{19}H_{17}N_2O_5^+$: 353.1132, found 353.1124 $[M + H]^+$.

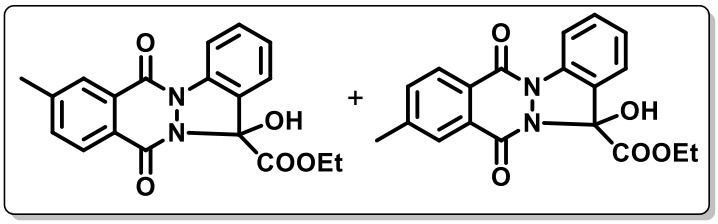

Methyl 13-hydroxy-8-methyl-6,11-dioxo-6,11-dihydro-13*H*-indazolo[1,2-*b*]phthalazine-13-carboxylate + Methyl 13-hydroxy-9-methyl-6,11-dioxo-6,11-dihydro-13*H*-indazolo[1,2-*b*]phthalazine-13-carboxylate (56ib) (1:0.8 or 0.8:1). White solid; yield: 59 mg (88%); mp 187−188 °C; ^{1}H NMR (400 MHz, $CDCl_3$) δ 8.45 – 8.38 (m, 1.8H), 8.35 (d, J = 8.0 Hz, 0.8H), 8.26 (s, 1H), 8.22 (d, J = 8.0 Hz, 1H), 8.13 (s, 0.8 H), 7.74 – 7.66 (m, 1.8H), 7.64 – 7.58 (m, 1.8H), 7.52 (dd, J = 7.9, 1.3 Hz, 1.8H), 7.40 – 7.32 (m, 1.8H), 5.61 (s, 1.7H), 3.83 (s, 5H), 2.60 (s, 3H), 2.58 (s, 2.4H); ^{13}C NMR (100 MHz, $CDCl_3$) δ 168.2, 155.8, 154.3, 145.5, 145.1, 136.3, 135.2, 134.9, 132.0, 130.2, 128.1, 128.1, 127.8, 127.7, 126.4, 126.3, 125.8, 124.7, 124.5, 123.2, 115.8, 115.9, 89.3, 89.2, 54.4, 21.9, 21.8; HRMS (ESI-TOF) (*m/z*) calculated $C_{18}H_{15}N_2O_5^+$: 339.0975, found 339.0976 $[M + H]^+$.

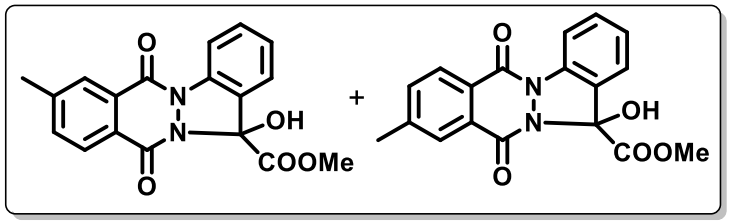

Diethyl 2-(2-(1,4-dioxo-3,4-dihydrophthalazin-2(1*H*)-yl)phenyl)malonate (56′af). White solid; yield: 65 mg (78%); mp 162−163 °C; ^{1}H NMR (400 MHz, $CDCl_3$) δ 8.48 – 8.42 (m, 1H), 8.10 – 8.03 (m, 1H), 7.90 – 7.83 (m, 2H), 7.75 – 7.70 (m, 1H), 7.56 – 7.43 (m, 3H), 4.76 (s, 1H), 4.22 – 4.12 (m, 4H), 1.22 – 1.15 (m, 6H); ^{13}C NMR (100 MHz, $CDCl_3$) δ 167.8, 157.0, 152.2, 139.2, 133.5, 133.1, 130.9, 130.4, 129.6, 129.4, 129.3, 128.3, 127.8, 125.5, 125.3, 62.1, 53.1, 13.9; HRMS (ESI-TOF) (*m/z*) calculated $C_{21}H_{21}N_2O_6^+$: 397.1394, found 397.1394 $[M + H]^+$.

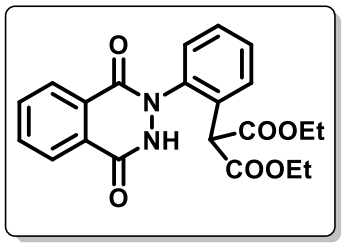

Ethyl 6-methyl-8,13-dioxo-8,13-dihydrophthalazino[2,3-*a*]cinnoline-5-carboxylate (57aa). Yellow solid; yield: 60 mg (82%); mp 112−113 °C; ^{1}H NMR (400 MHz, $CDCl_3$) δ 8.47 – 8.40 (m, 1H), 8.33 (dd, J = 7.6, 1.5 Hz, 1H), 7.96 – 7.83 (m, 3H), 7.35 – 7.28 (m, 2H), 7.23 (td, J = 7.5, 1.3 Hz, 1H), 4.43 (q, J = 7.2 Hz, 2H), 2.43 (s, 3H), 1.42 (t, J = 7.1 Hz, 3H); ^{13}C NMR (100 MHz, $CDCl_3$) δ 166.0, 157.3, 157.2, 140.8, 135.3, 134.3, 133.0, 129.7, 129.2, 128.4, 128.1, 127.9, 126.4, 124.7, 123.5, 119.5, 119.1, 61.6, 17.5, 14.2; HRMS (ESI-TOF) (*m/z*) calculated $C_{20}H_{17}N_2O_4^+$: 349.1183, found 349.1189 $[M + H]^+$.

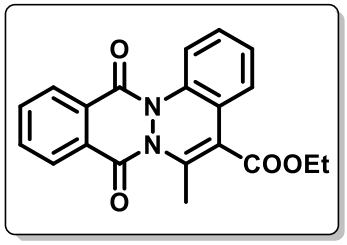

Methyl 6-methyl-8,13-dioxo-8,13-dihydrophthalazino[2,3-*a*]cinnoline-5-carboxylate (57ab). Yellow solid; yield: 54 mg (77%); mp 161−162 °C; ^{1}H NMR (400 MHz, $CDCl_3$) δ 8.49 – 8.40 (m, 1H), 8.37 – 8.29 (m, 1H), 7.97 – 7.83 (m, 3H), 7.34 – 7.29 (m, 2H), 7.26 – 7.21 (m, 1H), 3.95 (s, 3H), 2.44 (s, 3H); ^{13}C NMR (100 MHz, $CDCl_3$) δ 166.5, 157.3, 157.2, 141.4, 135.3, 134.4, 134.0, 129.7, 129.2, 128.4, 129.2, 127.9, 126.4, 124.8, 123.4, 119.4, 118.7, 52.4, 17.6; HRMS (ESI-TOF) (*m/z*) calculated $C_{19}H_{15}N_2O_4^+$: 335.1026, found 335.1028 $[M + H]^+$.

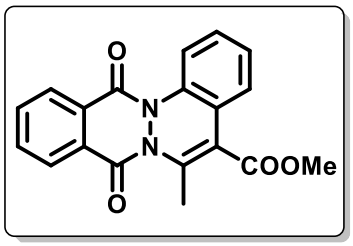

Ethyl 8,13-dioxo-6-phenyl-8,13-dihydrophthalazino[2,3-*a*]cinnoline-5-carboxylate (57ae). Yellow solid; yield: 61 mg (70%); mp 174−175 °C; ^{1}H NMR (400 MHz, $CDCl_3$) δ 8.53 – 8.46 (m, 1H), 8.22 – 8.11 (m, 1H), 7.98 – 7.88 (m, 3H), 7.87 – 7.82 (m, 1H), 7.81 – 7.78 (m, 1H), 7.40 – 7.29 (m, 6H), 4.00 (q, *J* = 7.1 Hz, 2H), 0.87 (t, *J* = 7.1 Hz, 3H); ^{13}C NMR (100 MHz, $CDCl_3$) δ 165.4, 157.6, 156.7, 140.8, 135.5, 134.3, 134.1, 133.0, 129.8, 129.6, 129.3, 129.1, 128.8, 128.6, 128.4, 128.0, 127.8, 126.6, 125.1, 124.5, 123.6, 123.0, 120.1, 119.2, 61.5, 13.5; HRMS (ESI-TOF) (*m/z*) calculated $C_{25}H_{19}N_2O_4^+$: 411.1339, found 411.1336 $[M + H]^+$.

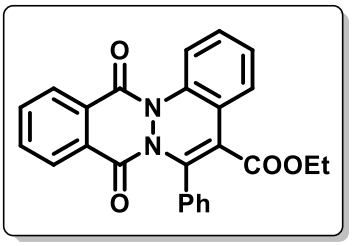

Ethyl 3,6-dimethyl-8,13-dioxo-8,13-dihydrophthalazino[2,3-*a*]cinnoline-5-carboxylate (57ba). Yellow solid; yield: 56 mg (78%); mp 167−168 °C; ^{1}H NMR (400 MHz, $CDCl_3$) δ 8.45 – 8.40 (m, 1H), 8.34 – 8.29 (m, 1H), 7.94 – 7.84 (m, 2H), 7.77 – 7.72 (m, 1H), 7.13 – 7.06 (m, 2H), 4.44 (q, *J* = 7.1 Hz, 2H), 2.41 (s, 3H), 2.36 (s, 3H), 1.42 (t, *J* = 7.1 Hz, 3H); ^{13}C NMR (100 MHz, $CDCl_3$) δ 166.1, 157.3, 157.1, 140.2, 136.3, 134.3, 133.8, 132.8, 129.7, 129.2, 128.8, 128.3, 127.8, 124.9, 123.2, 119.3, 119.1, 61.6, 21.2, 17.4, 14.2; HRMS (ESI-TOF) (*m/z*) calculated $C_{21}H_{19}N_2O_4^+$: 363.1339, found 363.1333 $[M + H]^+$.

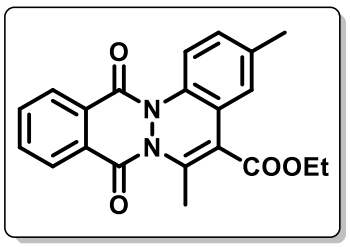

Methyl 3,6-dimethyl-8,13-dioxo-8,13-dihydrophthalazino[2,3-a]cinnoline-5-carboxylate (57bb). Yellow solid; yield: 53 mg (76%); mp 172−174 °C; ^{1}H NMR (400 MHz, $CDCl_3$) δ 8.46 – 8.40 (m, 1H), 8.35 – 8.29 (m, 1H), 7.95 – 7.85 (m, 2H), 7.75 (d, J = 8.4 Hz, 1H), 7.14 – 7.06 (m, 2H), 3.96 (s, 3H), 2.41 (s, 3H), 2.37 (s, 3H); ^{13}C NMR (100 MHz, $CDCl_3$) δ 166.6, 157.3, 157.1, 140.7, 136.4, 134.3, 133.9, 132.8, 129.7, 129.1, 128.9, 128.4, 127.8, 124.9, 123.1, 119.4, 118.9, 52.4, 21.2, 17.6; HRMS (ESI-TOF) (*m/z*) calculated $C_{20}H_{17}N_2O_4^+$: 349.1183, found 349.1182 $[M + H]^+$.

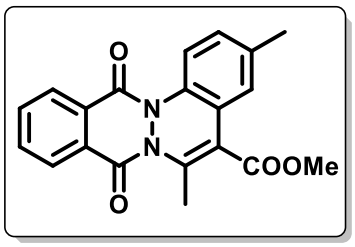

Ethyl 3-fluoro-6-methyl-8,13-dioxo-8,13-dihydrophthalazino[2,3-*a*]cinnoline-5-carboxylate (57ca). Yellow solid; yield: 59 mg (83%); mp 154−155 °C; ^{1}H NMR (400 MHz, $CDCl_3$) δ 8.46 – 8.40 (m, 1H), 8.33 (dd, J = 7.7, 1.5 Hz, 1H), 7.96 – 7.87 (m, 2H), 7.82 (dd, J = 9.1, 5.0 Hz, 1H), 7.10 (dd, J = 9.3, 2.9 Hz, 1H), 7.03 – 6.96 (m, 1H), 4.44 (q, J = 7.2 Hz, 2H), 2.45 (s, 3H), 1.59 (s, 2H), 1.42 (t, J = 7.1 Hz, 3H); ^{13}C NMR (100 MHz, $CDCl_3$) δ 165.5, 160.4 ($^{1}J_{C\text{-}F}$ = *244.8* Hz), 157.4, 157.1, 142.8, 134.5, 134.0, 131.0, 129.6, 129.1, 128.4, 127.9, 125.6 ($^{3}J_{C\text{-}F}$ = 8.9 Hz), 121.4 ($^{3}J_{C\text{-}F}$ = 8.5 Hz), 117.8, 114.8 ($^{2}J_{C\text{-}F}$ = 23 Hz), 111.5 ($^{2}J_{C\text{-}F}$ = 25.4 Hz), 61.8, 17.5, 14.2; HRMS (ESI-TOF) (*m/z*) calculated $C_{20}H_{16}FN_2O_4^+$ 367.1089, found 367.1088 $[M + H]^+$.

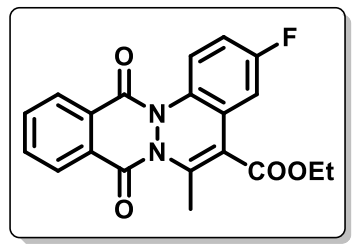

Methyl 3-fluoro-6-methyl-8,13-dioxo-8,13-dihydrophthalazino[2,3-*a*]cinnoline-5-carboxylate (57cb). Yellow solid; yield: 56 mg (81%); mp 175−176 °C; ^{1}H NMR (400 MHz, $CDCl_3$) δ 8.45 – 8.40 (m, 1H), 8.36 – 8.31 (m, 1H), 7.97 – 7.87 (m, 2H), 7.82 (dd, J = 9.1, 5.0 Hz, 1H), 7.09 (dd, J = 9.4, 2.8 Hz, 1H), 7.01 – 6.96 (m, 1H), 3.96 (s, 3H), 2.46 (s, 3H); ^{13}C NMR (100 MHz, $CDCl_3$) δ 165.9, 160. 3 ($^{1}J_{C\text{-}F}$ = 244.5 Hz), 157.4, 157.1, 143.4, 134.5, 134.1, 129.5, 129.1, 128.5, 128.0, 125.5, 121.5 ($^{3}J_{C\text{-}F}$ = 8.4 Hz), 114.8 ($^{2}J_{C\text{-}F}$ = 23.2 Hz), 111.7 ($^{2}J_{C\text{-}F}$ = 25.2 Hz), 52.5, 17.6; HRMS (ESI-TOF) (*m/z*) calculated $C_{19}H_{14}FN_2O_4^+$ 353.0932, found 353.0932 $[M + H]^+$.

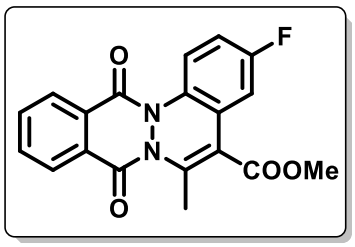

Ethyl 3-chloro-6-methyl-8,13-dioxo-8,13-dihydrophthalazino[2,3-*a*]cinnoline-5-carboxylate (57da). Yellow solid; yield: 58 mg (82%); mp 183−184 °C; ^{1}H NMR (400 MHz, $CDCl_3$) δ 8.43 – 8.40 (m, 1H), 8.34 – 8.31 (m, 1H), 7.95 – 7.88 (m, 2H), 7.78 (d, J = 8.8 Hz, 1H), 7.34 (d, J = 2.3 Hz, 1H), 7.25 (dd, J = 8.9, 2.4 Hz, 1H), 4.44 (q, J = 7.1 Hz, 2H), 2.44 (s, 3H), 1.43 (t, J = 7.1 Hz, 3H); ^{13}C NMR (100 MHz, $CDCl_3$) δ 165.4, 157.3, 157.2, 142.6, 134.5, 134.1, 133.6, 131.9, 129.5, 129.1, 128.5, 128.0, 127.9, 125.1, 124.6, 120.9, 117.8, 61.8, 17.6, 14.2; HRMS (ESI-TOF) (*m/z*) calculated $C_{20}H_{16}ClN_2O_4^+$: 385.0772, found 385.0776 $[M + H]^+$.

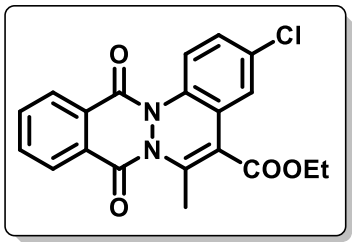

Methyl 3-chloro-6-methyl-8,13-dioxo-8,13-dihydrophthalazino[2,3-*a*]cinnoline-5 carboxylate (57db). Yellow solid; yield: 51 mg (76%); mp 221−222 °C; ^{1}H NMR (400 MHz, $CDCl_3$) δ 8.45 – 8.40 (m, 1H), 8.35 – 8.30 (m, 1H), 7.97 – 7.88 (m, 2H), 7.78 (d, J = 8.9 Hz, 1H), 7.33 (d, J = 2.3 Hz, 1H), 7.26 (dd, J = 8.9, 2.4 Hz, 1H), 3.97 (s, 3H), 2.44 (s, 3H); ^{13}C NMR (100 MHz, $CDCl_3$) δ 165.9, 157.3, 157.1, 143.1, 134.5, 134.2, 133.7, 131.9, 129.5, 129.1, 128.5, 128.0, 125.1, 124.7, 120.9, 117.5, 52.5, 17.7; HRMS (ESI-TOF) (*m/z*) calculated $C_{19}H_{14}ClN_2O_4^+$: 371.0615, found 371.0604 $[M + H]^+$.

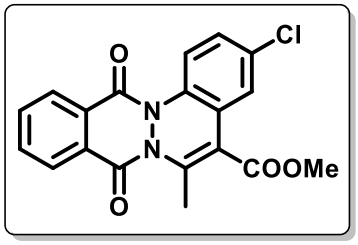

Ethyl 3-bromo-6-methyl-8,13-dioxo-8,13-dihydrophthalazino[2,3-*a*]cinnoline-5-carboxylate (57ea). Yellow solid; yield: 52 mg (77%); mp 186−188 °C; ^{1}H NMR (400 MHz, $CDCl_3$) δ 8.45 – 8.39 (m, 1H), 8.36 – 8.30 (m, 1H), 7.97 – 7.85 (m, 2H), 7.73 (d, J = 8.8 Hz, 1H), 7.50 (d, J = 2.2 Hz, 1H), 7.40 (dd, J = 8.8, 2.2 Hz, 1H), 4.44 (q, J = 7.2 Hz, 2H), 2.44 (s, 3H), 1.43 (t, J = 7.2 Hz, 3H); ^{13}C NMR (100 MHz, $CDCl_3$) δ 165.4, 157.2, 157.2, 142.6, 134.5, 134.2, 134.2, 130.8, 129.5, 129.1, 128.5, 128.0, 127.6, 125.4, 121.1, 119.6, 117.7, 61.8, 17.6, 14.2; HRMS (ESI-TOF) (*m/z*) calculated $C_{20}H_{16}BrN_2O_4^+$: 427.0288, found 427.0285 $[M + H]^+$.

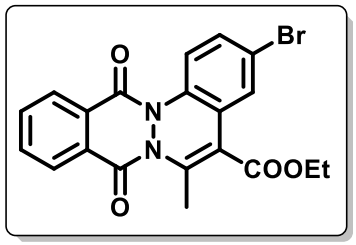

Methyl 3-bromo-6-methyl-8,13-dioxo-8,13-dihydrophthalazino[2,3-*a*]cinnoline-5-carboxylate (57eb). Yellow solid; yield: 50 mg (76%); mp 238−239 °C; ^{1}H NMR (400 MHz, $CDCl_3$) δ 8.44 – 8.39 (m, 1H), 8.36 – 8.27 (m, 1H), 7.97 – 7.87 (m, 2H), 7.72 (d, J = 8.8 Hz, 1H), 7.47 (d, J = 2.2 Hz, 1H), 7.40 (dd, J = 8.8, 2.2 Hz, 1H), 3.97 (s, 3H), 2.44 (s, 3H); ^{13}C NMR (100 MHz, $CDCl_3$) δ 165.9, 157.3, 157.1, 143.1, 134.5, 134.2, 130.9, 129.5, 129.1, 128.5, 128.0, 127.6, 125.4, 121.1, 119.7, 117.4, 52.6, 17.7; HRMS (ESI-TOF) (*m/z*) calculated $C_{19}H_{14}BrN_2O_4^+$: 415.0113, found 415.0101 $[M + H]^+$.

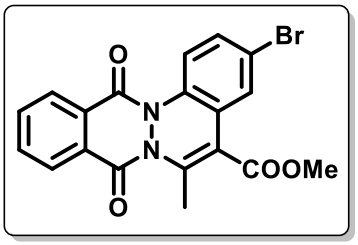

Ethyl 2-chloro-3,6-dimethyl-8,13-dioxo-8,13-dihydrophthalazino[2,3-*a*]cinnoline-5-carboxylate (57ga). Yellow solid; yield: 51 mg (75%); mp 216−217 °C; ^{1}H NMR (400 MHz, $CDCl_3$) δ 8.43 (dd, J = 7.2, 1.7 Hz, 1H), 8.35 – 8.30 (m, 1H), 7.96 – 7.86 (m, 3H), 7.18 (s, 1H), 4.43 (q, J = 7.1 Hz, 2H), 2.42 (s, 3H), 2.38 (s, 3H), 1.42 (t, J = 7.1 Hz, 3H); ^{13}C NMR (100 MHz, $CDCl_3$) δ 166.8, 157.2, 157.1, 143.9, 140.9, 134.4, 134.1, 133.8, 133.8, 129.5, 129.1, 128.5, 127.9, 126.4, 121.9, 120.0, 118.5, 61.7, 20.0, 17.6, 14.2; HRMS (ESI-TOF) (*m/z*) calculated $C_{21}H_{18}ClN_2O_4^+$: 397.0950, found 397.0946 $[M + H]^+$.

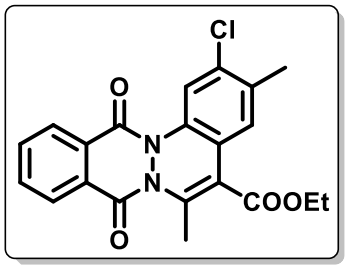

Methyl 2-chloro-3,6-dimethyl-8,13-dioxo-8,13-dihydrophthalazino[2,3-*a*]cinnoline-5-carboxylate (57gb). Yellow solid; yield: 47 mg (73%); mp 232−233 °C; ^{1}H NMR (400 MHz, $CDCl_3$) δ 8.46 – 8.41 (m, 1H), 8.36 – 8.30 (m, 1H), 7.98 – 7.86 (m, 3H), 7.16 (s, 1H), 3.96 (s, 3H), 2.41 (s, 3H), 2.38 (s, 3H); ^{13}C NMR (100 MHz, $CDCl_3$) δ 166.3, 157.2, 157.1, 141.4, 134.5, 134.1, 133.9, 133.8, 129.5, 129.1, 128.5, 127.9, 126.5, 121.8, 120.0, 118.2, 52.5, 20.0, 17.7; HRMS (ESI-TOF) (*m/z*) calculated $C_{20}H_{16}ClN_2O_4^+$: 383.0793, found 383.0803 $[M + H]^+$.

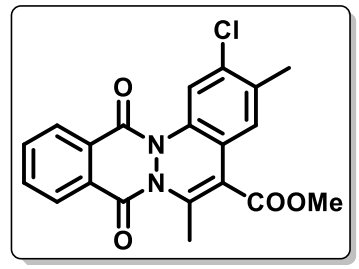

Ethyl 6,10-dimethyl-8,13-dioxo-8,13-dihydrophthalazino[2,3-*a*]cinnoline-5-carboxylate + Ethyl 6,11-dimethyl-8,13-dioxo-8,13-dihydrophthalazino[2,3-*a*]cinnoline-5-carboxylate (57ia) (1: 0.15 or 0.15:1). Yellow solid; yield: 54 mg (75%); mp 166−167 °C; ^{1}H NMR (400 MHz, $CDCl_3$) δ 8.32 (d, J = 8.0 Hz, 0.15H), 8.24 – 8.20 (m, 2H), 8.13 (s, 0.15H),

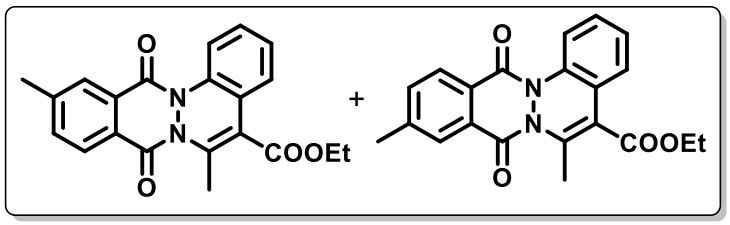

7.85 – 7.80 (m, 1.15H), 7.73 – 7.67 (m, 1.15H), 7.34 – 7.29 (m, 2.3H), 7.25 – 7.19 (m, 1.15H), 4.43 (q, *J* = 7.2 Hz, 2.3H), 2.61 (s, 3H), 2.60 (s, 0.45H), 2.43 (s, 3.45H), 1.41 (t, *J* = 7.1 Hz, 3.45H); ^{13}C NMR (100 MHz, $CDCl_3$) δ 166.1, 157.4, 157.4, 145.7, 141.0, 135.4, 135.3, 135.0, 129.6, 128.5, 128.1, 128.0, 128.0, 127.9, 126.8, 126.4, 126.2, 124.7, 123.6, 119.5, 119.4, 118.8, 61.6, 21.9, 21.9, 17.5, 17.5, 14.2; HRMS (ESI-TOF) (*m/z*) calculated $C_{21}H_{19}N_2O_4^+$: 363.1339, found 363.1343 $[M + H]^+$.

Methyl 6,10-dimethyl-8,13-dioxo-8,13-dihydrophthalazino[2,3-*a*]cinnoline-5-carboxylate + Methyl 6,11-dimethyl-8,13-dioxo-8,13-dihydrophthalazino[2,3-*a*]cinnoline-5-carboxylate (57ib) (1:0.6 or 0.6:1). Yellow solid; yield: 50 mg (72%); mp 190−191 °C; ^{1}H NMR (400 MHz, $CDCl_3$) δ 8.32 d, *J* = 8.0 Hz, 0.6H), 8.24 – 8.19 (m, 2H), 8.12 (s, 0.6H), 7.86 – 7.80 (m, 1.6H), 7.73 – 7.66 (m, 1.6H), 7.33 – 7.27 (m, 3.2H), 7.22 (m, 1.6H), 3.95 (s, 5H), 2.60 (s, 3H), 2.58 (s, 2H), 2.43 (s, 5H); ^{13}C NMR (100 MHz, $CDCl_3$) δ 166.5, 166.5, 157.4, 157.4, 145.8, 145.4, 141.7, 141.5, 135.5, 135.4, 135.3, 135.0, 129.6, 129.1, 128.5, 128.2, 128.1, 128.0, 127.9, 127.2, 126.8, 126.4, 126.3, 124.8, 123.5, 123.4, 119.5, 119.4, 118.8, 118.5, 52.3, 21.9, 21.9, 17.6, 17.6; HRMS (ESI-TOF) (*m/z*) calculated $C_{20}H_{17}N_2O_4^+$: 349.1183, found 349.1179 $[M + H]^+$.

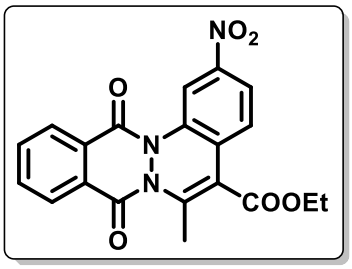

Ethyl 6-methyl-2-nitro-8,13-dioxo-8,13-dihydrophthalazino[2,3-*a*]cinnoline-5-carboxylate (57ja). Yellow solid; yield: 10 mg (15%); mp 221− 223 °C; ^{1}H NMR (400 MHz, $CDCl_3$) δ 8.70 (d, *J* = 2.3 Hz, 1H), 8.47 (dd, *J* = 7.3, 1.6 Hz, 1H), 8.38 – 8.29 (m, 1H), 8.09 (dd, *J* = 8.8, 2.3 Hz, 1H), 8.04 – 7.87 (m, 2H), 7.51 (d, *J* = 8.7 Hz, 1H), 4.45 (q, *J* = 7.1 Hz, 2H), 2.50 (s, 3H), 1.43 (t, *J* = 7.1 Hz, 3H); ^{13}C NMR (100 MHz, $CDCl_3$) δ 165.1, 157.3, 156.9, 145.4, 135.7, 134.9, 134.6, 129.6, 129.2, 129.1, 128.8, 128.2, 125.3, 121.3, 115.3, 62.0, 17.9, 14.2; HRMS (ESI-TOF) (*m/z*) calculated $C_{20}H_{16}N_3O_6^+$: 394.1034, found 394.1037 $[M + H]^+$.

Ethyl 6-methyl-3-nitro-8,13-dioxo-8,13-dihydrophthalazino[2,3-*a*]cinnoline-5-carboxylate (57la). Yellow solid; yield: 5 mg (8%); mp 156−157 °C; ^{1}H NMR (400 MHz, $CDCl_3$) δ 8.47 – 8.42 (m, 1H), 8.38 – 8.34 (m, 1H), 8.30 (d, J = 2.6 Hz, 1H), 8.15 (dd, J = 9.1, 2.6 Hz, 1H), 7.99 (s, 1H), 7.98 – 7.92 (m, 2H), 4.48 (q, J = 7.1 Hz, 2H), 2.50 (s, 3H), 1.45 (t, J = 7.1 Hz, 3H); ^{13}C NMR (100 MHz, $CDCl_3$) δ 164.9, 156.2, 155.2, 147.7, 145.2, 144.7, 134.7, 131.3, 129.2, 128.7, 128.2, 124.7, 123.2, 120.5, 120.0, 62.1, 17.8, 14.2; HRMS (ESI-TOF) (*m/z*) calculated $C_{20}H_{16}N_3O_6^+$: 394.1034, found 394.1033 $[M + H]^+$.

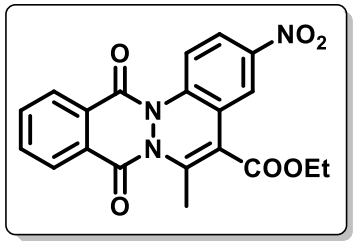

2,2-Dimethyl-2,3-dihydrobenzo[*c*]phthalazino[2,3-*a*]cinnoline-4,10,15(1*H*)-trione (57ag). Yellow solid; yield: 51 mg (68%); mp 200−202 °C; ^{1}H NMR (400 MHz, $CDCl_3$) δ 8.47 – 8.42 (m, 1H), 8.34 – 8.29 (m, 1H), 8.24 – 8.19 (m, 1H), 7.98 – 7.86 (m, 2H), 7.80 – 7.75 (m, 1H), 7.32 – 7.27 (m, 2H), 2.89 (s, 2H), 2.51 (s, 2H), 1.13 (s, 6H); ^{13}C NMR (100 MHz, $CDCl_3$) δ 195.8, 157.8, 156.9, 152.3, 135.3, 134.8, 134.0, 129.9, 128.8, 128.7, 128.1, 128.0, 127.0, 126.6, 122.3, 119.4, 117.8, 52.3, 40.8, 33.7, 28.2; HRMS (ESI-TOF) (*m/z*) calculated $C_{22}H_{19}N_2O_3^+$: 359.1390, found 359.1393 $[M + H]^+$.

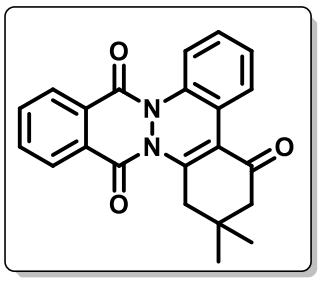

2,2,6-Trimethyl-2,3-dihydrobenzo[*c*]phthalazino[2,3-*a*]cinnoline-4,10,15(1*H*)-trione (57bg). Yellow solid; yield: 50 mg (65%); mp 223−224 °C; ^{1}H NMR (400 MHz, $CDCl_3$) δ 8.49 – 8.42 (m, 1H), 8.35 – 8.29 (m, 1H), 8.05 (d, J = 2.0 Hz, 1H), 7.98 – 7.86 (m, 2H), 7.69 (d, J = 8.4 Hz, 1H), 7.16 – 7.09 (m, 1H), 2.90 (s, 2H), 2.52 (s, 2H), 2.40 (s, 3H), 1.15 (s, 6H); ^{13}C NMR (100 MHz, $CDCl_3$) δ 195.9, 157.9, 156.8, 152.1, 136.5, 134.7, 133.9, 133.8, 130.0, 128.8, 128.7, 128.6, 128.0, 127.2, 122.1, 119.2, 117.8, 52.3, 40.8, 33.8, 28.2, 21.4; HRMS (ESI-TOF) (*m/z*) calculated $C_{23}H_{21}N_2O_3^+$: 373.1547, found 373.1547 $[M + H]^+$.

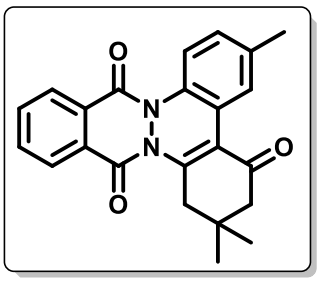

6-Fluoro-2,2-dimethyl-2,3-dihydrobenzo[*c*]phthalazino[2,3-*a*]cinnoline-4,10,15(1*H*)-trione (57cg). Yellow solid; yield: 48 mg (66%); mp 194−195 °C; ^{1}H NMR (400 MHz, $CDCl_3$) δ 8.45 (dd, J = 7.6, 1.5 Hz, 1H), 8.37 – 8.31 (m, 1H), 8.05 (dd, J = 10.3, 2.9 Hz, 1H), 8.02 – 7.90 (m, 2H), 7.77 (dd, J = 9.1, 5.1 Hz, 1H), 7.02 – 6.97 (m, 1H), 2.91 (s, 2H), 2.52 (s, 2H), 1.15 (s, 6H); ^{13}C NMR (100 MHz, $CDCl_3$) δ 195.4, 160.4 ($^{1}J_{C\text{-}F}$ = 244.1 Hz),

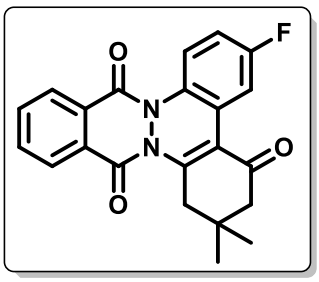

157.9, 156.8, 153.3, 135.0, 134.1, 129.7, 128.7, 128.1, 121.4, 121.3, 116.6, 115.0, 114.7, 113.9, 113.7, 52.0, 40.6, 33.7, 28.2; HRMS (ESI-TOF) (*m/z*) calculated $C_{22}H_{18}FN_2O_3^+$: 377.1296, found 377.1289 $[M + H]^+$.

Ethyl 2-(5-chloro-2-(1,4-dioxo-3,4-dihydrophthalazin-2(1*H*)-yl)phenyl)-3-oxobutanoate (E′) *(mixture of keto-enol tautomers, 2:1).* White solid; ^{1}H NMR (400 MHz, DMSO-d_6) δ 12.94 (s, 0.5H, -OH $_{\text{Enol form}}$), 11.94 (s, 1H, NH $_{\text{Keto form}}$), 11.73 (s, 0.5H, NH $_{\text{Enol form}}$), 8.28 (d, J = 7.8 Hz, 1H), 8.23 – 8.19 (m, 0.5H), 8.08 – 7.88 (m, 5H), 7.61 – 7.53 (m, 3H), 7.44 (t, J = 1.4 Hz, 0.5H), 7.38 (d, J = 2.4 Hz, 1H), 5.00 (s, 1H, $CH_{\text{Keto form}}$), 4.14 – 4.06 (m, 2H, $CH_{2\ \text{Keto form}}$), 3.95 (d, J = 7.1 Hz, 1H, -$CH_{2\ \text{Enol form}}$), 2.13 (s, 3H $Me_{\text{Keto form}}$), 2.09 (s, 1.5H $Me_{\text{Enol form}}$), 1.13 (t, J = 7.1 Hz, 3H, $CH_{3\ \text{Keto form}}$), 1.04 (t, J = 7.1 Hz, 1.5H, $CH_{3\ \text{Enol form}}$).

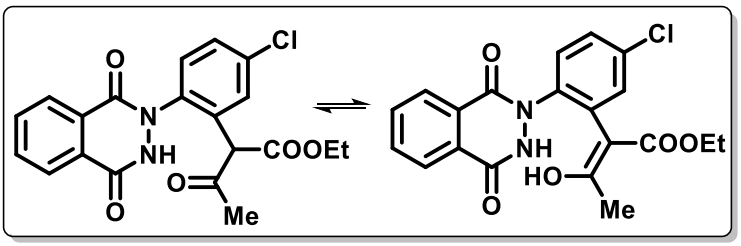

Ethyl 2-(2-(1,4-dioxo-3,4-dihydrophthalazin-2(1*H*)-yl)phenyl)-3-oxobutanoate (E) *(mixture of keto-enol tautomers).* White solid; yield: 108 mg (69%); ^{1}H NMR (400 MHz, DMSO-d_6) δ 12.95 (s, 0.33H, -$OH_{\text{Enol form}}$), 8.29 (d, J = 7.8 Hz, 1H), 8.22 (dd, J = 7.5, 1.2 Hz, 0.39H), 8.06 (d, J = 7.4 Hz, 1H), 8.02 (dd, J = 7.1, 1.4 Hz, 1H), 7.98 – 7.93 (m, 2H), 7.89 (ddd, J = 7.8, 6.9, 1.7 Hz, 1H), 7.54 – 7.49 (m, 4H), 7.49 – 7.42 (m, 1H), 7.39 – 7.36 (m, 1H), 7.34 – 7.31 (m, 0.4H), 4.89 (s, 1H, $CH_{\text{Keto form}}$), 4.10 – 4.07 (m, 1H, $CH_{2\ \text{Keto form}}$), 4.07 – 4.03 (m, 1H, $CH_{2\ \text{Keto form}}$), 3.97 – 3.90 (m, 1H, -$CH_{2\ \text{Enol form}}$), 2.08 (s, 3H, $Me_{\text{Keto form}}$), 1.24 (s, 1H, $Me_{\text{Enol form}}$), 1.11 (t, J = 7.1 Hz, 3H, $CH_{3\ \text{Keto form}}$), 1.03 (t, J = 7.1 Hz, 1H, $CH_{3\ \text{Enol form}}$); HRMS (ESI-TOF) (*m/z*) calculated $C_{20}H_{19}N_2O_5^+$: 367.1288, found 367.1283 $[M+H]^+$.

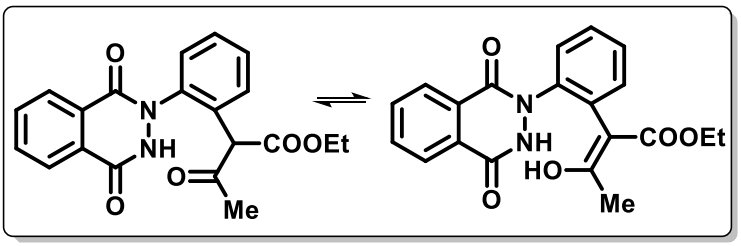

1.5 Single Crystal X-ray Diffraction Studies

In each case, a suitable crystal was mounted in a nylon loop attached to a goniometer head for initial crystal evaluation. Data were collected on a Kappa APEX II diffractometer equipped with a CCD detector (with the crystal-to-detector distance fixed at 60 mm) and sealed-tube monochromated MoKα radiation using the program APEX2.[112] Using the program SAINT[112] data was integrated, reflection profiles were fitted, and values of F^2 and $\sigma(F^2)$ for each reflection were

obtained. Lorentz and polarization effects were applied to the data. The subroutine XPREP[112] was used for the determination of space group, application of an absorption correction (SADABS),[112] merging of data, and generation of files necessary for solution and refinement. The crystal structures were solved by the direct method using the SHELXS program of the SHELXTL package and refined by full-matrix least square methods with SHELXL-2014.[113] Several full-matrix least-squares/difference Fourier cycles were performed for the convergence of refinement. All non-hydrogen atoms were refined with anisotropic displacement parameters. All hydrogen atoms were placed in ideal positions and refined as riding atoms with individual isotropic displacement parameters. All figures were drawn using MERCURY V 3.0[114].

1.5.1 Crystal data for 56ca (CCDC No. 1851226). $C_{18}H_{13}FN_2O_5$, M_r = 356.30, monoclinic, space group $P2_1/c$, a = 8.4553(15) Å, b = 21.077(4) Å, c = 8.8999(15) Å, α = 90°, β = 96.762(3)°, γ = 90°, V = 6345.7(4) Å^3, Z = 4, T = 296(2) K, D_{calc} = 1.503 g/cm^3; Full matrix least-square on F^2; R_1 = 0.0541, wR_2 = 0.1527 for 2138 observed reflections [I > 2σ(I)] and R_1 = 0.0738, wR_2 = 0.1775 for all 2784 reflections; GOF = 1.087.

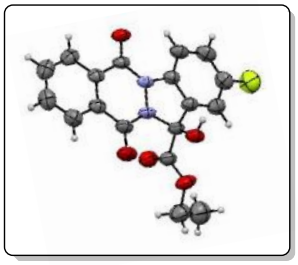

1.5.2 Crystal data for 57ba (CCDC No. 1851227). $C_{21}H_{18}N_2O_4$, M_r = 362.37, triclinic, space group $P\bar{1}$, a = 8.797(12) Å, b = 9.714(15) Å, c = 11.666(18) Å, α = 112.83(2)°, β = 99.88(2)°, γ = 102.02(2)°, V = 863(2) Å^3, Z = 2, D_{calc} = 1.395 g/cm^3, T = 296(2) K; Full matrix least-square on F^2; R_1 = 0.0446, wR_2 = 0.1323 for 2504 observed reflections [I > 2 σ(I)] and R_1 = 0.0553, wR_2 = 0.1418 for all 3099 reflections; GOF = 1.050.

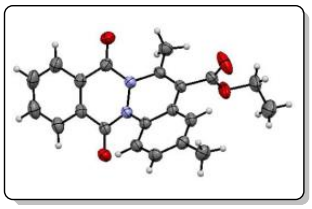

1.6 References

(1) Knölker, H.-J.; Reddy, K. R. *Chemical Reviews* **2002**, *102*, 4303-4428.

(2) Harvey, R. G. *Polycyclic Aromatic Hydrocarbons: Chemistry and Carcinogenicity*; CUP Archive, **1991**.

(3) Anthony, J. E. *Chemical Reviews* **2006**, *106*, 5028-5048.

(4) De Coen, L. M.; Heugebaert, T. S.; Garcia, D.; Stevens, C. V. *Chemical Reviews* **2016**, *116*, 80-139.

(5) Itoh, T. *Chemical Reviews* **2012**, *112*, 4541-4568.

(6) Romero, N. A.; Nicewicz, D. A. *Chemical Reviews* **2016**, *116*, 10075-10166.

(7) de Meijere, A.; Diederich, F.; *Metal-Catalyzed Cross-Coupling Reactions*, **2004**.

(8) Bolm, C.; Beller, M. *Transition Metals for Organic Synthesis*; Wiley-VCH: Weinheim, **2004**; Vol. 1.

(9) Heck, R. F.; Nolley Jr, J. *The Journal of Organic Chemistry* **1972**, *37*, 2320-2322.

(10) Miyaura, N.; Buchwald, S. L. *Cross-Coupling Reactions: A Practical Guide*; Springer, **2002**; Vol. 219.

(11) Hapke, M.; Brandt, L.; Lützen, A. *Chemical Society Reviews* **2008**, *37*, 2782-2797.

(12) Miyaura, N.; Suzuki, A. *Chemical Reviews* **1995**, *95*, 2457-2483.

(13) Suzuki, A. *Angewandte Chemie International Edition* **2011**, *50*, 6722-6737.

(14) Gandeepan, P.; Müller, T.; Zell, D.; Cera, G.; Warratz, S.; Ackermann, L. *Chemical Reviews* **2018**, *119*, 2192-2452.

(15) Ritleng, V.; Sirlin, C.; Pfeffer, M. *Chemical Reviews* **2002**, *102*, 1731-1770.

(16) Zhang, M.; Zhang, Y.; Jie, X.; Zhao, H.; Li, G.; Su, W. *Organic Chemistry Frontiers* **2014**, *1*, 843-895.

(17) Rouquet, G.; Chatani, N. *Angewandte Chemie International Edition* **2013**, *52*, 11726-11743.

(18) Das, R.; Kumar, G. S.; Kapur, M. *European Journal of Organic Chemistry* **2017**, *2017*, 5439-5459.

(19) Carvalho, R. L.; Dias, G. G.; Pereira, C. L.; Ghosh, P.; Maiti, D.; Silva Júnior, E. N. d. *Journal of the Brazilian Chemical Society* **2021**, *32*, 917-952.

(20) Gallego, D.; Baquero, E. A. *Open Chemistry* **2018**, *16*, 1001-1058.

(21) Alberico, D.; Scott, M. E.; Lautens, M. *Chemical Reviews* **2007**, *107*, 174-238.

(22) Liu, C.; Yuan, J.; Gao, M.; Tang, S.; Li, W.; Shi, R.; Lei, A. *Chemical Reviews* **2015**, *115*, 12138-12204.

(23) Yang, Y.; Lan, J.; You, J. *Chemical Reviews* **2017**, *117*, 8787-8863.

(24) Ackermann, L.; Vicente, R.; Kapdi, A. R. *Angewandte Chemie International Edition* **2009**, *48*, 9792-9826.

(25) Huang, H.; Ji, X.; Wu, W.; Jiang, H. *Chemical Society Reviews* **2015**, *44*, 1155-1171.

(26) Murai, S.; Kakiuchi, F.; Sekine, S.; Tanaka, Y.; Kamatani, A.; Sonoda, M.; Chatani, N. *Nature* **1993**, *366*, 529-531.

(27) Rej, S.; Das, A.; Chatani, N. *Coordination Chemistry Reviews* **2021**, *431*, 213683.

(28) Rej, S.; Chatani, N. *Angewandte Chemie International Edition* **2019**, *58*, 8304-8329.

(29) Chen, Z.; Wang, B.; Zhang, J.; Yu, W.; Liu, Z.; Zhang, Y. *Organic Chemistry Frontiers* **2015**, *2*, 1107-1295.

(30) Manan, R. S.; Zhao, P. *Nature communications* **2016**, *7*, 1-11.

(31) Sun, T.; Zhang, Y.; Qiu, B.; Wang, Y.; Qin, Y.; Dong, G.; Xu, T. *Angewandte Chemie* **2018**, *130*, 2909-2913.

(32) Wu, X.; Xiong, H.; Sun, S.; Cheng, J. *Organic Letters* **2018**, *20*, 1396-1399.

(33) Li, S.-S.; Qin, L.; Dong, L. *Organic & Biomolecular Chemistry* **2016**, *14*, 4554-4570.

(34) Yang, Z.; Yu, J.-T.; Pan, C. *Organic & Biomolecular Chemistry* **2021**, *19*, 8442-8465.

(35) Thoke, M. B.; Kang, Q. *Synthesis* **2019**, *51*, 2585-2631.

(36) Shibata, K.; Chatani, N. *Organic Letters* **2014**, *16*, 5148-5151.

(37) Li, J.; Liu, Y.; Tang, W.; Xue, D.; Li, C.; Xiao, J.; Wang, C. *Chemistry–A European Journal* **2017**, *23*, 14445-14449.

(38) Bouffard, J.; Itami, K. *C-H Activation* **2009**, 231-280.

(39) Ding, Q.; Zhou, X.; Pu, S.; Cao, B. *Tetrahedron* **2015**, *71*, 2376-2381.

(40) Stemmler, R. T.; Bolm, C. *Advanced Synthesis & Catalysis* **2007**, *349*, 1185-1198.

(41) Zhu, W.; Gunnoe, T. B. *Accounts of Chemical Research* **2020**, *53*, 920-936.

(42) Samanta, S.; Mondal, S.; Ghosh, D.; Hajra, A. *Organic Letters* **2019**, *21*, 4905-4909.

(43) Wang, W.; Wu, J.; Kuniyil, R.; Kopp, A.; Lima, R. N.; Ackermann, L. *Chem* **2020**, *6*, 3428-3439.

(44) Colby, D. A.; Tsai, A. S.; Bergman, R. G.; Ellman, J. A. *Accounts of Chemical Research* **2012**, *45*, 814-825.

(45) Van Leeuwen, P. W.; Claver, C. *Rhodium Catalyzed Hydroformylation*; Springer Science & Business Media, **2002**; Vol. 22.

(46) Tang, W.; Capacci, A. G.; White, A.; Ma, S.; Rodriguez, S.; Qu, B.; Savoie, J.; Patel, N. D.; Wei, X.; Haddad, N. *Organic Letters* **2010**, *12*, 1104-1107.

(47) Zhang, J.; Liu, C.; Wang, X.; Chen, J.; Zhang, Z.; Zhang, W. *Chemical Communications* **2018**, *54*, 6024-6027.

(48) Wang, H.; Yi, X.; Cui, Y.; Chen, W. *Organic & Biomolecular Chemistry* **2018**, *16*, 8191-8195.

(49) Tsuji, J. *Modern Rhodium-Catalyzed Organic Reactions*; John Wiley & Sons, **2005**.

(50) Zhu, H.; Zhao, S.; Zhou, Y.; Li, C.; Liu, H. *Catalysts* **2020**, *10*, 1253.

(51) Manikandan, R.; Jeganmohan, M. *Organic Letters* **2014**, *16*, 912-915.

(52) Ackermann, L. *Accounts of Chemical Research* **2014**, *47*, 281-295.

(53) Ackermann, L.; Novak, P.; Vicente, R.; Hofmann, N. *Angewandte Chemie International Edition* **2009**, *48*, 6045-6048.

(54) Chen, C.; Zhang, Y.; Hong, S. H. *The Journal of Organic Chemistry* **2011**, *76*, 10005-10010.

(55) De, S. K. *Tetrahedron Letters* **2004**, *45*, 2919-2922.

(56) Liu, W.; Ackermann, L. *Organic Letters* **2013**, *15*, 3484-3486.

(57) Barlow, H. L.; Teskey, C. J.; Greaney, M. F. *Organic Letters* **2017**, *19*, 6662-6665.

(58) Murahashi, S.-I.; Komiya, N.; Terai, H.; Nakae, T. *Journal of the American Chemical Society* **2003**, *125*, 15312-15313.

(59) Alizadeh, A.; Firuzyar, T.; Mikaeili, A. *Journal of Heterocyclic Chemistry* **2013**, *50*, 676-679.

(60) Zhang, J.; Kang, L. J.; Parker, T. C.; Blakey, S. B.; Luscombe, C. K.; Marder, S. R. *Molecules* **2018**, *23*, 922.

(61) Gilchrist, T. L. *Heterocyclic chemistry*; Prentice Hall, **1997**.

(62) Asif, M. *Current Medicinal Chemistry* **2012**, *19*, 2984-2991.

(63) Taek Han, Y.; Jung, J.-W.; Kim, N.-J. *Current Organic Chemistry* **2017**, *21*, 1265-1291.

(64) Khan, I.; Zaib, S.; Batool, S.; Abbas, N.; Ashraf, Z.; Iqbal, J.; Saeed, A. *Bioorganic & Medicinal Chemistry* **2016**, *24*, 2361-2381.

(65) Khan, I.; Ibrar, A.; Ahmed, W.; Saeed, A. *European Journal of Medicinal Chemistry* **2015**, *90*, 124-169.

(66) Lewgowd, W.; Stanczak, A. *Archiv der Pharmazie: An International Journal Pharmaceutical and Medicinal Chemistry* **2007**, *340*, 65-80.

(67) Pereira, J. A.; Pessoa, A. M.; Cordeiro, M. N. D.; Fernandes, R.; Prudêncio, C.; Noronha, J. P.; Vieira, M. *European Journal of Medicinal Chemistry* **2015**, *97*, 664-672.

(68) Tristan-Manzano, M.; Guirado, A.; Martínez-Esparza, M.; Galvez, J.; Garcia-Penarrubia, P.; J Ruiz-Alcaraz, A. *Current Medicinal Chemistry* **2015**, *22*, 3075-3108.

(69) Sangshetti, J.; Pathan, S. K.; Patil, R.; Ansari, S. A.; Chhajed, S.; Arote, R.; Shinde, D. B. *Bioorganic & Medicinal Chemistry* **2019**, *27*, 3979-3997.

(70) Xue, J.; Xin, L.; Hou, J.; Duan, L.; Wang, R.; Wei, Y.; Qiao, J. *Chemistry of Materials* **2017**, *29*, 4775-4782.

(71) Cho, J. Y.; Kwon, H. C.; Williams, P. G.; Jensen, P. R.; Fenical, W. *Organic Letters* **2006**, *8*, 2471-2474.

(72) Eldehna, W. M.; Ibrahim, H. S.; Abdel-Aziz, H. A.; Farrag, N. N.; Youssef, M. M. *European Journal of Medicinal Chemistry* **2015**, *89*, 549-560.

(73) Eldehna, W. M.; Abou-Seri, S. M.; El Kerdawy, A. M.; Ayyad, R. R.; Hamdy, A. M.; Ghabbour, H. A.; Ali, M. M.; Abou El Ella, D. A. *European Journal of Medicinal Chemistry* **2016**, *113*, 50-62.

(74) El-Helby, A. G. A.; Ayyad, R. R.; Sakr, H.; El-Adl, K.; Ali, M. M.; Khedr, F. *Archiv der Pharmazie* **2017**, *350*, 1700240.

(75) Russell, M. G.; Carling, R. W.; Atack, J. R.; Bromidge, F. A.; Cook, S. M.; Hunt, P.; Isted, C.; Lucas, M.; McKernan, R. M.; Mitchinson, A. *Journal of Medicinal Chemistry* **2005**, *48*, 1367-1383.

(76) El-Helby, A. G. A.; Ayyad, R. R.; Sakr, H. M.; Abdelrahim, A. S.; El-Adl, K.; Sherbiny, F. S.; Eissa, I. H.; Khalifa, M. M. *Journal of Molecular Structure* **2017**, *1130*, 333-351.

(77) Sun, X.-Y.; Wei, C.-X.; Deng, X.-Q.; Sun, Z.-G.; Quan, Z.-S. *Arzneimittelforschung* **2010**, *60*, 289-292.

(78) Bakale, R. P.; Naik, G. N.; Mangannavar, C. V.; Muchchandi, I. S.; Shcherbakov, I.; Frampton, C.; Gudasi, K. B. *European Journal of Medicinal Chemistry* **2014**, *73*, 38-45.

(79) Hegab, M. I.; Taleb, N. A. A.; Hasabelnaby, S. M.; Goudah, A. *European Journal of Medicinal Chemistry* **2010**, *45*, 1267-1277.

(80) Razvi, M.; Ramalingam, T.; Sattur, P. *Indian Journal of Chemistry* **1989**, *28B*, 987-989.

(81) Razvi, M.; Ramalingam, T.; Sattur, P. *Indian Journal of Chemistry* **1989**, *28B*, 695-697.

(82) NOMOTO, Y.; OBASE, H.; Takai, H.; Teranishi, M.; Nakamura, J.; Kubo, K. *Chemical and Pharmaceutical Bulletin* **1990**, *38*, 2179-2183.

(83) Khalil, A.; Berghot, M.; Gouda, M. *European Journal of Medicinal Chemistry* **2009**, *44*, 4448-4454.

(84) Ibrahim, H. S.; Eldehna, W. M.; Abdel-Aziz, H. A.; Elaasser, M. M.; Abdel-Aziz, M. M. *European Journal of Medicinal Chemistry* **2014**, *85*, 480-486.

(85) Sridhara, A. M.; Reddy, K. R. V.; Keshavayya, J.; Goud, P. S. K.; Somashekar, B. C.; Bose, P.; Peethambar, S. K.; Gaddam, S. K. *European Journal of Medicinal Chemistry* **2010**, *45*, 4983-4989.

(86) Wu, X.; Ji, H. *The Journal of Organic Chemistry* **2018**, *83*, 4650-4656.

(87) Gholamhosseyni, M.; Kianmehr, E. *Organic & Biomolecular Chemistry* **2018**, *16*, 5973-5978.

(88) Kim, K.; Han, S. H.; Jeoung, D.; Ghosh, P.; Kim, S.; Kim, S. J.; Ku, J.-M.; Mishra, N. K.; Kim, I. S. *The Journal of Organic Chemistry* **2020**, *85*, 2520-2531.

(89) Yin, C.; Zhong, T.; Zheng, X.; Li, L.; Zhou, J.; Yu, C. *Organic & Biomolecular Chemistry* **2021**, *19*, 7701-7705.

(90) Zhou, J.; Yin, C.; Zhong, T.; Zheng, X.; Yi, X.; Chen, J.; Yu, C. *Organic Chemistry Frontiers* **2021**, *8*, 5024-5031.

(91) Ford, A.; Miel, H.; Ring, A.; Slattery, C. N.; Maguire, A. R.; McKervey, M. A. *Chemical Reviews* **2015**, *115*, 9981-10080.

(92) Xia, Y.; Qiu, D.; Wang, J. *Chemical Reviews* **2017**, *117*, 13810-13889.

(93) Jha, N.; Khot, N. P.; Kapur, M. *The Chemical Record* **2021**, *21*, 4088-4122.

(94) Chan, W.-W.; Lo, S.-F.; Zhou, Z.; Yu, W.-Y. *Journal of the American Chemical Society* **2012**, *134*, 13565-13568.

(95) Dong, Y.; Chen, J.; Xu, H. *Chemical Communications* **2019**, *55*, 2027-2030.

(96) Tang, Z.; Mai, S.; Zhou, Y.; Song, Q. *Organic Chemistry Frontiers* **2018**, *5*, 2583-2587.

(97) Jiao, L.-Y.; Ning, Z.-H.; Yin, X.-M.; Hong, Q.; Liu, S.; Ma, X.-X. *Catalysis Communications* **2021**, *151*, 106278.

(98) Zhang, S.-S.; Jiang, C.-Y.; Wu, J.-Q.; Liu, X.-G.; Li, Q.; Huang, Z.-S.; Li, D.; Wang, H. *Chemical Communications* **2015**, *51*, 10240-10243.

(99) Ghosh, B.; Biswas, A.; Chakraborty, S.; Samanta, R. *Chemistry–An Asian Journal* **2018**, *13*, 2388-2392.

(100) Ghosh, B.; Samanta, R. *Chemical Communications* **2019**, *55*, 6886-6889.

(101) Yanagawa, M.; Harada, S.; Hirose, S.; Nemoto, T. *Advanced Synthesis & Catalysis* **2021**, *363*, 2189-2198.

(102) Li, B.; Zhang, B.; Zhang, X.; Fan, X. *Chemical Communications* **2017**, *53*, 1297-1300.

(103) Halskov, K. S.; Witten, M. R.; Hoang, G. L.; Mercado, B. Q.; Ellman, J. A. *Organic Letters* **2018**, *20*, 2464-2467.

(104) Ning, Y.; He, X.; Zuo, Y.; Wang, J.; Tang, Q.; Xie, M.; Li, R.; Shang, Y. *Organic & Biomolecular Chemistry* **2020**, *18*, 2893-2901.

(105) Song, C.; Yang, C.; Zhang, F.; Wang, J.; Zhu, J. *Organic Letters* **2016**, *18*, 4510-4513.

(106) Mahesha, C. K.; Agarwal, D. S.; Karishma, P.; Markad, D.; Mandal, S. K.; Sakhuja, R. *Organic & Biomolecular Chemistry* **2018**, *16*, 8585-8595.

(107) Su, L.; Yu, Z.; Ren, P.; Luo, Z.; Hou, W.; Xu, H. *Organic & Biomolecular Chemistry* **2018**, *16*, 7236-7244.

(108) Borah, G.; Patel, P. *Organic & Biomolecular Chemistry* **2019**, *17*, 2554-2563.

(109) Karishma, P.; Mahesha, C. K.; Agarwal, D. S.; Mandal, S. K.; Sakhuja, R. *The Journal of Organic Chemistry* **2018**, *83*, 11661-11673.

(110) Poli, D.; Catarzi, D.; Colotta, V.; Varano, F.; Filacchioni, G.; Daniele, S.; Trincavelli, L.; Martini, C.; Paoletta, S.; Moro, S. *Journal of Medicinal Chemistry* **2011**, *54*, 2102-2113.

(111) Presset, M.; Mailhol, D.; Coquerel, Y.; Rodriguez, J. *Synthesis* **2011**, *2011*, 2549-2552.

(112) *APEX2, SADABS and SAINT*; Bruker AXS inc: Madison, WI, USA, **2008**.

(113) Sheldrick, G. M. *SHELXTL* Version 2014/7. *https://shelx.uni-ac.gwdg.de/SHELX/index.php.*

(114) Macrae, C. F.; Bruno, I. J.; Chisholm, J. A.; Edgington, P. R.; McCabe, P.; Pidcock, E.; Rodriguez-Monge, L.; Taylor, R.; Streek, J.; Wood, P. A. *Journal of Applied Crystallography* **2008**, *41*, 466-470.

CHAPTER 2

Rhodium-Catalyzed Annulation of *N*-Aryl-2,3-dihydrophthalazine-1,4-diones with Nitroolefins

2.1 Introduction

Convergent synthetic strategies involving hybridization of two or more privileged heterocyclic moieties at the expense of transition-metal-catalyzed C-C/C-N annulations have witnessed remarkable progresses.[1-7] This has particularly become popular with the successful application of diversified directing groups such as *N*-heteroarenes, hydroxyl, amines, aldehydes, ketones, carboxylic acids, esters, imines, amides/thioamides, carbamates, nitriles, urea, oximes, hydrazines/hydrazones, sulfones and phosphine oxides/sulfides, enabling chelation-assisted selective C(sp^2)-H functionalization in a one pot-manner.[8-15] In this expedition, novel strategies for the synthesis of cinnolines have received prime interest due to the prevalence of cinnoline and cinnolone-fused heterocycles in several pharmacological active molecules[16,17] displaying anti-proliferative,[18] antibacterial,[19-22] antifungal,[23] anti-inflammatory,[24] anticancer[25-27] activities, and also found to act as *n*-channel semiconducting materials in organic photovoltaic cells[28] (Figure 2.1.1).

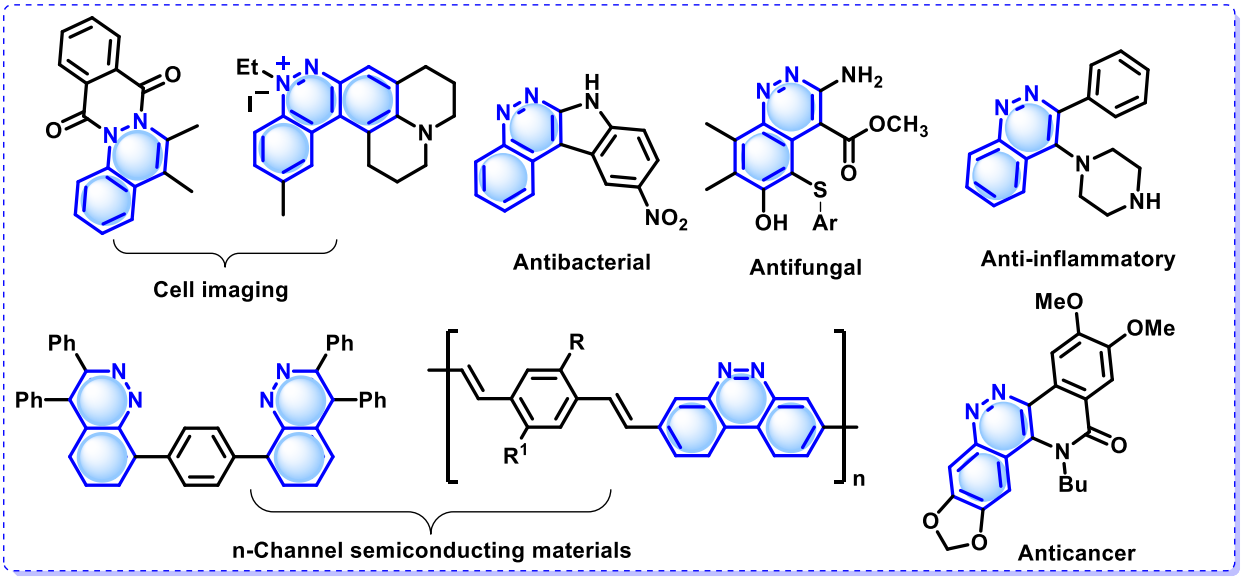

Figure 2.1.1 Selective examples of biologically active fused and functionalized cinnolines

In particular, the directing group potential of phthalazine-1,4-diones have been successfully explored in recent times for preparing functionally decorated fused-phthalazine-diones using variable coupling partners under Pd^{II}, Ir^{I}, Ru^{II} and Rh^{III} catalysis.[29] Moreover, focused advancements have been noticed towards the synthesis of phthalazino-fused cinnolines in recent years *via* C-H activation approach.

Along these lines, in 2016, Gandhi *et al.* disclosed a Ru(II)-catalyzed deoxygenation-oxidative annulation approach for the synthesis of phthalazino[2,3-*a*]cinnolines (**3**) from propargyl alcohols (**2**) and *N*-phenyl-2,3-dihydrophthalazine-1,4-diones (**1**) using $Cu(OAc)_2$ as an external oxidant. Excellent yields of tetracyclic fused-cinnolines were obtained by coupling diversely decorated substrates possessing electron-releasing and withdrawing substituents in acetic acid (Scheme 2.1.1).[30]

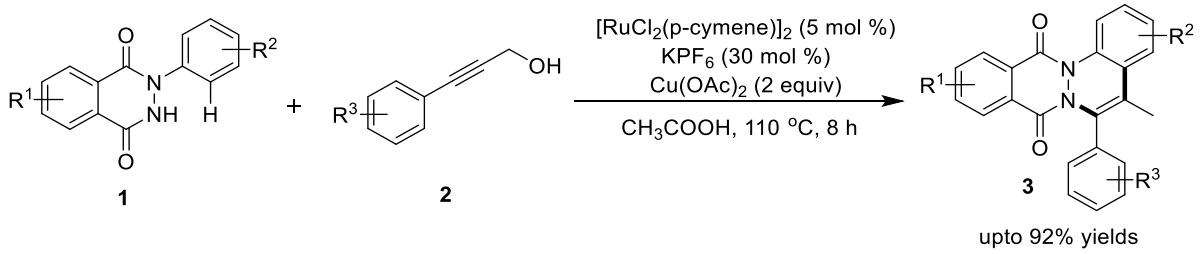

Scheme 2.1.1 Ruthenium-catalyzed annulation of *N*-aryl-2,3-dihydrophthalazine-1,4-diones (**1**) with propargyl alcohols (**2**)

Later, Perumal and coworkers reported Rh(III)-catalyzed dehydrogenative C-H/N-H functionalization to prepare substituted phthalazino[2,3-*a*]cinnolines (**5**) by the annulations of *N*-aryl-2,3-dihydrophthalazine-1,4-diones (**1**) and internal alkynes (**4**). This transformation was performed in presence of $[Cp^*RhCl_2]_2/AgSbF_6/Cu(OAc)_2$ catalytic system. Impressively, the synthesized compounds displayed good fluorescence properties in solid and aggregation states, thereby exhibiting applicability in cell imaging of various cancer cell lines (Scheme 2.1.2).[31]

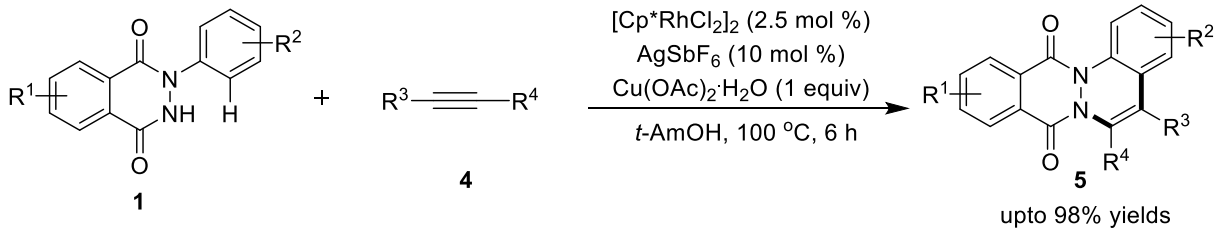

Scheme 2.1.2 Rhodium-catalyzed annulation of *N*-aryl-2,3-dihydrophthalazine-1,4-diones (**1**) with internal alkynes (**4**)

In 2018, Shang and coauthors accomplished the synthesis of phthalazino[2,3-*a*]cinnoline-8,13-diones (**7**) *via* Ir(III)-catalyzed C-H bond activation and annulation of *N*-aryl-2,3-dihydrophthalazine-1,4-diones (**1**) with cyclic 2-diazo-1,3-diketones (**6**) in DCE solvent

under inert atmosphere. Variedly decorated substrates tolerated the reaction conditions affording an array of pentacyclic fused-cinnolines in excellent yields (Scheme 2.1.3).[32]

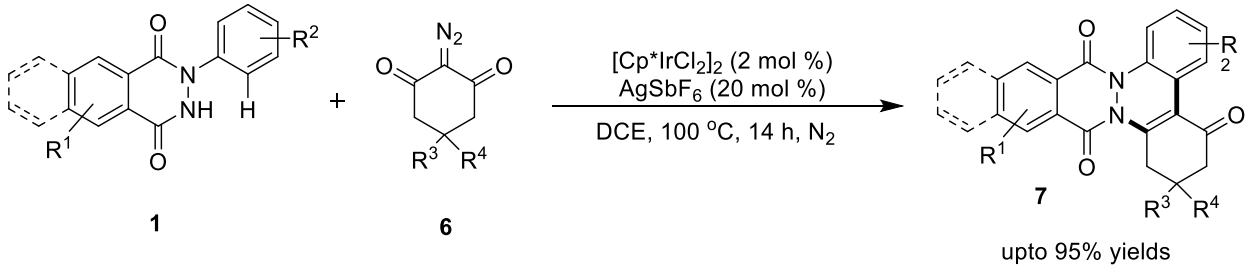

Scheme 2.1.3 Iridium-catalyzed annulation of *N*-aryl-2,3-dihydrophthalazine-1,4-diones (**1**) with cyclic 2-diazo-1,3-diketones (**6**)

In Strikingly contrast, nitroolefins are valued electrophilic synthons that have been extensively explored as Michael acceptors (Scheme 2.1.4).[33] Some of the examples includes: (a) L-proline-catalyzed addition of ketones (**9**) to nirostyrenes (**8**) producing *γ*-nitro ketones (**10**), (b) (*S*)-2-(morpholinomethyl)pyrrolidine- catalyzed enantio- and diastereoselective addition of aldehydes (**11**) to nitrolefins (**8**) yielding *γ*-nitro aldehydes (**12**), (c) 1,4-addition of formaldehyde dimethylhydrazone (**15**) to nitrolefins (**8**) delivering dimethyl-*β*-(3-nitropropylidene)hydrazine (**14**), (d) diastereoselective Michael addition of lithiated enantiopure sulfonates (**15**) with nitrolefins (**8**) using 1,2:5,6-di-*O*-isopropylidene-*α*-D-allofuranose as a chiral auxiliary to furnish *γ*-nitro sulfonates (**16**), and (e) 1,4-addition of enantiopure cyclohexanone enanimes (**17**) to nitroalkenes (**8)** to produce corresponding Michael adducts (**18**).

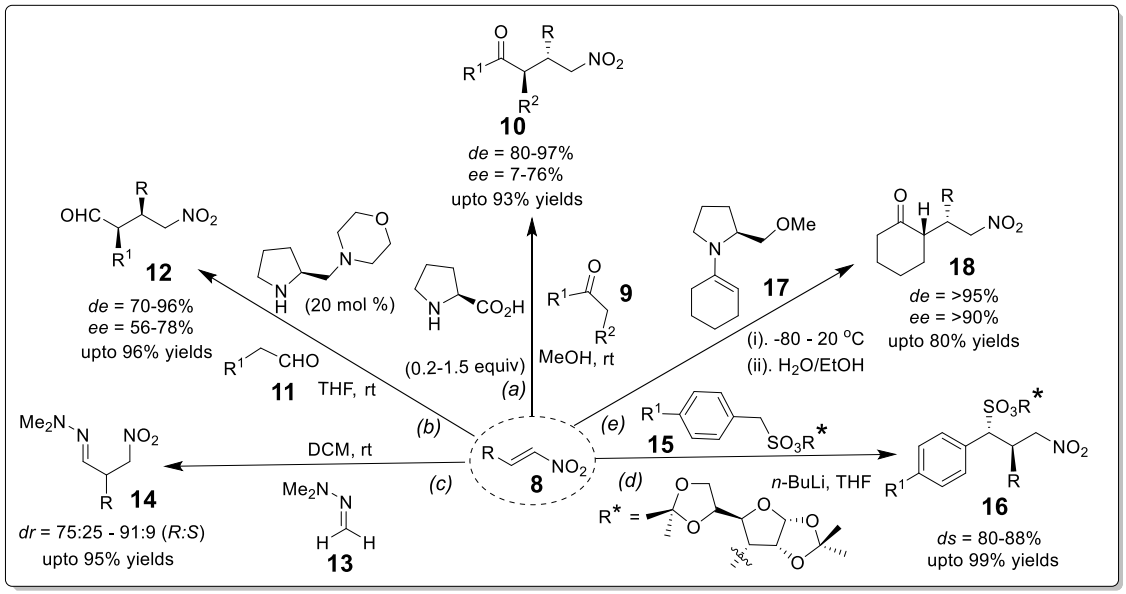

Scheme 2.1.4 Selective exemplification of nitroolefins as Michael acceptors

Furthermore, nitroolefins have also served as valued dienophiles in diversified cycloaddition reactions (Scheme 2.1.5).[34-41] Selective examples under this category includes: (a) formal [3+2] cycloaddition of 1,2 dicarbonyl compounds (or 2-ketophosphonate esters) (**19**) with *β*-halo-*β*-nitrolefins (**8**) to generate trisubstituted 2-carbonylfurans (or 2-phosphorylfurans) (**20**), (b) cycloaddition of isatin (**21**) and *N*-methylcarbamic acid (**22**) with nitroolefins (**8**) to give 3-spiropyrrolidines (**23**), (c) [3+2] cycloaddition of nitroolefins (**8**) with dipoles generated from sarcosine (**24**) and paraformaldehyde producing *N*-methylpyrrolidines (**25**), (d) 1,3-dipolar cycloaddition of diethyl 1-diazo-2-oxopropylphosphonate (**26**) to nitroalkenes (**8**) furnishing phosphonylpyrazoles (**27**), and (e) 1,3-dipolar cycloaddition reaction of imines (**28**) with nitroalkenes (**8**) affording pyrrolidine adducts (**29**).

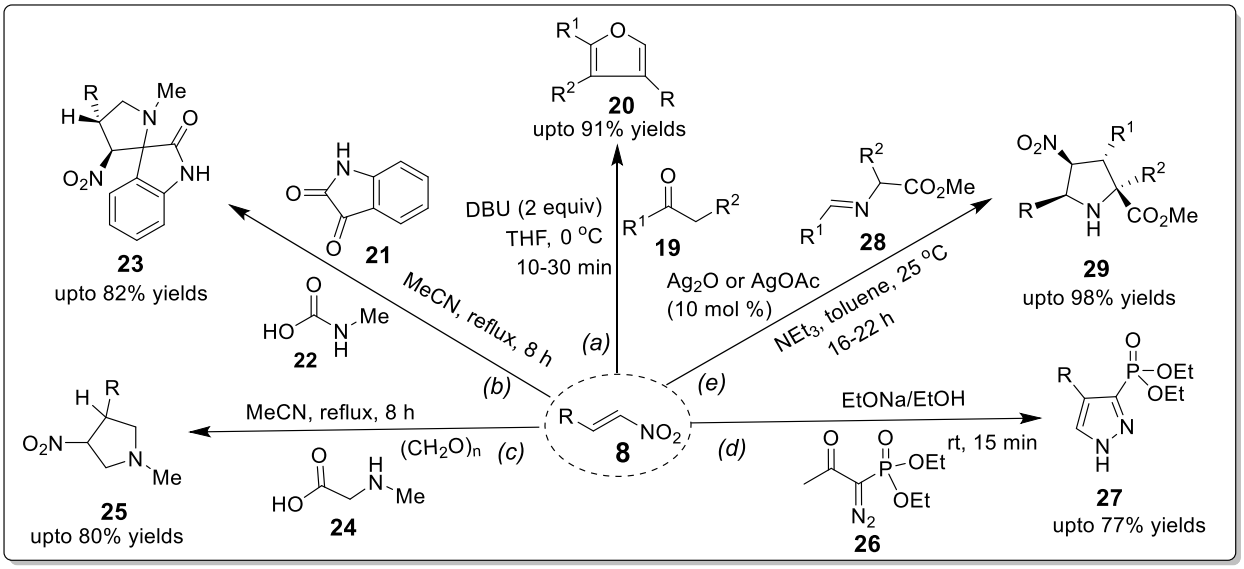

Scheme 2.1.5 Selective exemplification of nitroolefins in cycloaddition reactions

In disparity, the use of nitroolefins in transition-metal-catalyzed C-H functionalization has been explored only to a limited extent. For example, Ellman *et al.* reported a Rh(III)-catalyzed strategy for the addition of aryl and alkenyl C(sp^2)-H bonds (substrates: **30**) to niroalkenes (**8**) with the aid of appropriate directing groups. The developed method has the advantage of wide scope and functional group tolerability (Scheme 2.1.6).[42]

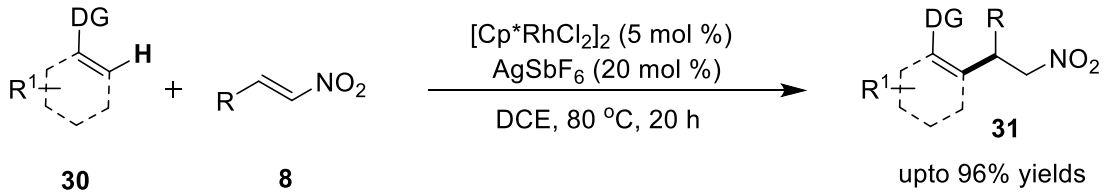

Scheme 2.1.6 Rhodium-catalyzed addition of aryl and alkenyl C(sp^2)-H bonds (substrates: **30**) to niroalkenes (**8**)

Chang, Li and coworkers in 2017, developed a simple and sustainable synthesis of nitro-functionalized indenes (**33**) under Rh(III)-catalyzed conditions through the annulation of arylnitrones (**32**) with nitroolefins (**8**). A variety of nitro-substituted indenes were synthesized in high yields *via* a sequential process involving C-H activation, migratory insertion of the olefin, protonolysis, followed by intramolecular Henry-type reaction (Scheme 2.1.7).[43]

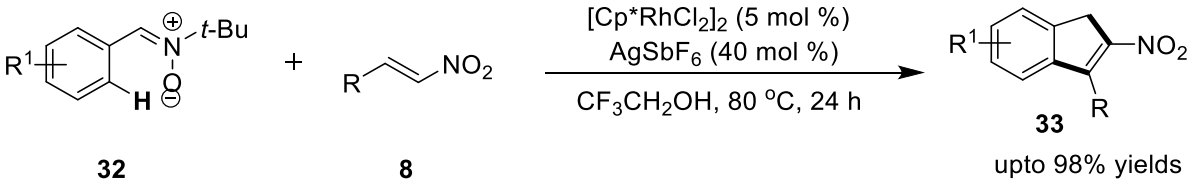

Scheme 2.1.7 Rhodium-catalyzed annulation of arylnitrones (**32**) with nitroolefins (**8**)

Ellman and Ward's group obtained 4-substituted isoquinolones and 2-pyridones (**35**) when *N*-methoxyamides (**34**) were allowed to react with nitroalkenes (**8**) under Rh(III)-catalyzed conditions in HFIP. This transformation was believed to proceed through a sequential concerted metalation and deprotonation process, generating rhodacyclic intermediate that in coordination with nitroalkenes provides rhodium nitronate, which undergoes $Cu(OAc)_2$ mediated cyclization and denitration provided isoquinolones (**35**) (Scheme 2.1.8).[44]

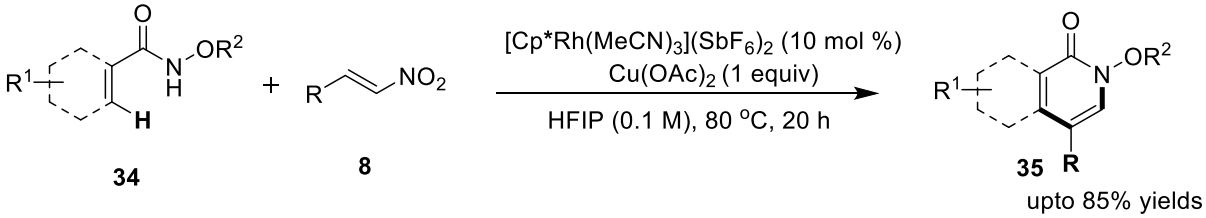

Scheme 2.1.8 Rhodium-catalyzed annulations of *N*-methoxyamides (**37**) with nitroalkenes (**8**)

Likewise, Zhang's group reported a facile and expeditious protocol for a Rh(III)-catalyzed annulation of benzimidates (**36**) and nitroalkenes (**8**) to furnish difunctionalized indenes (**37**) in moderate-to-good yields under ambient atmosphere (Scheme 2.1.9).[45]

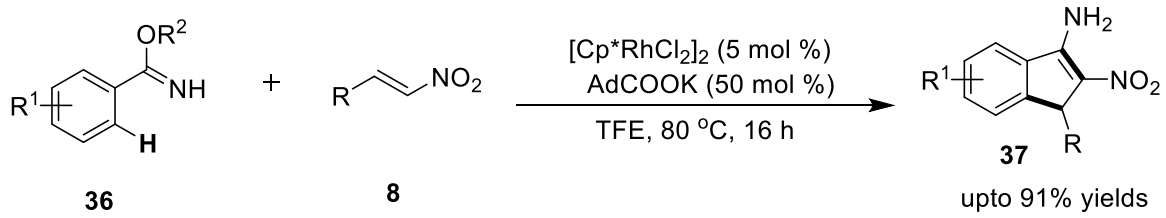

Scheme 2.1.9 Rhodium-catalyzed annulation of benzimidates (**36**) with nitroalkenes (**8**)

The preparation of nitro-functionalized spirocyclic benzosultams (**39**) have been documented by Deb's group through a Ir(III)-catalyzed annulative strategy, involving coupling between *N*-sulfonyl ketimines (**38**) and nitroalkenes (**8**) in TFE (Scheme 2.1.10).[46]

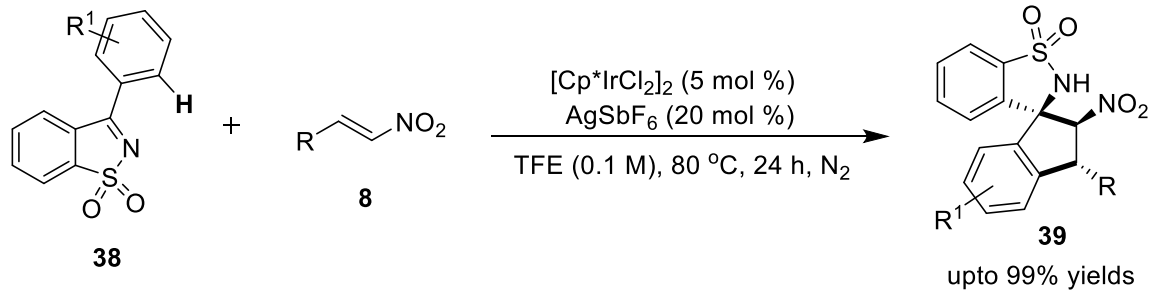

Scheme 2.1.10 Iridium-catalyzed spiroannulation of *N*-sulfonyl ketimines (**38**) with nitroalkenes (**8**)

Analogously, the same group reported another highly efficient and stereoselective synthesis of nitro-substituted spiro-2,3-dihydro-1,4-benzoxazine (**41**) derivatives using Rh(III)-catalyzed [3+2] annulation of benzoxazines (**40**) with nitroolefins (**8**) *via* redox-neutral C-H functionalization strategy (Scheme 2.1.11).[47]

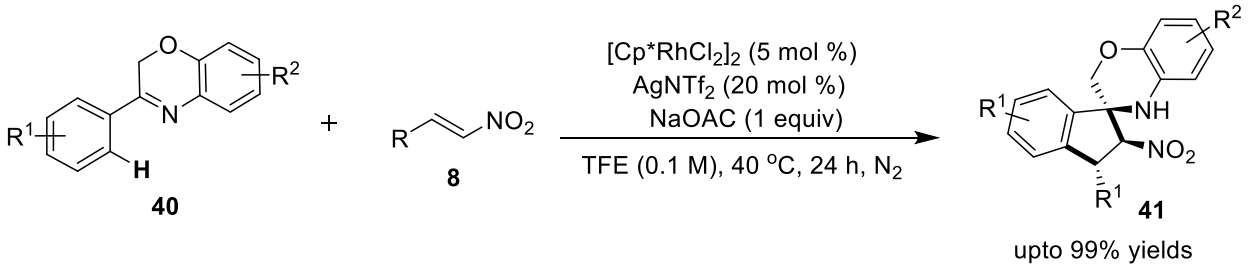

Scheme 2.1.11 Rhodium-catalyzed [3+2] annulation of benzoxazines (**41**) with nitroolefins (**8**)

Inspired from the biological importance and existing methods for the synthesis of phthalazino[2,3-*a*]cinnolines, we undertook and achieved the task of synthesizing hydroxyimino decorated phthalazino[2,3-*a*]cinnolines (**42**) by coupling from *N*-aryl-2,3-dihydrophthalazine-1,4- diones (**1**) with nitroolefins (**8**) under Rh(III)-catalysis (Scheme 2.1.12).[48]

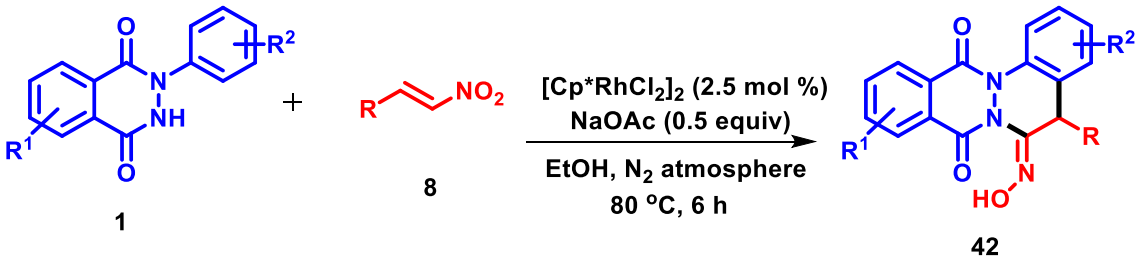

Scheme 2.1.12 Rhodium-catalyzed reductive annulation of *N*-aryl-2,3-dihydrophthalazine-1,4-diones (**1**) with nitroolefins (**8**)

2.2 Results and Discussion

The work commenced with optimizing the reaction condition for the coupling between 2-aryl-2,3-dihydrophthalazine-1,4-dione (**1a**) and *β*-nitrostyrene (**8a**) as model substrates, employing rhodium-catalysis (Table 2.2.1). Unfortunately, the coupling between the model substrates did not proceed using [Cp*****$RhCl_2$]$_2$ as a catalyst in ethanol at varied temperature conditions (Table 2.2.1, entry 1). The use of additives, such as $Cu(OAc)_2$, Cs_2CO_3 and $AgSbF_6$ remained ineffective to initiate any reaction under Rh-catalysis (Table 2.2.1, entries 2-4). Interestingly, a combination of [Cp*****$RhCl_2$]$_2$ with KPF_6 or NaOAc or CsOAc promoted the coupling reaction in ethanol at 40 ^oC under nitrogen atmosphere to afford 6-(hydroxyimino)-5-phenyl-5,6-dihydro-8*H*-indazolo[1,2-*a*]cinnolin-8-one (**42aa**) in 33%, 46% and 40% yields, respectively (Table 2.2.1, entries 5-7). The structure of **42aa** was unambiguously confirmed by its detailed spectroscopic analysis, including ^1H and ^{13}C NMR, COSY, HSQC, HMBC and HRMS. To our delight, 77% of **42aa** was obtained by carrying the coupling between **1a** and **8a** using [Cp*****$RhCl_2$]$_2$/NaOAc catalytic system at 80 °C in ethanol (Table 2.2.1, entry 8). Further optimization indicated that lowering of additive loading to 25 mol % produced a detrimental effect on the yield of **42aa**, while an increment in catalyst or additive loading did not produced any noticeable effect (Table 2.2.1, entries 9-11). Finally, solvent screening studies were persuaded that suggested the sensitivity of the reaction towards the choice of solvent. The use of TFE produced comparable results, while the yield of **42aa** drastically decreased when toluene, THF and ACN were used (Table 2.2.1, entries 12-15). On the other hand, polar aprotic solvents such as DMF and DMSO were complete unfavorable for this transformation (Table 2.2.1, entries 16-17). The coupling under air atmosphere furnished 45% of **42aa** (Table 2.2.1, entry 18). Unfortunately,

the reaction did not proceed at all using $[RuCl_2(p\text{-cymene})]_2$, $Co(OAc)_2$ and $[Ir(COD)Cl]_2$ as catalysts, under the described conditions (Table 2.2.1, entries 19-21).

Table 2.2.1 Selected optimization[a] of reaction conditions for the synthesis of **42aa**

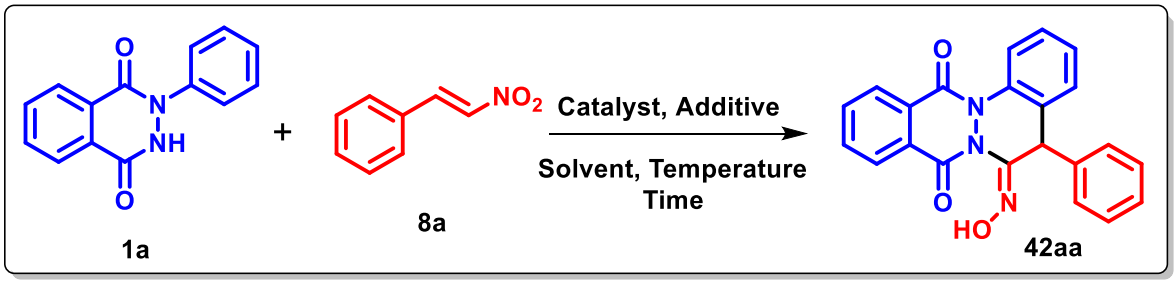

Entry	Catalyst (mol %)	Additive (mol %)	Solvent	Temp. (°C)	Yields (%)[b] **42aa**
1.	$[Cp^*RhCl_2]_2$ (2.5)	-	EtOH	25-80[c]	-
2.	$[Cp^*RhCl_2]_2$ (2.5)	$Cu(OAc)_2$ (50)	EtOH	40	-
3.	$[Cp^*RhCl_2]_2$ (2.5)	Cs_2CO_3 (50)	EtOH	40	-
4.	$[Cp^*RhCl_2]_2$ (2.5)	$AgSbF_6$ (50)	EtOH	40	-
5.	$[Cp^*RhCl_2]_2$ (2.5)	KPF_6 (50)	EtOH	40	33
6.	$[Cp^*RhCl_2]_2$ (2.5)	NaOAc (50)	EtOH	40	46
7.	$[Cp^*RhCl_2]_2$ (2.5)	CsOAc (50)	EtOH	40	40
8.	**$[Cp^*RhCl_2]_2$ (2.5)**	**NaOAc (50)**	**EtOH**	**80**	**77**
9.	$[Cp^*RhCl_2]_2$ (2.5)	NaOAc (25)	EtOH	80	53
10.	$[Cp^*RhCl_2]_2$ (2.5)	NaOAc (100)	EtOH	80	78
11.	$[Cp^*RhCl_2]_2$ (5)	NaOAc (50)	EtOH	80	75
12.	$[Cp^*RhCl_2]_2$ (2.5)	NaOAc (50)	TFE	80	71
13.	$[Cp^*RhCl_2]_2$ (2.5)	NaOAc (50)	Toluene	80	30
14.	$[Cp^*RhCl_2]_2$ (2.5)	NaOAc (50)	THF	80	25
15.	$[Cp^*RhCl_2]_2$ (2.5)	NaOAc (50)	ACN	80	20
16.	$[Cp^*RhCl_2]_2$ (2.5)	NaOAc (50)	DMF	80	-
17.	$[Cp^*RhCl_2]_2$ (2.5)	NaOAc (50)	DMSO	80	-
18.[d]	$[Cp^*RhCl_2]_2$ (2.5)	NaOAc (50)	EtOH	80	45[e]
19.	$[RuCl_2(p\text{-cymene})]_2$ (2.5)	NaOAc (50)	EtOH	80	-
20.	$Co(OAc)_2$ (2.5)	NaOAc (50)	EtOH	80	-
21.	$[Ir(COD)Cl]_2$ (2.5)	NaOAc (50)	EtOH	80	-

[a]Reaction conditions: The reactions are carried out with **1a** (0.24 mmol), **8a** (0.36 mmol) in the presence of catalyst/additive (as indicated in the table) in 5 mL of solvent at specified for 6 h under nitrogen atmosphere. [b]Isolated yields after column chromatography. [c]Reaction time = 12 h. [d]Under air atmosphere. [e]A number of minor spots appeared in addition to **42aa**.

With the optimized conditions in hand, we first examined the scope of the optimized strategy on a variety of *N*-aryl-2,3-dihydrophthalazine-1,4-diones (**1**) using *β*-nitrostyrene (**8a**) as a coupling partner. *N*-phenyl-2,3-dihydrophthalazine-1,4-dione (substrate: **1a**) reacted efficiently with **8a**

under standard conditions to produce hydroxyimino decorated phthalazino[2,3-*a*]cinnoline (**42aa**) in 77% yield. This thrives us to further explore the scope of this Rh-catalyzed reductive-annulation protocol with a variety of *N*-aryl-2,3-dihydrophthalazine-1,4-diones (**1b-l**) using **8a** as a coupling partner under the standard optimized conditions (Scheme 2.2.1). The annulation with *para* or *meta*-substituted *N*-aryl-2,3-dihydrophthalazine-1,4-diones bearing electron-donating groups (substrates: **1b-c**, **1e**) afforded the corresponding hydroxyiminated products (**42ba-ca, 42ea**) in 80-86% yields. In contrast, halo substituted *N*-aryl-2,3-dihydrophthalazine-1,4-diones (substrates: **1d, 1f**) gave comparatively lower yields of the desired products (**42da, 42fa**). Likewise, the annulation proceeded with great ease for *N*-aryl-2,3-dihydrophthalazine-1,4-diones bearing disubstitutions (substrates: **1g-h**), delivering the analogous products (**42ga-42ha**) in 78-87% yields. Further, we explored variedly decorated electron releasing and -withdrawing substituents on the phthalazine moiety (substrates: **1i-l**). Pleasingly, the corresponding products (**42ia-42la**) were obtained in 62-88% yields as inseparable regioisomeric mixtures in varied ratios. This is a result of using inseparable mixture of their *N*-aryl-2,3-dihydrophthalazine-1,4-diones (substrates: **1i-l**), which were synthesized by standard coupling reaction between phenylhydrazine and 5-methyl-, 5-methoxy-, 5-*t*-butyl and 5-bromophthalic anhydrides, respectively. Unfortunately, *N*-aryl-2,3-dihydrophthalazine-1,4-dione substrates possessing 2-Me, 2-Br, 4-NO_2, 4-CN substitutions on aryl ring, remained unreactive under described conditions. To assess the scalability of this Rh-catalyzed strategy, a representative gram-scale reaction was performed between **1a** and **8a** under optimized conditions to afford **42aa** in 74% (1.15 g) yield. The representative ^{1}H NMR and ^{13}C NMR of product **42aa** are shown in Figure 2.2.1 and Figure 2.2.2, respectively. As a representative example, single crystal of **42ba** were grown in chloroform to confirm the structure. ORTEP diagram of 21ba (CCDC 2040955) is given in Figure 2.2.3.

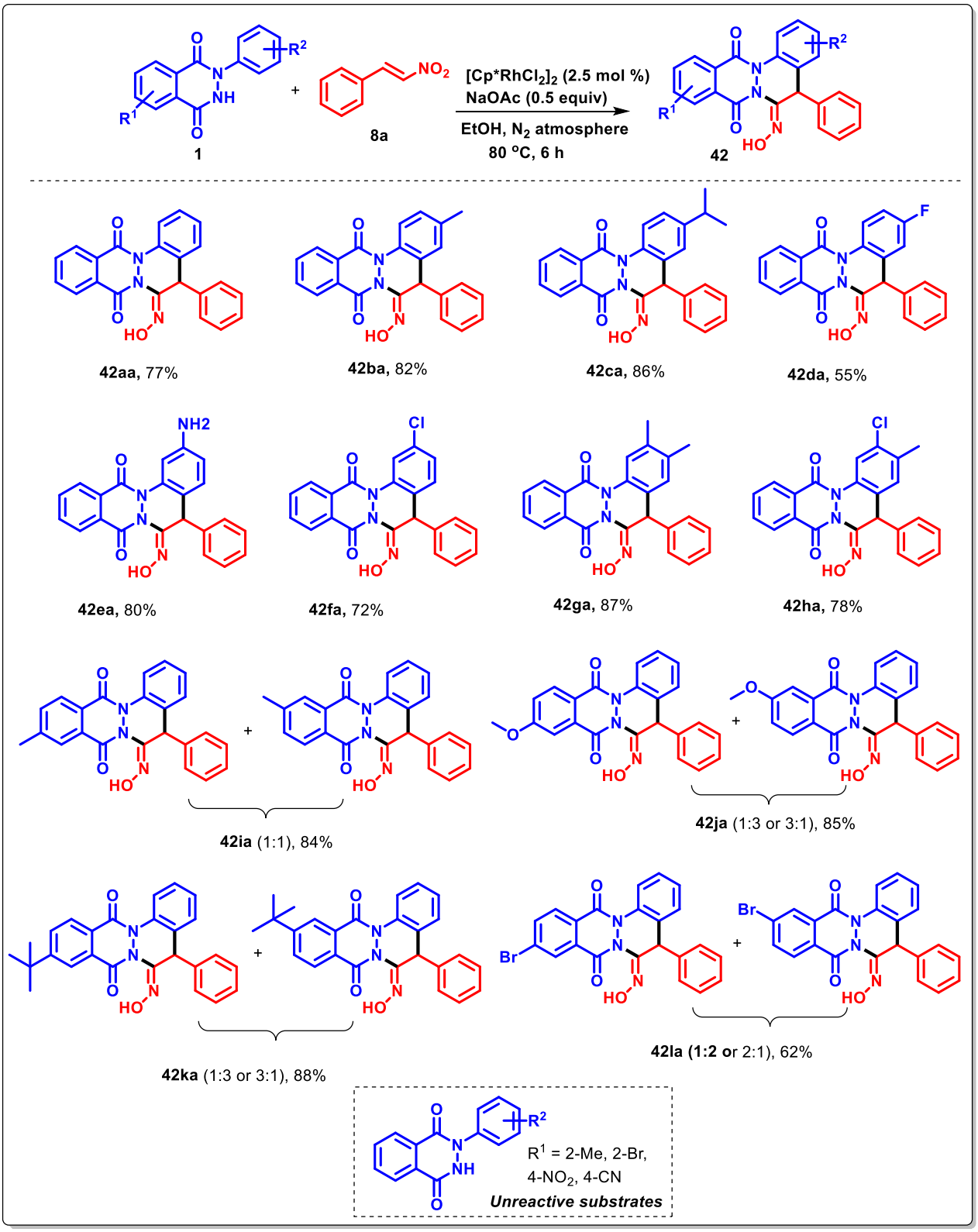

Scheme 2.2.1 Substrate scope of *N*-aryl-2,3-dihydrophthalazine-1,4-diones

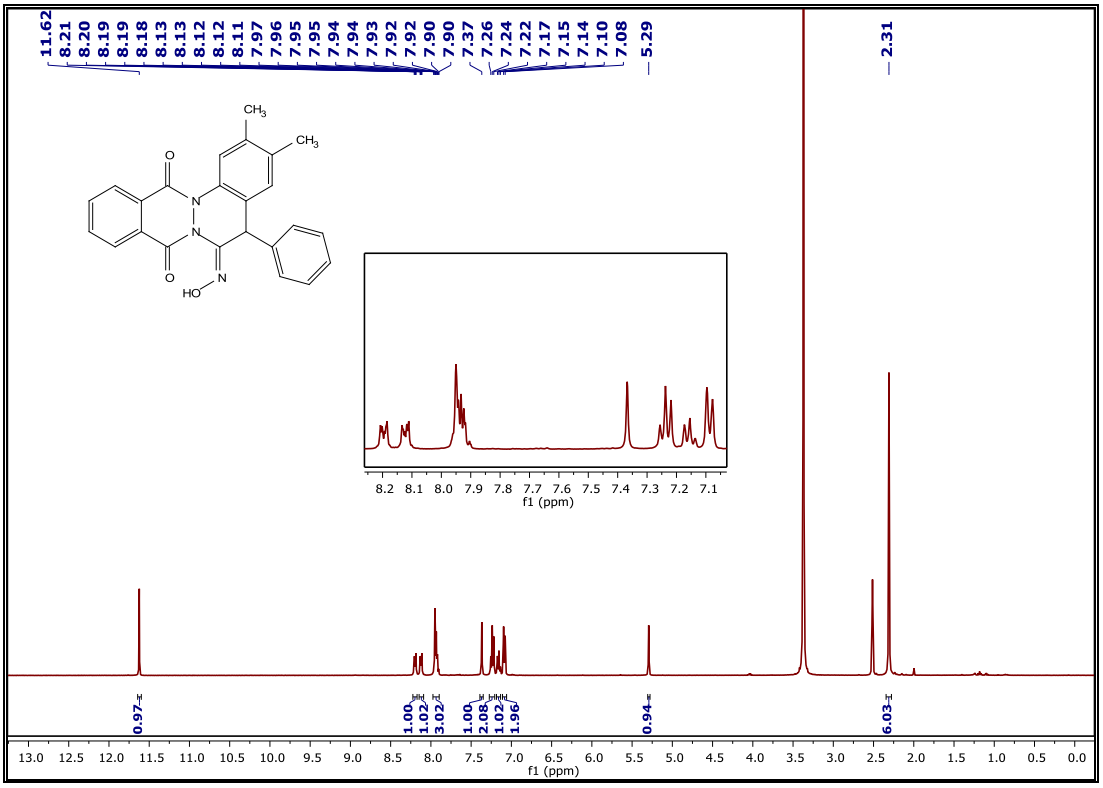

Figure 2.2.1 ^{1}H NMR spectra of **42aa**

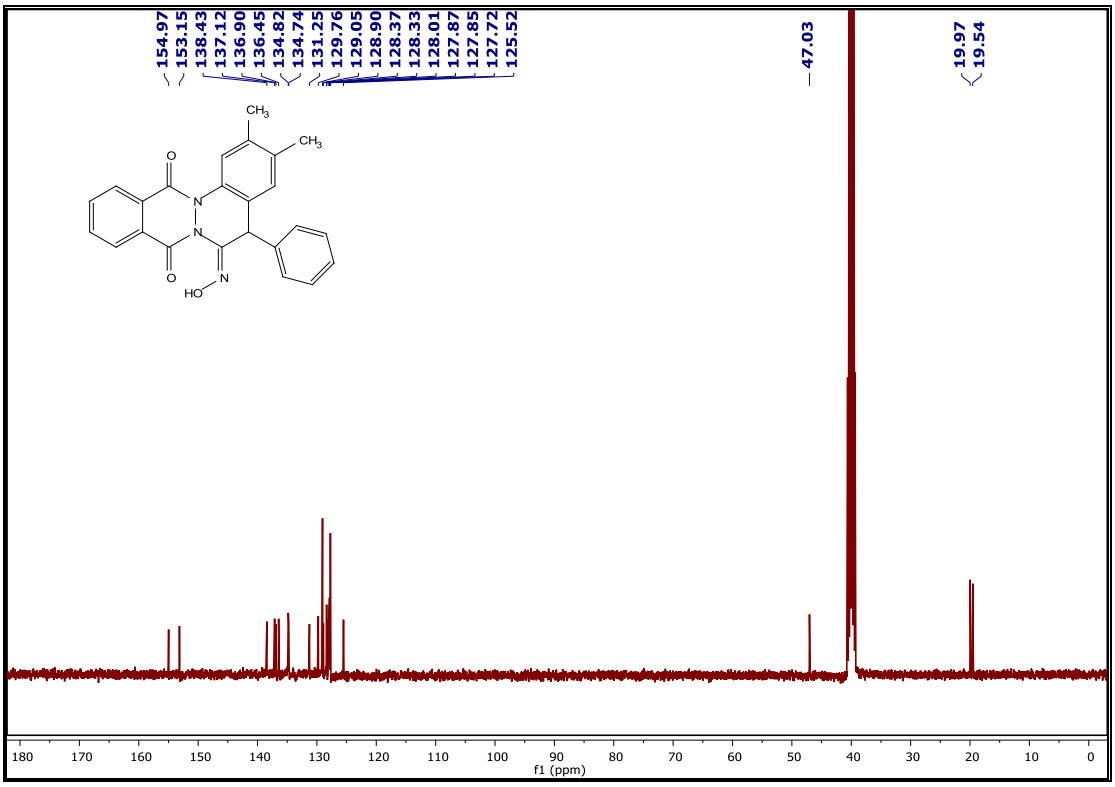

Figure 2.2.2 ^{13}C NMR spectra of **42aa**

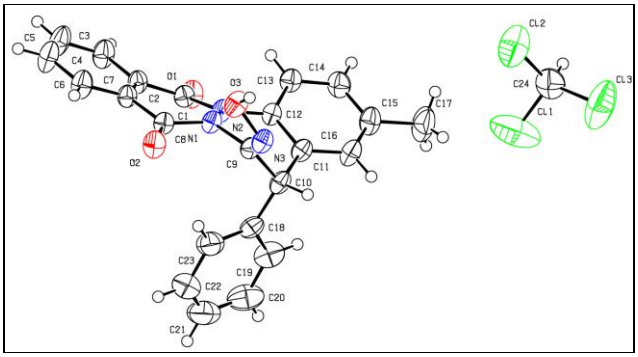

Figure 2.2.3 ORTEP diagram of **42ba·CHCl$_3$** with atom labelling scheme (thermal ellipsoids at 30% probability level)

We next focused our investigation on examining the use of diverse nitroolefins for this one-pot Rh-catalyzed reductive annulation strategy (Scheme 2.2.2). *para*-Substituted nitrostyrenes possessing electron-donating substituents (substrates: **8b-e**) showcased high reactivity with *N*-phenyl-2,3-dihydrophthalazine-1,4-dione (**1a**) to furnish respective fused-cinnolines (**42ab-42ae**) in 79-84% yields. While nitrostyrenes with moderate electron-withdrawing halogen substituents (substrates: **8f-g**) reacts with moderate reactivity with **1a** to produce the desired products (**42af-42ag**) in 60-61% yields. The trifluoromethyl-functionalized nitrostyrene (substrate: **8h**) showed poor reactivity with **1a** and the corresponding phthalazino-fused cinnoline (**42ah**) was observed on TLC in trace amounts. Pleasingly, 3-ethoxy-4-hydroxy, naphthyl, biphenyl bearing nitroolefins (substrates: **8i-k**) rendered the products (**42ai-ak**) in 78-88%. Additionally, the reaction was well tolerable with nitroolefins containing heterocyclic moieties such as thiophene, furan and indole (substrates: **8l-n**), affording their respective annulated products (**42al-an**) in 72-75% yields. Notably, the annulation of **1a** with nitro and cyano-substituted nitrostyrenes nitroolefins failed to react under the described conditions. It is most likely that the presence of electron-withdrawing groups on phenyl ring in nitrostyrenes decreases the nucleophilicity on C=C double bond, which further disfavors their coordination to rhodium. On the other hand, the previous observation was confirmed by treating **1a** with nitroolefin containing aliphatic long chain such as (*E*)-1-nitrooct-1-ene (substrate: **8o**), which under standard condition provided **42ao** with 56% yield.

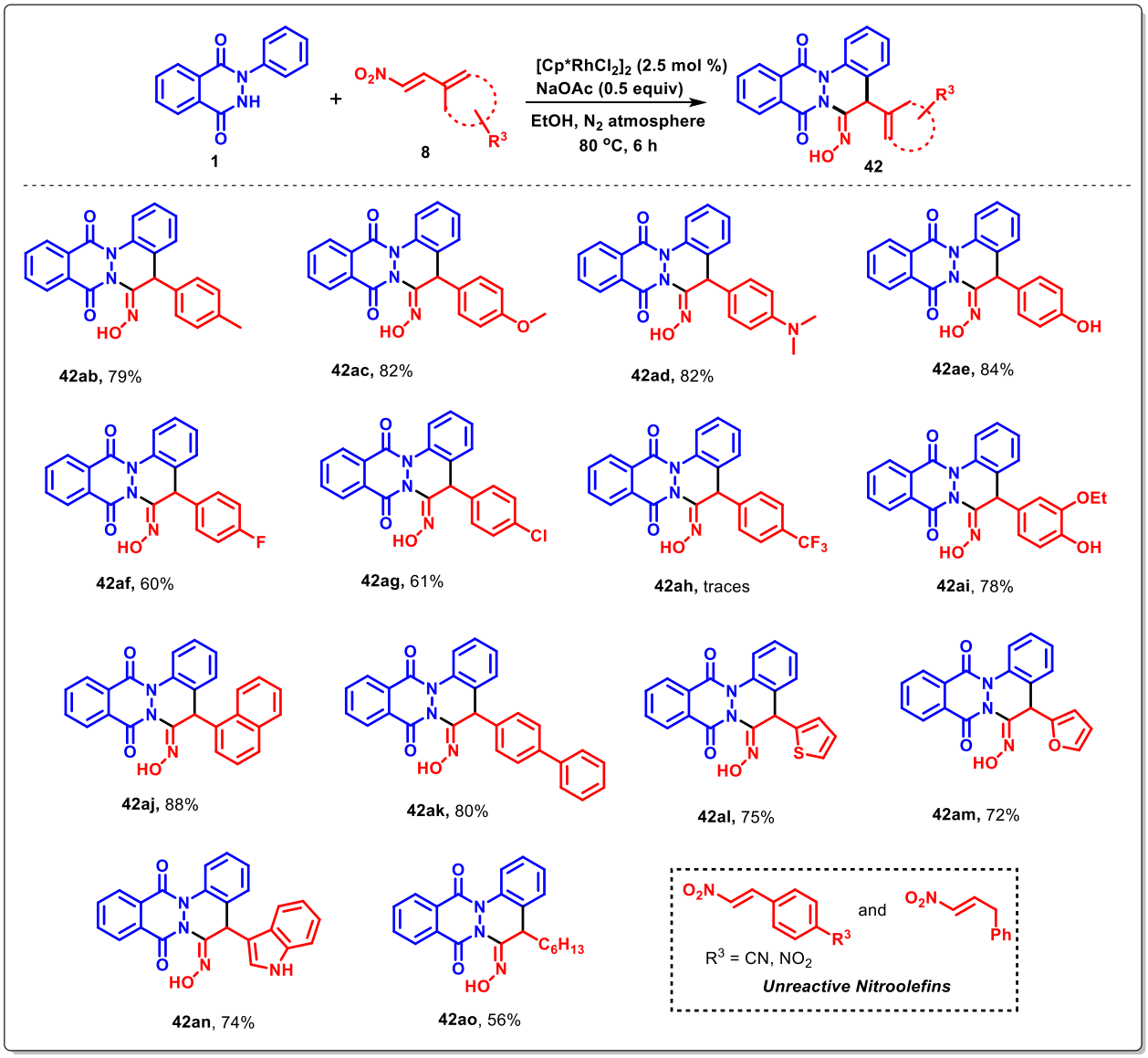

Scheme 2.2.2 Substrate scope of nitroolefins

A series of experiments were conducted to probe the mechanism of the strategy. An extensive incorporation (~72%) of deuterium atoms at the two *ortho* positions was observed by carrying the deuterium labelling experiment on **1b** under Rh-catalyzed optimized conditions in CD_3OD, which established the reversible nature of C-H cleavage step (Scheme 2.2.3i, Figure 2.2.4). In addition, Kinetic Isotope Effect study when performed by carrying two parallel reactions of **1b** and **1b-*d*$_2$** with **8a** under standard conditions, resulted in a Kinetic Isotope Effect (k_H/k_D) of 0.75 (Scheme 2.2.3ii, Figure 2.2.5 & 2.2.6). This inverse KIE value suggested C-H bond activation to be a rate-limiting step that might have progressed through an electrophilic aromatic substitution (S_EAr) mechanism.[49-52] In such cases, the reaction with detuterated substrates proceeds faster than the

non-deuterated substrates. Pleasingly, a key rhodacyclic intermediate (**42C′**) was isolated using DMSO as a stabilizing ligand, which successfully catalyzed the described annulation between **1a** and **8a** to produce **42aa** in 74% yield (Scheme 2.2.3iii, Figure 2.2.7 & Figure 2.2.8). In addition, a number of intermediates were detected during real-time *in situ* monitoring of the reaction progress by mass spectrometry. The species **42C**, **42D** and **42F** were detected in the ESI-MS of the crude reaction mixture obtained by reacting **1a** with **11a** under standard conditions at 25 ºC for 2 h (Scheme 2.2.3iv). The detection of species **42C**, **42D** and **42F** suggested the relevance of formation of a five-membered rhodacyclic complex, nitrostyrene coordinated rhodium complex and the possible mode of reduction mechanism. To further comprehend the source of hydrogen in the oxime functionality, a coupling reaction of **1b-*d*$_2$** with **8a** under standard conditions was carried. Interestingly, a minor deuterium incorporation (~10%) in oxime group (=NOH), along with the partial displacement of the second *ortho*-deuterium atom was observed in the final product (**42ba-*d*$_1$**). This provided an indication that AcOD generated by Rh-catalyzed C-H metallation of **1b-*d*$_2$** could be the source of deuterium in the reduction of nitro to oxime (Scheme 2.2.3v).

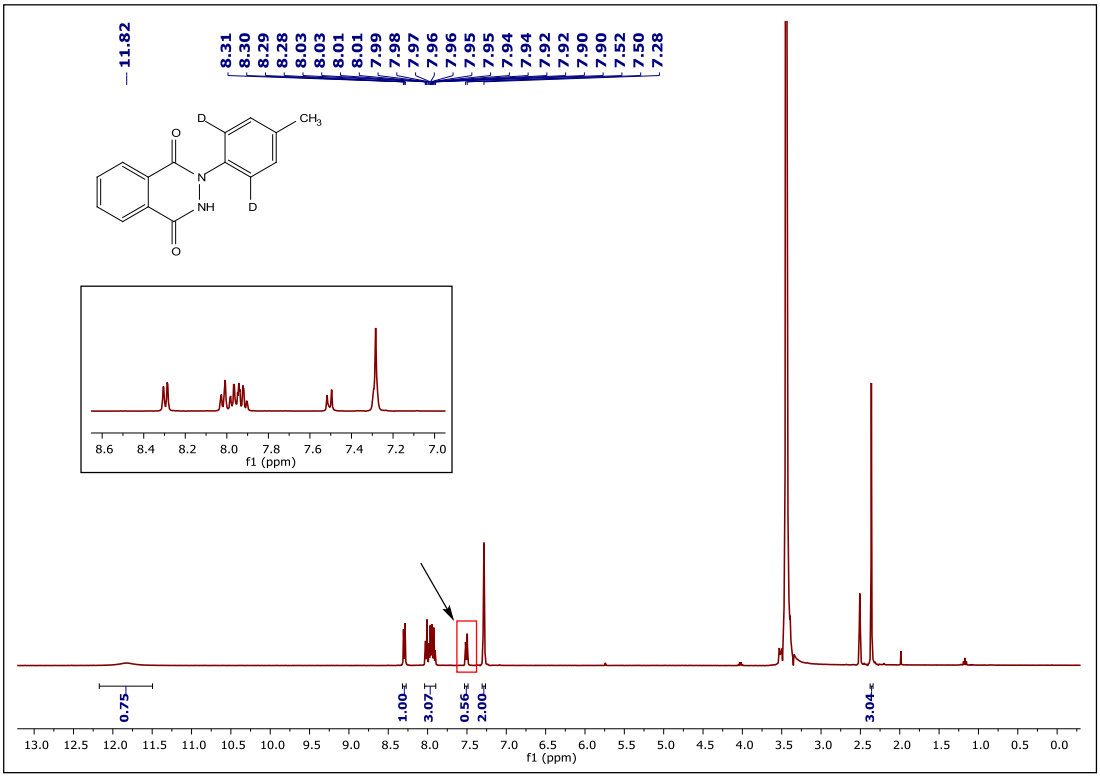

Figure 2.2.4 ^{1}H NMR of **1b/1b-*d*$_2$**

2.00-0.56/2.00 = 0.72*100 = ~72% D

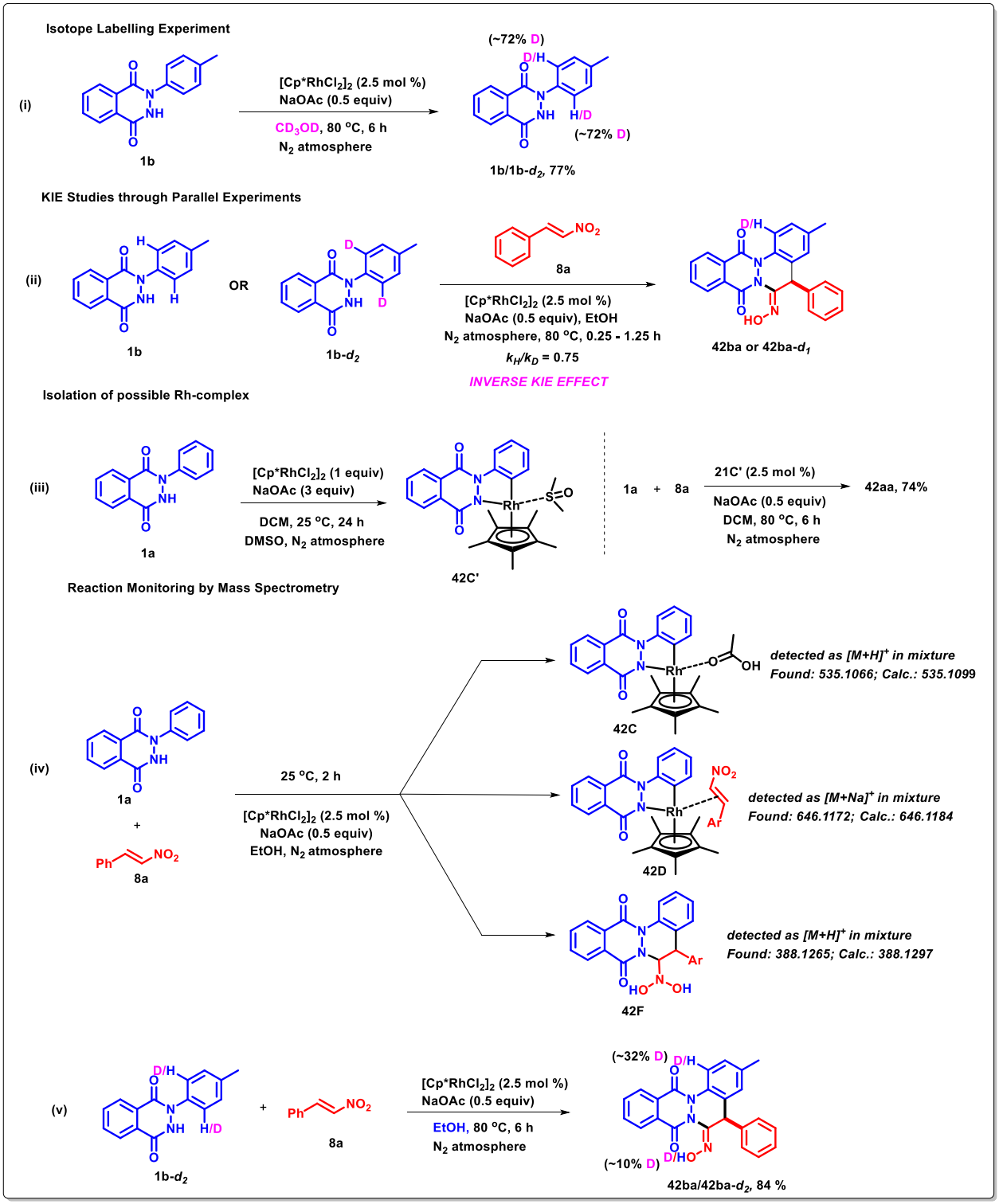

Scheme 2.2.3 Preliminary mechanistic investigations

Parallel Experiments

Time (Min)	15	30	45	60	75
^{1}H NMR Yield (%)	18.88	31.57	37.84	45.24	57.23

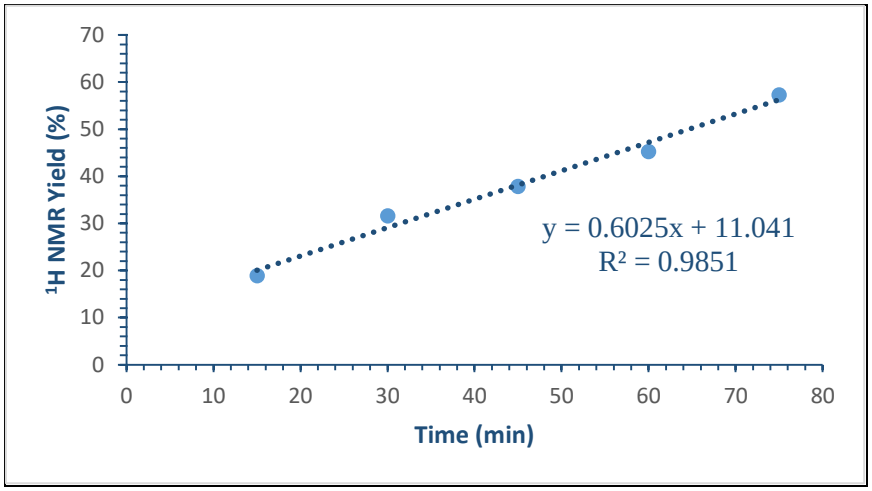

Figure 2.2.5 Protonated Kinetics

Time (Min)	15	30	45	60	75
^{1}H NMR Yield (%)	15.06	31.49	44.18	53.16	64.43

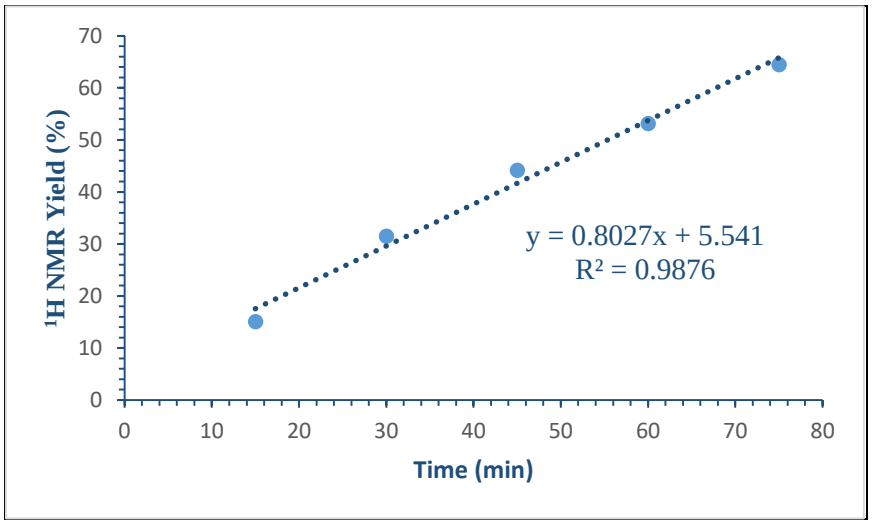

Figure 2.2.6 Deuterated Kinetics

KIE = k_H/k_D = 0.6025/0.8027= 0.75

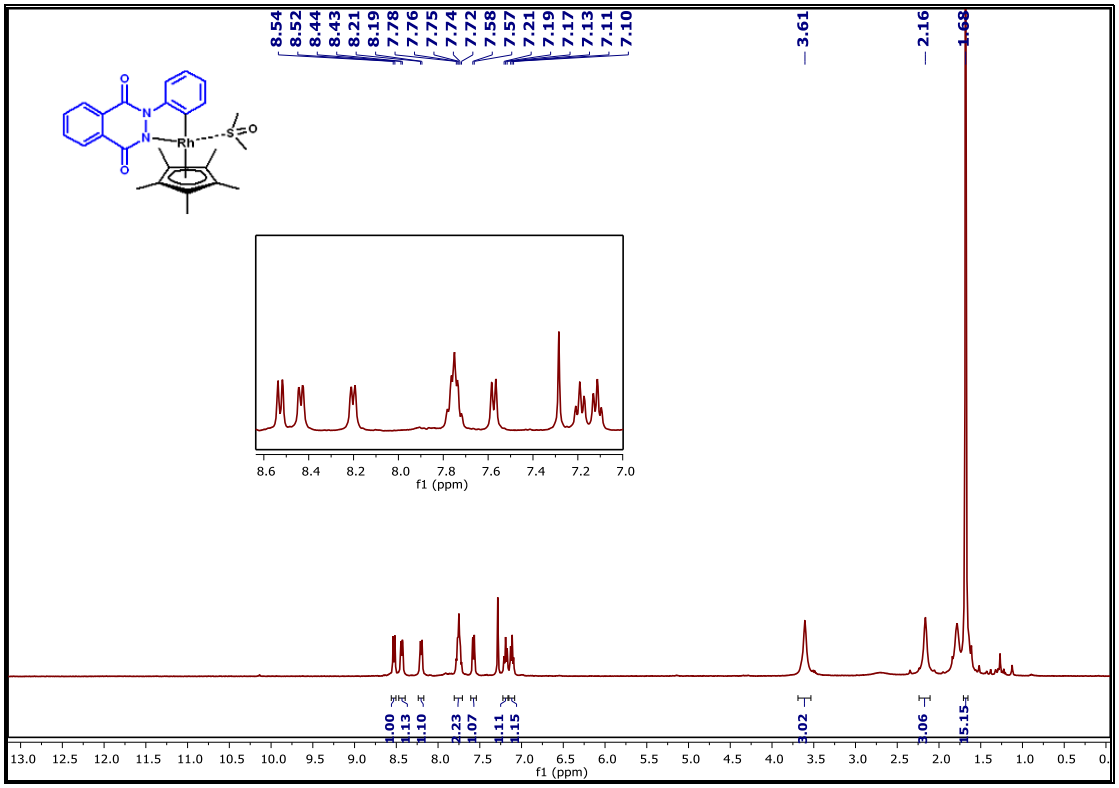

Figure 2.2.7 ^{1}H NMR spectra of **42C′**

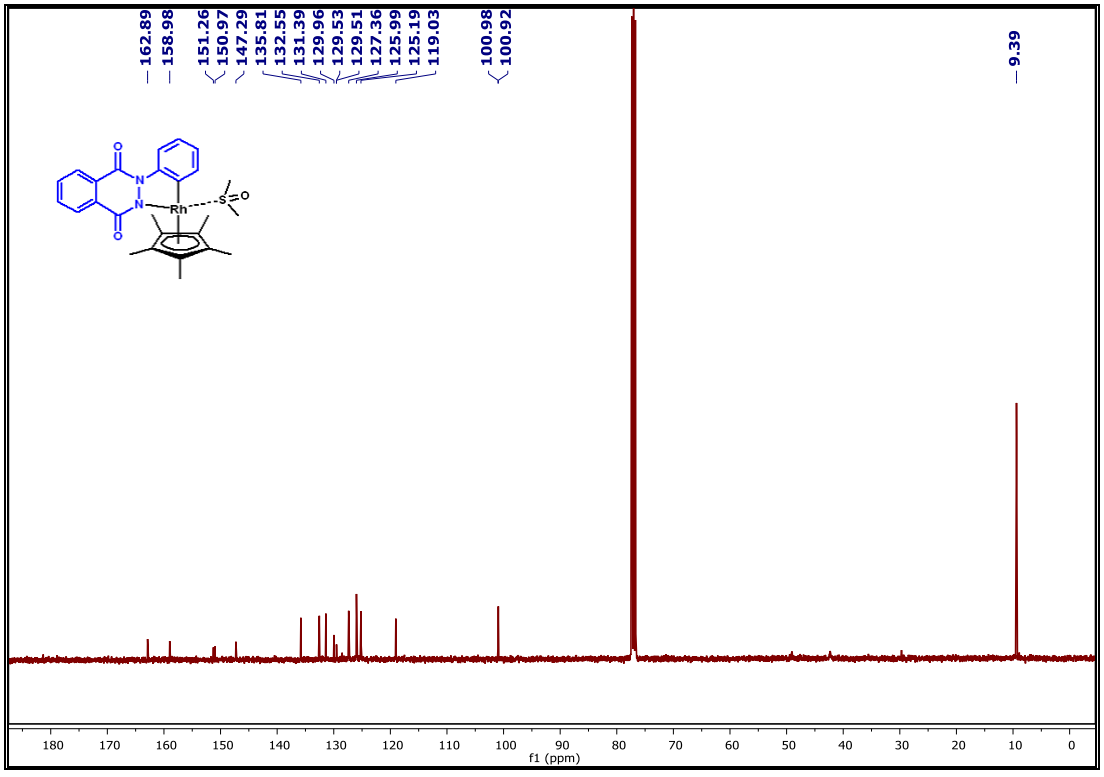

Figure 2.2.8 ^{13}C NMR spectra of **42C′**

On the basis of precedence literature and our preliminary mechanistic investigations, the reaction could be believed to be triggered by the formation of reactive [Cp*$Rh^{III}(OAc)_2$] species *via* acetate ion-mediated dissociation of dimeric $[Cp^*RhCl_2]_2$. This further activates the substrate (**1**) *via* N-H ligand exchange to produce species **A**, which subsequently furnishes a five-membered rhodacyclic intermediate (**C**) by C-H activation possibly through S_EAr mechanism *via* **B**. Next, the coordination of nitroalkene (**8**) followed by its insertion into C_{Ar}-Rh bond generates species **E** *via* **D**. Thereafter, acetate ion-mediated demetalation concomitant with the protonation of the two oxygen atoms of the nitro group produces **F**, along with the regeneration of active Rh(III) species for the next catalytic cycle. Finally, dehydration in **F** leads to the oxime decorated product (**42**) (Scheme 2.2.4)

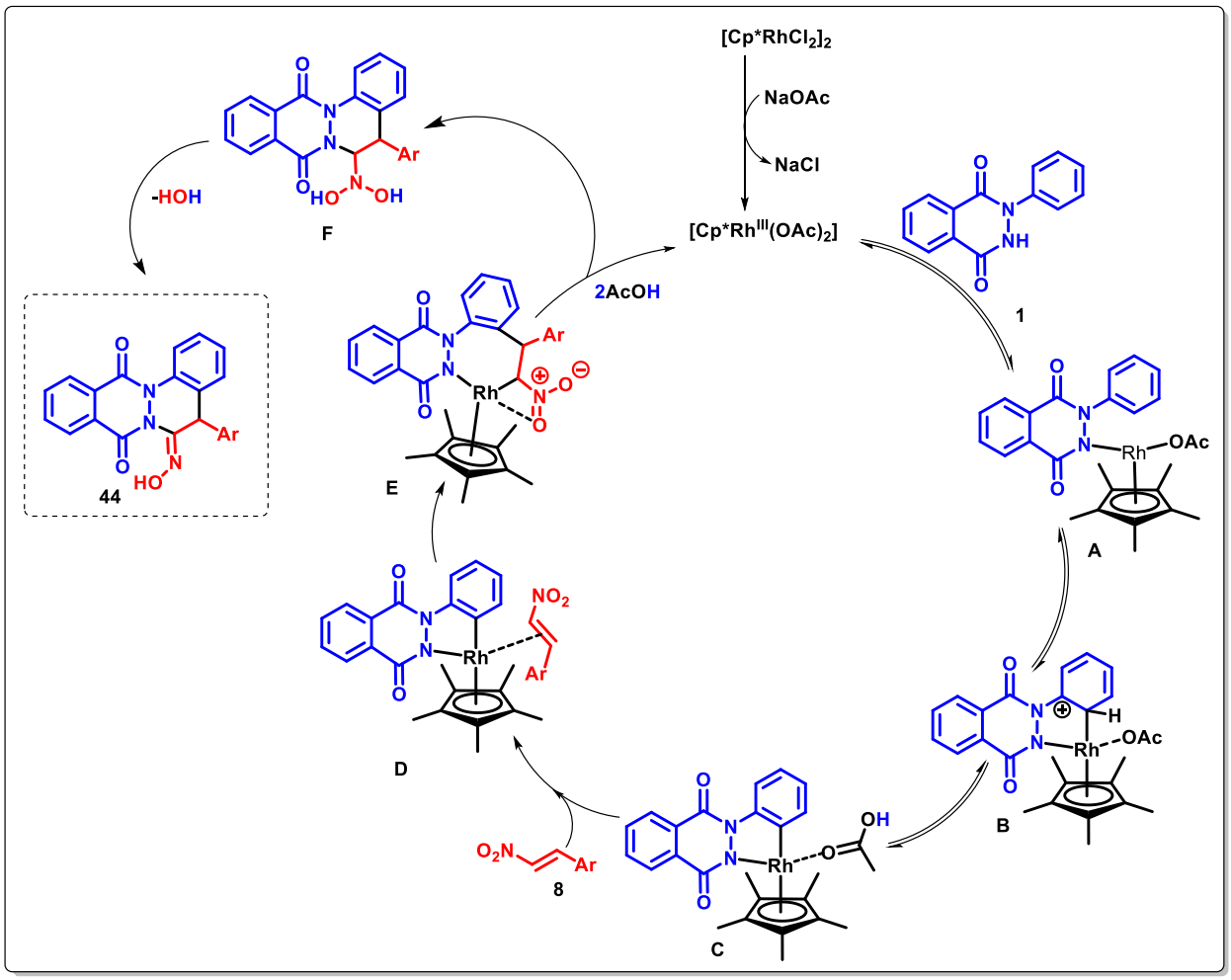

Scheme 2.2.4 Plausible mechanism

In summary, we have disclosed a facile strategy for the reductive [4+2] annulation of 2-aryl-2,3-dihydrophthalazine-1,4-diones with diversified nitroolefins to afford hydroxyimino decorated phthalazino[2,3-*a*]cinnolines under reducing agent free Rh-catalyzed conditions. The strategy provides a direct access to a variety of tetracyclic fused-cinnolines with potential applications in medicinal and material chemistry. Detailed mechanistic investigations indicated that the reaction proceeded through a sequential C-H activation/olefin insertion/reduction pathway *via* chelation-assisted directing group influence of phthalazine-dione groups, even in absence of a reducing agent.

2.3 Experimental Section

General Considerations

Commercially available reagents were used without purification. Commercially available solvents were dried by standard procedures prior to use. Nitrostyrenes (**8a** to **8c**; **8l** to **8n**; **8i** and **8o**),[53] **8d**,[54] **8e**,[55] (**8f** to **8h**; **8k**),[56] **8j**,[57] were prepared according to the reported procedures. Reactions were monitored by using thin layer chromatography (TLC) on 0.2 mm silica gel F254 plates (Merck). The chemical structures of final products and intermediates were characterized by nuclear magnetic resonance spectra (^{1}H NMR and ^{13}C NMR) were recorded on a 400 MHz spectrometer, and the chemical shifts are reported in δ units, parts per million (ppm), relative to residual chloroform (7.26 ppm) or DMSO (2.5 ppm) in the deuterated solvent. ^{13}C NMR spectra are fully decoupled. The following abbreviations were used to describe peak splitting patterns when appropriate: s = singlet, d = doublet, t = triplet, dd = doublet of doublets, and m = multiplet. Coupling constants *J* are reported in Hz. The ^{13}C NMR spectra are reported in ppm relative to deuterochloroform (77.0 ppm) or [d_6] DMSO (39.5 ppm). Melting points were determined on a capillary point apparatus equipped with a digital thermometer and are uncorrected. High-resolution mass spectra were recorded on Agilent Technologies 6545 Q-TOF LC/MS by using electrospray mode. Column chromatography was performed on silica gel (100-200) mesh using varying ratio of ethyl acetate/hexanes as eluent.

General procedure for the synthesis of hydroxyimino-decorated phthalazino[2,3-*a*]cinnolines (42)

To an oven-dried sealed tube with a screw cap (PTFE) containing *N*-aryl-2,3-dihydrophthalazine-1,4-one (**1**) (50 mg, 1 equiv) in EtOH (5 mL), nitroolefin (**8**) (1.5 equiv), [Cp*****$RhCl_2$]$_2$ (0.025

equiv), NaOAc (0.5 equiv) were added under a nitrogen atmosphere. The reaction mixture was stirred on a magnetic stirrer oil bath at 80 ºC for 6 h (traced by TLC). After the completion of the reaction, the reaction mixture was cooled to room temperature, concentrated, diluted with water and extracted with EtOAc (20 mL x 2). The organic layers were combined and concentrated under *vacuo* to afford a residue, which was purified by column chromatography (SiO_2 100−200 mesh) using hexanes/ethyl acetate as eluent systems to afford the desired product (**42**).

(*E*)-6-(Hydroxyimino)-5-phenyl-5,6-dihydrophthalazino[2,3-*a*]cinnoline-8,13-dione (42aa).

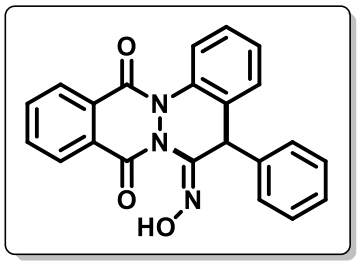

Pale yellow solid; yield: 60 mg (77%); mp 168−170 °C; ^{1}H NMR (400 MHz, DMSO-d_6) δ 11.69 (s, 1H), 8.22 – 8.18 (m, 1H), 8.17 – 8.11 (m, 2H), 7.98 – 7.89 (m, 2H), 7.62 (dd, J = 7.5, 1.8 Hz, 1H), 7.55 – 7.43 (m, 2H), 7.28 – 7.21 (m, 2H), 7.19 – 7.13 (m, 1H), 7.08 (d, J = 7.8 Hz, 2H), 5.42 (s, 1H); ^{13}C NMR (100 MHz, DMSO-d_6) δ 155.2, 153.2, 138.3, 136.9, 134.9, 133.5, 131.2, 129.3, 129.1, 128.8, 128.4, 128.3, 128.2, 128.0, 127.9, 127.9, 127.7, 125.1, 47.3; HRMS (ESI-TOF) (*m/z*) calculated $C_{22}H_{16}N_3O_3^+$: 370.1191, found 370.1177 $[M + H]^+$.

(*E*)-6-(Hydroxyimino)-3-methyl-5-phenyl-5,6-dihydrophthalazino[2,3-*a*]cinnoline-8,13-dione (42ba).

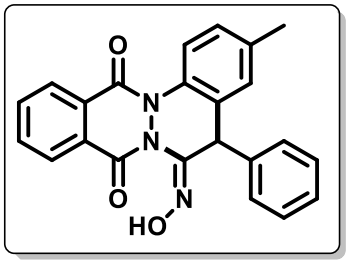

Pale yellow solid; yield: 62 mg (82%); mp 165−168 °C; ^{1}H NMR (400 MHz, DMSO-d_6) δ 11.66 (s, 1H), 8.22 – 8.16 (m, 1H), 8.14 – 8.10 (m, 1H), 8.04 (d, J = 8.4 Hz, 1H), 7.95 – 7.88 (m, 2H), 7.42 (d, J = 2.0 Hz, 1H), 7.32 (dd, J = 8.6, 1.2 Hz, 1H), 7.27 – 7.21 (m, 2H), 7.18 – 7.13 (m, 1H), 7.08 (d, J = 7.8 Hz, 2H), 5.34 (s, 1H), 2.40 (s, 3H); ^{13}C NMR (100 MHz, DMSO-d_6) δ 155.0, 153.1, 138.3, 138.0, 136.9, 134.8, 134.8, 131.1, 131.0, 129.5, 129.1, 128.9, 128.4, 128.0, 127.9, 127.9, 127.7, 124.9, 47.4, 21.1; HRMS (ESI-TOF) (*m/z*) calculated $C_{23}H_{18}N_3O_3^+$: 384.1348, found 384.1340 $[M + H]^+$.

(*E*)-6-(Hydroxyimino)-3-isopropyl-5-phenyl-5,6-dihydrophthalazino[2,3-*a*]cinnoline-8,13-dione (42ca). White solid; yield: 63 mg (86%); mp 187−189 °C; ^{1}H NMR (400 MHz, DMSO-d_6)

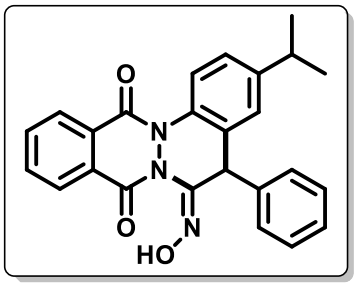

δ 11.69 (s, 1H), 8.22 – 8.17 (m, 1H), 8.15 – 8.10 (m, 1H), 8.05 (d, J = 8.6 Hz, 1H), 7.96 – 7.89 (m, 2H), 7.50 (d, J = 1.9 Hz, 1H), 7.40 (dd, J = 8.6, 2.0 Hz, 1H), 7.27 – 7.21 (m, 2H), 7.19 – 7.13 (m, 1H), 7.07 (d, J = 7.8 Hz, 2H), 5.37 (s, 1H), 3.05 – 2.94 (m, 1H), 1.27 (q, J = 3.6 Hz, 6H); ^{13}C NMR (100 MHz, DMSO-d_6) δ 155.0, 153.1,

148.9, 138.4, 136.8, 134.9, 134.8, 131.3, 131.1, 129.1, 128.8, 128.4, 128.0, 128.0, 127.9, 127.7, 126.9, 126.3, 125.2, 47.5, 33.6, 24.2; HRMS (ESI-TOF) (*m/z*) calculated $C_{25}H_{22}N_3O_3^+$: 412.1661, found 412.1656 $[M + H]^+$.

(*E*)-3-Fluoro-6-(hydroxyimino)-5-phenyl-5,6-dihydrophthalazino[2,3-*a*]cinnoline-8,13-dione (42da). Pale yellow solid; yield: 42 mg (55%); mp 170−172 °C; ^{1}H NMR (400 MHz, DMSO-d_6) δ 11.75 (s, 1H), 8.22 – 8.16 (m, 2H), 8.16 – 8.10 (m, 1H), 7.96 – 7.91 (m, 2H), 7.58 (dd, J = 8.6, 3.0 Hz, 1H), 7.40 (td, J = 8.8, 3.0 Hz, 1H), 7.29 – 7.23 (m, 2H), 7.21 – 7.15 (m, 1H), 7.08 (d, J = 7.8 Hz, 2H), 5.46 (s, 1H); ^{13}C NMR (100 MHz, DMSO-d_6) δ 160.7 ($^1J_{C\text{-}F}$ = 245.3 Hz), 155.2, 153.2, 137.9, 136.3, 134.9, 133.9, 129.3, 129.2, 128.7, 128.4, 128.1, 128.0, 127.9, 127.7, 127.6, 127.2, 115.8, 115.6, 115.5, 115.3, 47.2; ^{19}F NMR (376 MHz, DMSO-d_6) δ -113.06; HRMS (ESI-TOF) (*m/z*) calculated $C_{22}H_{15}FN_3O_3^+$: 388.1097, found 388.1072 $[M + H]^+$.

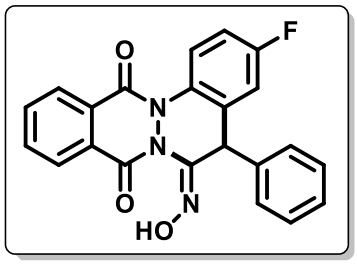

(*E*)-2-Amino-6-(hydroxyimino)-5-phenyl-5,6-dihydrophthalazino[2,3-*a*]cinnoline-8,13-dione (42ea). Yellow solid; yield: 61 mg (80%); mp 164−166 °C; ^{1}H NMR (400 MHz, DMSO-d_6) δ 11.44 (s, 1H), 8.19 (d, J = 6.6 Hz, 1H), 8.14 – 8.07 (m, 1H), 8.00 – 7.88 (m, 2H), 7.41 (s, 1H), 7.26 – 7.08 (m, 6H), 6.64 (dd, J = 8.1, 1.4 Hz, 1H), 5.41 (s, 2H), 5.14 (s, 1H); ^{13}C NMR (100 MHz, DMSO-d_6) δ 155.0, 153.2, 148.9, 139.0, 138.0, 134.8, 134.7, 134.1, 129.5, 129.1, 128.9, 128.3, 128.0, 127.8, 127.7, 127.7, 117.7, 114.1, 109.5, 46.7; HRMS (ESI-TOF) (*m/z*) calculated $C_{22}H_{17}N_4O_3^+$: 385.1300, found 385.1285 $[M + H]^+$.

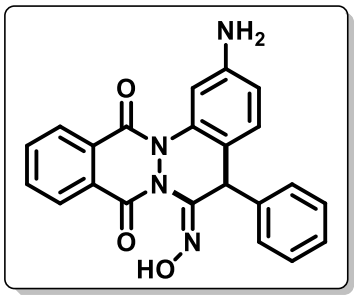

(*E*)-2-Chloro-6-(hydroxyimino)-5-phenyl-5,6-dihydrophthalazino[2,3-*a*]cinnoline-8,13-dione (42fa). Pale yellow solid; yield: 53 mg (72%); mp 116−117 °C; ^{1}H NMR (400 MHz, DMSO-d_6) δ 11.75 (s, 1H), 8.32 (d, J = 2.1 Hz, 1H), 8.25 – 8.21 (m, 1H), 8.15 – 8.11 (m, 1H), 7.99 – 7.93 (m, 2H), 7.63 (d, J = 8.3 Hz, 1H), 7.54 (dd, J = 8.2, 2.1 Hz, 1H), 7.29 – 7.24 (m, 2H), 7.21 – 7.16 (m, 1H), 7.10 (d, J = 7.7 Hz, 2H), 5.47 (s, 1H); ^{13}C NMR (100 MHz, DMSO-d_6) δ 155.7, 153.3, 138.0, 136.9, 135.1, 135.0, 134.4, 132.4, 131.0, 129.6, 129.2, 128.7, 128.6, 128.1, 128.0, 127.9, 127.8, 124.4, 46.8; HRMS (ESI-TOF) (*m/z*) calculated $C_{22}H_{15}ClN_3O_3^+$: 404.0801, found 404.0776 $[M + H]^+$.

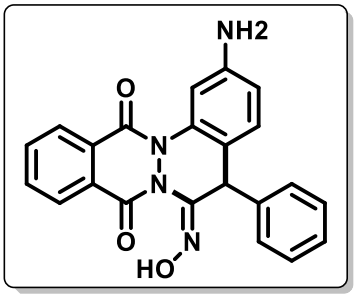

(*E*)-6-(Hydroxyimino)-2,3-dimethyl-5-phenyl-5,6-dihydrophthalazino[2,3-*a*]cinnoline-8,13-dione (42ga). White solid; yield: 65 mg (87%); mp 214−216 °C; ^{1}H NMR (400 MHz, DMSO-d_6) δ 11.62 (s, 1H), 8.22 – 8.17 (m, 1H), 8.14 – 8.09 (m, 1H),7.97 – 7.90 (m, 3H), 7.37 (s, 1H), 7.27– 7.20 (m, 2H), 7.18 – 7.13 (m, 1H), 7.09 (d, J = 7.7 Hz, 2H), 5.29 (s, 1H), 2.31 (s, 6H); ^{13}C NMR (100 MHz, DMSO-d_6) δ 155.0, 153.2, 138.4, 137.1, 136.9, 136.5, 134.8, 134.7, 131.3, 129.8, 129.1, 128.9, 128.4, 128.3, 128.0, 127.9, 127.9, 127.7, 125.5, 47.0, 20.0, 19.5; HRMS (ESI-TOF) (*m/z*) calculated $C_{24}H_{20}N_3O_3^+$: 398.1504, found 398.1482 $[M + H]^+$.

(*E*)-2-Chloro-6-(hydroxyimino)-3-methyl-5-phenyl-5,6-dihydrophthalazino[2,3-*a*]cinnoline-8,13-dione (42ha). Pale yellow solid; yield: 57 mg (78%); mp 217−219 °C; ^{1}H NMR (400 MHz, DMSO-d_6) δ 11.74 (s, 1H), 8.32 (s, 1H), 8.25 – 8.21 (m, 1H), 8.15 – 8.10 (m, 1H), 7.99 – 7.91 (m, 2H), 7.59 (s, 1H), 7.29 – 7.23 (m, 2H), 7.21 – 7.16 (m, 1H), 7.10 (d, J = 7.6 Hz, 2H), 5.38 (s, 1H), 2.41 (s, 3H); ^{13}C NMR (100 MHz, DMSO-d_6) δ 155.5, 153.2, 137.9, 136.9, 135.5, 135.0, 134.9, 132.5, 132.1, 131.4, 129.5, 129.2, 128.7, 128.5, 128.0, 128.0, 127.9, 127.8, 127.4, 124.7, 46.8, 19.8; HRMS (ESI-TOF) (*m/z*) calculated $C_{23}H_{17}ClN_3O_3^+$: 418.0958, found 418.0935 $[M + H]^+$.

(*E*)-6-(Hydroxyimino)-10-methyl-5-phenyl-5,6-dihydrophthalazino[2,3-*a*]cinnoline-8,13-dione + (*E*)-6-(Hydroxyimino)-11-methyl-5-phenyl-5,6-dihydrophthalazino[2,3-*a*]cinnoline-8,13-dione (1:1) (42ia). White solid; yield: 64 mg (84%); mp 121−124 °C; ^{1}H NMR (400 MHz, DMSO-d_6) δ 11.66 (s, 0.5H), 11.63 (s, 0.5H), 8.17 – 8.11 (m, 1H), 8.09 (d, J = 8.0 Hz, 0.5H), 8.04 – 8.00 (m, 1H), 7.95 – 7.92 (m, 0.5H), 7.77 – 7.75 (m, 0.5H), 7.74 – 7.72 (m, 0.5H), 7.63 – 7.62 (m, 0.5H), 7.61 – 7.59 (m, 0.5H), 7.55 – 7.49 (m, 1H), 7.48 – 7.43 (m, 1H), 7.27 – 7.21 (m, 2H), 7.19 – 7.13 (m, 1H), 7.09 – 7.05 (m, 2H), 5.40 (s, 1H), 2.50 (s, 3H); ^{13}C NMR (100 MHz, DMSO-d_6) δ 155.3, 153.2, 153.2, 145.7, 145.6, 138.4, 138.4, 137.0, 137.0, 135.7, 133.6, 133.6, 131.3, 131.1, 129.3, 129.3, 129.1, 128.7, 128.5, 128.3, 128.2, 128.2, 128.1, 128.0,

127.9, 127.8, 127.7, 126.4, 125.7, 125.2, 125.1, 47.4, 47.4, 21.7, 21.6; HRMS (ESI-TOF) (*m/z*) calculated $C_{23}H_{18}N_3O_3^+$: 384.1348, found 384.1339 $[M + H]^+$.

(*E*)-6-(Hydroxyimino)-10-methoxy-5-phenyl-5,6-dihydrophthalazino[2,3-*a*]cinnoline-8,13-dione + (E)-6-(Hydroxyimino)-11-methoxy-5-phenyl-5,6-dihydrophthalazino[2,3-*a*]cinnoline-8,13-dione (1:3) or (3:1) (42ja). White solid; yield: 63 mg (85%); mp 185−187 °C; ^{1}H NMR (400 MHz, DMSO-d_6) δ 11.67 (s, 0.3H), 11.59 (s, 1H), 8.18 – 8.11 (m, 1.6H), 8.06 (d, J = 8.7 Hz, 1H), 7.65 – 7.57 (m, 2H), 7.55 – 7.51 (m, 1.6H), 7.50 – 7.42 (m, 3H), 7.29 – 7.21 (m, 3H), 7.20 – 7.14 (m, 1.3H), 7.07 (d, J = 7.3 Hz, 2.6H), 5.40 (s, 1.3H), 3.94 (s, 4.2H); ^{13}C NMR (100 MHz, DMSO-d_6) δ 164.2, 164.1, 155.0, 155.0, 153.0, 152.9, 138.4, 138.3, 137.0, 137.0, 133.6, 133.6, 131.4, 130.9, 130.9, 130.8, 130.3, 130.1, 129.3, 129.1, 129.1, 128.3, 128.2, 128.0, 127.9, 127.7, 125.2, 125.0, 122.7, 122.5, 121.7, 121.0, 110.6, 109.9, 56.6, 56.5, 47.5, 47.4; HRMS (ESI-TOF) (*m/z*) calculated $C_{23}H_{18}N_3O_4^+$: 400.1297, found 400.1296 $[M + H]^+$.

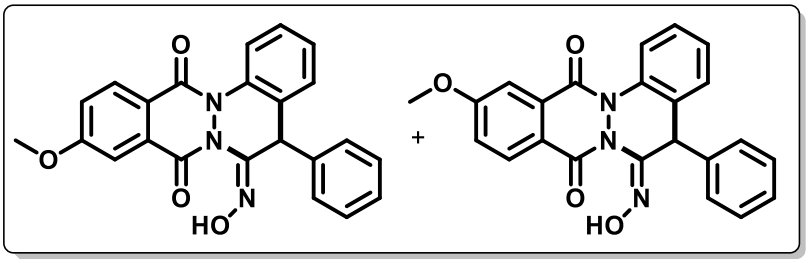

(*E*)-10-(*tert*-Butyl)-6-(hydroxyimino)-5-phenyl-5,6-dihydrophthalazino[2,3-*a*]cinnoline-8,13-dione + (*E*)-11-(*tert*-Butyl)-6-(hydroxyimino)-5-phenyl-5,6-dihydrophthalazino[2,3-*a*]cinnoline-8,13-dione (1:3) or (3:1) (42ka). White solid; yield: 63 mg (88%); mp 133−136 °C; ^{1}H NMR (400 MHz, DMSO-d_6) δ 11.78 (s, 1H), 11.66 (s, 0.3H), 8.19 – 8.15 (m, 0.6H), 8.14 – 8.10 (m, 2H), 8.07 – 8.05 (d, J = 1.7 Hz, 0.3H), 8.04 – 8.00 (m, 1H), 7.96 (dd, J = 8.2, 1.3 Hz, 1H), 7.66 (dd, J = 7.4, 1.4 Hz, 1H), 7.61 (dd, J = 7.4, 1.4 Hz, 0.3H), 7.52 (td, J = 7.6, 1.6 Hz, 1.3 H), 7.45 (td, J = 7.4, 1.2 Hz, 1.3H), 7.30 – 7.20 (m, 3H), 7.20 – 7.12 (m, 1.3 H), 7.10 – 7.07 (m, 0.6 H), 7.03 – 6.98 (m, 2H), 6.22 (s, 1H), 5.41 (s, 0.3H), 1.35 (s, 12H); ^{13}C NMR (100 MHz, DMSO-d_6) δ 158.3, 158.2, 156.1, 155.5, 147.1, 136.9, 136.8, 134.5, 133.5, 132.6, 130.9, 130.0, 129.6, 129.3, 129.1, 128.6, 128.4, 128.3, 128.3, 128.2, 128.0, 127.9, 127.8, 127.7, 127.3, 126.5, 126.3, 125.5, 125.0, 124.2, 123.6, 41.2, 35.7, 31.0, 31.0; HRMS (ESI-TOF) (*m/z*) calculated $C_{26}H_{24}N_3O_3^+$: 426.1817, found 426.1797 $[M + H]^+$.

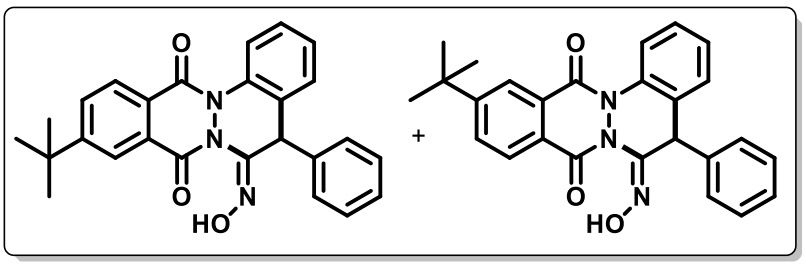

(*E*)-10-Bromo-6-(hydroxyimino)-5-phenyl-5,6-dihydrophthalazino[2,3-*a*]cinnoline-8,13-dione + (*E*)-11-Bromo-6-(hydroxyimino)-5-phenyl-5,6-dihydrophthalazino[2,3-*a*]cinnoline-8,13-dione (1:2) or (2:1) (42la). Pale yellow solid; yield: 44 mg (62%); mp 142−145 °C; ^{1}H NMR

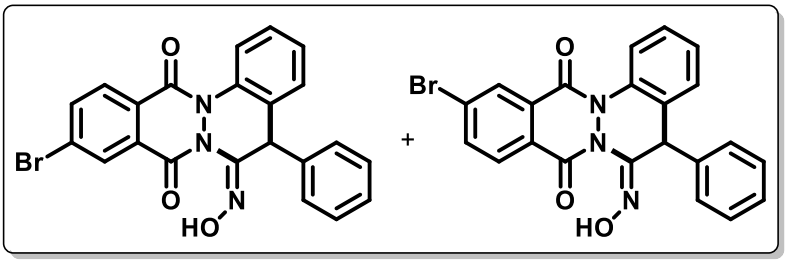

(400 MHz, DMSO-d_6) δ δ 11.83 (s, 0.5H), 11.74 (s, 1H), 8.32 – 8.24 (m, 1H), 8.19 – 8.02 (m, 4H), 7.96 (d, J = 7.9 Hz, 0.5H), 7.69 (d, J = 7.2 Hz, 0.5 H), 7.65 – 7.59 (d, J = 7.2 Hz, 1H), 7.57 – 7.45 (m, 3H), 7.31 – 7.14 (m, 5H), 7.08 (d, J = 7.5 Hz, 2H), 6.99 (d, J = 7.6 Hz, 1H), 6.23 (s, 0.5 H), 5.43 (s, 1H); ^{13}C NMR (100 MHz, DMSO-d_6) δ 154.1, 152.6, 146.9, 138.1, 137.8, 137.8, 136.8, 136.6, 134.3, 133.4, 131.2, 130.7, 130.6, 130.5, 130.4, 130.2, 130.2, 129.6, 129.4, 129.3, 129.1, 129.0, 128.9, 128.7, 128.5, 128.3, 128.0, 127.9, 127.7, 127.2, 127.0, 125.6, 125.1, 47.2; HRMS (ESI-TOF) (*m/z*) calculated $C_{22}H_{15}BrN_3O_3^+$: 448.0296, found 448.0280 $[M + H]^+$.

(*E*)-6-(Hydroxyimino)-5-(4-methylphenyl)-5,6-dihydrophthalazino[2,3-*a*]cinnoline-8,13-dione (42ab). White solid; yield: 63 mg (79%); mp 197−199 °C; ^{1}H NMR (400 MHz, DMSO-d_6) δ 11.76 (s, 1H), 8.22 – 8.15 (m, 2H), 8.00 – 7.90 (m, 3H), 7.64 (dd, J = 7.4, 1.3 Hz, 1H), 7.51 (td, J = 7.6, 1.6 Hz, 1H), 7.45 (td, J = 7.4, 1.2 Hz, 1H), 7.03 (d, J = 8.0 Hz, 2H), 6.88 (d, J = 8.0 Hz, 2H), 6.16 (s, 1H), 2.14 (s, 3H); ^{13}C NMR (100 MHz, DMSO-d_6) δ 155.8, 155.5, 147.1, 137.0, 134.9, 134.9, 134.4, 133.7, 130.3, 129.8, 129.6, 128.7, 128.6, 128.4, 128.4, 128.3, 128.3, 127.2, 125.6, 40.9, 20.9; HRMS (ESI-TOF) (*m/z*) calculated $C_{23}H_{18}N_3O_3^+$: 384.1348, found 384.1323 $[M + H]^+$.

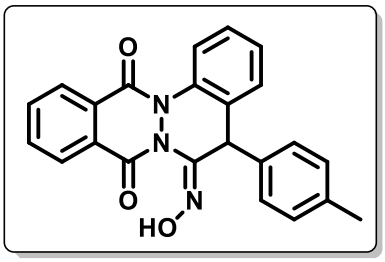

(*E*)-6-(Hydroxyimino)-5-(4-methoxyphenyl)-5,6-dihydrophthalazino[2,3-*a*]cinnoline-8,13-dione (42ac). White solid; yield: 69 mg (82%); mp 141−143 °C; ^{1}H NMR (400 MHz, DMSO-d_6) δ 11.63 (s, 1H), 8.24 – 8.20 (m, 1H), 8.18 – 8.12 (m, 2H), 7.96 – 7.91 (m, 2H), 7.59 (dd, J = 7.5, 1.7 Hz, 1H), 7.51 (td, J = 7.5, 1.7 Hz, 1H), 7.45 (td, J = 7.4, 1.3 Hz, 1H), 7.02 – 6.97 (m, 2H), 6.83 – 6.77 (m, 2H), 5.32 (s, 1H), 3.62 (s, 3H); ^{13}C NMR (100 MHz, DMSO-d_6) δ 158.9, 155.2, 153.1, 138.5, 134.9, 133.5,

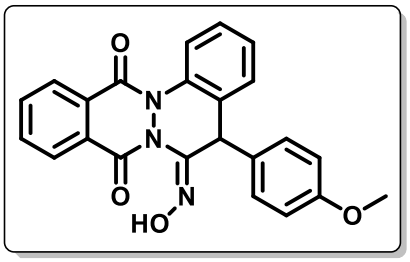

131.4, 129.3, 128.9, 128.7, 128.5, 128.2, 128.1, 127.9, 125.1, 114.5, 55.4, 46.7; HRMS (ESI-TOF) (*m/z*) calculated $C_{23}H_{18}N_3O_4^+$: 400.1297, found 400.1272 $[M + H]^+$.

(*E*)-5-(4-(Dimethylamino)phenyl)-6-(hydroxyimino)-5,6-dihydrophthalazino[2,3-*a*]cinnoline-8,13-dione (42ad). Pale yellow solid; yield: 71 mg (82%); mp 151−153 °C; ^{1}H NMR

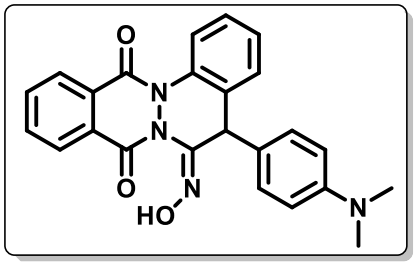

(400 MHz, DMSO-d_6) δ 11.60 (s, 1H), 8.25 – 8.20 (m, 1H), 8.19 – 8.11 (m, 2H), 8.02 – 7.91 (m, 2H), 7.57 (d, J = 7.2 Hz, 1H), 7.53 – 7.40 (m, 2H), 6.86 (d, J = 8.4 Hz, 2H), 6.55 (d, J = 8.5 Hz, 2H), 5.22 (s, 1H), 2.76 (s, 6H); ^{13}C NMR (100 MHz, DMSO-d_6) δ 155.2, 153.0, 149.9, 138.8, 134.9, 133.4, 131.8, 129.2, 128.9, 128.5, 128.3, 128.2, 128.1, 128.0, 127.9, 125.1, 123.7, 112.6, 46.7; HRMS (ESI-TOF) (*m/z*) calculated $C_{24}H_{21}N_4O_3^+$: 413.1613, found 413.1591 $[M + H]^+$.

(*E*)-6-(Hydroxyimino)-5-(4-hydroxyphenyl)-5,6-dihydrophthalazino[2,3-*a*]cinnoline-8,13-dione (42ae). Pale yellow solid; 68 mg (84%); mp 183−186 °C; ^{1}H NMR (400 MHz, DMSO-d_6)

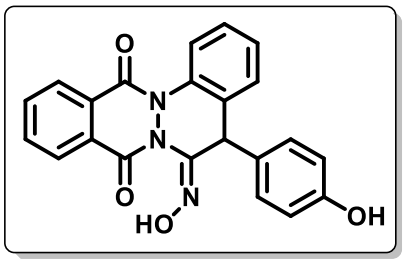

δ 11.58 (s, 1H), 9.36 (s, 1H), 8.25 – 8.19 (m, 1H), 8.16 – 8.10 (m, 2H), 8.00 – 7.90 (m, 2H), 7.58 (dd, J = 7.4 Hz, 1.8, 1H), 7.53 – 7.40 (m, 2H), 6.85 (d, J = 8.2 Hz, 2H), 6.63 – 6.55 (m, 2H), 5.25 (s, 1H); ^{13}C NMR (100 MHz, DMSO-d_6) δ 157.0, 155.2, 153.1, 138.7, 134.9, 133.4, 131.7, 129.2, 128.8, 128.4, 128.2, 128.1, 128.1, 127.9, 126.9, 125.2, 115.8, 46.8; HRMS (ESI-TOF) (*m/z*) calculated $C_{22}H_{16}N_3O_4^+$: 386.1140, found 386.1125 $[M + H]^+$.

(*E*)-5-(4-Fluorophenyl)-6-(hydroxyimino)-5,6-dihydrophthalazino[2,3-*a*]cinnoline-8,13-dione (42af). Pale yellow solid; yield: 49 mg (60%); mp 153−157 °C; ^{1}H NMR (400 MHz, DMSO-

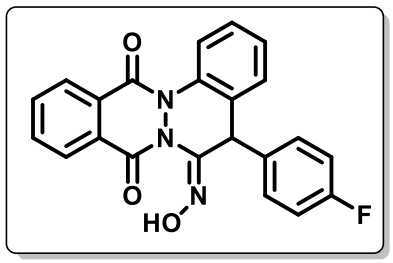

d_6) δ 11.71 (s, 1H), 8.25 – 8.11 (m, 3H), 7.99 – 7.90 (m, 2H), 7.59 (d, J = 7.4 Hz, 1H), 7.52 (t, J = 7.6 Hz, 1H), 7.45 (t, J = 7.4 Hz, 1H), 7.10 (d, J = 7.1 Hz, 4H), 5.42 (s, 1H); ^{13}C NMR (100 MHz, DMSO-d_6) δ 161.8 ($^1J_{C\text{-}F}$ = 242.4 Hz), 155.4, 153.3, 138.2, 134.9, 133.5, 133.3, 130.8, 129.9, 129.8, 129.3, 128.9, 128.5, 128.4, 128.2, 128.0, 127.9, 124.9, 116.0 ($^2J_{C\text{-}F}$ = 21.2 Hz), 46.6; ^{19}F NMR (376 MHz, DMSO-d_6) δ -110.18; HRMS (ESI-TOF) (*m/z*) calculated $C_{22}H_{15}FN_3O_3^+$: 388.1097, found 388.1064 $[M + H]^+$.

(*E*)-5-(4-Chlorophenyl)-6-(hydroxyimino)-5,6-dihydrophthalazino[2,3-*a*]cinnoline-8,13-dione (42ag). Pale yellow solid; yield: 52 mg (61%); mp 168−171 °C; ^{1}H NMR (400 MHz, DMSO-d_6) δ 11.77 (s, 1H), 8.25 – 8.18 (m, 2H), 8.16 – 8.12 (m, 1H), 8.00 – 7.92 (m, 2H), 7.59 (dd, J = 7.6, 1.7 Hz, 1H), 7.52 (td, J = 7.6, 1.4 Hz, 1H), 7.45 (td, J = 7.4, 1.0 Hz, 1H), 7.34 (d, J = 8.5 Hz, 2H), 7.10 (d, J = 8.4 Hz, 2H), 5.44 (s, 1H); ^{13}C NMR (100 MHz, DMSO-d_6) δ 155.4, 153.4, 138.0, 136.2, 135.0, 133.6, 132.7, 130.4, 129.7, 129.4, 129.2, 128.9, 128.5, 128.5, 128.2, 128.0, 127.9, 124.9, 46.7; HRMS (ESI-TOF) (*m/z*) calculated $C_{22}H_{15}ClN_3O_3^+$: 404.0801, found 404.0784 $[M + H]^+$.

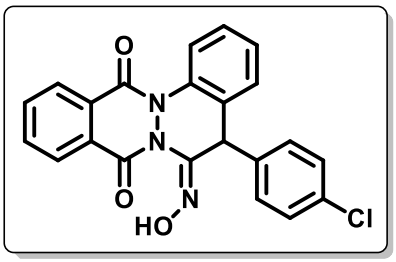

(*E*)-5-(3-Ethoxy-4-hydroxyphenyl)-6-(hydroxyimino)-5,6-dihydrophthalazino[2,3-*a*]cinnoline-8,13-dione (42ak). Pale yellow solid; yield: 70 mg (78%); mp 203−206 °C; ^{1}H NMR (400 MHz, DMSO-d_6) δ 11.58 (s, 1H), 8.88 (s, 1H), 8.23 – 8.19 (m, 1H), 8.17 – 8.13 (m, 1H), 8.10 (dd, J = 8.1, 1.3 Hz, 1H), 7.98 – 7.91 (m, 2H), 7.60 (dd, J = 7.4, 1.5 Hz, 1H), 7.51 (td, J = 7.6, 1.8 Hz, 1H), 7.45 (td, J = 7.4, 1.4 Hz, 1H), 6.63 (d, J = 2.6 Hz, 1H), 6.60 (d, J = 8.2 Hz, 1H), 6.36 (dd, J = 8.2, 1.3 Hz, 1H), 5.25 (s, 1H), 3.82 – 3.71 (m, 2H), 1.16 (t, J = 7 Hz, 3H); ^{13}C NMR (100 MHz, DMSO-d_6) δ 155.1, 153.2, 146.9, 146.5, 138.7, 134.9, 133.3, 131.9, 129.1, 128.8, 128.4, 128.3, 128.2, 128.1, 127.8, 127.3, 125.5, 120.3, 116.1, 113.2, 64.2, 47.0, 14.9; HRMS (ESI-TOF) (*m/z*) calculated $C_{24}H_{20}N_3O_5^+$: 430.1402, found 430.1388 $[M + H]^+$.

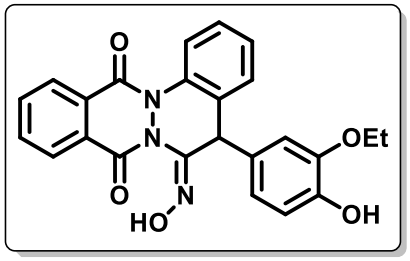

(*E*)-6-(Hydroxyimino)-5-(naphthalen-1-yl)-5,6-dihydrophthalazino[2,3-*a*]cinnoline-8,13-dione (42al). White solid; yield: 77 mg (88%); mp 202−204 °C; ^{1}H NMR (400 MHz, DMSO-d_6) δ 11.74 (s, 1H), 8.55 (d, J = 7.8 Hz, 1H), 8.29 (t, J = 8.2 Hz, 2H), 7.97 – 7.82 (m, 4H), 7.76 (d, J = 8.2 Hz, 1H), 7.67 (t, J = 7.5 Hz, 1H), 7.58 (t, J = 7.6 Hz, 3H), 7.46 (t, J = 7.6 Hz, 1H), 7.24 (t, J = 7.6 Hz, 1H), 6.80 (d, J = 6.5 Hz, 1H), 6.14 (s, 1H); ^{13}C NMR (100 MHz, DMSO-d_6) δ 155.5, 152.6, 138.7, 134.8, 134.8, 134.3, 134.0, 132.1, 131.9, 130.9, 129.3, 129.0, 128.9, 128.5, 128.4, 128.4, 127.9, 127.7, 126.8, 126.5, 125.5, 124.8, 124.7, 45.4; HRMS (ESI-TOF) (*m/z*) calculated $C_{26}H_{18}N_3O_3^+$: 420.1348, found 420.1333 $[M + H]^+$.

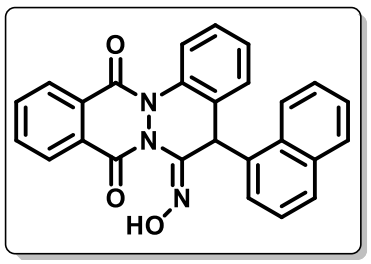

(*E*)-5-([1,1'-Biphenyl]-4-yl)-6-(hydroxyimino)-5,6-dihydrophthalazino[2,3-*a*]cinnoline-8,13-dione (42am). White solid; yield: 74 mg (80%); mp 176−177 °C; ^{1}H NMR (400 MHz, DMSO-d_6)

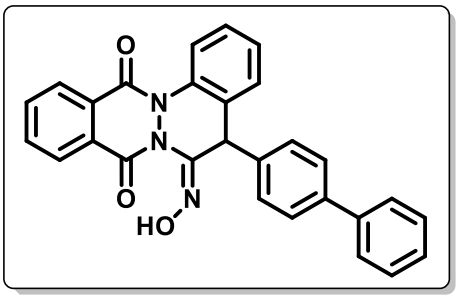

δ 11.72 (s, 1H), 8.26 – 8.18 (m, 2H), 8.17 – 8.11 (m, 1H), 7.98 – 7.91 (m, 2H), 7.66 – 7.44 (m, 7H), 7.39 (t, J = 7.4 Hz, 2H), 7.30 (t, J = 7.2 Hz, 1H), 7.18 (d, J = 8.0 Hz, 2H), 5.45 (s, 1H); ^{13}C NMR (100 MHz, DMSO-d_6) δ 155.4, 153.3, 139.6, 139.5, 138.2, 136.4, 134.9, 133.6, 130.9, 129.5, 129.3, 128.9, 128.5, 128.4, 128.3, 128.2, 128.1, 128.0, 127.9, 127.3, 127.0, 124.9, 47.1; HRMS (ESI-TOF) (*m/z*) calculated $C_{28}H_{20}N_3O_3^+$: 446.1504, found 446.1478 $[M + H]^+$.

(*E*)-6-(Hydroxyimino)-5-(thiophen-2-yl)-5,6-dihydrophthalazino[2,3-*a*]cinnoline-8,13-dione (42ao). Pale yellow solid; yield: 59 mg, (75%); mp 146−144 °C; ^{1}H NMR (400 MHz, DMSO-d_6)

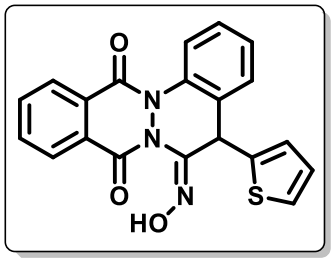

δ 11.72 (s, 1H), 8.31 – 8.24 (m, 1H), 8.21 – 8.13 (m, 2H), 8.02 – 7.94 (m, 2H), 7.63 (dd, J = 7.6, 1.7 Hz, 1H), 7.55 – 7.48 (m, 1H), 7.43 (td, J = 7.5, 1.3 Hz, 1H), 7.36 (dd, J = 5.0, 1.3 Hz, 1H), 6.92 – 6.87 (m, 1H), 6.85 – 6.79 (m, 1H), 5.64 (s, 1H); ^{13}C NMR (100 MHz, DMSO-d_6) δ 155.3, 153.2, 140.2, 137.6, 135.0, 132.9, 131.7, 129.0, 128.6, 128.5, 128.4, 128.2, 128.1, 127.9, 127.6, 126.8, 126.4, 125.4, 43.3; HRMS (ESI-TOF) (*m/z*) calculated $C_{20}H_{14}N_3O_3S^+$: 376.0755, found 376.0734 $[M + H]^+$.

(*E*)-5-(Furan-2-yl)-6-(hydroxyimino)-5,6-dihydrophthalazino[2,3-*a*]cinnoline-8,13-dione (42ap). Pale yellow solid; yield: 54 mg (72%); mp 170−171 °C; ^{1}H NMR (400 MHz, DMSO-d_6)

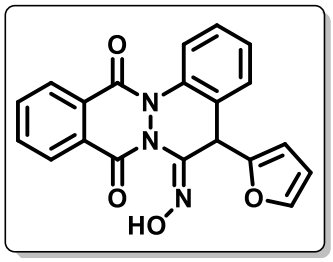

δ 11.76 (s, 1H), 8.32 – 8.27 (m, 1H), 8.21 – 8.14 (m, 2H), 8.04 – 7.95 (m, 2H), 7.60 (d, J = 7.1, 1H) 7.54 – 7.48 (m, 2H), 7.42 (t, J = 7.3 Hz, 1H), 6.32 – 6.27 (m, 1H), 6.04 (d, J = 3.0 Hz, 1H), 5.47 (s, 1H); ^{13}C NMR (100 MHz, DMSO-d_6) δ 155.5, 153.3, 150.4, 136.6, 134.9, 133.3, 129.4, 129.0, 128.7, 128.6, 128.4, 128.1, 128.1, 127.9, 125.0, 111.1, 107.9, 42.0; HRMS (ESI-TOF) (*m/z*) calculated $C_{20}H_{14}N_3O_4^+$: 360.0984, found 360.0977 $[M + H]^+$.

(*E*)-6-(Hydroxyimino)-5-(1*H*-indol-3-yl)-5,6-dihydrophthalazino[2,3-*a*]cinnoline-8,13-dione (42aq). Pale yellow solid; yield: 64 mg (74%); mp 147−148 °C; ^{1}H NMR (400 MHz, DMSO-d_6)

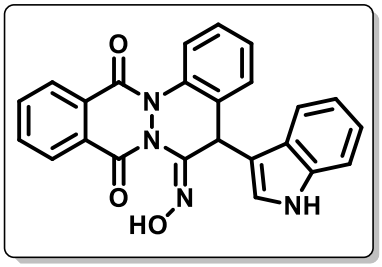

δ 11.55 (s, 1H), 10.87 (d, J = 2.6 Hz, 1H), 8.28 – 8.23 (m, 1H), 8.16 (dd, J = 8.3, 1.2 Hz, 1H), 8.08 – 8.03 (m, 1H), 7.98 – 7.88 (m, 2H), 7.64 – 7.57 (m, 2H), 7.51 (td, J = 7.6, 1.7 Hz, 1H), 7.43 (td, J = 7.4, 1.1 Hz, 1H), 7.27 (d, J = 8.0 Hz, 1H), 7.10 – 7.04 (m, 1H), 7.02 – 6.97 (m, 1H), 6.64 (d, J = 1.7 Hz, 1H), 5.49 (s, 1H); ^{13}C NMR (100 MHz, DMSO-d_6) δ 155.5, 152.8, 138.9, 136.8, 134.8, 133.5, 132.2, 128.9, 128.6, 128.4, 128.2, 128.2, 127.9, 127.9, 126.6, 125.2, 123.4, 122.0, 119.4, 119.3, 112.0, 110.4, 40.7; HRMS (ESI-TOF) (*m/z*) calculated $C_{24}H_{17}N_4O_3^+$: 409.1300, found 409.1276 $[M + H]^+$.

(*Z*)-5-Hexyl-6-(hydroxyimino)-5,6-dihydrophthalazino[2,3-*a*]cinnoline-8,13-dione (42ar).

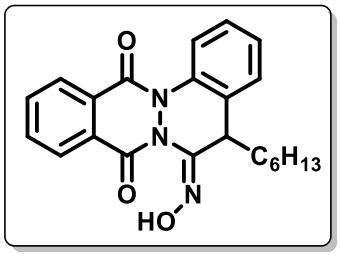

White solid; yield: 44 mg (56%); mp 62–63 °C; ^{1}H NMR (400 MHz, DMSO-d_6) δ 11.44 (s, 1H), 8.32 – 8.20 (m, 3H), 8.01 – 7.99 (m, 2H), 7.44 – 7.33 (m, 3H), 3.89 – 3.85 (m, 1H), 1.73 – 1.65 (m, 2H), 1.45 – 1.19 (m, 8H), 0.79 (t, J = 6.7 Hz, 3H); ^{13}C NMR (100 MHz, DMSO-d_6) δ 155.7, 153.4, 138.9, 134.7, 134.7, 133.0, 132.4, 129.5, 128.5, 128.5, 128.2, 127.8, 127.6, 127.5, 124.2, 43.0, 31.5, 31.4, 28.5, 27.1, 22.4, 14.3; HRMS (ESI-TOF) (*m/z*) calculated $C_{22}H_{24}N_3O_3^+$: 378.1812, found 378.1778 $[M + H]^+$.

Procedure for the synthesis of [Cp*Rh(Phthalazine-dione)DMSO] complex (44C′)]

To an oven-dried sealed tube with a screw cap (PTFE), **1a** (2 equiv), $[Cp^*RhCl_2]_2$ (1 equiv), NaOAc (5 equiv), Na_2CO_3 (2 equiv) and DCM (5 mL) were added. The sealed tube was tightly capped after purging with N_2 gas and the reaction was allowed to stir on a magnetic stirrer at 25 °C for 12 h. The reaction mixture was filtered through celite pad and washed with excess DCM. The combined organic layers were concentrated under reduced pressure to reduced its volume of 1 mL. To this, DMSO (1 mL) was added and the reaction was allowed to settle down for 12 h. Later, the reaction mixture quenched with water and extracted with DCM (2 x 15 mL). The organic layers were combined, dried over anhydrous sodium sulphate and concentrated under reduced pressure afforded the desired complex in 71% yield.

Orange solid; yield: 41 mg (71%); mp 165−166 °C; ^{1}H NMR (400 MHz, $CDCl_3$) δ 8.53 (d, J = 8 Hz, 1H), 8.47 – 8.39 (m, 1H), 8.24 – 8.17 (m, 1H), 7.80 – 7.70 (m, 2H), 7.57 (d, J = 7.1 Hz, 1H), 7.19 (t, J = 7.2 Hz, 1H), 7.11 (t, J = 7.0 Hz, 1H), 3.61 (s, 3H), 2.16 (s, 3H), 1.68 (s, 15H); ^{13}C NMR (100 MHz, $CDCl_3$) δ 162.9, 159.0, 151.3, 151.0, 147.3, 135.8, 132.6, 131.4, 130.0, 129.5, 129.5, 127.4, 126.0, 125.2, 119.0, 101.0, 100.9, 9.4; HRMS (ESI-TOF) (*m/z*) calculated $C_{26}H_{30}RhSN_2O_3^+$: 553.1032, found 553.1062 $[M + H]^+$.

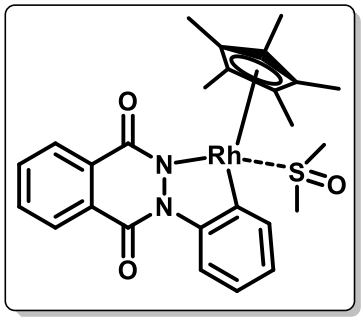

Isotope labelling experiment

To an oven-dried sealed tube with a screw cap (PTFE) containing **1b** (50 mg, 1 equiv) in CD_3OD (2 mL), $[Cp^*RhCl_2]_2$ (0.025 equiv), NaOAc (0.5 equiv) were added under a nitrogen atmosphere. The reaction was allowed to stir at 80 ºC for 6 h. The reaction was cooled to room temperature, quenched with water and extracted with DCM (2 x 15 mL). The organic layers were combined, dried over anhydrous sodium sulphate and concentrated under reduced pressure. Purification by column chromatography using ethyl acetate/hexanes (3:7) as eluent afforded the desired product (**1b**/**1b**-***d*$_2$**) in 77% yield. The deuteration content was confirmed using ^{1}H NMR analysis.

Kinetic Isotope Effect studies using parallel experiments

For the first set, to an oven-dried sealed tube with a screw cap (PTFE), **1b** (25.23 mg, 0.1 mmol), $[Cp^*RhCl_2]_2$ (1.54 mg, 0.0025 mmol), NaOAc (4.13 mg, 0.05 mmol), nitrostyrene (**8a**) (22.37 mg, 0.15 mmol) and ethanol (5 mL) were added under nitrogen atmosphere. For the parallel second set, **1b**-***d*$_2$** (25.43 mg, 0.1 mmol) was used (instead of **1b**) under standard conditions. The sealed tubes were capped and the reaction mixtures were allowed to stir at 80 ºC for 15, 30, 45, 60 and 75 mins. Reaction fractions were collected at regular time intervals, filtered and concentrated under reduced pressure. The product conversion percentage was determined by ^{1}H NMR analysis. The KIE was calculated as k_H/k_D = 0.75.

2.4 Single Crystal X-ray Diffraction Studies

Using a suitable crystal mounted in a nylon loop that was attached to a goniometer head, initial crystal evaluation and data collection of each compound were performed on a Kappa APEX II diffractometer equipped with a CCD detector (with the crystal-to-detector distance fixed at 60 mm) and sealed-tube monochromated Mo$K\alpha$ radiation using the program APEX2.[58] Data were integrated, reflections were fitted and values of F^2 and $\sigma(F^2)$ for each reflection were obtained by

using the program SAINT.[58] Data were also corrected for Lorentz and polarization effects. The subroutine XPREP[58] was used for the processing of data that included determination of space group, application of an absorption correction (SADABS),[58] merging of data, and generation of files necessary for solution and refinement. The crystal structure was solved by direct methods using the SHELXS program of the SHELXTL package and was refined using SHELXL.[59,60] All non-hydrogen atoms were refined with anisotropic displacement parameters. All hydrogen atoms for **42ba** were placed in ideal positions and refined as riding atoms with individual isotropic displacement parameters. All figures were drawn using MERCURY V 3.0.[61]

2.4.1 Crystal data for 42ba·CHCl$_3$ (CCDC No. 2040955). $C_{24}H_{18}Cl_3N_3O_3$, Mr = 502.76 g/mol,

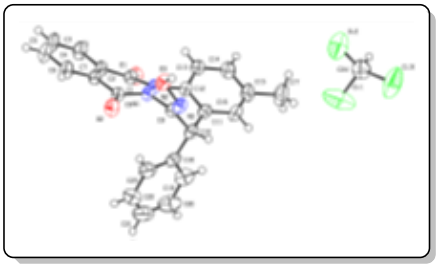

triclinic, space group $P\bar{1}$, a = 8.6451(14) Å, b = 11.0685(5) Å, c = 12.210(2) Å, α = 92.777(2)°, β = 102.505(2)°, γ = 90.319(2)°, V = 1139.1(3) Å^3, Z = 2, D_{calcd} = 1.466 g/cm^3, T = 296(2) K; Full matrix least-square on F^2; R_1 = 0.0551, wR_2 = 0.1482 for 3525 observed reflections [$I > 2\sigma(I)$] and R_1 = 0.0616, wR_2 = 0.1543 for all 4033 reflections; GOF = 1.043.

2.5 References

(1) Daugulis, O.; Roane, J.; Tran, L. D. *Accounts of Chemical Research* **2015**, *48*, 1053-1064.

(2) Ghorai, D.; Dutta, C.; Choudhury, J. *ACS Catalysis* **2016**, *6*, 709-713.

(3) Chen, F.; Wang, T.; Jiao, N. *Chemical Reviews* **2014**, *114*, 8613-8661.

(4) Yamaguchi, J.; Yamaguchi, A. D.; Itami, K. *Angewandte Chemie International Edition* **2012**, *51*, 8960-9009.

(5) Gensch, T.; Hopkinson, M.; Glorius, F.; Wencel-Delord, J. *Chemical Society Reviews* **2016**, *45*, 2900-2936.

(6) Satoh, T.; Miura, M. *Chemistry–A European Journal* **2010**, *16*, 11212-11222.

(7) Song, G.; Wang, F.; Li, X. *Chemical Society Reviews* **2012**, *41*, 3651-3678.

(8) Yang, L.; Huang, H. *Chemical Reviews* **2015**, *115*, 3468-3517.

(9) Ye, B.; Cramer, N. *Accounts of Chemical Research* **2015**, *48*, 1308-1318.

(10) Chen, Z.; Wang, B.; Zhang, J.; Yu, W.; Liu, Z.; Zhang, Y. *Organic Chemistry Frontiers* **2015**, *2*, 1107-1295.

(11) Sambiagio, C.; Schönbauer, D.; Blieck, R.; Dao-Huy, T.; Pototschnig, G.; Schaaf, P.; Wiesinger, T.; Zia, M. F.; Wencel-Delord, J.; Besset, T. *Chemical Society Reviews* **2018**, *47*, 6603-6743.

(12) Colby, D. A.; Tsai, A. S.; Bergman, R. G.; Ellman, J. A. *Accounts of Chemical Research* **2012**, *45*, 814-825.

(13) Kuhl, N.; Schroeder, N.; Glorius, F. *Advanced Synthesis & Catalysis* **2014**, *356*, 1443-1460.

(14) Song, G.; Li, X. *Accounts of Chemical Research* **2015**, *48*, 1007-1020.

(15) Wang, F.; Yu, S.; Li, X. *Chemical Society Reviews* **2016**, *45*, 6462-6477.

(16) Lewgowd, W.; Stanczak, A. *Archiv der Pharmazie: An International Journal Pharmaceutical and Medicinal Chemistry* **2007**, *340*, 65-80.

(17) Barraja, P.; Diana, P.; Lauria, A.; Passannanti, A.; Almerico, A. M.; Minnei, C.; Longu, S.; Congiu, D.; Musiu, C.; La Colla, P. *Bioorganic & Medicinal Chemistry* **1999**, *7*, 1591-1596.

(18) Zhang, X.; Bai, R.; Xiong, H.; Xu, H.; Hou, W. *Bioorganic & Medicinal Chemistry Letters* **2020**, *30*, 126916.

(19) Parasuraman, P.; Shanmugarajan, R.; Aravazhi, T.; Nehru, K.; Mathiazhaga, T.; Rajakumari, R. *International Journal of Pharmacy & Life Sciences* **2012**, *3*.

(20) Bommagani, M. B.; Mokenapelli, S.; Yerrabelli, J. R.; Boda, S. K.; Chitneni, P. R. *Synthetic Communications* **2020**, *50*, 1016-1025.

(21) Gavini, E.; Juliano, C.; Mulè, A.; Pirisino, G.; Murineddu, G.; Pinna, G. A. *Archiv der Pharmazie: An International Journal Pharmaceutical and Medicinal Chemistry* **2000**, *333*, 341-346.

(22) Stańczak, A.; Ochocki, Z.; Martynowski, D.; Główka, M.; Nawrot, E. *Archiv der Pharmazie: An International Journal Pharmaceutical and Medicinal Chemistry* **2003**, *336*, 18-30.

(23) Ryu, C.-K.; Lee, J. Y. *Bioorganic & Medicinal Chemistry Letters* **2006**, *16*, 1850-1853.

(24) Tonk, R. K.; Bawa, S.; Chawla, G.; Deora, G. S.; Kumar, S.; Rathore, V.; Mulakayala, N.; Rajaram, A.; Kalle, A. M.; Afzal, O. *European Journal of Medicinal Chemistry* **2012**, *57*, 176-184.

(25) Stefańska, B.; Arciemiuk, M.; Bontemps-Gracz, M. M.; Dzieduszycka, M.; Kupiec, A.; Martelli, S.; Borowski, E. *Bioorganic & Medicinal Chemistry* **2003**, *11*, 561-572.

(26) Ruchelman, A. L.; Singh, S. K.; Ray, A.; Wu, X.; Yang, J.-M.; Zhou, N.; Liu, A.; Liu, L. F.; LaVoie, E. J. *Bioorganic & Medicinal Chemistry* **2004**, *12*, 795-806.

(27) Yu, Y.; Singh, S. K.; Liu, A.; Li, T.-K.; Liu, L. F.; LaVoie, E. J. *Bioorganic & Medicinal Chemistry* **2003**, *11*, 1475-1491.

(28) Tsuji, H.; Yokoi, Y.; Sato, Y.; Tanaka, H.; Nakamura, E. *Chemistry–An Asian Journal* **2011**, *6*, 2005-2008.

(29) Sivaraj, C.; Ramkumar, A.; Sankaran, N.; Gandhi, T. *Organic & Biomolecular Chemistry* **2021**, *19*, 8165-8183.

(30) Rajkumar, S.; Savarimuthu, S. A.; Kumaran, R. S.; Nagaraja, C.; Gandhi, T. *Chemical Communications* **2016**, *52*, 2509-2512.

(31) Mayakrishnan, S.; Arun, Y.; Balachandran, C.; Emi, N.; Muralidharan, D.; Perumal, P. T. *Organic & Biomolecular Chemistry* **2016**, *14*, 1958-1968.

(32) Cai, P.; Zhang, E.; Wu, Y.; Fang, T.; Li, Q.; Yang, C.; Wang, J.; Shang, Y. *ACS Omega* **2018**, *3*, 14575-14584.

(33) Berner, O. M.; Tedeschi, L.; Enders, D. *European Journal of Organic Chemistry* **2002**, *2002*, 1877-1894.

(34) Nair, D. K.; Kumar, T.; Namboothiri, I. N. *Synlett* **2016**, *27*, 2425-2442.

(35) Halimehjani, A. Z.; Namboothiri, I. N.; Hooshmand, S. E. *RSC Advances* **2014**, *4*, 31261-31299.

(36) Denmark, S. E.; Thorarensen, A. *Chemical Reviews* **1996**, *96*, 137-166.

(37) Barrett, A. G.; Graboski, G. G. *Chemical Reviews* **1986**, *86*, 751-762.

(38) FEUER, H.; MILLER, R.; LAWYER, C. B. *The Journal of Organic Chemistry* **1961**, *26*, 1357-1360.

(39) Ono, N.; Kamimura, A.; Kaji, A. *The Journal of Organic Chemistry* **1988**, *53*, 251-258.

(40) DRAKE, N. L.; ROSS, A. B. *The Journal of Organic Chemistry* **1958**, *23*, 717-720.

(41) Varma, R.; Kabalka, G. *Heterocycles (Sendai)* **1986**, *24*, 2645-2677.

(42) Potter, T. J.; Kamber, D. N.; Mercado, B. Q.; Ellman, J. A. *ACS Catalysis* **2017**, *7*, 150-153.

(43) Bai, D.; Jia, Q.; Xu, T.; Zhang, Q.; Wu, F.; Ma, C.; Liu, B.; Chang, J.; Li, X. *The Journal of Organic Chemistry* **2017**, *82*, 9877-9884.

(44) Potter, T. J.; Li, Y.; Ward, M. D.; Ellman, J. A. *European Journal of Organic Chemistry* **2018**, *2018*, 4381-4388.

(45) Lv, N.; Chen, Z.; Liu, Y.; Liu, Z.; Zhang, Y. *Advanced Synthesis & Catalysis* **2019**, *361*, 4140-4146.

(46) Mishra, A.; Mukherjee, U.; Sarkar, W.; Meduri, S. L.; Bhowmik, A.; Deb, I. *Organic Letters* **2019**, *21*, 2056-2059.

(47) Mishra, A.; Bhowmik, A.; Samanta, S.; Sarkar, W.; Das, S.; Deb, I. *Organic Letters* **2020**, *22*, 1340-1344.

(48) Karishma, P.; Mahesha, C. K.; Mandal, S. K.; Sakhuja, R. *The Journal of Organic Chemistry* **2021**, *86*, 2734-2747.

(49) Shi, X. Y.; Renzetti, A.; Kundu, S.; Li, C. J. *Advanced Synthesis & Catalysis* **2014**, *356*, 723-728.

(50) Li, J.; Ackermann, L. *Angewandte Chemie International Edition* **2015**, *54*, 8551-8554.

(51) Tunge, J. A.; Foresee, L. N. *Organometallics* **2005**, *24*, 6440-6444.

(52) Park, C. P.; Nagle, A.; Yoon, C. H.; Chen, C.; Jung, K. W. *The Journal of Organic Chemistry* **2009**, *74*, 6231-6236.

(53) Jalal, S.; Sarkar, S.; Bera, K.; Maiti, S.; Jana, U. *European Journal of Organic Chemistry* **2013**, *2013*, 4823-4828.

(54) Wang, C.; Wang, S. *Synthetic Communications* **2002**, *32*, 3481-3486.

(55) Kumar, M. S.; Rajanna, K.; Reddy, K. R.; Venkateswarlu, M.; Venkanna, P. *Synthetic Communications* **2013**, *43*, 2672-2677.

(56) Ambala, S.; Singh, R.; Singh, M.; Cham, P. S.; Gupta, R.; Munagala, G.; Yempalla, K. R.; Vishwakarma, R. A.; Singh, P. P. *RSC Advances* **2019**, *9*, 30428-30431.

(57) Venkatanna, K.; Kumar, S. Y.; Karthick, M.; Padmanaban, R.; Ramanathan, C. R. *Organic & Biomolecular Chemistry* **2019**, *17*, 4077-4086.

(58) *APEX2*, *SADABS and SAINT*; Bruker AXS inc: Madison, WI, USA, **2008**.

(59) Sheldrick, G. M. *Acta Crystallographica Section A: Foundations and Advances* **2015**, *71*, 3-8.

(60) Sheldrick, G. M. *Acta Crystallographica Section C: Structural Chemistry* **2015**, *71*, 3-8.

(61) Macrae, C. F.; Bruno, I. J.; Chisholm, J. A.; Edgington, P. R.; McCabe, P.; Pidcock, E.; Rodriguez-Monge, L.; Taylor, R.; Streek, J.; Wood, P. A. *Journal of Applied Crystallography* **2008**, *41*, 466-470.

CHAPTER 3

Rhodium-Catalyzed Spirocyclization of *N*-Aryl-2,3-dihydrophthalazine-1,4-diones with Maleimides

3.1 Introduction

Oxidative C–H bond functionalization provides a fascinating and atom-economic process for constructing pharmaceutically and medicinally important compounds.[1-8] In the past two decades, several α,β-unsaturated systems have been used as efficient coupling partners in C-H alkylation and alkenylation reactions.[9-13] In this context, maleimide (an α,β-unsaturated imide) has been recognized as a privileged structural motif that forms an integral part of numerous pharmaceuticals and functional materials.[14-21] Moreover, maleimides can readily be transformed into biologically relevant succinimides, γ-lactams, pyrrolidines and other synthetically modified derivatives, making them one of the most promising organic entities.[22-24] Among these synthetically manipulated organic analogues, succinimide constitute an integral part of many natural products[25-27] such as salfredin C-1, palasimide and potent drugs,[28-37] including phensuximide, lurasidone and thalidomide. Apart from this, succinimide exhibits profound applications in the field of material science,[38] sensors,[39-41] dyes,[42,43] polymers[44] and macromolecules[45]. In addition, numerous spiro-succinimides have been identified as orally potent aldose reductase inhibitors[46] (Figure 3.1.1).

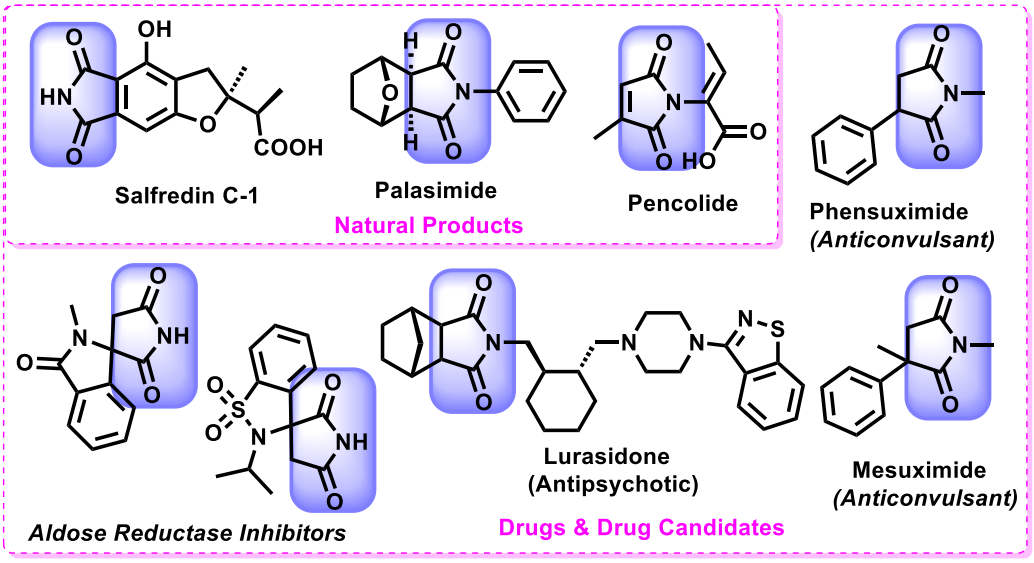

Figure 3.1.1 Succinimide containing natural products, drugs and drug candidates

The delocalization of the double bond with either of the two carbonyl groups provides electron acceptor and dienophile characteristics to the maleimide, which have been successfully explored for the introduction of succinimide moiety *via* cycloaddition,[47,48] conjugate addition,[49-52] anionic/radical polymerization[53] and cross-coupling reactions.[54-56] In addition, substantial efforts have been devoted towards hydroarylation, alkenylation, annulation and spirocyclization of

(hetero)arenes with maleimides *via* transition metal-catalyzed chelation-assisted direct C*(sp²)*–H bond functionalization aided by diversified directing groups (DGs) (Figure 3.1.2).[57,58]

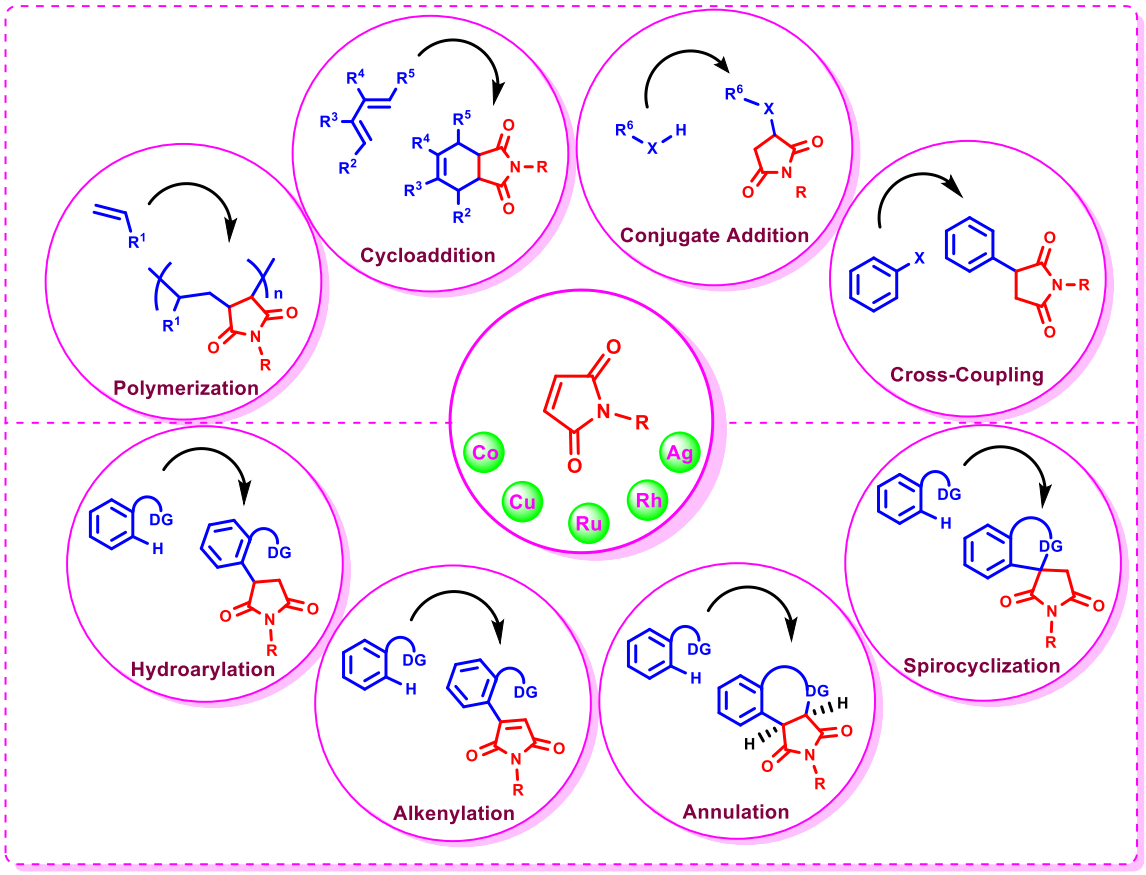

Figure 3.1.2 A pictorial representation depicting various chemical applications of maleimides

For example, in 2015 Miura and coworkers reported 8-aminoquinoline-directed Cu(II)-catalyzed oxidative coupling of benzamides (**1**) with maleimides (**2**) to afford spirocyclized products (**3**) using Cy_2NMe as a base, which enhanced the chemoselectivity and accelerated the reaction (Scheme 3.1.1).[59]

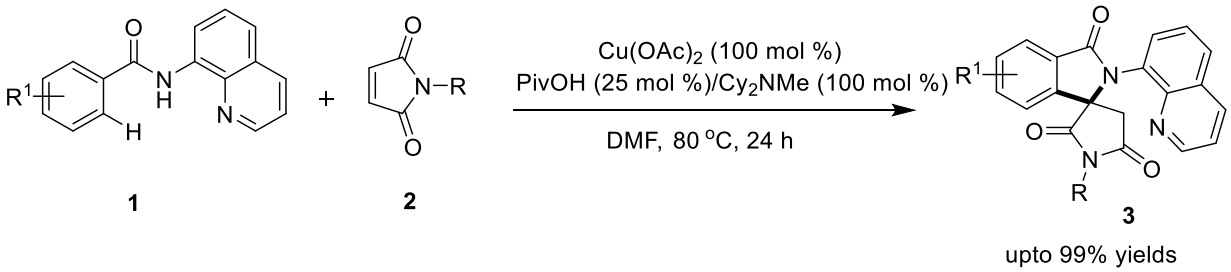

Scheme 3.1.1 Copper-catalyzed spirocyclization of benzamides (**1**) with maleimides (**2**)

In 2018, Zhai's group developed an efficient strategy for the synthesis of regioselective spirosuccinimides (**5**) in high yields *via* Co(II)-catalyzed C*(sp²)*-H functionalization of benzoic

hydrazides (**4**) with maleimides (**2**) (Scheme 3.1.2).[60] The application of 2-(1-methyl-hydrazinyl)pyridine as a directing group enhanced the catalytic efficiency, and could be expediently removed in one step under mild conditions.

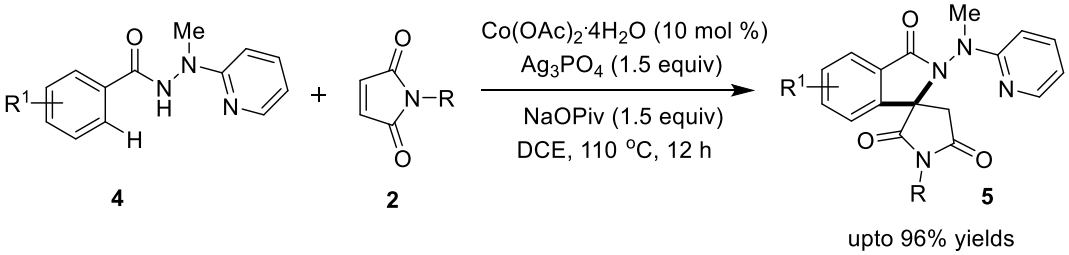

Scheme 3.1.2 Cobalt-catalyzed spirocyclization of benzoic hydrazides (**4**) with maleimides (**2**)

In the same year, Luo *et al.* developed a Rh(III)/Cu(II)-catalyzed [3+2] annulation of cyclic/acyclic aldimines and ketimines (**6**) with maleimides (**2**) leading to tricyclic/tetracyclic spiroannulated products (**7**) in high diastereoselectivity (Scheme 3.1.3).[61]

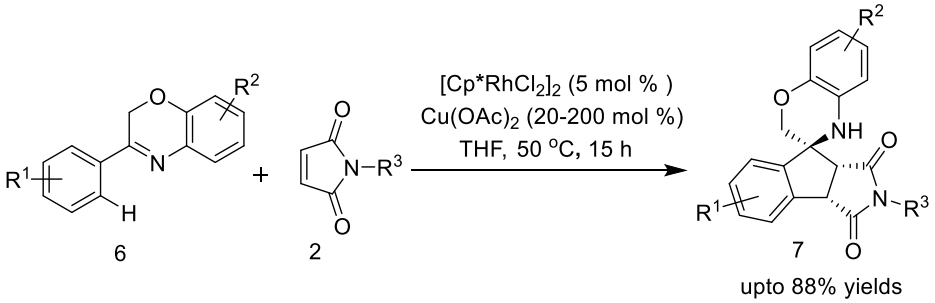

Scheme 3.1.3 Rhodium/Copper-catalyzed spiroannulation of aldimines/ketimines (**6**) with maleimides (**2**)

In contrast, the alkylation of the methyl group in 8-methylquinolines (**8**) was achieved with maleimide (**2**) by Kim's group under Rh(III)-catalyzed C*(sp^3)*–H bond activation (Scheme 3.1.4).[62]

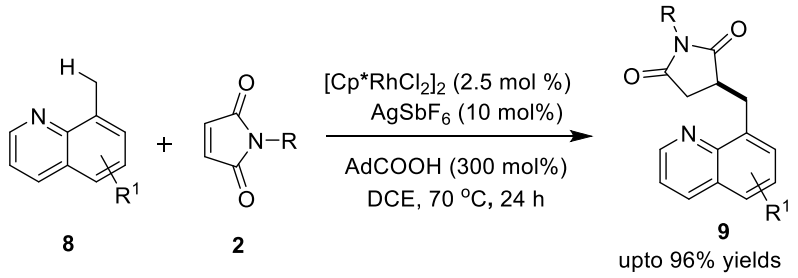

Scheme 3.1.4 Rhodium-catalyzed alkylation of 8-methylquinolines (**8**) with maleimides (**2**)

The same group further accomplished Rh(III)-catalyzed site-selective alkylation of chromones, naphthoquinones and xanthones (**10**) with maleimides (**2**) in appreciable yields (Scheme 3.1.5).[63]

The synthesized derivatives showed a high cytotoxic effect against human breast adenocarcinoma MCF-7 cell lines, with an activity competitive with anticancer agent doxorubicin.

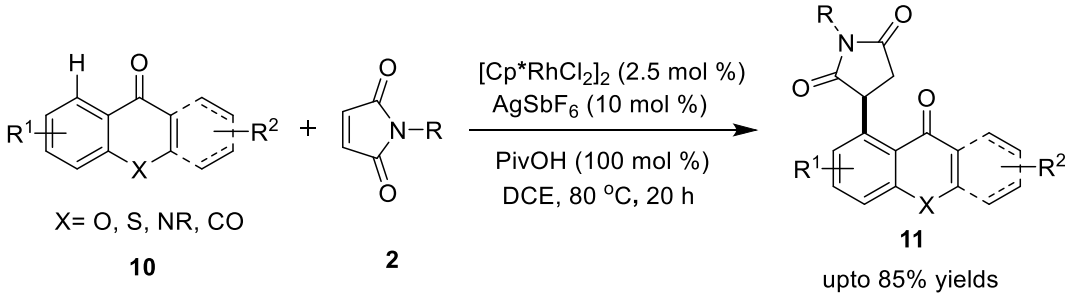

Scheme 3.1.5 Rhodium-catalyzed alkylation of chromones, naphthoquinones and xanthones (**10**) with maleimides (**2**)

Prabhu and co-workers reported elegant Rh(III)-catalyzed switchable strategies for the C-4 alkylation and alkenylation of 3-(trifluoroacetyl)indoles (**12**) with maleimides (**2**), producing oxidative Heck-type alkylative products (**13**) and conjugated addition products (**14**) respectively, using $COCF_3$ as a weak directing group. Acid additive promoted the formation of hydroarylated products (**14**), whereas a base additive paved way for the formation of Heck-type products (**13**) (Scheme 3.1.6).[64]

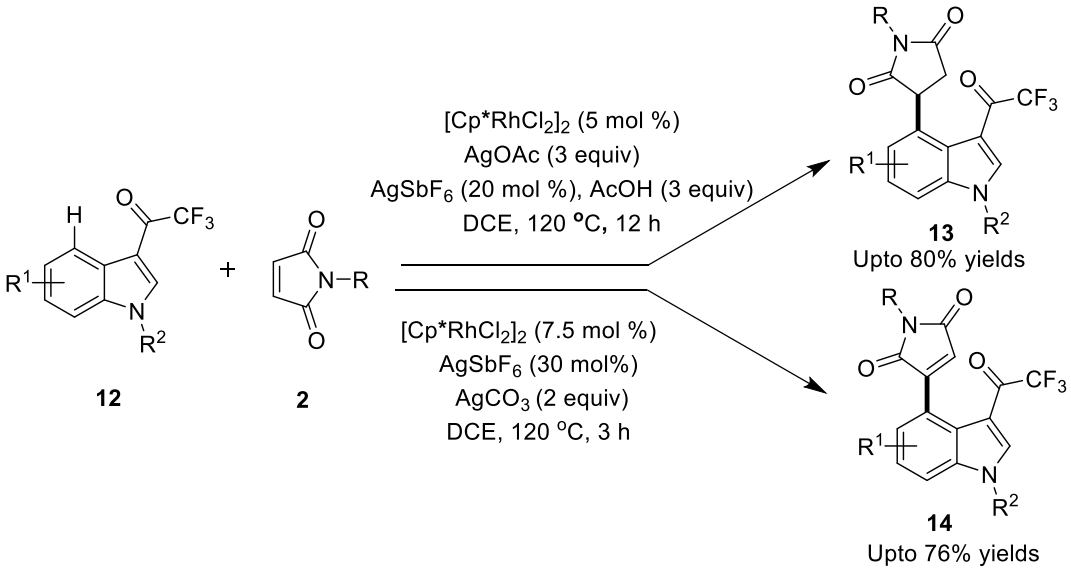

Scheme 3.1.6 Rhodium-catalyzed C-4 alkylation and alkenylation of 3-(trifluoroacetyl)indoles (**14**) with maleimides (**2**)

Prabhu *et al.* disclosed an efficient protocol for the Co(III)-facilitated 1,4-addition of maleimides (**2**) on azobenzenes (**15**) by exploiting the directing group influence of an azo group (Scheme

3.1.7).[65] The catalyst displayed high functional group tolerance and is compatible with a broad substrate scope with symmetric and asymmetric azobenzenes.

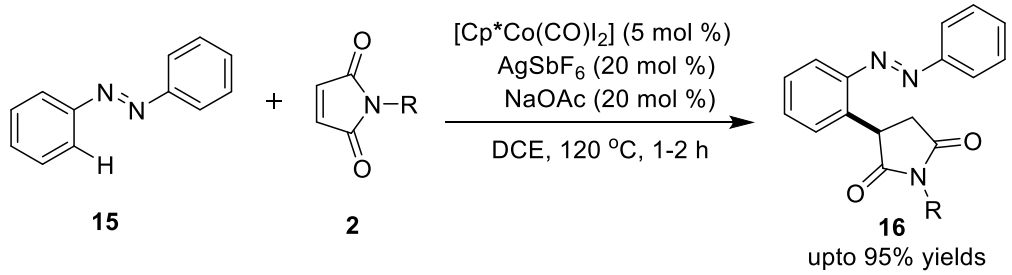

Scheme 3.1.7 Cobalt-catalyzed alkylation of azobenzenes (**15**) with maleimides (**2**)

Li and Fan presented a ubiquitous strategy for the efficient synthesis of pharmaceutically important maleimide-fused benzocarbazoles (**18**) and imidazo(1,2-*a*)pyridines (**20**) by the oxidative [4+2] annulation of 2-arylindoles (**17**) and 2-arylimidazo(1,2-*a*)pyridines (**19**) with maleimides (**2**) under Rh(III)-catalyzed conditions (Scheme 3.1.8).[66] The mechanism was proposed to proceed *via* a concerted pathway involving the formation of five-membered rhodacyclic intermediate followed by insertion of maleimide. Subsequent C3-H activation producing a seven-membered intermediate followed by reductive elimination and oxidative dehydrogenation afforded the respective products (**18**) and (**20**).

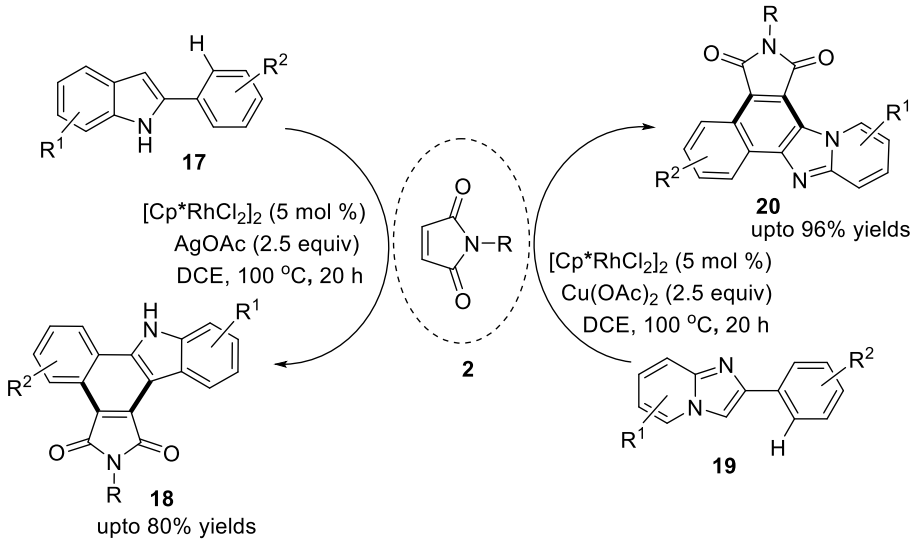

Scheme 3.1.8 Rhodium-catalyzed oxidative [4+2] annulations of 2-arylindoles (**17**) and 2-arylimidazo(1,2-*a*)pyridines (**19**) with maleimides (**2**)

In 2020, Hajra *et al.* demonstrated additive-driven switchable Rh(III)-catalyzed strategies for the hydroarylation and oxidative arylation of 2-arylindazoles (**21**) with maleimides (**2**). The developed

strategies showed showcased wide functional group tolerance with good yields of *ortho*-alkylated and *ortho*-alkenylated products (Scheme 3.1.9).[67]

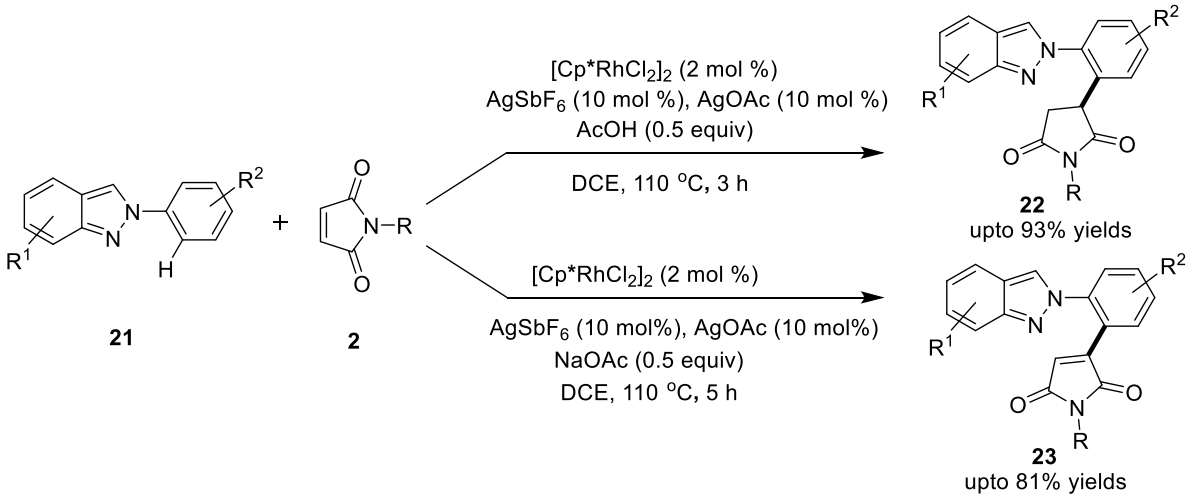

Scheme 3.1.9 Rhodium-catalyzed additive-driven hydroarylation and alkenylation of 2-arylindazoles (**21**) with maleimides (**2**)

In 2019, Zhang and Fan presented selective synthetic approaches for the formation of pentacyclic fused products (**24**) and spirocyclized products (**25**) by the reaction between 2-arylindazoles (**21**) with maleimides (**2**) under slightly modified Rh(III)-catalyzed conditions. Intriguingly, the selectivity could be switched by resorting to different additives (Scheme 3.1.10).[68]

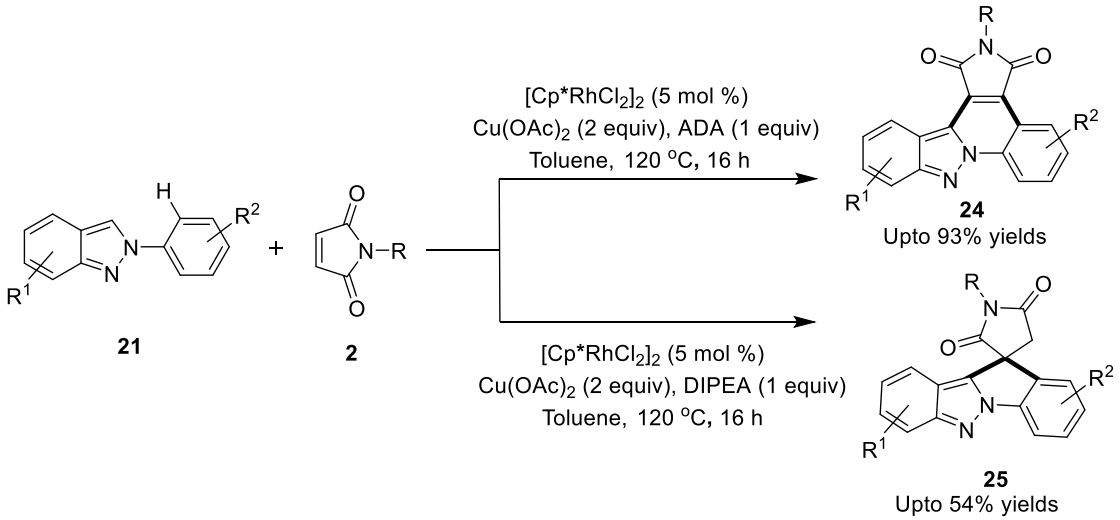

Scheme 3.1.10 Rhodium-catalyzed additive-driven oxidative coupling of 2-arylindazoles (**19**) with maleimides (**2**)

Prabhu and co-workers reported interesting Rh(III)-catalyzed coupling protocols between Li^+/Na^+ salts of carboxylic acid (**26**) with maleimides (**2**) under solvent-modulated conditions to furnish

decarboxylative Heck-type products (**27**) in THF, and [4+1] spiro-annulated products (**28**) in TFE, respectively. The authors demonstrated the directing group ability of a weakly coordinating carboxylate group whereby solvents played a pivotal role in switching selectivity. (Scheme 3.1.11).[69]

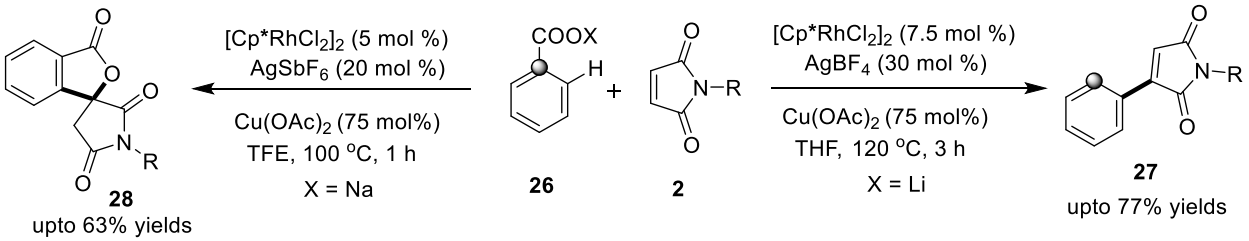

Scheme 3.1.11 Rhodium-catalyzed solvent-modulated coupling of Na^+/Li^+ salts of carboxylic acid (**26**) with maleimides (**2**)

The reaction of *N*-aryl acrylamides (**29**) with maleimides (**2**) under Ru(II)-catalyzed conditions was developed by Jeganmohan's group. An array of hydroarylated products (**30**) were synthesized in moderate-to-good yields by a sequence of alkylation and subsequent intramolecular oxidative cyclization (Scheme 3.1.12).[70]

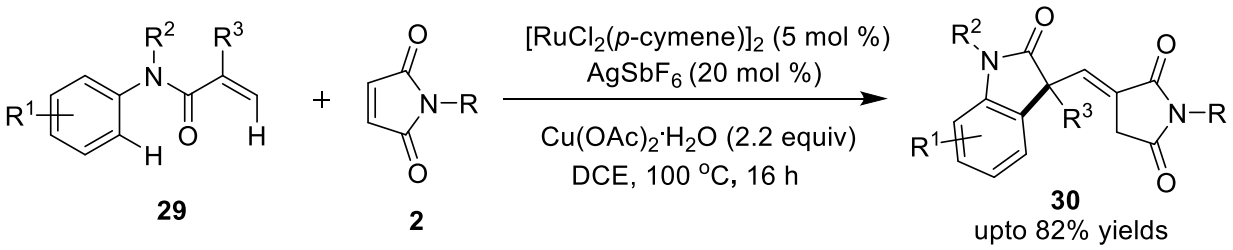

Scheme 3.1.12 Ruthenium-catalyzed alkylation of *N*-aryl acrylamides (**29**) with maleimides (**2**)

Likewise, Kim *et al.* described an efficient protocol for the C–H alkylation of acrylamides (**31**) with maleimides (**2**). Integration of cationic rhodium catalyst with PivOH significantly promoted this reaction. A thermodynamically stable olefin (**32**) with high diastereoselectivity was produced in high yields (Scheme 3.1.13).[71]

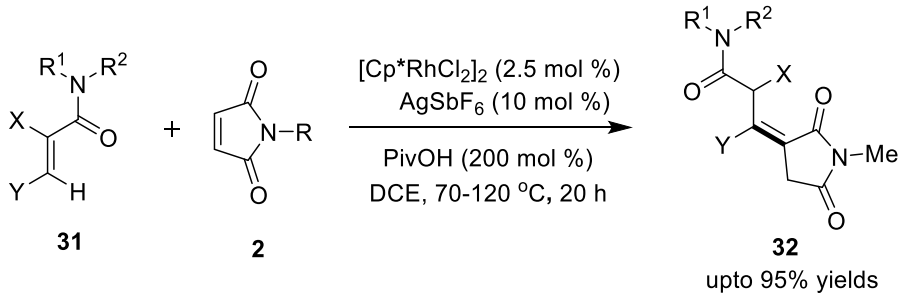

Scheme 3.1.13 Rhodium-catalyzed alkenylation of acrylamides (**29**) with maleimides (**2**)

Muniraj and Prabhu reported a Co(III)-catalyzed [4+2] annulation reaction of *N*-chlorobenzamides (**33**) with maleimides (**2**) using internally oxidizable *N*-chloroamide as a directing group. The reaction employed an air-stable, cost-effective and highly abundant cobalt catalyst that afforded the annulated products (**34**) in high yields at room temperature, albeit under argon atmosphere (Scheme 3.1.14).[72]

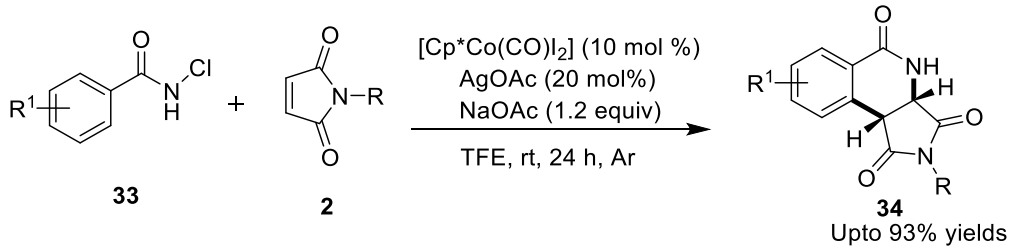

Scheme 3.1.14 Cobalt-catalyzed catalyzed [4+2] annulation of *N*-chlorobenzamides (**17**) with maleimides (**2**)

Cui and coworkers disclosed a facile protocol for the synthesis of 3,4-dihydroisoquinolines (**36**) by a tandem C–C and C–N bond formation *via* Rh(III)-catalyzed [4+2] annulation of 3-aryl-5-isoxazolone (**35**) and maleimides (**2**). The developed method exhibited wide functional group compatibility on the two substrates (Scheme 3.1.15).[73]

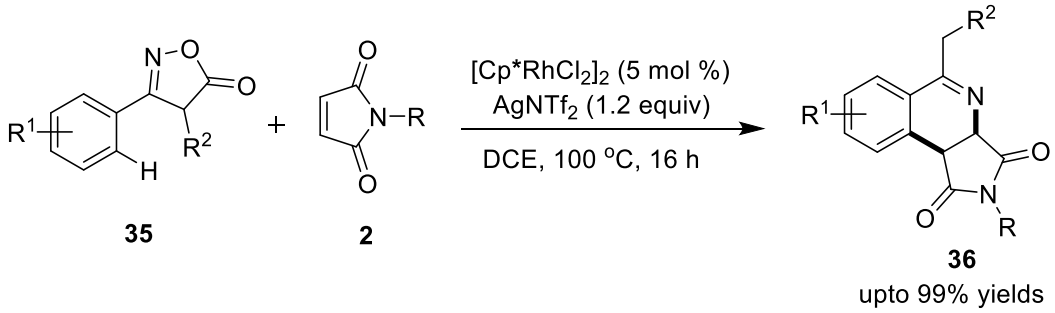

Scheme 3.1.15 Rhodium-catalyzed [4+2] annulation of 3-aryl-5-isoxazolone (**35**) with maleimides (**2**)

Wang and Liu reported an efficient protocol for the synthesis of maleimide decorated tryptophan and tryptophan-containing peptides by coupling *N*-(2-pyridyl)tryptophan derivatives (**37**) with malemides (**2**) to deliver Heck-type products (**38**) *via* Rh(III)-catalyzed C*(sp^2-H)* bond activation (Scheme 3.1.16).[74] A broad range of dipeptides, tripeptides, tetrapeptides, pentapeptides, hexapeptides and macrocyclic peptides were successfully transformed into desired C-2 alkenylated products.

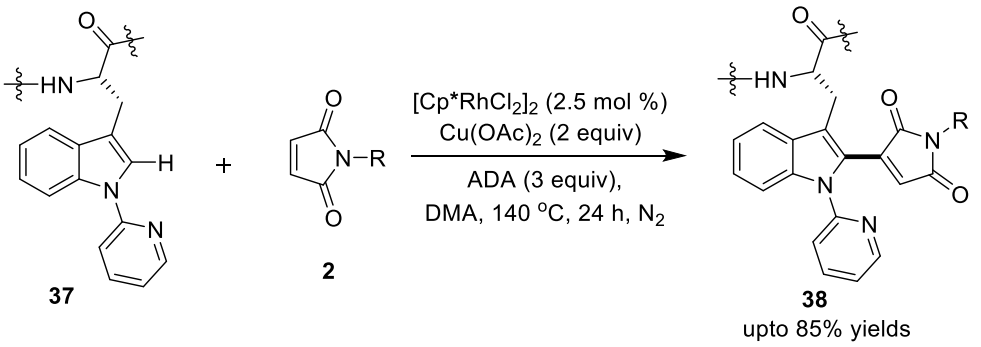

Scheme 3.1.16 Rhodium-catalyzed C-2 alkenylation of tryptophan-containing peptides (**38**) with maleimides (**2**)

In 2021, Hajra *et al.* reported Ru(II)-catalyzed strategies for the coupling of 2-arylquinoxalines (**39**) with maleimides (**2**) to furnish hydroarylated (**40**) and spirocyclized products (**41**) under slightly modified conditions. The transformation featured excellent yields, high atom economy, broad functional group tolerance (Scheme 3.1.17).[75]

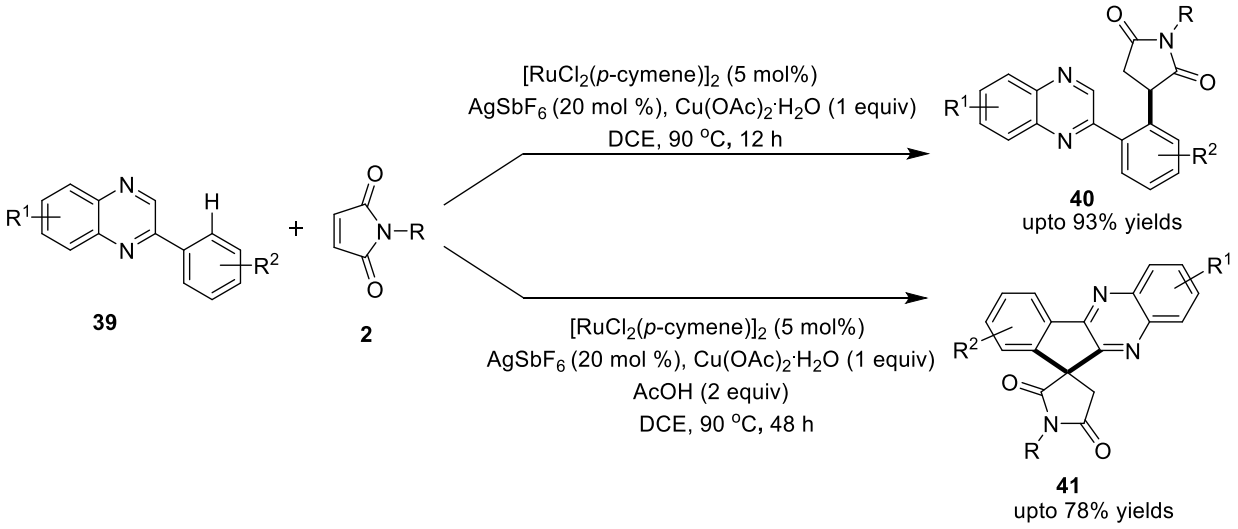

Scheme 3.1.17 Ruthenium-catalyzed hydroarylation and spirocyclization of 2-arylquinoxalines (**39**) with maleimides (**2**)

Very recently, Kim *et al.* reported the synthesis of spirosuccinimide bearing 2-arylindazolones (**43**) *via* the reaction between 2-arylindazol-3-ols (**42**) and maleimides (**2**) under Rh(III)-catalyzed conditions (Scheme 3.1.18).[76] The developed methodology highlighted by the synthesis of spirosuccinimides containing bioactive molecule-linked and chemical probe-linked maleimides.

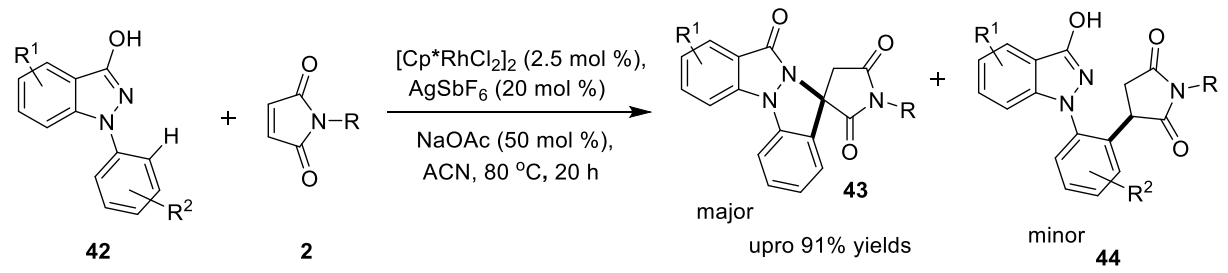

Scheme 3.1.18 Rhodium-catalyzed coupling of 2-arylindazol-3-ols (**42**) with maleimides (**2**)

Kim's group also achieved *ortho*-C-H alkylation of *N*-aryl-2-3-dihydrophthlazine-diones (**45**) with maleimide (**2**) in good-to-excellent yields by using Rh(III)/$AgSbF_6$ catalytic system (Scheme 3.1.19).[77] The reaction was believed to progress *via* rhodacyclic intermediate formation followed by coordination, migratory insertion of maleimide and finally proton demetalation to furnish the functionalized products (**46**).

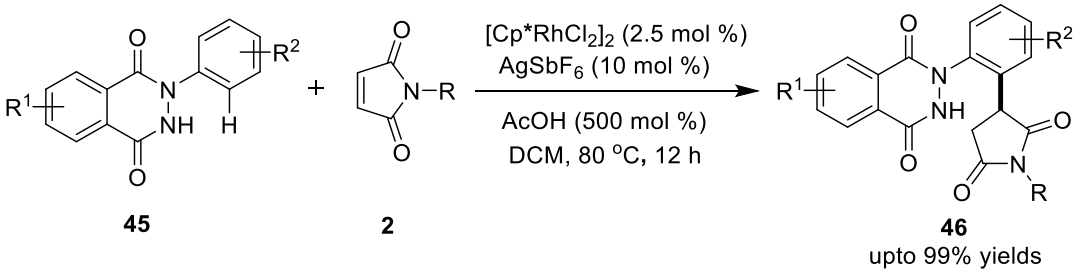

Scheme 3.1.19 Rhodium-catalyzed *ortho*-C-H alkylation of *N*-aryl-2,3-dihydrophthlazinediones (**45**) with maleimide (**2**)

In the backdrop of the above discussion, we anticipated to develop a novel strategy for the annulation of *N*-aryl-2,3-dihydrophthalazine-1,4-diones (**47**) with maleimides (**2**). The synthetic methods for spirocyclic products usually demand the use of complex starting materials, limited substrate scope or multistep operation. On the contrary, we have developed a facile methodology for the direct oxidative spirocyclization of *N*-aryl-2,3-dihydrophthalazine-1,4-diones (**47**) with maleimides (**2**) in excellent yields (Scheme 3.1.20)[78]

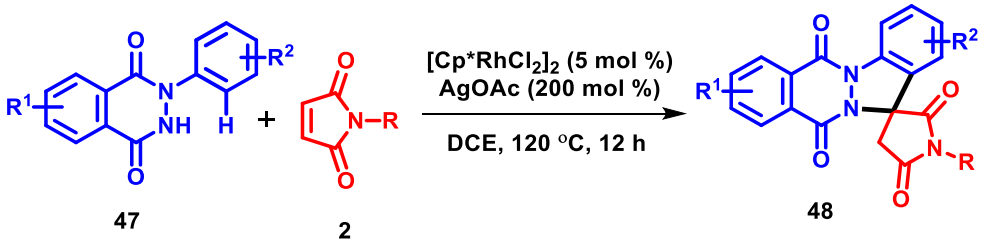

Scheme 3.1.20 Rhodium-catalyzed oxidative spirocyclization of *N*-aryl-2,3-dihydrophthalazine-1,4-diones (**47**) with maleimides (**2**)

3.2 Results and Discussion

The proposed work was initiated by systematically optimizing the reaction conditions for the possible annulation/cyclization between 2-phenyl-2,3-dihydrophthalazine-1,4-dione (**47a**) and *N*-phenylmaleimide (**2a**) (Table 3.2.1). The model substrates (**47a** and **2a**) failed to produce any product in the presence of AgOAc (50 mol %) and DCE at varied temperatures (Table 5.2.1, entry 1). Using $[Cp^{*}RhCl_2]_2$ (2.5 mol %) as a catalyst, the model substrates did not react at temperatures ranging from 25-120 ^{o}C to yield any product (Table 3.2.1, entry 2). The use of additives such as $Cu(OAc)_2$, NaOAc, $AgSbF_6$ and KPF_6 with $[Cp^{*}RhCl_2]_2$ (2.5 mol %) were also ineffective in coupling the substrates to produce any product at varied temperatures (Table 5.2.1, entries 3–6). However, the use of Ag_2CO_3 (50 mol %) in combination with $[Cp^{*}RhCl_2]_2$ (2.5 mol %) triggered the coupling between **47a** and **2a** in DCE at 120 ^{o}C to furnish a solid product **48aa** in 32% yield (Table 3.2.1, entry 7). Careful analysis of ^{1}H, ^{13}C NMR, COSY and HSQC of **48aa** confirmed the formation of spirocyclized product, characterized as 1'-phenylspiro[indazolo[1,2-*b*]phthalazine-13,3'-pyrrolidine]-2',5',6,11-tetraone. Thereafter, attempts were made to improve the yields of the product. Replacing Ag_2CO_3 with AgOAc (50 mol %) resulted in the formation of **48aa** in 45% yield (Table 3.2.1, entry 8). Independent studies of increasing the reaction time did not prove any beneficial effect on the yield of **48aa**, while increasing AgOAc loading to 100 mol % and 200 mol % enhanced the yield of **48aa** to 58% and 76%, respectively (Table 3.2.1, entries 9-10). Delightfully, a significant increment in the yield of **48aa** to 91% was observed by employing 5 mol % of the catalyst in a combination of 200 mol % of AgOAc (Table 3.2.1, entry 11). Solvent screening studies indicated ACN, dioxane, THF, toluene, DMF and DMSO to be moderately effective for this transformation, producing **48aa** in 58-79% yields (Table 3.2.1, entries 12-17). In contrast, ethanol was completely ineffective due to hydrolysis of maleimide under standard conditions (Table 3.2.1, entry 18). Unfortunately, the reaction between model substrates afforded very low yield of the product, when 5 mol % of Ru(II) catalyst and 200 mol % of AgOAc was used in DCE (Table 3.2.1, entry 19).

Table 3.2.1 Selected optimization[a] of reaction conditions for the synthesis of **48aa**

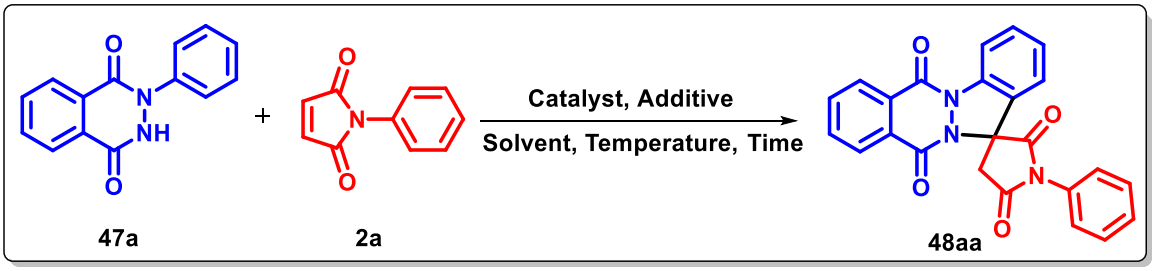

Entry No.	Catalyst (mol %)	Additive (mol %)	Solvent	Temp. (°C)	Yields (%)[b] **48aa**
1.	-	AgOAc (50)	DCE	25-120	-
2.	$[Cp^*RhCl_2]_2$ (2.5)	-	DCE	25-120	-
3.	$[Cp^*RhCl_2]_2$ (2.5)	$Cu(OAc)_2$ (50)	DCE	25-120	-
4.	$[Cp^*RhCl_2]_2$ (2.5)	NaOAc (50)	DCE	25-120	-
5.	$[Cp^*RhCl_2]_2$ (2.5)	$AgSbF_6$ (50)	DCE	25-120	-
6.	$[Cp^*RhCl_2]_2$ (2.5)	KPF_6 (50)	DCE	25-120	-
7.	$[Cp^*RhCl_2]_2$ (2.5)	$AgCO_3$ (50)	DCE	120	32
8.	$[Cp^*RhCl_2]_2$ (2.5)	AgOAc (50)	DCE	120	45
9.	$[Cp^*RhCl_2]_2$ (2.5)	AgOAc (100)	DCE	120	58
10.	$[Cp^*RhCl_2]_2$ (2.5)	AgOAc (200)	DCE	120	76
11.	**$[Cp^*RhCl_2]_2$ (5.0)**	**AgOAc (200)**	**DCE**	**120**	**91**
12.	$[Cp^*RhCl_2]_2$ (5.0)	AgOAc (200)	ACN	120	79
13.	$[Cp^*RhCl_2]_2$ (5.0)	AgOAc (200)	Dioxane	120	74
14.	$[Cp^*RhCl_2]_2$ (5.0)	AgOAc (200)	THF	120	65
15.	$[Cp^*RhCl_2]_2$ (5.0)	AgOAc (200)	Toluene	120	58
16.	$[Cp^*RhCl_2]_2$ (5.0)	AgOAc (200)	DMF	120	70
17.	$[Cp^*RhCl_2]_2$ (5.0)	AgOAc (200)	DMSO	120	66
18.	$[Cp^*RhCl_2]_2$ (5.0)	AgOAc (200)	EtOH	120	-
19.	$[RuCl_2(p\text{-cymene})]_2$ (5.0)	AgOAc (200)	DCE	120	22

[a]Reaction conditions: The reactions were carried out with **47a** (0.21 mmol) and **2a** (0.42 mmol) in the presence of catalyst/additive (as indicated in the table) in sealed tube using 3 mL of solvent at specified temperature for 12 h. [b]Isolated yields.

After the best conditions were established, we explored the generality of the optimized strategy using a variety of *N*-aryl-2,3-dihydrophthalazine-1,4-diones (**47b-l**), which reacted with *N*-phenylmaleimide (**2a**) with great ease to afford excellent yields of the desired products (Scheme 3.2.1). In particular, *N*-aryl-2,3-dihydrophthalazine-1,4-diones with electron-donating groups (substrates: **47b** & **47c)** on the aryl moiety showcased slightly better reactivity over electron-withdrawing groups (substrates: **47d** & **47e**), furnishing **48ba-48ca** and **48da-48ea** in 89-93% and 82-86% yields, respectively. The presence of disubstitutions at *meta-para* or at *ortho-para*

positions of the aryl moiety with electronically-rich and/or weakly-deficient groups (same/different) (substrates: **47f-h**) showcased negligible difference in their reactivity with **2a,** delivering their respective products **48fa-48ha** in 88-93% yields.

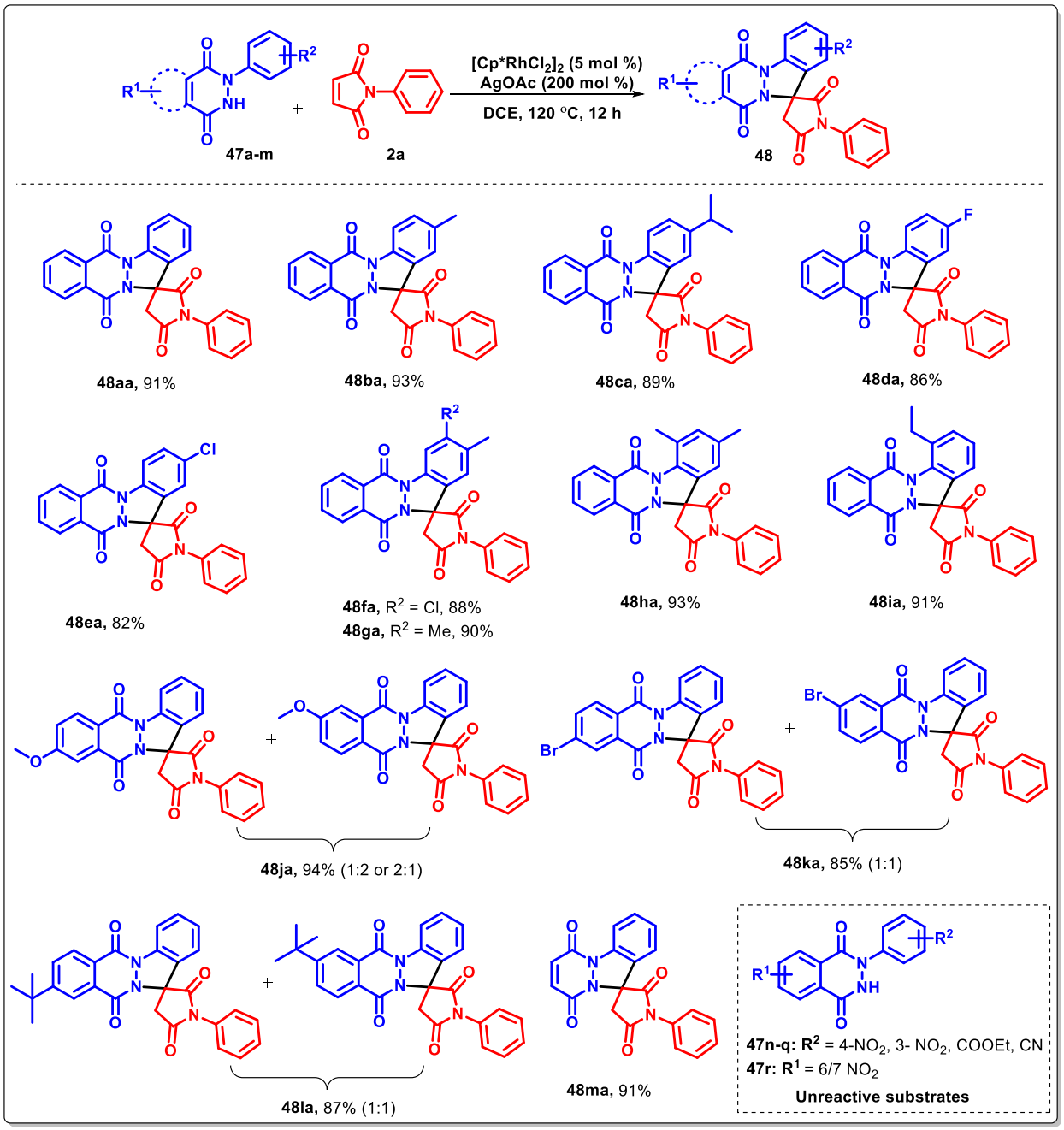

Scheme 3.2.1 Substrate scope of *N*-aryl-2,3-dihydrophthalazine-1,4-diones

Furthermore, *ortho*-ethyl substituted *N*-phenyl-2,3-dihydrophthalazine-1,4-dione (substrate: **47i**) smoothly underwent the cyclization with **2a** to afford corresponding spiro-product (**48ia**) in 91% yield. Similarly, *N*-aryl-2,3-dihydrophthalazine-1,4-diones with electron-donating/withdrawing

groups (substrates: **47j**, **47k** & **47l**) on the phthalazine moiety reacted comfortably with **2a** under described conditions to produce their corresponding products (**48ja-48la**) in 85-94% yields. Noteworthy, **48ja-48la** were obtained as a mixture of two regioisomers in varied ratios, as their substrates, **47j-47l** were prepared as an inseparable 6/7-substituted regioisomeric mixtus from 5-OMe/5-Br/5-*t*-Bu phthalic anhydride and phenylhydrazine. Moreover, the reaction of **2a** was also compatible with 1-phenyl-1,2-dihydropyridazine-3,6-dione (**47m**) yielding the spirocyclized product (**48ma**) in 91%. Unfortunately, strongly electron-withdrawing groups placed at different positions of aryl/phthalazine moieties (substrates: **47n-47r**)] were found to be unsuitable to afford any product under the described conditions (the starting materials were recovered as such). It is most likely that the electron-deficient nature of substrates disfavors its nucleophilic attack on Rh, thereby indicating the possibility of S_EAr pathway to be involved in the C-H metallation step. The representative ^{1}H NMR and ^{13}C NMR spectra of **48aa** are shown in Figure 3.2.1 and Figure 3.2.2, respectively.

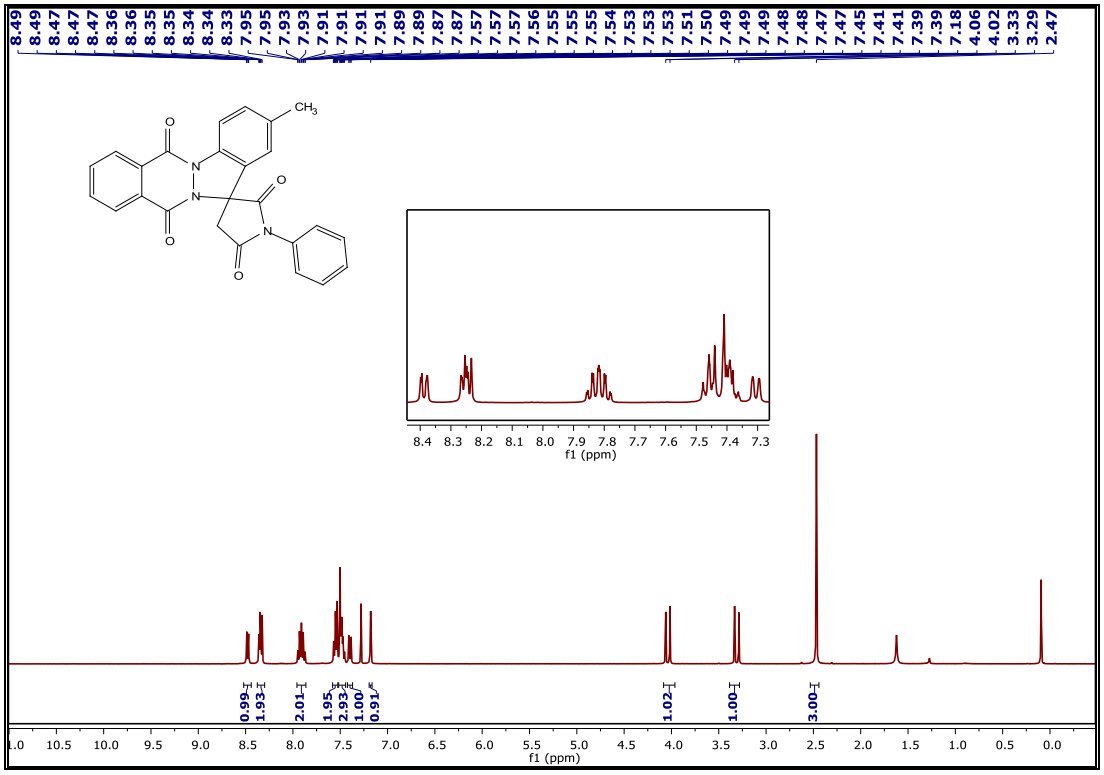

Figure 3.2.1 ^{1}H NMR spectra of **48aa**

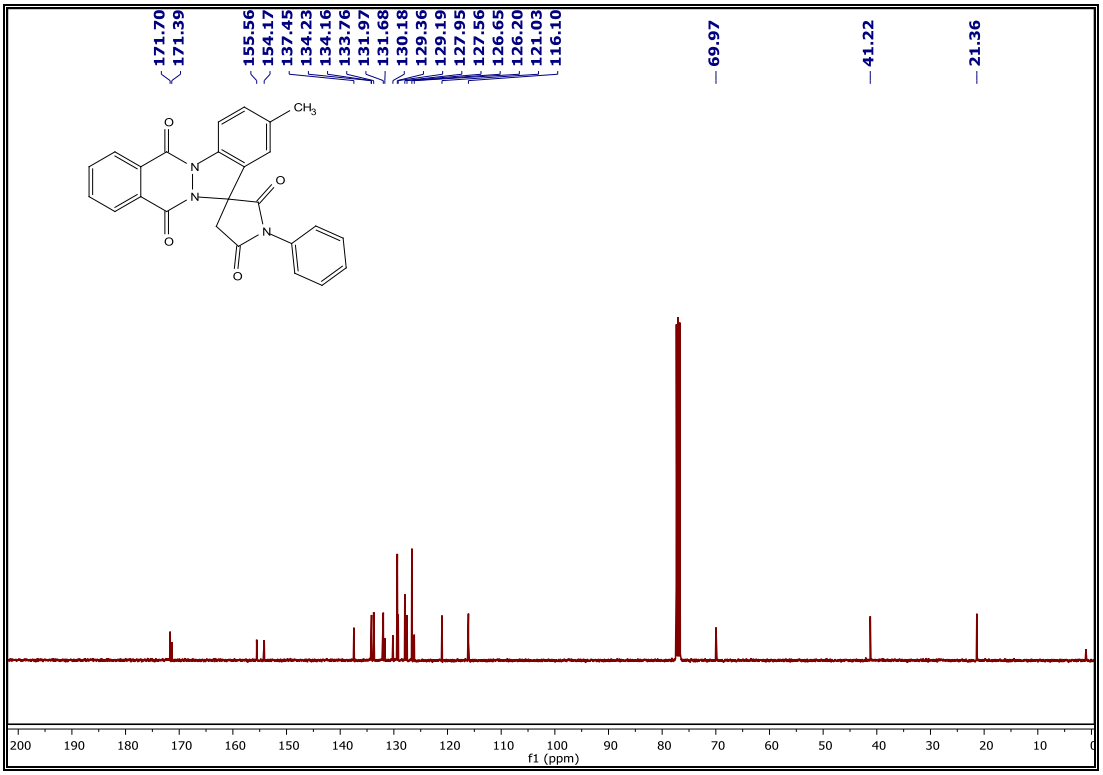

Figure 3.2.2 ^{13}C NMR spectra of **48aa**

To further expand the scope of this oxidative cyclization, the coupling abilities of variedly decorated *N*-aryl/alkyl maleimides (**2b-2s**) were examined (Scheme 3.2.2). Of these, a wide range of electronically-rich and -deficient *p*-substituted *N*-arylmaleimides {R^3 = 4-Me (**2b**), 4-OMe (**2c**), 4-F (**2d**), 4-Cl (**2e**), 4-Br (**2f**), 4-NO_2 (**2g**), 4-CF_3 (**2h**)} showcased excellent reactivity with **47a** to furnish spiro-cyclized products (**48ab-48ah**) in 82-97% yields. A comparative study on the positioning of the substituent when performed using *para*, *meta* and *ortho*-methyl substituted *N*-arylmaleimides (**2b, 2i** & **2j**) with **47a** under described conditions indicated minor reactivity difference, affording their respective spiro-succinimides (**48ab, 48ai** & **48aj**) in 96%, 92% and 88% yields, respectively. Interestingly, the coupling of *N*-naphthylmaleimide (**2k**) with **47a** produces the desired product **48ak** in 94% yield, albeit as a mixture of two rotamers. Delightfully, *N*-benzylmaleimide (**2l**) reacted smoothly with **47a** to furnish **48al** in 95% yield, while *N*-cyclohexylmaleimide (**2m**), *N*-methylmaleimide (**2n**) and *N*-propylmaleimide (**2o**) reacted smoothly with **47a** under optimized conditions to yield desired spiro-succinimides, **48am-48ao** in 73-86% yields. Also, *N*-allylmaleimide (**2p**) gave the desired product (**3ap**) in 83% yield. Gratifyingly, the reaction of maleimide (**2q**) with **1a** yielded the spirocyclized product (**3aq**) in 54% yield. Morever, ethyl 2,5-dioxo-2,5-dihydro-1*H*-pyrrole-1-carboxylate (**2r**) reacted easily

with **47a** to deliver corresponding spirocyclizedcyclized product (**48ar**) in 68% yield. Also, the reaction of glycine amino ester bearing malemide (ethyl 2-(2,5-dioxo-2,5-dihydro-1*H*-pyrrol-1-yl)acetate, (**2s**) with **47a** resulted in the formation of the desired spirocyclized product (**48as**) in 65% yield. Unfortunately, diethyl maleate failed to produce the desired product under optimized conditions (Scheme 3.2.2).

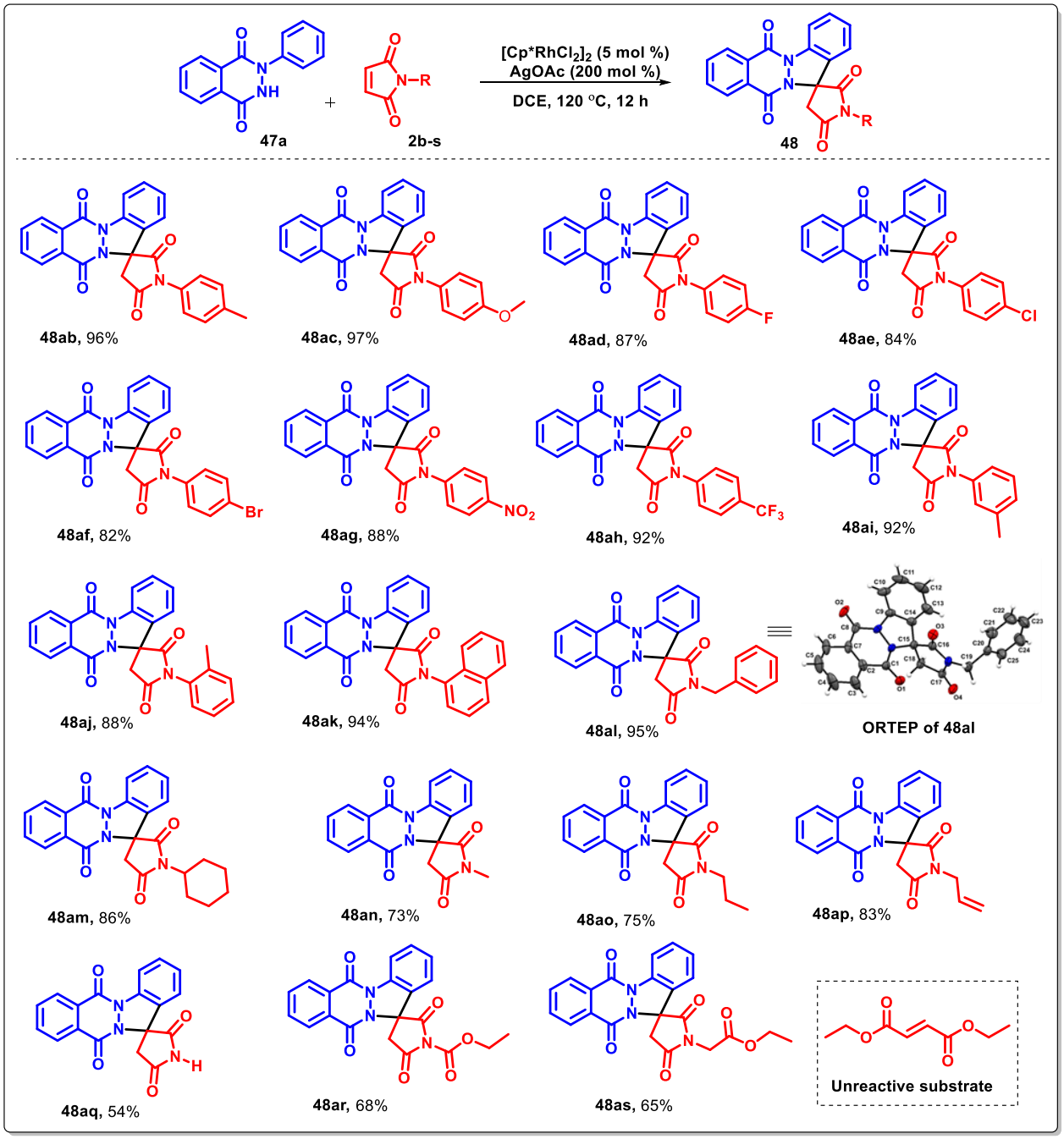

Scheme 3.2.2. Substrate scope of *N*-aryl/alkyl maleimides

Moreover, crystals of **48al** were grown in chloroform *via* single solvent slow evaporation at room temperature. As a representative example, the assigned structure of **48al** was furthur confirmed by X-ray diffraction (XRD) studies (Scheme 3.2.2).

After successful synthesis of variedly substituted spiro derivatives, a scaling up reaction was performed to demonstrate the industrial efficacy of the process. Hence, the reaction of **47a** (2.1 mmol, 0.5 g) with **2a** (4.2 mmol) under optimized reaction conditions afforded **48aa** in 88% yield (Scheme 3.2.3).

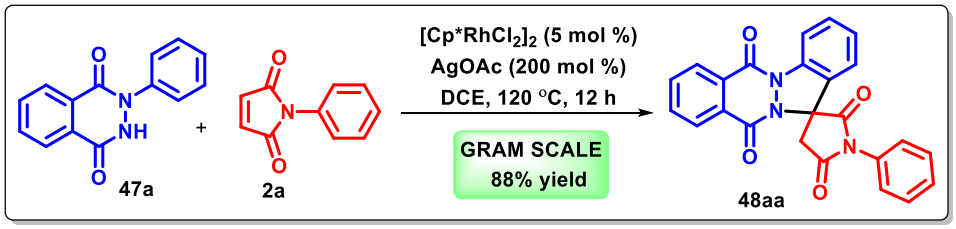

Scheme 3.2.3 Gram scale synthesis of **48aa**

To gain the insight of the mechanism, selective experiments were performed (Scheme 3.2.4). One-pot competitive experiment between electronically-rich and -deficient *N*-aryl-2,3-dihydrophthalazine-1,4-diones (**47b** and **47d**) with **2a** under standard conditions produced a mixture of their corresponding oxidative spirocyclized products (**48ba : 48da**) in 2:1 ratio (Scheme 3.2.4i). Likewise, the reaction of **47a** with 1:1 mixture of **2b** and **2f** under similar reaction conditions furnished a mixture of their corresponding products (**48ab : 48af**) in almost equivalent ratio (Scheme 3.2.4i). Similarly, the reaction of **47a** with 1:1 mixture of **2b** and **2g** under optimized conditions resulted in a mixture of corresponding spirocyclized products (**48ab : 48ag**) in 1:3 ratio (Scheme 3.2.4i). Deuterium labelling experiment was next performed by reacting **47b** with $[Cp^*RhCl_2]_2$/AgOAc in a mixture of CD_3COOD, MeOD and DCE. Interestingly, a remarkable deuterium exchange (~72%) at the two *ortho* hydrogen atoms was observed, affording mixture of deuterated and non-deuterated substrates (**47b**/**47b-*d*$_2$**) in 75% yield (Figure 3.2.3). This clearly indicated the possibility of reversible nature of C−H bond dissociation step (Scheme 3.2.4ii). Kinetic Isotopic Studies computed a P_H/P_D of 3.0 (Figure 3.2.4), when an intermolecular competitive experiment of **47b** and **47b-*d*$_2$** was carried with **2a** under standard conditions (Scheme 3.2.4iii). Further, two parallel reactions of **47b** and **47b-*d*$_2$** with **2a** under standard reaction conditions resulted in a Kinetic Isotope Effect (k_H/k_D) of 1.12 (Scheme 3.2.4iv, Figure 3.2.5 & Figure 3.2.6). These results clearly indicated that C–H activation step might be involved in the rate-determining step.

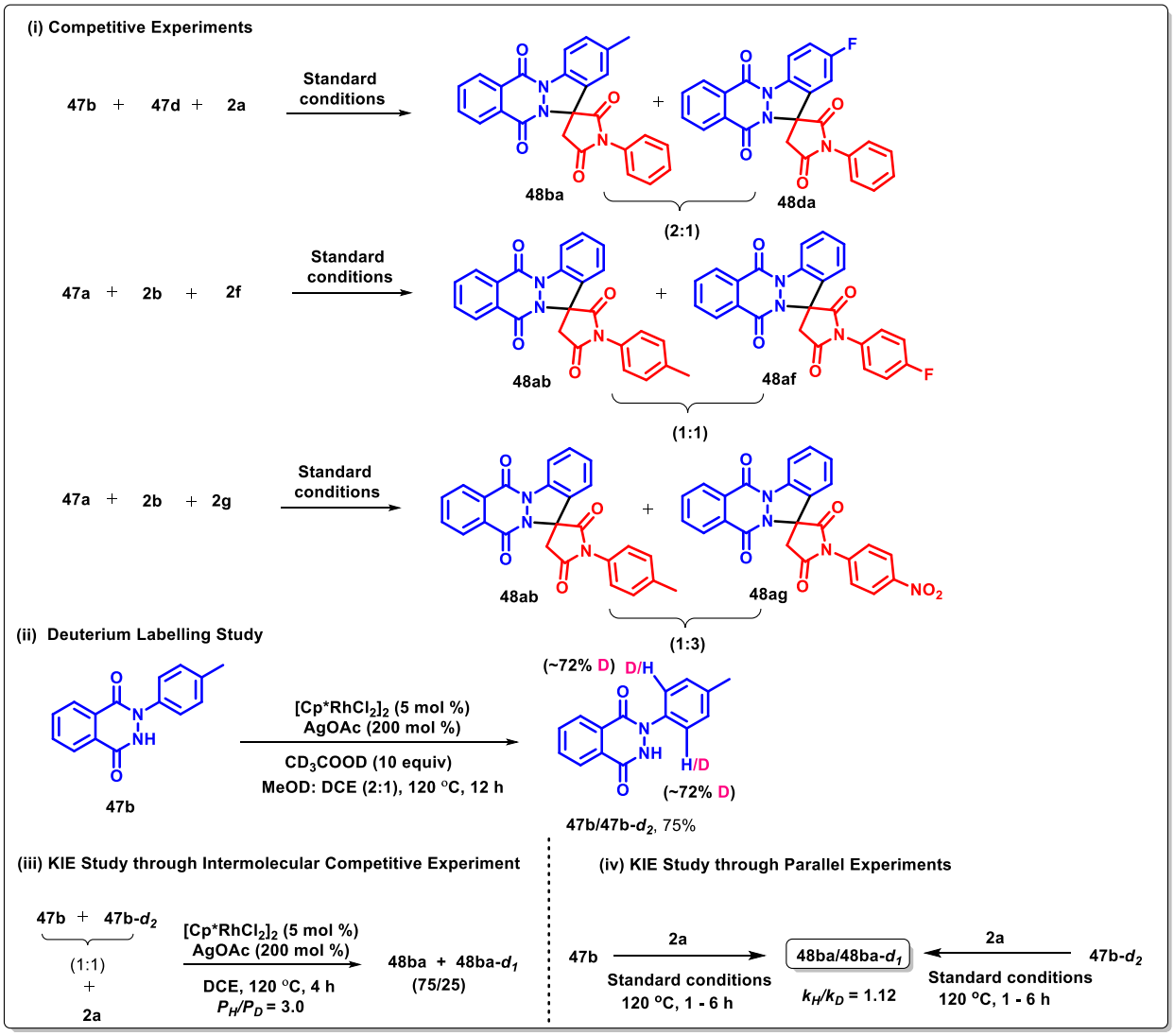

Scheme 3.2.4 Preliminary mechanistic investigations

Further, a stoichiometric reaction of [Cp*$RhCl_2$]$_2$ (1 equiv) with AgOAc (2.5 equiv) in DCE at room temperature for 6 h afforded a yellow solid, whose ^{1}H NMR indicated the formation of [Cp*Rh$(OAc)_2$] (Scheme 3.2.5i). However, attempts to purify this further leads to its decomposition. Parallelly, further reaction of crude [Cp*Rh$(OAc)_2$] with *N*-phenylphthalazine-1,4-dione (**47a**) at room temperature and subsequent warming to 60 °C up to 12 h leads to a orange coloured complex mixture that could not be purified, in spite of several attempts.

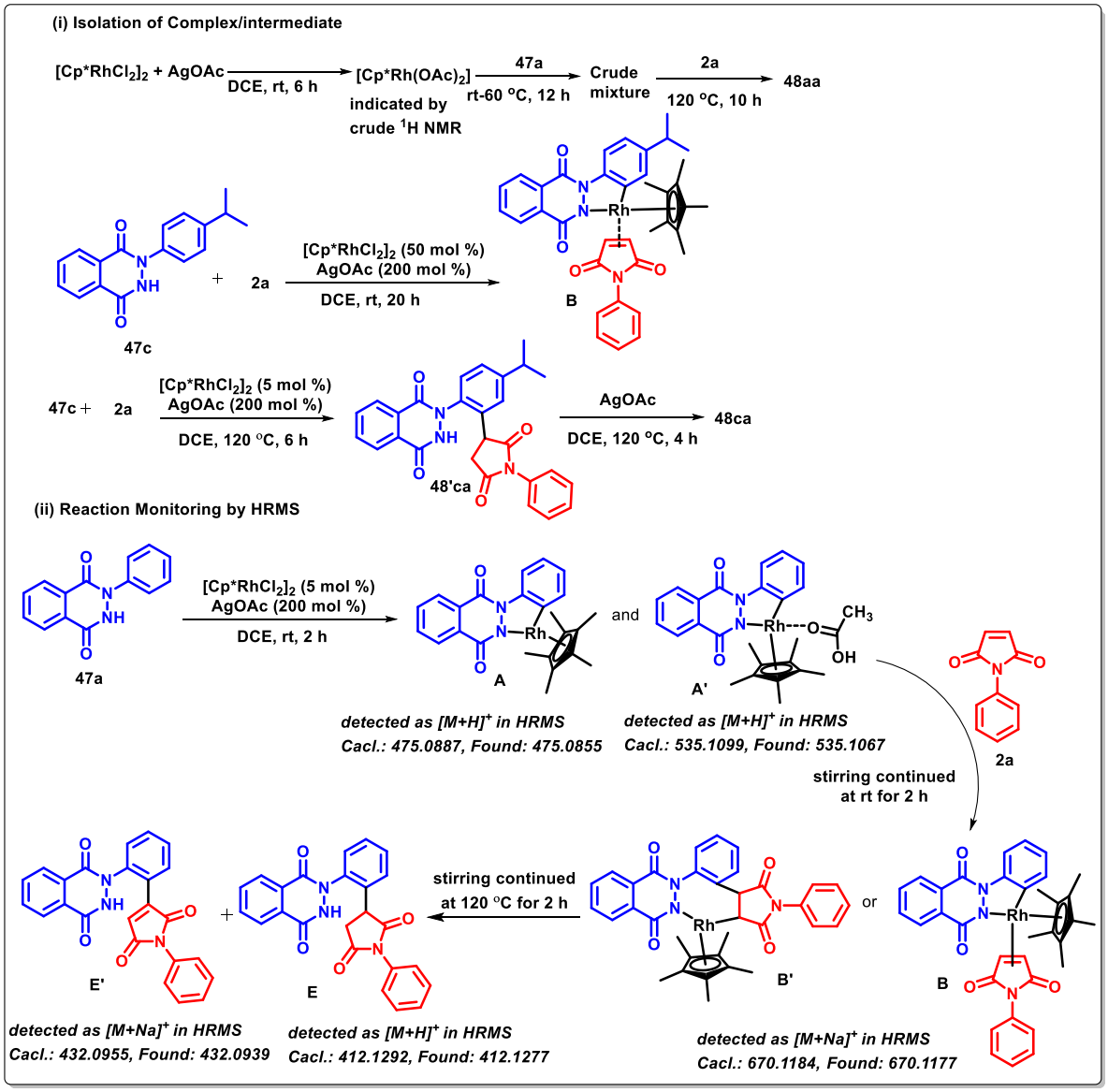

Scheme 3.2.5 Preliminary mechanistic investigations

On the other hand, subsequent addition of *N*-phenyl maleimide (**47a**) to the above crude mixture and its continued heating at 120 °C for 10 h furnished **48aa** in major amounts (Scheme 3.2.5i). Pleasingly, a maleimide coordinated five-membered rhodacyclic intermediate **B** was isolated by reacting **47c** and **2a** using stoichiometric amounts of $[Cp^*RhCl_2]_2$ and AgOAc in DCE at room temperature for 20 h. The structure of the complex **B** was confirmed by ^1H, ^{13}C NMR and HRMS analysis (Scheme 3.2.5i, Figure 3.2.7 & Figure 3.2.8). Interestingly, the reaction between **47c** and **2a** using $[Cp^*RhCl_2]_2$/AgOAc catalytic system in DCE at 120 °C for 6 h afforded the formation of *ortho*-alkylated product (**48′ca**) in appreciable yield. Purification of **48′ca** by column chromatography followed by its subsequent heating in DCE for 4 h produced **48ca**, thereby

indicating *ortho*-alkylated product to be an intermediate (Figure 3.2.9 & Figure 3.2.10). Finally real-time monitoring of the reaction in a sequential manner indicated the presence of intermediates **A**, **A'**, **B**, **B'**, **E** and **E′** in the HRMS of the mixture (Scheme 3.2.5ii).

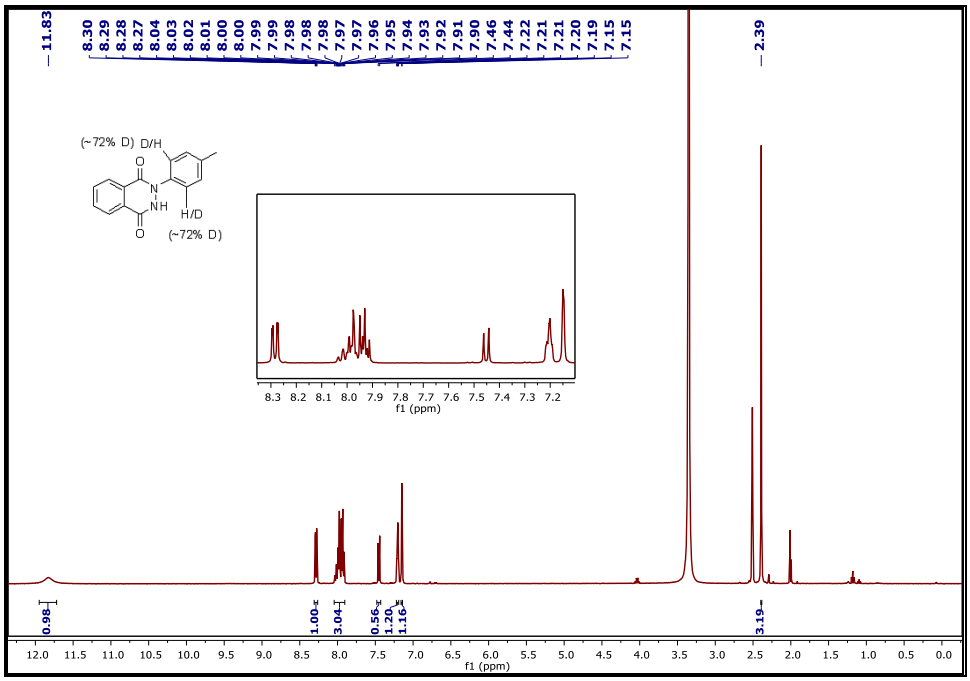

Figure 3.2.3 ^{1}H NMR of **47b**/**47b-*d*$_2$**

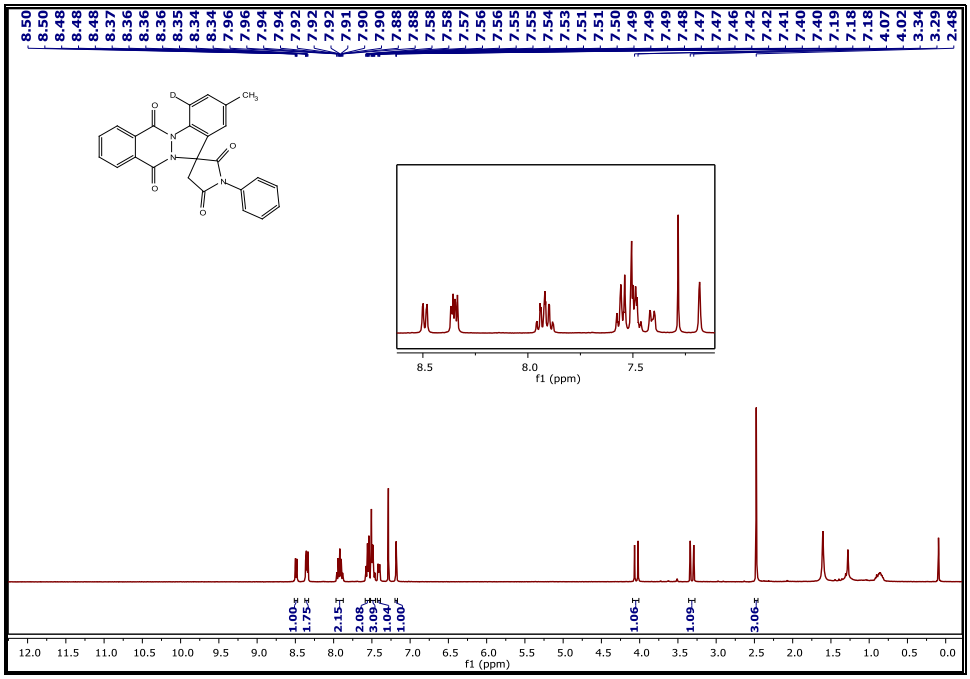

Figure 3.2.4 ^{1}H NMR of **48ba**+**48ba-*d*$_1$**

$$P_H/P_D = 0.75/0.25 = 3.0$$

Parallel Experiments

Time (h)	1	2	3	4	5	6
^{1}H NMR Yield (%)	7.87	14.47	19.01	22.53	26.86	31.83

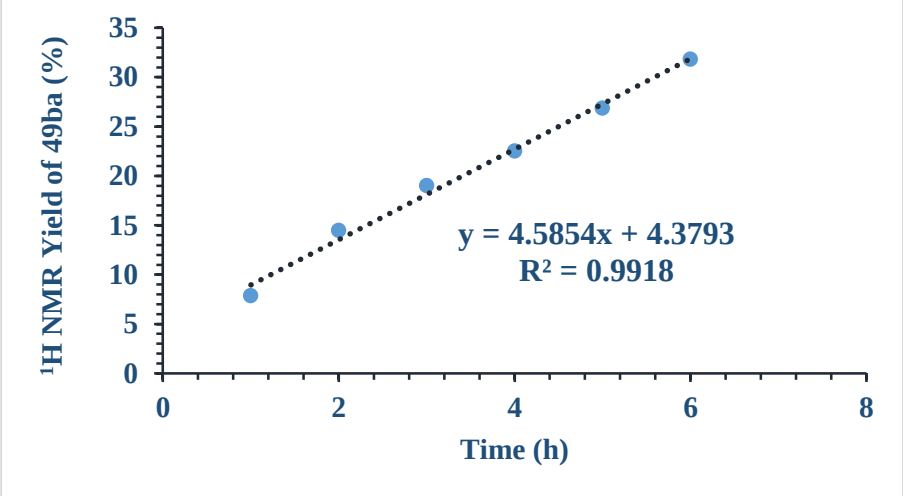

Figure 3.2.5 Protonated Kinetics

Time (h)	1	2	3	4	5	6
^{1}H NMR Yield (%)	6.70	10.98	16.08	19.37	23.07	27.38

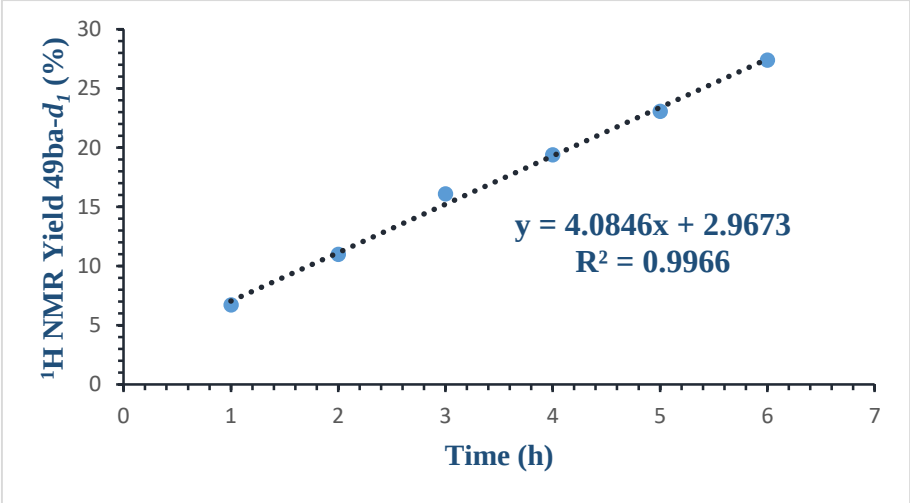

Figure 3.2.6 Deuterated Kinetics

KIE = k_H/k_D = 4.5854/4.0846= 1.12

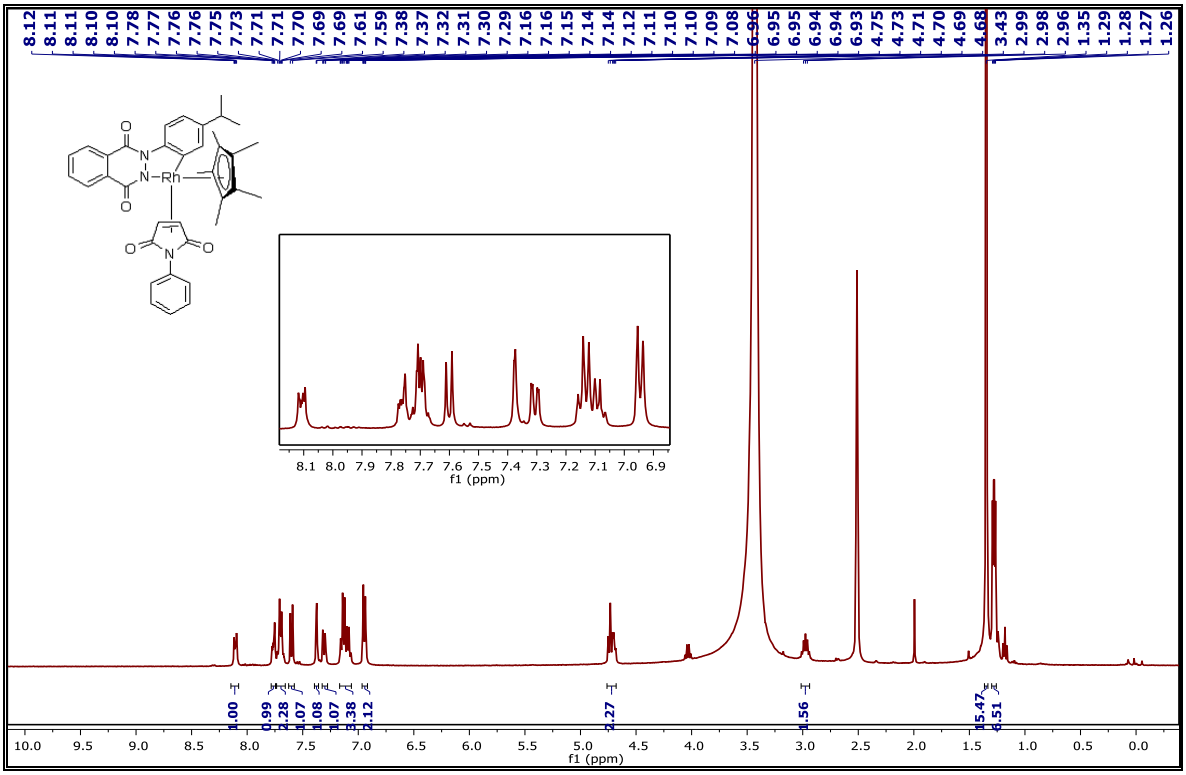

Figure 3.2.7 ^{1}H NMR spectra of **B**

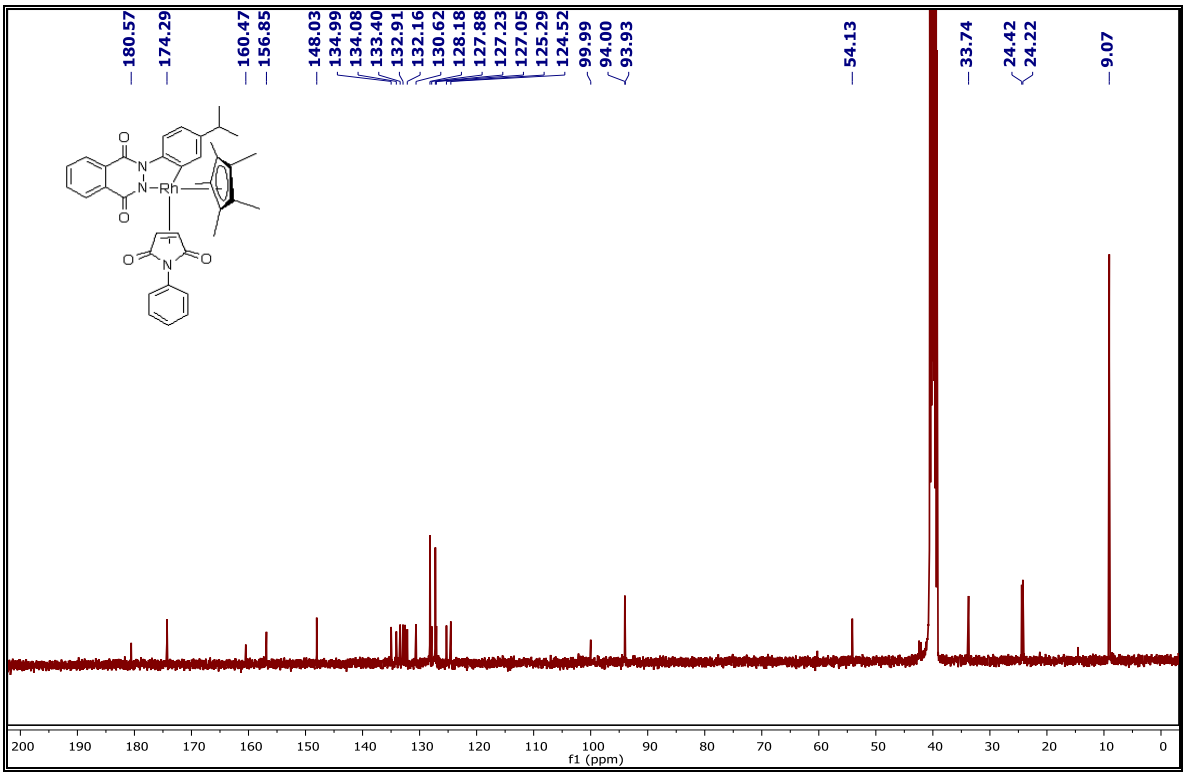

Figure 3.2.8 ^{13}C NMR spectra of **B**

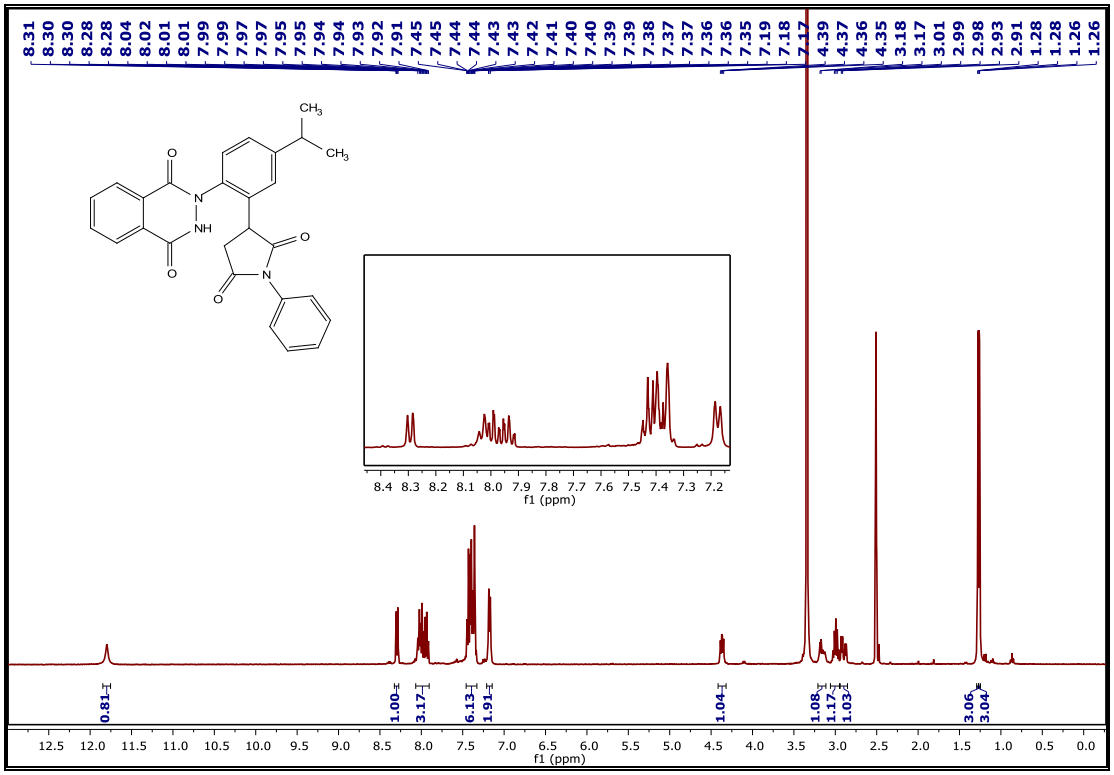

Figure 3.2.9 ^{1}H NMR spectra of **48′ca**

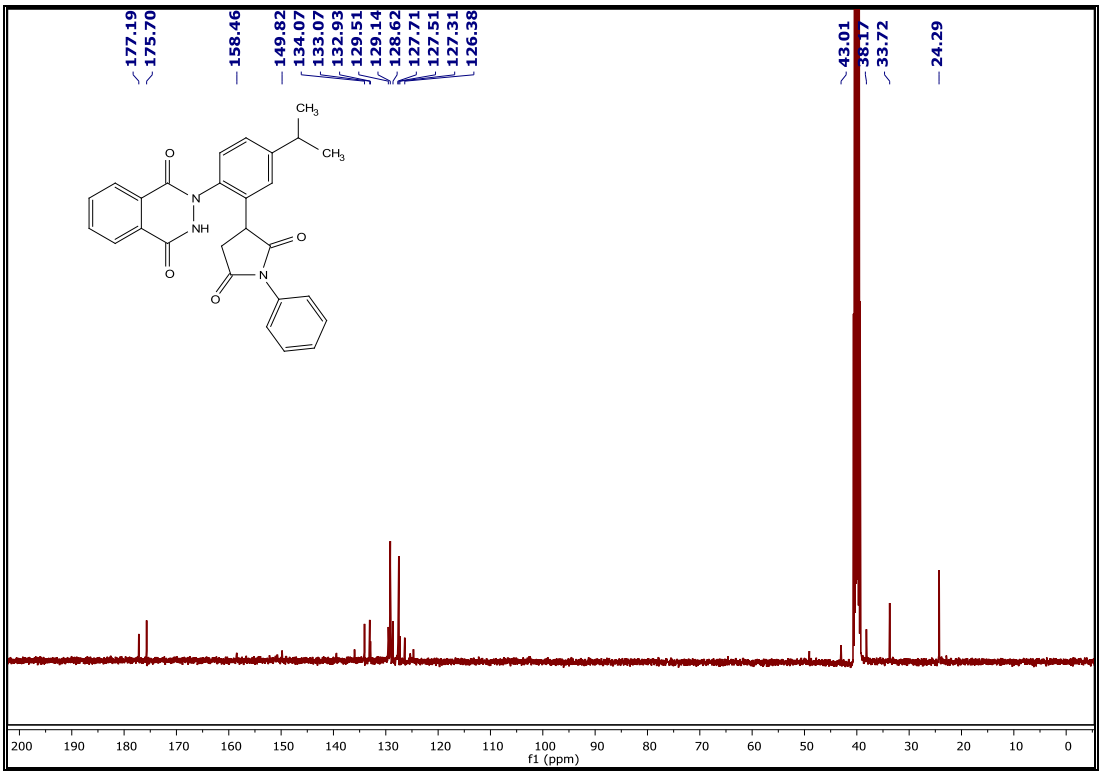

Figure 3.2.10 ^{13}C NMR spectra of **48′ca**

Based on the above mentioned results and previous literature precedence[69,79] a plausible reaction mechanism is proposed (Scheme 3.2.6). The deprotonation of the N−H bond and acetate-mediated C-H bond cleavage in **47a** to an active Rh(III) monomeric species [Cp*Rh(OAc)$_2$] obtained by the dissociation of [Cp*RhCl$_2$]$_2$ with OAc$^-$ commenced the catalytic cycle to generate a five-membered rhodacyclic intermediate **A**. Coordinative insertion of double bond maleimide into C$_{Ar}$–Rh bond generates the species **C** *via* intermediate **B**. Epimerization of **C** to **D** followed by protonation produces the *ortho*-functionalized intermediate **E**. Subsequently, oxidation and intramolecular aza-Michael-type addition/protonation sequence (**E′→49**) afforded the spiro-succinimide product.

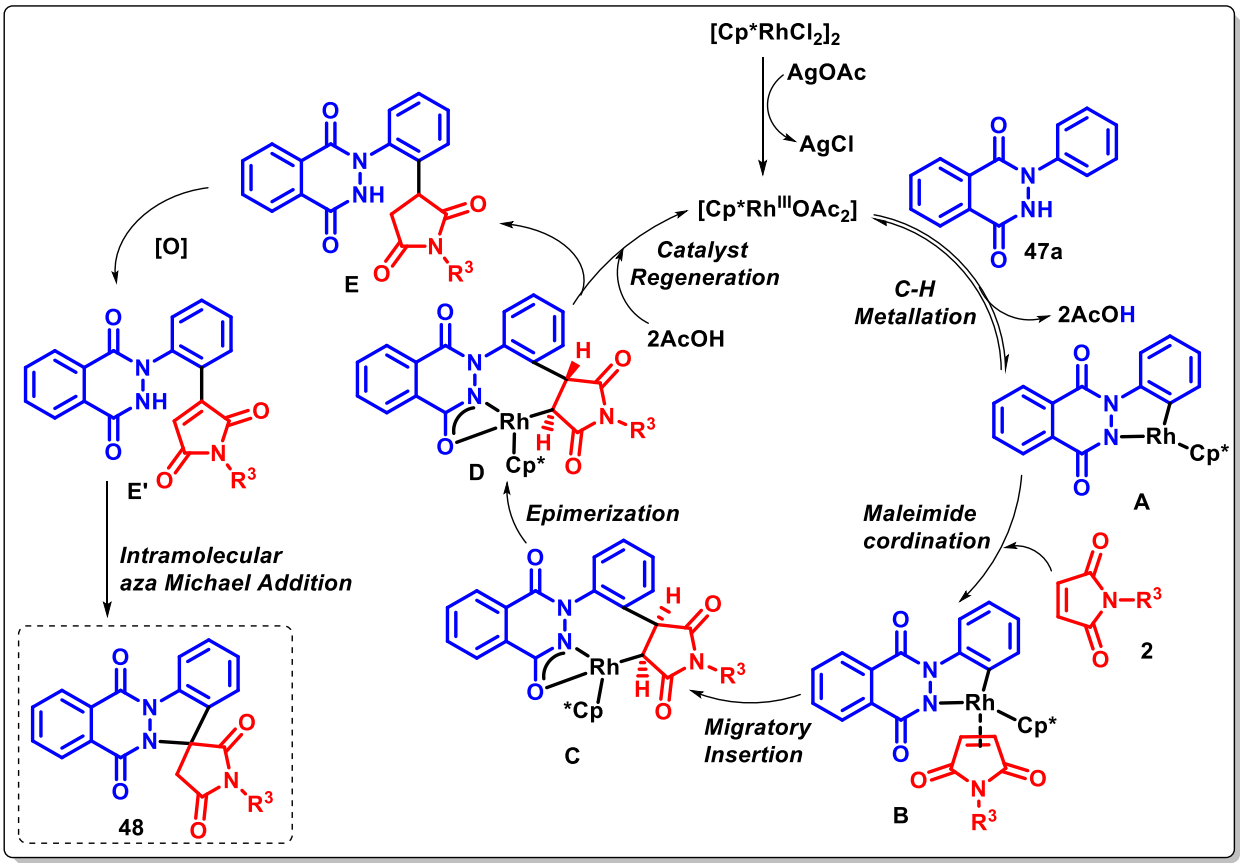

Scheme 3.2.6 Plausible mechanism

In summary, we have demonstrated a Rh(III)-catalyzed strategy for the oxidative spiro-cyclization of 2-aryl-2,3-dihydrophthalazine-1,4-diones with maleimides. The present protocol allows an efficient route for the synthesis of a series of spiro[indazolo[1,2-b]phthalazine-13,3'-pyrrolidine]-2',5',6,11-tetraones from diversely decorated *N*-arylphthalazine-diones and *N*-aryl/alkylmaleimides in good-to-excellent yields. Mechanistic invertigations suggested that the

oxidative spirocyclization reaction proceeds through a sequential ortho-alkenylation followed by an intramolecular aza-Michael-type addition/protonation process.

3.3 Experimental Section

General Considerations

Commercially available reagents were used without purification. Commercially available solvents were dried by standard procedures prior to use. *N*-aryl/alkyl maleimides (**2a-m**, **2o-p**),[80] (**2r**),[81] (**2s**)[82] were prepared according to the reported procedures. Reactions were monitored by using thin layer chromatography (TLC) on 0.2 mm silica gel F254 plates (Merck). The chemical structures of final products and intermediates were characterized by nuclear magnetic resonance spectra (^{1}H NMR and ^{13}C NMR) recorded on a 400 MHz spectrometer, and the chemical shifts are reported in δ units, parts per million (ppm), relative to residual chloroform (7.26 ppm) or DMSO (2.5 ppm) in the deuterated solvent. ^{13}C NMR spectra are fully decoupled. The following abbreviations were used to describe peak splitting patterns when appropriate: s = singlet, d = doublet, t = triplet, dd = doublet of doublets, and m = multiplet. Coupling constants *J* are reported in Hz. The ^{13}C NMR spectra are reported in ppm relative to deuterochloroform (77.0 ppm) or [d_6] DMSO (39.5 ppm). Melting points were determined on a capillary point apparatus equipped with a digital thermometer and are uncorrected. High-resolution mass spectra were recorded on Agilent Technologies 6545 Q-TOF LC/MS by using electrospray mode. Column chromatography was performed on silica gel (100-200 mesh) using varying ratio of ethyl acetate/hexanes as eluent.

General procedure for the synthesis of *N*-aryl/alkyl spiro[indazolo[1,2-*b*]phthalazine-13,3'-pyrrolidines (48)

To an oven-dried sealed tube with a screw cap (PTFE) charged with 2-aryl-2,3-dihydrophthalazine-1,4-dione (**47**) (50 mg, 1 equiv), [Cp*****$RhCl_2$]$_2$ (0.05 equiv) and AgOAc (2 equiv) in DCE (3 mL), *N*-aryl/alkyl maleimide (**2**) (2.0 equiv) was added. The reaction mixture was to allowed to stirr at 120 ºC for 12 h. On completion of the reaction as indicated by TLC, the reaction mixture was cooled to room temperature, diluted with DCM (5 mL), filtered through celite. The reaction was quenched with water and extracted with DCM (2 x 15 mL). The organic layers were combined, dried over anhydrous sodium sulphate and concentrated *in vacuo.* Purification by column chromatography using hexanes/ethyl acetate (8:2 to 7:3) as eluent afforded the desired product (**48**).

1'-Phenylspiro[indazolo[1,2-*b*]phthalazine-13,3'-pyrrolidine]-2',5',6,11-tetraone (48aa).

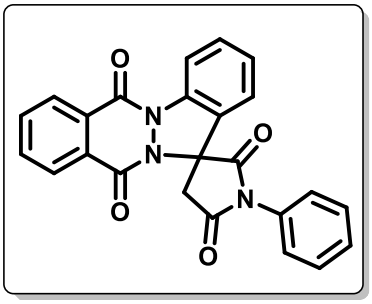

White solid; yield: 78 mg (91%); mp 254−255 °C; ^{1}H NMR (400 MHz, $CDCl_3$) δ 8.52 – 8.46 (m, 2H), 8.36 (dd, J = 7.2, 1.9 Hz, 1H), 7.98 – 7.88 (m, 2H), 7.66 – 7.60 (m, 1H), 7.58 – 7.52 (m, 2H), 7.51 – 7.47 (m, 3H), 7.42 (d, J = 4.3 Hz, 2H), 4.06 (d, J = 18.2 Hz, 1H), 3.33 (d, J = 18.2 Hz, 1H); ^{13}C NMR (100 MHz, $CDCl_3$) δ 171.6, 171.3, 155.6, 154.5, 136.4, 134.2, 133.9, 131.6, 131.4, 130.1, 129.4, 129.2, 128.1, 128.0, 127.6, 127.0, 126.7, 126.1, 120.7, 116.4, 70.0, 41.3; HRMS (ESI-TOF) (*m/z*) calculated $C_{24}H_{16}N_3O_4^+$: 410.1140, found 410.1134 $[M + H]^+$.

2-Methyl-1'-phenylspiro[indazolo[1,2-*b*]phthalazine-13,3'-pyrrolidine]-2',5',6,11-tetraone (48ba). White solid; yield: 78 mg (93%); mp 304−305 °C; ^{1}H NMR (400 MHz, $CDCl_3$) δ 8.50 –

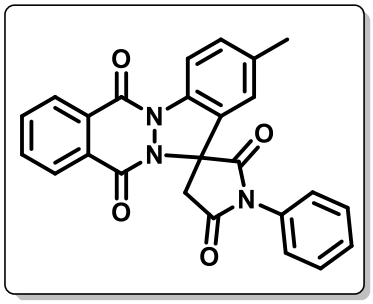

8.46 (m, 1H), 8.37 – 8.31 (m, 2H), 7.96 – 7.86 (m, 2H), 7.58 – 7.52 (m, 2H), 7.51 – 7.45 (m, 3H), 7.40 (dd, J = 8.3, 0.8 Hz, 1H), 7.18 (t, J = 0.96 Hz, 1H), 4.03 (d, J = 18.2 Hz, 1H), 3.31 (d, J = 18.2 Hz, 1H), 2.47 (s, 3H); ^{13}C NMR (100 MHz, $CDCl_3$) δ 171.7, 171.4, 155.6, 154.2, 137.5, 134.2, 134.2, 133.8, 132.0, 131.7, 130.2, 129.4, 129.2, 128.0, 127.6, 126.7, 126.2, 121.0, 116.1, 70.0, 41.2, 21.4; HRMS (ESI-TOF) (*m/z*) calculated $C_{25}H_{18}N_3O_4^+$: 424.1297, found 424.1292 $[M + H]^+$.

2-Isopropyl-1'-phenylspiro[indazolo[1,2-*b*]phthalazine-13,3'-pyrrolidine]-2',5',6,11-tetraone (48ca). White solid; yield: 72 mg (89%); mp 290−291 °C; ^{1}H NMR (400 MHz, $CDCl_3$)

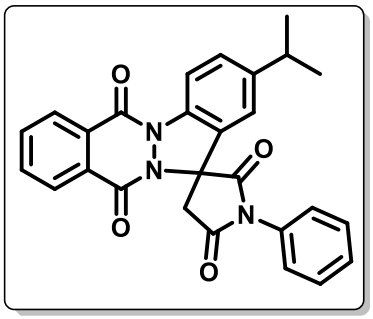

δ 8.52 – 8.47 (m, 1H), 8.40 – 8.33 (m, 2H), 7.97 – 7.87 (m, 2H), 7.60 – 7.54 (m, 2H), 7.52 – 746 (m, 4H), 7.20 (s, 1H), 4.05 (d, J = 18.2 Hz, 1H), 3.34 (d, J = 18.2 Hz, 1H), 3.10 – 2.98 (m, 1H), 1.32 (d, J = 6.8 Hz, 6H); ^{13}C NMR (100 MHz, $CDCl_3$) δ 171.8, 171.5, 155.6, 154.2, 148.7, 134.4, 134.2, 133.8, 131.7, 130.2, 129.5, 129.4, 129.2, 128.0, 127.9, 127.6, 126.6, 126.1, 118.4, 116.3, 70.1, 41.3, 34.1, 24.1; HRMS (ESI-TOF) (*m/z*) calculated $C_{27}H_{22}N_3O_4^+$: 452.1610, found 452.1607 $[M + H]^+$.

2-Fluoro-1'-phenylspiro[indazolo[1,2-*b*]phthalazine-13,3'-pyrrolidine]-2',5',6,11-tetraone (48da).White solid; yield: 72 mg (86%); mp 280−281 °C; ^{1}H NMR (400 MHz, $CDCl_3$) δ 8.51 – 8.44 (m, 2H), 8.38 – 8.33 (m, 1H), 7.98− 7.89 (m, 2H), 7.60 – 7.53 (m, 2H), 7.52 – 7.45 (m, 3H), 7.35 – 7.29 (m, 1H), 7.13 (dd, *J* = 7.2, 2.6 Hz, 1H), 4.04 (d, *J* = 18.3 Hz, 1H), 3.32 (d, *J* = 18.3 Hz, 1H); ^{13}C NMR (100 MHz, $CDCl_3$) δ 171.2, 170.8, 160.9 ($^{1}J_{C\text{-}F}$ = 247.4 Hz), 155.6, 154.3, 134.3, 134.0, 132.8, 132.7, 131.5, 129.9, 129.4, 129.3, 128.0, 127.9, 127.7, 127.6, 127.5, 126.6, 118.4 ($^{2}J_{C\text{-}F}$ = 23.3 Hz), 117.9 ($^{3}J_{C\text{-}F}$ = 8.2 Hz), 108.5 ($^{2}J_{C\text{-}F}$ = 26.0 Hz), 69.9 ($^{4}J_{C\text{-}F}$ = 2.5 Hz), 41.1; ^{19}F NMR (376 MHz, $CDCl_3$) δ -112.31; HRMS (ESI-TOF) (*m/z*) calculated $C_{24}H_{15}FN_3O_4^+$: 428.1046, found 428.1030 $[M + H]^+$.

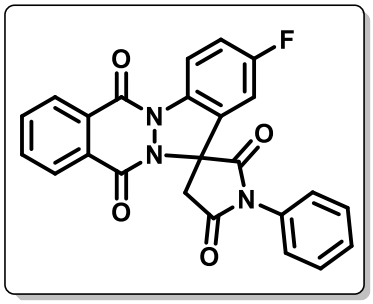

2-Chloro-1'-phenylspiro[indazolo[1,2-*b*]phthalazine-13,3'-pyrrolidine]-2',5',6,11-tetraone (48ea). White solid; yield: 67 mg (82%); mp 318−320 °C; ^{1}H NMR (400 MHz, $CDCl_3$) δ 8.51 – 8.46 (m, 1H), 8.42 (d, *J* = 8.8 Hz, 1H), 8.38 – 8.34 (m, 1H), 7.98 – 7.89 (m, 2H), 7.60 – 7.54 (m, 3H), 7.52 – 7.47 (m, 3H), 7.38 (d, *J* = 2.0 Hz, 1H), 4.03 (d, *J* = 18.3 Hz, 1H), 3.32 (d, *J* = 18.3 Hz, 1H); ^{13}C NMR (100 MHz, $CDCl_3$) δ 171.2, 170.9, 155.5, 154.4, 135.0, 134.4, 134.1, 132.3, 131.6, 131.5, 129.8, 129.4, 129.3, 128.1, 127.9, 127.7, 127.6, 126.6, 121.2, 117.3, 69.8, 41.2; HRMS (ESI-TOF) (*m/z*) calculated $C_{24}H_{15}ClN_3O_4^+$: 444.0751, found 444.0730 $[M + H]^+$.

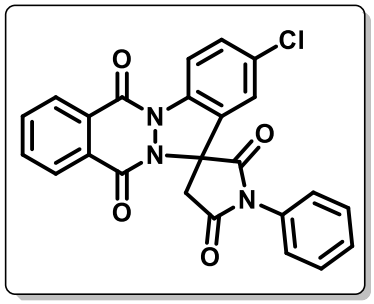

3-Chloro-2-methyl-1'-phenylspiro[indazolo[1,2-*b*]phthalazine-13,3'-pyrrolidine]-2',5',6,11-tetraone (48fa). White solid; yield: 70 mg (88%); mp 297−298 °C; ^{1}H NMR (400 MHz, $CDCl_3$) δ 8.53 – 8.45 (m, 2H), 8.38 – 8.33 (m, 1H), 7.98 – 7.89 (m, 2H), 7.59 – 7.53 (m, 2H), 7.52 − 7.46 (m, 3H), 7.24 (s, 1H), 4.03 (d, *J* = 18.3 Hz, 1H), 3.30 (d, *J* = 18.3 Hz, 1H), 2.48 (s, 3H); ^{13}C NMR (100 MHz, $CDCl_3$) δ 171.5, 171.1, 155.5, 154.3, 137.3, 135.4, 135.1, 134.3, 134.1, 131.6, 129.8, 129.4, 129.3, 128.1, 128.0, 127.7, 126.6, 124.5, 122.5, 116.8, 69.8, 41.2, 20.4; HRMS (ESI-TOF) (*m/z*) calculated $C_{25}H_{17}ClN_3O_4^+$: 458.0902, found 458.0894 $[M + H]^+$.

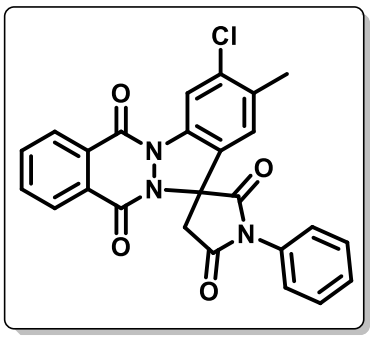

2,3-Dimethyl-1'-phenylspiro[indazolo[1,2-*b*]phthalazine-13,3'-pyrrolidine]-2',5',6,11-tetraone (48ga). White solid; yield: 74 mg (90%); mp 359−360 °C; ^{1}H NMR (400 MHz, $CDCl_3$)

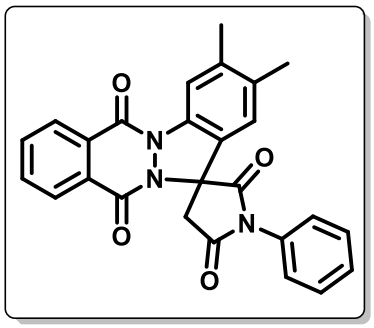

δ 8.48 (dd, J = 7.4, 1.6 Hz, 1H), 8.35 (dd, J = 7.4, 1.6 Hz, 1H), 8.28 (s, 1H), 7.96 – 7.87 (m, 2H), 7.59 – 7.53 (m, 2H), 7.52 – 7.45 (m, 3H), 7.13 (s, 1H), 4.03 (d, J = 18.2 Hz, 1H), 3.30 (d, J = 18.2 Hz, 1H), 2.41 (s, 3H), 2.36 (s, 3H); ^{13}C NMR (100 MHz, $CDCl_3$) δ 171.8, 171.6, 155.6, 154.1, 140.6, 136.2, 134.5, 134.1, 133.7, 131.7, 130.2, 129.4, 129.2, 128.0, 127.5, 126.7, 123.5, 121.3, 117.1, 69.9, 41.2, 20.4, 20.1; HRMS (ESI-TOF) (*m/z*) calculated $C_{26}H_{20}N_3O_4^+$: 438.1448, found 438.1443 $[M + H]^+$.

2,4-Dimethyl-1'-phenylspiro[indazolo[1,2-*b*]phthalazine-13,3'-pyrrolidine]-2',5',6,11-tetraone (48ha). White solid; yield: 76 mg (93%); mp 272−274 °C; ^{1}H NMR (400 MHz, $CDCl_3$)

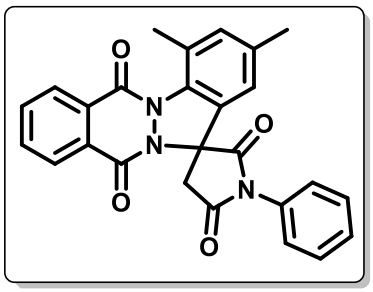

δ 8.44 – 8.40 (m, 1H), 8.32 – 8.28 (m, 1H), 7.94 – 7.86 (m, 2H), 7.57 – 7.52 (m, 2H), 7.50 – 7.44 (m, 3H), 7.21 (s, 1H), 6.97 (s, 1H), 3.98 (d, J = 18.2 Hz, 1H), 3.26 (d, J = 18.2 Hz, 1H), 2.67 (s, 3H), 2.42 (s, 3H); ^{13}C NMR (100 MHz, $CDCl_3$) δ 172.0, 171.9, 156.5, 155.5, 138.0, 135.3, 134.1, 133.7, 133.5, 131.7, 130.7, 129.3, 129.1, 128.3, 128.2, 128.2, 127.5, 127.3, 118.4, 70.0, 41.7, 22.8, 21.0; HRMS (ESI-TOF) (*m/z*) calculated $C_{26}H_{20}N_3O_4^+$: 438.1453, found 438.1421 $[M + H]^+$.

4-Ethyl-1'-phenylspiro[indazolo[1,2-*b*]phthalazine-13,3'-pyrrolidine]-2',5',6,11-tetraone (48ia). White solid; yield: 75 mg (91%); mp 269−270 °C; ^{1}H NMR (400 MHz, $CDCl_3$) δ 8.47 –

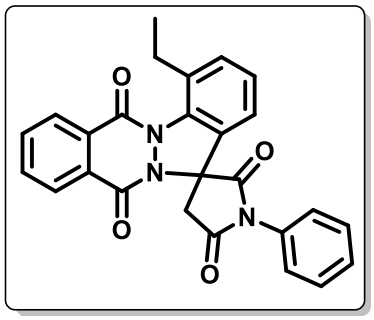

8.43 (m, 1H), 8.33 – 8.29 (m, 1H), 7.95 – 7.87 (m, 2H), 7.58 – 7.51 (m, 2H), 7.49 – 7.44 (m, 4H), 7.43 – 7.37 (m, 1H), 7.21 (dd, J = 7.6, 1.3 Hz, 1H), 4.01 (d, J = 18.2 Hz, 1H), 3.28 (d, J = 18.2 Hz, 1H), 3.18 – 3.10 (m, 2H), 1.32 (t, J = 7.5 Hz, 3H); ^{13}C NMR (100 MHz, $CDCl_3$) δ 171.9, 171.8, 156.7, 155.9, 134.9, 134.1, 134.0, 133.8, 133.0, 131.7, 130.6, 129.3, 129.1, 128.4, 128.3, 128.2, 127.8, 127.3, 126.6, 118.0, 70.0, 41.8, 28.5, 14.9; HRMS (ESI-TOF) (*m/z*) calculated $C_{26}H_{20}N_3O_4^+$: 438.1448, found 438.1428 $[M + H]^+$.

9-Methoxy-1'-phenylspiro[indazolo[1,2-*b*]phthalazine-13,3'-pyrrolidine]-2',5',6,11-tetraone + 8-Methoxy-1'-phenylspiro[indazolo[1,2-*b*]phthalazine-13,3'-pyrrolidine]-2',5',6,11-tetraone (1:2 or 2:1) (48ja). White solid; yield: 77 mg (94%); mp 274−275 °C; ^{1}H NMR (400 MHz, $CDCl_3$) δ 8.49 – 8.43 (m, 1.5H), 8.39 (d, J = 8.8 Hz, 0.5H), 8.26 (d, J = 8.7 Hz, 1H), 7.87 (d, J = 2.6 Hz, 1H), 7.74 (d, J = 2.6 Hz, 0.5H), 7.64 – 7.56 (m, 2.5H), 7.55 – 7.52 (m, 2H), 7.50 – 7.46 (m, 4H), 7.44 – 7.37 (m, 5H), 4.09 – 4.02 (m, 0.75H), 4.04 – 4.02 (m, 3.75H), 4.00 (s, 1.5H), 3.32 (two dd, J = 18.2 each, 1.5H); ^{13}C NMR (100 MHz, $CDCl_3$) δ 171.7, 171.6, 171.5, 171.3, 164.4, 164.2, 155.5, 155.4, 154.5, 154.4, 136.6, 136.4, 132.2, 131.7, 131.3, 131.3, 130.1, 130.1, 129.6, 129.4, 129.4, 129.2, 129.2, 127.0, 126.7, 126.7, 126.6, 126.4, 125.8, 123.0, 122.7, 122.2, 121.0, 120.8, 120.7, 116.4, 116.2, 109.8, 109.2, 70.0, 69.8, 56.1, 41.4, 41.3; HRMS (ESI-TOF) (*m/z*) calculated $C_{25}H_{18}N_3O_5^+$: 440.1246, found 440.1214 $[M + H]^+$.

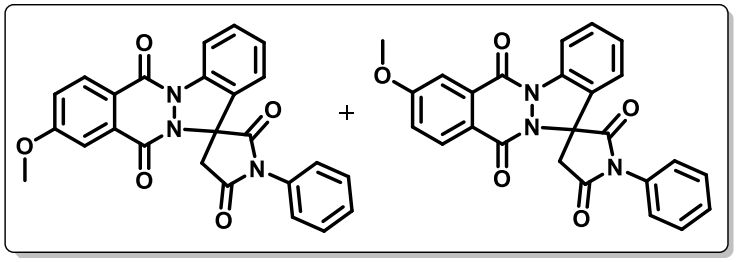

9-Bromo-1'-phenylspiro[indazolo[1,2-*b*]phthalazine-13,3'-pyrrolidine]-2',5',6,11-tetraone + 8-Bromo-1'-phenylspiro[indazolo[1,2-*b*]phthalazine-13,3'-pyrrolidine]-2',5',6,11-tetraone (1:1) (48ka). White solid; yield: 65 mg (85%); mp 268−269 °C; ^{1}H NMR (400 MHz, $CDCl_3$) δ 8.62 (d, J = 2.0 Hz, 1H), 8.50 (d, J = 2.0 Hz, 1H), 8.45 (dd, J = 8.2, 2.4 Hz, 2H), 8.34 (d, J = 8.4 Hz, 1H), 8.21 (d, J = 8.4 Hz, 1H), 8.06 – 7.99 (m, 2H), 7.65 – 7.59 (m, 2H), 7.58 – 7.53 (m, 4H), 7.51 – 7.45 (m, 6H), 7.44 – 7.39 (m, 4H), 4.03 (dd, J = 18.2, 4.8 Hz, 2H), 3.33 (dd, J = 18.2, 1.8 Hz, 2H); ^{13}C NMR (100 MHz, $CDCl_3$) δ 171.5, 171.1, 171.1, 155.0, 154.3, 153.8, 153.1, 137.5, 137.2, 136.2, 136.2, 131.4, 131.4, 131.0, 130.6, 129.8, 129.7, 129.4, 129.4, 129.3, 129.3, 129.3, 129.2, 128.8, 127.3, 127.2, 126.7, 126.6, 126.1, 126.0, 120.8, 120.8, 1106.5, 116.4, 70.2, 70.1, 41.2; HRMS (ESI-TOF) (*m/z*) calculated $C_{24}H_{15}BrN_3O_4^+$: 488.0240, found 488.0216 $[M + H]^+$.

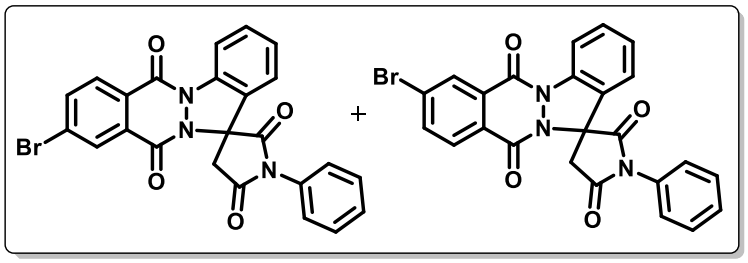

9-(*tert*-Butyl)-1'-phenylspiro[indazolo[1,2-*b*]phthalazine-13,3'-pyrrolidine]-2',5',6,11-tetraone + 8-(*tert*-Butyl)-1'-phenylspiro[indazolo[1,2-*b*]phthalazine-13,3'-pyrrolidine]-2',5',6,11-tetraone (1:1) (48la). White solid; yield: 69 mg (87%); mp 267−268 °C; ^{1}H NMR (400 MHz, $CDCl_3$) δ 8.52 – 8.46 (m, 3H), 8.42 (d, J = 8.3 Hz, 1H), 8.37 (d, J = 1.8 Hz, 1H), 8.28 (d, J = 8.3 Hz, 1H), 7.99 – 7.92 (m, 2H), 7.65 – 7.59 (m, 2H), 7.58 – 7.52 (m, 4H), 7.51 – 7.46 (m, 6H), 7.43 – 7.39 (m, 4H), 4.05 (d, J = 17.9 Hz, 2H), 3.32 (dd, J = 18.2, 2.7 Hz, 2H), 1.46 (s, 9H), 1.44 (s, 9H); ^{13}C NMR (100 MHz, $CDCl_3$) δ 171.7, 171.6, 171.4, 171.3, 158.7, 158.4, 155.7, 154.9, 136.5, 136.5, 131.8, 131.7, 131.5, 131.3, 129.8, 129.4, 129.2, 128.0, 127.7, 127.5, 127.5, 126.9, 126.8, 126.6, 126.2, 126.1, 125.5, 124.6, 124.2, 120.7, 120.7, 116.4, 116.3, 70.0, 69.9, 41.3, 35.8, 35.7, 31.1, 31.0; HRMS (ESI-TOF) (*m/z*) calculated $C_{28}H_{24}N_3O_4^+$: 466.1761, found 466.1738 $[M + H]^+$.

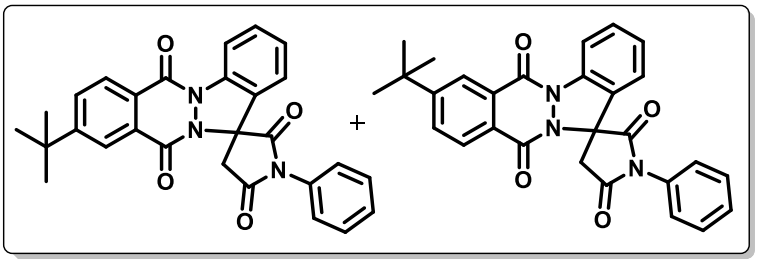

1'-Phenylspiro[pyridazino[1,2-*a*]indazole-11,3'-pyrrolidine]-2',5',6,9-tetraone (48ma). White solid; yield: 87 mg (91%); mp 261−262 °C; ^{1}H NMR (400 MHz, DMSO-d_6) δ 8.19 (d, J = 8.0 Hz, 1H), 8.03 (d, J = 7.6 Hz, 1H), 7.64 (td, J = 7.7, 1.2 Hz, 1H), 7.60 – 7.54 (m, 2H), 7.53 – 7.45 (m, 2H), 7.42 – 7.36 (m, 2H), 7.26 (d, J = 10.3 Hz, 1H), 7.17 (d, J = 10.3 Hz, 1H), 3.83 (d, J = 18.8 Hz, 1H), 3.50 (d, J = 18.8 Hz, 1H); ^{13}C NMR (100 MHz, DMSO-d_6) δ 172.9, 172.2, 154.6, 153.8, 137.2, 136.1, 134.6, 132.5, 131.4, 129.7, 129.6, 127.6, 127.6, 126.6, 123.8, 114.8, 70.7, 40.6; HRMS (ESI-TOF) (*m/z*) calculated $C_{20}H_{14}N_3O_4^+$: 360.0979, found 360.0952 $[M + H]^+$.

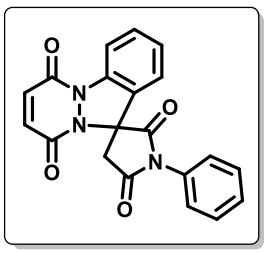

1'-(*p*-Methylphenyl)spiro[indazolo[1,2-*b*]phthalazine-13,3'-pyrrolidine]-2',5',6,11-tetraone (48ab). White solid; yield: 85 mg (96%); mp 323−324 °C; ^{1}H NMR (400 MHz, DMSO-d_6) δ 8.40 – 8.36 (m, 1H), 8.32 (d, J = 8.1 Hz, 1H), 8.30 – 8.26 (m, 1H), 8.08 – 8.02 (m, 2H), 7.99 (d, J = 7.8 Hz, 1H), 7.66 (td, J = 7.7, 1.2 Hz, 1H), 7.41 – 7.35 (m, 2H), 7.47 (td, J = 7.7, 1.0 Hz, 1H), 7.34 – 7.28 (m, 2H), 3.91 (d, J = 18.8 Hz, 1H), 3.50 (d, J = 18.8 Hz, 1H), 2.38 (s, 3H); ^{13}C NMR (100 MHz, DMSO-d_6) δ 173.2, 172.8, 155.2, 154.4, 139.3, 136.3, 135.0, 134.8, 131.5, 130.2, 129.9, 128.1, 127.9, 127.6, 127.5, 127.5, 126.8,

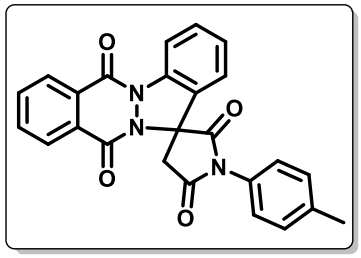

123.5, 115.3, 70.5, 41.3, 21.2; HRMS (ESI-TOF) (*m/z*) calculated $C_{25}H_{18}N_3O_4^+$: 424.1297, found 424.1287 $[M + H]^+$.

1'-(4-Methoxyphenyl)spiro[indazolo[1,2-*b*]phthalazine-13,3'-pyrrolidine]-2',5',6,11-tetraone (48ac). White solid; yield: 89 mg (97%); mp 305−306 °C; ^{1}H NMR (400 MHz, $CDCl_3$)

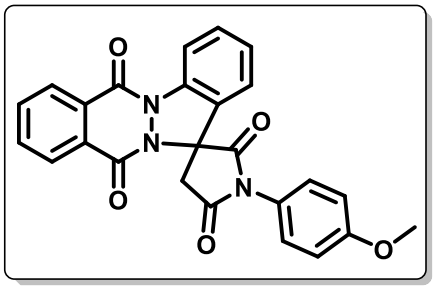

δ 8.52 – 8.46 (m, 2H), 8.38 – 8.34 (m, 1H), 7.98 – 7.88 (m, 2H), 7.65 – 7.58 (m, 1H), 7.44 – 7.36 (m, 4H), 7.08 – 7.02 (m, 2H), 4.04 (d, J = 18.2 Hz, 1H), 3.87 (s, 3H), 3.31 (d, J = 18.2 Hz, 1H); ^{13}C NMR (100 MHz, $CDCl_3$) δ 171.9, 171.5, 160.0, 155.5, 154.5, 136.4, 134.2, 133.9, 131.3, 130.1, 128.0, 127.9, 127.6, 127.0, 126.2, 124.2, 120.7, 116.4, 114.7, 70.0, 55.6, 41.2; HRMS (ESI-TOF) (*m/z*) calculated $C_{25}H_{18}N_3O_5^+$: 440.1246, found 440.1252 $[M + H]^+$.

1'-(4-Fluorophenyl)spiro[indazolo[1,2-*b*]phthalazine-13,3'-pyrrolidine]-2',5',6,11-tetraone (48ad). White solid; yield: 78 mg (87%); mp 247−248 °C; ^{1}H NMR (400 MHz, $CDCl_3$) δ 8.53 –

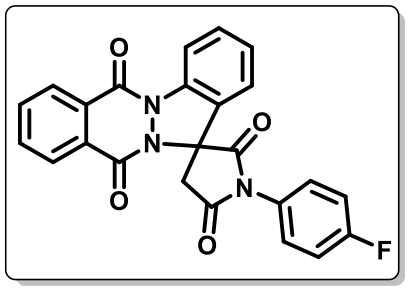

8.46 (m, 2H), 8.38 – 8.33 (m, 1H), 7.98 – 7.89 (m, 2H), 7.65 – 7.59 (m, 1H), 7.52 – 7.45 (m, 2H), 7.44 – 7.37 (m, 2H), 7.27 – 7.20 (m, 2H), 4.03 (d, J = 18.3 Hz, 1H), 3.33 (d, J = 18.3 Hz, 1H); ^{13}C NMR (100 MHz, $CDCl_3$) δ 171.5, 171.3, 162.6 ($^1J_{C\text{-}F}$ = 247.9 Hz), 155.6, 154.5, 136.4, 134.3, 134.0, 131.4, 130.1, 128.6 ($^3J_{C\text{-}F}$ = 8.8 Hz), 128.1, 127.9, 127.6, 127.5, 127.5, 127.0, 125.9, 120.7, 116.6, 116.4 ($^2J_{C\text{-}F}$ = 22.4 Hz), 70.0, 41.3; ^{19}F NMR (376 MHz, $CDCl_3$) δ -111.32; HRMS (ESI-TOF) (*m/z*) calculated $C_{24}H_{15}FN_3O_4^+$: 428.1046, found 428.1019 $[M + H]^+$.

1'-(4-Chlorophenyl)spiro[indazolo[1,2-*b*]phthalazine-13,3'-pyrrolidine]-2',5',6,11-tetraone (48ae). White solid; yield: 78 mg (84%); mp 290−291 °C; ^{1}H NMR (400 MHz, $CDCl_3$ + DMSO-

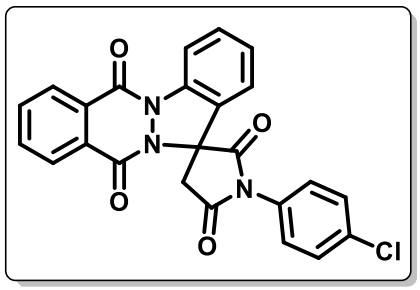

d_6) δ 8.44 – 8.37 (m, 2H), 8.29 – 8.24 (m ,1H), 7.91 – 7.81 (m, 2H), 7.58 – 7.51 (m, 1H), 7.48 – 7.41 (m, 2H), 7.40 – 7.32 (m, 4H), 3.94 (d, J = 18.4 Hz, 1H), 3.28 (d, J = 18.4 Hz, 1H); ^{13}C NMR (100 MHz, $CDCl_3$ + DMSO-d_6) δ 171.3, 171.2, 155.5, 154.4, 136.4, 135.0, 134.3, 133.9, 131.3, 130.1, 130.0, 129.5, 127.9, 127.8, 127.5, 127.0, 125.8, 120.9, 116.2, 69.9, 41.2; HRMS (ESI-TOF) (*m/z*) calculated $C_{24}H_{15}ClN_3O_4^+$: 444.0746, found 444.0751 $[M + H]^+$.

1'-(4-Bromophenyl)spiro[indazolo[1,2-*b*]phthalazine-13,3'-pyrrolidine]-2',5',6,11-tetraone (48af). White solid; yield: 84 mg (82%); mp 314−315 °C; ^{1}H NMR (400 MHz, $CDCl_3$) δ 8.52 – 8.46 (m, 2H), 8.37 – 8.33 (m, 1H), 7.98 – 7.88 (m, 2H), 7.70 – 7.66 (m, 2H), 7.65 – 7.60 (m, 1H), 7.46 – 7.35 (m, 4H), 4.03 (d, *J* = 18.3 Hz, 1H), 3.33 (d, *J* = 18.3 Hz, 1H); ^{13}C NMR (100 MHz, $CDCl_3$) *δ* 171.3, 171.1, 155.6, 154.5, 136.4, 134.3, 134.0, 132.6, 131.5, 130.6, 130.1, 128.2, 128.1, 127.9, 127.6, 127.0, 125.8, 123.2, 120.7, 116.4, 70.0, 41.3; HRMS (ESI-TOF) (*m/z*) calculated $C_{24}H_{15}BrN_3O_4^+$: 488.0240, found 488.0229 $[M + H]^+$.

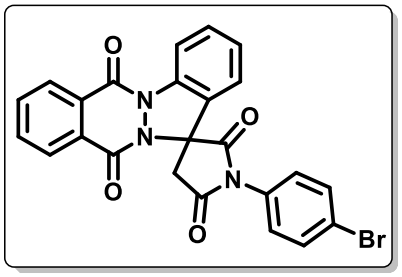

1'-(4-Nitrophenyl)spiro[indazolo[1,2-*b*]phthalazine-13,3'-pyrrolidine]-2',5',6,11-tetraone (48ag). Pale yellow solid; yield: 84 mg (88%); mp 266−267 °C; ^{1}H NMR (400 MHz, $CDCl_3$) *δ* 8.50 – 8.45 (m, 2H), 8.40 – 8.36 (m, 1H), 8.32 (d, *J* = 8.2 Hz, 1H), 8.29 – 8.25 (m, 1H), 8.10 (d, *J* = 7.5 Hz, 1H), 8.08 – 8.00 (m, 2H), 7.81 – 7.76 (m, 2H), 7.70 – 7.65 (m, 1H), 7.48 (td, *J* = 7.7, 1.1 Hz, 1H), 3.98 (d, *J* = 19.0 Hz, 1H), 3.58 (d, *J* = 18.8 Hz, 1H); ^{13}C NMR (100 MHz, $CDCl_3$) *δ* 172.6, 172.2, 155.3, 154.4, 147.7, 138.0, 136.5, 135.0, 134.7, 131.5, 130.0, 128.6, 128.2, 127.9, 127.6, 127.3, 126.5, 125.1, 124.0, 115.2, 70.6, 41.6; HRMS (ESI-TOF) (*m/z*) calculated $C_{24}H_{15}N_4O_6^+$: 455.0986, found 455.0956 $[M + H]^+$.

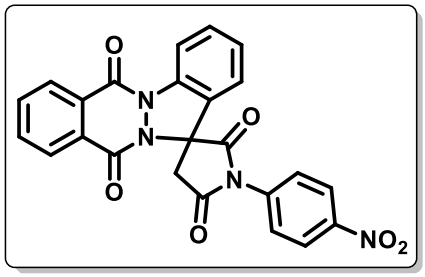

1'-(4-(Trifluoromethyl)phenyl)spiro[indazolo[1,2-*b*]phthalazine-13,3'-pyrrolidine]-2',5',6,11-tetraone (48ah). White solid; yield: 92 mg (92%); mp 292−293 °C; ^{1}H NMR (400 MHz, $CDCl_3$) *δ* 8.54 – 8.46 (m, 2H), 8.38 – 8.32 (m, 1H), 7.99 – 7.90 (m, 2H), 7.82 (d, *J* = 8.4 Hz, 2H), 7.69 – 7.60 (m, 3H), 7.46 – 7.39 (m, 2H), 4.05 (d, *J* = 18.3 Hz, 1H), 3.36 (d, *J* = 18.4 Hz, 1H); ^{13}C NMR (100 MHz, $CDCl_3$) *δ* 171.1, 171.0, 155.7, 154.4, 136.5, 134.3, 134.0, 131.5, 130.1, 128.1, 127.9, 127.6, 127.0, 127.0, 126.5 (q, $J_{C\text{-}F}$ = 3.7 Hz), 125.7, 120.8, 116.4, 70.0, 41.3; ^{19}F NMR (376 MHz, $CDCl_3$) *δ* -62.78; HRMS (ESI-TOF) (*m/z*) calculated $C_{25}H_{15}F_3N_3O_4^+$: 478.1009, found 478.0988 $[M + H]^+$.

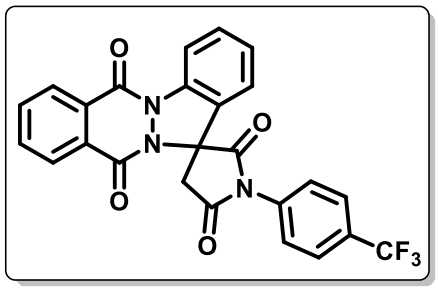

1'-(3-Methylphenyl)spiro[indazolo[1,2-*b*]phthalazine-13,3'-pyrrolidine]-2',5',6,11-tetraone (48ai). White solid; yield: 82 mg (92%); mp 264−265 °C; ^{1}H NMR (400 MHz, $CDCl_3$) δ 8.52 – 8.46 (m, 2H), 8.40 – 8.35 (m, 1H), 7.98 – 7.88 (m, 2H), 7.65 – 7.58 (m, 1H), 7.46 – 7.39 (m, 3H), 7.30 – 7.24 (m, 3H), 4.06 (d, J = 18.2 Hz, 1H), 3.32 (d, J = 18.2 Hz, 1H), 2.45 (s, 3H); ^{13}C NMR (100 MHz, $CDCl_3$) δ 171.7, 171.3, 155.6, 154.5, 139.6, 136.4, 134.2, 133.9, 131.5, 131.3, 130.1, 130.1, 129.2, 128.1, 128.0, 127.6, 127.2, 127.0, 126.2, 123.7, 120.7, 116.4, 70.1, 41.3, 21.3; HRMS (ESI-TOF) (*m*/z) calculated $C_{25}H_{18}N_3O_4^+$: 424.1292, found 424.1258 [M + H]$^+$.

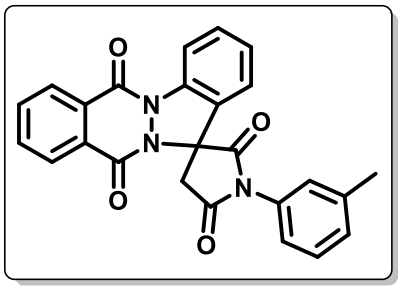

1'-(2-Methylphenyl)spiro[indazolo[1,2-*b*]phthalazine-13,3'-pyrrolidine]-2',5',6,11-tetraone (48aj). (Mixture of two rotamers, 1:1) White solid; yield: 78 mg (88%); mp 314−315 °C; ^{1}H NMR (400 MHz, $CDCl_3$) δ 8.53 – 8.45 (m, 4H), 8.38 (d, J = 7.2 Hz, 2H), 7.98 – 7.88 (m, 4H), 7.66 – 7.59 (m, 2H), 7.47 – 7.32 (m, 11H), 7.15 (d, J = 7.6 Hz, 1H), 4.22 (d, J = 18.0 Hz, 1H), 4.04 (d, J = 18.4 Hz, 1H), 3.37 (d, J = 18.4 Hz, 1H), 3.29 (d, J = 18.0 Hz), 2.47 (s, 3H), 2.32 (s, 3H); ^{13}C NMR (100 MHz, $CDCl_3$) δ 171.6, 171.4, 171.2, 171.2, 155.6, 155.4, 154.5, 154.5, 137.1, 136.5, 136.3, 135.1, 134.2, 134.2, 133.9, 133.9, 131.6, 131.3, 131.3, 131.0, 130.9, 130.6, 130.1, 130.0, 130.0, 128.3, 128.1, 128.0, 128.0, 127.7, 127.6, 127.4, 127.0, 127.0, 126.8, 126.4, 126.1, 120.7, 120.4, 116.5, 116.4, 70.2, 70.2, 41.6, 41.0, 18.0, 17.9; HRMS (ESI-TOF) (*m/z*) calculated $C_{25}H_{18}N_3O_4^+$: 424.1292, found 424.1263 [M + H]$^+$.

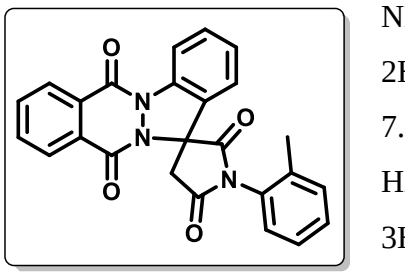

1'-(Naphthalen-1-yl)spiro[indazolo[1,2-*b*]phthalazine-13,3'-pyrrolidine]-2',5',6,11-tetraone (48ak). (Mixture of two rotamers, 1:1) White solid; yield: 91 mg (94%); mp 344−345 °C; ^{1}H NMR (400 MHz, $CDCl_3$) δ 8.43 – 8.39 (m, 3H), 8.37 – 8.31 (m, 4H), 8.21 – 8.13 (m, 4H), 8.12 – 8.05 (m, 6H), 8.04 – 8.00 (m, 1H), 7.81 (d, J = 6.7 Hz, 1H), 7.78 – 7.61 (m, 9H), 7.57 (d, J = 7.3 Hz, 1H), 7.54 – 7.49 (m, 1H), 4.17 (d, J = 18.9 Hz, 1H), 4.00 (d, J = 18.8 Hz, 1H), 3.88 (d, J = 18.8 Hz, 1H), 3.60 (d, J = 18.9 Hz, 1H); ^{13}C NMR (100 MHz, $CDCl_3$) δ 173.7, 173.3, 173.2, 173.1, 155.4, 155.2, 154.4, 154.4, 136.6, 136.3, 135.0, 134.8, 134.3, 134.2, 131.5, 131.5, 130.6,

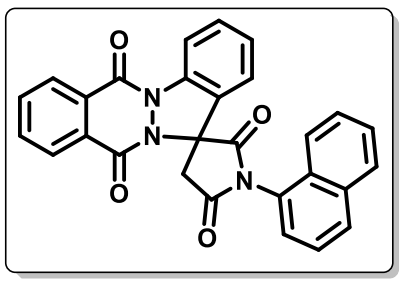

130.4, 130.2, 130.1, 130.0, 129.6, 129.5, 129.4, 128.9, 128.7, 128.2, 127.9, 127.8, 127.7, 127.7, 127.5, 127.5, 127.5, 127.3, 127.2, 127.2, 126.7, 126.2, 126.0, 123.7, 123.6, 123.5, 122.8, 115.3, 115.3, 71.0, 70.6, 41.6, 41.5; HRMS (ESI-TOF) (*m/z*) calculated $C_{28}H_{18}N_3O_4^+$: 460.1292, found 460.1258 $[M + H]^+$.

1'-Benzylspiro[indazolo[1,2-*b*]phthalazine-13,3'-pyrrolidine]-2',5',6,11-tetraone (48al). White solid; yield: 84 mg (95%); mp 275−276 °C; ^{1}H NMR (400 MHz, $CDCl_3$) δ 8.51 – 8.46 (m, 1H), 8.43 (d, J = 8.2 Hz, 1H), 8.36 – 8.30 (m, 1H), 7.97 – 7.86 (m, 2H), 7.58 – 7.51 (m, 1H), 7.48 – 7.44 (m, 2H), 7.42 – 7.32 (m, 3H), 7.28 – 7.24 (td, J = 6.6, 1.0 Hz, 1H), 6.98 (d, J = 7.7 Hz, 1H), 4.95 (overlapped doublets, J = 14.2 Hz, 2H), 3.95 (d, J = 18.0 Hz, 1H), 3.11 (d, J = 18.0 Hz, 1H); ^{13}C NMR (100 MHz, $CDCl_3$) δ 172.0, 171.8, 155.4, 154.5, 136.2, 135.2, 134.2, 133.9, 131.2, 130.0, 128.8, 128.5, 128.2, 128.0, 127.6, 126.9, 126.2, 120.5, 116.3, 70.0, 43.4, 41.0; HRMS (ESI-TOF) (*m/z*) calculated $C_{25}H_{18}N_3O_4^+$: 424.1297, found 424.1302 $[M + H]^+$.

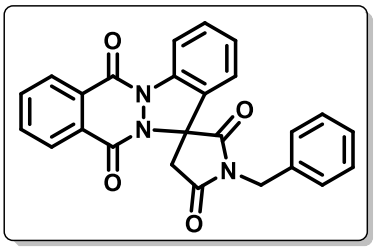

1'-Cyclohexylspiro[indazolo[1,2-*b*]phthalazine-13,3'-pyrrolidine]-2',5',6,11-tetraone (48am). White solid; yield: 75 mg (86%); mp 227−229 °C; ^{1}H NMR (400 MHz, $CDCl_3$) δ 8.50 – 8.43 (m, 2H), 8.36 – 8.31 (m, 1H), 7.95 – 7.86 (m, 2H), 7.60 – 7.54 (m, 1H), 7.35 (td, J = 7.7, 1.0 Hz, 1H), 7.23 – 7.19 (m, 1H), 4.24 – 4.11 (m, 1H), 3.86 (d, J = 17.9 Hz, 1H), 3.07 (d, J = 18.0 Hz, 1H), 2.34 – 2.17 (m, 2H), 1.94 – 1.78 (m, 4H), 1.46 – 1.20 (m, 4H); ^{13}C NMR (100 MHz, $CDCl_3$) δ 172.5, 172.0, 155.3, 154.5, 136.3, 134.1, 133.8, 131.1, 130.0, 128.1, 128.0, 127.6, 126.9, 126.5, 120.4, 116.3, 69.6, 53.1, 40.9, 29.0, 28.7, 25.8, 25.0; HRMS (ESI-TOF) (*m/z*) calculated $C_{24}H_{22}N_3O_4^+$: 416.1605, found 416.1590 $[M + H]^+$.

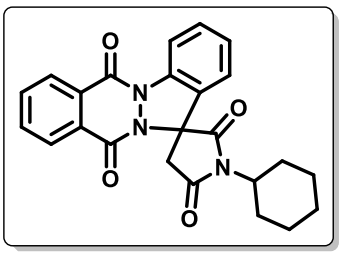

1'-Methylspiro[indazolo[1,2-*b*]phthalazine-13,3'-pyrrolidine]-2',5',6,11-tetraone (48an). White solid; yield: 53 mg (73%); mp 345−346 °C; ^{1}H NMR (400 MHz, $CDCl_3$) δ 8.52 – 8.44 (m, 2H), 8.34 – 8.29 (m, 1H), 7.97 – 7.88 (m, 2H), 7.59 (td, J = 7.4, 1.2 Hz, 1H), 7.37 (td, J = 7.7, 1.0 Hz, 1H), 7.26 (d, J = 7.7 Hz, 1H), 3.89 (d, J = 18.0 Hz, 1H), 3.27 (s, 3H), 3.16 (d, J = 18.1 Hz, 1H); ^{13}C NMR (100 MHz, $CDCl_3$) δ 172.5, 172.2, 155.4, 154.5, 136.3, 134.2, 133.9, 131.2, 130.1, 128.0, 127.9, 127.5, 126.9, 126.0,

120.7, 116.3, 70.1, 41.2, 25.8; HRMS (ESI-TOF) (*m/z*) calculated $C_{19}H_{14}N_3O_4^+$: 348.0984, found 348.0964 $[M + H]^+$.

1'-Propylspiro[indazolo[1,2-*b*]phthalazine-13,3'-pyrrolidine]-2',5',6,11-tetraone (48ao). White solid; yield: 59 mg (75%); mp 240−241 °C; ^{1}H NMR (400 MHz, $CDCl_3$) δ 8.50 − 8.44 (m, 2H), 8.34 – 8.31 (m, 1H), 7.96 – 7.86 (m, 2H), 7.61 – 7.55 (m, 1H), 7.37 (td, *J* = 7.6, 1.0 Hz, 1H), 7.23 (d, *J* = 7.7 Hz, 1H), 3.91 (d, *J* = 18.0 Hz, 1H), 3.78 – 3.67 (m, 2H), 3.13 (d, *J* = 18.0 Hz, 1H), 1.85 – 1.75 (m, 2H), 1.03 (t, *J* = 7.4 Hz, 3H); ^{13}C NMR (100 MHz, $CDCl_3$) δ 172.5, 172.1, 155.3, 154.5, 136.3, 134.1, 133.9, 131.2, 130.0, 128.0, 128.0, 127.6, 126.9, 126.3, 120.5, 116.3, 70.0, 41.6, 41.1, 21.0, 11.3; HRMS (ESI-TOF) (*m/z*) calculated $C_{21}H_{18}N_3O_4^+$: 376.1297, found 376.1300 $[M + H]^+$.

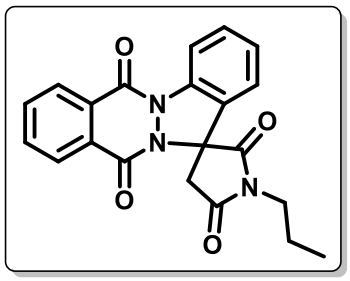

1'-Allylspiro[indazolo[1,2-*b*]phthalazine-13,3'-pyrrolidine]-2',5',6,11-tetraone (48ap). White solid; yield: 65 mg (83%); mp 227−228 °C; ^{1}H NMR (400 MHz, $CDCl_3$) δ 8.51 – 8.43 (m, 2H), 8.35 – 8.30 (m, 1H), 7.96 – 7.87 (m, 2H), 7.61 – 7.55 (m, 1H), 7.37 (td, *J* = 7.6, 1.0 Hz, 1H), 7.26 – 7.22 (m, 1H), 6.01 – 5.86 (m, 1H), 5.46 (dq, *J* = 17.1, 1.4 Hz, 1H), 5.33 (dq, *J* = 10.3, 1.2 Hz, 1H), 4.40 – 4.32 (m, 2H), 3.95 (d, *J* = 18.0 Hz, 1H), 3.16 (d, *J* = 18.0 Hz, 1H); ^{13}C NMR (100 MHz, $CDCl_3$) δ 171.9, 171.7, 155.4, 154.5, 136.3, 134.2, 133.9, 131.2, 130.0, 129.9, 128.0, 127.6, 126.9, 126.1, 120.6, 119.1, 116.3, 70.0, 41.9, 41.1; HRMS (ESI-TOF) (*m/z*) calculated $C_{21}H_{16}N_3O_4^+$: 374.1135, found 374.1108 $[M + H]^+$.

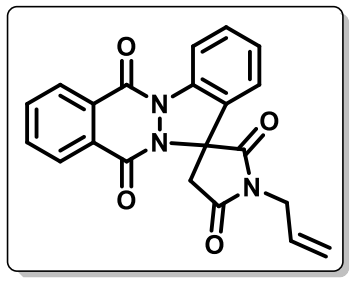

Spiro[indazolo[1,2-*b*]phthalazine-13,3'-pyrrolidine]-2',5',6,11-tetraone (48aq). White solid; yield: 38 mg (54%); mp 255−257 °C; ^{1}H NMR (400 MHz, DMSO-d_6) δ 12.33 (s, 1H), 8.39 – 8.33 (m, 1H), 8.29 (d, *J* = 8.1 Hz, 1H), 8.25 – 8.21 (m, 1H), 8.07 – 7.99 (m, 2H), 7.75 (d, *J* = 7.6 Hz, 1H), 7.65 – 7.60 (m, 1H), 7.42 (td, *J* = 7.3, 0.6 Hz, 1H), 3.72 (d, *J* = 18.6 Hz, 1H), 3.22 (d, *J* = 18.6 Hz, 1H); ^{13}C NMR (100 MHz, DMSO-d_6) δ 175.1, 174.5, 154.8, 154.3, 136.2, 134.8, 134.7, 131.2, 129.9, 128.3, 127.9, 127.5, 127.3, 127.3, 122.9, 115.2, 71.6, 42.1; HRMS (ESI-TOF) (*m/z*) calculated $C_{18}H_{12}N_3O_4^+$: 334.0822, found 334.0792 $[M + H]^+$.

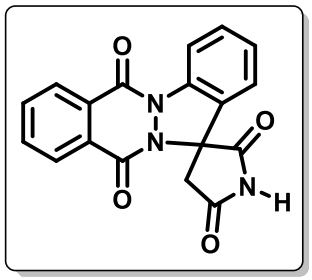

Ethyl 2',5',6,11-tetraoxo-6,11-dihydrospiro[indazolo[1,2-*b*]phthalazine-13,3'-pyrrolidine]-1'-carboxylate (48ar). Pale yellow solid; yield: 58 mg (68%); mp 274−276 °C; ^{1}H NMR (400 MHz, DMSO-d_6) δ 8.38 – 8.34 (m, 1H), 8.29 (d, J = 8.2 Hz, 1H), 8.25 – 8.21 (m, 1H), 8.08 – 8.00 (m ,2H), 7.94 (d, 7.5 Hz, 1H), 7.69 – 7.63 (m, 1H), 7.45 (td, J = 7.7, 1.0 Hz, 1H), 4.43 (q, 7.1 Hz, 2H), 3.85 (d, J = 18.9 Hz, 1H), 3.50 (d, J = 18.9 Hz, 1H), 1.33 (t, J = 7.1 Hz, 3H); ^{13}C NMR (100 MHz, DMSO-d_6) δ 169.7, 169.5, 155.1, 154.3, 147.9, 136.4, 135.0, 134.8, 131.6, 130.0, 128.0, 127.9, 127.6, 127.3, 126.2, 123.8, 115.2, 70.2, 65.1, 41.2, 14.3; HRMS (ESI-TOF) (*m/z*) calculated $C_{21}H_{16}N_3O_6^+$: 406.1034, found 406.1045 $[M + H]^+$.

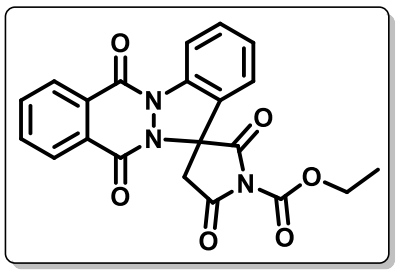

Ethyl 2-(2',5',6,11-tetraoxo-6,11-dihydrospiro[indazolo[1,2-b]phthalazine-13,3'-pyrrolidin]-1'-yl)acetate (48as). Pale yellow solid; yield: 57 mg (65%); mp 291−293 °C; ^{1}H NMR (400 MHz, DMSO-d_6) δ 8.40 – 8.36 (m, 1H), 8.31 (d, J = 8.1 Hz, 1H), 8.24 – 8.20 (m, 1H), 8.09 – 8.00 (m, 2H), 7.69 – 7.64 (m, 1H), 8.61 – 8.57 (m, 1H), 7.48 (td, J = 7.6, 1.0 Hz, 1H), 4.57 (d, J = 17.3 Hz, 1H), 4.43 (d, J = 17.3 Hz, 1H), 4.25 – 4.17 (m, 2H), 3.94 (d, J = 18.8 Hz, 1H), 3.42 (d, J = 18.8 Hz, 1H), 1.25 (t, 7.1 Hz, 3H); ^{13}C NMR (100 MHz, DMSO-d_6) δ 172.7, 172.3, 167.1, 154.8, 154.4, 136.2, 134.9, 134.8, 131.5, 130.0, 128.2, 27.9, 127.5, 127.4, 126.8, 122.7, 115.4, 70.1, 62.2, 40.4, 39.5, 14.4; HRMS (ESI-TOF) (*m/z*) calculated $C_{22}H_{18}N_3O_6^+$: 420.1190, found 420.420.1215 $[M + H]^+$.

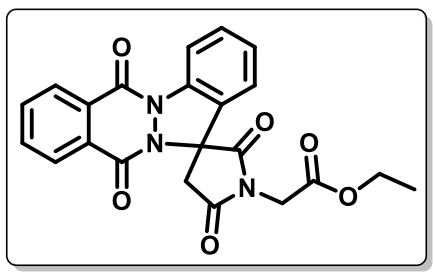

2-(2-(2,5-Dioxo-1-phenylpyrrolidin-3-yl)-4-isopropylphenyl)-2,3-dihydrophthalazine-1,4-dione (48'ca). To an oven-dried sealed tube with a screw cap (PTFE) charged with **47c** (50 mg, 1 equiv), [Cp*****$RhCl_2$]$_2$ (0.05 equiv) and AgOAc (2 equiv) in DCE (3 mL), **2a** (2.0 equiv) was added. The reaction mixture was allowed to stirr at 120 ºC for 6 h. The reaction was cooled to room temperature, diluted with DCM (5 mL), filtered through celite. The reaction was quenched with water and extracted with DCM (2 x 15 mL). The organic layers were combined, dried over anhydrous sodium sulphate and concentrated *in vacuo*. Purification by column chromatography (hexanes/ethyl acetate = 7:3) afforded compound **48'ca** as White solid; yield: 74 mg (92%); mp

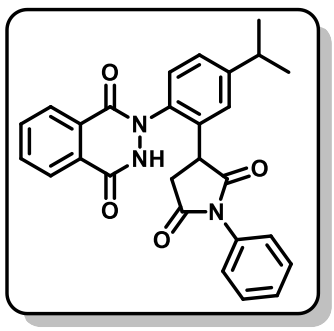

160−162 °C; ^{1}H NMR (400 MHz, DMSO-d_6) δ 11.80 (s, 1H), 8.31 – 8.27 (m, 1H), 8.06 – 7.91 (m, 3H), 7.33 – 7.46 (m, 6H), 7.20 – 7.14 (m, 2H), 4.40 – 4.32 (m, 1H), 3.20 – 3.12 (m, 1H), 3.06 – 2.96 (m, 1H), 2.94 – 2.85 (m, 1H), 1.28 (d, J = 1.9 Hz, 3H), 1.26 (d, J = 1.9 Hz, 3H); ^{13}C NMR (100 MHz, DMSO-d_6) δ 177.2, 175.7, 158.5, 149.8, 134.1, 133.1, 132.9, 129.5, 129.1, 128.6, 127.7, 127.5, 127.3, 126.4, 43.0, 38.2, 33.7, 24.3; HRMS (ESI-TOF) (m/z) calculated $C_{27}H_{24}N_3O_4^+$: 454.1761, found 454.1744 $[M + H]^+$.

Procedure for deuterium labelling study. To an oven-dried sealed tube with a screw cap (PTFE) charged with 2-(4-methylphenyl)-2,3-dihydrophthalazine-1,4-dione (**47b**) (50 mg, 1 equiv) in CD_3COOD (10 equiv), MeOD (1 mL) and DCE (0.5 mL), $[Cp^*RhCl_2]_2$ (0.05 equiv) and AgOAc (2 equiv) were added. The reaction mixture was allowed to stirr at 120 ºC for 12 h. The reaction was cooled to room temperature, diluted with DCM (5 mL), filtered through celite. The reaction was quenched with water and extracted with DCM (2 x 15 mL). The organic layers were combined, dried over anhydrous sodium sulphate and concentrated *in vacuo*. Purification by column chromatography using ethyl acetate/hexanes (3:7) as eluent afforded the desired product (**47b-*d*$_2$**) in 75% yield with ~72% deuterium incorporation at the two *ortho* positions of aryl ring.

Procedure for parallel experiments

For the first set, to an oven-dried sealed tube with a screw cap (PTFE), **47b** (25.23 mg, 0.1 mmol), $[Cp^*RhCl_2]_2$ (0.05 equiv), AgOAc (2 equiv), *N*-phenyl maleimide (**2a**) (34.63 mg, 0.2 mmol) and DCE (5 mL) were added. For the parallel second set, 1b-d_2 was used (instead of **47b**) under standard conditions. The sealed tubes were capped and the reaction mixtures were allowed to stir at 120 ºC for 1 h, 2 h, 3 h, 4 h, 5 h and 6 h. Reaction fractions were collected at regular time intervals, filtered and concentrated under reduced pressure. The product conversion percentage was determined by ^{1}H NMR analysis. The KIE was calculated as k_H/k_D = 1.12.

Procedure for intermolecular competitive experiment

To an oven-dried sealed tube with a screw cap (PTFE) charged with **47b** (25.23 mg, 0.1 mmol), (**47b-*d*$_2$**) (25.43 mg, 0.1 mmol), $[Cp^*RhCl_2]_2$ (0.05 equiv), AgOAc (2 equiv), *N*-phenyl maleimide (**2a**) (34.63 mg, 0.2 mmol) and DCE (3 mL) were added. The sealed tube was capped and the reaction mixture was allowed to stir at 120 ºC for 4 h, the reaction was cooled to room temperature, diluted with DCM (5 mL), filtered through celite. The reaction was quenched with water and extracted with DCM (2 x 15 mL). The organic layers were combined, dried over anhydrous sodium sulphate and concentrated *in vacuo*. The crude residue was purified by column chromatography

using ethyl acetate/hexanes (1:9 to 2:8) as eluent afforded the desired product in combined yield (**48ba : 48ba-*d*$_1$**) in 31% yield. The intermolecular P_H/P_D was found to be 3.0.

Procedure for the isolation of [Rh(Cp)*(OAc)$_2$] complex

To an oven-dried sealed tube with a screw cap (PTFE) charged with [Cp*****RhCl$_2$]$_2$ (1 equiv), AgOAc (2.5 equiv) and DCE (3 mL) were added and the reaction was stirred at room temperature for 6 h. A fraction of reaction mixture was collected, filtered and dried. ^{1}H NMR analysis of the crude reaction mixture indicated the presence of [Rh(Cp)*****(OAc)$_2$] complex intermediate.

[Rh(Cp)*(OAc)$_2$] complex. ^{1}H NMR (Crude reaction mixture) (400 MHz, DMSO-*d*$_6$) δ 1.97 (s, 6H), 1.73 (s, 15H); HRMS (ESI-TOF) (*m/z*) calculated $C_{14}H_{22}O_4Rh^+$: 357.0568, found 357.0544 $[M + H]^+$.

Procedure for the synthesis of [Rh(Cp)*(4-isopropylphenyl)phthalazine-dione)maleimide] complex (B)

To an oven-dried sealed tube with a screw cap (PTFE) charged with 2-(4-isopropylphenyl)-2,3-dihydrophthalazine-1,4-dione (**48c**) (50 mg, 1 equiv) in DCE (3 mL) at room temperature, [Cp*****RhCl$_2$]$_2$ (0.5 equiv) and AgOAc (2 equiv), *N*-phenylmaleimide (**2a**) (2.0 equiv) was added. The stirring was continued for additional 20 h, after which diluted with DCM (5 mL), filtered through celite. The reaction was quenched with water and extracted with DCM (2 x 15 mL). The organic layers were combined, dried over anhydrous sodium sulphate and concentrated *in vacuo*. Purification by column chromatography using ethyl acetate/hexanes (1:1) as eluent afforded the desired product (**B**) in 43% yield.

[Rh(Cp)*(4-isopropylphenyl)phthalazine-dione)maleimide] complex (B). Orange solid; yield: 26 mg (43%); mp 257−258 °C; ^{1}H NMR (400 MHz, DMSO-*d*$_6$) δ 8.14 − 8.07 (m, 1H), 7.78 – 7.74 (m, 1H), 7.73 – 7.66 (m, 2H), 7.60 (d, *J* = 8.1 Hz, 1H), 7.37 (d, *J* = 2.1 Hz, 1H), 7.30 (dd, *J* = 8.1, 2.0 Hz, 1H), 7.17 – 7.06 (m, 3H), 6.96 – 6.92 (m, 2H), 4.76 – 4.68 (m, 2H), 3.01 – 2.94 (m, 2H), 1.35 (s, 15H), 1.28 (overlapped doublets, *J* = 4.0 Hz, 6H); ^{13}C NMR (100 MHz, DMSO-*d*$_6$) δ 180.6, 174.3, 160.5, 156.9, 148.0, 135.0, 134.1, 133.4, 132.9, 132.2, 130.6, 128.2, 127.9, 127.2, 127.1, 125.3, 124.5, 100.0, 94.0, 93.9, 54.1, 33.7, 24.4, 24.2, 9.1; HRMS (ESI-TOF) (*m/z*) calculated $C_{37}H_{37}N_3O_4Rh^+$: 690.1839, found 690.1808 $[M + H]^+$.

3.4 Single Crystal X-ray Diffraction Studies

After choosing a suitable crystal with the help of a light microscope, it was mounted in a nylon loop to attach to a goniometer head for centering, initial crystal evaluation and data collection

using a Kappa APEX II diffractometer equipped with a CCD detector (with the crystal-to-detector distance fixed at 60 mm) and sealed-tube monochromated MoKα radiation using the program APEX2.[83] With data integrated, reflections were fitted and values of F^2 and $\sigma(F^2)$ for each reflection were obtained by using the program SAINT.[83] Further correction to data were applied for Lorentz and polarization effects. Using the subroutine XPREP[83] for the processing of data that included determination of space group, application of an absorption correction (SADABS)[83], merging of data, necessary files were generated for solution and refinement. Its structure was solved by direct methods using the SHELXS program of the SHELXTL package and was refined using SHELXL.[84,85] All non-hydrogen atoms were refined with anisotropic displacement parameters. All hydrogen atoms were placed in ideal positions and refined as riding atoms with individual isotropic displacement parameters. All figures were drawn using MERCURY V 3.0[86]

3.4.1 Crystal data for 48al (CCDC No. 2085563). $C_{25}H_{17}N_3O_4$, Mr = 423.42 g/mol, monoclinic, space group *P*-1 (No. 2), a = 9.703(3) Å, b = 9.990(3) Å, c = 11.609(3) Å, α = 99.013(6)°, β = 108.540(6)°, γ = 94.588(6)°, V = 1043.5(5) Å^3, Z = 2, D_{calcd} = 1.348 g/cm^3, T = 296(2) K; Full matrix least-square on F^2; R_1 = 0.075, wR_2 = 0.202 for 2894 observed reflections [I > 2σ(I)] and R_1 = 0.0858, wR_2 = 0.2193 for all 3695 reflections; number of parameters = 290; GOF = 1.056.

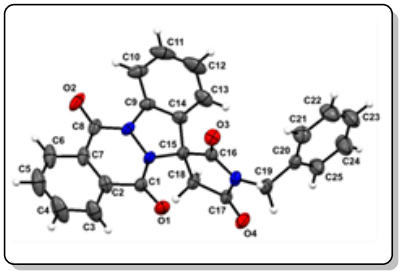

3.5 References

(1) Ritleng, V.; Sirlin, C.; Pfeffer, M. *Chemical Reviews* **2002**, *102*, 1731-1770.

(2) Wencel-Delord, J.; Dröge, T.; Liu, F.; Glorius, F. *Chemical Society Reviews* **2011**, *40*, 4740-4761.

(3) Yang, L.; Huang, H. *Chemical Reviews* **2015**, *115*, 3468-3517.

(4) Gensch, T.; Hopkinson, M.; Glorius, F.; Wencel-Delord, J. *Chemical Society Reviews* **2016**, *45*, 2900-2936.

(5) Arockiam, P. B.; Bruneau, C.; Dixneuf, P. H. *Chemical Reviews* **2012**, *112*, 5879-5918.

(6) Manikandan, R.; Jeganmohan, M. *Chemical Communications* **2017**, *53*, 8931-8947.

(7) Nareddy, P.; Jordan, F.; Szostak, M. *ACS Catalysis* **2017**, *7*, 5721-5745.

(8) Song, G.; Wang, F.; Li, X. *Chemical Society Reviews* **2012**, *41*, 3651-3678.

(9) Huang, Z.; Lim, H. N.; Mo, F.; Young, M. C.; Dong, G. *Chemical Society Reviews* **2015**, *44*, 7764-7786.

(10) Zhang, Z.; Tanaka, K.; Yu, J.-Q. *Nature* **2017**, *543*, 538-542.

(11) Rouquet, G.; Chatani, N. *Chemical Science* **2013**, *4*, 2201-2208.

(12) Liu, B.; Hu, P.; Zhou, X.; Bai, D.; Chang, J.; Li, X. *Organic Letters* **2017**, *19*, 2086-2089.

(13) Bachon, A. K.; Hermann, A.; Bolm, C. *Chemistry–A European Journal* **2019**, *25*, 5889-5892.

(14) Deslandes, S.; Chassaing, S.; Delfourne, E. *Marine Drugs* **2009**, *7*, 754-786.

(15) Wu, M.-D.; Cheng, M.-J.; Wang, B.-C.; Yech, Y.-J.; Lai, J.-T.; Kuo, Y.-H.; Yuan, G.-F.; Chen, I.-S. *Journal of Natural Products* **2008**, *71*, 1258-1261.

(16) Yue, H.; Lu, F.; Shen, C.; Quan, J.-M. *Bioorganic Chemistry* **2015**, *61*, 21-27.

(17) Hu, K.; Patnaik, D.; Collier, T. L.; Lee, K. N.; Gao, H.; Swoyer, M. R.; Rotstein, B. H.; Krishnan, H. S.; Liang, S. H.; Wang, J. *ACS Medicinal Chemistry Letters* **2017**, *8*, 287-292.

(18) Ichikawa, S.; Tatebayashi, N.; Matsuda, A. *The Journal of Organic Chemistry* **2013**, *78*, 12065-12075.

(19) Csávás, M.; Miskovics, A.; Szűcs, Z.; Rőth, E.; Nagy, Z. L.; Bereczki, I.; Herczeg, M.; Batta, G.; Nemes-Nikodém, É.; Ostorházi, E. *The Journal of Antibiotics* **2015**, *68*, 579-585.

(20) Lauer, M. H.; Drekener, R. L.; Correia, C. R. D.; Gehlen, M. H. *Photochemical & Photobiological Sciences* **2014**, *13*, 859-866.

(21) Mahmood, Z.; Zhao, J. *The Journal of Organic Chemistry* **2016**, *81*, 587-594.

(22) Liu, J.; Zhang, H.-R.; Lin, X.-R.; Yan, S.-J.; Lin, J. *RSC Advances* **2014**, *4*, 27582-27590.

(23) Marsh, B. J.; Adams, H.; Barker, M. D.; Kutama, I. U.; Jones, S. *Organic Letters* **2014**, *16*, 3780-3783.

(24) Han, S. H.; Mishra, N. K.; Jo, H.; Oh, Y.; Jeon, M.; Kim, S.; Kim, W. J.; Lee, J. S.; Kim, H. S.; Kim, I. S. *Advanced Synthesis & Catalysis* **2017**, *359*, 2396-2401.

(25) Matsumoto, K.; Nagashima, K.; Kamigauchi, T.; Kawamura, Y.; Yasuda, Y.; Ishii, K.; Uotani, N.; Sato, T.; Nakai, H.; Terui, Y. *The Journal of Antibiotics* **1995**, *48*, 439-446.

(26) Peter, M. G.; Snatzke, G.; Snatzke, F.; Nagarajan, K.; Schmid, H. *Helvetica Chimica Acta* **1974**, *57*, 32-64.

(27) Bochis, R. J.; Fisher, M. H. *Tetrahedron Letters* **1968**, *9*, 1971-1974.

(28) Deeks, E. D. *Drugs* **2015**, *75*, 1393-1403.

(29) Ishiyama, T.; Tokuda, K.; Ishibashi, T.; Ito, A.; Toma, S.; Ohno, Y. *European Journal of Pharmacology* **2007**, *572*, 160-170.

(30) Nakamura, M.; Ogasa, M.; Guarino, J.; Phillips, D.; Severs, J.; Loebel, A. *The Journal of Clinical Psychiatry* **2009**, *70*, 10941.

(31) Miller, C.; Long, L. M. *Journal of the American Chemical Society* **1951**, *73*, 4895-4898.

(32) Crider, A. M.; Kolczynski, T. M.; Yates, K. M. *Journal of Medicinal Chemistry* **1980**, *23*, 324-326.

(33) Shoji, A.; Kuwahara, M.; Ozaki, H.; Sawai, H. *Journal of the American Chemical Society* **2007**, *129*, 1456-1464.

(34) Luzzio, F. A.; Duveau, D. Y.; Lepper, E. R.; Figg, W. D. *The Journal of Organic Chemistry* **2005**, *70*, 10117-10120.

(35) Rankin, G. O.; Cressey-Veneziano, K.; Wang, R. T.; Brown, P. I. *Journal of Applied Toxicology* **1986**, *6*, 349-356.

(36) Deshpande, M. N.; Cain, M. H.; Patel, S. R.; Singam, P. R.; Brown, D.; Gupta, A.; Barkalow, J.; Callen, G.; Patel, K.; Koops, R. *Organic Process Research & Development* **1998**, *2*, 351-356.

(37) Bharkavi, C.; Kumar, S. V.; Ali, M. A.; Osman, H.; Muthusubramanian, S.; Perumal, S. *Bioorganic & Medicinal Chemistry Letters* **2017**, *27*, 3071-3075.

(38) Tasdelen, M. A. *Polymer Chemistry* **2011**, *2*, 2133-2145.

(39) Huo, F.; Kang, J.; Yin, C.; Zhang, Y.; Chao, J. *Sensors and Actuators B: Chemical* **2015**, *207*, 139-143.

(40) Zhang, Y.; Huo, F.; Yin, C.; Yue, Y.; Hao, J.; Chao, J.; Liu, D. *Sensors and Actuators B: Chemical* **2015**, *207*, 59-65.

(41) Xue, G.; Yu, S.; Qiang, Z.; Xiuying, L.; Jiangrong, L. *Analytica Chimica Acta* **2020**, *1108*, 46-53.

(42) Fleischmann, C.; Lievenbrück, M.; Ritter, H. *Polymers* **2015**, *7*, 717-746.

(43) Xie, Y.; Husband, J. T.; Torrent-Sucarrat, M.; Yang, H.; Liu, W.; O'Reilly, R. K. *Chemical Communications* **2018**, *54*, 3339-3342.

(44) Chen, G.-Q.; Wu, Z.-Q.; Wu, J.-R.; Li, Z.-C.; Li, F.-M. *Macromolecules* **2000**, *33*, 232-234.

(45) Gandini, A. *Progress in Polymer Science* **2013**, *38*, 1-29.

(46) Wrobel, J.; Dietrich, A.; Woolson, S. A.; Millen, J.; McCaleb, M.; Harrison, M. C.; Hohman, T. C.; Sredy, J.; Sullivan, D. *Journal of Medicinal Chemistry* **1992**, *35*, 4613-4627.

(47) Tamizmani, M.; Ramesh, B.; Jeganmohan, M. *The Journal of Organic Chemistry* **2018**, *83*, 3746-3755.

(48) Yang, J.; Zhao, B.; Xi, Y.; Sun, S.; Yang, Z.; Ye, Y.; Jiang, K.; Wei, Y. *Organic Letters* **2018**, *20*, 1216-1219.

(49) Muniraj, N.; Prabhu, K. R. *ACS Omega* **2017**, *2*, 4470-4479.

(50) Gopula, B.; Yang, S. H.; Kuo, T. S.; Hsieh, J. C.; Wu, P. Y.; Henschke, J. P.; Wu, H. L. *Chemistry–A European Journal* **2015**, *21*, 11050-11055.

(51) Chen, X.; Ren, J.; Xie, H.; Sun, W.; Sun, M.; Wu, B. *Organic Chemistry Frontiers* **2018**, *5*, 184-188.

(52) Zhang, Z.; Han, S.; Tang, M.; Ackermann, L.; Li, J. *Organic Letters* **2017**, *19*, 3315-3318.

(53) Dolci, E.; Froidevaux, V.; Joly-Duhamel, C.; Auvergne, R.; Boutevin, B.; Caillol, S. *Polymer Reviews* **2016**, *56*, 512-556.

(54) Yu, W.; Zhang, W.; Liu, Y.; Liu, Z.; Zhang, Y. *Organic Chemistry Frontiers* **2017**, *4*, 77-80.

(55) Morita, T.; Akita, M.; Satoh, T.; Kakiuchi, F.; Miura, M. *Organic Letters* **2016**, *18*, 4598-4601.

(56) Gao, X.; Tang, L.; Huang, L.; Huang, Z.-S.; Ma, Y.; Wu, G. *Organic Letters* **2019**, *21*, 745-748.

(57) Manoharan, R.; Jeganmohan, M. *Asian Journal of Organic Chemistry* **2019**, *8*, 1949-1969.

(58) Kumar, S. V.; Banerjee, S.; Punniyamurthy, T. *Organic Chemistry Frontiers* **2020**, *7*, 1527-1569.

(59) Miura, W.; Hirano, K.; Miura, M. *Organic Letters* **2015**, *17*, 4034-4037.

(60) Zhao, H.; Shao, X.; Wang, T.; Zhai, S.; Qiu, S.; Tao, C.; Wang, H.; Zhai, H. *Chemical Communications* **2018**, *54*, 4927-4930.

(61) Zhu, C.; Luan, J.; Fang, J.; Zhao, X.; Wu, X.; Li, Y.; Luo, Y. *Organic Letters* **2018**, *20*, 5960-5963.

(62) Han, S.; Park, J.; Kim, S.; Lee, S. H.; Sharma, S.; Mishra, N. K.; Jung, Y. H.; Kim, I. S. *Organic Letters* **2016**, *18*, 4666-4669.

(63) Han, S. H.; Kim, S.; De, U.; Mishra, N. K.; Park, J.; Sharma, S.; Kwak, J. H.; Han, S.; Kim, H. S.; Kim, I. S. *The Journal of Organic Chemistry* **2016**, *81*, 12416-12425.

(64) Sherikar, M. S.; Kapanaiah, R.; Lanke, V.; Prabhu, K. R. *Chemical Communications* **2018**, *54*, 11200-11203.

(65) Muniraj, N.; Prabhu, K. R. *The Journal of Organic Chemistry* **2017**, *82*, 6913-6921.

(66) Li, B.; Guo, C.; Shen, N.; Zhang, X.; Fan, X. *Organic Chemistry Frontiers* **2020**, *7*, 3698-3704.

(67) Ghosh, A. K.; Samanta, S.; Ghosh, P.; Neogi, S.; Hajra, A. *Organic & Biomolecular Chemistry* **2020**, *18*, 3093-3097.

(68) Guo, C.; Li, B.; Liu, H.; Zhang, X.; Zhang, X.; Fan, X. *Organic Letters* **2019**, *21*, 7189-7193.

(69) Sherikar, M. S.; Prabhu, K. R. *Organic Letters* **2019**, *21*, 4525-4530.

(70) Manoharan, R.; Logeswaran, R.; Jeganmohan, M. *The Journal of Organic Chemistry* **2019**, *84*, 14830-14843.

(71) Sharma, S.; Han, S. H.; Oh, Y.; Mishra, N. K.; Lee, S. H.; Oh, J. S.; Kim, I. S. *Organic Letters* **2016**, *18*, 2568-2571.

(72) Muniraj, N.; Prabhu, K. R. *Organic Letters* **2019**, *21*, 1068-1072.

(73) Wan, T.; Pi, C.; Wu, Y.; Cui, X. *Organic Letters* **2020**, *22*, 6484-6488.

(74) Peng, J.; Li, C.; Khamrakulov, M.; Wang, J.; Liu, H. *Organic Letters* **2020**, *22*, 1535-1541.

(75) Laru, S.; Bhattacharjee, S.; Singsardar, M.; Samanta, S.; Hajra, A. *The Journal of Organic Chemistry* **2021**, *86*, 2784-2795.

(76) Kang, J. Y.; An, W.; Kim, S.; Kwon, N. Y.; Jeong, T.; Ghosh, P.; Kim, H. S.; Mishra, N. K.; Kim, I. S. *Chemical Communications* **2021**, *57*, 10947-10950.

(77) Cho, Y. S.; Kim, H. D.; Kim, E.; Han, S. H.; Han, S. B.; Mishra, N. K.; Jung, Y. H.; Jeong, T.; Kim, I. S. *Asian Journal of Organic Chemistry* **2021**, *10*, 202-209.

(78) Karishma, P.; Mandal, S. K.; Sakhuja, R. *Asian Journal of Organic Chemistry* **2021**, *10*, 2580-2590.

(79) Lv, N.; Liu, Y.; Xiong, C.; Liu, Z.; Zhang, Y. *Organic Letters* **2017**, *19*, 4640-4643.

(80) Mandal, R.; Emayavaramban, B.; Sundararaju, B. *Organic Letters* **2018**, *20*, 2835-2838.

(81) Sengoku, T.; Murata, Y.; Aso, Y.; Kawakami, A.; Inuzuka, T.; Sakamoto, M.; Takahashi, M.; Yoda, H. *Organic Letters* **2015**, *17*, 5846-5849.

(82) Nikitas, N. F.; Theodoropoulou, M. A.; Kokotos, C. G. *European Journal of Organic Chemistry* **2021**, *2021*, 1168-1173.

(83) *APEX2, SADABS and SAINT*; Bruker AXS inc: Madison, WI, USA, **2008**.

(84) Sheldrick, G. M. *Acta Crystallographica Section A: Foundations and Advances* **2015**, *71*, 3-8.

(85) Sheldrick, G. M. *Acta Crystallographica Section C: Structural Chemistry* **2015**, *71*, 3-8.

(86) Macrae, C. F.; Bruno, I. J.; Chisholm, J. A.; Edgington, P. R.; McCabe, P.; Pidcock, E.; Rodriguez-Monge, L.; Taylor, R.; Streek, J.; Wood, P. A. *Journal of Applied Crystallography* **2008**, *41*, 466-470.

CHAPTER 4

Ruthenium Catalyzed C-H Acylmethylation of *N*-Arylphthalazine-1,4-diones with *α*-Carbonyl Sulfoxonium Ylides

4.1 Introduction

Transition metal-catalyzed C-C and C-N bond-forming strategies have completely astonished the scientific community with the spectacular mechanistic engagements of metal ions, endowing complex chemical entities from simple starting materials.[1-3] In particular, the impact of chelation-assisted directed group C(*sp*^{2})-H functionalization have received an overwhelming response on multiple heterocyclic architectures using a variety of transition-metals, including Cu, Pd, Rh, Ru, Ir and Co.[4-13] Of these, Ru-catalyzed C-H functionalization/annulation strategies are prominent in tailoring unprecedented heterocyclic architectures.[14-17] Owing to its high catalytic activity and low cost, ruthenium has become an appealing metal catalyst for C-H bond activation in the synthesis of *N*-heterocyclic compounds.[18-20]

In striking contrast, sulfur ylides are reactive coupling partners that have witnessed a renaissance in contemporary catalysis such as in C-H functionalization,[21-24] insertion,[25-30] cyclopropanation, aziridation and epoxidation reactions.[31-33] The chemistry of sulfur ylides was first disclosed in the early 1930s by Ingold and Jessop.[34] However, the synthetic prowess of these reagents gained much importance in 1960s after the pioneering works by Corey and Chaykovsky towards the synthesis of strained rings.[35] Based on the oxidation state of the sulfur atom, sulfur ylides have been categorized into two main classes: sulfonium and sulfoxonium ylides (stable carbenoids). In particular, the prodigious advancement observed in the chemistry of sulfoxonium ylides in the last few years is due to its structural resemblance and chemical similarities with the diazo compounds.[22,36] In general, sulfoxonium ylides are more stable and less nucleophilic than sulfonium ylides. However, these are more stable and nucleophilic than diazo compounds (Figure 4.1.1).

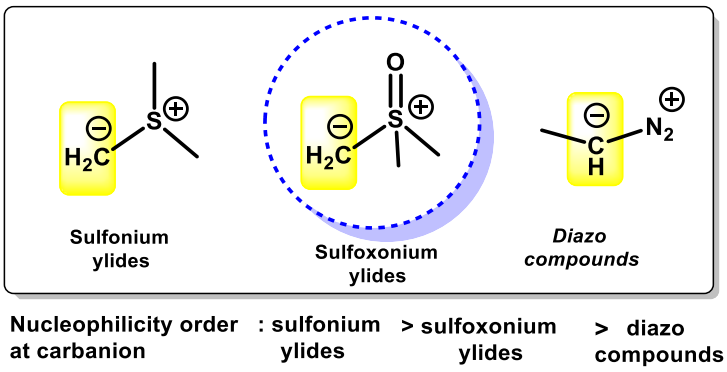

Figure 4.1.1 Structure/nucleophilicity comparison of sulfonium ylides, sulfoxonium ylides and diazo compounds

In the past, sulfoxonium ylides have been mainly used for the incorporation of methylene synthons to construct small rings such as cyclopropanes, epoxides, aziridines using electrophilic partners such as aldehydes, enones and imines.[37-39] This have been typically achieved *via* two prominent pathways, (a) sulfoxonium ylides directly undergoing insertion reactions into a X-H bond (X = C, N, O, S), (b) sulfoxonium ylides functioning as precursors to transition metal-carbene complexes. Under the influence of an appropriate directing groups, the cycloaddition of sulfoxonium ylides to a variety of nucleophilic metal-associated intermediates for the *o*-acylmethylation and annulation of different aromatic and heteroaromatic scaffolds have been mainly observed using Rh/Ir/Ru catalysts. A schematic representation depicting the possible mechanistic pathways for the above two processes is described below (Scheme 4.1.1).

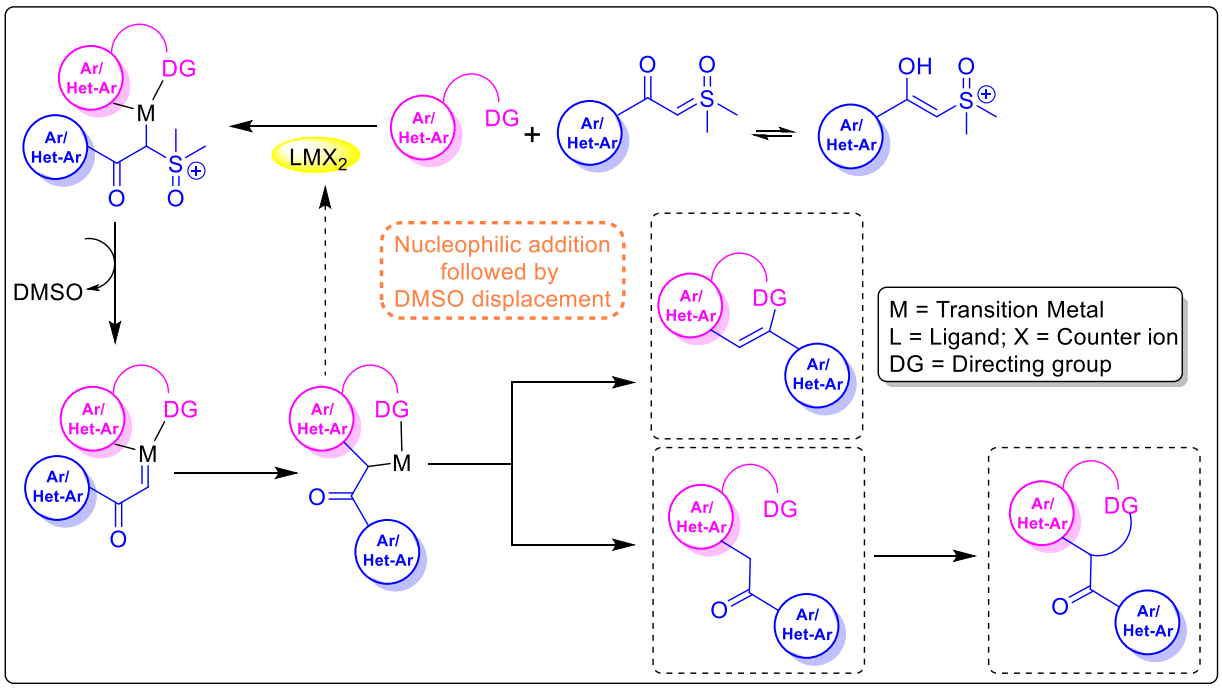

Scheme 4.1.1 General mechanistic pathways for directing group-aided functionalization/annulation of (hetero)arenes with sulfoxonium ylides under transition metal-catalysis

Under this realm, the first report on metal-catalyzed C-H functionalization using *α*-carbonyl sulfoxonium ylides as a coupling partner was reported in 2017 by Aïssa and co-workers. This acylmethylation approach showcased efficient cross-coupling reactions of *α*-carbonyl sulfoxonium ylides (**2**) with C(sp^2)-H bond of 2-arylpyridines (**1**) under Rh(II)-catalysis (Scheme 4.1.2).[40]

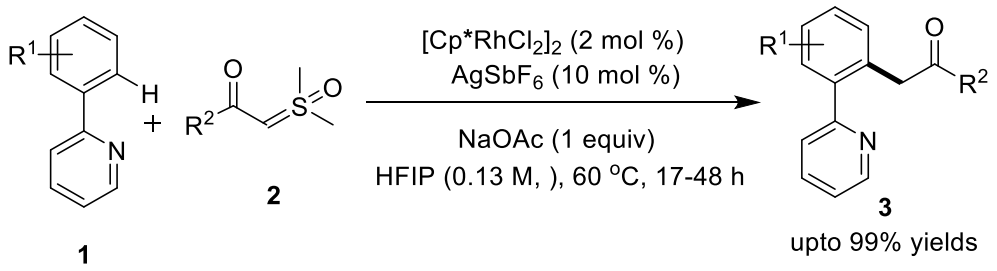

Scheme 4.1.2 Rhodium-catalyzed cross-coupling of 2-arylpyridines (**1**) with sulfoxonium ylides (**2**)

Ever since this work, metal-catalyzed functionalization and annulations using sulfoxonium ylides have been extensively explored. For example, in 2018, Maulide *et al.* presented a novel cross-olefination of diazo compounds (**4**) with sulfoxonium ylides (**2**) under Ru(II)-catalyzed conditions to afford substituted *Z*-olefins (**5**) in appreciable yields under Ru(II)-catalysis (Scheme 4.1.3).[41] The authors also studied the intrinsic responses in the reactivities of diazo compounds and sulfoxonium ylides as carbene precursors and nucleophiles, respectively.

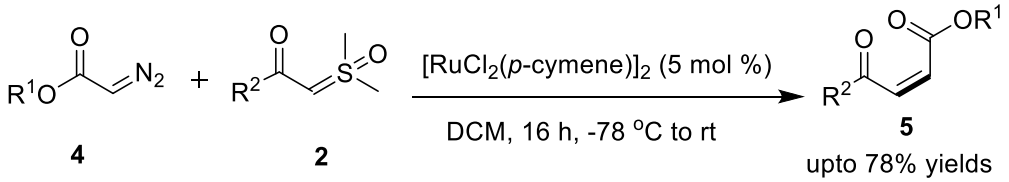

Scheme 4.1.3 Ruthenium-catalyzed cross-olefination of diazo compounds (**4**) with sulfoxonium ylides (**2**)

In the same year, Wang's group developed a Ru(II)-catalyzed C–H functionalization/annulation cascade process for the synthesis of isoquinolines (**7**) in moderate-to-good yields from sulfoxonium ylides (**2**) and benzimidates (**6**) using mesitylenic acid as an organic acid additive (Scheme 4.1.4).[42]

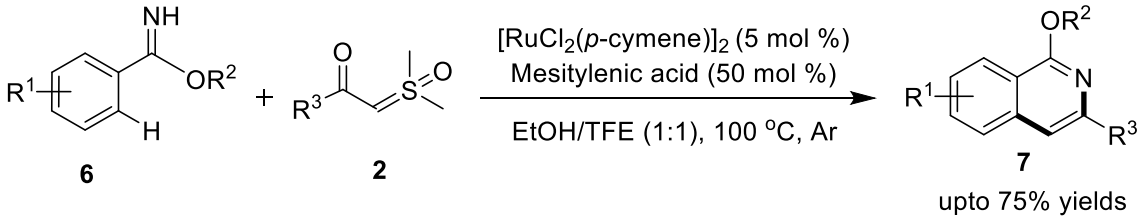

Scheme 4.1.4 Ruthenium-catalyzed C–H functionalization/annulation of benzimidates (**6**) with sulfoxonium ylides (**2**)

Likewise, Zeng *et al.* disclosed Ru(II)-catalyzed coupling of *S*-arylsulfoximines (**8**) with *α*-carbonyl sulfoxonium ylides (**2**) to obtain 1,2-benzothiazines (**9**) in good yields and moderate functional group tolerance (Scheme 4.1.5).[43]

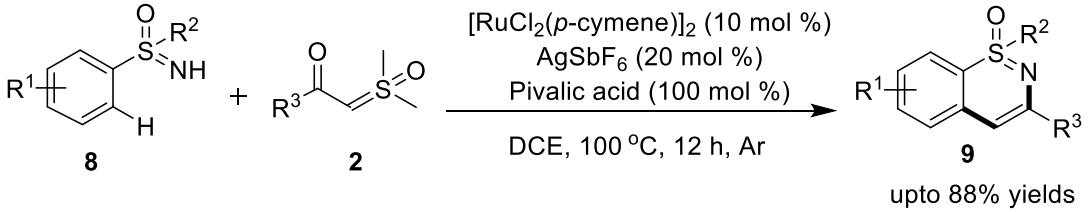

Scheme 4.1.5 Ruthenium-catalyzed coupling of *S*-arylsulfoximines (**8**) with sulfoxonium ylides (**2**)

Furthermore, Kim and Park established the Rh(III)-catalyzed [4+1]-annulation of azobenzenes (**10**) with *α*-carbonyl sulfoxonium ylides (**2**) for the synthesis of biologically active indazolone derivatives (**11**) (Scheme 4.1.6a).[44] Later, Cheng and co-workers reported the same protocol with slight modification in the strategy. The method exhibited an array of C-3 acylated indazoles in moderate-to-good yields (Scheme 4.1.6b).[45]

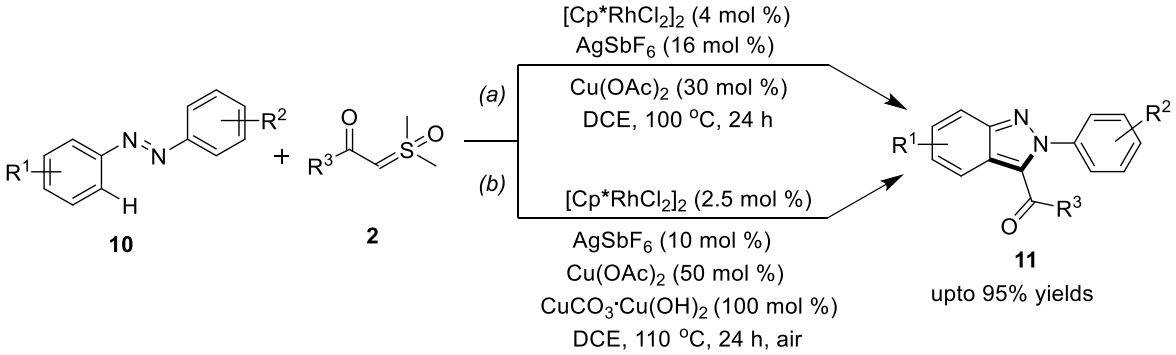

Scheme 4.1.6 Rhodium-catalyzed [4+1]-annulation of azobenzenes (**10**) with sulfoxonium ylides (**2**)

In 2019, Zhou and Liu's group employed Ru(II)-catalyzed selective C–H bond activation of imidamides (**12**) and annulation with sulfoxonium ylides (**2**) to furnish 3-ketoindole derivatives (**13**) in impressive yields and good functional group compatibility (Scheme 4.1.7).[46] This protocol generated a series of indole scaffolds by C-N and C-S bond cleavages. Besides, the synthetic applicability of this method was demonstrated by executing a gram-scale reaction and synthesizing an anti-inflammatory drug, Clometacin.

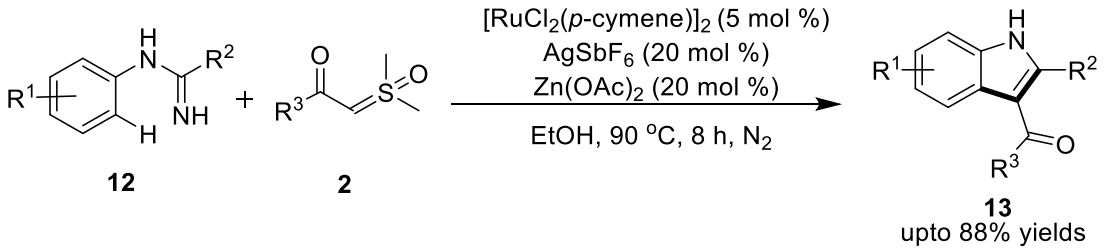

Scheme 4.1.7 Ruthenium-catalyzed annulation of imidamides (**12**) with sulfoxonium ylides (**2**)

Furthermore, Wang's group used a cationic Rh(III)-complex as an efficient catalytic system for the synthesis of multi-substituted naphthalenes (**15**) *via* annulation of enaminones (**14**) with *α*-carbonyl sulfoxonium ylides **(2**) (Scheme 4.1.8).[47] The procedure featured enaminone playing dual-functionality as a directing group and as a cyclizing group.

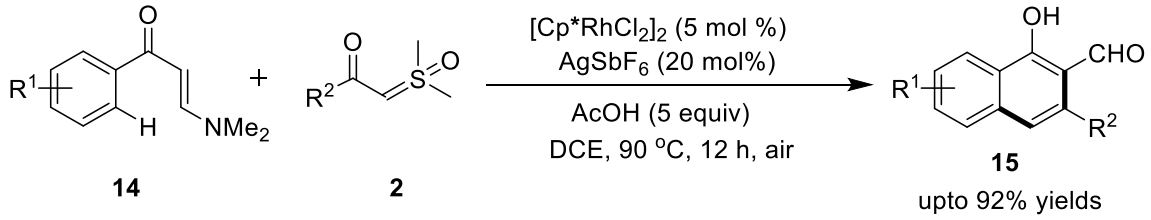

Scheme 4.1.8 Rhodium-catalyzed annulation of enaminones (**14**) with sulfoxonium ylides (**2**)

Notably, Huang *et al.* implemented a Rh(III)-catalyzed one-pot strategy for the aldehydic C-H functionalization in salicylaldehydes derivatives (**16**), followed by dehydrative cyclization with *α*-carbonyl sulfoxonium ylides (**2**) to obtain flavanoids (**17**) with ample substrate scope (Scheme 4.1.9).[48]

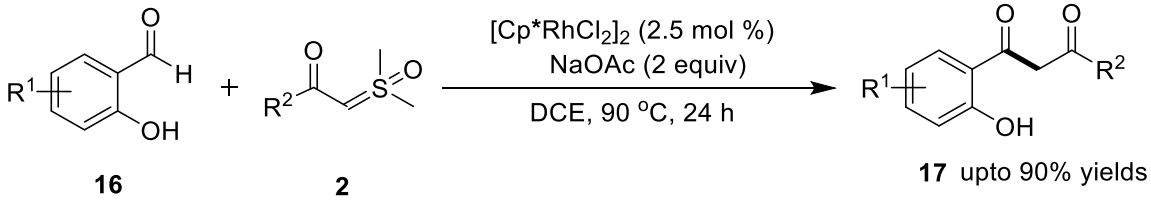

Scheme 4.1.9 Rhodium-catalyzed aldehydic C-H functionalization in salicylaldehydes derivatives (**16**) with sulfoxonium ylides (**2**)

Later, Ru(II)-catalyzed [5+1] annulation of 2-alkenylanilines (**18**) with sulfoxonium ylides (**2**) as effective carbene precursors for the assembly of various 2-acylquinolines has been achieved by Nan and Ma group, with good yields and excellent functional group tolerance (Scheme 4.1.10).[49]

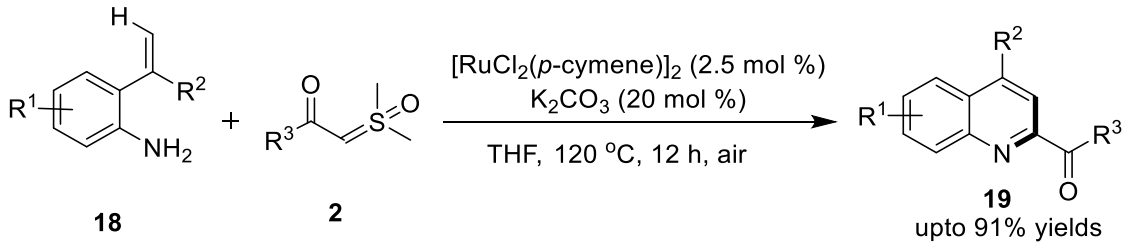

Scheme 4.1.10 Ruthenium-catalyzed [5+1] annulation of 2-alkenylanilines (**18**) with sulfoxonium ylides (**2**)

Cheng *et al.* proposed a Rh(III)-catalyzed regioselective acylmethylation of [2,2′-bipyridine]-6-carboxamides (**20**) with sulfoxonium ylides (**2**) in impressive yields (Scheme 4.1.11).[50] The reaction was presumed to occur by the rollover cyclometallation pathway by ingeniously utilizing the *trans* effect of an acylamino group at the C6-position.

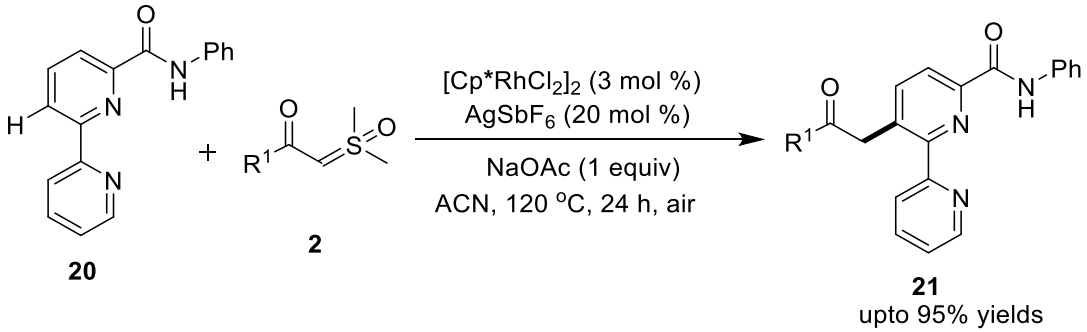

Scheme 4.1.11 Rhodium-catalyzed C3-H acylmethylation of bipyridine-6-carboxamides (**20**) with sulfoxonium ylides (**2**)

In the year 2020, [Cp*****$IrCl_2$] was found to be effective catalyst for the site-selective direct C-4 acylmethylation of indole benzenoids (**22**) with *α*-carbonyl sulfoxonium ylides (**2**) using sulfur directing groups (Scheme 4.1.12).[51] Intriguingly, the synthetic utility of the coupled products was emphasized upon the synthesis of C3-C4 looped medium-sized ring scaffolds that are widely found in biologically important molecules.

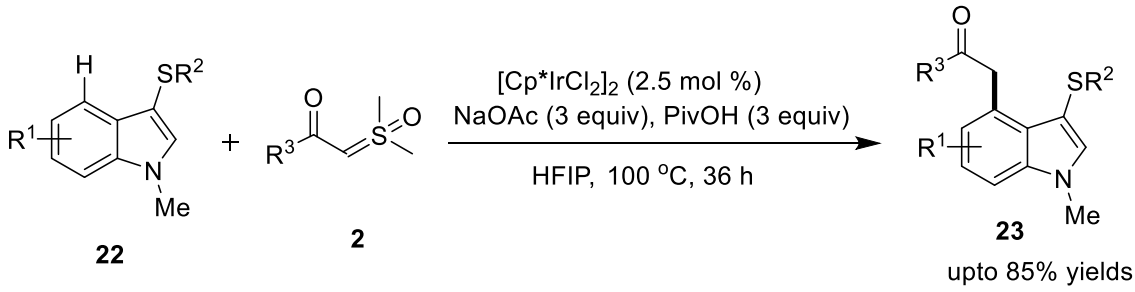

Scheme 4.1.12 Iridium-catalyzed acylmethylation of indoles (**22**) with sulfoxonium ylides (**2**)

Very recently, Chen and Zhu have developed a facile Rh(III)-catalyzed method for the acylmethylation and annulation of 2,2′-bipyridine (**24**) with sulfoxonium ylides (**2**) by introducing a removable group like Br at the 6-position (Scheme 4.1.13).[52] The authors reported the synthetic transformations of the prepared compounds by delivering diversely functionalized heterocycles.

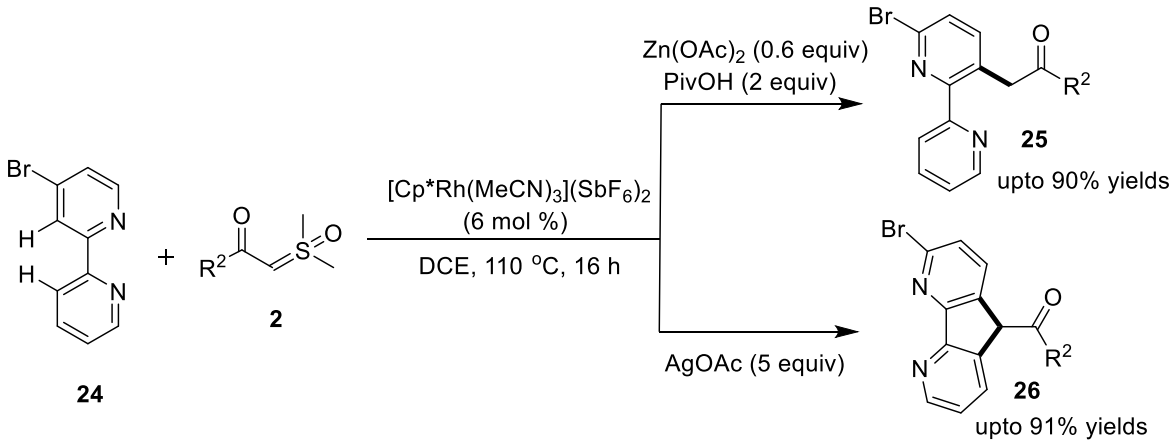

Scheme 4.1.13 Rhodium-catalyzed C-H functionalization and annulation of 2,2′-bipyridine (**24**) with sulfoxonium ylides (**2**)

In striking contrast, sulfoxonium ylides have also been used as a carbenoid-based directing group in several metal-catalyzed C-H activation protocols; whereby functionalization and annulation are consecutively occurring in a tandem fashion to construct carbocyclic and heterocyclic entities of paramount importance. A schematic representation depicting the possible mechanistic pathway for the C-H functionalization/cyclization of sulfoxonium ylide *via* inbuilt directing group capability of sulfoxonium ylide, is shown below (Scheme 4.1.14).

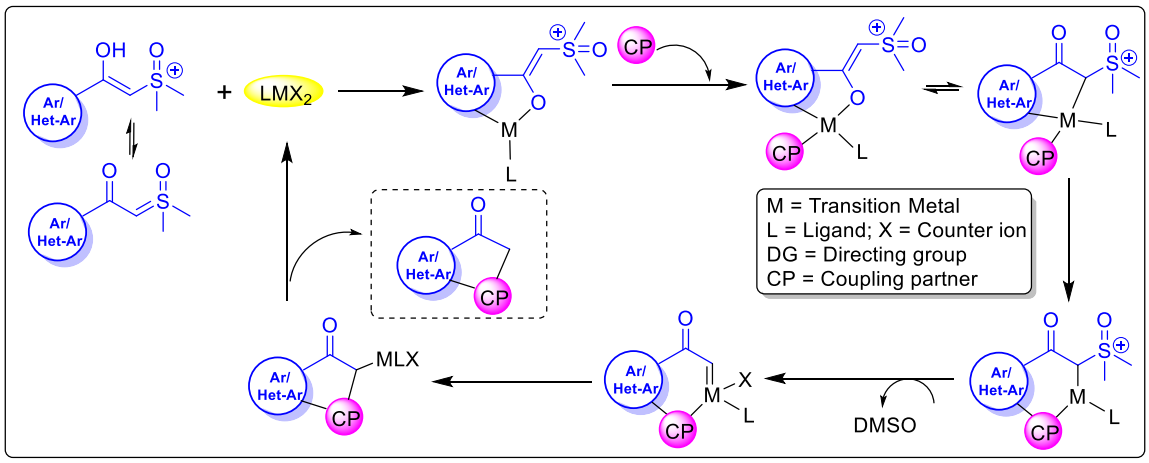

Scheme 4.1.14 General mechanistic pathway for inbuilt directing group-aided functionalization/annulation of sulfoxonium ylides under transition metal-catalysis

With the anticipation to insert metal-carbenoids into electrophilic coupling partners, several research groups have extended their contribution towards the construction of C-C and C-X (hetero atom) bonds. For instance, Li and coworkers team reported a direct and efficient Rh(III)-catalyzed synthesis of 1-naphthols (**28**) using *α*-carbonyl sulfoxonium ylides (**2)** and alkynes (**27**) as the starting materials (Scheme 4.1.15a).[53] Later, Tan *et al.* disclosed the synthesis of naphthol derivatives from the same starting materials using [Cp*****Co(CO)I_2]/AgOTf/AgOAc catalytic system (Scheme 4.1.15b).[54]

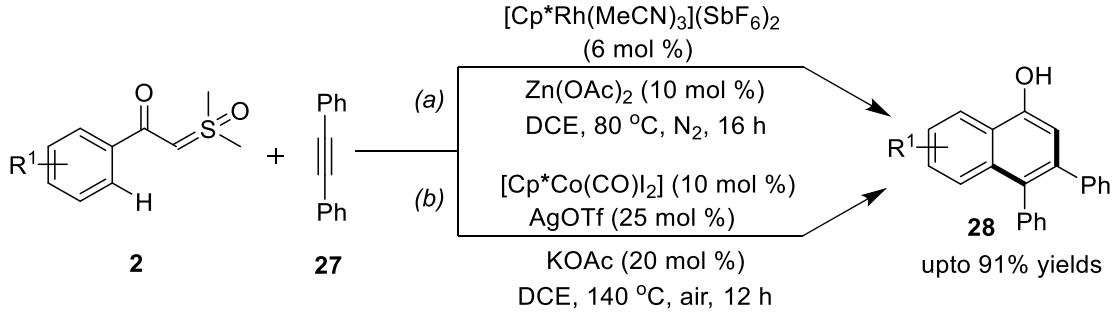

Scheme 4.1.15 Rhodium/Cobalt-catalyzed coupling of sulfoxonium ylides (**2)** with alkynes (**27**)

Further, weakly coordinating *α*-carbonyl sulfoxonium ylides (**2**) was found to undergo homocoupling in the presence of [$RuCl_2$(*p*-cymene)]$_2$/$AgSbF_6$/AcOH catalytic system to produce a series of 3-substituted isocoumarins (**29**). In this strategy, sulfoxonium ylides act both as an acylmethylating reagent as well as an aromatic counterpart (Scheme 4.1.16).[55]

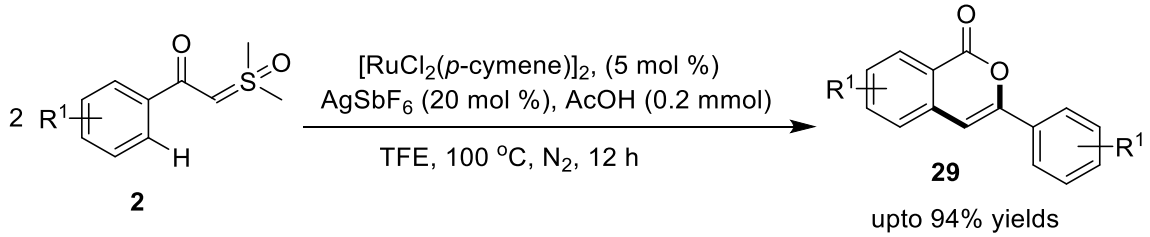

Scheme 4.1.16 Ruthenium-catalyzed homocoupling of sulfoxonium ylides (**2)**

In 2019, Xang and Fan illustrated a Rh(III)-catalyzed coupling reaction of *α*-carbonyl sulfoxonium ylides (**2**) with *α*-diazo carbonyl compounds (**4**) in TFE at 100 ℃, furnishing naphthalenones (**30**) in decent yields. While, switching the solvent to toluene at 80 ℃ furnished acylmethylated naphthalenones (**31**) in comparatively better yields. The diverse synthetic potential of the annulated species was also reported (Scheme 4.1.17).[56]

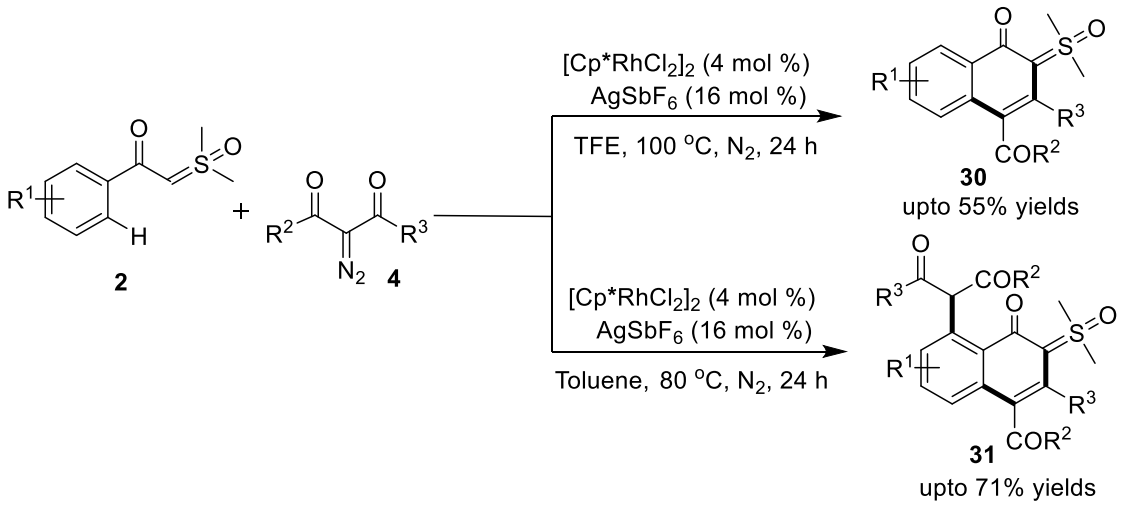

Scheme 4.1.17 Rhodium-catalyzed solvent-driven coupling of sulfoxonium ylides (**2**) with *α*-diazo carbonyl compounds (**4**)

Kong and Li *et al.* demonstrated Co(III)-catalyzed C-H amidation of *α*-carbonyl sulfoxonium ylides (**2**) with 1,4,2-dioxazol-5-ones (**32**). The mechanism proceeded through the chelation-assisted C–H activation→nitrenoid formation, which followed by migratory insertion of the Rh-C(aryl) into the nitrene, furnished the corresponding *ortho*-amidated products (**33**) in good-to-excellent yields (Scheme 4.1.18).[57]

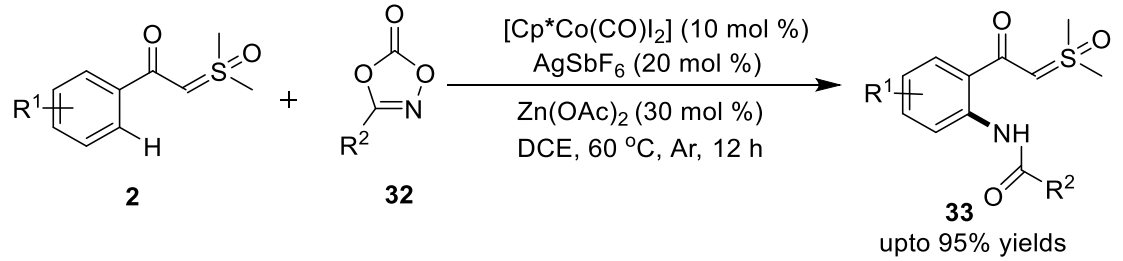

Scheme 4.1.18 Cobalt-catalyzed *ortho*-midation of sulfoxonium ylides with 1,4,2-dioxazol-5-ones (**32**)

Another interesting application of chelation-assisted C-H activation was reported by Zhou and Yu, where 2*H*-cyclopropa[*b*]-naphthalen-2-ones (**35**) bearing a quaternary carbon center were prepared by the coupling of *α*-carbonyl sulfoxonium ylides (**2**) with allenoates (**34**) (Scheme 4.1.19).[58] The mechanism featured C-H activation and cascade cyclopropanation, involving sulfoxonium ylide functionality as a traceless bifunctional directing group and C4 synthon. The methodology exhibits excellent diastereoselectivity with high functional group tolerance.

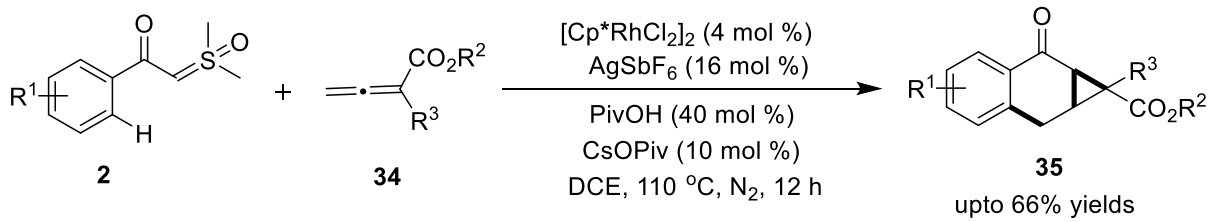

Scheme 4.1.19 Rhodium-catalyzed cascade cyclopropanation of sulfoxonium ylides with allenoates (**34**)

Sun and Li achieved naphthalen-1(2*H*)-one (**37**) framework through the Rh(III)-catalyzed [4+2] annulation of sulfoxonium ylides (**2**) with oxa/azabicyclic olefins (**36**), while divergent C-H functionalized products (**38**), along with [4+2]-annulated products were obtained in excellent yields by using $[Cp^*RhCl_2]_2$/$AgSbF_6$/PivOH catalytic system (Scheme 4.1.20).[59]

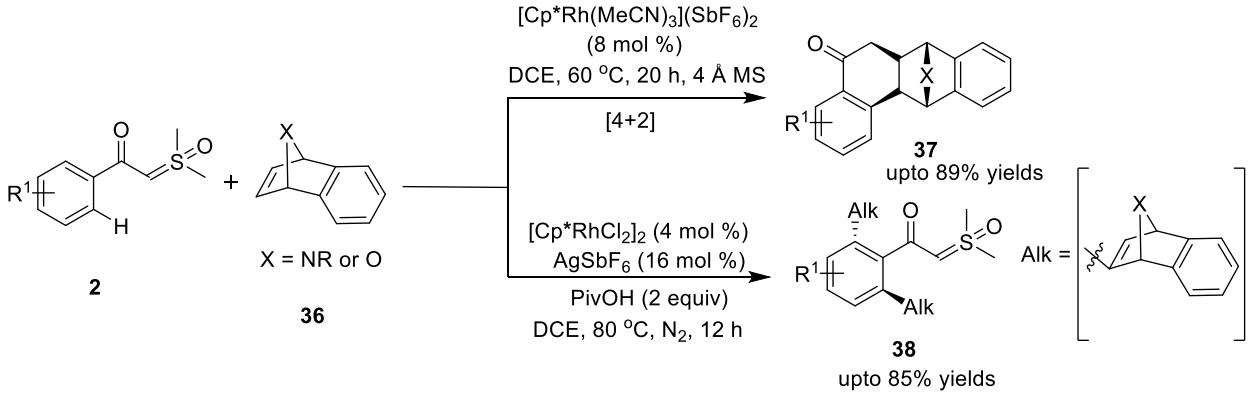

Scheme 4.1.20 Rhodium-catalyzed C-H functionalization/ [4+2] annulation of sulfoxonium ylides (**2**) with strained olefins (**36**)

Prabhu and coworkers utilized highly functionalized unsymmetrical internal alkynes or 4-hydroxy-2-alkynoates (**39**) and sulfoxonium ylides (**2**) for furnishing furanone-fused naphthol scaffolds (**40**) in domino fashion under Rh(III)-catalysis (Scheme 4.1.21).[60] Additionally, the synthesis of analogs of natural product fimbricalyx lactone A and bromo-derivatives of furanone-fused naphthol that are used as an intermediate in developing photochromic-dichroic materials, were also synthesized.

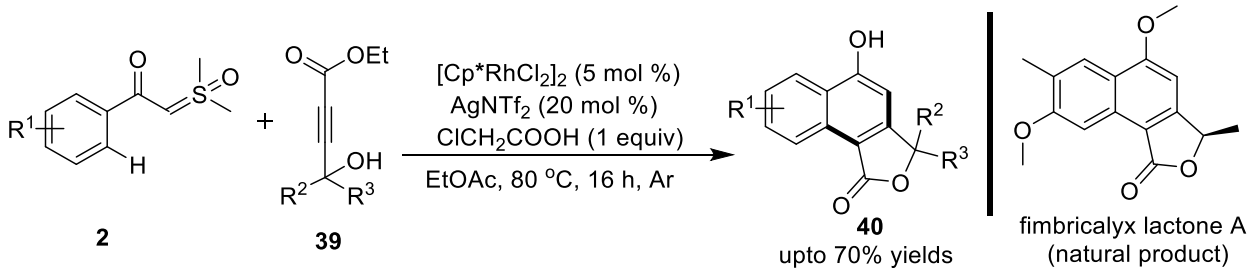

Scheme 4.1.21 Rhodium-catalyzed coupling of functionalized unsymmetrical internal alkynes or 4-hydroxy-2-alkynoates (**39**) and sulfoxonium ylides (**2**)

In the year 2019, Cheng *et al.* reported an unprecedented Rh(III)-catalyzed [4+1] annulation of *α*-carbonyl sulfoxonium ylides (**2**) and anthranils (**41**) to synthesize indolone derivatives (**42**) in good-to-excellent yields. The reaction produced ample derivatives with broad substrate scope and functional group tolerance (Scheme 4.1.22).[61]

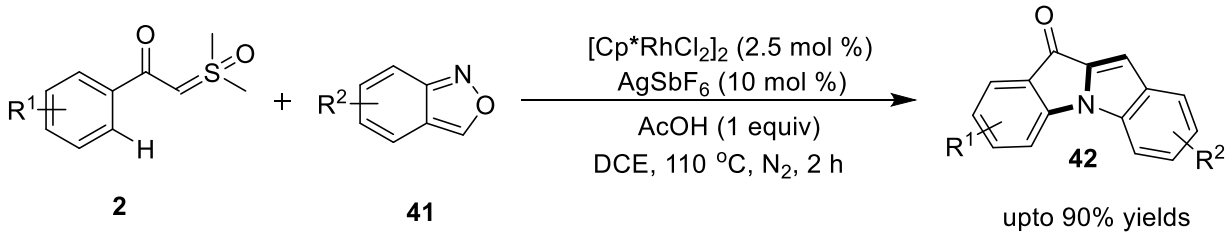

Scheme 4.1.22 Rhodium-catalyzed [4+1] annulation of sulfoxonium ylides (**2**) and anthranils (**41**)

Chatani and coworkers presented a high-yielding approach for the Rh(III)-catalyzed [4+1] cycloaddition reaction of substituted benzoyl sulfoxonium ylides (**2**) with activated alkenes (**43**), furnishing a variety of indanone derivatives (**44**) in excellent yields (Scheme 4.1.23).[62]

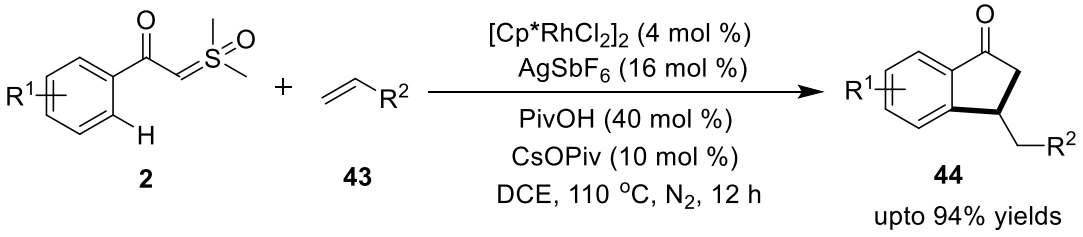

Scheme 4.1.23 Rhodium-catalyzed [4+1] cycloaddition of benzoyl sulfoxonium ylides (**2**) with activated alkenes (**43**)

A highly efficient Ir(III)-catalyzed cross-coupling reaction of benzoyl sulfoxonium ylides (**2**) with arylboronic acids (**45)** was accomplished by Zhang's group towards the construction of *α*-phenylacetophenones (**46**). The developed strategy involved C-H activation under redox-neutral conditions with wide substrate scope (Scheme 4.1.24).[63]

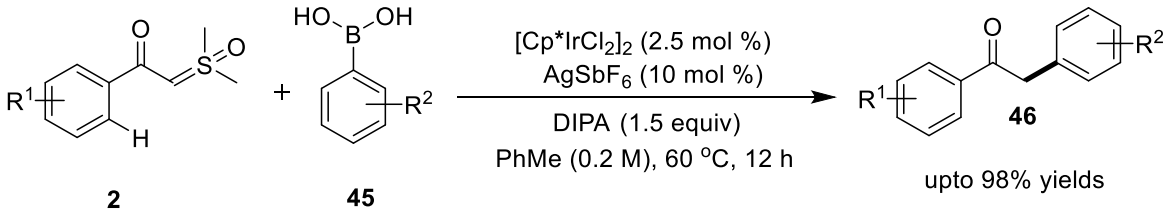

Scheme 4.1.24 Iridium-catalyzed cross-coupling of benzoyl sulfoxonium ylides (**2**) with arylboronic acids (**45**)

Fascinated by the varied chemical reactivities of sulfoxonium ylides (**2**), and in continuation with our on-going interest towards exploring the inbuilt directing group capability of *N*-aryl-2,3-dihyrophthalazine-1,4-dione by coupling it with different coupling partners, we developed an efficient Ru(II)-catalyzed strategy for the coupling of *N*-aryl-2,3-dihydrophthalazine-1,4-diones with *α*-carbonyl sulfoxonium ylides to furnish *o*-acylmethylated products, which acted as an active reservoir to assemble diversely functionalized phthalazino-fused cinnolines under Lawesson's reagent and $BF_3{\cdot}OEt_2$-mediated conditions (Scheme 4.1.25).[64]

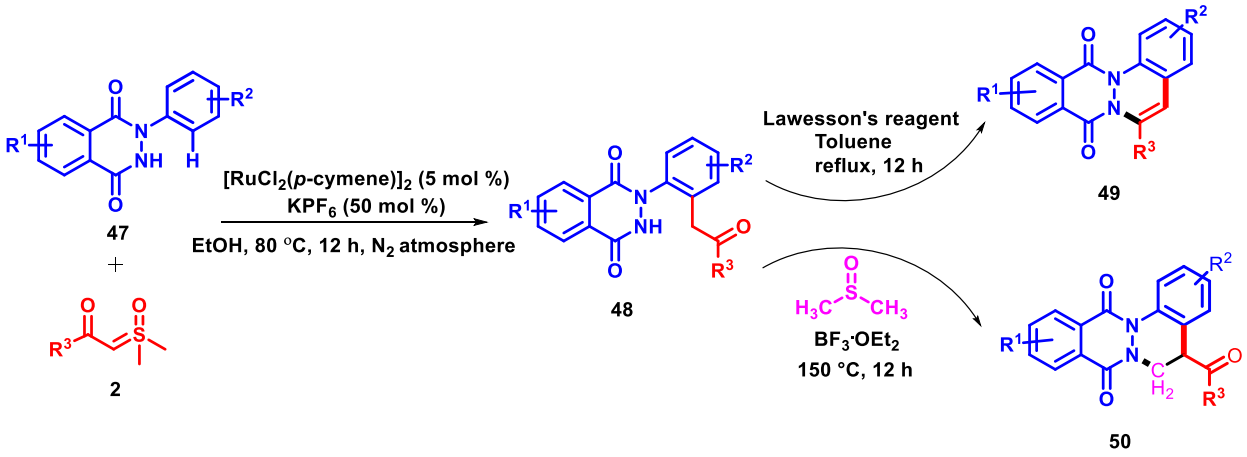

Scheme 4.1.25 Ruthenium-catalyzed *o*-acylmethylation of 2-aryl-2,3-dihydrophthalazine-1,4-diones (**47**) with *α*-carbonyl sulfoxonium ylides **(2**) and its subsequent cyclization.

4.2 Results and Discussion

Initially, the transition-metal-catalyzed optimization studies for the coupling between *N*-phenyl-2,3-dihydrophthalazine-1,4-dione (**47a**) and 2-(dimethyl(oxo)-λ^6-sulfanylidene)-1-phenylethan-1-one (**2a**) as model substrates were studied to afford the envisioned *o*-acylmethylated product (Table 4.2.1). Unfortunately, no product formation was observed by using $[Cp^*RhCl_2]_2$ or $[Cp^*IrCl_2]_2$ in presence or absence of $AgSbF_6$ in ethanol at 80 °C for 12 h (Table 4.2.1, entries 1-4). Strikingly, the use of 5 mol % of $[RuCl_2(p\text{-cymene})]_2$ probed the reaction between the two

model substrates (**47a** & **2a**) in ethanol at 80 °C under nitrogen atmosphere to afford 48% of *o*-acylmethylated product (**48aa**) (Table 4.2.1, entry 5), which was fully characterized using ^{1}H and ^{13}C NMR, COSY, HSQC and HRMS analysis.

Table 4.2.1 Selected optimization[a] of reaction conditions for the synthesis of **48aa**

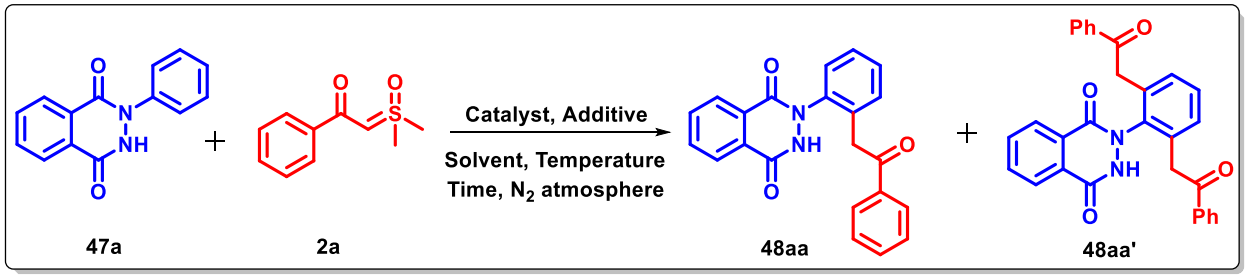

Entry No.	Catalyst (mol %)	Additive (mol %)	Solvent	Yields (%)[b]	
				48aa	**48aa′**
1.	[Cp*$RhCl_2$]$_2$ (5)	-	EtOH	-	-
2.	[Cp*$RhCl_2$]$_2$ (5)	$AgSbF_6$ (50)	EtOH	-	-
3.	[Cp*$IrCl_2$]$_2$ (5)	-	EtOH	-	-
4.	[Cp*$IrCl_2$]$_2$ (5)	$AgSbF_6$ (50)	EtOH	-	-
5.	[$RuCl_2$(*p*-cymene)]$_2$ (5)	-	EtOH	48	-
6.	[$RuCl_2$(*p*-cymene)]$_2$ (5)	$AgSbF_6$ (50)	EtOH	70	-
7.	[$RuCl_2$(*p*-cymene)]$_2$ (5)	$Cu(OAc)_2$ (50)	EtOH	66	-
8.	**[$RuCl_2$(*p*-cymene)]$_2$ (5)**	**KPF_6 (50)**	**EtOH**	**82**	**-**
9.	[$RuCl_2$(*p*-cymene)]$_2$ (5)	NaOAc (50)	EtOH	38	22
10.	[$RuCl_2$(*p*-cymene)]$_2$ (5)	KOAc (50)	EtOH	32	20
11.	[$RuCl_2$(*p*-cymene)]$_2$ (5)	CsOAc (50)	EtOH	30	30
12.	[$RuCl_2$(*p*-cymene)]$_2$ (5)	KPF_6 (40)	EtOH	78	-
13.	[$RuCl_2$(*p*-cymene)]$_2$ (5)	KPF_6 (30)	EtOH	70	-
14.	[$RuCl_2$(*p*-cymene)]$_2$ (5)	KPF_6 (70)	EtOH	83	-
15.	[$RuCl_2$(*p*-cymene)]$_2$ (5)	KPF_6 (50)	*t*-Amyl alcohol	67	-
16.	[$RuCl_2$(*p*-cymene)]$_2$ (5)	KPF_6 (50)	*t*- BuOH	63	-
17.	[$RuCl_2$(*p*-cymene)]$_2$ (5)	KPF_6 (50)	TFE	65	-
18.	[$RuCl_2$(*p*-cymene)]$_2$ (5)	KPF_6 (50)	Toluene	-	-
19.	[$RuCl_2$(*p*-cymene)]$_2$ (5)	KPF_6 (50)	THF	-	-
20.	[$RuCl_2$(*p*-cymene)]$_2$ (5)	KPF_6 (50)	DCE	-	-
21.	[$RuCl_2$(*p*-cymene)]$_2$ (5)	KPF_6 (50)	DMF	-	-
22.	[$RuCl_2$(*p*-cymene)]$_2$ (5)	KPF_6 (50)	DMSO	-	-
23.[c]	[$RuCl_2$(*p*-cymene)]$_2$ (5)	KPF_6 (50)	EtOH	48	-
24.[d]	[$RuCl_2$(*p*-cymene)]$_2$ (5)	KPF_6 (50)	EtOH	40	-

[a]Reaction conditions: The reactions were carried out with **47a** (0.20 mmol) and **2a** (0.25 mmol) in the presence of catalyst/additive (as indicated in the table) in 5 mL of solvent at 80 °C for 12 h under N_2 atmosphere. [b]Isolated yields. [c]Under air. [d]At room temperature for 24 h.

Further, an amelioration in the yield of **48aa** to 70% and 66% was observed by using 50 mol % of $AgSbF_6$ and $Cu(OAc)_2$, respectively as additives (Table 4.2.1, entries 6-7). Delightfully, the use of KPF_6 (50 mol %) was found to be momentous for the *o*-acylmethylation of **47a** using **2a** under Ru(II)-catalyzed conditions, furnishing **48aa** in 82% yield (Table 4.2.1, entry 8). In contrast, the use of other additives such as NaOAc, KOAc and CsOAc produced **48aa** in lower yields, along with the isolation of minor amounts of bis(*o*-acylmethylated) product (**48aa′**) (Table 4.2.1, entries 9-11). Also, **48aa** was isolated in comparatively lower yields when the KPF_6 loading was reduced, while no significant elevation was observed by increasing the additive loading (Table 4.2.1, entries 12-14). Solvent screening studies were next investigated, and it was found the Ru-catalyzed *o*-acylmethylation of **47a** produced inferior results in other alcoholic solvents such as *t*-amyl alcohol, *t*-butyl alcohol and trifluoroethanol (TFE), while the reaction was not favourable at all in toluene, THF, DCE, DMF and DMSO (Table 4.2.1, entries 15-22). When the optimized reaction in ethanol was carried out in presence of air, only 48% of **48aa** was produced (Table 4.2.1, entry 23), while the reaction did not embark to completion at room temperature even after 24 h, affording 40% yield of **48aa** (Table 4.2.1, entry 24).

With the optimized conditions in hand, we determined the generality of the reaction with respect to various substituted *N*-aryl-2,3-dihydrophthalazine-1,4-diones (**47b-k**) with **2a** under optimized conditions (Scheme 4.2.1). As summarized in Scheme 4.2.1, excellent yields (78-88%) of the *o*-acylmethylated products (**48ba-48ea**) have recurred when *N*-aryl-2,3-dihydrophthalazine-1,4-diones substituted with electronically differentiated groups (Me, F, Cl, Br) on the aryl moiety (substrates: **47b-e**) were coupled with **2a**. The presence of disubstitution at *meta* and *para*-positions of aryl moiety with electronically-rich and/or weakly-deficient groups (same/different) (substrates: **47f−h**) showcased negligible difference in their reactivity with **2a**, furnishing the corresponding *o*-acylmethylated products (**48fa-48ga**) in 79-80% yields. In addition, *N*-phenyl methyl-substituted 2,3-dihydrophthalazine-1,4-dione (**47h**) successfully reacted with **2a** to afford expected product **48ha** in 76% yield. Notably, **48ha** was obtained as a mixture of two regioisomers (1:2), as **47h** itself was prepared as an inseparable 6 & 7-substituted regioisomeric mixture from 5-methylphthalic anhydride and phenylhydrazine. Likewise, *N*-phenyl OMe and Br-substituted 2,3-dihyrophthalazine-diones (substrates: **47i-j**: mixture of 6 & 7 substituted isomers obtained from 5-methoxy/5-bromophthalic anhydride) produced their corresponding *o*-acylmethylated products (**48ia-48ja**) in high yields as a mixture of two regioisomers. While, *N*-phenyl (5 or 8)-

fluoro-substituted 2,3-dihydrophthalazine-1,4-dione (**47k**, obtained from 4-fluorophthalic anhydride) produced **48ka** in 80% yield. In striking contrast, *N*-aryl-2,3-dihydrophthalazine-1,4-diones possessing Me and Cl substituents at *ortho* and *para*-positions of aryl moiety (substrates: **47l-m**) and strongly electron-withdrawing groups (NO_2, COOEt) at *para*-position (substrates: **47n-o**) failed to react with **2a** under the optimized Ru(II)-catalyzed conditions. Finally, **47p** was also found to be an unreactive substrate for the desired functionalization. Representative ^{1}H NMR and ^{13}C NMR spectra of the *o*-acylmethylated product **48aa** are shown in Figure 4.2.1 and Figure 4.2.2, respectively.

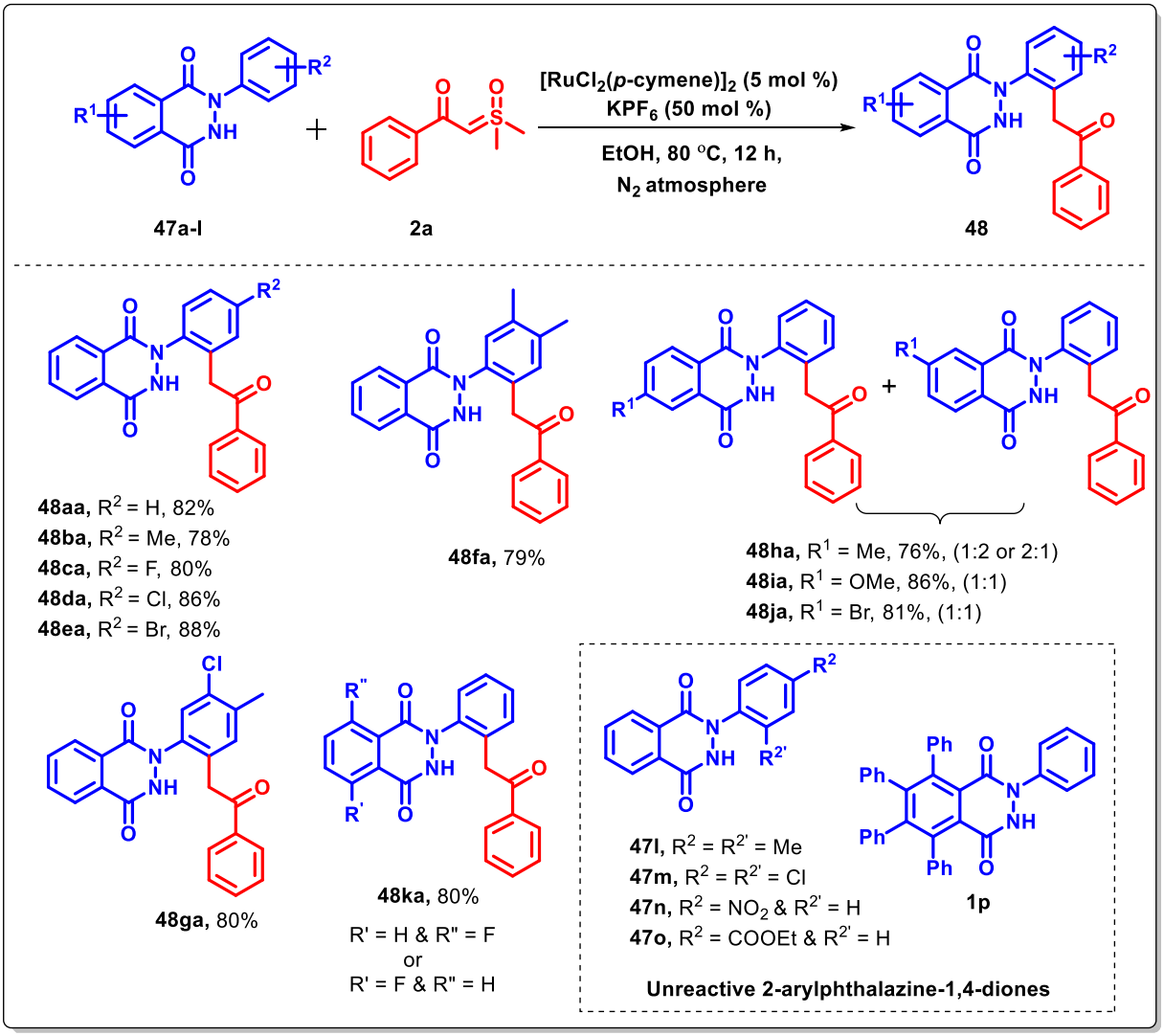

Scheme 4.2.1 Substrate scope of *N*-aryl-2,3-dihydrophthalazine-1,4-diones

To further expand the scope of this transformation, the coupling abilities of various α-carbonyl sulfoxonium ylides (**2b-q**) were explored (Scheme 4.2.2). A variety of aroyl sulfoxonium ylides

possessing electron-donating (substrates: **2b-d**, **2h**) and electron-withdrawing substituents (substrates: **2e-g**, **2i-k**) coupled efficiently with **47a**, affording the corresponding *o*-acylmethylated products (products: **48ab**-**48ak**) in 73-85% yields. Further, comparative studies of coupling of **47a** with *ortho*, *meta* and *para*-functionalized methyl and chloro substituted aroyl sulfoxonium ylides (substrates: **2b-d** & **2e-g**) showcased very little influence on the product's yield (products: **48ab-48ad** & **48ae-48ag**).

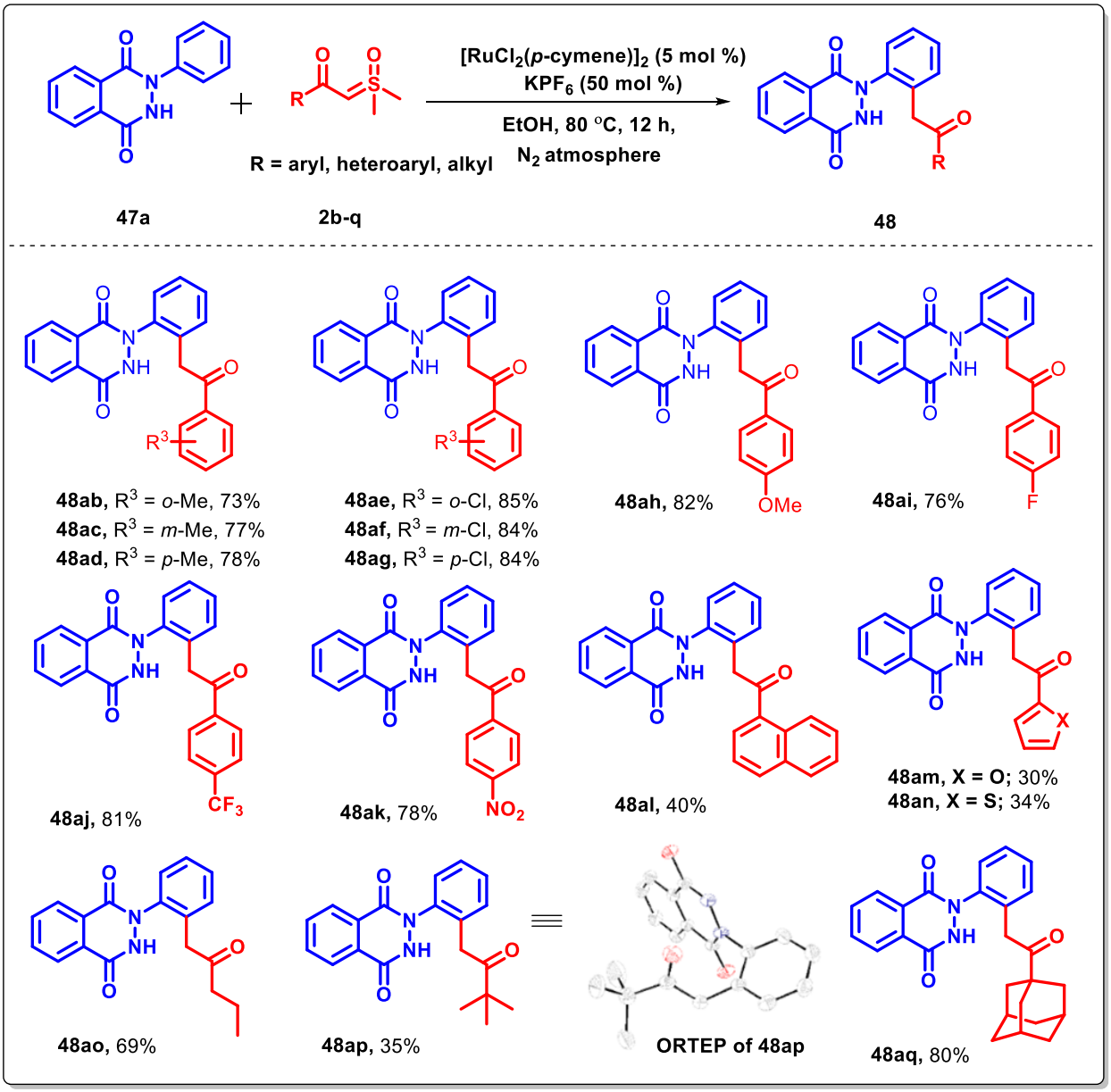

Scheme 4.2.2 Substrate scope of *α*-carbonyl sulfoxonium ylides

Delightfully, aroyl sulfoxonium ylides bearing strong electron-withdrawing groups, such as trifluoromethyl and nitro (substrates: **2j** & **2k**) underwent smooth coupling with **47a** to give the

functionalized products (**48aj** & **48ak**) in 81% and 78% yields, respectively. Naphthalene and heteroaryl, in particular, furan and thiophene functionalized sulfoxonium ylides (substrates: **2l-n**) also participated in this coupling process, albeit producing moderate yields of the desired products (**48al-48an**). Interestingly, alkyl substituted *α*-carbonyl sulfoxonium ylides, including *n*-propyl, *t*-butyl and admantanyl (substrates: **2o-q**) were also proved to be effective coupling partners for the *o*-acylmethyation of **47a**, delivering their corresponding products (**48ao-48aq**) in moderate-to-good yields. Also, single crystals of **48ap** were grown from chloroform for X-ray diffraction (XRD) studies as a representative example, which further confirmed the assigned structure of **48**. An ORTEP diagram (CCDC no. 1937966) of **48ap** is shown in Scheme 4.2.2.

To assess the scalability of Ru(II)-catalyzed *o*-acylmethylation, a gram-scale reaction was performed between **47a** and **2a** under the optimized conditions to afford **48aa** in 86% (1.28 g) yield, which was concordant to that obtained on a smaller scale (Scheme 4.2.3i). The synthetic utility of *o*-acylmethylated product **48aa** was further demonstrated by carrying its reduction with $NaBH_4$ in methanol at room temperature to furnish the corresponding hydroxyalkyated product (**48′aa**) in 64% (Scheme 4.2.3ii).

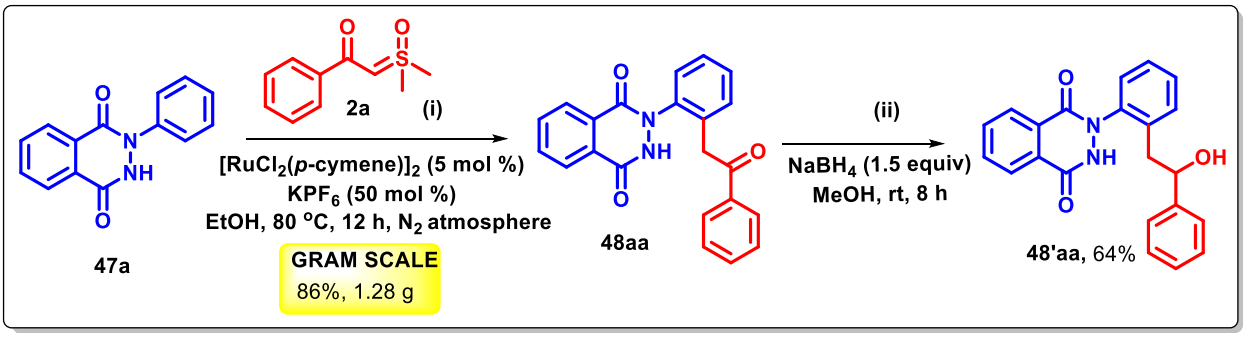

Scheme 4.2.3 Gram scale synthesis of **48aa** and its synthetic application

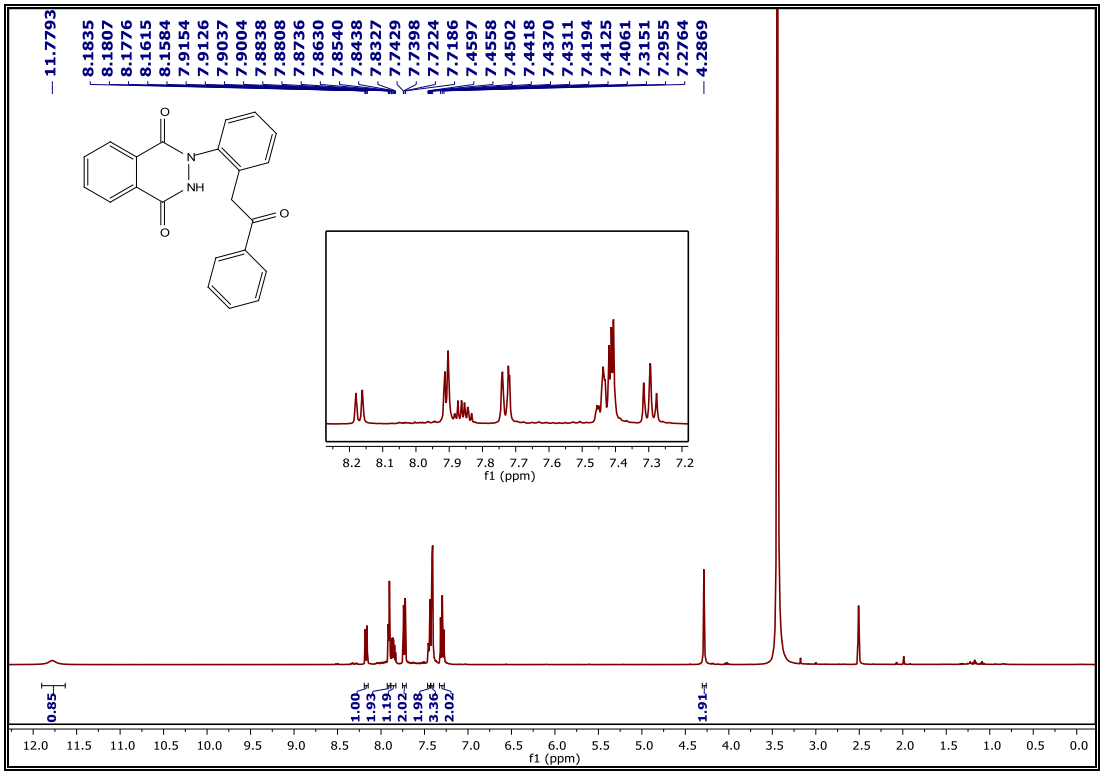

Figure 4.2.1 ^{1}H NMR spectra of **48aa**

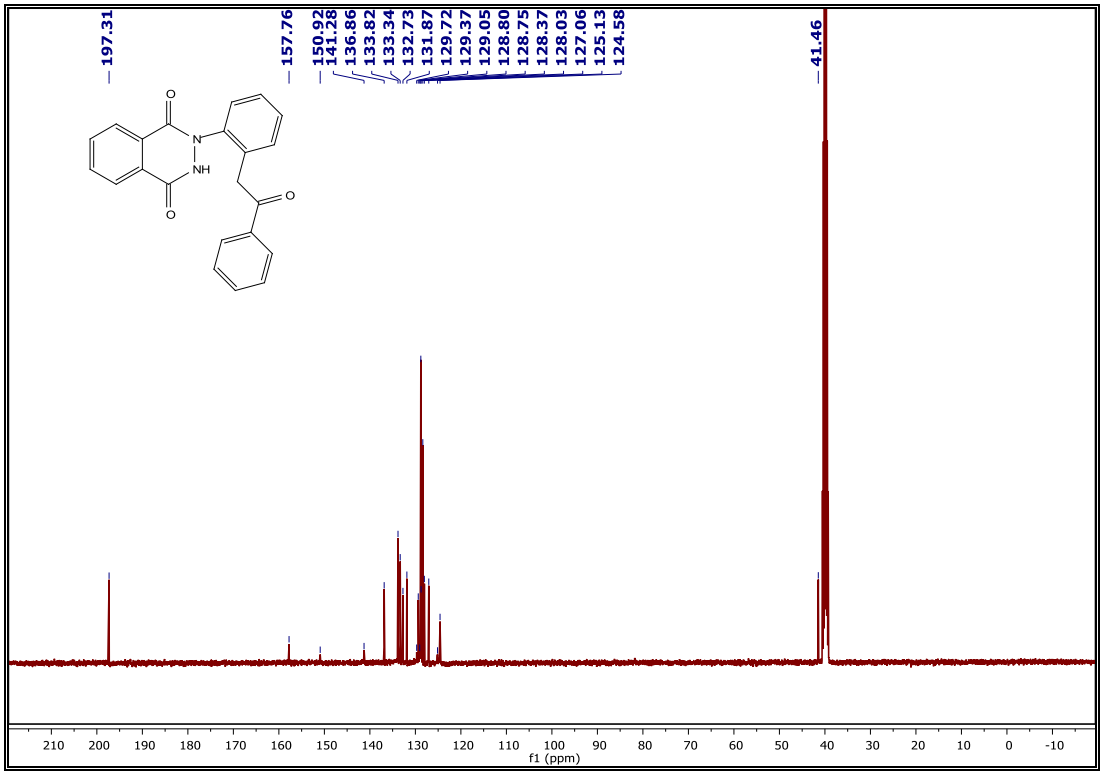

Figure 4.2.2 ^{13}C NMR spectra of **48aa**

We next focused our attention towards achieving intramolecular cyclization in **48aa** under acid-mediated conditions to obtain phthalazino-fused cinnolines (Table 4.2.2). Notably, the use of Lewis acids [$Yb(OTf)_3$ and $Zn(OTf)_2$] and Bronsted acids [AcOH, PivOH and TFA] did not furnish any cyclized product by heating **48aa** in DMA at 160 °C up to 12 h (Table 4.2.2, entries 1-5). While, the use of $TsOH{\cdot}H_2O$ and $BF_3{\cdot}OEt_2$ afforded 6-phenylphthalazino[2,3-*a*]cinnoline-8,13-dione (**49aa**) in extremely low yields (<10% & 14% yield) (Table 4.2.2, entries 6-7).

Table 4.2.2 Selected optimization[a] of reaction conditions for the synthesis of **49aa** or **50aa**

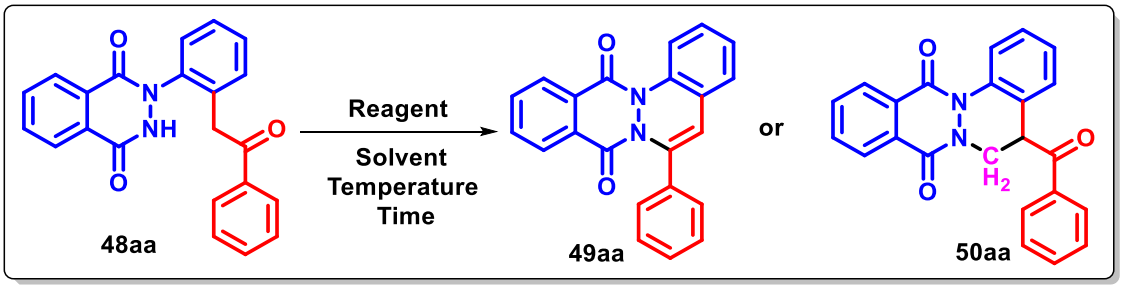

Entry	Reagent (equiv)	Solvent	Temp., Time	Yields (%)[b] **49aa**	Yields (%)[b] **50aa**
1.	$Yb(OTf)_3$ (1)	DMA	160 °C, 12 h	-	-
2.	$Zn(OTf)_2$ (1)	DMA	160 °C, 12 h	-	-
3.	CH_3COOH (1)	DMA	160 °C, 12 h	-	-
4.	PivOH (1)	DMA	160 °C, 12 h	-	-
5.	CF_3COOH (1)	DMA	160 °C, 12 h	-	-
6.	$TsOH{\cdot}H_2O$ (1)	DMA	160 °C, 12 h	<10	-
7.	$BF_3{\cdot}OEt_2$ (1)	DMA	160 °C, 12 h	14	-
8.	$BF_3{\cdot}OEt_2$ (1)	Ethanol	80 °C, 12 h	-	-
9.	$BF_3{\cdot}OEt_2$ (1)	Toluene	110 °C, 12 h	27	-
10.	LR (1)	Toluene	110 °C, 12 h	53	-
11.	**LR (2)**	**Toluene**	**110 °C, 12 h**	**92**	**-**
12.	LR (3)	Toluene	110 °C, 12 h	93	-
13.	$BF_3{\cdot}OEt_2$ (1)	DMF	150 °C, 12 h	-	45
14.	$BF_3{\cdot}OEt_2$ (1)	DMSO	150 °C, 12 h	-	55
15.	$BF_3{\cdot}OEt_2$ (2)	DMSO	150 °C, 12 h	-	81
16.	**$BF_3{\cdot}OEt_2$ (3)**	**DMSO**	**150 °C, 12 h**	**-**	**80**

[a]Reaction conditions: The reactions were carried out with **48aa** (0.14 mmol) in the presence of reagent (as indicated in the table) in 5 mL of solvent under ambient conditions. [b]Isolated yields. LR: Lawesson's Reagent

Solvent screening experiments proved ethanol to be completely ineffective, while toluene to be comparatively better than DMA under $BF_3{\cdot}OEt_2$-mediated conditions, producing **49aa** in 27% yield (Table 4.2.2, entries 8-9). Thus, realizing the incompetence of the carbonyl group in 2-(*o*-

acylmethylphenyl)-2,3-dihydrophthalazine-1,4-dione (**48aa**) to undergo nucleophilic addition (or cyclization) in presence of a variety of weak and strong acids, we anticipated that converting carbonyl to thiocarbonyl might increase its reactivity for envisioned nucleophilic attack by the amide group on it. To our delight, the reaction of **48aa** with Lawesson's reagent (1 equiv) in toluene at 110 ^{o}C for 12 h under ambient conditions afforded **49aa** in 53% yield, which further got elevated to 92% by using 2 equiv of Lawesson's reagent (Table 4.2.2, entries 10-11). No further yield enhancement of **49aa** was observed by increasing the reagent's equivalents (Table 4.2.2, entry 12). Thereafter, various *o*-acylmethylated 2-aryl-2,3-dihydrophhalazine-1,4-diones (**48**) were subjected to Lawesson's reagent-mediated cyclization in toluene under the optimized conditions (Scheme 4.2.4). The scope with respect to substitutions on acyl and aryl groups in *o*-acylmethylated 2-aryl-2,3-dihyrophhalazine1,4-diones (**48**) was found to be excellent towards the Lawesson's reagent-mediated cyclization. Electron-donating as well as electron-withdrawing groups present on acyl/aryl moieties (substrates: **48ga**, **48ab**, **48ah**, **48ai**, **48aj**) were well tolerated, furnishing their corresponding 6-arylphthalazino[2,3-*a*]cinnoline-8,13-diones (products: **49ga**, **49ab**, **49ah**, **49ai**, **49aj**) in 88-93% yields. The ^{1}H NMR and ^{13}C NMR spectra of **49aa** are depicted in 4.2.3 and 4.2.4 respectively. As a representative example, the structure of **49ab** are unambiguously confirmed by single crystal X-ray analysis. An ORTEP diagram (CCDC no. 1937967) of **49ab** is shown in Scheme 4.2.4.

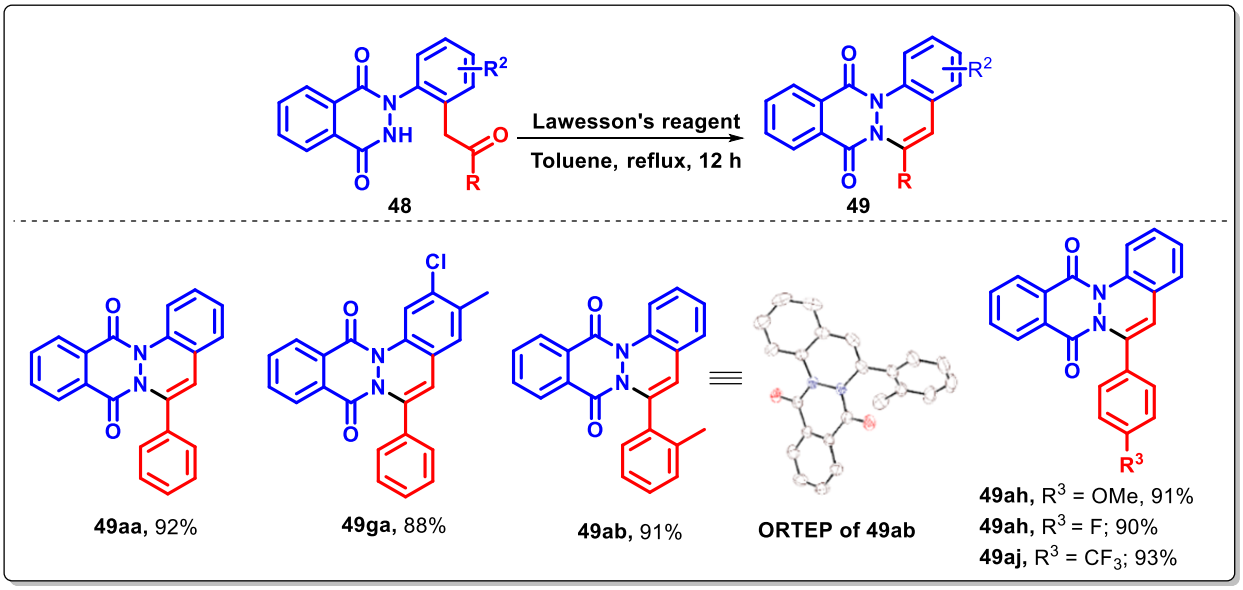

Scheme 4.2.4 Synthesis of 6-arylphthalazino[2,3-*a*]cinnoline-8,13-diones (**49**)

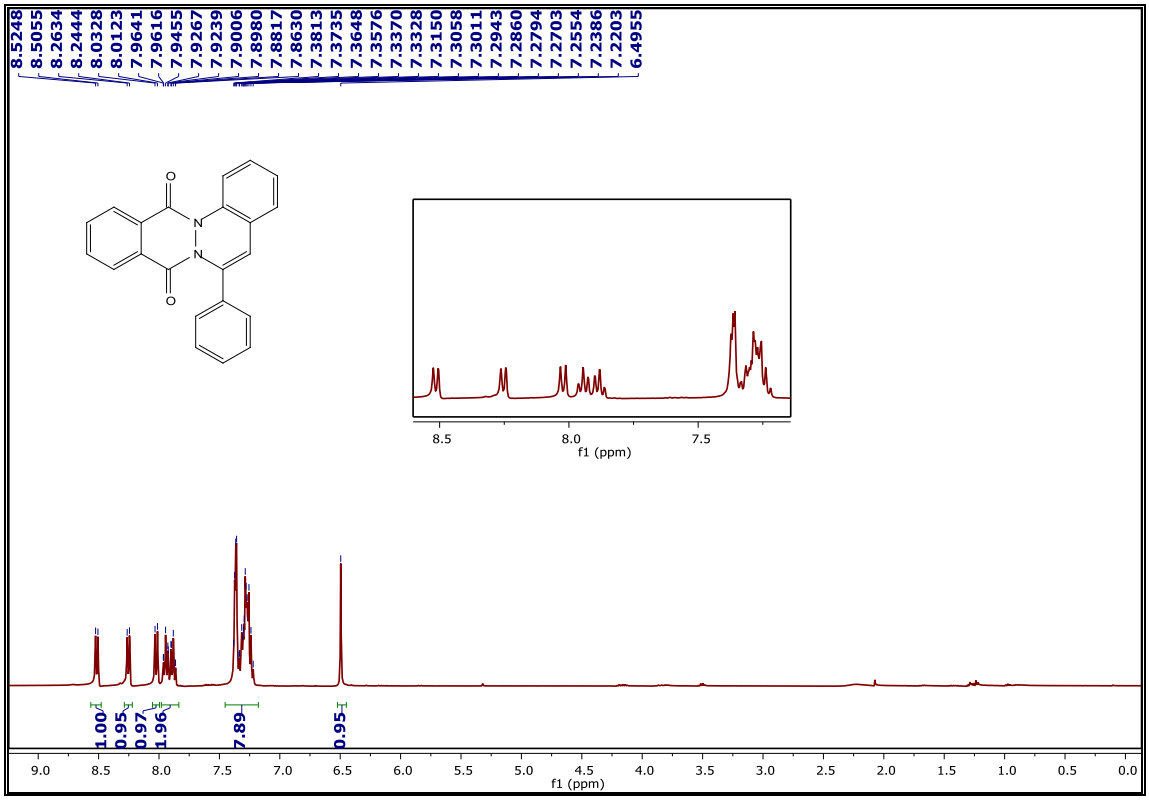

Figure 4.2.3 ^{1}H NMR spectra of **49aa**

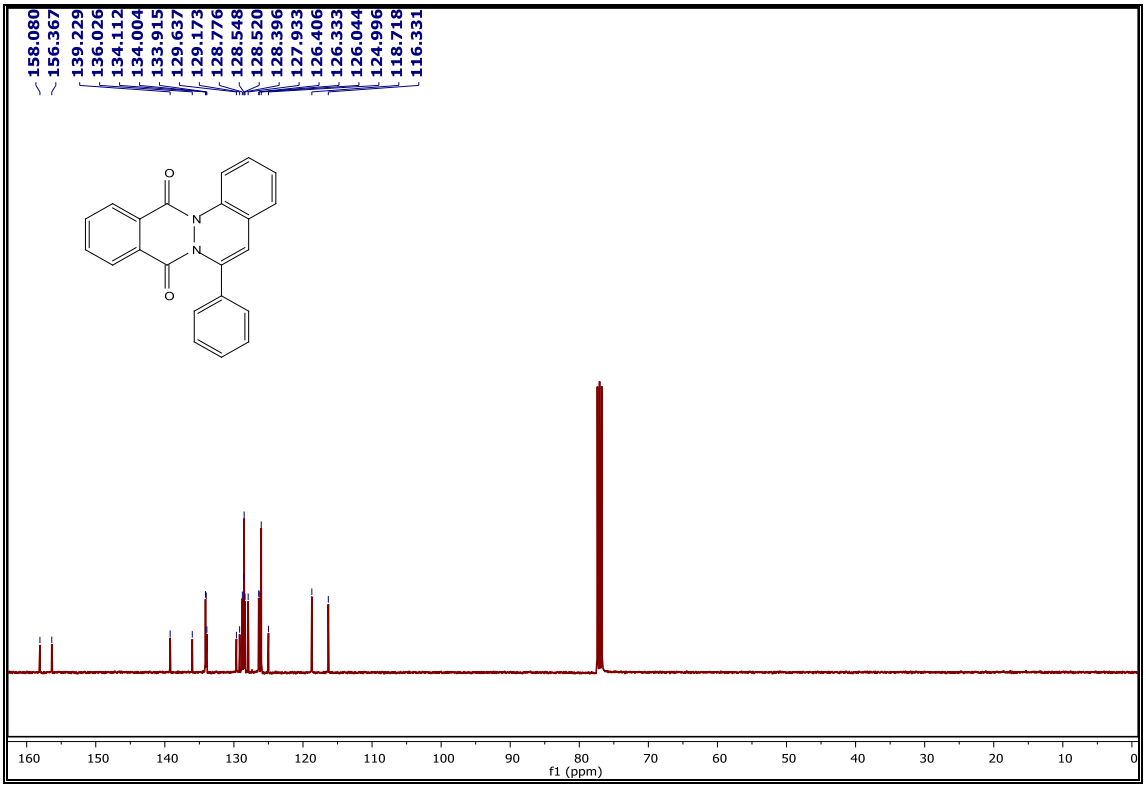

Figure 4.2.4 ^{13}C NMR spectra of **49aa**

Interestingly, during one of the attempted cyclization studies on **48aa**, the use of $BF_3{\cdot}OEt_2$ (1 equiv) in DMF under heating conditions at 150 ^oC under ambient conditions afforded 5-benzoyl-5,6-dihydrophthalazino[2,3-*a*]cinnoline-8,13-dione (**50aa**) in 45% yield (Table 4.2.2, entry 13). Replacing DMF with DMSO provided **50aa** in 55% yield, which further got significantly inflated to 81% by using 2 equiv of $BF_3{\cdot}OEt_2$ (Table 4.2.2, entries 14-15). Albeit no further change was observed by using 3 equiv of $BF_3{\cdot}OEt_2$ (Table 4.2.2, entry 16). This unprecedented formation of dihydrophthalazino-fused cinnoline scaffold clearly suggested the role of DMSO as a methylene source,[65,66] resulting in tandem C-N and C-C bond formations under $BF_3{\cdot}OEt_2$-mediated conditions.

With the established DMSO impelled $BF_3{\cdot}OEt_2$-mediated cyclization conditions, the scope of several *o*-acylmethylated 2-aryl-2,3-dihydrophthalazine-1,4-diones (**48**) were evaluated (Scheme 4.2.5). Initiated by varying the substrate scope on the acyl part of acylmethylated 2-arylphhalazine-1,4-diones **48**, the reaction was found to be compatible to a wide variety of functionalities. Of these, both electron-donating (substrate: **48ba**) and electron-withdrawing substituents (substrates: **48ca**, **48da**) showed good tolerance, recurring their corresponding cyclized products in 66-78% yields. The presence of disubstitutions (similar/dissimilar) on the *meta* and *para* positions of aryl ring of **48** (substrates: **48fa**-**48ga**) ensued methylene inserted cinnolines (**50fa**-**50ga**) in 76-78% yields. As stated earlier, since **48ha** was obtained in a regioisomeric form, its corresponding cyclized product **50ha** was also isolated as a regioisomer mixture in 62% yield. The representative ^1H NMR and ^{13}C NMR spectra of the *o*-acylmethylated product **50fa** are shown in Figure 4.2.5 and Figure 4.2.6, respectively.

It is noteworthy that attempts to perform the *o*-acylmethylation of **47**, and any of the above two described cyclizations in a one-step manner did not produced the desired fused-cinnolines under a variety of conditions. However, sequential one-pot *o*-acylmethylation of **47** in ethanol, and thereafter cyclization using Lawesson's reagent in toluene or $BF_3{\cdot}OEt_2$ in DMSO furnished the expected phthalazine-fused cinnolines in slightly better yields over the showcased two-step strategies.

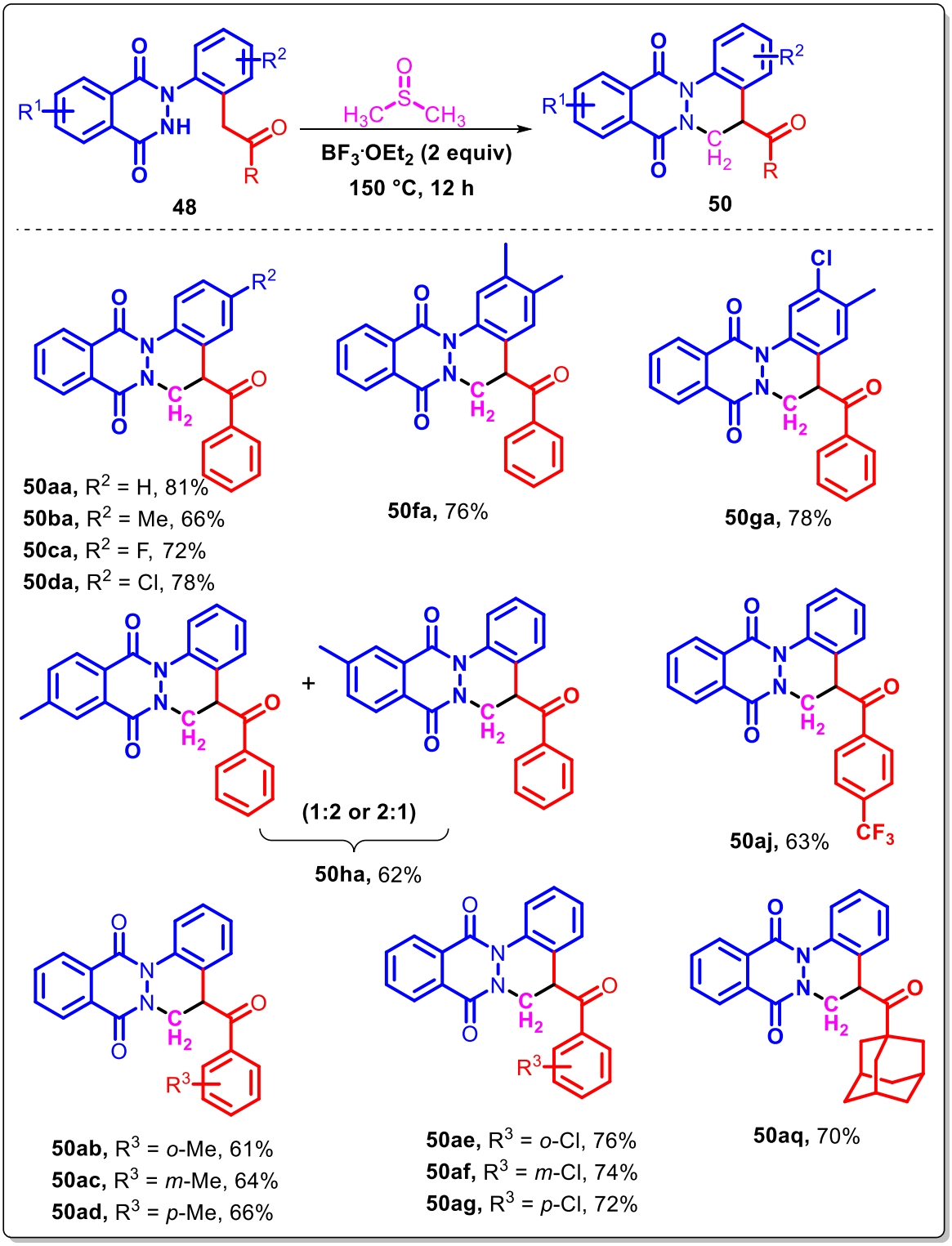

Scheme 4.2.5 Synthesis of 5-acyl-5,6-dihydrophthalazino[2,3-*a*]cinnoline-8,13-diones (**50**)

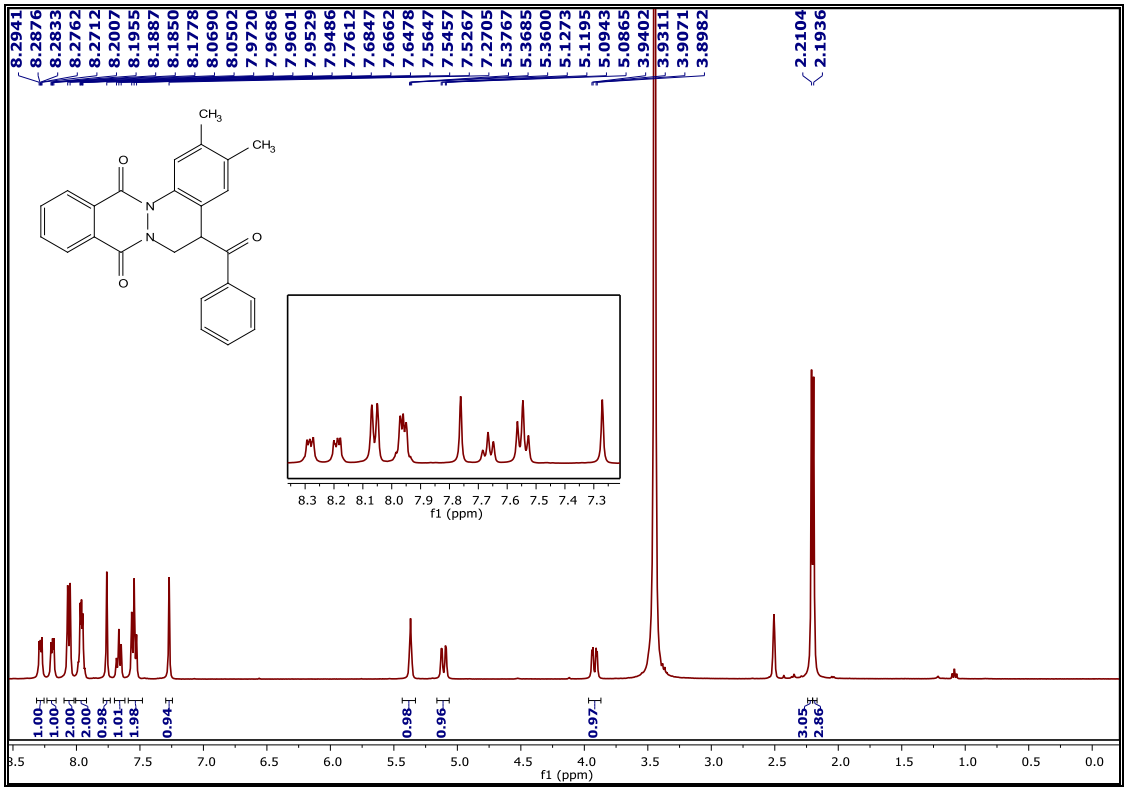

Figure 4.2.5 ^{1}H NMR spectra of **50fa**

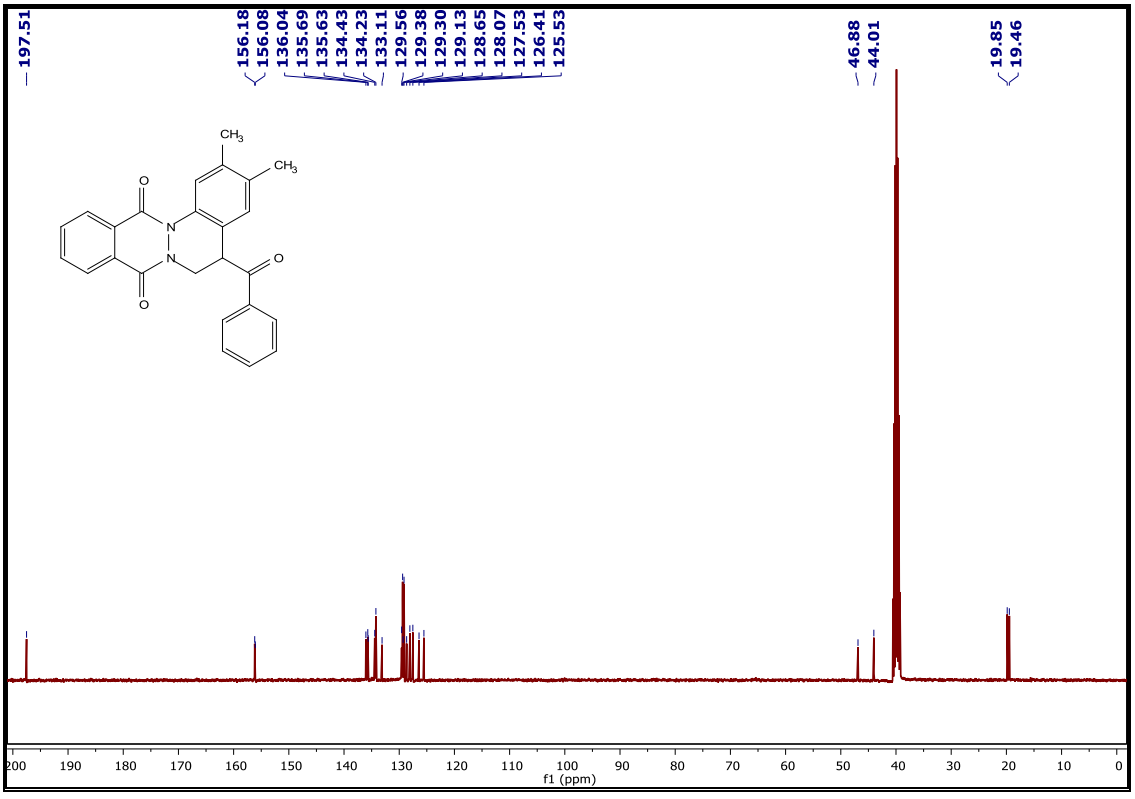

Figure 4.2.6 ^{13}C NMR spectra of **50fa**

In order to probe the mechanism of the different transformations disclosed, several control experiments were investigated (Scheme 4.2.6 & 4.2.7). Firstly, **48aa** was not formed at all in absence of $[RuCl_2(p\text{-cymene})]_2$ using KPF_6 in ethanol at 80 °C (Scheme 4.2.6i). One-pot competitive experiment between electronically rich and deficient 2-aryl-2,3-dihydrophthalazine-1,4-diones (**47b** and **47d**) with **2a** produced their corresponding *o*-acylmethylated products (**48ba:48da**, 1:1) in almost equivalent ratio under optimized conditions (Scheme 4.2.6i).

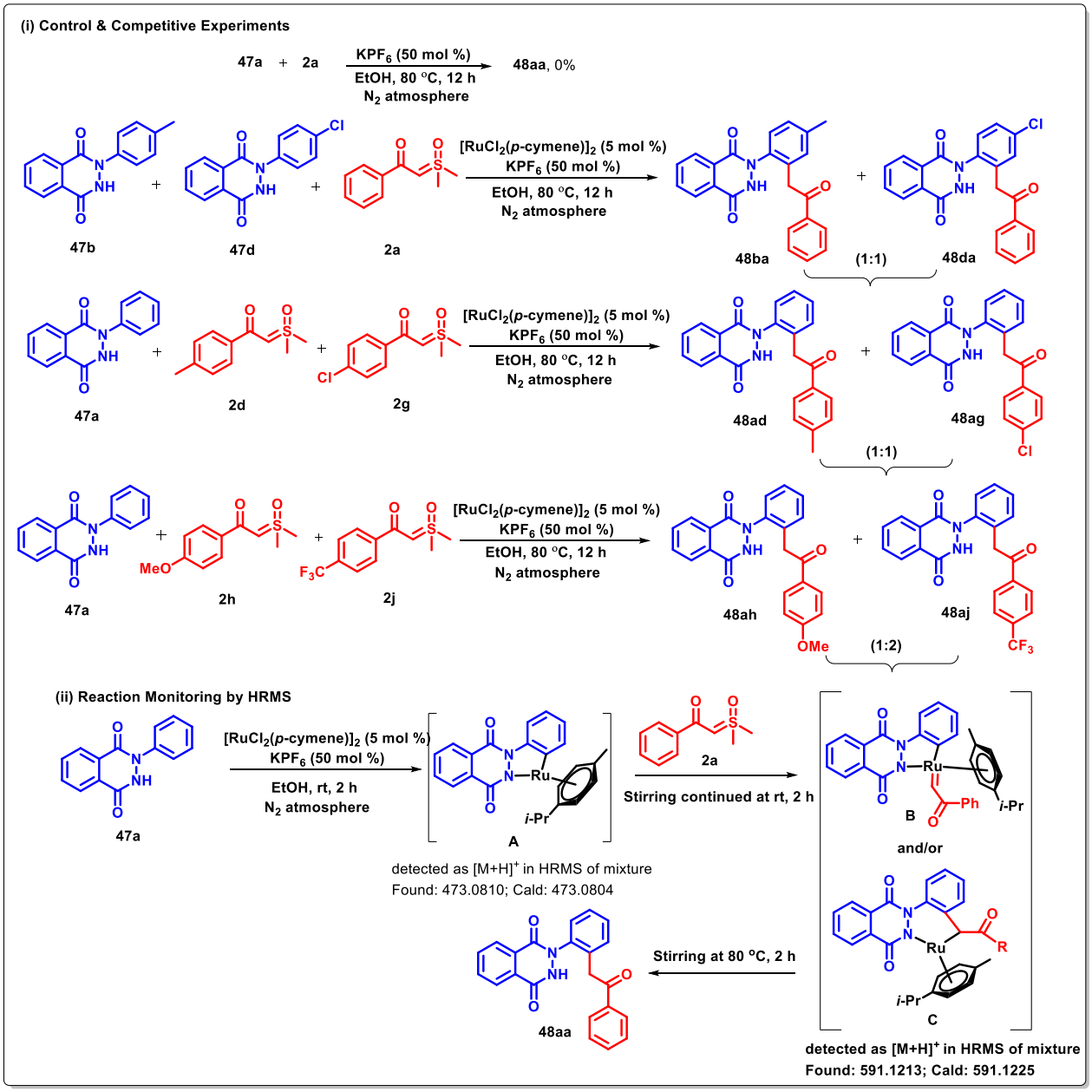

Scheme 4.2.6 Preliminary mechanistic investigations

Similarly, a competitive experiment between electronically rich and deficient *α*-carbonyl sulfoxonium ylides (**2d** and **2g**) with **47a** furnished their corresponding *o*-acylmethylated products (**48ad:48ag**, 1:1) in almost equivalent ratio (Scheme 4.2.6i). However, a competitive experiment between -OMe and -CF_3 substituted *α*-carbonyl sulfoxonium ylides (**2h** and **2j**) with **47a** furnished the corresponding *o*-acylmethylated products (**48ah:48aj**) in 1:2 ratio, respectively (Scheme 4.2.6i). Interestingly, during real-time and *in situ* monitoring of the reaction progress by mass spectrometry, the presence of five-membered ruthenacyclic species **A** was detected in ESI-MS, after 2 h of the reaction of **47a** under Ru(II)-catalyzed conditions at room temperature (Scheme 4.2.6ii). Further, the formation of species **B** and/or **C** were also detected in the ESI-MS of the crude reaction mixture, after 2 h of addition of **2a** to the precedent mixture (Scheme 4.2.6ii). The detection of species **A-C** clearly indicated the relevance of C-H activation and possible mode(s) of coordination of ruthenium with sulfoxonium ylide. Subsequently, **48aa** was detected (in minor amounts on TLC) in ESI-MS after stirring the same reaction mixture at 80 ^oC for 2 h (Scheme 4.2.6ii).

To shed some light on the mechanisms of Lawesson's reagent and $BF_3{\cdot}OEt_2$-mediated cyclizations of **48**, few more studies were carried (Scheme 4.2.7). During *in situ* monitoring of Lawesson's reagent-mediated cyclization of **48aa** by mass spectrometry, *o*-thioacylmethylated 2-arylphthalazine-1,4-dione (species **D**) was detected in ESI-MS, however, it could not be isolated by column chromatography even after numerous attempts (Scheme 4.2.7i). On the other hand, *in situ* monitoring of $BF_3{\cdot}OEt_2$-mediated cyclization of **48aa** by mass spectrometry, species **E** and **F** were detected in ESI-MS after 4 h, indicating that their formations might be involved in the reaction pathway (Scheme 4.2.7i). Notably, both the cyclization reactions proceeded comfortably to afford their corresponding products in high yields in presence of radical scavenger TEMPO (3 equiv). This clearly advocates about the non-involvement of radical pathways for the two cyclization strategies (Scheme 4.2.7ii). Finally, the formation of **50aa-*d_2*** in presence of deuterated DMSO-d_6 affirmed DMSO as a methylene source and solvent in the disclosed $BF_3{\cdot}OEt_2$-mediated cyclizations of **48aa** (Scheme 4.2.7iii).

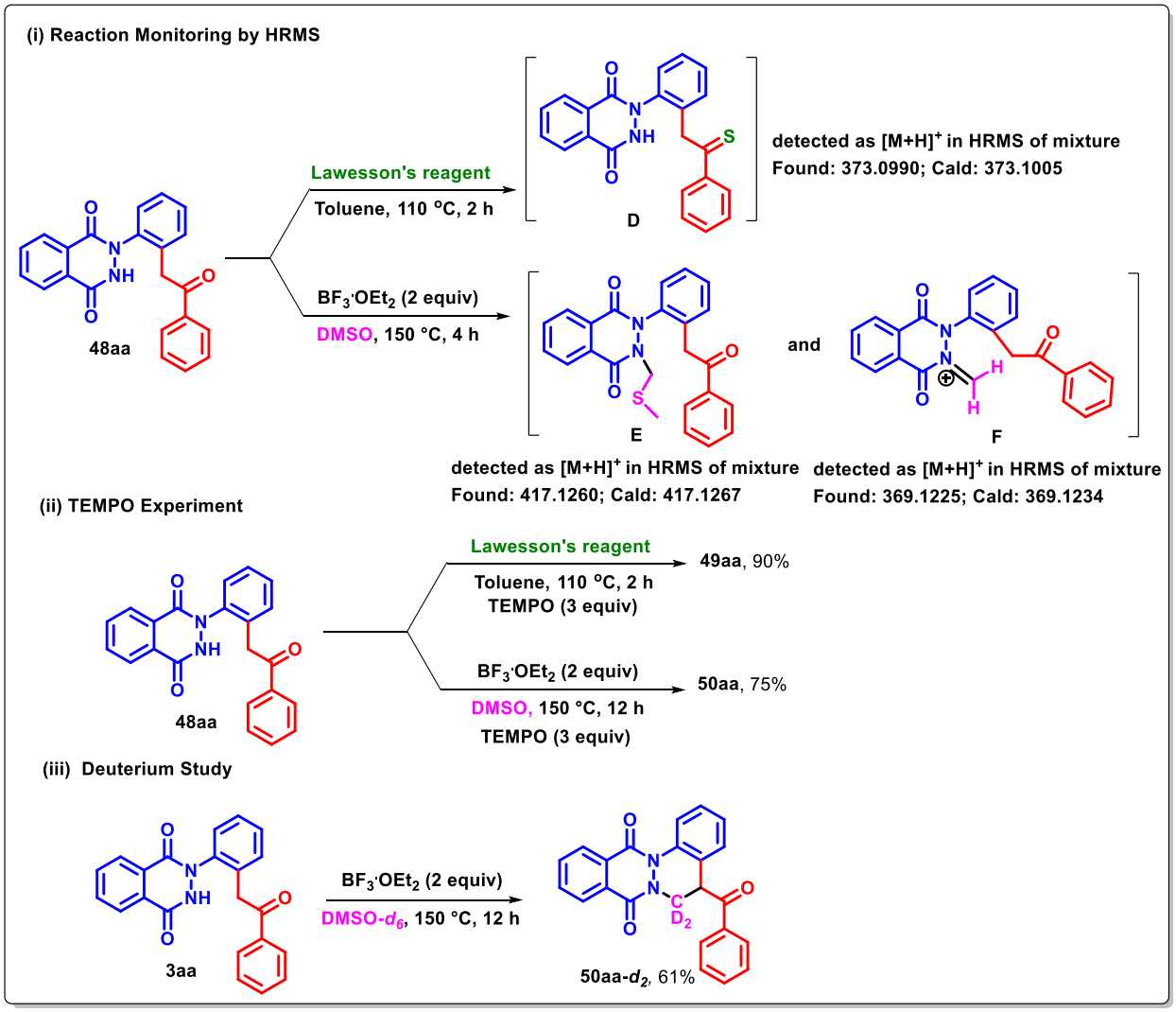

Scheme 4.2.7 Preliminary mechanistic investigations

On the basis of our preliminary mechanistic results and literature precedents,[41,43,67,68] a plausible mechanism for the *o*-acylmethylation and the two disclosed cyclizations are proposed (Scheme 4.2.8). The reaction is believed to be initiated by the formation of active monomeric Ru(II) catalyst, {[RuX_2(*p*-cymene)]; X = PF_6 and/or Cl} by the dissociation of dimeric [$RuCl_2$(*p*-cymene)]$_2$ with KPF_6. Cyclometalation of this Ru(II) catalyst with **47a** generates the five-membered ruthenacyclic intermediate **A** *via* C-H activation, which upon coordination with sulfoxonium ylide (**2**) and subsequent elimination of DMSO furnishes a ruthenium *α*-oxo carbene species **B**. Thereafter, migratory insertion of the activated carbene into Ru–aryl bond gives a six-membered ruthenacyclic intermediate **C**, which upon protonolysis of the Ru–N and Ru–C bonds produces *o*-acylmethylated product **48**, along with the regeneration of the active catalyst. For the Lawesson's reagent-mediated

cyclization, it is likely that thionation of carbonyl functionality in **48** with Lawesson's reagent affords *o*-thioacylmethylated 2-aryl-2,3-dihydrophthalazine-1,4-dione **D**, which on intramolecular nucleophilic attack by the amide group, followed by H_2S elimination generates **49**. While the $BF_3{\cdot}OEt_2$-mediated cyclization is believed to be initiated by activation of DMSO by $BF_3{\cdot}OEt_2$ to generate electrophilic thionium ion, which on interception with **48** gives the alkylsulfurized intermediate **E**. **E** subsequent on demethylthioation affords the iminium species **F**, which undergoes acid-mediated intramolecular cyclization *via* **G** to deliver the desired product **50**.

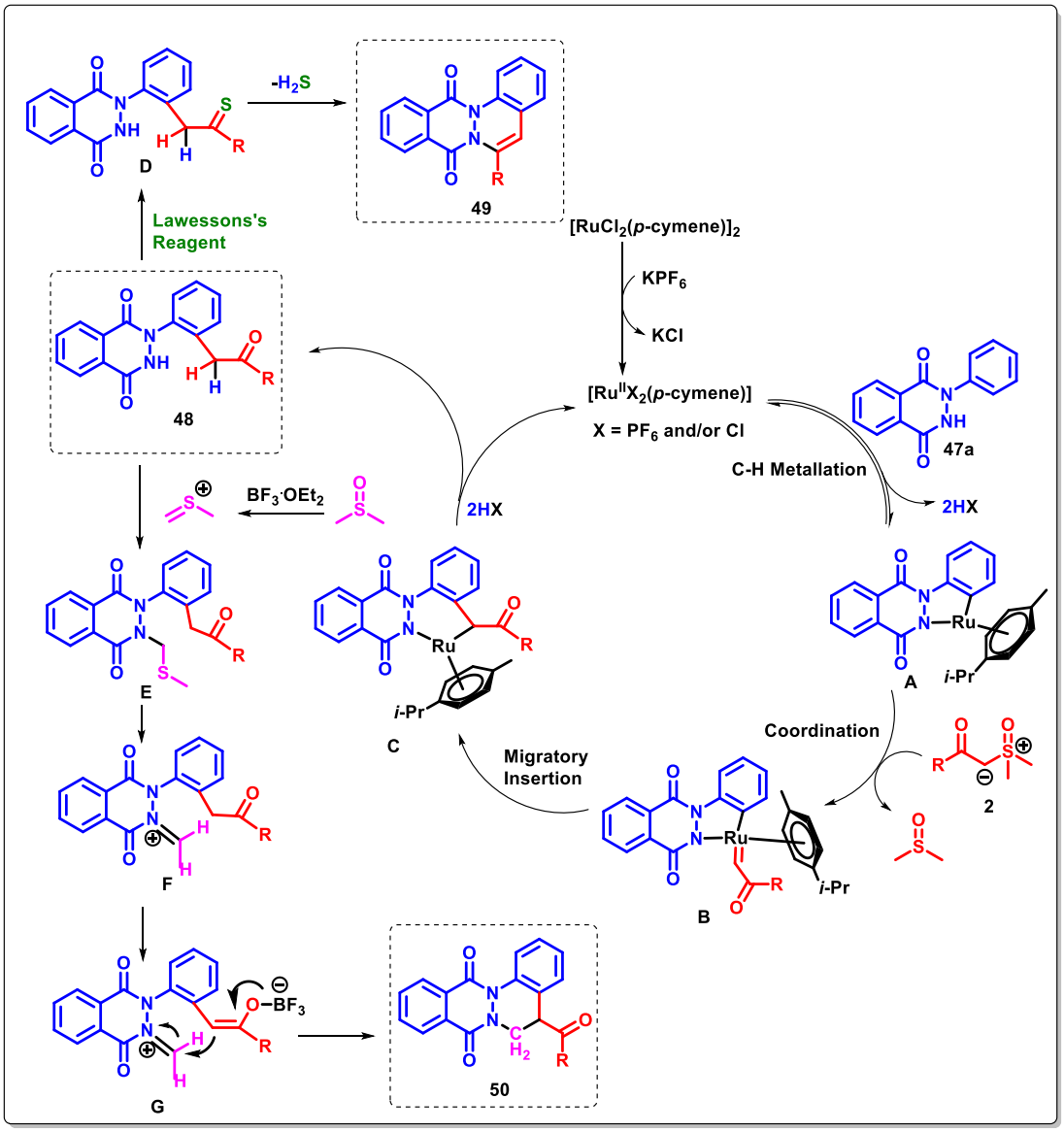

Scheme 4.2.8 Plausible mechanism for *o*-acylmethylation and Lawesson's reagent and $BF_3{\cdot}OEt_2$-mediated cyclization

In summary, we have developed a Ru(II)-catalyzed strategy for the *ortho*-Csp^2-H acylmethylation of 2-aryl-2,3-dihydrophthalazine-1,4-diones with *α*-carbonyl sulfoxonium ylides. The synthesized 2-(*o*-acylmethylaryl)-2,3-dihydrophthalazine-1,4-diones further underwent cyclization using Lawesson's reagent in refluxing toluene under ambient conditions to afford 6-arylphthalazino[2,3-*a*]cinnoline-8,13-dione in excellent yields. While 5-acyl-5,6-dihydrophthalazino[2,3-*a*]cinnoline-8,13-diones were obtained by $BF_3{\cdot}OEt_2$-mediated cyclization of 2-(*o*-acylmethylaryl)-2,3-dihydrophthalazine-1,4-diones using DMSO as a solvent and a methylene source *via* dual C-C and C-N bond formations.

4.3 Experimental Section

General Considerations

Commercially available reagents were used without purification. Commercially available solvents were dried by standard procedures prior to use. *α*-carbonyl sulfoxonium ylides[40] were prepared according to the reported procedures. Reactions were monitored by using thin layer chromatography (TLC) on 0.2 mm silica gel F254 plates (Merck). The chemical structures of final products and intermediates were characterized by nuclear magnetic resonance spectra (^{1}H NMR and ^{13}C NMR) were recorded on a 400 MHz spectrometer, and the chemical shifts are reported in *δ* units, parts per million (ppm), relative to residual chloroform (7.26 ppm) or DMSO (2.5 ppm) in the deuterated solvent. ^{13}C NMR spectra are fully decoupled. The following abbreviations were used to describe peak splitting patterns when appropriate: s = singlet, d = doublet, t = triplet, dd = doublet of doublets, and m = multiplet. Coupling constants, *J*, are reported in hertz (Hz). The ^{13}C NMR spectra are reported in ppm relative to $CDCl_3$ (77.0 ppm) or DMSO-d_6 (39.5 ppm). Melting points were determined on a capillary point apparatus equipped with a digital thermometer and are uncorrected. High resolution mass spectra were recorded on an Agilent Technologies 6545 Q-TOF LC/MS by using electrospray mode. Column chromatography was performed on silica gel (100−200 mesh) using a varying ratio of ethyl acetate/hexanes as an eluent.

General procedure for *o*-acylmethylation of 2-aryl-2,3-dihydrophthalazine-1,4-diones

To a stirred solution of *N*-aryl-2,3-dihydrophthalazine-1,4-dione (**47**) (100 mg, 1 equiv) in ethanol (10 mL) under nitrogen atmosphere, $[RuCl_2(p\text{-cymene})]_2$ (0.05 equiv), KPF_6 (0.5 equiv) and *α*-carbonyl sulfoxonium ylide (**2**) (1.5 equiv) were added at room temperature. The reaction was stirred at 80 °C for 12 h, and the progress of the reaction was monitored by TLC. After the completion of the reaction, ethanol was evaporated under reduced pressure, and water was added

to the reaction mixture. The mixture was extracted with EtOAc (3 × 15 mL), and the combined organic layers were separated, dried over anhydrous sodium sulfate, and concentrated under vacuum to yield a crude mixture. The crude mixture was purified by column chromatography using ethyl acetate/hexanes (3:7) as an eluent system to afford the desired product (**48**).

2-(2-(2-Oxo-2-phenylethyl)phenyl)-2,3-dihydrophthalazine-1,4-dione (48aa). White solid,

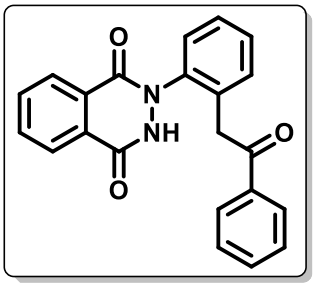

122 mg (82% yield); mp 151−153 °C; ^{1}H NMR (400 MHz, DMSO-d_6) δ 11.78 (s, 1H), 8.19 – 8.15 (m, 1H), 7.93 – 7.89 (m, 2H), 7.88 – 7.83 (m, 1H), 7.73 (dd, J = 8.2, 1.2 Hz, 2H), 7.46 – 7.43 (m, 2H), 7.43 – 7.39 (m, 3H), 7.29 (t, J = 7.8 Hz, 2H), 4.29 (s, 2H); ^{13}C NMR (100 MHz, DMSO-d_6) δ 197.3, 157.8, 150.9, 141.3, 136.9, 133.8, 133.3, 132.7, 131.9, 129.7, 129.4, 129.1, 128.8, 128.8, 128.4, 128.0, 127.1, 125.1, 124.6, 41.5; HRMS (ESI-TOF) (*m/z*) calculated $C_{22}H_{17}N_2O_3^+$ 357.1234, found 357.1221 $[M + H]^+$.

2-(2,6-Bis(2-oxo-2-phenylethyl)phenyl)-2,3-dihydrophthalazine-1,4-dione (48aa′). White

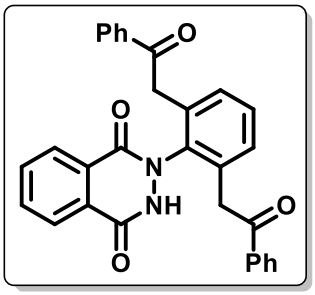

solid; mp 180−181 °C; ^{1}H NMR (400 MHz, DMSO-d_6) δ 11.67 (s, 1H), 8.06 (d, J = 7.6 Hz, 1H), 7.85 – 7.73 (m, 3H), 7.69 (d, J = 7.6 Hz, 4H), 7.44 – 7.38 (m, 3H), 7.37 – 7.33 (m, 2H), 7.26 (t, J = 7.6 Hz, 4H), 4.26 – 4.12 (m, 4H); ^{13}C NMR (100 MHz, DMSO-d_6) δ 197.2, 157.8, 151.4, 139.9, 138.2, 136.8, 135.9, 134.9, 134.6, 133.6, 133.3, 132.4, 130.7, 129.3, 128.8, 128.8, 128.4, 126.9, 125.5, 124.5, 41.3; HRMS (ESI-TOF) (*m/z*) calculated $C_{30}H_{23}N_2O_4^+$ 475.1652, found 475.1653 $[M + H]^+$.

2-(4-Methyl-2-(2-oxo-2-phenylethyl)phenyl)-2,3-dihydrophthalazine-1,4-dione (48ba). White

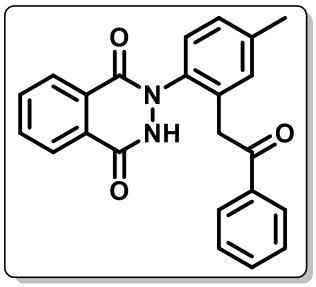

solid, 114 mg (78% yield); mp 140−141 °C; ^{1}H NMR (400 MHz, DMSO-d_6) δ 11.76 (s, 1H), 8.16 (d, J = 7.7 Hz, 1H), 7.93 – 7.88 (m, 2H), 7.87 – 7.82 (m, 1H), 7.72 (d, J = 6.9 Hz, 2H), 7.46 – 7.41 (m, 1H), 7.32 – 7.25 (m, 3H), 7.25 – 7.18 (m, 2H), 4.23 (s, 2H), 2.36 (s, 3H); ^{13}C NMR (100 MHz, DMSO-d_6) δ 197.4, 157.8, 150.8, 138.8, 138.0, 136.9, 133.8, 133.5, 133.3, 132.7, 132.2, 131.4, 129.4, 128.8, 128.5, 128.4, 127.1, 124.6, 41.3, 21.2; HRMS (ESI-TOF) (*m/z*) calculated $C_{23}H_{19}N_2O_3^+$ 371.1390, found 371.1392 $[M + H]^+$.

2-(4-Fluoro-2-(2-oxo-2-phenylethyl)phenyl)-2,3-dihydrophthalazine-1,4-dione (48ca). White

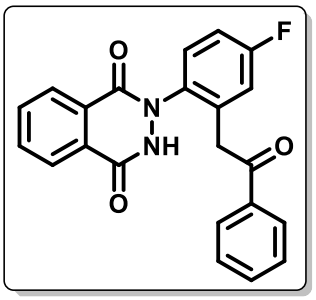

solid, 116 mg (80% yield); mp 139−140 °C; ^{1}H NMR (400 MHz, DMSO-d_6) δ 11.82 (s, 1H), 8.15 (d, J = 7.7 Hz, 1H), 7.92 – 7.88 (m, 2H), 7.87 – 7.82 (m, 1H), 7.74 (d, J = 7.3 Hz, 2H), 7.51 – 7.41 (m, 2H), 7.38 – 7.22 (m, 4H), 4.32 (s, 2H); ^{13}C NMR (100 MHz, DMSO-d_6) δ 196.6, 161.5 ($^{1}J_{C–F}$ = 242.9 Hz), 157.9, 151.0, 137.7, 136.7, 136.5 ($^{3}J_{C–F}$ = 8.9 Hz), 133.9, 133.5, 132.8, 130.8 ($^{3}J_{C–F}$ = 9.0 Hz), 129.7, 129.3, 128.8, 128.3, 127.0, 125.2, 124.6, 118.6 ($^{2}J_{C–F}$ = 22.9 Hz), 114.8 ($^{2}J_{C–F}$ = 22.4 Hz), 41.2; ^{19}F NMR (376 MHz, DMSO-d_6) δ -113.9 ; HRMS (ESI-TOF) (*m/z*) calculated $C_{22}H_{16}FN_2O_3^+$ 375.1139, found 375.1139 $[M + H]^+$.

2-(4-Chloro-2-(2-oxo-2-phenylethyl)phenyl)-2,3-dihydrophthalazine-1,4-dione (48da). White

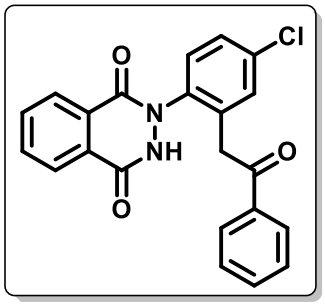

solid, 123 mg (86% yield); mp 170−171 °C; ^{1}H NMR (400 MHz, DMSO-d_6) δ 11.83 (s, 1H), 8.14 (d, J = 7.7 Hz, 1H), 7.93 – 7.88 (m, 2H), 7.87 – 7.82 (m, 1H), 7.74 (d, J = 6.9 Hz, 2H), 7.57 (d, J = 2.1 Hz, 1H), 7.51 – 7.43 (m, 3H), 7.31 (t, J = 7.6 Hz, 2H), 4.34 (s, 2H); ^{13}C NMR (100 MHz, DMSO-d_6) δ 196.6, 157.8, 150.9, 140.3, 136.7, 136.1, 133.9, 133.5, 132.8, 132.7, 131.8, 130.6, 129.2, 128.9, 128.3, 127.9, 127.0, 125.1, 124.6, 41.0; HRMS (ESI-TOF) (*m/z*) calculated $C_{22}H_{16}ClN_2O_3^+$ 391.0844, found 391.0844 $[M + H]^+$.

2-(4-Bromo-2-(2-oxo-2-phenylethyl)phenyl)-2,3-dihydrophthalazine-1,4-dione (48ea). White

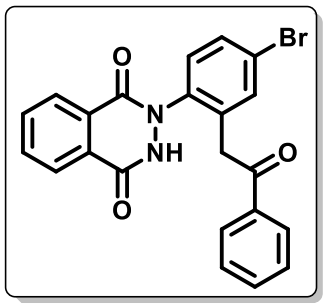

solid, 121 mg (88% yield); mp 169−170 °C; ^{1}H NMR (400 MHz, DMSO-d_6) δ 11.83 (s, 1H), 8.13 (d, J = 7.6 Hz, 1H), 7.91 – 7.87 (m, 2H), 7.86 – 7.81 (m, 1H), 7.74 (brs, 1H), 7.73 – 7.69 (m, 2H), 7.62 (dd, J = 8.4, 2.3 Hz, 1H), 7.48 – 7.43 (m, 1H), 7.40 (d, J = 8.4 Hz, 1H), 7.31 (t, J = 7.8 Hz, 2H), 4.34 (s, 2H); ^{13}C NMR (100 MHz, DMSO-d_6) δ 196.7, 157.8, 151.0, 140.7, 136.7, 136.4, 134.7, 133.9, 133.5, 132.8, 130.9, 130.9, 129.7, 129.2, 129.1, 128.9, 128.3, 127.0, 124.6, 121.3, 40.9; HRMS (ESI-TOF) (*m/z*) calculated for $C_{22}H_{16}BrN_2O_3^+$ 435.0339, found 435.0343 $[M + H]^+$.

2-(4,5-Dimethyl-2-(2-oxo-2-phenylethyl)phenyl)-2,3-dihydrophthalazine-1,4-dione (48fa).

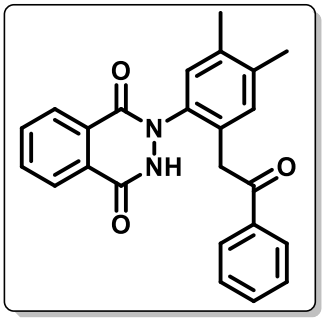

White solid, 114 mg (79% yield); mp 197−198 °C; ^{1}H NMR (400 MHz, DMSO-d_6) δ 11.72 (s, 1H), 8.16 (d, J = 7.7 Hz, 1H), 7.94 – 7.79 (m, 3H), 7.72 (d, J = 7.7 Hz, 2H), 7.43 (t, J = 7.4 Hz, 1H), 7.29 (t, J = 7.6 Hz, 2H), 7.16 (s, 2H), 4.18 (s, 2H), 2.25 (s, 3H), 2.22 (s, 3H); ^{13}C NMR (100 MHz, DMSO-d_6) δ 197.5, 157.7, 150.8, 138.7, 136.9, 136.7, 136.0, 134.4, 133.7, 133.3, 132.7, 132.5, 130.6, 129.5, 129.4, 128.8, 128.4, 127.1, 125.2, 124.6, 41.1, 19.5, 19.3; HRMS (ESI-TOF) (*m/z*) calculated for $C_{24}H_{21}N_2O_3^+$ 385.1547, found 385.1545 $[M + H]^+$.

2-(5-Chloro-4-methyl-2-(2-oxo-2-phenylethyl)phenyl)-2,3-dihydrophthalazine-1,4-dione

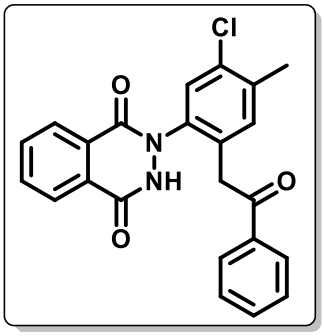

(48ga). White solid, 113 mg (80% yield); mp 208−209 °C; ^{1}H NMR (400 MHz, DMSO-d_6) δ 11.79 (s, 1H), 8.14 (td, J = 7.7, 1.1 Hz, 1H), 7.91 – 7.88 (m, 2H), 7.87 – 7.81 (m, 1H), 7.73 (d, J = 7.1 Hz, 2H), 7.53 (s, 1H), 7.47 – 7.44 (m, 1H), 7.43 (s, 1H), 7.30 (t, J = 7.7 Hz, 2H), 4.27 (s, 2H), 2.38 (s, 3H); ^{13}C NMR (100 MHz, DMSO-d_6) δ 196.9, 157.8, 151.0, 140.1, 136.8, 135.8, 134.3, 133.9, 133.4, 132.8, 131.9, 129.3, 128.9, 128.8, 128.3, 127.1, 125.1, 124.6, 40.8, 19.8; HRMS (ESI-TOF) (*m/z*) calculated $C_{23}H_{18}ClN_2O_3^+$ 405.1000, found 405.0996 $[M + H]^+$.

6-Methyl-2-(2-(2-oxo-2-phenylethyl)phenyl)-2,3-dihydrophthalazine-1,4-dione + 7-Methyl-2-(2-(2-oxo-2-phenylethyl)phenyl)-2,3-dihydrophthalazine-1,4-dione (1:2 or 2:1) (48ha).

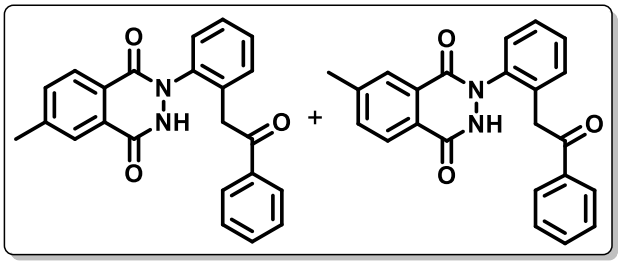

White solid, 111 mg (76% yield); mp 193−194 °C; ^{1}H NMR (400 MHz, DMSO-d_6) δ 11.70 (s, 1.5H), 8.06 (d, J = 8.1 Hz, 0.5H), 7.96 (s, 1H), 7.81 (d, J = 8.1 Hz, 1H), 7.76 – 7.70 (m, 4.5H), 7.69 – 7.65 (m, 0.5H), 7.48 – 7.36 (m, 7.5H), 7.35 – 7.28 (m, 3H), 4.27 (s, 3H), 2.50 (s, 4.5H); ^{13}C NMR (100 MHz, DMSO-d_6) δ 197.3, 157.8, 151.0, 144.4, 143.2, 141.4, 136.8, 134.9, 133.9, 133.8, 133.3, 131.8, 129.3, 128.8, 128.7, 128.4, 128.0, 127.1, 126.8, 124.6, 124.2, 41.5, 41.5, 21.8, 21.8; HRMS (ESI-TOF) (*m/z*) calculated $C_{23}H_{19}N_2O_3^+$ 371.1390, found 371.1392 $[M + H]^+$.

6-Methoxy-2-(2-(2-oxo-2-phenylethyl)phenyl)-2,3-dihydrophthalazine-1,4-dione + 7-Methoxy-2-(2-(2-oxo-2-phenylethyl)phenyl)-2,3-dihydrophthalazine-1,4-dione (1:1) (48ia).

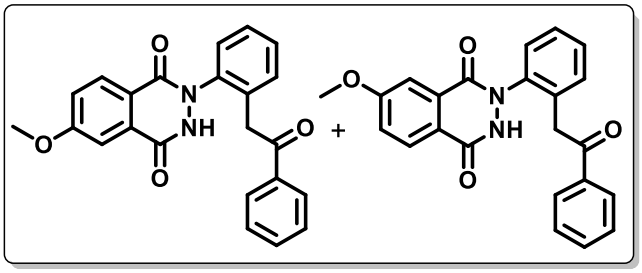

White solid, 124 mg (86% yield); mp 180−181 °C; ^{1}H NMR (400 MHz, DMSO-d_6) δ 11.68 (s, 2H), 8.09 (d, J = 8.8 Hz, 1H), 7.85 (d, J = 8.8 Hz, 1H), 7.74 (d, J = 7.6 Hz, 4H), 7.54 (d, J = 2.6 Hz, 1H), 7.49 – 7.38 (m, 12H), 7.35 – 7.29 (m, 4H), 7.26 (d, J = 2.6 Hz, 1H), 4.27 (s, 4H), 3.93 (s, 3H), 3.92 (s, 3H); ^{13}C NMR (100 MHz, DMSO-d_6) δ 197.3, 197.3, 163.4, 162.7, 157.6, 136.9, 133.8, 133.8, 133.3, 131.8, 131.8, 131.4, 129.4, 128.8, 128.8, 128.8, 128.7, 128.6, 128.4, 128.4, 128.0, 128.0, 126.8, 122.9, 122.5, 121.3, 108.3, 106.0, 56.4, 56.3, 41.5, 41.4; HRMS (ESI-TOF) (*m/z*) calculated $C_{23}H_{19}N_2O_4^+$ 387.1339, found 387.1327 $[M + H]^+$.

6-Bromo-2-(2-(2-oxo-2-phenylethyl)phenyl)-2,3-dihydrophthalazine-1,4-dione + 7-Bromo-2-(2-(2-oxo-2-phenylethyl)phenyl)-2,3-dihydrophthalazine-1,4-dione (1:1) (48ja). White solid,

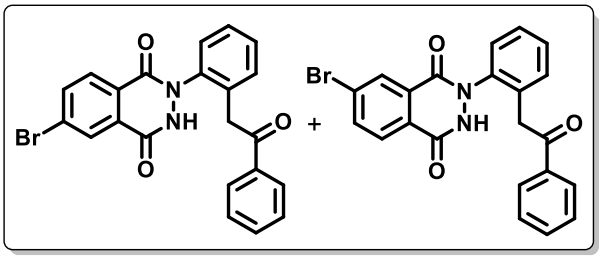

111 mg (81% yield); mp 222−224 °C; ^{1}H NMR (400 MHz, DMSO-d_6) δ 11.96 (s, 2H), 8.20 (d, J = 2.0 Hz, 1H), 8.10 – 8.05 (m, 2H), 8.03 (d, J = 2.0 Hz, 1H), 8.02 –7.98 (m, 1H), 7.83 (d, J = 8.5 Hz, 1H), 7.76 – 7.71 (m, 4H), 7.49 – 7.38 (m, 10H), 7.34 – 7.27 (m, 4H), 4.29 (s, 4H); ^{13}C NMR (100 MHz, DMSO-d_6) δ 197.3, 158.3, 156.6, 141.0, 136.9, 136.8, 135.7, 133.9, 133.3, 133.3, 132.0, 131.0, 129.5, 129.4, 128.9, 128.8, 128.8, 128.7, 128.4, 128.1, 127.7, 127.0, 126.4, 41.4, 41.3; HRMS (ESI-TOF) (*m/z*) calculated $C_{22}H_{16}BrN_2O_3^+$ 435.0339 ,found 435.0358 $[M + H]^+$.

5-Fluoro-2-(2-(2-oxo-2-phenylethyl)phenyl)-2,3-dihydrophthalazine-1,4-dione or 8-Fluoro-2-(2-(2-oxo-2-phenylethyl)phenyl)-2,3-dihydrophthalazine-1,4-dione (48ka). White solid, 117

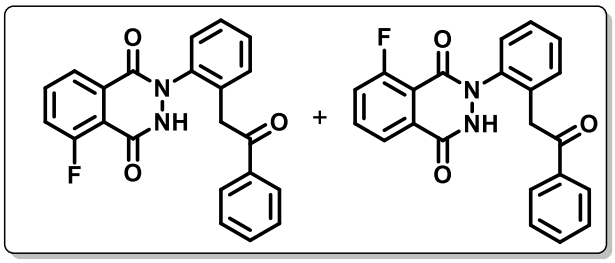

mg (80% yield); mp 193−194 °C; ^{1}H NMR (400 MHz, DMSO-d_6) δ 11.75 (s, 1H), 8.01 (dd, J = 7.9, 1.1 Hz, 1H), 7.89 – 7.82 (m, 1H), 7.77 – 7.72 (m, 2H), 7.71 – 7.67 (m, 1H), 7.48 – 7.40 (m, 5H), 7.30 (t, J = 8.8 Hz, 2H), 4.29 (s, 2H); ^{13}C NMR (100 MHz, DMSO-d_6) δ 197.4, 159.3, 156.7, 156.5, 148.8, 140.9, 136.9, 134.2 ($^{2}J_{C–F}$ =

9.11 Hz), 133.9, 133.3, 132.0, 131.6, 128.9, 128.8, 128.7, 128.4, 128.1, 123.5 ($^3J_{C–F}$ = 3.7 Hz), 121.1, 120.9, 41.3; ^{19}F NMR (376 MHz, DMSO-d_6) δ -110.6; HRMS (ESI-TOF) (*m/z*) calculated $C_{22}H_{16}FN_2O_3^+$ 375.1139, found 375.1160 $[M + H]^+$.

2-(2-(2-Oxo-2-(2-methyl)-ethyl)phenyl)-2,3-dihydrophthalazine-1,4-dione (48ab). White solid, 114 mg (73% yield); mp 150−151 °C; ^{1}H NMR (400 MHz, DMSO-d_6) δ 11.84 (s, 1H), 8.18 (d, *J* = 7.7 Hz, 1H), 7.96 – 7.84 (m, 3H), 7.59 (d, *J* = 7.2 Hz, 1H), 7.48 – 7.39 (m, 4H), 7.24 – 7.19 (m, 1H), 7.11 – 7.02 (m, 2H), 4.26 (s, 2H), 2.17 (s, 3H); ^{13}C NMR (100 MHz, DMSO-d_6) δ 200.5, 157.7, 150.9, 141.4, 137.7, 137.6, 133.9, 133.5, 132.8, 132.2, 131.9, 131.5, 129.3, 129.0, 128.8, 128.7, 128.4, 128.0, 127.1, 125.9, 124.6, 44.6, 20.8; HRMS (ESI-TOF) (*m/z*) calculated $C_{23}H_{19}N_2O_3^+$ 371.1390, found 371.1388 $[M + H]^+$.

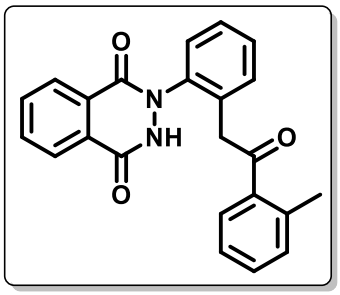

2-(2-(2-Oxo-2-(3-methyl)ethyl)phenyl)-2,3-dihydrophthalazine-1,4-dione (48ac). White solid, 119 mg (77% yield); mp 171−173 °C; ^{1}H NMR (400 MHz, DMSO-d_6) δ 11.79 (s, 1H), 8.16 (d, *J* = 7.7 Hz, 1H), 7.93 – 7.89 (m, 2H), 7.88 – 7.83 (m, 1H), 7.52 (d, *J* = 7.6 Hz, 1H), 7.48 – 7.40 (m, 5H), 7.23–7.12 (m, 2H), 4.26 (s, 2H), 2.17 (s, 3H); ^{13}C NMR (100 MHz, DMSO-d_6) δ 197.5, 157.7, 150.9, 141.2, 138.1, 137.0, 134.1, 133.9, 133.8, 132.7, 131.9, 129.3, 128.8, 128.8, 128.7, 128.0, 127.0, 125.6, 124.5, 41.3, 21.2; HRMS (ESI-TOF) (*m/z*) calculated $C_{23}H_{19}N_2O_3^+$ 371.1390, found 371.1389 $[M + H]^+$.

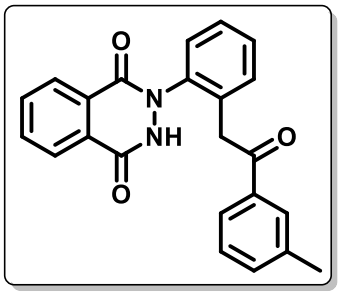

2-(2-(2-Oxo-2-(4-methyl)ethyl)phenyl)-2,3-dihydrophthalazine-1,4-dione (48ad). White solid, 121 mg (78% yield); mp 198−200 °C; ^{1}H NMR (400 MHz, DMSO-d_6) δ 11.77 (s, 1H), 8.15 (d, *J* = 7.7 Hz, 1H), 7.94 – 7.82 (m, 3H), 7.61 (d, *J* = 8.2 Hz, 2H), 7.45 – 7.38 (m, 4H), 7.05 (d, *J* = 7.9 Hz, 2H), 4.24 (s, 2H), 2.22 (s, 3H); ^{13}C NMR (100 MHz, DMSO-d_6) δ 196.9, 157.7, 150.8, 143.7, 141.2, 134.4, 134.2, 133.7, 132.6, 131.9, 129.3, 129.3, 128.8, 128.7, 128.5, 128.0, 127.1, 125.1, 124.5, 41.3, 21.5; HRMS (ESI-TOF) (*m/z*) calculated $C_{23}H_{19}N_2O_3^+$ 371.1390, found 371.1386 $[M + H]^+$.

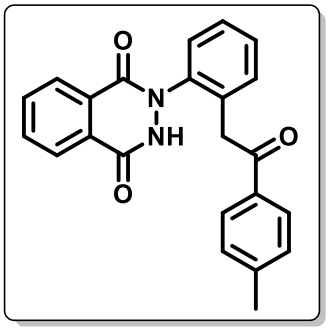

2-(2-(2-(2-Chlorophenyl)-2-oxoethyl)phenyl)-2,3-dihydrophthalazine-1,4-dione (48ae).

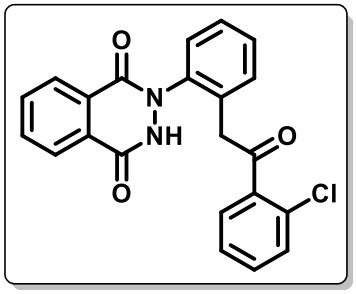

White solid, 139 mg (85% yield); mp 149−150 °C; ^{1}H NMR (400 MHz, DMSO-d_6) δ 11.87 (s, 1H), 8.21 (d, J = 7.8 Hz, 1H), 7.99 – 7.87 (m, 3H), 7.47 – 7.38 (m, 5H), 7.37 – 7.31 (m, 2H), 7.28 – 7.17 (m, 1H), 4.31 (s, 2H); ^{13}C NMR (100 MHz, DMSO-d_6); δ 199.4, 157.7, 151.0, 141.5, 139.0, 134.0, 132.8, 132.5, 132.3, 132.2, 130.5, 129.7, 129.4, 128.8, 128.7, 128.3, 127.5, 127.1, 125.2, 124.6, 45.7; HRMS (ESI-TOF) (*m/z*) calculated $C_{22}H_{16}ClN_2O_3^+$ 391.0844, found 391.0840 $[M + H]^+$.

2-(2-(2-(3-Chlorophenyl)-2-oxoethyl)phenyl)-2,3-dihydrophthalazine-1,4-dione (48af).

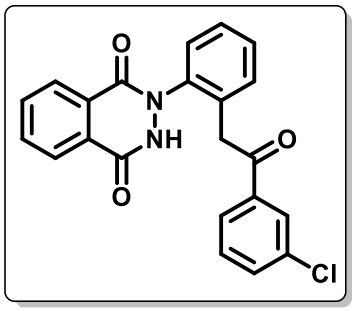

White solid, 138 mg (84% yield); mp 213−215 °C; ^{1}H NMR (400 MHz, DMSO-d_6) δ 11.79 (s, 1H), 8.14 (d, J = 7.8 Hz, 1H), 7.93–7.90 (m, 2H), 7.88 – 7.82 (m, 1H), 7.70 – 7.64 (m, 2H), 7.49 – 7.42 (m, 3H), 7.42 – 7.39 (m, 2H), 7.31 (t, J = 7.8 Hz, 1H), 4.30 (s, 2H); ^{13}C NMR (100 MHz, DMSO-d_6) δ 196.4, 157.7, 151.0, 141.2, 138.7, 133.8, 133.7, 133.0, 132.7, 132.1, 130.7, 129.3, 128.8, 128.8, 128.2, 127.9, 127.0, 41.5; HRMS (ESI-TOF) (*m/z*) calculated $C_{22}H_{16}ClN_2O_3^+$ 391.0844, found 391.0842 $[M + H]^+$.

2-(2-(2-(4-Chlorophenyl)-2-oxoethyl)phenyl)-2,3-dihydrophthalazine-1,4-dione (48ag).

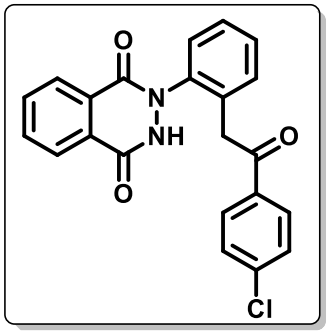

White solid, 137 mg (84% yield); mp 229−230 °C; ^{1}H NMR (400 MHz, DMSO-d_6) δ 11.77 (s, 1H), 8.14 (d, J = 7.7 Hz, 1H), 7.94 – 7.83 (m, 3H), 7.71 (d, J = 8.6 Hz, 2H), 7.48 – 7.39 (m, 4H), 7.31 (d, J = 8.6 Hz, 2H), 4.27 (s, 2H); ^{13}C NMR (100 MHz, DMSO-d_6) δ 196.5, 157.7, 150.9, 141.2, 138.3, 135.5, 133.9, 133.8, 132.7, 132.0, 130.2, 129.3, 128.8, 128.8, 128.1, 127.0, 125.1, 124.5, 41.4; HRMS (ESI-TOF) (*m/z*) calculated $C_{22}H_{16}ClN_2O_3^+$ 391.0844, found 391.0838 $[M + H]^+$.

2-(2-(2-(4-Methoxyphenyl)-2-oxoethyl)phenyl)-2,3-dihydrophthalazine-1,4-dione (48ah).

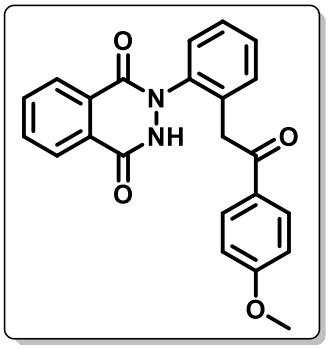

White solid, 133 mg (82% yield); mp 112−115 °C; ^{1}H NMR (400 MHz, DMSO-d_6) δ 11.78 (s, 1H), 8.16 (d, J = 7.6 Hz, 1H), 7.91 – 7.88 (m, 2H), 7.87 – 7.82 (m, 1H), 7.7 (d, J = 8.8 Hz, 2H), 7.43 – 7.36 (m, 4H), 6.75 (d, J = 8.9 Hz, 2H), 4.20 (s, 2H), 3.71 (s, 3H); ^{13}C NMR (100 MHz, DMSO-d_6) δ 195.7, 163.2, 157.8, 150.9, 141.2, 134.4, 133.7, 132.6, 131.8, 130.7, 129.8, 129.4, 128.8, 128.8, 127.9, 127.1, 125.2, 124.5, 113.9, 55.8, 41.0; HRMS (ESI-TOF) (*m/z*) calculated $C_{23}H_{19}N_2O_4^+$ 387.1339, found 387.1336 $[M + H]^+$.

2-(2-(2-(4-Fluorophenyl)-2-oxoethyl)phenyl)-2,3-dihydrophthalazine-1,4-dione (48ai). White solid, 119 mg (76% yield); mp 228−229 °C; ^{1}H NMR (400 MHz, DMSO-d_6) δ 11.75 (s, 1H), 8.15 (d, J = 7.7 Hz, 1H), 7.93 – 7.89 (m, 2H), 7.88 – 7.83 (m, 1H), 7.82 – 7.76 (m, 2H), 7.46 – 7.39 (m, 4H), 7.08 (t, J = 8.8 Hz, 2H), 4.27 (s, 2H); ^{13}C NMR (100 MHz, DMSO-d_6) δ 196.0, 165.2 ($^{1}J_{C–F}$ = 250.1 Hz), 157.7, 150.8, 141.2, 133.9, 133.8, 133.6 ($^{4}J_{C–F}$ = 2.8 Hz), 132.7, 131.9, 131.4 ($^{3}J_{C–F}$ = 9.4 Hz), 129.3, 128.8, 128.8, 128.1, 127.0, 124.5, 115.7 ($^{2}J_{C–F}$ = 21.8 Hz), 41.4; ^{19}F NMR (376 MHz, DMSO-d_6) δ -106.2; HRMS (ESI-TOF) (*m/z*) calculated $C_{22}H_{16}FN_2O_3^+$ 375.1139, found 375.1149 $[M + H]^+$.

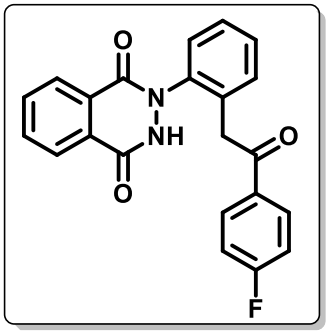

2-(2-(2-Oxo-2-(4-(Trifluoromethyl)phenyl)ethyl)phenyl)-2,3-dihydrophthalazine-1,4-dione (48aj). White solid, 114 mg (81% yield); mp 241−243 °C; ^{1}H NMR (400 MHz, DMSO-d_6) δ 11.76 (s, 1H), 8.12–8.08 (m, 1H), 7.91 – 7.86 (m, 4H), 7.85 – 7.80 (m, 1H), 7.62 (d, J = 8.2 Hz, 2H), 7.51 – 7.47 (m, 1H), 7.46 – 7.43 (m, 1H), 7.42 – 7.39 (m, 2H), 4.34 (s, 2H); ^{13}C NMR (100 MHz, DMSO-d_6) δ 196.9, 157.7, 150.9, 140.0, 133.8, 133.7, 132.8, 132.7, 132.5, 132.1, 129.3, 129.1, 128.8, 128.2, 127.0, 125.7 (q, $^{3}J_{C–F}$ = 3.6 Hz), 125.4, 124.5, 122.7, 41.6; ^{19}F NMR (376 MHz, DMSO-d_6) δ -61.6; HRMS (ESI-TOF) (*m/z*) calculated $C_{23}H_{16}F_3N_2O_3^+$ 425.1108, found 425.1121 $[M + H]^+$.

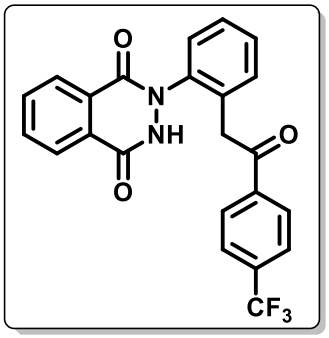

2-(2-(2-(4-Nitrophenyl)-2-oxoethyl)phenyl)-2,3-dihydrophthalazine-1,4-dione (48ak). Pale yellow solid, 131 mg (78% yield); mp 250−252 °C; ^{1}H NMR (400 MHz, DMSO-d_6) δ 11.77 (s, 1H), 8.12 – 8.03 (m, 3H), 7.92 (d, J = 8.9 Hz, 2H), 7.88 – 7.79 (m, 3H), 7.52 – 7.48 (m, 1H), 7.46 – 7.38 (m, 3H), 4.35 (s, 2H); ^{13}C NMR (100 MHz, DMSO-d_6) δ 196.8, 157.7, 151.0, 149.9, 141.6, 141.2, 133.8, 133.5, 132.7, 132.1, 129.7, 129.2, 128.9, 128.3, 127.0, 124.5, 123.8, 41.9; HRMS (ESI-TOF) (*m/z*) calculated $C_{22}H_{16}N_3O_5^+$ 402.1084, found 402.1098 $[M + H]^+$.

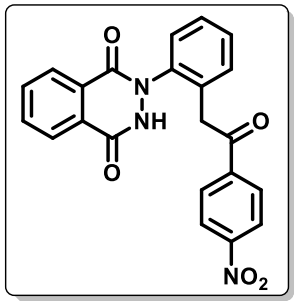

2-(2-(2-(Naphthalen-1-yl)-2-oxoethyl)phenyl)-2,3-dihydrophthalazine-1,4-dione (48al). White solid, 68 mg (40% yield); mp 105−106 °C; ^{1}H NMR (400 MHz, DMSO-d_6) δ 11.78 (s, 1H), 8.09 (dd, J = 8.6, 5.1 Hz, 2H), 7.95 – 7.83 (m, 5H), 7.82 – 7.77 (m, 1H), 7.54 – 7.51 (m, 1H), 7.49 – 7.42 (m, 4H), 7.40 – 7.32 (m, 2H), 4.45 (s, 2H); ^{13}C NMR (100 MHz, DMSO-d_6) δ 200.8, 157.7, 151.0, 141.8, 135.7, 133.8, 133.7, 133.5, 132.7, 132.6, 132.2, 129.6, 129.3, 128.8, 128.7, 128.6, 128.1, 128.1, 127.8, 127.0, 126.6, 125.7, 124.8, 124.5, 45.3; HRMS (ESI-TOF) (*m/z*) calculated $C_{26}H_{19}N_2O_3^+$ 407.1390, found 407.1384 $[M + H]^+$.

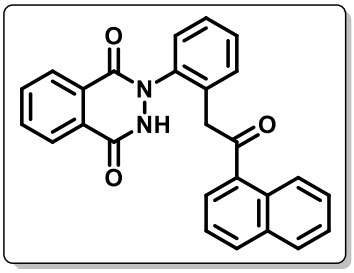

2-(2-(2-(Furan-2-yl)-2-oxoethyl)phenyl)-2,3-dihydrophthalazine-1,4-dione (48am). White solid, 44 mg (30% yield); mp 154−155 °C; ^{1}H NMR (400 MHz, DMSO-d_6) δ 11.79 (s, 1H), 8.20 (d, J = 7.5 Hz, 1H), 7.97 – 7.93 (m, 2H), 7.92 – 7.86 (m, 1H), 7.67 – 7.64 (m, 1H), 7.48 – 7.38 (m, 4H), 7.16 (d, J = 3.6 Hz, 1H), 7.46 – 7.41 (m, 1H), 4.08 (s, 2H); ^{13}C NMR (100 MHz, DMSO-d_6) δ 185.2, 157.8, 152.0, 150.2, 147.9, 133.9, 133.3, 132.8, 132.0, 129.4, 128.8, 128.8, 128.2, 127.1, 124.6, 118.8, 116.1, 112.7, 40.9; HRMS (ESI-TOF) (*m/z*) calculated $C_{20}H_{15}N_2O_4^+$ 347.1026, found 347.1013 $[M + H]^+$.

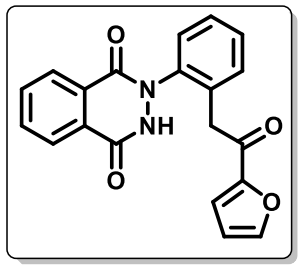

2-(2-(2-Oxo-2-(thiophen-2-yl)ethyl)phenyl)-2,3-dihydrophthalazine-1,4-dione (48an). White solid, 52 mg (34% yield); mp 158−159 °C; ^{1}H NMR (400 MHz, DMSO-d_6) δ 11.77 (s, 1H), 8.18 (d, J = 7.7 Hz, 1H), 7.93 – 7.89 (m, 2H), 7.88 – 7.84 (m, 1H), 7.78 (dd, J = 4.9, 1.1 Hz, 1H), 7.65 (dd, J = 3.5, 1.0 Hz, 1H), 7.48 – 7.40 (m, 4H), 6.94 – 6.89 (m, 1H), 4.21 (s, 2H); ^{13}C NMR (100 MHz, DMSO-d_6) δ 190.1, 157.9, 151.1, 143.9, 141.3, 135.5, 135.4, 134.0,

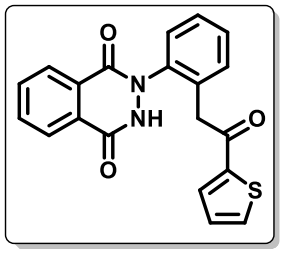

133.8, 133.8, 133.7, 132.9, 132.0, 129.4, 129.0, 128.8, 128.3, 127.2, 124.7, 42.0 ; HRMS (ESI-TOF) (*m/z*) calculated $C_{20}H_{15}N_2O_3S^+$ 363.0798, found 363.0787 $[M + H]^+$.

2-(2-(2-Oxopentyl)phenyl)-2,3-dihydrophthalazine-1,4-dione (48ao). White solid, 93 mg (69% yield); mp 150−152 °C; ^{1}H NMR (400 MHz, DMSO-d_6) δ 11.80 (s, 1H), 8.26 (d, J = 7.2 Hz, 1H), 8.05 – 7.90 (m, 3H), 7.45 – 7.37 (m, 4H), 3.63 (s, 2H), 2.22 (t, J = 7.1 Hz, 2H), 1.31 – 1.21 (m, 2H), 0.62 (t, J = 7.4 Hz, 3H); ^{13}C NMR (100 MHz, DMSO-d_6) δ 207.2, 157.8, 150.9, 141.3, 134.1, 133.2, 133.0, 132.0, 129.4, 128.8, 128.8, 128.1, 127.2, 125.3, 124.7, 45.7, 43.8, 16.8, 13.8; HRMS (ESI-TOF) (*m/z*) calculated $C_{19}H_{19}N_2O_3^+$ 323.1390, found 323.1387 $[M + H]^+$.

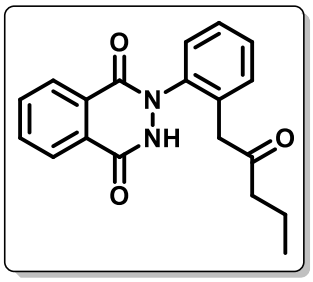

2-(2-(3,3-Dimethyl-2-oxobutyl)phenyl)-2,3-dihydrophthalazine-1,4-dione (48ap). White solid, 49 mg (35% yield); mp 180−183 °C; ^{1}H NMR (400 MHz, DMSO-d_6) δ 11.87 (s, 1H), 8.27 (d, J = 7.3 Hz, 1H), 8.03 – 7.90 (m, 3H), 7.41 – 7.36 (m, 3H), 7.33 – 7.28 (m, 1H), 3.86 (s, 2H), 0.86 (s, 9H); ^{13}C NMR (100 MHz, DMSO-d_6) δ 211.1, 157.6, 150.8, 141.3, 134.1, 133.5, 133.0, 132.5, 129.5, 128.6, 128.4, 127.7, 127.1, 125.2, 124.7, 44.1, 26.4; HRMS (ESI-TOF) (*m/z*) calculated $C_{20}H_{21}N_2O_3^+$ 337.1547, found 337.1541 $[M + H]^+$.

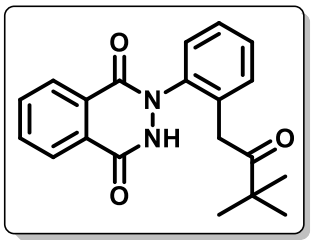

2-(2-(2-((3r,5r,7r)-Adamantan-1-yl)-2-oxoethyl)phenyl)-2,3-dihydrophthalazine-1,4-dione (48aq). White solid, 139 mg (80% yield); mp 201−202 °C; ^{1}H NMR (400 MHz, DMSO-d_6) δ 11.87 (s, 1H), 8.28 (d, J = 7.2 Hz, 1H), 8.03 – 7.90 (m, 3H), 7.40 – 7.36 (m, 3H), 7.31 – 7.26 (m, 1H), 3.79 (d, J = 20.6 Hz, 2H), 1.74 (brs, 3H), 1.58 – 1.52 (m, 3H), 1.47 (d, J = 2.1 Hz, 6H), 1.44–1.38 (m, 3H); ^{13}C NMR (100 MHz, DMSO-d_6) δ 210.6, 157.6, 150.9, 141.2, 134.0, 133.5, 132.9, 132.5, 129.6, 128.5, 128.4, 127.7, 127.1, 125.2, 124.6, 46.1, 39.2, 38.0, 36.3, 27.7; HRMS (ESI-TOF) (*m/z*) calculated $C_{26}H_{27}N_2O_3^+$ 415.2016, found 415.2015 $[M + H]^+$.

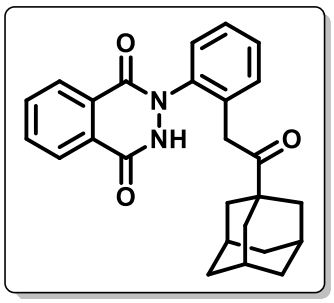

2-(2-(2-Hydroxy-2-phenylethyl)phenyl)-2,3-dihydrophthalazine-1,4-dione (48′aa). White

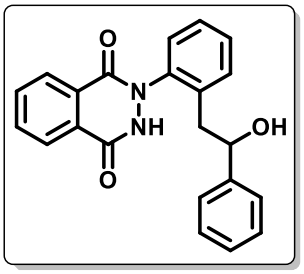

solid, 19 mg (from 30 mg of 48aa) (64%); ^{1}H NMR (400 MHz, DMSO-d_6) δ 8.22 (d, J = 7.8 Hz, 1H), 8.10 (d, J = 7.8 Hz, 1H), 7.92 – 7.78 (m, 2H), 7.37 – 7.24 (m, 4H), 7.20 – 7.06 (m, 5H), 4.72 (d, J = 6.7 Hz, 1H), 2.81 – 2.65 (m, 2H); HRMS (ESI-TOF) (*m/z*) calculated $C_{22}H_{19}N_2O_3^+$ 359.1390, found 359.1390 $[M + H]^+$.

General procedure for the synthesis of 6-arylphthalazino[2,3-*a*]cinnoline-8,13-diones

To a stirred solution of 2-(*o*-acylmethylaryl)-2,3-dihydrophthalazine-1,4-dione (**48**) (30 mg, 1 equiv) in toluene (5 mL), Lawesson's reagent (2 equiv) was added at room temperature. The reaction was stirred at 110 ^{o}C for 12 h. The progress of the reaction was monitored by TLC. After the completion of the reaction, the reaction was quenched by adding water, and the aqueous layer was extracted with EtOAc (3 × 15 mL). The combined organic layers were separated, dried over anhydrous sodium sulfate, and concentrated under reduced pressure to give crude mixture. The crude mixture was purified by column chromatography using ethyl acetate/hexanes (1:9) as an eluent system to afford the desired product (**49**).

6-Phenylphthalazino[2,3-*a*]cinnoline-8,13-dione (49aa). Yellow solid, 26 mg (92%); mp

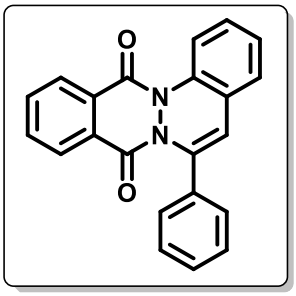

154−155 °C; ^{1}H NMR (400 MHz, $CDCl_3$) δ 8.51 (d, J = 7.4 Hz, 1H), 8.25 (d, J = 7.6 Hz, 1H), 8.02 (d, J = 8.2 Hz, 1H), 7.98 – 7.83 (m, 2H), 7.45 – 7.17 (m, 8H), 6.50 (s, 1H); ^{13}C NMR (100 MHz, $CDCl_3$) δ 158.1, 156.4, 139.2, 136.0, 134.1, 134.0, 133.9, 129.6, 129.2, 128.8, 128.5, 128.5, 128.4, 127.9, 126.4, 126.3, 126.0, 125.0, 118.7, 116.3; HRMS (ESI-TOF) (*m/z*) calculated $C_{22}H_{15}N_2O_2^+$ 339.1128, found 339.1125 $[M + H]^+$.

2-Chloro-3-methyl-6-phenylphthalazino[2,3-*a*]cinnoline-8,13-dione (49ga). Yellow solid, 25

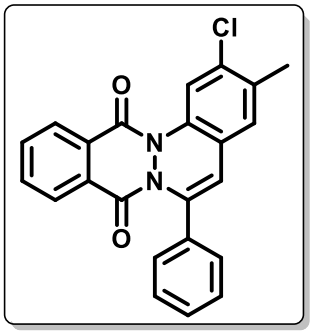

mg (88%); mp 254−255 °C; ^{1}H NMR (400 MHz, $CDCl_3$) δ 8.50 (dd, J = 7.8, 1.1 Hz, 1H), 8.24 (dd, J = 7.6, 1.0 Hz, 1H), 8.08 (s, 1H), 7.99 – 7.85 (m, 2H), 7.39 – 7.32 (m, 3H), 7.27 – 7.21 (m, 2H), 7.13 (s, 1H), 6.42 (s, 1H), 2.40 (s, 3H); ^{13}C NMR (100 MHz, $CDCl_3$) δ 158.0, 156.4, 139.3, 134.5, 134.3, 134.2, 134.1, 133.9, 133.8, 129.4, 129.1, 128.9, 128.6, 128.6, 128.0, 127.9, 126.0, 123.5, 119.4, 115.6, 19.7; HRMS (ESI-TOF) (*m/z*) calculated $C_{23}H_{16}ClN_2O_2^+$ 387.0895, found 387.0881 $[M + H]^+$.

6-(2-methyl)phthalazino[2,3-*a*]cinnoline-8,13-dione (49ab). Yellow solid, 26 mg (91%); mp 174−176 °C; ^{1}H NMR (400 MHz, $CDCl_3$) δ 8.49 (d, J = 7.6 Hz, 1H), 8.20 (d, J = 7.5 Hz, 1H), 8.02 (d, J = 8.2 Hz, 1H), 7.92 (t, J = 6.7 Hz, 1H), 7.84 (t, J = 6.8 Hz, 1H), 7.46 – 7.40 (m, 1H), 7.36 – 7.23 (m, 5H), 7.17 – 7.09 (m, 1H), 6.30 (s, 1H), 2.07 (s, 3H); ^{13}C NMR (100 MHz, $CDCl_3$) δ 157.7, 155.4, 139.5, 135.6, 134.8, 134.4, 134.0, 133.9, 130.0, 129.5, 129.0, 128.8, 128.7, 128.4, 128.3, 127.9, 126.6, 126.1, 126.1, 125.2, 119.4, 116.7, 19.7; HRMS (ESI-TOF) (*m/z*) calculated $C_{23}H_{17}N_2O_2^+$ 353.1285, found 353.1266 $[M + H]^+$.

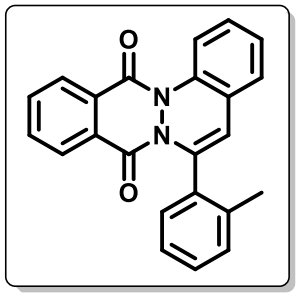

6-(4-Methoxyphenyl)phthalazino[2,3-*a*]cinnoline-8,13-dione (49ah). Yellow solid, 26 mg (91%); mp 135−136 °C; ^{1}H NMR (400 MHz, $CDCl_3$) δ 8.50 (dd, J = 7.8, 1.0 Hz, 1H), 8.25 (dd, J = 7.5, 1.0 Hz, 1H), 8.06 – 7.82 (m, 3H), 7.34 – 7.15 (m, 5H), 7.88 (d, J = 8.8 Hz, 2H), 6.42 (s, 1H), 3.83 (s, 3H); ^{13}C NMR (100 MHz, $CDCl_3$) δ 159.9, 158.1, 156.5, 139.1, 136.0, 134.1, 134.0, 129.6, 129.2, 128.5, 128.1, 127.9, 127.4, 126.4, 126.2, 126.1, 125.3, 118.7, 115.1, 55.3; HRMS (ESI-TOF) (*m/z*) calcd for $C_{23}H_{17}N_2O_3^+$ 369.1234, found 369.1223 $[M + H]^+$.

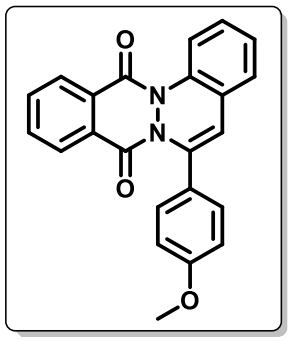

6-(4-Fluorophenyl)phthalazino[2,3-*a*]cinnoline-8,13-dione (49ai). Yellow solid, 26 mg (90%); mp 242−243 °C; ^{1}H NMR (400 MHz, $CDCl_3$) δ 8.51 (dd, J = 7.8, 1.1 Hz, 1H), 8.24 (dd, J = 7.6, 1.0 Hz, 1H), 8.01 (d, J = 8.2 Hz, 1H), 7.97 – 7.87 (m, 2H), 7.34 – 7.22 (m, 5H), 7.09 – 7.02 (m, 2H), 6.45 (s, 1H); ^{13}C NMR (100 MHz, $CDCl_3$) δ 162.7 ($^{1}J_{C–F}$ = 247.5 Hz), 158.1, 156.4, 138.2, 136.0, 134.2, 134.1, 130.0, 130.0, 129.6, 129.0, 128.6, 128.5, 127.9, 127.8, 126.4 ($^{3}J_{C–F}$ = 15.1 Hz), 124.8, 118.7, 116.3, 115.6 ($^{2}J_{C–F}$ = 21.9 Hz); ^{19}F NMR (376 MHz, DMSO-d_6) δ -114.5; HRMS (ESI-TOF) (*m/z*) calculated $C_{22}H_{14}FN_2O_2^+$ 357.1039, found 357.1020 $[M + H]^+$.

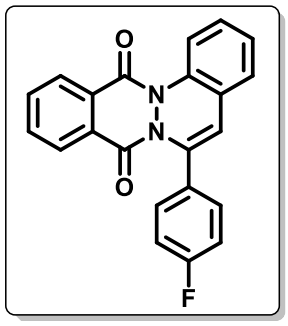

6-(4-(Trifluoromethyl)phenyl)phthalazino[2,3-*a*]cinnoline-8,13-dione (49aj). Yellow solid, 27 mg (93%); mp 200−201 °C; ^{1}H NMR (400 MHz, $CDCl_3$) δ 8.52 (d, J = 7.6 Hz, 1H), 8.24 (d, J = 7.5 Hz, 1H), 8.03 (d, J = 8.2 Hz, 1H), 7.97 (t, J = 7.1 Hz, 1H), 7.90 (t, J = 7.5 Hz, 1H), 7.62 (d, J = 8.1 Hz, 2H), 7.39 – 7.24 (m, 5H), 6.55 (s, 1H); ^{13}C NMR (100 MHz, $CDCl_3$) δ 158.0, 156.3, 137.6, 137.5, 136.1, 134.3 ($^{4}J_{C-F}$ = 4.9 Hz), 130.4 (q, $^{2}J_{C-F}$ = 32.5 Hz), 129.6, 129.0, 128.8, 128.7,

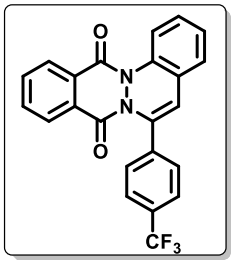

127.9, 126.5 ($^3J_{C-F}$ = 13.9 Hz), 126.3, 125.6 (q, $^4J_{C-F}$ = 3.7 Hz), 125.2, 124.4, 122.5, 118.7, 117.9; ^{19}F NMR (376 MHz, DMSO-d_6) δ -61.7; HRMS (ESI-TOF) (*m/z*) calculated $C_{23}H_{14}F_3N_2O_2^+$ 407.1002, found 407.0985 $[M + H]^+$.

General procedure for the synthesis of 5-acyl-5,6-dihydrophthalazino[2,3-*a*]cinnoline-8,13-diones

To a stirred solution of 2-(*o*-acylmethylaryl)-2,3-dihydrophthalazine-1,4-dione (**48**) (50 mg, 1 equiv) in DMSO (5 mL), $BF_3{\cdot}OEt_2$ (2 equiv) was added at 0 °C. The reaction was stirred at 150 °C for 12 h. The progress of the reaction was monitored by TLC. After the completion of the reaction, the reaction was quenched by adding saturated sodium bicarbonate solution, and the aqueous layer was extracted with EtOAc (3 × 15 mL). The combined organic layers were separated, dried over anhydrous sodium sulfate, and concentrated under reduced pressure to give crude mixture. The crude mixture was purified by column chromatography using ethyl acetate/hexanes (3:7) as an eluent system to afford the desired product (**50**).

5-Benzoyl-5,6-dihydrophthalazino[2,3-*a*]cinnoline-8,13-dione (50aa). White solid, 42 mg (81% yield); mp 211−212 °C; ^{1}H NMR (400 MHz, DMSO-d_6) δ 8.34 – 8.29 (m, 1H), 8.23 – 8.18 (m, 1H), 8.11 – 8.06 (m, 2H), 8.02 (d, *J* = 1.2 Hz, 1H), 8.00 – 7.96 (m, 2H), 7.71 – 7.66 (m, 1H), 7.56 (t, *J* = 7.9 Hz, 2H), 7.50 (dd, *J* = 7.6, 1.6 Hz, 1H), 7.43 – 7.37 (m, 1H), 7.32 – 7.27 (m, 1H), 5.48 (t, *J* = 3.4 Hz, 1H), 5.12 (dd, *J* = 13.3, 3.4 Hz, 1H), 4.02 (dd, J = 13.3, 3.7 Hz, 1H); ^{13}C NMR (100 MHz, DMSO-d_6) δ 197.4, 156.3, 156.1, 135.6, 135.4, 134.6, 134.3, 134.3, 129.4, 129.3, 129.3, 129.2, 129.0, 128.7, 128.2, 127.9, 127.6, 127.1, 125.1, 46.8, 44.5; HRMS (ESI-TOF) (*m/z*) calculated $C_{23}H_{17}N_2O_3^+$ 369.1234, found 369.1224 $[M + H]^+$.

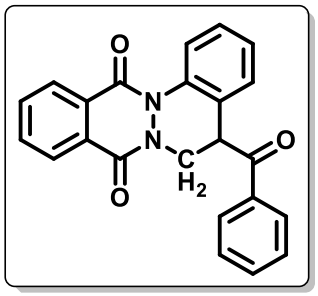

5-Benzoyl-3-methyl-5,6-dihydrophthalazino[2,3-a]cinnoline-8,13-dione (50ba). White solid, 34 mg (66% yield); mp 206−207 °C; ^{1}H NMR (400 MHz, DMSO-d_6) δ 8.31 – 8.27 (m, 1H), 8.21 – 8.16 (m, 1H), 8.07 (d, J = 7.4 Hz, 2H), 8.00 – 7.94 (m, 2H), 7.90 (d, J = 8.4 Hz, 1H), 7.71 – 7.65 (m, 1H), 7.56 (t, J = 7.6 Hz, 2H), 7.30 (s, 1H), 7.20 (dd, J = 8.5, 2.0 Hz, 1H), 5.42 (t, J = 3.4 Hz, 1H), 5.12 (dd, J = 13.3, 3.3 Hz, 1H), 3.97 (dd, J = 13.3, 3.6 Hz, 1H), 2.30 (s, 3H); ^{13}C NMR (100 MHz, DMSO-d_6) δ 197.5, 156.1, 136.6, 135.6, 134.5, 134.3, 134.3, 133.0, 129.4, 129.3, 129.2, 129.2, 129.0, 128.6, 128.5, 128.1, 127.5, 124.8, 46.7, 44.4, 21.0; HRMS (ESI-TOF) (*m/z*) calculated $C_{24}H_{19}N_2O_3^+$ 383.1390, found 383.1387 $[M + H]^+$.

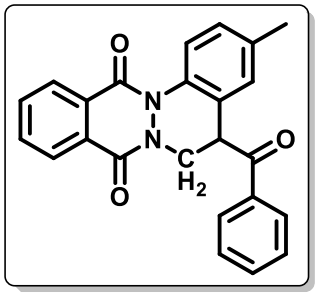

5-Benzoyl-3-fluoro-5,6-dihydrophthalazino[2,3-*a*]cinnoline-8,13-dione (50ca). White solid, 37 mg (72% yield); mp 173−175 °C; ^{1}H NMR (400 MHz, DMSO-d_6) δ 8.33 – 8.28 (m, 1H), 8.21 – 8.16 (m, 1H), 8.11 – 8.03 (m, 3H), 8.03 – 7.93 (m, 2H), 7.69 (t, J = 7.4 Hz, 1H), 7.56 (t, J = 7.6 Hz, 2H), 7.47 (dd, J = 8.8, 3.0 Hz, 1H), 7.31 – 7.21 (m, 1H), 5.48 (t, J = 3.2 Hz, 1H), 5.21 (dd, J = 13.4, 2.9 Hz, 1H), 3.96 (dd, J = 13.4, 3.6 Hz, 1H); ^{13}C NMR (100 MHz, DMSO-d_6) δ 196.8, 159.5 ($^{1}J_{C–F}$ = 243.8 Hz), 156.2, 156.1, 135.3, 134.6, 134.4 ($^{3}J_{C–F}$ = 5.9 Hz), 131.8 ($^{4}J_{C–F}$ = 2.8 Hz), 131.7, 131.6, 129.5, 129.2, 129.1, 128.6, 128.2, 127.6, 127.3, 127.2, 115.7 ($^{2}J_{C–F}$ = 23.3 Hz), 114.9 ($^{2}J_{C–F}$ = 22.6 Hz), 46.7, 44.8; ^{19}F NMR (376 MHz, DMSO-d_6) δ -112.1; HRMS (ESI-TOF) (*m/z*) calculated $C_{23}H_{16}FN_2O_3^+$ 387.1139, found 387.1145 $[M + H]^+$.

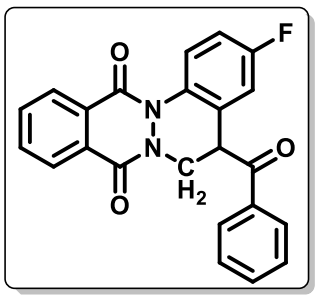

5-Benzoyl-3-chloro-5,6-dihydrophthalazino[2,3-*a*]cinnoline-8,13-dione (50da). White solid, 40 mg (78% yield); mp 168−170 °C; ^{1}H NMR (400 MHz, DMSO-d_6) δ 8.33 – 8.28 (m, 1H), 8.19 – 8.15 (m, 1H), 8.13 – 8.05 (m, 3H), 8.01 – 7.93 (m, 2H), 7.69 (t, J = 7.3 Hz, 1H), 7.65 (d, J = 2.5 Hz, 1H), 7.57 (t, J = 7.6 Hz, 2H), 7.48 (dd, J = 8.9, 2.5 Hz, 1H), 5.50 (t, J = 3.2 Hz, 1H), 5.24 (dd, J = 13.5, 2.9 Hz, 1H), 3.96 (dd, J = 13.5, 3.6 Hz, 1H); ^{13}C NMR (100 MHz, DMSO-d_6) δ 197.0, 156.4, 156.0, 135.3, 134.7, 134.4, 134.4, 134.3, 131.0, 130.7, 129.5, 129.2, 129.0, 128.8, 128.5, 128.2, 127.8, 127.6, 126.5, 46.3, 44.6; HRMS (ESI-TOF) (*m/z*) calculated $C_{23}H_{16}ClN_2O_3^+$ 403.0844, found 403.0847 $[M + H]^+$.

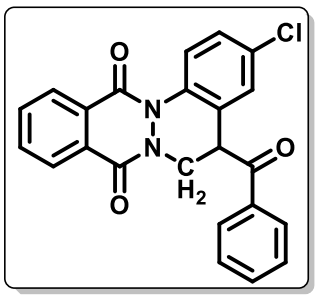

5-Benzoyl-2,3-dimethyl-5,6-dihydrophthalazino[2,3-*a*]cinnoline-8,13-dione (50fa). White solid, 39 mg (76% yield); mp 172−174 °C; ^{1}H NMR (400 MHz, DMSO-d_6) δ 8.31 – 8.26 (m, 1H), 8.23 – 8.16 (m, 1H), 8.06 (d, J = 7.5 Hz, 2H), 8.01 – 7.92 (m, 2H), 7.76 (s, 1H), 7.67 (t, J = 7.4 Hz, 1H), 7.55 (t, J = 7.6 Hz, 2H), 7.27 (s, 1H), 5.37 (t, J = 3.3 Hz, 1H), 5.11 (dd, J = 13.2, 3.1 Hz, 1H), 3.92 (dd, J = 13.2, 3.6 Hz, 1H), 2.21 (s, 3H), 2.19 (s, 3H); ^{13}C NMR (100 MHz, DMSO-d_6) δ 197.5, 156.2, 156.1, 136.0, 135.7, 135.6, 134.4, 134.2, 133.1, 129.6, 129.4, 129.3, 129.1, 128.7, 128.1, 127.5, 126.4, 125.5, 46.9, 44.0, 19.9, 19.5; HRMS (ESI-TOF) (*m/z*) calculated $C_{25}H_{21}N_2O_3^+$ 397.1547, found 397.1546 $[M + H]^+$.

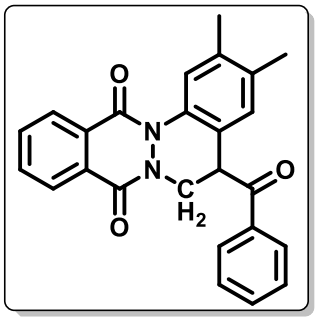

5-Benzoyl-2-chloro-3-methyl-5,6-dihydrophthalazino[2,3-*a*]cinnoline-8,13-dione (50ga). White solid, 40 mg (78% yield); mp 166−168 °C; ^{1}H NMR (400 MHz, DMSO-d_6) δ 8.34 – 8.27 (m, 1H), 8.20 (s, 1H), 8.19 – 8.13 (m, 1H), 8.07 (d, J = 7.7 Hz, 2H), 8.03 – 7.91 (m, 2H), 7.70 (t, J = 7.5 Hz, 1H), 7.57 (t, J = 7.6 Hz, 2H), 7.49 (s, 1H), 5.45 (brs, 1H), 5.28 – 5.16 (m, 1H), 3.94 (dd, J = 13.5, 3.6 Hz, 1H), 2.32 (s, 3H); ^{13}C NMR (100 MHz, DMSO-d_6) δ 197.3, 156.4, 156.0, 135.4, 134.7, 134.4, 134.4, 134.1, 134.1, 132.1, 131.2, 129.5, 129.2, 129.0, 128.5, 128.3, 127.6, 124.5, 46.2, 44.3, 19.6; HRMS (ESI-TOF) (*m/z*) calculated $C_{24}H_{18}ClN_2O_3^+$ 417.1000, found 417.0999 $[M + H]^+$.

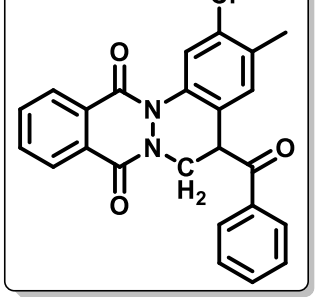

5-Benzoyl-10-methyl-5,6-dihydrophthalazino[2,3-*a*]cinnoline-8,13-dione + 5-Benzoyl-11-methyl-5,6-dihydrophthalazino[2,3-*a*]cinnoline-8,13-dione (1:2 or 2:1) (50ha). White solid, 32 mg (62% yield); mp 150−151 °C; ^{1}H NMR (400 MHz, DMSO-d_6) δ 8.19 (d, J = 8.1 Hz, 1H), 8.13 – 8.03 (m, 5H), 8.01 – 7.96 (m, 2H), 7.78 (d, J = 8.0 Hz, 1.5H), 7.67 (t, J = 7.4 Hz, 1.5H), 7.55 (t, J = 7.6 Hz, 3H), 7.49 (d, J = 7.6 Hz, 1.5H), 7.39 (t, J = 7.9 Hz, 1.5H), 7.28 (t, J = 7.2 Hz, 1H), 5.47 (t, J = 3.4 Hz, 1.5H), 5.16–5.07 (m, 1.5H), 3.98 (dd, J = 13.6, 3.6 Hz, 1.5H), 2.53 (d, J = 5.5 Hz, 4.5H); ^{13}C NMR (100 MHz, DMSO-d_6) δ 197.4, 156.4, 156.2, 145.3, 144.9, 135.7, 135.5, 135.2, 134.3, 129.4, 129.2, 129.0, 128.3, 128.0, 127.9, 127.7, 127.4, 127.1,

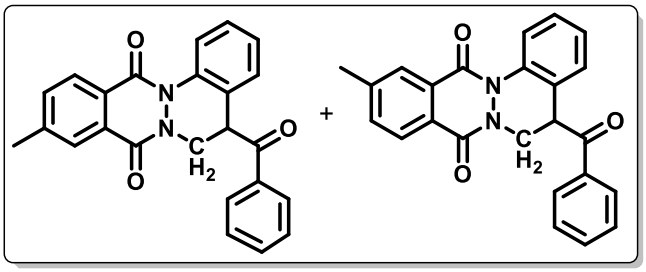

127.0, 126.3, 125.1, 46.8, 44.6, 21.8; HRMS (ESI-TOF) (*m/z*) calculated $C_{24}H_{19}N_2O_3^+$ 383.1390, found 383.1388 $[M + H]^+$.

5-(2-Methylbenzoyl)-5,6-dihydrophthalazino[2,3-*a*]cinnoline-8,13-dione (50ab). White solid, 31 mg (61% yield); mp 158−160 °C; ^{1}H NMR (400 MHz, DMSO-d_6) δ 8.33 – 8.28 (m, 1H), 8.26 – 8.22 (m, 1H), 8.03 – 7.96 (m, 3H), 7.87 (d, J = 7.4 Hz, 1H), 7.45 – 7.37 (m, 2H), 7.37 – 7.32 (m, 2H), 7.28 – 7.23 (m, 1H), 7.18 (d, J = 7.2 Hz, 1H), 5.30 (t, J = 2.9 Hz, 1H), 5.22 (dd, J = 13.1, 2.5 Hz, 1H), 3.81 (dd, J = 13.1, 3.6 Hz, 1H), 1.93 (s, 3H); ^{13}C NMR (100 MHz, DMSO-d_6) δ 200.7, 156.4, 156.2, 137.3, 137.0, 135.3, 134.7, 134.3, 131.9, 131.8, 129.6, 129.2, 129.0, 128.8, 128.7, 128.2, 127.9, 127.6, 127.4, 126.1, 125.0, 47.7, 46.6, 19.9; HRMS (ESI-TOF) (*m/z*) calculated $C_{24}H_{19}N_2O_3^+$ 383.1390, found 383.1374 $[M + H]^+$.

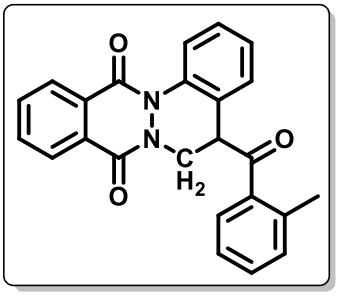

5-(3-Methylbenzoyl)-5,6-dihydrophthalazino[2,3-*a*]cinnoline-8,13-dione (50ac). White solid, 33 mg (64% yield); mp 192−193 °C; ^{1}H NMR (400 MHz, DMSO-d_6) δ 8.34 – 8.28 (m, 1H), 8.24 – 8.17 (m, 1H), 8.03 – 7.95 (m, 3H), 7.91 (d, J = 7.6 Hz, 1H), 7.86 (s, 1H), 7.51 – 7.36 (m, 4H), 7.31 – 7.26 (m, 1H), 5.47 (t, J = 3.5 Hz, 1H), 5.09 (dd, J = 13.3, 3.5 Hz, 1H), 4.06 – 3.99 (m, 1H), 2.37 (s, 3H); ^{13}C NMR (100 MHz, DMSO-d_6) δ 197.5, 156.3, 156.1, 138.9, 135.7, 135.4, 135.0, 134.6, 134.3, 129.4, 129.4, 129.3, 129.3, 128.9, 128.7, 128.2, 127.8, 127.6, 127.1, 126.5, 125.1, 46.8, 44.5, 21.3; HRMS (ESI-TOF) (*m/z*) calculated $C_{24}H_{19}N_2O_3^+$ 383.1390, found 383.1377 $[M + H]^+$.

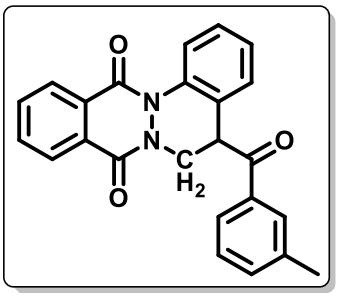

5-(4-Methylbenzoyl)-5,6-dihydrophthalazino[2,3-*a*]cinnoline-8,13-dione (50ad). White solid, 34 mg (66% yield); mp 207−209 °C; ^{1}H NMR (400 MHz, DMSO-d_6) δ 8.33 – 8.29 (m, 1H), 8.23 – 8.18 (m, 1H), 8.02 – 7.95 (m, 5H), 7.47 (dd, J = 7.7, 1.6 Hz, 1H), 7.41 – 7.34 (m, 3H), 7.31 – 7.25 (m, 1H), 5.44 (t, J = 3.5 Hz, 1H), 5.10 – 5.04 (m, 1H), 4.02 (dd, J = 13.2, 3.6 Hz, 1H), 2.39 (s, 3H); ^{13}C NMR (100 MHz, DMSO-d_6) δ 196.9, 156.3, 156.1, 144.9, 135.3, 134.6, 134.3, 133.2, 130.0, 129.5, 129.3, 129.3, 128.9, 128.7, 128.2, 127.8, 127.6, 127.1, 125.2, 125.1, 46.9, 44.3, 21.7; HRMS (ESI-TOF) (*m/z*) calculated $C_{24}H_{19}N_2O_3^+$ 383.1390, found 383.1371 $[M + H]^+$.

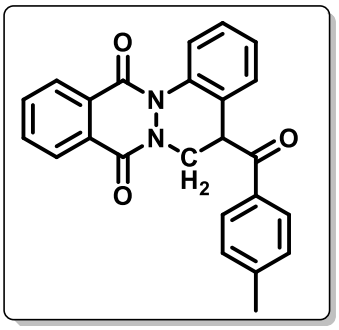

5-(2-Chlorobenzoyl)-5,6-dihydrophthalazino[2,3-*a*]cinnoline-8,13-dione (50ae). White solid, 39 mg (76% yield); mp 237−238 °C; ^{1}H NMR (400 MHz, DMSO-d_6) δ 8.32 – 8.27 (m, 1H), 8.26 – 8.21 (m, 1H), 8.01 – 7.91 (m, 3H), 7.80 (dd, J = 7.0, 1.7 Hz, 1H), 7.51 – 7.36 (m, 5H), 7.29 – 7.23 (m, 1H), 5.32 (dd, J = 13.3, 2.3 Hz, 1H), 5.19 (t, J = 2.9 Hz, 1H), 3.77 (dd, J = 13.3, 3.6 Hz, 1H); ^{13}C NMR (100 MHz, DMSO-d_6) δ 199.1, 156.2, 156.0, 137.4, 135.2, 134.6, 134.3, 132.9, 130.8, 130.1, 129.5, 129.2, 129.1, 128.7, 128.4, 128.2, 128.2, 127.6, 127.6, 127.2, 125.0, 48.9, 45.9; HRMS (ESI-TOF) (*m/z*) calculated $C_{23}H_{16}ClN_2O_3^+$ 403.0844, found 403.0827 $[M + H]^+$.

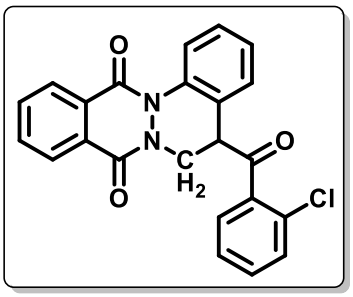

5-(3-Chlorobenzoyl)-5,6-dihydrophthalazino[2,3-*a*]cinnoline-8,13-dione (50af). White solid, 38 mg (74% yield); mp 214−216 °C; ^{1}H NMR (400 MHz, DMSO-d_6) δ 8.34 – 8.29 (m, 1H), 8.23 – 8.17 (m, 1H), 8.09 (t, J = 1.9 Hz, 1H), 8.06 – 8.01 (m, 2H), 8.00 – 7.95 (m, 2H), 7.76 (dd, J = 7.9, 1.2 Hz, 1H), 7.59 (t, J = 7.9 Hz, 1H), 7.49 (dd, J = 7.7, 1.6 Hz, 1H), 7.43 – 7.37 (m, 1H), 7.33 – 7.26 (m, 1H), 5.50 (t, J = 3.4 Hz, 1H), 5.12 (dd, J = 13.3, 3.4 Hz, 1H), 4.01 (dd, J = 13.4, 3.6 Hz, 1H); ^{13}C NMR (100 MHz, DMSO-d_6) δ 196.5, 156.3, 156.1, 137.5, 135.4, 134.6, 134.3, 134.0, 131.5, 129.2, 129.0, 128.8, 128.7, 128.6, 128.2, 128.0, 127.9, 127.6, 127.1, 125.7, 125.0, 46.6, 44.8; HRMS (ESI-TOF) (*m/z*) calculated $C_{23}H_{16}ClN_2O_3^+$ 403.0844, found 403.0836 $[M + H]^+$.

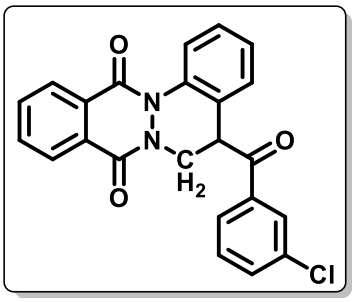

5-(4-Chlorobenzoyl)-5,6-dihydrophthalazino[2,3-*a*]cinnoline-8,13-dione (50ag). White solid, 37 mg (72% yield); mp 229−230 °C; ^{1}H NMR (400 MHz, DMSO-d_6) δ 8.33 – 8.28 (m, 1H), 8.22 – 8.17 (m, 1H), 8.09 (d, J = 8.6 Hz, 2H), 8.02 (d, J = 8.2 Hz, 1H), 8.00 – 7.95 (m, 2H), 7.63 (d, J = 8.6 Hz, 2H), 7.49 (dd, J = 7.6, 1.6 Hz, 1H), 7.43 – 7.37 (m, 1H), 7.32 – 7.26 (m, 1H), 5.46 (t, J = 3.5 Hz, 1H), 5.11 (dd, J = 13.3, 3.4 Hz, 1H), 4.01 (dd, J = 13.3, 3.7 Hz, 1H); ^{13}C NMR (100 MHz, DMSO-d_6) δ 196.5, 156.3, 156.1, 139.3, 135.4, 134.6, 134.3, 134.3, 131.1, 129.6, 129.2, 129.0, 129.0, 128.7, 128.2, 128.0, 127.6, 127.1, 125.0, 46.7, 44.6; HRMS (ESI-TOF) (*m/z*) calculated $C_{23}H_{16}ClN_2O_3^+$ 403.0844, found 403.0828 $[M + H]^+$.

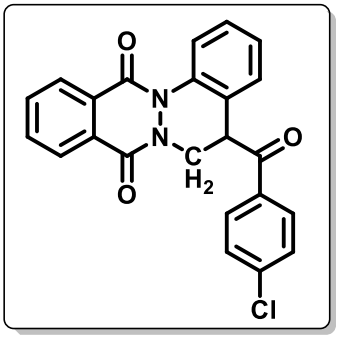

5-(4-(Trifluoromethyl)benzoyl)-5,6-dihydrophthalazino[2,3-*a*]cinnoline-8,13-dione (50aj). White solid, 65 mg (63% yield); mp 150−151 °C; ^{1}H NMR (400 MHz, DMSO-d_6) δ 8.34 – 8.29

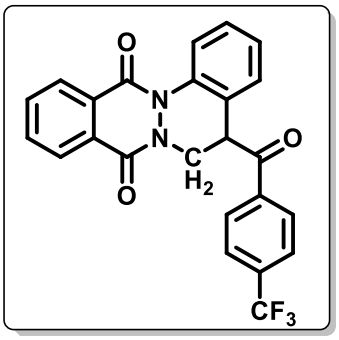

(m, 1H), 8.26 (d, *J* = 8.2 Hz, 2H), 8.23 – 8.18 (m, 1H), 8.02 (dd, 8.4, 1.2 Hz, 1H), 8.00 – 7.95 (m, 2H), 7.93 (d, *J* = 8.2 Hz, 2H), 7.52 (dd, *J* = 7.7, 1.6 Hz, 1H), 7.43 – 7.38 (m, 1H), 7.32 – 7.27 (m, 1H), 5.52 (t, *J* = 3.3 Hz, 1H), 5.16 (dd, *J* = 13.3, 3.2 Hz, 1H), 4.01 (dd, *J* = 13.3, 3.6 Hz, 1H); ^{13}C NMR (100 MHz, DMSO-*d*$_6$) *δ* 197.0, 156.4, 156.2, 138.9, 135.4, 134.6, 134.3, 133.5, 133.2, 130.0, 129.2 ($^{3}J_{C\text{-}F}$ = 7.1 Hz, 1H), 128.7 (q, $^{3}J_{C\text{-}F}$ = 5.6 Hz), 128.2, 128.1, 127.6, 127.2, 126.4 ($^{4}J_{C\text{-}F}$ = 3.8 Hz), 125.0, 122.8, 46.6, 45.1; ^{19}F NMR (376 MHz, DMSO-*d*$_6$) *δ* -62.6; HRMS (ESI-TOF) (*m/z*) calculated $C_{24}H_{16}F_3N_2O_3^+$ 437.1108, found 437.1087 $[M + H]^+$.

5-((3*r*,5*r*,7*r*)-Adamantane-1-carbonyl)-5,6-dihydrophthalazino[2,3-*a*]cinnoline-8,13-dione (50aq). White solid, 72 mg (70% yield); mp 156−157 °C; ^{1}H NMR (400 MHz, DMSO-*d*$_6$) *δ* 8.34 – 8.29 (m, 1H), 8.24 – 8.18 (m, 1H), 8.10 (d, *J* = 8.2 Hz, 1H), 8.01 – 7.95 (m, 2H), 7.43 – 7.36 (m, 1H), 7.28 (d, *J* = 4.0 Hz, 2H), 4.94 (t, *J* = 3.8 Hz, 1H), 4.84 (dd, *J* = 13.2, 4.2 Hz, 1H), 3.88 (dd, *J* = 13.4, 3.5Hz, 1H), 2.06 – 1.98 (m, 3H), 1.91 – 1.81 (m, 6H), 1.73 – 1.64 (m, 6H); ^{13}C NMR (100 MHz, DMSO-*d*$_6$) *δ* 212.0, 156.4, 155.9, 135.5, 134.5, 134.3, 129.9, 129.4, 128.7, 128.2, 127.6, 126.6, 125.0, 47.7, 46.1, 42.2, 37.2, 36.3, 27.6; HRMS (ESI-TOF) (*m/z*) calculated $C_{27}H_{27}N_2O_3^+$ 427.2016, found 427.2004 $[M + H]^+$.

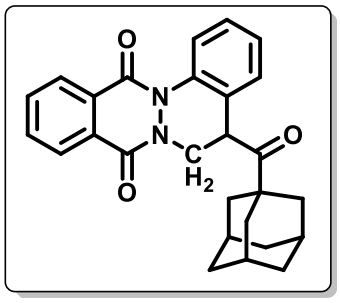

5-Benzoyl-5,6-dihydrophthalazino[2,3-*a*]cinnoline-8,13-dione-6,6-*d*$_2$ (50aa-*d*$_2$). White solid, 32 mg (61% yield); ^{1}H NMR (400 MHz, DMSO-*d*$_6$) *δ* 8.34 – 8.29 (m, 1H), 8.24 – 8.18 (m, 1H), 8.12 – 8.05 (m, 2H), 8.03 – 7.95 (m, 3H), 7.72 – 7.65 (m, 1H), 7.55 (t, *J* = 7.7 Hz, 2H), 7.50 (dd, *J* = 7.7, 1.5 Hz, 1H), 7.43 – 7.36 (m, 1H), 7.32 – 7.26 (m, 1H), 5.47 (s, 1H); ^{13}C NMR (100 MHz, DMSO-*d*$_6$) *δ* 197.5, 156.3, 156.2, 135.5, 135.3, 134.7, 134.4, 134.3, 129.5, 129.2, 129.1, 128.6, 128.2, 128.0, 127.6, 127.3, 126.6, 125.1, 46.1, 44.4; HRMS (ESI-TOF) (*m/z*) calculated $C_{23}H_{15}D_2N_2O_3^+$ 371.1359, found 371.1357 $[M + H]^+$.

4.4 Single Crystal X-ray Diffraction Studies

After screening the crystals of **48ap** and **49ab** under a microscope, one suitable crystal in each case was mounted in a nylon loop attached to a goniometer head. Initial crystal evaluation and data collection were performed on a Kappa APEX II diffractometer equipped with a CCD detector (with the crystal-to-detector distance fixed at 60 mm) and sealed-tube monochromated MoKα radiation using the program APEX2.[69] Data were integrated, reflections were fitted and values of F^2 and $\sigma(F^2)$ for each reflection were obtained by using the program SAINT.[69] Data were also corrected for Lorentz and polarization effects. The subroutine XPREP[69] was used for the processing of data that included determination of space group, application of an absorption correction (SADABS),[69] merging of data, and generation of files necessary for solution and refinement. The crystal structure was solved and refined using SHELX 97.[70] In each case, the space group was chosen based on systematic absences and confirmed by the successful refinement of the structure. Positions of most of the non-hydrogen atoms were obtained from a direct methods solution. Several full-matrix least-squares/difference Fourier cycles were performed, locating the remainder of the non-hydrogen atoms. All non-hydrogen atoms were refined with anisotropic displacement parameters. All hydrogen atoms were placed in ideal positions and refined as riding atoms with individual isotropic displacement parameters. In case of **48ap**, there were two independent molecules in the asymmetric unit. For **49ab**, the *o*-tolyl group was found to be disordered and modelled over two positions. All figures were drawn using MERCURY V 3.0[71] and Platon.[72]

4.4.1 Crystal data for 48ap (CCDC No. 1937966). $C_{20}H_{20}N_2O_3$, M_r = 336.38 g/mol, monoclinic, space group $P2_1$, a = 9.8634(4) Å, b = 14.7615(6) Å, c = 13.0625(4) Å, α = 90°, β = 108.155(2)°, γ = 90°, V = 1807.2(1) $Å^3$, Z = 4, D_{calcd} = 1.236 g/cm^3, T = 296(2) K; Full matrix least-square on F^2; R_1 = 0.0509, wR_2 = 0.1378 for 4527 observed reflections [I > 2σ(I)] and R_1 = 0.0654, wR_2 = 0.1605 for all 5494 reflections; GOF = 1.082.

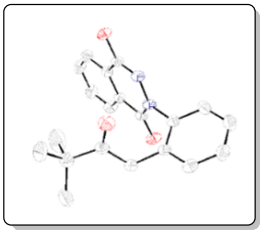

4.4.2 Crystal data for 49ab (CCDC No. 1937967). $C_{23}H_{16}N_2O_2$, Mr = 352.38 g/mol, monoclinic, space group $P2_1/n$, a = 10.698(2) Å, b = 15.404(3) Å, c = 10.784(2) Å, α = 90°, β = 92.007(12)°, γ = 90°, V = 1776(1) $Å^3$, Z = 4, D_{calcd} = 1.318 g/cm^3, T = 296(2) K; Full matrix least-square on F^2; R_1 = 0.0523, wR_2 = 0.1392 for 2117 observed reflections [I > 2σ(I)] and R_1 = 0.0695, wR_2 = 0.1499 for all 2802 reflections; GOF = 1.061.

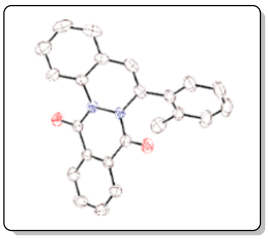

4.5 References

(1) Ruiz-Castillo, P.; Buchwald, S. L. *Chemical Reviews* **2016**, *116*, 12564-12649.

(2) Wu, X.-F. *Transition Metal-Catalyzed Heterocycle Synthesis via C-H Activation*; John Wiley & Sons, **2015**.

(3) Yi, H.; Zhang, G.; Wang, H.; Huang, Z.; Wang, J.; Singh, A. K.; Lei, A. *Chemical Reviews* **2017**, *117*, 9016-9085.

(4) Sambiagio, C.; Schönbauer, D.; Blieck, R.; Dao-Huy, T.; Pototschnig, G.; Schaaf, P.; Wiesinger, T.; Zia, M. F.; Wencel-Delord, J.; Besset, T. *Chemical Society Reviews* **2018**, *47*, 6603-6743.

(5) Rao, W.-H.; Shi, B.-F. *Organic Chemistry Frontiers* **2016**, *3*, 1028-1047.

(6) Zhao, B.; Shi, Z.; Yuan, Y. *The Chemical Record* **2016**, *16*, 886-896.

(7) Colby, D. A.; Tsai, A. S.; Bergman, R. G.; Ellman, J. A. *Accounts of Chemical Research* **2012**, *45*, 814-825.

(8) Colby, D. A.; Bergman, R. G.; Ellman, J. A. *Chemical Reviews* **2010**, *110*, 624-655.

(9) Ackermann, L. *Chemical Reviews* **2011**, *111*, 1315-1345.

(10) Kapdi, A. R.; Maiti, D. *Strategies for Palladium-Catalyzed Non-directed and Directed C-H Bond Functionalization*; *Elsevier*, **2017**.

(11) Gandeepan, P.; Ackermann, L. *Chem* **2018**, *4*, 199-222.

(12) Zhang, M.; Zhang, Y.; Jie, X.; Zhao, H.; Li, G.; Su, W. *Organic Chemistry Frontiers* **2014**, *1*, 843-895.

(13) Yang, J. *Organic & Biomolecular Chemistry* **2015**, *13*, 1930-1941.

(14) Gramage-Doria, R.; Bruneau, C. *Coordination Chemistry Reviews* **2021**, *428*, 213602.

(15) Khan, F. F.; Sinha, S. K.; Lahiri, G. K.; Maiti, D. *Chemistry–An Asian Journal* **2018**, *13*, 2243-2256.

(16) Singh, K. S. *Catalysts* **2019**, *9*, 173.

(17) Manikandan, R.; Jeganmohan, M. *Organic & Biomolecular Chemistry* **2015**, *13*, 10420-10436.

(18) Dhawa, U.; Zell, D.; Yin, R.; Okumura, S.; Murakami, M.; Ackermann, L. *Journal of Catalysis* **2018**, *364*, 14-18.

(19) Zhu, H.; Zhao, S.; Zhou, Y.; Li, C.; Liu, H. *Catalysts* **2020**, *10*, 1253.

(20) Arockiam, P. B.; Bruneau, C.; Dixneuf, P. H. *Chemical Reviews* **2012**, *112*, 5879-5918.

(21) Wu, X.; Sun, S.; Yu, J.-T.; Cheng, J. *Synlett* **2019**, *30*, 21-29.

(22) Kumar, A.; Sherikar, M. S.; Hanchate, V.; Prabhu, K. R. *Tetrahedron* **2021**, *101*, 132478.

(23) Quintana, J.; Torres, M.; Serratosa, F. *Tetrahedron* **1973**, *29*, 2065-2076.

(24) Baldwin, J. E.; Adlington, R. M.; Godfrey, C. R.; Gollins, D. W.; Vaughan, J. G. *Journal of the Chemical Society, Chemical Communications* **1993**, 1434-1435.

(25) Mangion, I. K.; Nwamba, I. K.; Shevlin, M.; Huffman, M. A. *Organic Letters* **2009**, *11*, 3566-3569.

(26) Dias, R. M.; Burtoloso, A. C. *Organic Letters* **2016**, *18*, 3034-3037.

(27) Tian, Y.; Kong, X.-Q.; Niu, J.; Huang, Y.-B.; Wu, Z.-H.; Xu, B. *Tetrahedron Letters* **2020**, *61*, 151627.

(28) Li, H.; Wu, C.; Liu, H.; Wang, J. *The Journal of Organic Chemistry* **2019**, *84*, 13262-13275.

(29) Chen, Z.; Kong, X.; Xu, B. *ChemistrySelect* **2020**, *5*, 2465-2468.

(30) Fu, Y.; Wang, Z.; Zhang, Q.; Li, Z.; Liu, H.; Bi, X.; Wang, J. *RSC Advances* **2020**, *10*, 6351-6355.

(31) Wang, L.; Cao, W.; Mei, H.; Hu, L.; Feng, X. *Advanced Synthesis & Catalysis* **2018**, *360*, 4089-4093.

(32) Mishra, U. K.; Patel, K.; Ramasastry, S. *Organic Letters* **2018**, *21*, 175-179.

(33) Patel, K.; Mishra, U. K.; Mukhopadhyay, D.; Ramasastry, S. *Chemistry–An Asian Journal* **2019**, *14*, 4568-4571.

(34) Ingold, C. K.; Jessop, J. A. *Journal of the Chemical Society (Resumed)* **1930**, 713-718.

(35) Corey, E.; Chaykovsky, M. *Journal of the American Chemical Society* **1964**, *86*, 1640-1641.

(36) Vaitla, J.; Bayer, A. *Synthesis* **2019**, *51*, 612-628.

(37) Li, A.-H.; Dai, L.-X.; Aggarwal, V. K. *Chemical Reviews* **1997**, *97*, 2341-2372.

(38) Corey, E.; Chaykovsky, M. *Journal of the American Chemical Society* **1965**, *87*, 1353-1364.

(39) Helmkamp, G. K., *Sulfur Ylides. Emerging Synthetic Intermediates* (Trost, Barry M.; Melvn, Lawrence S.). ACS Publications: **1976**.

(40) Barday, M.; Janot, C.; Halcovitch, N. R.; Muir, J.; Aïssa, C. *Angewandte Chemie* **2017**, *129*, 13297-13301.

(41) Neuhaus, J. D.; Bauer, A.; Pinto, A.; Maulide, N. *Angewandte Chemie International Edition* **2018**, *57*, 16215-16218.

(42) Shi, X.; Wang, R.; Zeng, X.; Zhang, Y.; Hu, H.; Xie, C.; Wang, M. *Advanced Synthesis & Catalysis* **2018**, *360*, 4049-4053.

(43) Xie, H.; Lan, J.; Gui, J.; Chen, F.; Jiang, H.; Zeng, W. *Advanced Synthesis & Catalysis* **2018**, *360*, 3534-3543.

(44) Oh, H.; Han, S.; Pandey, A. K.; Han, S. H.; Mishra, N. K.; Kim, S.; Chun, R.; Kim, H. S.; Park, J.; Kim, I. S. *The Journal of Organic Chemistry* **2018**, *83*, 4070-4077.

(45) Zhu, J.; Sun, S.; Cheng, J. *Tetrahedron Letters* **2018**, *59*, 2284-2287.

(46) Wu, C.; Zhou, J.; He, G.; Li, H.; Yang, Q.; Wang, R.; Zhou, Y.; Liu, H. *Organic Chemistry Frontiers* **2019**, *6*, 1183-1188.

(47) Wang, Z.; Xu, H. *Tetrahedron Letters* **2019**, *60*, 664-667.

(48) Xu, G. D.; Huang, K. L.; Huang, Z. Z. *Advanced Synthesis & Catalysis* **2019**, *361*, 3318-3323.

(49) Chen, P.; Nan, J.; Hu, Y.; Ma, Q.; Ma, Y. *Organic Letters* **2019**, *21*, 4812-4815.

(50) Yu, J.; Wen, S.; Ba, D.; Lv, W.; Chen, Y.; Cheng, G. *Organic Letters* **2019**, *21*, 6366-6369.

(51) Kona, C. N.; Nishii, Y.; Miura, M. *Organic Letters* **2020**, *22*, 4806-4811.

(52) Chen, M.; Meng, H.; Yang, F.; Wang, Y.; Chen, C.; Zhu, B. *Organic & Biomolecular Chemistry* **2021**, *19*, 4268-4271.

(53) Xu, Y.; Yang, X.; Zhou, X.; Kong, L.; Li, X. *Organic Letters* **2017**, *19*, 4307-4310.

(54) Yu, Y.; Wu, Q.; Liu, D.; Yu, L.; Tan, Z.; Zhu, G. *Organic Chemistry Frontiers* **2019**, *6*, 3868-3873.

(55) Zhou, M. D.; Peng, Z.; Wang, H.; Wang, Z. H.; Hao, D. J.; Li, L. *Advanced Synthesis & Catalysis* **2019**, *361*, 5191-5197.

(56) Chen, X.; Wang, M.; Zhang, X.; Fan, X. *Organic Letters* **2019**, *21*, 2541-2545.

(57) Jia, Q.; Kong, L.; Li, X. *Organic Chemistry Frontiers* **2019**, *6*, 741-745.

(58) Lou, J.; Wang, Q.; Zhou, Y.-G.; Yu, Z. *Organic Letters* **2019**, *21*, 9217-9222.

(59) Wang, P.; Xu, Y.; Sun, J.; Li, X. *Organic Letters* **2019**, *21*, 8459-8463.

(60) Hanchate, V.; Kumar, A.; Prabhu, K. R. *Organic Letters* **2019**, *21*, 8424-8428.

(61) Wu, X.; Xiao, Y.; Sun, S.; Yu, J.-T.; Cheng, J. *Organic Letters* **2019**, *21*, 6653-6657.

(62) Kommagalla, Y.; Ando, S.; Chatani, N. *Organic Letters* **2020**, *22*, 1375-1379.

(63) Shu, B.; Wang, X.-T.; Shen, Z.-X.; Che, T.; Zhong, M.; Song, J.-L.; Kang, H.-J.; Xie, H.; Zhang, L.; Zhang, S.-S. *Organic Chemistry Frontiers* **2020**, *7*, 1802-1808.

(64) Karishma, P.; Agarwal, D. S.; Laha, B.; Mandal, S. K.; Sakhuja, R. *Chemistry–An Asian Journal* **2019**, *14*, 4274-4288.

(65) Jiang, S.; Yang, Z.; Guo, Z.; Li, Y.; Chen, L.; Zhu, Z.; Chen, X. *Organic & Biomolecular Chemistry* **2019**, *17*, 7416-7424.

(66) Yang, P.; Xu, W.; Wang, R.; Zhang, M.; Xie, C.; Zeng, X.; Wang, M. *Organic Letters* **2019**, *21*, 3658-3662.

(67) Wu, X. F.; Natte, K. *Advanced Synthesis & Catalysis* **2016**, *358*, 336-352.

(68) Sun, K.; Wang, X.; Jiang, Y.; Lv, Y.; Zhang, L.; Xiao, B.; Li, D.; Zhu, Z.; Liu, L. *Chemistry–An Asian Journal* **2015**, *10*, 536-539.

(69) *APEX2*, *SADABS and SAINT*; Bruker AXS inc: Madison, WI, USA, **2008**.

(70) Sheldrick, G. M. *Acta Crystallographica Section C: Structural Chemistry* **2015**, *71*, 3-8.

(71) Macrae, C. F.; Bruno, I. J.; Chisholm, J. A.; Edgington, P. R.; McCabe, P.; Pidcock, E.; Rodriguez-Monge, L.; Taylor, R.; Streek, J.; Wood, P. A. *Journal of Applied Crystallography* **2008**, *41*, 466-470.

(72) Spek, A. L. *PLATON, Version 1.62*, University of Utrecht, **1999**.

CHAPTER 5

Ruthenium Catalyzed C-H Amidation and Carbocyclization of *N*-Aryl-2,3-dihydrophthalazine-1,4-diones with Isocyanates

5.1 Introduction

Amide bonds are ubiquitous in nature, and also accounts for their presence in more than 25% of known drugs as per Comprehensive Medicinal Chemistry (CMC) database (Figure 5.1.1). Their distinct role in synthetic materials and biologically active compounds makes the synthesis of amide-containing heterocyclic molecules one of the regularly performed reactions in organic synthesis.[1-5] In addition, amide linkages have been introduced as an essential component to synthetic drugs such as Procaine, Lidocaine and Tocainide to increase their metabolic stability. Amide linkage has been also known to impose degradable character, good thermal and mechanical characteristics to biodegradable poly (amide)s polymers.[6] Furthermore, amides have served as the reactive precursors and intermediates for synthetic manipulations.[7] Generally, acid activation as acyl halides, acyl azides, anhydrides or esters, followed by nucleophilic substitution by an appropriate amine are among the most common strategies employed for the construction of an amide bond. However, continued expedition towards developing newer amide bond forming strategies and direct amido group inserting reagents remain desirable.

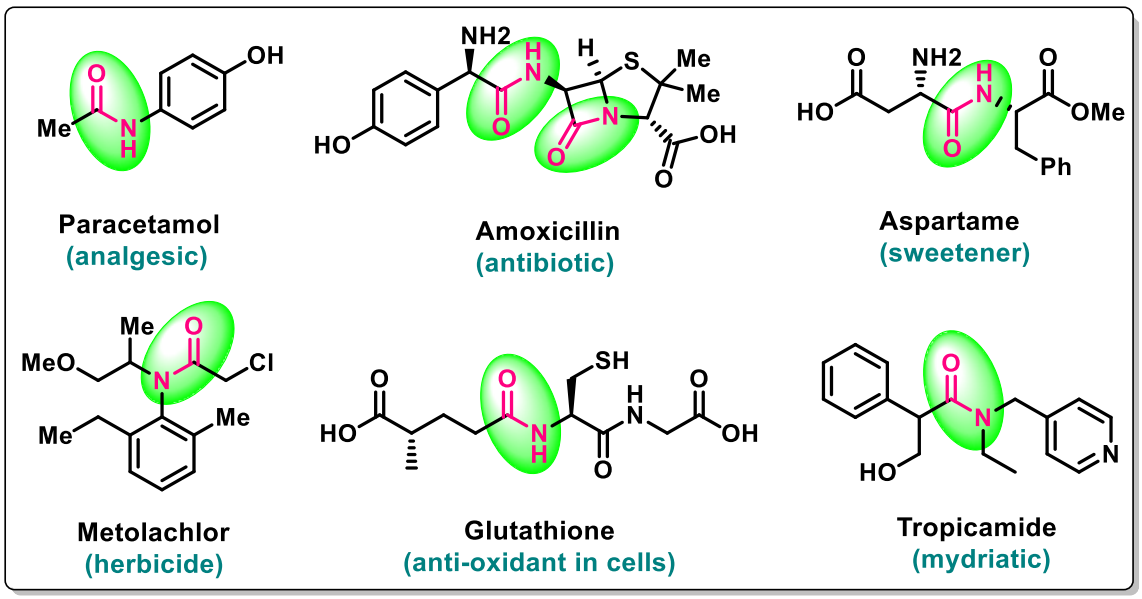

Figure 5.1.1 Selective examples of amide-containing drugs

In contrast, transition metal-catalyzed directing group-assisted inert C(sp^2)-H functionalization has pooled up powerful strategies into modern chemistry toolbox in the last decade.[8-14] Such strategies in conjunction with subsequent intramolecular C-C/C-N cyclizations have been successfully applied for the synthesis of unprecedented fused heterocycles in an atom-economical manner.[15-18] Of these, transient directing group-assisted carbonyl insertion strategies using different carbonyl

surrogates have gained particular interest.[19,20] For example, carbon monoxide (CO) has been used as a direct carbonyl source widely used for the cyclocarbonylation of different (hetero)arenes, employing different functionalities as directing groups under Pd,[21] Cu,[22-24] Ni,[25] Ru,[26,27] Rh,[28] and Co[29-31] catalysis. Due to requirement of high pressure equipment for handling toxic and flammable CO, other solid or liquid carbonyl surrogates that are capable of generating CO in a controlled manner such as nitromethane,[32] *N*,*N*-dimethylformamide (DMF),[33,34] azodicarboxylate (DIAD & DEAD),[35-37] benzene-1,3,5-triyl triformate (TFBen),[38,39] aldehydes[40,41] and Langlois reagent (CF_3SO_2Na)[42] have been subsequently optimized for the cyclocarbonylation of different substrates under metal-catalyzed conditions (Figure 5.1.2). Unfortunately, the thermal decomposition of some of these carbonyl surrogates such as nitromethane, DMF and DEAD to CO requires elevated temperatures and acidic conditions. Thus, greater anticipation exists for developing newer carbonyl surrogates with wider applicability of cyclocarbonylation on different aromatic/heteroaromatic frameworks.

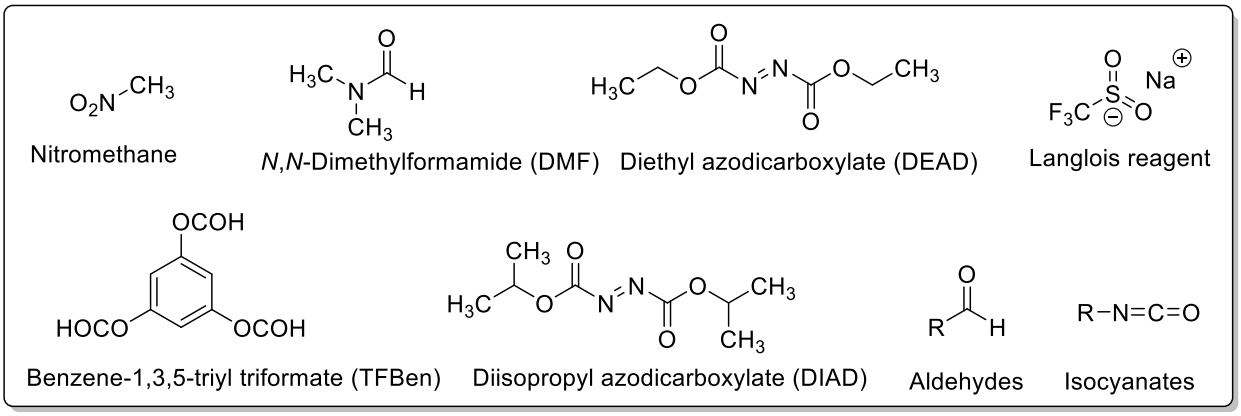

Figure 5.1.2 Selective examples of carbonyl surrogates

Interestingly, isocyanates are inexpensive commercially available reagents that readily undergo nucleophilic addition. They have proven valuable amidating agents for the aminocarbonylation of (hetero)arenes under Ru,[43,44] Re,[45] Rh,[46,47] Co[48] and Mn[49] catalysis. The coordination of isocyanates to metal centers has been established *via* η^2-C,N and η^2-C,O fashion, with the former being the most common binding mode (Figure 5.1.3).[50-52] Regardless of the binding mode, the coordination of isocyanate with the metal center changes its geometry, thus the deviation from linearity lowers its activation energy and enables its coupling with the nucleophilic counterpart.

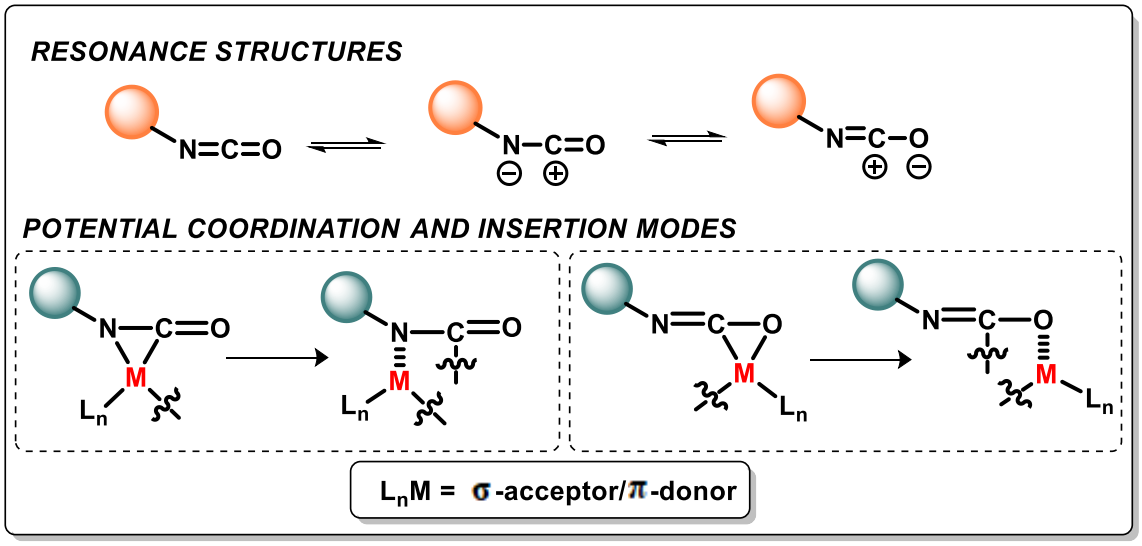

Figure 5.1.3 Possible modes of coordination of isocyanates to metal centres

In the early 2000s, Kuninobu and Takai have succeeded in the Re(I)-catalyzed intermolecular annulation of aromatic aldimines (**1**) with aryl isocyanates (**2**) to give phthalimidine (**3**) derivatives in quantitative yields. The reactions was proposed to proceed *via* a series of steps involving C–H bond activation, isocyanate insertion, intramolecular nucleophilic cyclization of the generated amido-rhenium species to the aldmines and reductive elimination (Scheme 5.1.1).[53]

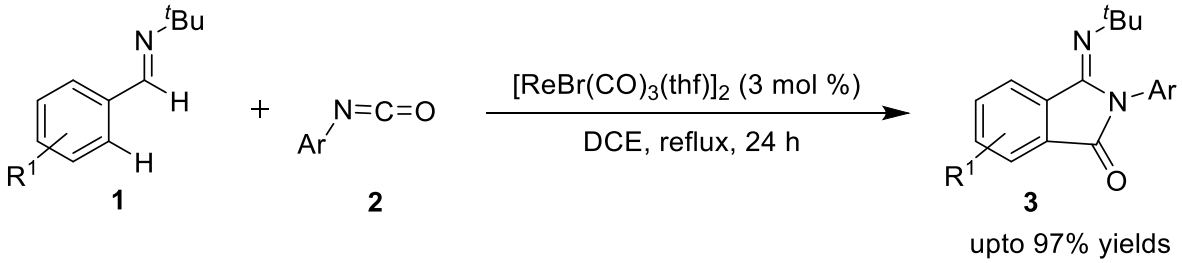

Scheme 5.1.1 Rhenium-catalyzed annulation of aldimines (**1**) with isocyanates (**2**)

Jamison *et al.* developed a synthetic protocol for the preparation of acrylamides (**6**) *via* Ni(0)-IPr mediated reaction of *α*-olefins (**4**) with isocyanates (**2**) (Scheme 5.1.2a). Furthermore, deprotection of *N*-*tert*-butyl amides was achieved by the acid treatment under reflux conditions to furnish primary amides in excellent yields.[54] Similarly, Murakami's group designed a new synthetic route for preparing 1,3,5-trisubstituted hydantoins (**8**) from acrylates (**5**) and isocyanates (**2**) using Nickel(0)/SIPr catalytic system. The mechanism was initiated by a one-pot *N*-substituted fumaramate formation, and its subsequent cyclization with another molecule of isocyanate (Scheme 5.1.2b).[55]

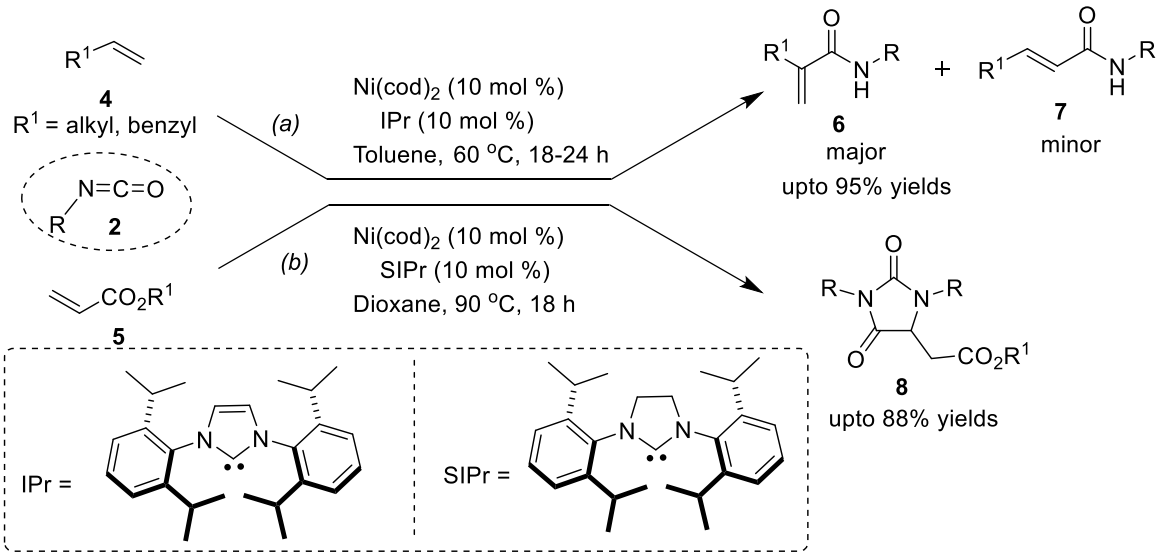

Scheme 5.1.2 Nickel-catalyzed functionalization/annulation of olefins (**4** & **5**) with isocyanates (**2**)

In 2011, Bergman and Ellman group reported a Rh(III)-catalyzed C-H bond amidation of anilide and enamide (**9**) with isocyanates (**2**) producing a broad range of anthranilamides and enamide amides (**10**), respectively (Scheme 5.1.3).[56]

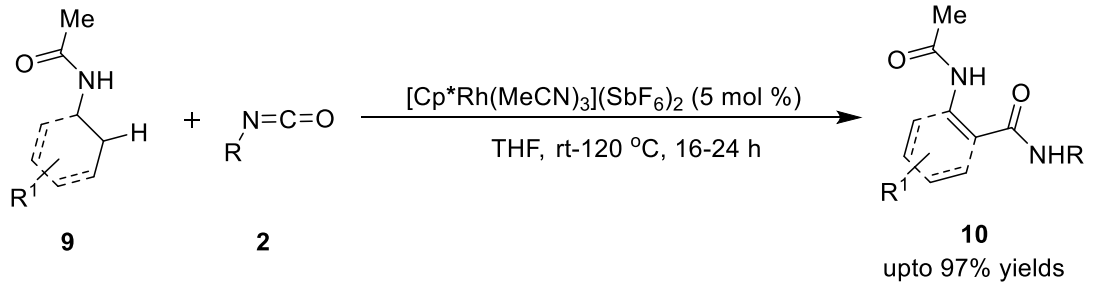

Scheme 5.1.3 Rhodium-catalyzed amidation of anilides and enamides (**9**) with isocyanates (**2**)

The following year, Cheng *et al.* described Ru(II)-catalyzed amidation of 2-aryl pyridines (**11**) with isocyanates (**2**) as an amidating partner using sodium acetate as an additive. A series of amidated derivatives (**12**) was reported in good to excellent yields (Scheme 5.1.4).[43]

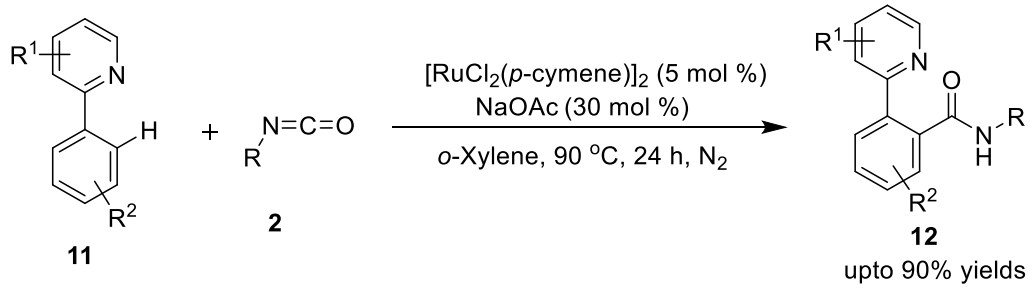

Scheme 5.1.4 Ru-catalyzed amidation of 2-arylpyridines (**11**) with isocyanates (**2**)

Furthermore, Ackermann's group employed a versatile Mn(I)-catalyst for the C-H aminocarbonylation of heteroarenes (**13**) suing aryl as well as alkyl isocyanates (**2**) with ample substrate scope in moderate-to-good yields. The mechanism demonstrated an initial organometallic C-H manganesation step that upon rate-determining migratory insertion followed by deprotonation produced the amidated product (**14**) (Scheme 5.1.5).[49]

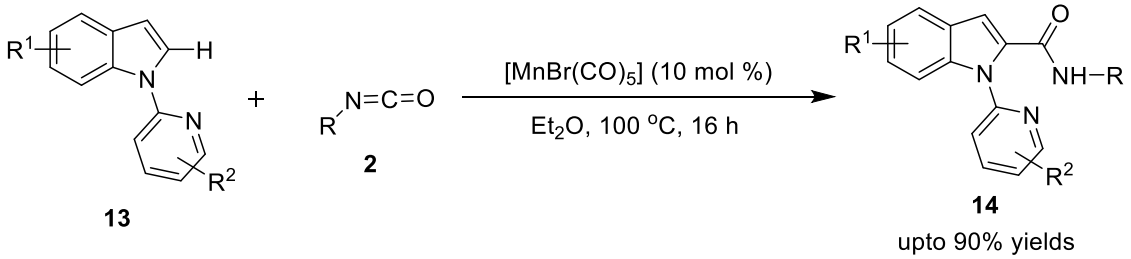

Scheme 5.1.5 Manganese-catalyzed aminocarbonylation of heteroarenes (**13**) with isocyanates (**2**)

The same group also accomplished the synthesis of phthalimide derivatives (**16** & **18**) through Ru(II)-catalyzed reaction between easily accessible benzamides (**15**) and heteroaromatic amides (**17**) with isocyanates (**2**). The reaction mechanism includes insertion of cycloruthenated species into the C-Het bond of isocyanate affording the target compounds in moderate-to-good yields (Scheme 5.1.6).[57]

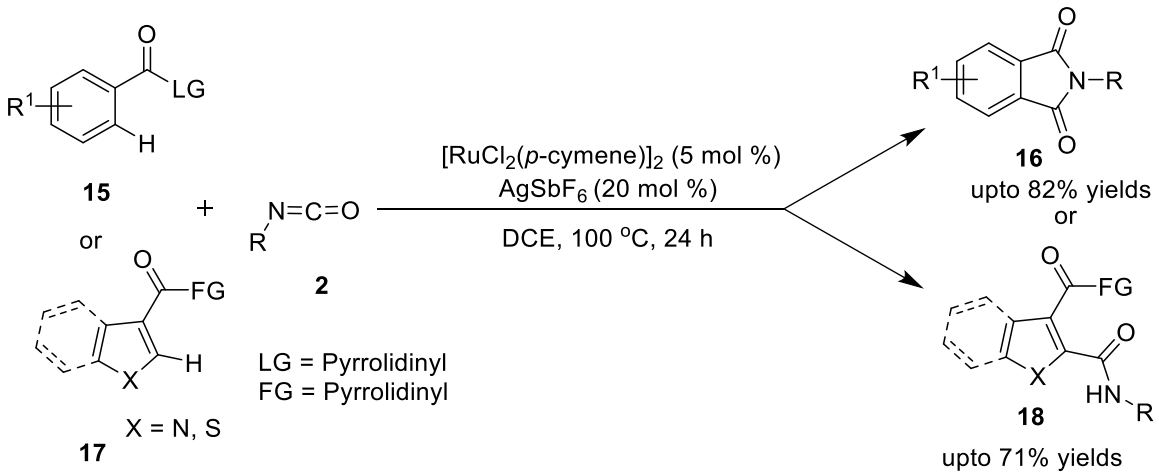

Scheme 5.1.6 Ruthenium-catalyzed reaction of benzamides (**15**) and heteroaromatic amides (**17**) with isocyanates (**2**)

Likewise, Ellman documented an elegant Co(III)-catalyzed strategy for the amidation of N-arylpyrazoles (**19**) with isocyantes (**2**). The presented work was equally effective with a variety of electron-rich and electron-deficient isocyanates, furnishing the target molecules (**20**) in excellent yields (Scheme 5.1.7).[48]

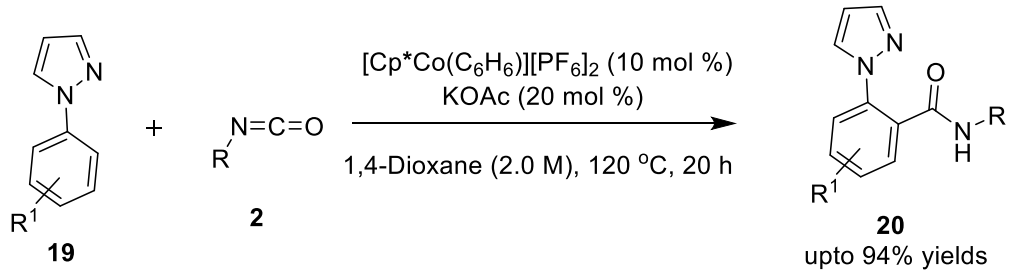

Scheme 5.1.7 Cobalt-catalyzed amidation of *N*-arylpyrazoles (**19**) with isocyantes (**2**)

Later, Kim *et al.* described a facile and efficient approach for the C2-amidation of indoles (**21**) with isocyanates (**2**) under Rh(III)/$AgSbF_6$ catalysis, with excellent chemoselectivity and good functional group tolerance (Scheme 5.1.8).[47]

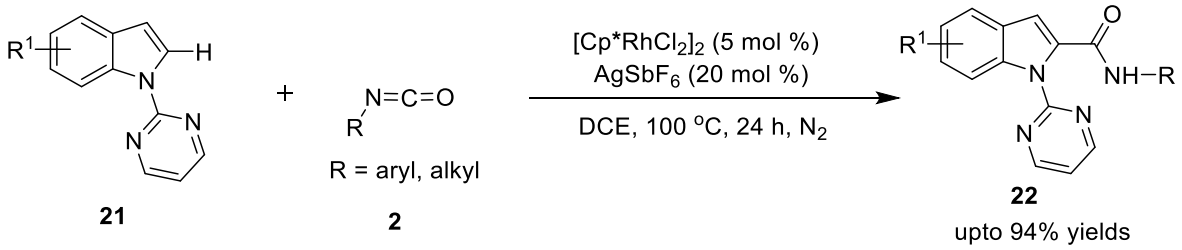

Scheme 5.1.8 Rhodium-catalyzed C2-amidation of indoles (**21**) with isocyanates (**2)**

In 2015, the same group successfully achieved the Rh(III)-catalyzed direct C-H *ortho*-amidation and *N*-sulfonyl amidation of azobenzenes (**23**) with aryl and alkyl isocyanates (**2**) and arylsulfonyl isocyanates, respectively (Scheme 5.1.9a).[46] Similarly, Wang and coworkers performed high chemo- and regioselective approach for the aminocarbonylation of azoarenes (**23**) with isocyanates (**2**) by the catalytic use of rhenium and sodium acetate in toluene in good yields (Scheme 5.1.9b).[45]

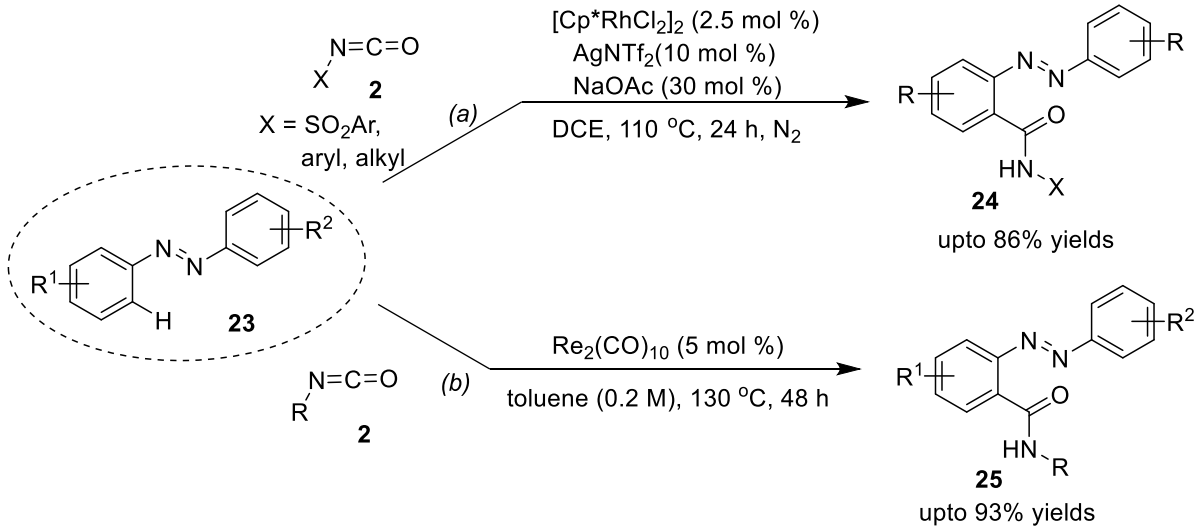

Scheme 5.1.9 Rhodium/Rhenium catalyzed *o*-amidation of azoarenes (**23**) with isocyanates (**2**)

Li and coworkers described the synthesis of *N*-substituted phthalimidines (**27**) from benzoic acids (**26**) and isocyanates (**2**) under Rh(III) catalysis. The reaction proceeded through a cascade rhodium-catalyzed C-H amidation followed by intramolecular cyclization. The developed protocol was examined with different substituted benzoic acids and isocyanates, delivering aminocarbonylated products (**27**) in moderate-to-good yields (Scheme 5.1.10a).[58] Subsequently, the same group disclosed another approach by tuning the reaction conditions to furnish a series of *N*-arylbenzamides (**28**) from the same coupling partners in the presence of Rh(III)/Cu_2O/K_2HPO_4 catalytic system. The mechanism was proposed to involve a series of steps including K_2HPO_4-mediated rhodacycle formation→*ortho*-C-H bond amidation→decarboxylation. (Scheme 5.1.10b).[59]

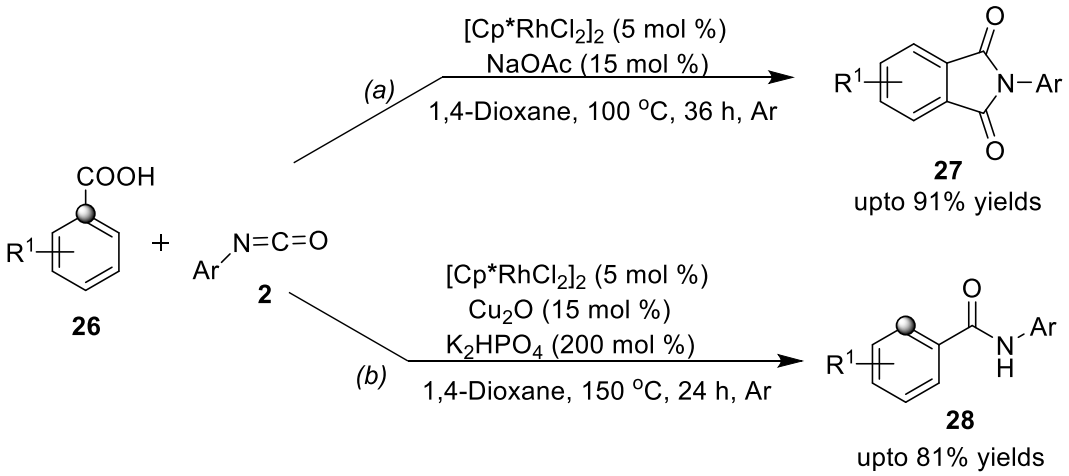

Scheme 5.1.10 Rhodium-catalyzed aminocarbonylation of benzoic acids (**26**) with isocyanates (**2**)

Our group reported a convergent method for the direct *ortho*-amidation of 2-arylimidazo- [1,2-*a*]pyridines (**29**) with aryl isocyanates (**2**) under Ru(II)-catalyzed conditions using KPF_6 as an additive in DCE. The developed strategy facilitated great flexibility of the substituted pattern on isocyanates and 2-arylimidazo-heterocycles and afforded the desired amidated products (**30**) in good-to-excellent yields (Scheme 5.1.11).[44]

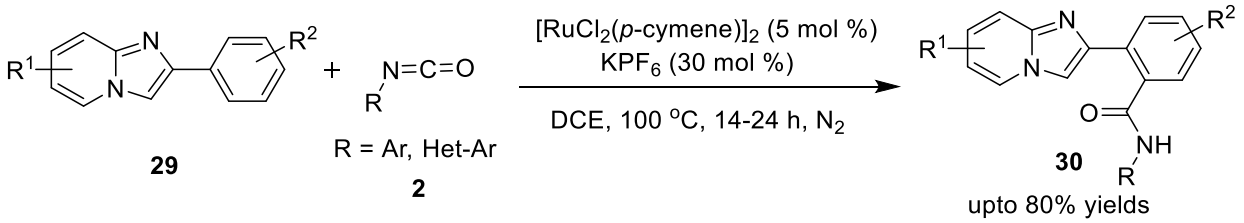

Scheme 5.1.11 Ruthenium-catalyzed amidation of 2-arylimidazo[1,2-*a*]pyridines (**29**) with isocyanates (**2**)

Copper-catalyzed borylative carboxamidation reaction of vinylarenes (**31**) with isocyanates (**2**) has been developed by Mazet's group, producing *α*-chiral amides (**32**) with high stereospecificity. The reaction was adequately explored with a broad range of substituted vinylarenes and isocyanates, leading to corresponding amidated products in appreciable yields (Scheme 5.1.12).[60]

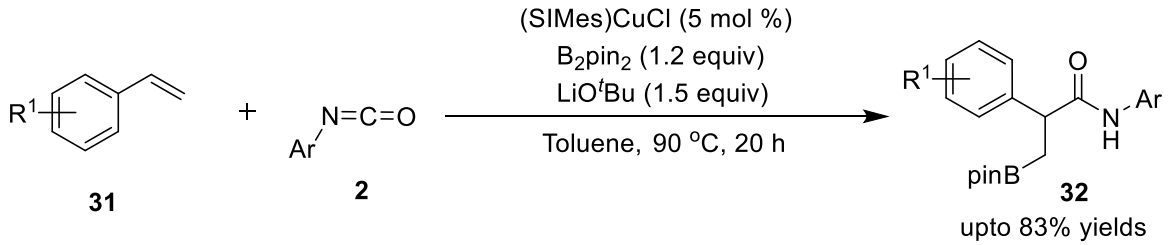

Scheme 5.1.12 Copper-catalyzed carboxamidation of vinylarenes (**31**) with isocyanates (**2**)

Recently, Zhao and Shi proposed a novel Ru(II)-catalyzed carbonylation of oxalyl amide-protected benzylamines (**33**) with isocyanates (**2**). The reaction showcased a wide range of substituent tolerance with various benzylamines providing a gallery of carbonylated products (**34**) in moderate-to-excellent yields (Scheme 5.1.13).[61]

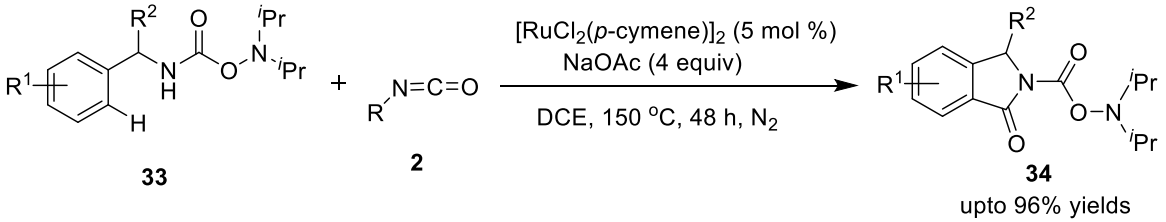

Scheme 5.1.13 Ruthenium-catalyzed carbonylation of *N*-protected benzylamines (**33**) with isocyanates (**2**)

Moreover, transition metal-catalyzed strategies for the synthesis of indazolo-phthalazines and other related fused phthalazines have received considerable attention in recent years due to their applications as an anti-inflammatory,[62] antitumor,[63] antibacterial[64] agents (Figure 5.1.4).

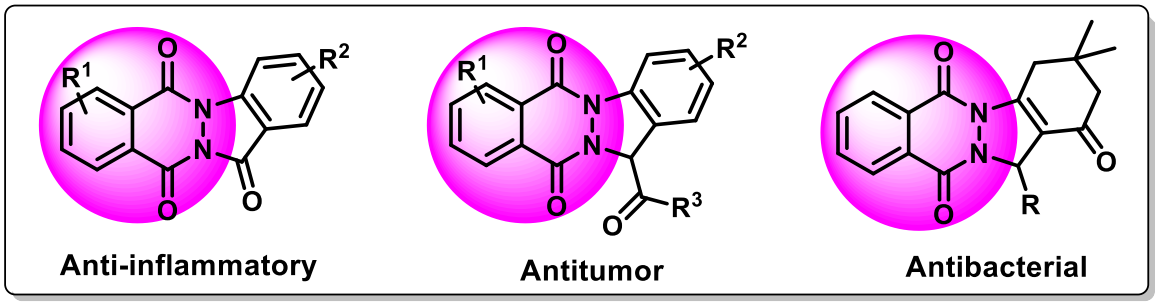

Figure 5.1.4 Selective examples of bioactive indazolo-phthalazines

Inspired by divergent chemical reactivities of isocyanates as amide-introducing reagent and a carbonyl surrogate, and the valuable medicinal importance of indazolo-fused phthalazines, we developed efficient strategies to synthesize amidated *N*-aryl-2,3-dihydrophthalazine-1,4-diones and indazolo[1,2-*b*]phthalazine-triones as a potential pharmaceutical lead (Scheme 5.1.14).[65]

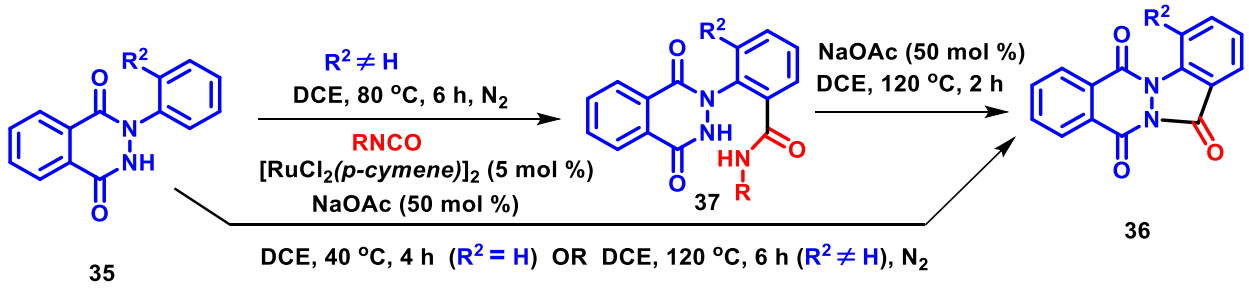

Scheme 5.1.14 Ruthenium-catalyzed carbocyclization and *o*-amidation of *N*-aryl-2,3-dihydrophthalazine-1,4-diones (**35**) using isocyanates (**2**)

5.2 Results and Discussion

At the outset of the proposed work, we commenced optimizing the reaction conditions for the coupling between *N*-phenyl-2,3-dihydrophthalazine-1,4-dione (**35a**) and phenyl isocyanate (**2a**) as model substrates, under ruthenium catalysis (Table 5.2.1). Initially, the reaction did not proceed using $RuCl_3 \cdot xH_2O$ as a catalyst, in absence or presence of additives in DCE at varied range of temperatures (Table 5.2.1, entries 1-4). However, replacing $RuCl_3 \cdot xH_2O$ with $[RuCl_2(p\text{-cymene})]_2$ in combination with KPF_6 promoted the coupling between **35a** and **2a** at room temperature to afford 28% of cyclocarbonylative product (**36aa**) after 8 h (Table 5.2.1, entry 5). The structure of **36aa** was unambiguously confirmed by its detailed spectroscopic analysis. Substitution of KPF_6 with $AgSbF_6$ and NaOAc afforded **36aa** in 46% and 53% yields, respectively (Table 5.2.1, entries 6-7). To our delight, the reactivity between the model substrates significantly increased by using 50 mol % of NaOAc in DCE at 40 °C for 4 h, furnishing **36aa** in 87% yield (Table 5.2.1, entry 8). Unfortunately, reducing the catalyst loading to 2.5 mol % had a detrimental effect, while no considerable increment in the yield of **36aa** was observed by further increasing the catalyst/additive loading (Table 5.2.1, entries 9-11). The use of other acetate additives (CsOAc and KOAc) displayed no positive effect, resulting in lower yields of **36aa** (Table 5.2.1, entries 12-13). Finally, solvent screening studies revealed DCM and toluene to be also suitable reaction media for this transformation, albeit producing **36aa** in slightly inferior yields, whereas acetonitrile (ACN) and tetrahydrofuran (THF) were found be less desirable (Table 5.2.1, entries 14-17). On

the other hand, dioxane, ethanol (EtOH), *N*,*N*-dimethylformamide (DMF), dimethylsulfoxide (DMSO) and dimethylacetamide (DMA) were completely unfavorable for this transformation (Table 5.2.1, entries 18-22).

Table 5.2.1 Selected Optimization[a] of Reaction Conditions for the Synthesis of **36aa**

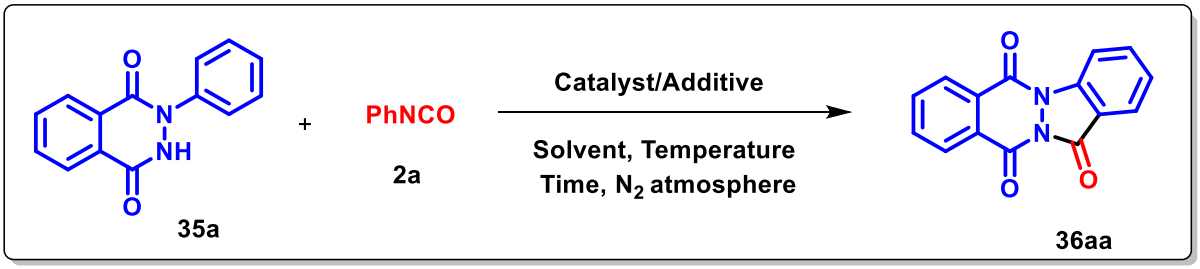

Entry No.	Catalyst (mol %)	Additive (mol %)	Solvent	Temp. (°C)	Yields (%)[b] **36aa**
1.	$RuCl_3 \cdot xH_2O$ (5)	-	DCE	25-80[c]	-
2.	$RuCl_3 \cdot xH_2O$ (5)	$AgSbF_6$ (20)	DCE	25-80[c]	-
3.	$RuCl_3 \cdot xH_2O$ (5)	KPF_6 (20)	DCE	25-80[c]	-
4.	$RuCl_3 \cdot xH_2O$ (5)	NaOAc (20)	DCE	25-80[c]	-
5.	$[RuCl_2(p\text{-cymene})]_2$ (5)	KPF_6 (20)	DCE	25[c]	28
6.	$[RuCl_2(p\text{-cymene})]_2$ (5)	$AgSbF_6$ (20)	DCE	25[c]	46
7.	$[RuCl_2(p\text{-cymene})]_2$ (5)	NaOAc (20)	DCE	25[c]	53
8.	$[RuCl_2(p\text{-cymene})]_2$ (5)	NaOAc (50)	DCE	40	87
9.	$[RuCl_2(p\text{-cymene})]_2$ (2.5)	NaOAc (50)	DCE	40	72
10.	$[RuCl_2(p\text{-cymene})]_2$ (10)	NaOAc (50)	DCE	40	86
11.	$[RuCl_2(p\text{-cymene})]_2$ (5)	NaOAc (100)	DCE	40	88
12.	$[RuCl_2(p\text{-cymene})]_2$ (5)	CsOAc (50)	DCE	40	73
13.	$[RuCl_2(p\text{-cymene})]_2$ (5)	KOAc (50)	DCE	40	70
14.	$[RuCl_2(p\text{-cymene})]_2$ (5)	NaOAc (50)	DCM	40	81
15.	$[RuCl_2(p\text{-cymene})]_2$ (5)	NaOAc (50)	Toluene	40	79
16.	$[RuCl_2(p\text{-cymene})]_2$ (5)	NaOAc (50)	ACN	40	46
17.	$[RuCl_2(p\text{-cymene})]_2$ (5)	NaOAc (50)	THF	40	44
18.	$[RuCl_2(p\text{-cymene})]_2$ (5)	NaOAc (50)	Dioxane	40	<10
19.	$[RuCl_2(p\text{-cymene})]_2$ (5)	NaOAc (50)	EtOH	40	-
20.	$[RuCl_2(p\text{-cymene})]_2$ (5)	NaOAc (50)	DMF	40	-
21.	$[RuCl_2(p\text{-cymene})]_2$ (5)	NaOAc (50)	DMSO	40	-
22.	$[RuCl_2(p\text{-cymene})]_2$ (5)	NaOAc (50)	DMA	40	-

[a]Reaction conditions: The reactions were carried out with **35a** (0.20 mmol) and **2a** (0.31 mmol) in the presence of catalyst/additive (as indicated in the table) in sealed tube in 3 mL of solvent at specified temperature for 4 h under N_2 atmosphere. [b]Isolated yields. [c]Reaction time = 8 h.

With the optimal reaction conditions established, we investigated the scope of this one-pot carbocyclization protocol on a variety of *N*-aryl-2,3-dihydrophthalazine-1,4-diones (substrates: **35b-y**) using phenyl isocyanate (**2a**) as a carbonyl source (Scheme 5.2.1). The *meta* and *para*

substituted *N*-aryl-2,3-dihydrophthalazine-1,4-diones possessing electron-donating (substrates: **35b-c**) and electron-withdrawing substituents (substrates: **35d-h**) on aryl moiety were readily converted to their corresponding carbocyclized products (**36ba-ha**) in 72-93% yields under optimized conditions, while *ortho*-substituted *N*-aryl-2,3-dihydrophthalazine-1,4-diones (substrates: **35i-k**) underwent carbocyclization in DCE at 120 °C for 6 h to furnish the desired tetracyclic products (**36ia-ka**) in 50-94% yields.

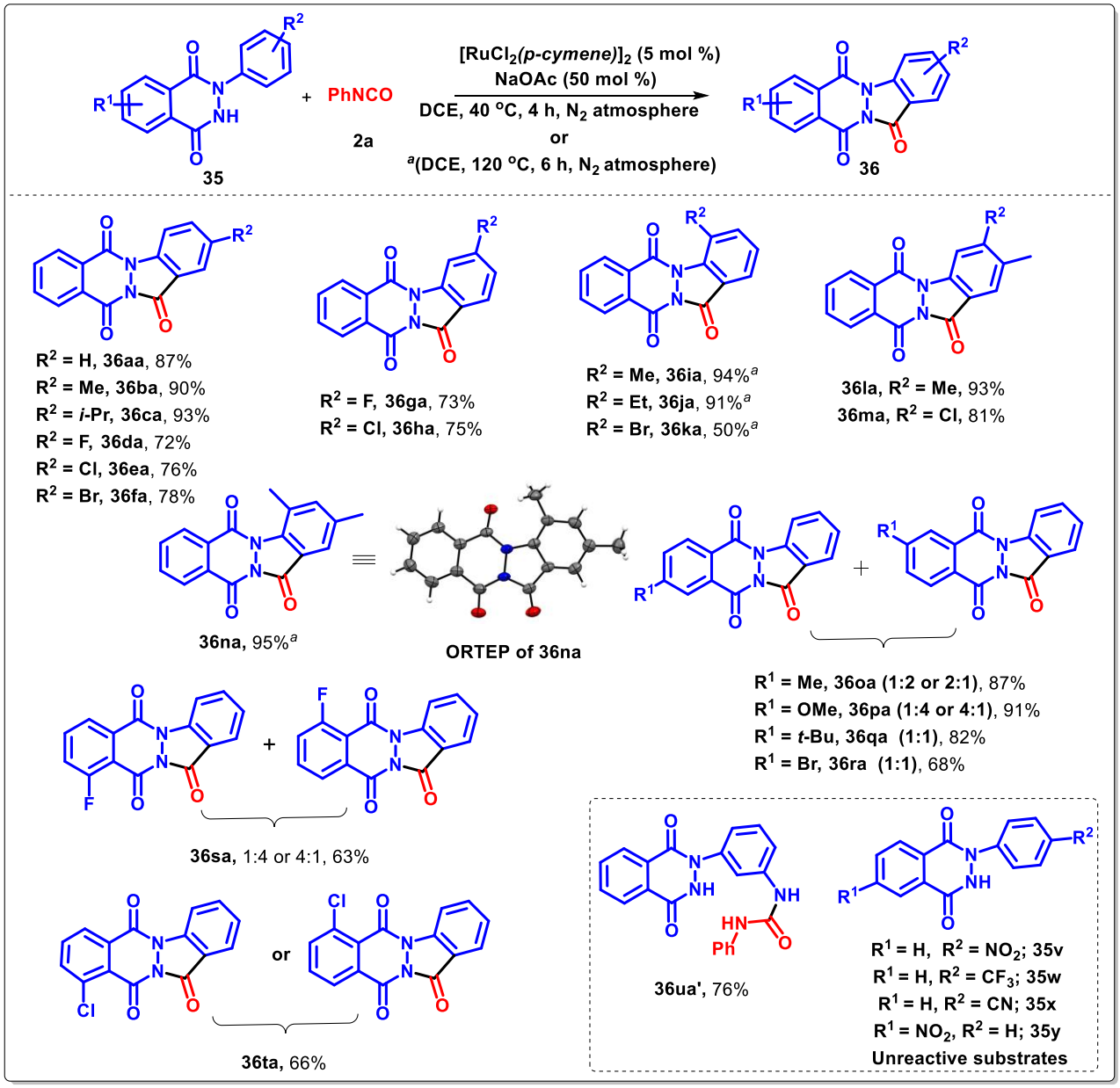

Scheme 5.2.1 Substrate scope of 2-arylphthalazine-1,4-diones

Additionally, the disubstituted *N*-aryl-2,3-dihydrophthalazine-1,4-diones (substrates: **35l-m**) were well tolerated to provide a smooth transformation to their corresponding carbonyl inserted products (**36la-ma**) in 81-93% yields, while, 2-(2,4-dimethylphenyl)-2,3-dihyrophthalazine-1,4-dione (substrate: **35n**) produced corresponding carbocyclized product (**36na**) in 95% yield, only after heating at 120 ^{o}C in DCE for 6 h. For variedly decorated electron-donating and -withdrawing substitutions on phthalazine moiety (substrates: **35o-t**), smooth transformations were observed to access good-to-excellent yields of the desired products (**36oa-ta**). Of these, the products (**36oa-sa**) were obtained as mixtures of two regioisomers in varying ratio, as their starting substrates (substrates: **35o-s**) themselves were prepared as an inseparable regioisomeric mixture. For example, inseparable mixtures of 6/7-methyl-, 6/7-methoxy-, 6/7-*t*-butyl, 6/7-bromo-, 5/8-fluoro *N*-phenyl-2,3-dihydrophthalazine-1,4-diones (**35o-s**) were obtained by standard coupling reaction between phenylhydrazine with 5-methyl-, 5-methoxy-, 5-*t*-butyl, 5-bromo-, 4-fluoro-phthalic anhydrides, respectively. In disparity, we could successfully isolate **36ta** as a single regioisomer in 66% yield by performing the reaction of 5/8-chloro-2-phenyl-2,3-dihydrophthalazine-1,4-dione (substrate: **35t**) with **2a** under standard conditions. It is worth mentioning that in all the above transformations, electron-rich substrates displayed higher reactivity over electron-deficient substrates, irrespective of their positions. Notably, attempts to achieve carbocyclization on 2-(3-aminophenyl)-2,3-dihydrophthalalazine-1,4-diones (substrate: **35u**) with **2a** under standard conditions afforded *N*-phenylurea derivative (**36ua**′) in 76% yield (Scheme 5.2.1), while nitro, trifluoromethyl or cyano substitutions on arylphthalazine moieties (substrates, **35v-y**) failed to react with **2a** under standard conditions. We envisioned that the presence of such electron-withdrawing substituents on the arylphthalazine moieties will disfavour the nucleophilic attack of **35** on the ruthenium metal ion, thereby suggesting the possibility of a S_EAr pathway to be involved in the reaction. The representative ^{1}H NMR and ^{13}C NMR spectra of carbocyclized product **36aa** are shown in Figure 5.2.1 and Figure 5.2.2, respectively. As a representative example, single crystals of **36na** were grown in chloroform to determine its structure. An ORTEP diagram of **36na** (CCDC 2023522) is given in Scheme 5.2.1.

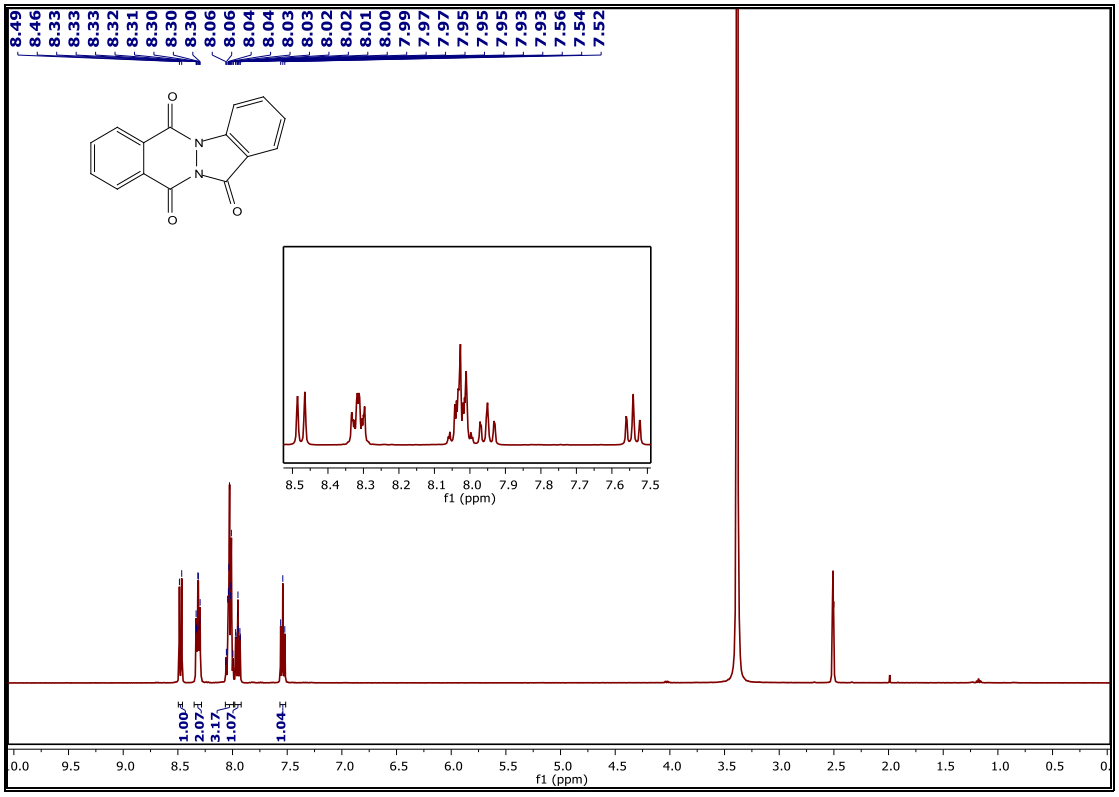

Figure 5.2.1 ^{1}H NMR spectra of **36aa**

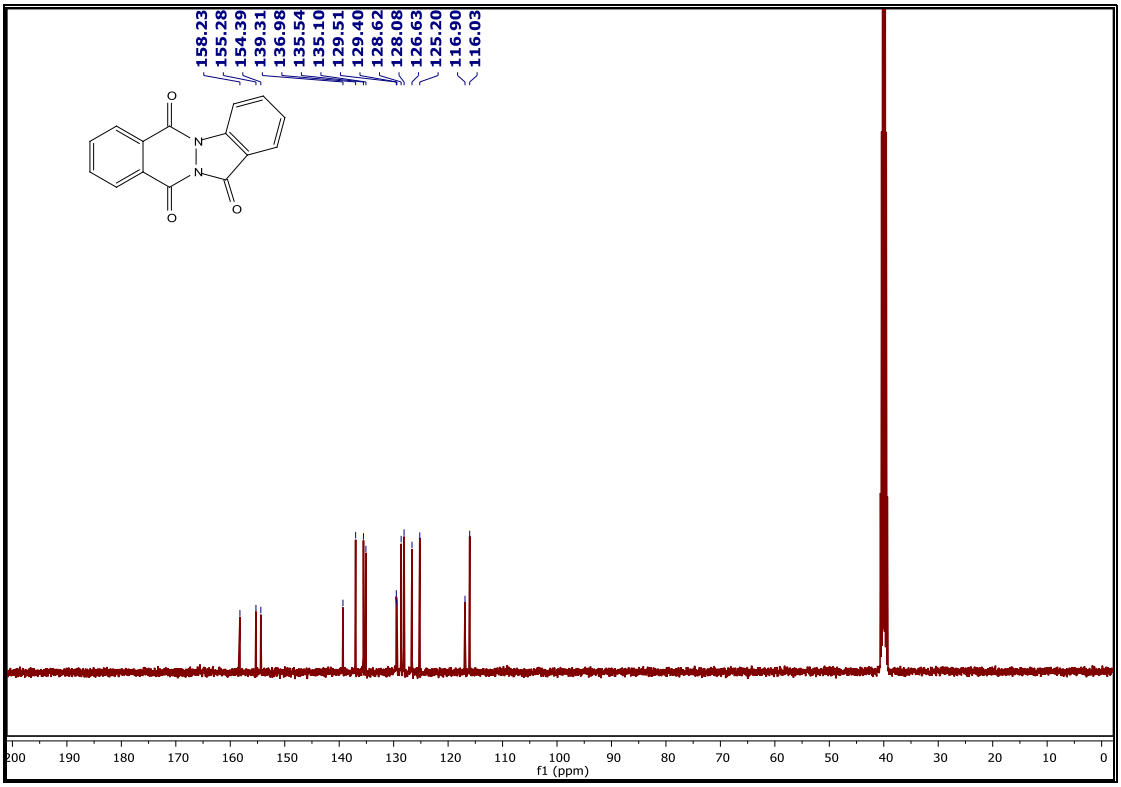

Figure 5.2.2 ^{13}C NMR spectra of **36aa**

Subsequently, the reactivity of several other commercially available isocyanates (**2b-f**) was examined towards carbocyclization of **35a** under the optimized conditions (Scheme 5.2.2). The results of this screening revealed slightly higher reactivity of electron-rich aryl isocyanates (substrates: **2e-f**) over electron-deficient aryl isocyanates (substrates: **2b-d**) towards this Ru-catalyzed carbocyclization protocol.

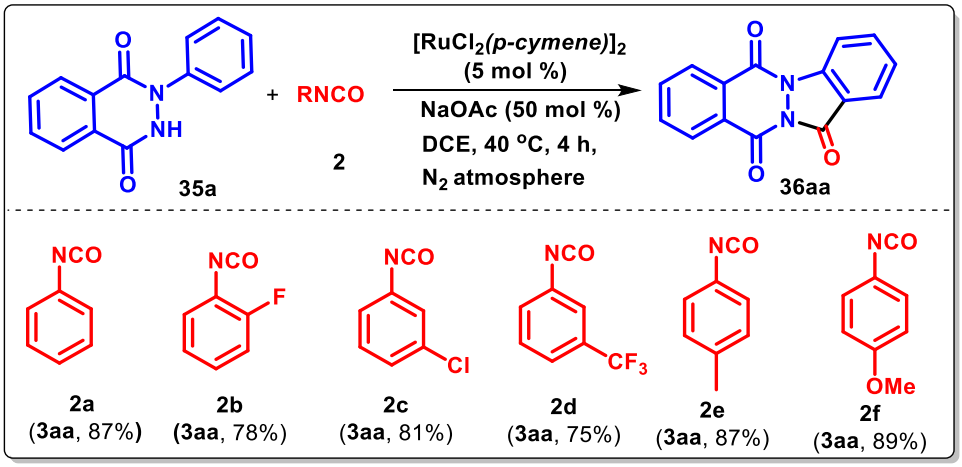

Scheme 5.2.2 Isocyanates screening for carbocyclization with **35a**

Since amides constitute an integral part of several marketed drugs and biologically active natural products, we spur our interest towards synthesizing amido functionalized 2-phenyl-2,3-dihydrophthalazine-1.4-diones using phenyl isocyanate (**2a**). Foreseeing site selective *ortho*-C-H amidated phenyl-2,3-dihydrophthalazine-1.4-dione as a possible intermediate in the above optimized strategy, attempts were made to isolate it in major amounts by tuning the reaction conditions. Thus, Ru-catalyzed coupling between **35a** and **2a** was performed at comparatively lower temperature or for lesser duration of time. However, in spite of several modifications in the reaction conditions, we failed to isolate the amide derivative, and ended up in isolating carbocyclized product only. It is worth mentioning that appearance of a polar spot was observed on TLC (ethyl acetate/hexanes, 3:7) after 2 h commencement of the reaction; however, its simultaneous consumption to the carbocyclized product's spot was observed with the progression of the reaction, even at room temperature, while no reaction was observed at low temperature. In fact, similar results were obtained by performing the coupling of **2a** with numerous other *N*-aryl-2,3-dihydrophthalazine-1.4-diones (**35b-h**). Interestingly, the reaction of 2-(2-methylphenyl)-2,3-dihydrophthalazine-1,4-dione (**35i**) with **2a** under Ru-catalyzed conditions in DCE at 80 °C fruitfully resulted in the formation of *ortho*-amidated product (**37ia**) in 96% yield (Scheme 5.2.3).

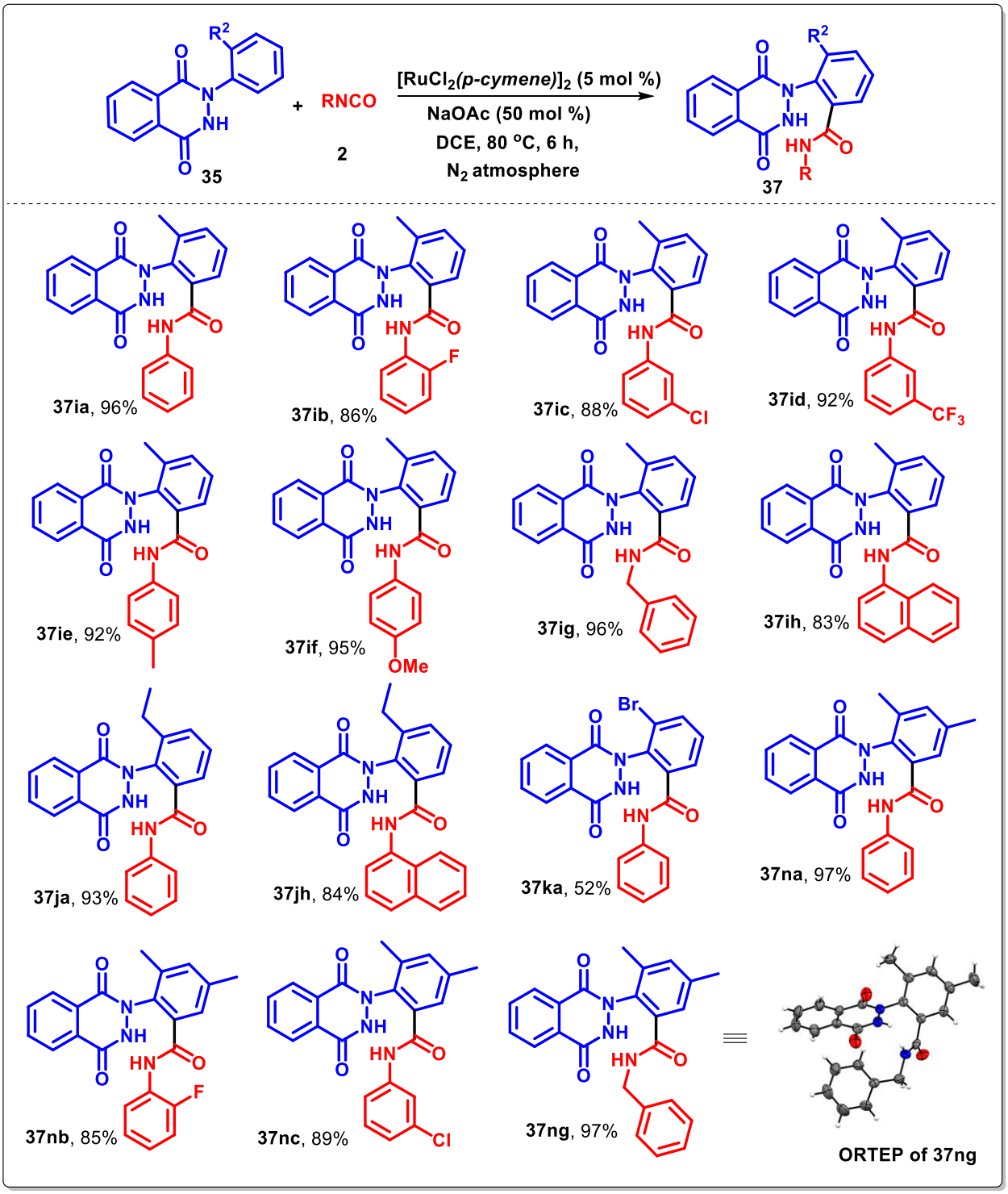

Scheme 5.2.3 *Ortho*-amidation of *N*-(*ortho*-substituted aryl)-2,3-dihydrophthalazine-1,4-diones with isocyanates

More appealing, the reaction of **35i** with electron-deficient (substrates: **2b-d**) and electron-rich (substrates: **2e-f**) aryl isocyanates comfortably furnished their respective *ortho*-amidated products

(**37ib-if**) in 86–95% yields. Benzyl isocyanate (substarte: **2g**) and naphthyl isocyanate (substrate: **2h**) also actively participated in *ortho*-amidation reaction on **35i**, producing **37ig** and **37ih** in 96% and 83% yields, respectively. On similar lines, a variety of isocyanates underwent *ortho*-amidation on 2-(2-ethylphenyl)-2,3-dihydrophthalazine-1,4-dione (**35j**) and 2-(2,4-di-methylphenyl)-2,3-dihydrophthalazine-1,4-dione (**35n**) to produce the desired amides (**37ja**, **37jh** & **37na-nc**, **37ng**) in 84-97% yields. Unfortunately, 2-(2-bromophenyl)-2,3-dihydrophthalazine-1,4-dione (**35k**) showcased moderate reactivity for coupling with **2a**, providing the corresponding amide (**37ka**) in 52% yield (Scheme 5.2.3). The representative ^{1}H NMR and ^{13}C NMR spectra of *ortho*-amidated product **37aa** are shown in Figure 5.2.3 and Figure 5.2.4, respectively. As a representative example, single crystals of **37ng** were grown in ethyl acetate and methanol to determine its structure. An ORTEP diagram of **37ng** (CCDC 2023523) is given in Scheme 5.2.3.

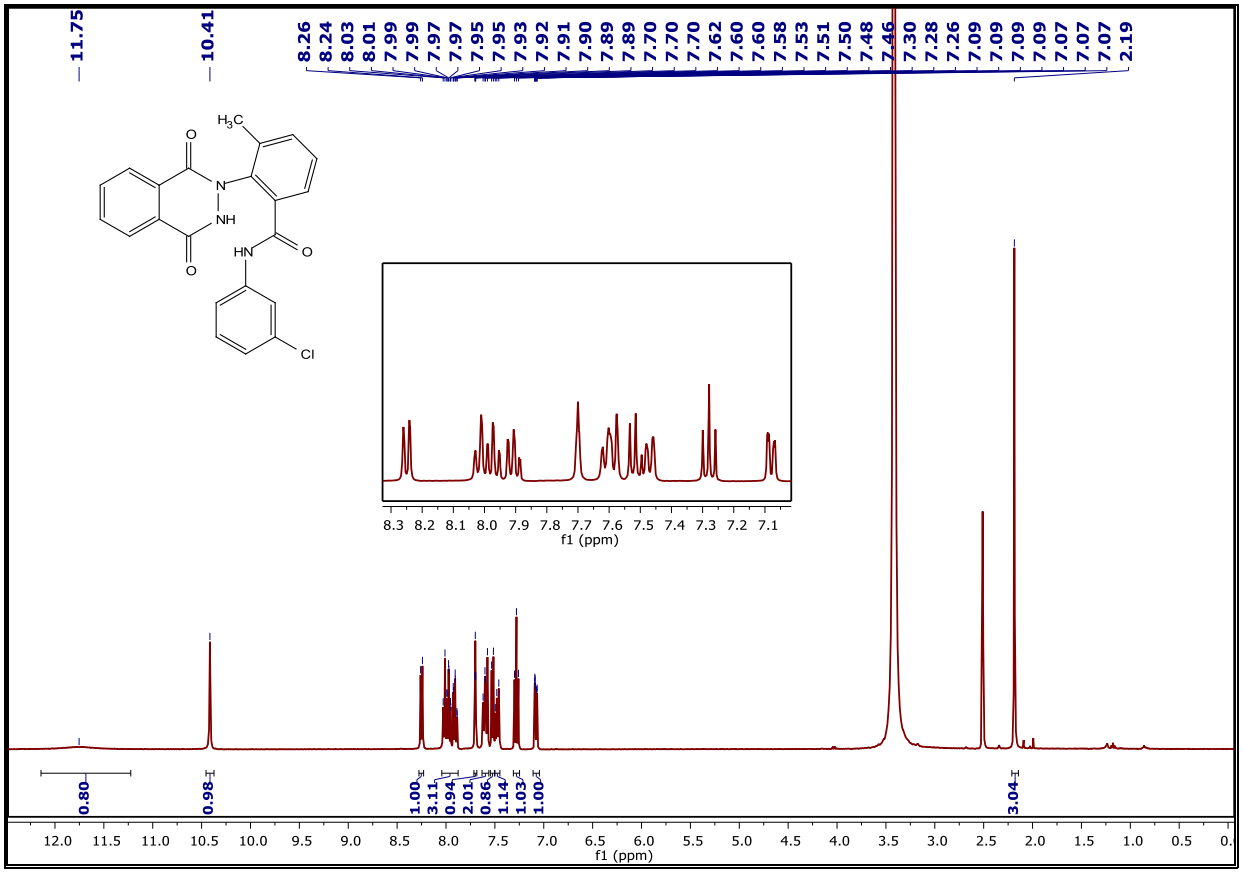

Figure 5.2.3 ^{1}H NMR spectra of **37aa**

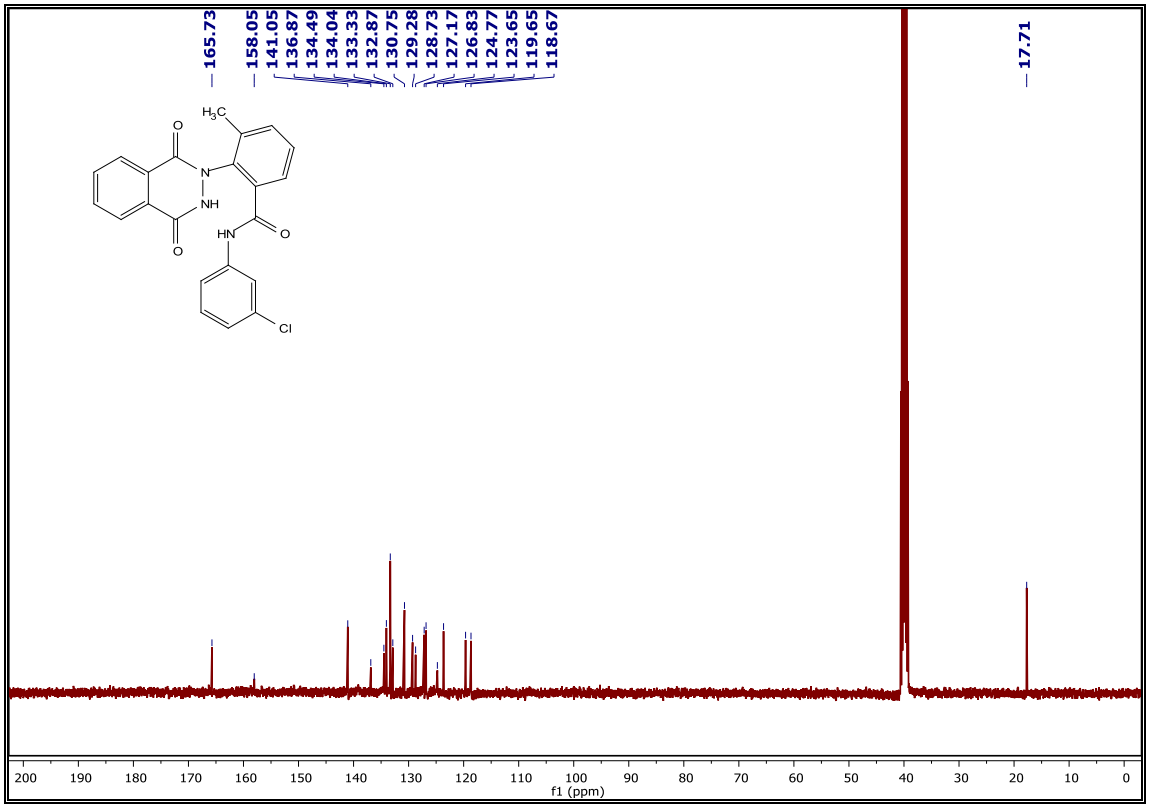

Figure 5.2.4 ^{13}C NMR spectra of **37aa**

To demonstrate the chemical applicability of the carbocyclized and *ortho*-amidated products, a few transformations of **36aa** and **37ia** were performed (Scheme 5.2.4). For example, **36aa** on reduction with alumninum hydride (LAH) in THF at 25 ^{o}C for 4 h afforded the corresponding amidol (**36aa′**) in 72% yield, while its reaction with Lawesson's reagent in toluene under reflux conditions for 4 h smoothly gave 13-thioxo-13*H*-indazolo[1,2-*b*]phthalazine-6,11-dione (**36aa′′**) in 93% yield. Similarly, **37ia** on reaction with Lawesson's reagent in toluene under reflux conditions for 4 h afforded 13-thioxo-13*H*-indazolo[1,2-*b*]phthalazine-6,11-dione (**37ia′′**) in 89% yield. Very interestingly, phenyliodine(III) diacetate (PIDA)-mediated cyclization of **37ia** in trifluoroethanol (TFE) at 0 ^{o}C afforded 1-methyl-6-phenylbenzo[5,6][1,2,3]triazino[1,2-*b*]phthalazine-5,8,13(6*H*)-trione (**37ia′**) in 95% yield. Notably, the *ortho*-amidated product (**37ia**) was comfortably converted to corresponding cyclized product (**36ia**) either using NaOAc in DCE at 120 ^{O}C for 2 h or using $POCl_3$ in toluene at 80 ^{o}C for 4 h.

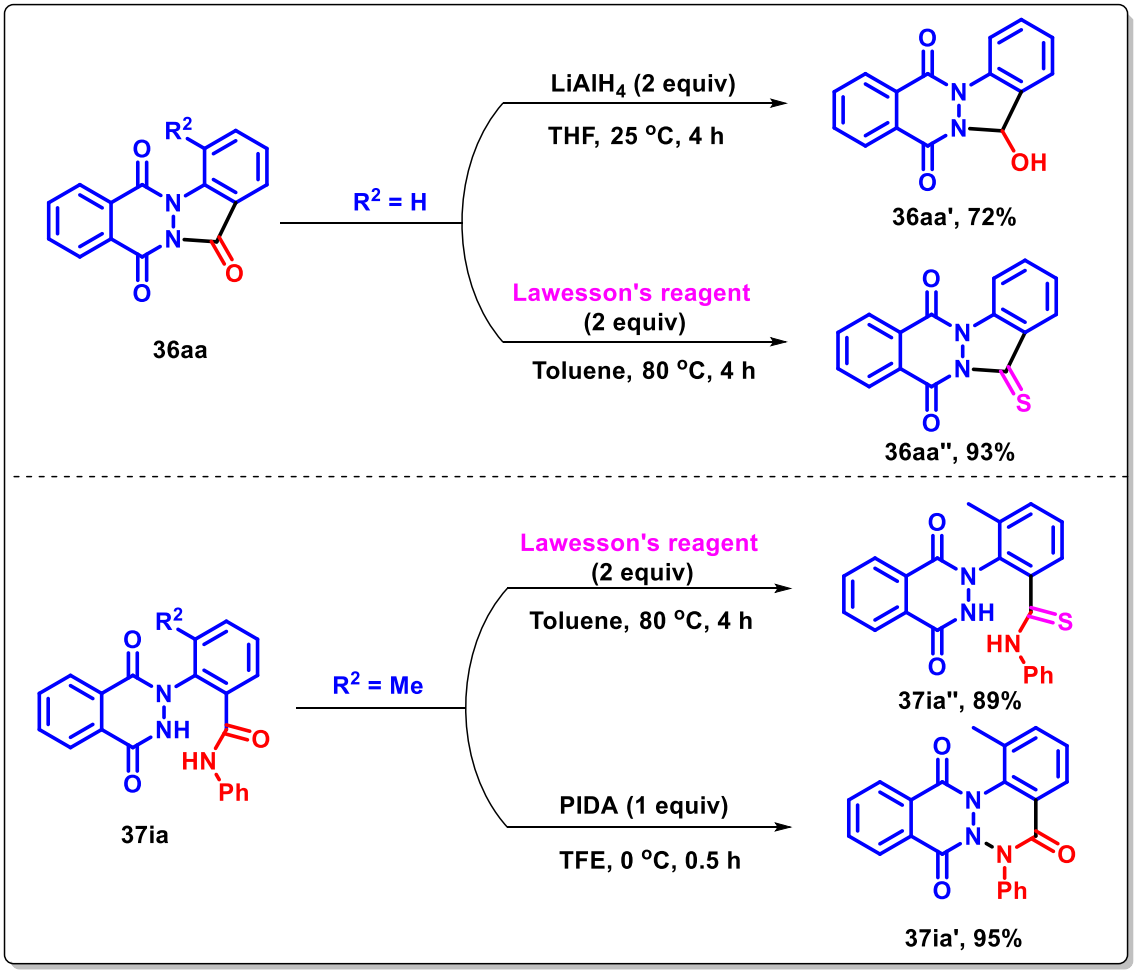

Scheme 5.2.4 Chemical transformations of **36aa** and **37ia**

To obtain mechanistic insight of the disclosed strategy, independent deuterium labelling experiments were performed by reacting **35b** and **35i** under Ru-catalyzed optimized conditions using D_2O as a co-solvent, in two different reaction pots for 4 h (Scheme 5.2.5i-ii). Interestingly, remarkable deuterium exchange (~98% and ~99%) at the *ortho* hydrogen atom(s) were observed affording corresponding mixtures of deuterated and non-deuterated substrates (**35b**/**35b-*d*$_2$** and **35i**/**35i-*d*$_1$**) in 77% and 74% yields, respectively (Figure 5.2.5 & Figure 5.2.6). This clearly indicated the possibility of reversible nature of C−H bond dissociation step. Further, two parallel reactions of **35i** and *deuterio*-**35i** with **2a** under standard reaction conditions resulted in a kinetic isotope effect (k_H/k_D) of 1.52, while, P_H/P_D of 3.2 was observed by carrying an intermolecular competitive reaction of **35b** and **35b-*d*$_2$** with **2a** under standard conditions at 40 °C for 2 h (Scheme 5.2.5iii-iv, Figure 5.2.7, Figure 5.2.8 & Figure 5.2.9). These set of reactions indicated that C−H bond cleavage might be involved in the rate-limiting step. Attempts to isolate possible ruthenium

complex intermediate by carrying reaction of **35a** with stoichiometric amounts of [$RuCl_2$(*p*-cymene)]$_2$ and NaOAc in DCE at room temperature were not fruitful. However, an isolable cycloruthenium complex **B′** was obtained by reacting [$RuCl_2$(*p*-cymene)]$_2$ (1 equiv) with **35a** (1.5 equiv) and NaOAc (2.5 equiv) in dichloromethane (DCM) at room temperature using pyridine as an external stabilizing ligand (Scheme 5.2.5v, Figure 5.2.10 and Figure 5.2.11). Further, complex **B′** when used as a catalyst for the coupling between **35a** and **2a** in DCE at 40 °C for 4 h produced **36aa** in 85% yield (Scheme 5.2.5vi).

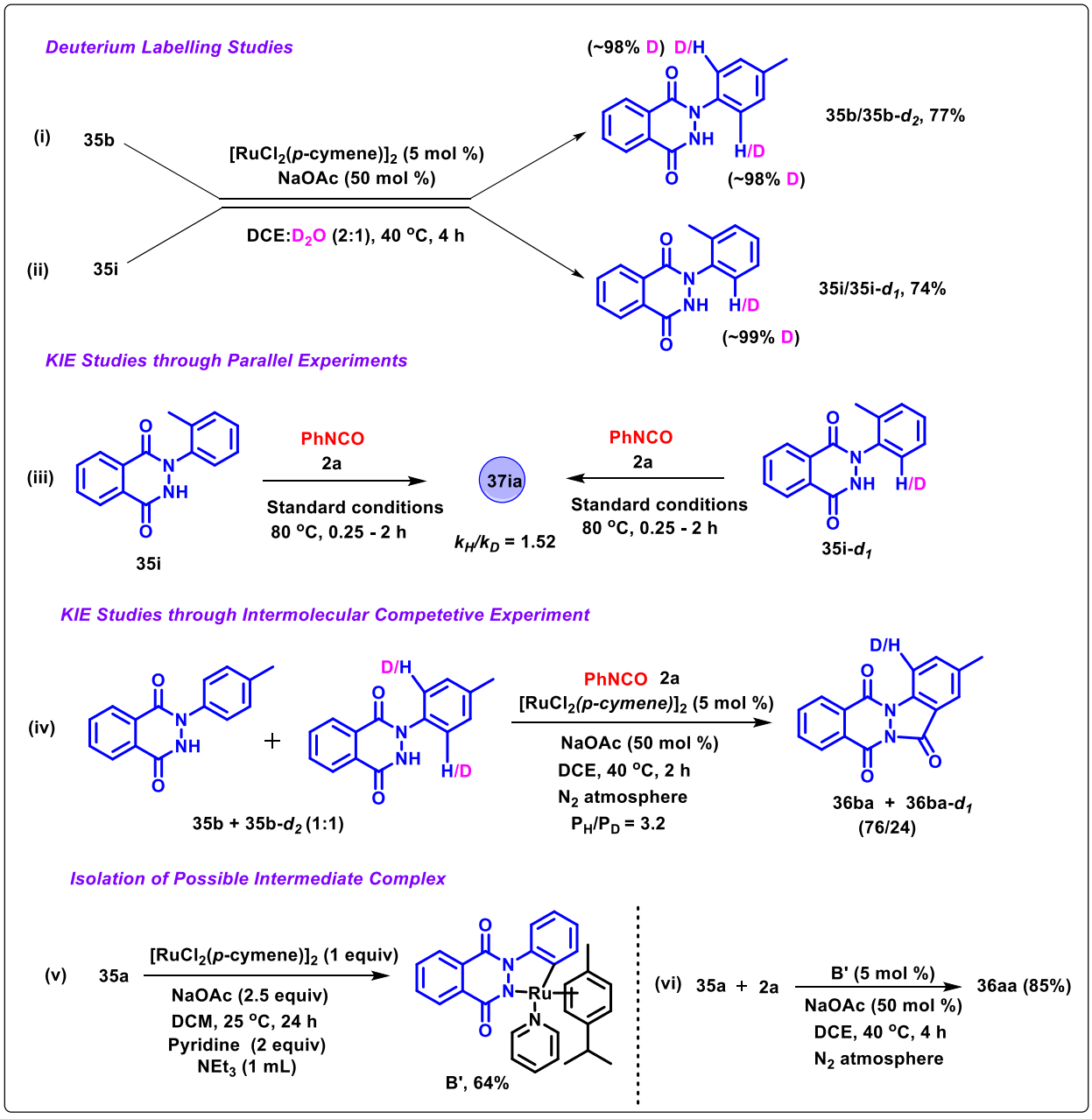

Scheme 5.2.5 Preliminary mechanistic investigations

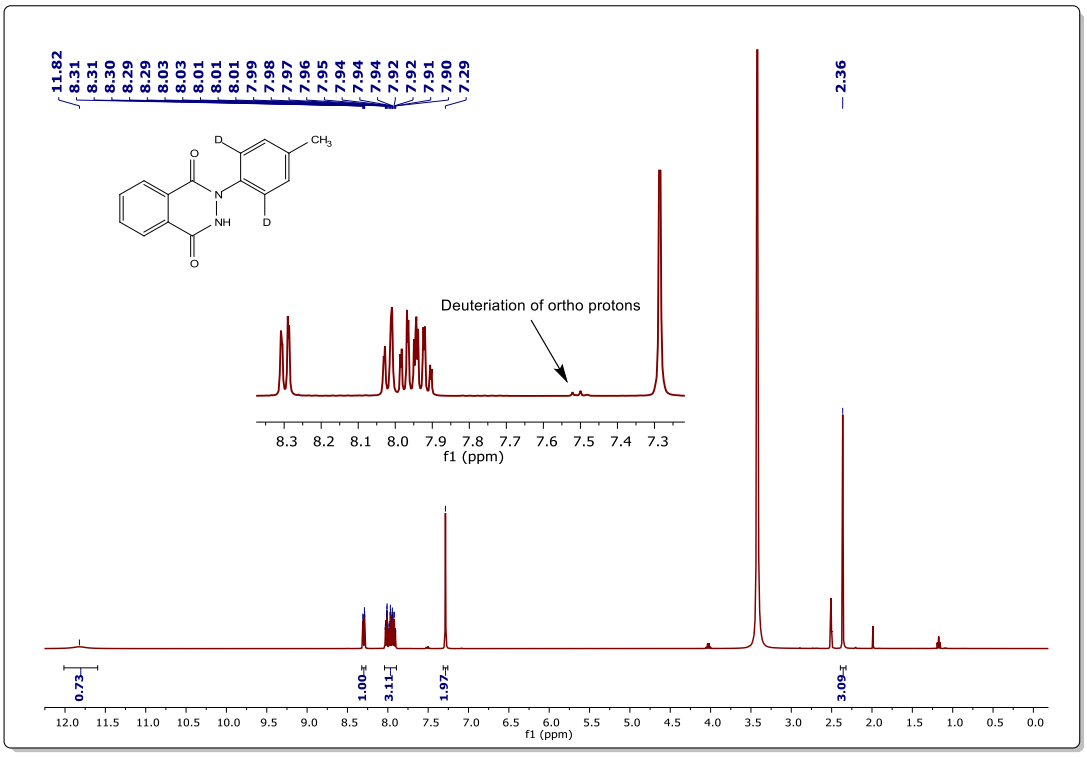

Figure 5.2.5 ^{1}H NMR of **35b/35b-*d*$_2$**

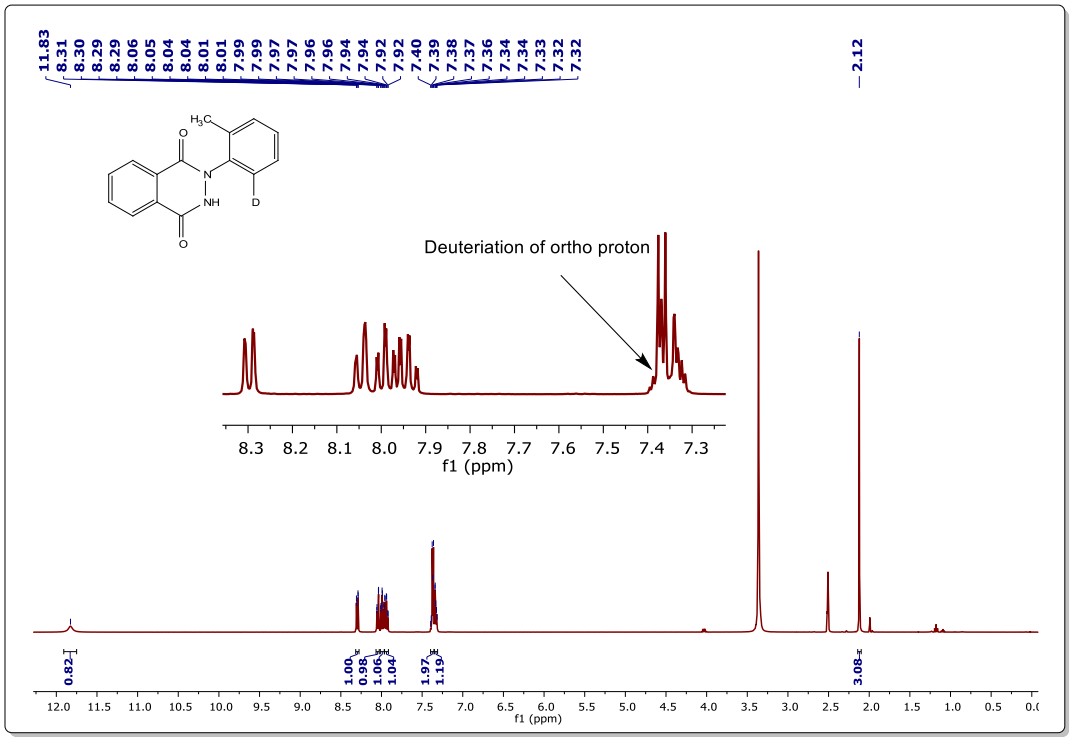

Figure 5.2.6 ^{1}H NMR of **35i/35i-*d*$_1$**

Intermolecular Competitive Experiment

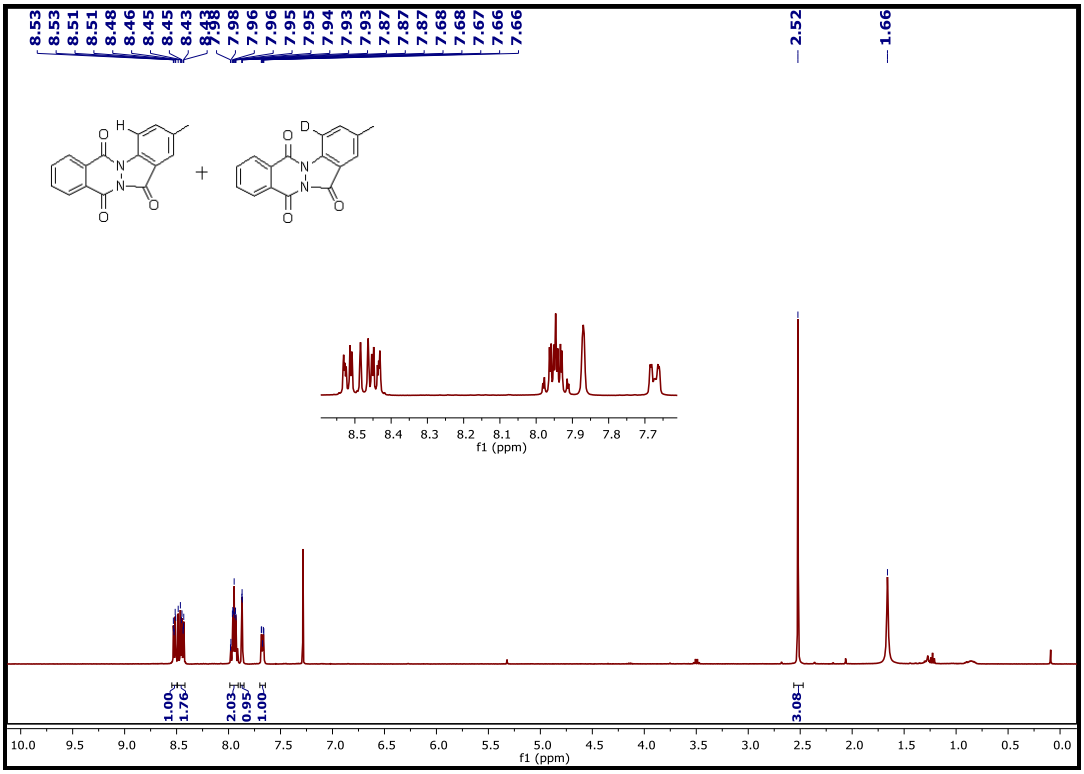

Figure 5.2.7 ^{1}H NMR of **36ba+36ba-*d*$_1$**

$$P_H/P_D = 0.76/0.24 = 3.2$$

Parallel Experiments

Time (Min)	15	30	60	90	120
^{1}H NMR Yield of 37ia (%)	0	8.86	24.97	37.62	48.22

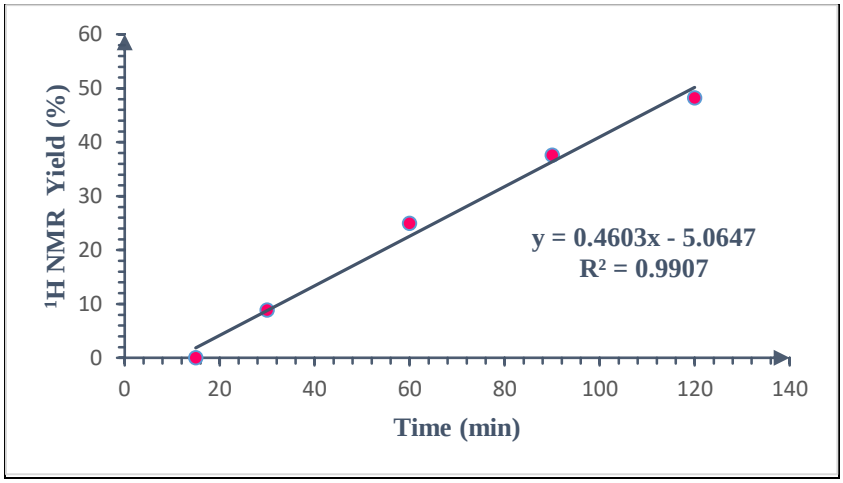

Figure 5.2.8 Protonated Kinetics

Time (Min)	15	30	60	90	120
^{1}H NMR Yield of 37ia (%)	0	4.75	13.63	19.73	33.26

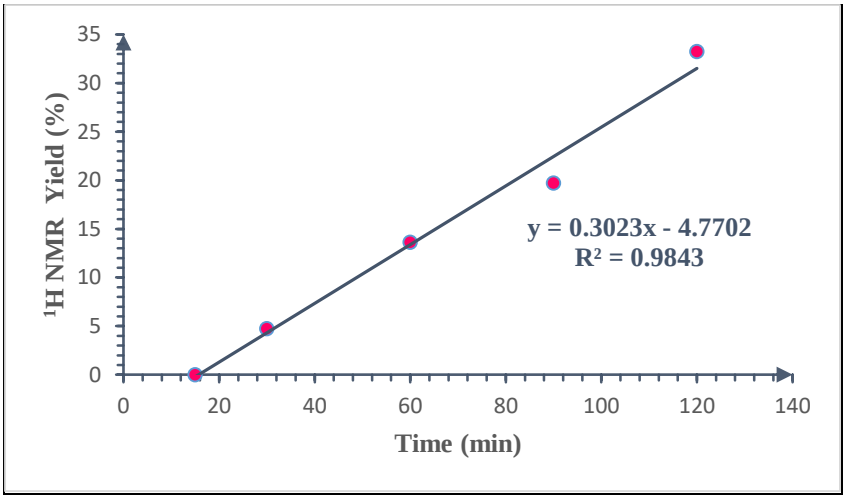

Figure 5.2.9 Deuterated Kinetics

KIE = k_H/k_D = 0.4603/0.3023= 1.52

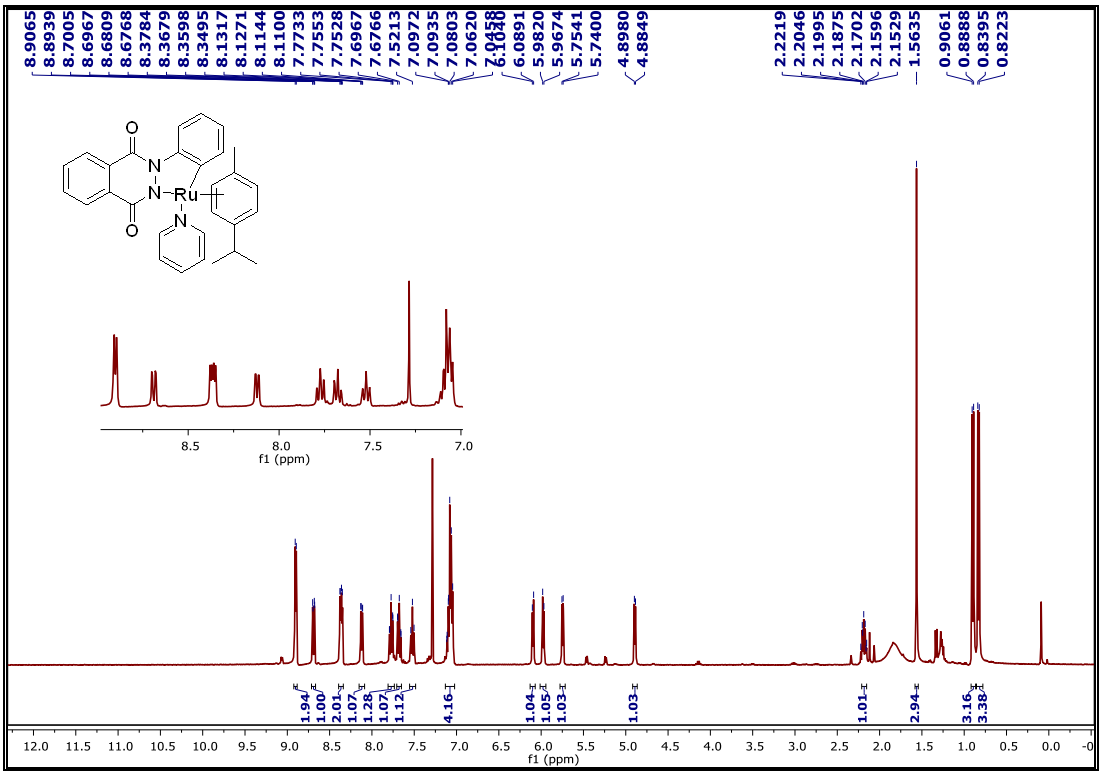

Figure 5.2.10 ^{1}H NMR spectra of intermediate [Ru(*p*-Cymene)Py] Complex (**B′**)

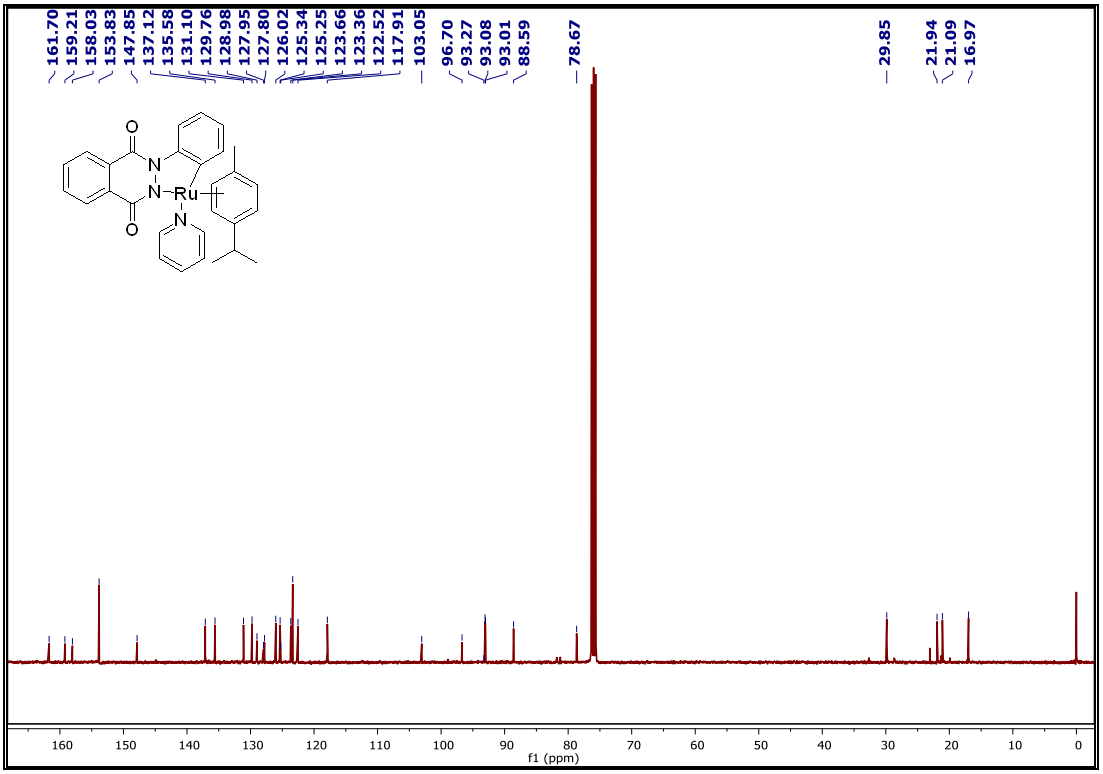

Figure 5.2.11 ^{13}C NMR spectra of intermediate [Ru(*p*-Cymene)Py] Complex (**B′**)

On the basis of precedence literature reports[58,66,67] and our preliminary mechanistic investigations, a plausible reaction mechanism is proposed (Scheme 5.2.6). The reaction is believed to proceed by formation of monomeric [$Ru^{II}OAc_2$(*p*-cymene)] species by acetate ion-mediated dissociation of dimeric [$RuCl_2$(*p*-cymene)]$_2$ catalyst. This Ru(II) active species undergoes ligand exchange with N-H of **35** to furnish **A**, which facilitate C-H metallation to produce five-membered ruthenacyclic complex **B**. Further, coordination of Ru with –C=N double bond of aryl isocyanate (**2**) and subsequent migratory insertion of –C=N into Ru-Ar bond generates species **D** *via* **C**. Protonolysis of the two nitrogens in species **D** furnishes *ortho*-amidated intermediate **37,** along with the regeneration of the active Ru(II) species for the next catalytic cycle. Finally, intramolecular nucleophilic substitution provides tetracyclic carbocyclized product (**35**).

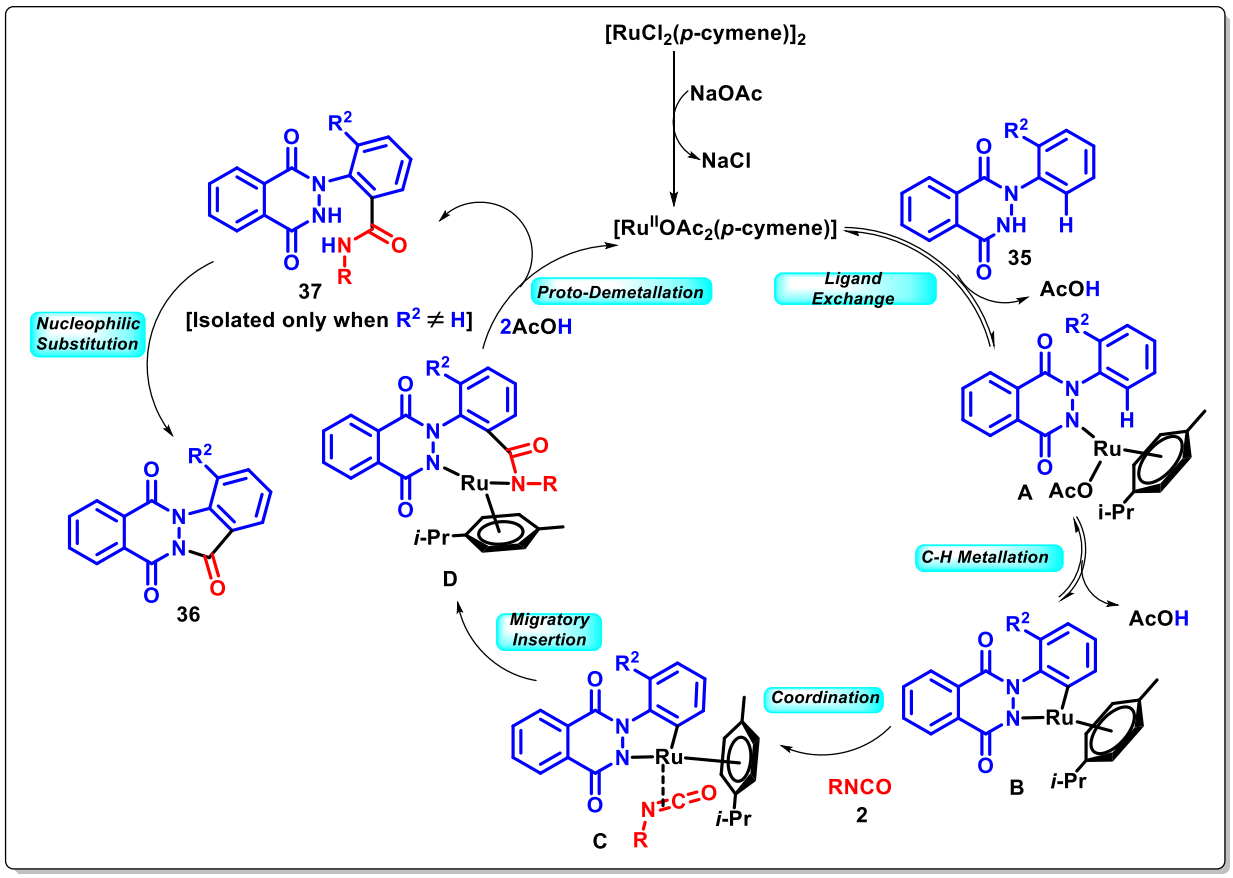

Scheme 5.2.6 Plausible mechanism

In summary, we have developed a mild and efficient Ru(II)-catalyzed strategy for the direct carbocyclization of 2-aryl-2,3-dihydrophthalazine-1,4-diones using isocyanates as a carbonyl source *via* sequential C-C/C-N bond formations. Interestingly, a series of diversely decorated 2-phenylphthalazine-1,4-dione amides were isolated by coupling substituted aryl isocyanates with

ortho-substituted *N*-aryl-2,3-dihydrophthalazine-1,4-diones under slightly modified reaction conditions. Successful transformations of the carbocyclized and *ortho*-amidated products resulted in chemically divergent fused and functionalized phthalazinones.

5.3 Experimental Section

General Considerations

Commercially available reagents were used without purification. Commercially available solvents were dried by standard procedures prior to use. Commercially available aryl isocyanates were used without purification. Reactions were monitored by using thin layer chromatography (TLC) on 0.2 mm silica gel F254 plates (Merck). The chemical structures of final products and intermediates were characterized by nuclear magnetic resonance spectra (^{1}H NMR and ^{13}C NMR) were recorded on a 400 MHz spectrometer, and the chemical shifts are reported in δ units, parts per million (ppm), relative to residual chloroform (7.26 ppm) or DMSO (2.5 ppm) in the deuterated solvent. ^{13}C NMR spectra are fully decoupled. The following abbreviations were used to describe peak splitting patterns when appropriate: s = singlet, d = doublet, t = triplet, dd = doublet of doublets, and m = multiplet. Coupling constants *J* are reported in Hz. The ^{13}C NMR spectra are reported in ppm relative to deuterochloroform (77.0 ppm) or [d_6] DMSO (39.5 ppm). Melting points were determined on a capillary point apparatus equipped with a digital thermometer and are uncorrected. High-resolution mass spectra were recorded on Agilent Technologies 6545 Q-TOF LC/MS by using electrospray mode. Column chromatography was performed on silica gel (100-200) mesh using varying ratio of ethyl acetate/hexanes as eluent.

General procedure for the synthesis of indazolo-fused phthalazine-diones (36)

To an oven-dried sealed tube with a screw cap (PTFE) charged with 2-aryl-2,3-dihydrophthalazine-1,4-dione (**35**) (50 mg, 1 equiv), $[RuCl_2(p\text{-cymene})]_2$ (0.05 equiv) and NaOAc (0.5 equiv) were added phenyl isocyanate (**2a**) (1.5 equiv) and DCE (3 mL) under N_2 atmosphere. The reaction mixture was to allowed stirr at 40 ºC for 4 h (or 120 ºC for 6 h). On completion of the reaction as indicated by TLC, the reaction was cooled to room temperature, diluted with DCM (5 mL), filtered through celite the reaction was quenched with water and extracted with DCM (2 x 15 mL). The organic layers were combined, dried over anhydrous sodium sulphate and concentrated in vacuo. Purification by column chromatography using ethyl acetate/hexanes (1:9 to 2:8) as eluent afforded the desired product (**36**).

13*H*-Indazolo[1,2-*b*]phthalazine-6,11,13-trione (36aa). Pale yellow solid; yield: 48 mg (87%, from **2a**), 43 mg (78%, from **2b**), 45 mg (81%, from **2c**), 42 mg (75%, from **2d**), 48 mg (87%, from **2e**), 49 mg (89%, from **2f**); mp 212−213 °C; ^{1}H NMR (400 MHz, DMSO-d_6) δ 8.47 (d, J = 8.4 Hz, 1H), 8.35 – 8.28 (m, 2H), 8.06 – 7.99 (m, 3H), 7.98 – 7.92 (m, 1H), 7.54 (t, J = 7.9 Hz, 1H); ^{13}C NMR (100 MHz, DMSO-d_6) δ 158.2, 155.3, 154.4, 139.3, 137.0, 135.5, 135.1, 129.5, 129.4, 128.6, 128.1, 126.6, 125.2, 116.9, 116.0; HRMS (ESI-TOF) (*m/z*) calculated $C_{15}H_9N_2O_3^+$: 265.0608, found 265.0609 $[M + H]^+$.

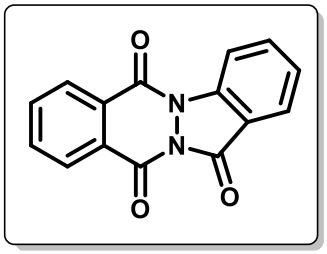

2-Methyl-13*H*-indazolo[1,2-*b*]phthalazine-6,11,13-trione (36ba). Pale yellow solid; yield: 50 mg (90%); mp 223−224 °C; ^{1}H NMR (400 MHz, $CDCl_3$) δ 8.53 – 8.49 (m, 1H), 8.47 – 8.40 (m, 2H), 7.98 – 7.90 (m, 2H), 7.85 (s, 1H), 7.66 (dd, J = 8.5, 1.8 Hz, 1H), 2.51 (s, 3H); ^{13}C NMR (100 MHz, $CDCl_3$) δ 158.2, 154.9, 153.6, 137.8, 137.5, 136.8, 135.1, 134.5, 129.2, 129.1, 128.9, 128.3, 124.9, 116.7, 115.9, 21.1; HRMS (ESI-TOF) (*m/z*) calculated $C_{16}H_{11}N_2O_3^+$: 279.0764, found 279.0764 $[M + H]^+$.

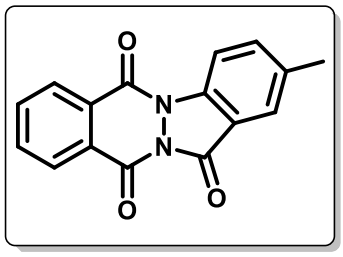

2-Isopropyl-13*H*-indazolo[1,2-*b*]phthalazine-6,11,13-trione (36ca). Pale yellow solid; yield: 51 mg (93%); mp 212−215 °C; ^{1}H NMR (400 MHz, $CDCl_3$) δ 8.55 – 8.49 (m, 2H), 8.46 – 8.42 (m, 1H), 7.99 – 7.90 (m, 3H), 7.74 (dd, J = 8.6, 1.8 Hz, 1H), 3.09 (sep, J = 6.8 Hz, 1H), 1.35 (d, J = 6.8, Hz, 6H); ^{13}C NMR (100 MHz, $CDCl_3$) δ 158.4, 154.9, 153.6, 147.9, 137.7, 135.8, 135.1, 134.5, 129.2, 129.1, 128.9, 128.3, 122.4, 116.7, 116.1, 33.9, 23.9; HRMS (ESI-TOF) (*m/z*) calculated $C_{18}H_{15}N_2O_3^+$: 307.1077, found 307.1071 $[M + H]^+$.

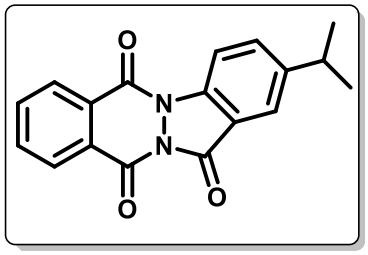

2-Fluoro-13*H*-indazolo[1,2-*b*]phthalazine-6,11,13-trione (36da). Pale yellow solid; yield: 40 mg (72%); mp 198−200 °C; ^{1}H NMR (400 MHz, $CDCl_3$) δ 8.63 (dd, J = 9.0, 4.0 Hz, 1H), 8.56 – 8.51 (m, 1H), 8.49 – 8.43 (m, 1H), 8.03 – 7.93 (m, 2H), 7.75 (dd, J = 6.8, 2.6 Hz, 1H), 7.60 (td, J = 8.8, 2.6 Hz, 1H); ^{13}C NMR (100 MHz, $CDCl_3$) δ 160.5 ($^1J_{C\text{-}F}$ = 247.7 Hz), 157.2 ($^4J_{C\text{-}F}$ = 3.7 Hz), 154.8, 153.7, 135.6, 135.3, 134.8, 129.4, 129.2, 128.8 ($^3J_{C\text{-}F}$ = 6.7 Hz) , 128.4, 124.6 ($^2J_{C\text{-}F}$ = 24.7 Hz), 120.8, 118.2 ($^3J_{C\text{-}F}$ = 7.9 Hz), 111.2

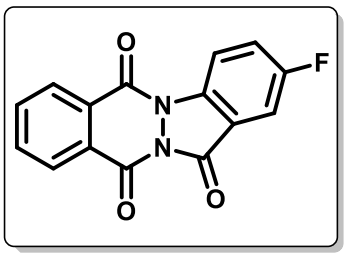

($^{2}J_{C\text{-}F}$ = 24.8 Hz); ^{19}F NMR (376 MHz, $CDCl_3$) δ -113.06; HRMS (ESI-TOF) (*m/z*) calculated $C_{15}H_8FN_2O_3^+$: 283.0513, found 283.0511 $[M + H]^+$.

2-Chloro-13*H*-indazolo[1,2-*b*]phthalazine-6,11,13-trione (36ea). Pale yellow solid; yield: 42 mg (76%); mp 290−292 °C; ^{1}H NMR (400 MHz, $CDCl_3$) δ 8.57 (d, J = 8.8 Hz, 1H), 8.55 – 8.50 (m, 1H), 8.47 – 8.41 (m, 1H), 8.06 (d, J = 2.2 Hz, 1H), 8.02 – 7.93 (m, 2H), 7.81 (dd, J = 8.8, 2.2 Hz, 1H), ; ^{13}C NMR (100 MHz, $CDCl_3$) δ 156.8, 154.7, 153.8, 137.5, 136.7, 135.3, 134.9, 132.4, 129.4, 128.8, 128.7, 128.5, 124.9, 118.1, 117.5; HRMS (ESI-TOF) (*m/z*) calculated $C_{15}H_8ClN_2O_3^+$: 299.0218, found 299.0217 $[M + H]^+$.

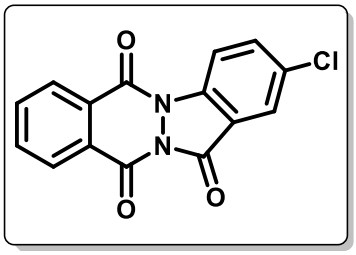

2-Bromo-13*H*-indazolo[1,2-*b*]phthalazine-6,11,13-trione (36fa). Pale yellow solid; yield: 42 mg (78%); mp 154−156 °C; ^{1}H NMR (400 MHz, $CDCl_3$) δ 8.55 – 8.49 (m, 2H), 8.47 – 8.42 (m, 1H), 8.22 (d, J = 1.8 Hz, 1H), 8.01 – 7.93 (m, 3H); ^{13}C NMR (100 MHz, $CDCl_3$) δ 156.7, 154.7, 153.8, 139.4, 137.9, 135.3, 134.9, 129.4, 128.8, 128.7, 128.5, 128.0, 119.7, 118.4, 117.8; HRMS (ESI-TOF) (*m/z*) calculated $C_{15}H_8BrN_2O_3^+$: 342.9713, found 342.9705 $[M + H]^+$.

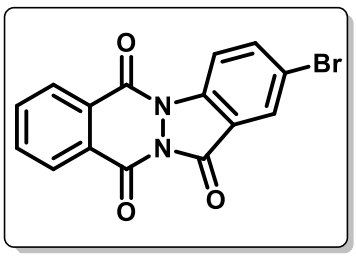

3-Fluoro-13*H*-indazolo[1,2-*b*]phthalazine-6,11,13-trione (36ga). White solid; yield: 40 mg (73%); mp 281−282 °C; ^{1}H NMR (400 MHz, $CDCl_3$) δ 8.56 – 8.51 (m, 1H), 8.49 – 8.43 (m, 1H), 8.33 (dd, J = 9.0, 2.2 Hz, 1H), 8.09 (dd, J = 5.2, 3.4 Hz, 1H), 8.01 – 7.94 (m, 2H), 7.22 (td, J = 8.6, 2.2 Hz, 1H); ^{13}C NMR (100 MHz, $CDCl_3$) δ 167.8 ($^{1}J_{C\text{-}F}$ = 255.6 Hz), 157.1, 154.6, 154.0, 140.4 ($^{3}J_{C\text{-}F}$ = 14.6 Hz), 135.2, 135.0, 129.4, 128.9, 128.6, 128.5, 127.7 ($^{3}J_{C\text{-}F}$ = 11.3 Hz), 115.1 ($^{2}J_{C\text{-}F}$ = 24.5 Hz), 112.8 ($^{4}J_{C\text{-}F}$ = 1.6 Hz), 103.9 ($^{2}J_{C\text{-}F}$ = 29.8 Hz); ^{19}F NMR (376 MHz, $CDCl_3$) δ -97.11; HRMS (ESI-TOF) (*m/z*) calculated $C_{15}H_8FN_2O_3^+$: 283.0513, found 283.0503 $[M + H]^+$.

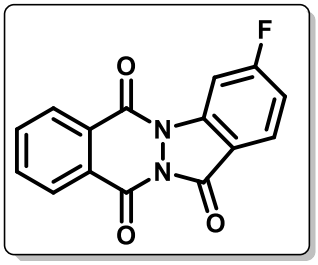

3-Chloro-13*H*-indazolo[1,2-*b*]phthalazine-6,11,13-trione (36ha). Pale yellow solid; yield: 41 mg (75%); mp 189−190 °C; ^{1}H NMR (400 MHz, DMSO-d_6) δ 8.49 (s, 1H), 8.41 – 8.28 (m, 2H), 8.15 – 7.98 (m, 3H), 7.61 (d, J = 7.6 Hz, 1H); ^{13}C NMR (100 MHz, DMSO-d_6) δ 157.4, 155.2, 154.7, 141.3, 139.7, 135.7, 135.4, 129.5, 129.1, 128.7, 128.2, 127.0, 127.0, 115.9, 115.6;

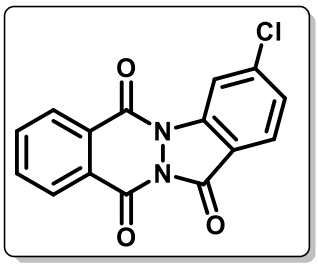

HRMS (ESI-TOF) (*m/z*) calculated $C_{15}H_8ClN_2O_3^+$: 299.0218, found 299.0215 $[M + H]^+$.

4-Methyl-13*H*-indazolo[1,2-*b*]phthalazine-6,11,13-trione (36ia). White solid; yield: 52 mg (94%); mp 210−211 °C; ^{1}H NMR (400 MHz, $CDCl_3$) δ 8.50 – 8.46 (m, 1H), 8.40 – 8.36 (m, 1H), 7.97 – 7.90 (m, 3H), 7.65 (d, *J* = 7.4 Hz, 1H), 7.4 (t, *J* = 7.6 Hz, 1H), 2.70 (s, 3H); ^{13}C NMR (100 MHz, $CDCl_3$) δ 158.9, 155.9, 155.8, 139.8, 139.2, 135.0, 134.5, 129.7, 129.0, 128.9, 128.6, 128.0, 127.1, 122.9, 119.5, 22.2; HRMS (ESI-TOF) (*m/z*) calculated $C_{16}H_{11}N_2O_3^+$: 279.0764, found 279.0771 $[M + H]^+$.

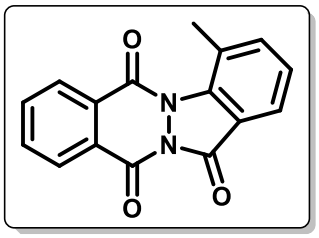

4-Ethyl-13*H*-indazolo[1,2-*b*]phthalazine-6,11,13-trione (36ja). White solid; yield: 50 mg (91%); mp 118−119 °C; ^{1}H NMR (400 MHz, DMSO-d_6) δ 8.31 – 8.27 (m, 2H), 8.06 – 7.97 (m, 2H), 7.88 – 7.80 (m, 2H), 7.54 (t, *J* = 7.6 Hz, 1H), 3.02 (q, *J* = 7.4 Hz, 2H), 1.20 (t, *J* = 7.4 Hz, 3H); ^{13}C NMR (100 MHz, DMSO-d_6) δ 159.0, 156.5, 156.3, 139.2, 137.6, 135.6, 134.9, 134.0, 130.2, 129.2, 128.5, 128.3, 127.7, 122.7, 120.3, 27.9, 14.7; HRMS (ESI-TOF) (*m/z*) calculated $C_{17}H_{13}N_2O_3^+$: 293.0921, found 293.0925 $[M + H]^+$.

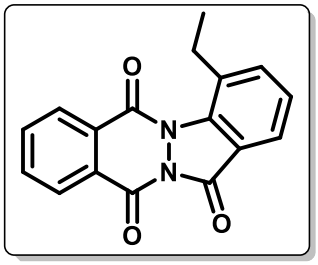

4-Bromo-13*H*-indazolo[1,2-*b*]phthalazine-6,11,13-trione (36ka). White solid; yield: 23 mg (50%); mp 165−168 °C; ^{1}H NMR (400 MHz, DMSO-d_6) δ 8.32 – 8.25 (m, 2H), 8.18 (d, *J* = 8.1 Hz, 1H), 8.09 – 8.00 (m, 3H), 7.52 (t, *J* = 7.7 Hz, 1H); ^{13}C NMR (100 MHz, DMSO-d_6) δ 158.0, 156.3, 156.1, 141.2, 140.5, 135.7, 135.2, 130.2, 129.2, 128.8, 128.8, 128.2, 124.5, 123.2, 110.4; HRMS (ESI-TOF) (*m/z*) calculated $C_{15}H_8BrN_2O_3^+$: 342.9713, found 342.9706 $[M + H]^+$.

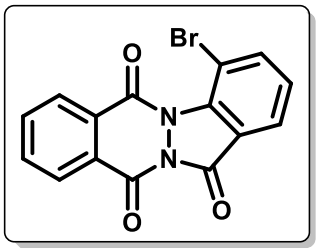

2,3-Dimethyl-13*H*-indazolo[1,2-*b*]phthalazine-6,11,13-trione (36la). Pale yellow solid; yield: 51 mg (93%); mp 254−255 °C; ^{1}H NMR (400 MHz, $CDCl_3$) δ 8.52 – 8.49 (m, 1H), 8.43 – 8.40 (m, 1H), 8.36 (s, 1H), 7.97 – 7.90 (m, 2H), 7.79 (s,1H), 2.48 (s, 3H), 2.40 (s, 3H); ^{13}C NMR (100 MHz, $CDCl_3$) δ 158.2, 154.9, 153.6, 147.6, 138.1, 136.1, 135.0, 134.4, 129.1, 129.1, 129.0, 128.2, 125.1, 116.5, 114.4, 21.4, 19.9; HRMS (ESI-TOF) (*m/z*) calculated $C_{17}H_{13}N_2O_3^+$: 293.0921, found 293.0916 $[M + H]^+$.

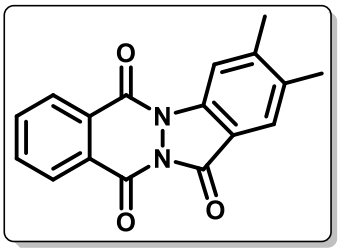

3-Chloro-2-methyl-13*H*-indazolo[1,2-*b*]phthalazine-6,11,13-trione (36ma). Pale yellow solid;

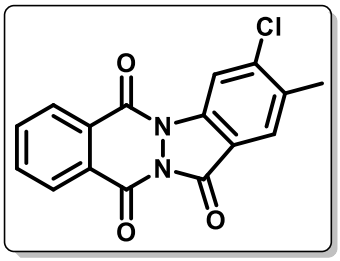

yield: 44 mg (81%); mp 212−213 °C; ^{1}H NMR (400 MHz, DMSO-d_6) δ 8.47 (s, 1H), 8.36 – 8.30 (m, 2H), 7.94 – 7.81 (m, 3H), 2.47 (s, 3H); ^{13}C NMR (100 MHz, DMSO-d_6) δ 157.5, 155.2, 154.4, 141.8, 137.9, 135.7, 135.3, 134.7, 129.5, 129.1, 128.7, 128.1, 126.9, 116.0, 115.9; HRMS (ESI-TOF) (*m/z*) calculated $C_{16}H_{10}ClN_2O_3^+$: 313.0374, found 313.0369 $[M + H]^+$.

2,4-Dimethyl-13*H*-indazolo[1,2-*b*]phthalazine-6,11,13-trione (36na). White solid; yield: 52 mg

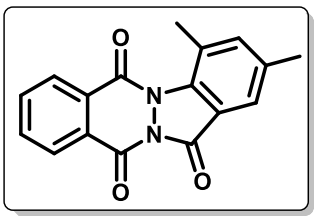

(95%); mp 182−183 °C; ^{1}H NMR (400 MHz, $CDCl_3$) δ 8.51 – 8.46 (m, 1H), 8.41 – 8.35 (m, 1H), 7.97 – 7.89 (m, 2H), 7.72 (s, 1H), 7.48 (s, 1H), 2.66 (s, 3H), 2.48 (s, 3H); ^{13}C NMR (100 MHz, $CDCl_3$) δ 158.9, 155.9, 155.6, 140.4, 138.0, 137.5, 134.9, 134.4, 129.7, 128.9, 128.5, 127.6, 122.6, 119.6, 22.2, 20.8; HRMS (ESI-TOF) (*m/z*) calculated $C_{17}H_{13}N_2O_3^+$: 293.0921, found 293.0906 $[M + H]^+$.

8-Methyl-13*H*-indazolo[1,2-*b*]phthalazine-6,11,13-trione + 9-Methyl-13*H*-indazolo[1,2-*b*]phthalazine-6,11,13-trione (1:2 or 2:1) (36oa). Pale yellow solid; yield: 48 mg (87%); mp

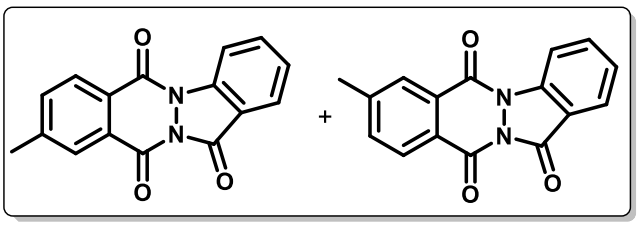

186−187 °C; ^{1}H NMR (400 MHz, $CDCl_3$) δ 8.58 (dd, J = 8.4, 2.6 Hz, 1.5H), 8.38 (d, J = 8.0 Hz, 1H), 8.32 – 8.28 (m, 1H), 8.21 (s, 1H), 8.07 (d, J = 7.8 Hz, 1.5H), 7.87 – 7.82 (m, 1.5H), 7.73 (td, J = 7.8, 1.0 Hz, 1.5H), 7.51 – 7.45 (m, 1.5H), 2.61 (s, 4.5H); ^{13}C NMR (100 MHz, $CDCl_3$) δ 158.2, 158.1, 155.0, 154.9, 154.0, 154.0, 146.8, 146.2, 139.3, 139.2, 136.5, 136.4, 136.1, 135.6, 129.3, 129.3, 128.8, 128.8, 128.5, 128.4, 126.4, 126.4, 126.3, 126.2, 125.3, 116.7, 116.6, 116.2, 116.2, 22.0, 21.9; HRMS (ESI-TOF) (*m/z*) calculated $C_{16}H_{11}N_2O_3^+$: 279.0764, found 279.0762 $[M + H]^+$.

8-Methoxy-13*H*-indazolo[1,2-*b*]phthalazine-6,11,13-trione + 9-Methoxy-13*H*-indazolo[1,2-*b*]phthalazine-6,11,13-trione (1:4 or 4:1) (36pa). Pale yellow solid; yield: 50 mg (91%); mp

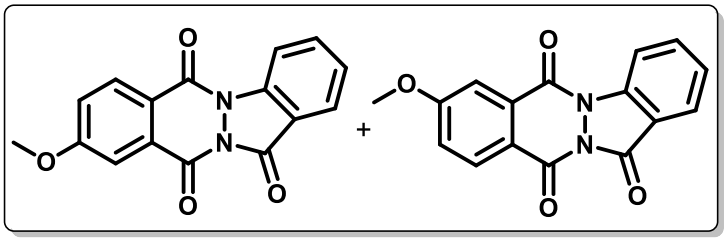

233−234 °C; ^{1}H NMR (400 MHz, $CDCl_3$) δ 8.57 (dd, J = 8.4, 2.7 Hz, 1.25H), 8.41 (d, J = 8.4 Hz, 1H), 8.33 (d, J = 8.8 Hz, 0.25H), 8.10 – 8.04 (m,

1.25H), 7.89 – 7.80 (m, 2.5H), 7.52 – 7.45 (m, 1.25H), 7.44 – 7.36 (m, 1.25H), 4.03 (s, 3.75H); ^{13}C NMR (100 MHz, $CDCl_3$) δ 165.1, 164.7, 158.2, 158.0, 154.6, 153.8, 139.4, 139.1, 136.5, 136.3, 131.4, 131.1, 131.0, 130.4, 126.4, 126.1, 125.4, 125.3, 122.9, 122.3, 121.7, 121.6, 116.9, 116.4, 116.2, 116.1, 111.4, 110.7, 56.3, 56.2; HRMS (ESI-TOF) (*m/z*) calculated $C_{16}H_{11}N_2O_4^+$: 295.0713, found 295.0712 $[M + H]^+$.

8-(*tert*-Butyl)-13*H*-indazolo[1,2-*b*]phthalazine-6,11,13-trione + 9-(*tert*-Butyl)-13*H*-indazolo[1,2-*b*]phthalazine-6,11,13-trione (1:1) (36qa). Pale yellow solid; yield : 45 mg (82%);

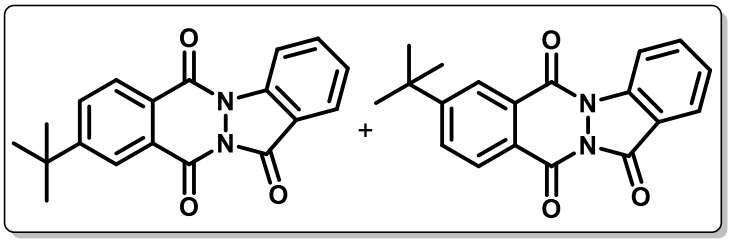

mp 193−195°C; ^{1}H NMR (400 MHz, $CDCl_3$ + DMSO-d_6) δ 8.50 – 8.42 (m, 2H), 8.36 – 8.26 (m, 3H), 8.22 (dd, *J* = 8.2, 2.3 Hz, 1H), 7.97 – 7.90 (m, 2H), 7.89 – 7.81 (m, 2H), 7.77 – 7.70 (m, 2H), 7.40 – 7.34 (m, 2H), 1.35 – 1.30 (m, 18H); ^{13}C NMR (100 MHz, $CDCl_3$ + DMSO-d_6) δ 159.7, 159.1, 158.1, 155.2, 154.8, 154.2, 153.8, 139.2, 136.4, 136.4, 132.6, 132.1, 129.1, 128.6, 128.5, 128.3, 126.3, 126.3, 126.2, 125.6, 125.1, 125.1, 124.9, 116.6, 116.5, 116.1, 116.1, 35.7, 35.7, 30.9; HRMS (ESI-TOF) (*m/z*) calculated $C_{19}H_{17}N_2O_3^+$: 321.1234, found 321.1219 $[M + H]^+$.

8-Bromo-13*H*-indazolo[1,2-*b*]phthalazine-6,11,13-trione + 9-Bromo-13*H*-indazolo[1,2-*b*]phthalazine-6,11,13-trione (1:1) (36ra). Pale yellow solid; yield: 37 mg (68%); mp

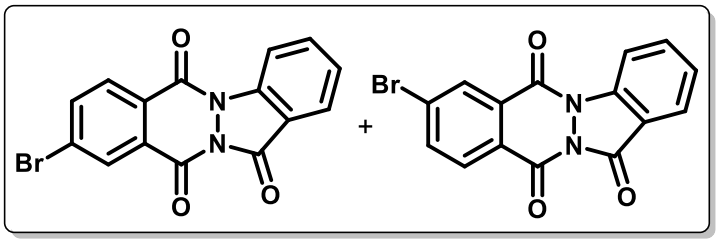

218−219 °C; ^{1}H NMR (400 MHz, $CDCl_3$) δ 8.63 – 8.58 (m, 2H), 8.37 (d, *J* = 8.3 Hz, 1H), 8.10 (d, *J* = 7.8 Hz, 1H), 8.05 (dd, *J* = 8.3, 1.9Hz, 1H), 7.92 – 7.87 (m, 1H), 7.55 – 7.51 (m, 1H), 7.41 – 7.32 (m, 5H), 7.16 – 7.11 (m, 1H), 6.73 (brs, 1H); ^{13}C NMR (100 MHz, $CDCl_3$) δ 158.0, 154.3, 152.6, 139.2, 138.0, 137.9, 136.7, 131.3, 131.0, 130.7, 130.3, 129.3, 127.6, 126.7, 125.5, 124.3, 121.2, 116.6, 116.3; HRMS (ESI-TOF) (*m/z*) calculated $C_{15}H_8BrN_2O_3^+$: 342.9713, found 342.9699 $[M + H]^+$.

7-Fluoro-13*H*-indazolo[1,2-*b*]phthalazine-6,11,13-trione + 10-Fluoro-13*H*-indazolo[1,2-*b*]phthalazine-6,11,13-trione (1:4 or 4:1) (36sa). Pale yellow solid; yield: 35 mg (63%); mp 225−226 °C; ^{1}H NMR (400 MHz, $CDCl_3$ + DMSO-d_6) δ 8.59 (d, J = 8.4 Hz, 0.25H), 8.56 (d, J = 8.4 Hz, 1H), 8.36 (d, J = 7.8 Hz, 0.25H), 8.28 (d, J = 7.8 Hz, 1H), 8.06 (d, 7.8 Hz, 1.25H), 7.95 – 7.89 (m, 1.25H), 7.88 – 7.83 (m, 1.25H), 7.63 – 7.56 (m, 1.25H), 7.52 – 7.46 (m, 1.25H); ^{13}C NMR (100 MHz, $CDCl_3$ + DMSO-d_6) δ 164.2, 157.9, 152.7, 138.8, 136.8, 136.6 ($^{3}J_{C\text{-}F}$ = 9.9 Hz), 136.5, 130.8, 126.7, 126.5, 125.4 ($^{4}J_{C\text{-}F}$ = 1.7 Hz), 124.6 ($^{4}J_{C\text{-}F}$ = 4.0 Hz), 123.2 ($^{2}J_{C\text{-}F}$ = 21.1 Hz), 116.6 ($^{2}J_{C\text{-}F}$ = 36.0 Hz), 116.3; ^{19}F NMR (376 MHz, $CDCl_3$ + DMSO-d_6) δ -106.43, -108.41; HRMS (ESI-TOF) (*m/z*) calculated $C_{15}H_8FN_2O_3^+$: 283.0513, found 283.0510 $[M + H]^+$.

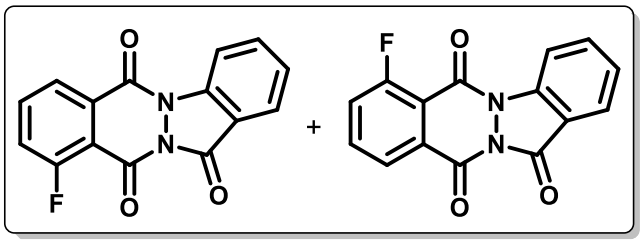

7-Chloro-13*H*-indazolo[1,2-*b*]phthalazine-6,11,13-trione or 10-Chloro-13*H*-indazolo[1,2-*b*]phthalazine-6,11,13-trione (36ta). Pale yellow solid; yield: 36 mg (66%); mp 210−211 °C; ^{1}H NMR (400 MHz, DMSO-d_6) δ 8.47 (d, J = 8.3 Hz, 1H), 8.34 (dd, J = 7.7, 1.4 Hz, 1H), 8.08 – 8.03 (m, 2H), 8.01 – 7.95 (m, 2H), 7.57 (t, J = 7.7 Hz, 1H); ^{13}C NMR (100 MHz, DMSO-d_6) δ 158.2, 153.5, 153.3, 138.7, 138.1, 137.0, 135.7, 135.5, 132.4, 127.7, 126.9, 125.5, 125.2, 117.1, 116.1; HRMS (ESI-TOF) (*m/z*) calculated $C_{15}H_8ClN_2O_3^+$: 299.0218, found 299.0222 $[M + H]^+$.

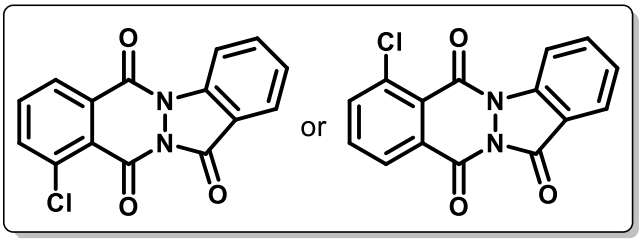

1-(3-(1,4-Dioxo-3,4-dihydrophthalazin-2(1*H*)-yl)phenyl)-3-phenylurea (36ua′). Pale Yellow solid; yield: 56 mg (76%); mp 240−241 °C; ^{1}H NMR (400 MHz, DMSO-d_6) δ 8.60 (s, 1H), 8.57 (s. 1H), 8.54 (s, 1H), 8.01 – 7.92 (m, 4H), 7.39 (d, J = 7.7 Hz, 2H), 7.26 (t, J = 7.5 Hz, 2H), 7.07 (t, J = 8.5 Hz, 1H), 6.95 (t, J = 7.3 Hz, 1H), 6.92 – 6.86 (m, 2H), 6.35 (dd, J = 7.6, 1.5 Hz 1H); ^{13}C NMR (100 MHz, DMSO-d_6) δ 167.0, 152.8, 147.9, 141.0, 140.1, 135.6, 129.9, 129.2, 124.0, 122.3, 118.6, 110.3, 106.4, 102.3; HRMS (ESI-TOF) (*m/z*) calculated $C_{21}H_{17}N_4O_3^+$: 373.1295, found 373.1292 $[M + H]^+$.

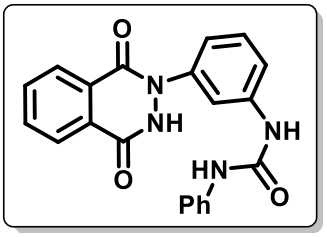

General procedure for the synthesis of *ortho*-amidated *N*-aryl-2,3-dihydrophthalazine-1,4-dione (37)

To an oven-dried sealed tube, *ortho*-substituted 2-aryl-2,3-dihydrophthalazine-1,4-dione (**35i-k,n**) (50 mg, 1 equiv), $[RuCl_2(p\text{-cymene})]_2$ (0.05 equiv), NaOAc (0.5 equiv) and aryl isocyanate (**2**) (1.5 equiv) in DCE (3 mL) were added under N_2 atmosphere. The reaction mixture was allowed to stirr at 80 ^oC for 6 h. On completion of the reaction as indicated by TLC, the reaction was quenched with water and extracted with DCM (2 x 10 mL). The organic layers were combined, dried over anhydrous sodium sulphate and concentrated under reduced pressure to give a crude mixture. The crude mixture was purified by column chromatography using ethyl acetate/hexanes (3:7 to 4:6) as eluent system to afford the desired product (**37**).

2-(1,4-Dioxo-3,4-dihydrophthalazin-2(1*H*)-yl)-3-methyl-*N*-phenylbenzamide (37ia). White solid; yield: 71 mg (96%); mp 210−211 °C; ^{1}H NMR (400 MHz, DMSO-d_6) δ 11.75 (brs, 1H), 10.14 (s, 1H), 8.26 (d, J = 7.6 Hz, 1H), 8.03 – 7.87 (m, 3H), 7.64 – 7.48 (m, 5H), 7.23 (t, J = 7.6 Hz, 2H), 7.01 (J = 7.4 Hz, 1H), 2.18 (s, 3H); ^{13}C NMR (100 MHz, DMSO-d_6) δ 165.4, 163.7, 158.1, 139.6, 136.8, 134.9, 134.0, 133.1, 132.8, 129.3, 129.0, 128.7, 127.2, 126.9, 124.8, 123.9, 120.3, 17.7; HRMS (ESI-TOF) (*m/z*) calculated $C_{22}H_{18}N_3O_3^+$: 372.1343, found 372.1349 $[M + H]^+$.

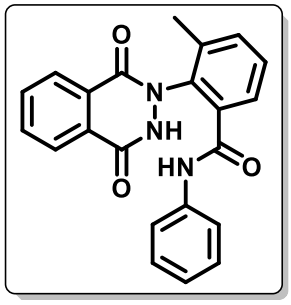

2-(1,4-Dioxo-3,4-dihydrophthalazin-2(1*H*)-yl)-*N*-(2-fluorophenyl)-3-methylbenzamide (37ib). White solid; yield: 66 mg (86%); mp 145−147 °C; ^{1}H NMR (400 MHz, DMSO-d_6) δ 11.83 (brs, 1H), 9.80 (s, 1H), 8.26 (d, J = 7.5 Hz, 1H), 8.05 – 7.87 (m, 3H), 7.68 – 7.48 (m, 4H), 7.26 – 7.04 (m, 3H), 2.17 (s, 3H); ^{13}C NMR (100 MHz, DMSO-d_6) δ 165.4, 158.2, 155.3 ($^1J_{C\text{-}F}$ = 245.4 Hz), 136.9, 134.2, 134.0, 133.3, 132.9, 129.3, 129.0, 128.9, 127.1, 127.1, 126.9 ($^3J_{C\text{-}F}$ = 7.1 Hz), 126.3, 126.0 ($^3J_{C\text{-}F}$ = 11.9 Hz), 124.8, 124.7, 124.6, 120.3, 116.1 ($^2J_{C\text{-}F}$ = 19.5 Hz), 17.6; ^{19}F NMR (376 MHz, DMSO-d_6) δ -122.34; HRMS (ESI-TOF) (*m/z*) calculated $C_{22}H_{17}FN_3O_3^+$: 390.1248, found 372.1227 $[M + H]^+$.

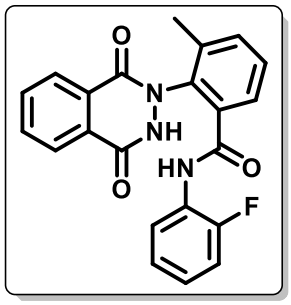

***N*-(3-Chlorophenyl)-2-(1,4-dioxo-3,4-dihydrophthalazin-2(1*H*)-yl)-3-methylbenzamide**

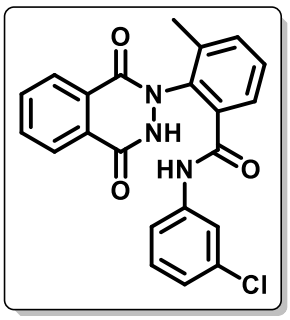

(37ic). White solid; yield: 71 mg (88%); mp 153−154 °C; ^{1}H NMR (400 MHz, DMSO-d_6) δ 11.75 (brs, 1H), 10.41 (s, 1H), 8.25 (d, J = 7.7 Hz, 1H), 8.04 – 7.88 (m, 3H), 7.70 (t, J = 1.6 Hz, 1H), 7.63 – 7.56 (m, 2H), 7.52 (d, J = 7.5 Hz, 1H), 7.50 – 7.44 (m, 1H), 7.28 (t, J = 8.1 Hz, 1H), 7.11 – 7.04 (m, 1H), 2.19 (s, 3H); ^{13}C NMR (100 MHz, DMSO-d_6) δ 165.7, 158.1, 141.1, 136.9, 134.5, 134.0, 133.3, 132.9, 130.8, 129.3, 128.7, 127.2, 126.8, 124.8, 123.7, 119.7, 118.7, 17.7; HRMS (ESI-TOF) (*m/z*) calculated $C_{22}H_{17}ClN_3O_3^+$: 406.0953, found 406.0966 $[M + H]^+$.

2-(1,4-Dioxo-3,4-dihydrophthalazin-2(1*H*)-yl)-3-methyl-*N*-(3(trifluoromethyl)phenyl) benzamide (37id). White solid; yield: 80 mg (92%); mp 155−156 °C; ^{1}H NMR (400 MHz,

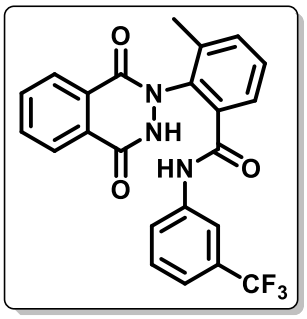

DMSO-d_6) δ 11.76 (brs, 1H), 10.56 (s, 1H), 8.24 (d, J = 7.6 Hz, 1H), 8.03 – 7.88 (m, 4H), 7.81 (d, J = 8.3 Hz, 1H), 7.64 (d, J = 7.2 Hz, 1H), 7.59 (d, J = 6.8 Hz, 1H), 7.55 – 7.46 (m, 2H), 7.37 (d, J = 7.8 Hz, 1H), 2.19 (s, 3H); ^{13}C NMR (100 MHz, DMSO-d_6) δ 165.9, 158.0, 140.3, 136.9, 134.4, 134.0, 133.4, 132.9, 130.3, 129.9, 129.6, 129.3, 128.7, 127.2, 126.8, 125.8, 124.7 (q, $J_{C\text{-}F}$ = 7.5 Hz), 123.8, 123.1, 120.3, 116.4, 17.7; ^{19}F NMR (376 MHz, DMSO-d_6) δ -61.32; HRMS (ESI-TOF) (*m/z*) calculated $C_{23}H_{17}F_3N_3O_3^+$: 440.1217, found 440.1225 $[M + H]^+$.

2-**(1,4-Dioxo-3,4-dihydrophthalazin-2(1*H*)-yl)-3-methyl-*N*-(*p*-tolyl)benzamide (37ie).** White

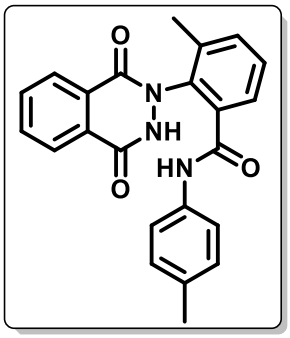

solid; yield: 71 mg (92%); mp 161−162 °C; ^{1}H NMR (400 MHz, DMSO-d_6) δ 11.78 (brs, 1H), 10.08 (s, 1H), 8.25 (d, J = 7.5 Hz, 1H), 8.04 – 7.87 (m, 3H), 7.62 – 7.54 (m, 2H), 7.50 (t, J = 7.5 Hz, 1H), 7.42 (d, J = 8.4 Hz, 2H), 7.03 (d, J = 8.3 Hz, 2H), 2.21 (s, 3H), 2.17 (s, 3H); ^{13}C NMR (100 MHz, DMSO-d_6) δ 165.2, 158.0, 137.1, 136.8, 135.0, 134.0, 133.0, 132.9, 132.8, 129.4, 128.7, 127.2, 126.9, 124.8, 120.2, 20.9, 17.7; HRMS (ESI-TOF) (*m/z*) calculated $C_{23}H_{20}N_3O_3^+$: 386.1499, found 386.1499 $[M + H]^+$.

2-(1,4-Dioxo-3,4-dihydrophthalazin-2(1*H*)-yl)-*N*-(4-methoxyphenyl)-3-methylbenzamide

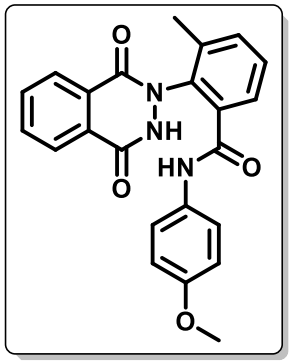

(37if). White solid; yield: 76 mg (95%); mp 172−173 °C; ^{1}H NMR (400 MHz, DMSO-d_6) δ 11.77 (brs, 1H), 10.01 (s, 1H), 8.25 (d, J = 7.6 Hz, 1H), 8.04 – 7.87 (m, 3H), 7.62 – 7.47 (m, 3H), 7.43 (d, J = 9.0 Hz, 2H), 6.81 (d, J = 9.0 Hz, 2H), 3.68 (s, 3H), 2.17 (s, 1H); ^{13}C NMR (100 MHz, DMSO-d_6) δ 165.0, 155.9, 136.8, 135.1, 134.0, 132.9, 132.8, 132.6, 129.3, 128.7, 127.2, 126.8, 124.7, 121.9, 120.4, 114.4, 114.2, 55.6, 17.7; HRMS (ESI-TOF) (*m/z*) calculated $C_{23}H_{20}N_3O_4^+$: 402.1448, found 404.1444 $[M + H]^+$.

***N*-Benzyl-2-(1,4-dioxo-3,4-dihydrophthalazin-2(1*H*)-yl)-3-methylbenzamide (37ig).** White solid; yield: 73 mg (96%); mp 173−174 °C; ^{1}H NMR (400 MHz, DMSO-d_6) δ 11.81 (brs, 1H), 8.56 (t, J = 6.0 Hz, 1H), 8.25 (d, J = 7.6 Hz, 1H), 8.05 – 7.89 (m, 3H), 7.54 – 7.43 (m, 3H), 7.12 (brs, 5H), 4.35 (dd, J = 15.5, 6.5 Hz, 1H), 4.21 (dd, J = 15.4, 5.8 Hz, 1H), 2.14 (s, 3H); ^{13}C NMR (100 MHz, DMSO-d_6) δ 166.8, 158.2, 139.6, 136.7, 135.2, 133.9, 132.8, 132.7, 129.4, 128.9, 128.5, 127.2, 127.1, 126.9, 126.6, 124.7, 42.7, 17.6; HRMS (ESI-TOF) (*m/z*) calculated $C_{23}H_{20}N_3O_3^+$: 386.1499, found 386.1499 $[M + H]^+$.

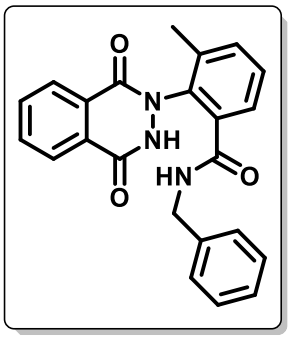

2-(1,4-Dioxo-3,4-dihydrophthalazin-2(1*H*)-yl)-3-methyl-*N*-(naphthalen-1-yl)benzamide

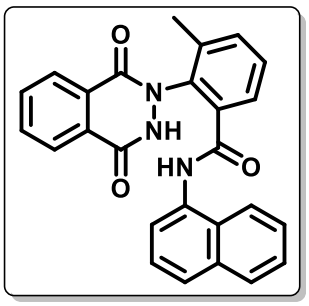

(37ih). White solid; yield: 71 mg (83%); mp 190−191 °C; ^{1}H NMR (400 MHz, DMSO-d_6) δ 11.84 (brs, 1H), 10.25 (s, 1H), 8.32 (d, J = 7.3 Hz, 1H), 8.02 – 7.86 (m, 5H), 7.79 (t, J = 7.4 Hz, 2H), 7.62 – 7.52 (m, 2H), 7.50 – 7.41 (m, 3H), 7.37 (t, J = 7.8 Hz, 1H), 2.23 (s, 3H); ^{13}C NMR (100 MHz, DMSO-d_6) δ 166.6, 158.2, 136.8, 135.3, 134.1, 134.1, 134.0, 132.9, 132.8, 129.7, 129.4, 128.9, 128.3, 127.2, 126.8, 126.8, 126.5, 126.5, 126.4, 126.4, 125.9, 124.7, 124.1, 123.5, 121.9, 118.1, 17.7; HRMS (ESI-TOF) (*m/z*) calculated $C_{26}H_{20}N_3O_3^+$: 422.1499, found 422.1500 $[M + H]^+$.

2-(1,4-Dioxo-3,4-dihydrophthalazin-2(1*H*)-yl)-3-ethyl-*N*-phenylbenzamide (37ja). White solid; yield: 67 mg (93%); mp 189−190 °C; ^{1}H NMR (400 MHz, DMSO-d_6) δ 11.76 (brs, 1H), 10.17 (s, 1H), 8.25 (d, J = 7.7 Hz, 1H), 8.04 – 7.87 (m, 3H), 7.62 – 7.50 (m, 5H), 7.23 (t, J = 7.6 Hz, 2H), 7.01 (t, J = 7.3 Hz, 1H), 2.54 (q, J = 3.4 Hz, 2H), 1.09 (t, J = 7.6 Hz, 3H); ^{13}C NMR (100 MHz, DMSO-d_6) δ 165.5, 158.4, 142.5, 139.6, 135.1, 134.0, 132.9, 131.6, 129.3, 129.0, 127.2, 126.9, 124.7, 123.9, 120.2, 24.3, 14.9; HRMS (ESI-TOF) (*m/z*) calculated $C_{23}H_{20}N_3O_3^+$: 386.1499, found 386.1498 [M + H]$^+$.

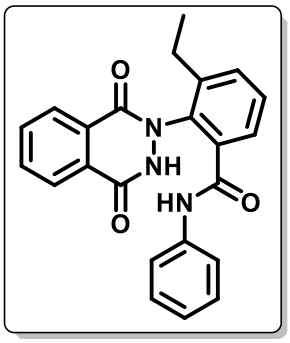

2-(1,4-Dioxo-3,4-dihydrophthalazin-2(1*H*)-yl)-3-ethyl-*N*-(naphthalen-1-yl)benzamide (37jh). White solid; yield: 69 mg (84%); mp 204−205 °C; ^{1}H NMR (400 MHz, DMSO-d_6) δ 11.83 (brs, 1H), 10.26 (s, 1H), 8.32 (J = 7.4 Hz, 1H), 8.00 (d, J = 7.8 Hz, 2H), 7.97 – 7.85 (m, 3H), 7.82 – 7.73 (m, 2H), 7.64 – 7.58 (m, 2H), 7.51 – 7.42 (m, 3H), 7.38 (t, J = 7.8 Hz, 1H), 2.63 – 2.54 (m, 2H), 1.14 (t, J = 7.5 Hz, 3H); ^{13}C NMR (100 MHz, DMSO-d_6) δ 166.7, 158.6, 142.5, 135.5, 134.8, 134.2, 134.2, 134.1, 134.0, 132.8, 131.5, 129.8, 129.4, 129.1, 128.9, 128.2, 127.2, 126.8, 126.4, 126.3, 125.9, 124.2, 124.1, 123.4, 121.9, 118.0, 24.3, 14.9; HRMS (ESI-TOF) (*m/z*) calculated $C_{27}H_{22}N_3O_3^+$: 436.1656, found 436.1638 [M + H]$^+$.

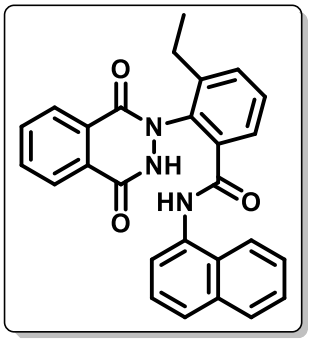

3-Bromo-2-(1,4-dioxo-3,4-dihydrophthalazin-2(1*H*)-yl)-*N*-phenylbenzamide (37ka). White solid; yield: 36 mg (52%); mp 249−250 °C; ^{1}H NMR (400 MHz, DMSO-d_6) δ) 11.87 (brs, 1H), 10.32 (s, 1H), 8.25 (d, J = 7.8 Hz, 1H), 8.04 – 7.95 (m, 3H), 7.93 – 7.88 (m, 1H), 7.81 (d, J = 7.6 Hz, 1H), 7.60 – 7.51 (m, 3H), 7.25 (t, J = 7.6 Hz, 2H), 7.03 (t, J = 7.4 Hz, 1H); ^{13}C NMR (100 MHz, DMSO-d_6) δ 164.1, 157.9, 139.3, 137.1, 135.3, 134.3, 133.0, 130.8, 129.1, 128.7, 127.2, 124.9, 124.2, 123.9, 120.3; HRMS (ESI-TOF) (*m/z*) calculated $C_{21}H_{15}BrN_3O_3^+$: 436.0291, found 436.0271 [M + H]$^+$.

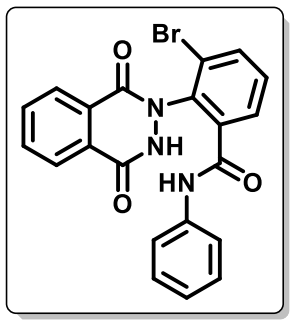

2-(1,4-Dioxo-3,4-dihydrophthalazin-2(1*H*)-yl)-3,5-dimethyl-*N*-phenylbenzamide (37na).

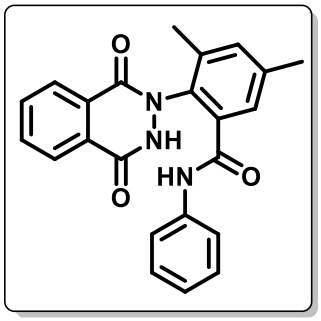

White solid; yield: 70 mg (97%); mp 275−276 °C; ^{1}H NMR (400 MHz, DMSO-d_6) δ 11.72 (brs, 1H), 10.10 (s, 1H), 8.24 (d, J = 7.6 Hz, 1H), 8.03 – 7.86 (m, 3H), 7.53 (d, J = 7.9 Hz, 2H), 7.42 (s, 1H), 7.37 (s, 1H), 7.23 (t, J = 7.6 Hz, 2H), 7.01 (t, J = 7.4 Hz, 1H), 2.42 (s, 3H), 2.13 (s, 3H); ^{13}C NMR (100 MHz, DMSO-d_6) δ 165.4, 158.1, 139.6, 138.2, 136.5, 134.7, 133.9, 133.4, 132.8, 129.3, 129.0, 127.3, 127.2, 124.8, 123.9, 120.2, 21.1, 17.6; HRMS (ESI-TOF) (*m/z*) calculated $C_{23}H_{20}N_3O_3^+$: 386.1499, found 386.1502 $[M + H]^+$.

2-(1,4-Dioxo-3,4-dihydrophthalazin-2(1*H*)-yl)-*N*-(2-fluorophenyl)-3,5-dimethylbenzamide (37nb). White solid; yield: 64 mg (85%); mp 202−203 °C; ^{1}H NMR (400 MHz, DMSO-d_6) δ 11.79

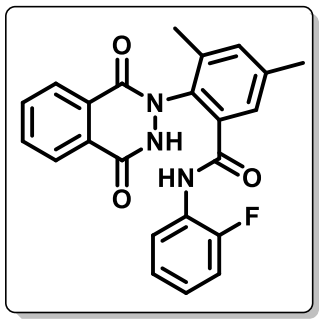

(brs, 1H), 9.72 (s, 1H), 8.26 (d, J = 7.5 Hz, 1H), 8.03 – 7.87 (m, 3H), 7.52 (t, J = 8.6 Hz, 1H), 7.48 (s, 1H), 7.39 (s, 1H), 7.20 – 7.13 (m, 2H), 7.12 – 7.06 (m, 1H), 2.43 (s, 3H), 2.13 (s, 3H); ^{13}C NMR (100 MHz, DMSO-d_6) δ 165.5, 158.3, 155.2 ($^{1}J_{C\text{-}F}$ = 245 Hz), 138.4, 136.6, 134.7, 134.0, 133.7, 132.8, 129.3, 129.0, 127.2, 127.6, 126.8 ($^{3}J_{C\text{-}F}$ = 7.6 Hz), 126.1, 126.0, 124.8, 124.7, 124.6, 120.2, 116.1 ($^{2}J_{C\text{-}F}$ = 19.4 Hz), 21.1, 17.6; ^{19}F NMR (376 MHz, DMSO-d_6) δ -122.48; HRMS (ESI-TOF) (*m/z*) calculated $C_{23}H_{19}FN_3O_3^+$: 404.1405, found 404.1415 $[M + H]^+$.

***N*-(3-Chlorophenyl)-2-(1,4-dioxo-3,4-dihydrophthalazin-2(1*H*)-yl)-3,5-dimethylbenzamide**

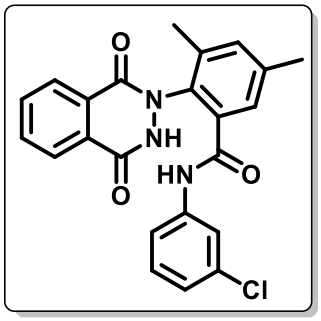

(37nc). White solid; yield: 70 mg (89%); mp 231−232 °C; ^{1}H NMR (400 MHz, DMSO-d_6) δ 11.73 (brs, 1H), 10.38 (s, 1H), 8.24 (d, J = 7.7 Hz, 1H), 8.04 – 7.87 (m, 3H), 7.70 (t, J = 2.2 Hz, 1H), 7.47 (d, J = 8.4 Hz, 1H), 7.42 (s, 1H), 7.39 (s, 1H), 7.28 (t, J = 8.1 Hz, 1H), 7.08 (dd, J = 7.8, 1.1 Hz, 1H), 2.43 (s, 3H), 2.14 (s, 3H); ^{13}C NMR (100 MHz, DMSO-d_6) δ 165.8, 158.1, 141.1, 138.2, 136.6, 134.2, 134.0, 133.7, 133.3, 132.8, 130.7, 129.3, 127.3, 127.2, 124.8, 123.6, 119.6, 118.6, 21.1, 17.6; HRMS (ESI-TOF) (*m/z*) calculated $C_{23}H_{19}ClN_3O_3^+$: 420.1109, found 420.1118 $[M + H]^+$.

***N*-Benzyl-2-(1,4-dioxo-3,4-dihydrophthalazin-2(1*H*)-yl)-3,5-dimethylbenzamide (37ng)**.

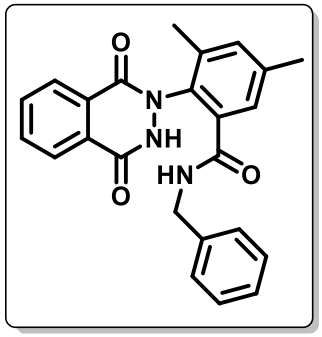

White solid; yield: 73 mg (97%); mp 172−173 °C; ^{1}H NMR (400 MHz, DMSO-d_6) δ 11.77 (brs, 1H), 8.52 (t, J = 6.1 Hz, 1H), 8.24 (d, J = 7.4 Hz, 1H), 8.05 – 7.87 (m, 3H), 7.32 (s, 2H), 7.11 (s, 5H), 4.34 (dd, J = 15.4, 6.4 Hz, 1H), 4.18 (dd, J = 15.4, 5.7 Hz, 1H), 2.38 (s, 3H), 2.09 (s, 3H); ^{13}C NMR (100 MHz, DMSO-d_6) δ 166.9, 158.6, 141.3, 139.6, 138.3, 136.4, 134.9, 133.8, 133.1, 132.7, 129.4, 128.7, 128.5, 127.5, 127.2, 127.1, 127.1, 127.0, 126.9, 124.8, 42.7, 21.1, 17.5; HRMS (ESI-TOF) (*m/z*) calculated $C_{24}H_{22}N_3O_3^+$: 400.1656, found 400.1639 $[M + H]^+$.

Procedure for the synthesis of 36aa′

To an oven-dried sealed tube with a screw cap (PTFE) charged with **36aa** (30 mg, 1 equiv) in distilled THF (3 mL) at 0 °C, lithium aluminium hydride (2 equiv) was added. The reaction mixture was allowed to stir at 25 °C for 4 h. On completion of the reaction as indicated by TLC, the reaction was quenched with water and extracted with DCM (2 x 10 mL). The organic layers were combined, dried over anhydrous sodium sulphate and concentrated under reduced pressure. The crude mixture was purified by column chromatography using ethyl acetate/hexanes (3:7) as eluent system to afford the desired product (**36aa′**).

13-Hydroxy-13*H*-indazolo[1,2-*b*]phthalazine-6,11-dione (36aa'). White solid; yield: 22 mg (72%); mp 122−124 °C; ^{1}H NMR (400 MHz, DMSO-d_6) δ 8.41 (d, J = 8.2 Hz, 1H), 8.17 (d, J = 7.7 Hz, 1H), 7.95 (d, J = 7.8 Hz, 1H), 7.88 (t, J = 8.1 Hz, 1H), 7.84 – 7.75 (m, 2H), 7.69 (t, J = 7.6 Hz, 1H), 7.55 – 7.48 (m, 2H), 6.86 (d, J = 7.2 Hz, 1H); ^{13}C NMR (100 MHz, DMSO-d_6) δ 161.6, 157.4, 140.8, 137.3, 135.2, 134.8, 130.3, 128.4, 127.9, 126.1, 125.5, 124.3, 118.4, 115.9, 72.9; HRMS (ESI-TOF) (*m/z*) calculated $C_{15}H_{11}N_2O_3^+$: 267.0764, found 267.0765 $[M + H]^+$.

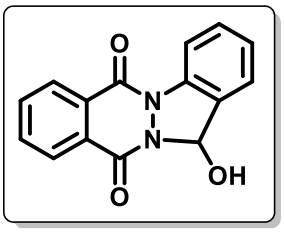

Procedure for the synthesis of 36aa″ or 37ia″

To an oven-dried sealed tube with a screw cap (PTFE) charged with **36aa** or **37ia** (30 mg, 1 equiv) in toluene (3 mL), Lawesson's reagent (2 equiv) was added. The reaction mixture was allowed to stir at 80 °C for 4 h. On completion of the reaction as indicated by TLC , the reaction was quenched with water, and extracted with DCM (2 x 10 mL). The organic layers were combined, dried over anhydrous sodium sulphate and concentrated under reduced pressure. The crude mixture was

purified by column chromatography using ethyl acetate/hexanes (1:9) as eluent system to afford the desired product (**36aa′′ or 37ia′′**).

13-Thioxo-13*H*-indazolo[1,2-*b*]phthalazine-6,11-dione (36aa′′). Yellow solid; yield: 29 mg (93%); mp 230−231 °C; ^{1}H NMR (400 MHz, $CDCl_3$) δ 8.65 – 8.58 (m, 2H), 8.52 – 8.46 (m, 1H), 8.17 (d, J = 7.9 Hz, 1H), 8.03 – 7.95 (m, 2H), 7.87 (t, J = 7.8 Hz, 1H), 7.50 (t, J = 7.6 Hz, 1H); ^{13}C NMR (100 MHz, $CDCl_3$) δ 179.6, 155.3, 152.9, 137.8, 135.7, 135.2, 134.9, 129.9, 129.1, 128.4, 128.3, 128.1, 126.9, 125.7, 115.9; HRMS (ESI-TOF) (*m/z*) calculated $C_{15}H_9N_2O_2S^+$: 281.0379, found 281.0379 $[M + H]^+$.

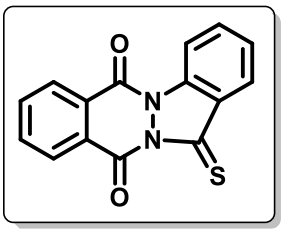

2-(1,4-Dioxo-3,4-dihydrophthalazin-2(1*H*)-yl)-3-methyl-*N*-phenylbenzothioamide (37ia′′). Yellow solid; yield: 28 mg (89%); mp 152−153 °C; ^{1}H NMR (400 MHz, $CDCl_3$) δ 9.95 (s, 1H), 8.52 (d, J = 7.7 Hz, 1H), 8.36 (s, 1H), 7.92 – 7.82 (m, 2H), 7.80 – 7.70 (m, 3H), 7.65 (d, J = 6.6 Hz, 1H), 7.49 – 7.40 (m, 2H), 7.25 (t, J = 7.6 Hz, 2H), 7.12 (t, J = 7.4 Hz, 1H), 2.13 (s, 3H); ^{13}C NMR (100 MHz, $CDCl_3$) δ 195.4, 161.1, 143.4, 139.8, 138.7, 136.2, 134.6, 134.1, 132.3, 131.9, 129.8, 129.6, 128.7, 127.8, 127.6, 126.8, 126.6, 126.4, 122.3, 17.5; HRMS (ESI-TOF) (*m/z*) calculated $C_{22}H_{18}N_3O_2S^+$: 388.1114, found 388.1118 $[M + H]^+$.

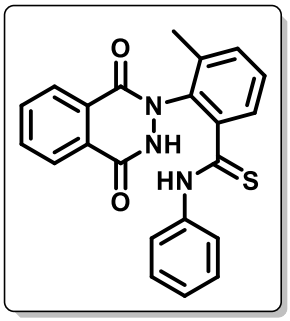

Procedure for the synthesis of 37ia′

To an oven-dried sealed tube with a screw cap (PTFE) charged with **37ia** (30 mg, 1 equiv) in TFE (3 mL) at 0 ºC, PIDA (1 equiv) was added. The reaction mixture was allowed to stir at 0 ºC for 0.5 h. On completion of the reaction as indicated by TLC, the reaction was quenched with water, and extracted with DCM (2 x 10 mL). The organic layers were combined, dried over anhydrous sodium sulphate and concentrated under reduced pressure to afford pure desired product (**37ia′**).

1-Methyl-6-phenylbenzo[5,6][1,2,3]triazino[1,2-*b*]phthalazine-5,8,13(6*H*)-trione (37ia′). Pale yellow solid; yield: 28 mg (95%); mp 235−237 °C; ^{1}H NMR (400 MHz, $CDCl_3$) δ 7.90 (dd, J = 7.2, 0.8 Hz, 1H), 7.84 – 7.74 (m, 6H), 7.46 – 7.37 (m, 4H), 7.27 – 7.22 (m, 1H), 2.28 (s, 3H); ^{13}C NMR (100 MHz, $CDCl_3$) δ 164.1, 161.2, 148.0, 135.1, 133.9, 129.0, 128.9, 126.9, 126.6, 124.5, 124.1, 123.6, 122.3, 122.1, 16.3; HRMS (ESI-TOF) (*m/z*) calculated $C_{22}H_{16}N_3O_3^+$: 370.1186, found 370.1178 $[M + H]^+$.

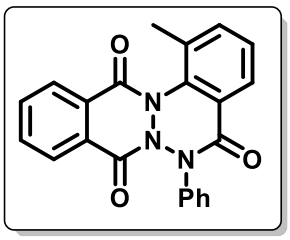

Procedure for the synthesis of [Ru(*p*-Cymene)(Phthalazine-dione)Py] complex (B′)[68]

To an oven-dried sealed tube with a screw cap (PTFE) charged with $[RuCl_2(p\text{-cymene})]_2$ (50 mg, 1 equiv) in DCM (20 mL) at room temperature, pyridine (12.91 mg, 2 equiv) was added. After vigorous stirring for 4 h, NaOAc (16.86 mg, 2.5 equiv), **35a** (29.06 mg, 1.5 equiv) and NEt_3 (1 mL) were added to the solution. The stirring was continued for additional 20 h, after which silica gel (60-120 mesh) was added to the flask and the solvent was concentrated under reduced pressure to obtain a dry slurry, whcih was subjected to column chromatography using ethyl acetate/hexanes (1:1) as eluent system to afford **B′** in 64% yield.

[Ru(*p*-Cymene)(Phthalazine-dione)Py] complex. Dark green solid; yield: 74 mg (64%); mp 195−200 °C ^{1}H NMR (400 MHz, $CDCl_3$) δ 8.90 (d, J = 5.0 Hz, 2H), 8.69 (dd, J = 1.5, 7.8 Hz, 1H),

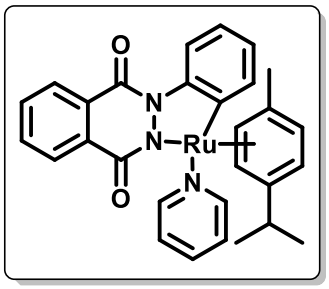

8.39 – 8.34 (m, 2H), 8.12 (dd, J = 7.8, 1.5 Hz, 1H), 7.81 – 7.74 (m, 1H), 7.70 – 7.65 (m, 1H), 7.75 – 7.48 (m, 1H), 7.13 – 7.02 (m, 4H), 6.10 (d, J = 5.9 Hz, 1H), 5.97 (d, J = 5.8 Hz, 1H), 5.75 (d, J = 5.6 Hz, 1H), 4.89 (d, J = 5.2 Hz, 1H), 2.21 – 2.15 (m, 1H), 1.56 (s, 3H), 0.89 (d, J = 6.9 Hz, 3H), 0.83 (d, J = 6.9 Hz, 3H); ^{13}C NMR (100 MHz, $CDCl_3$) δ 161.7, 159.2, 158.0, 153.8, 147.9, 137.1, 135.6, 131.1, 129.8, 129.0, 128.0, 127.8, 126.0, 125.3, 125.3, 123.7, 123.4, 122.5, 117.9, 103.1, 96.7, 93.3, 93.1, 93.0, 88.6, 78.7, 29.9, 21.9, 21.1, 17.0; HRMS (ESI-TOF) (*m/z*) calculated $C_{29}H_{28}N_3O_2Ru^+$: 570.1061, found 570.1106 $[M + H]^+$.

Procedure for deuterium labelling studies

To an oven-dried sealed tube charged with 3 mL of DCE:D_2O (2:1), **35b** or **35i** (1 equiv), $[RuCl_2(p\text{-cymene})]_2$ (0.05 equiv), NaOAc (0.5 equiv) were added. The reaction was allowed to stir at 40 ºC for 4 h. The reaction was cooled to room temperature, quenched with water and extracted with DCM (2 x 15 mL). The organic layers were combined, dried over anhydrous sodium sulphate and concentrated under reduced pressure. Purification by column chromatography using ethyl acetate/hexanes (3:7) as eluent afforded the desired product (**35b**/**35b-*d*$_2$**) in 77% yield or **35i**/**35i-*d*$_1$** in 74% yield. The deuteration content was confirmed using ^{1}H NMR analysis.

Parallel Experiments

For the first set, to an oven-dried sealed tube with a screw cap (PTFE), **35i** (25.23 mg, 0.1 mmol), $[RuCl_2(p\text{-cymene})]_2$ (3.06 mg, 0.005 mmol), NaOAc (4.13 mg, 0.05 mmol), phenyl isocyanate (**2a**) (17.86 mg, 0.15 mmol) and DCE (3 mL) were added under N_2 atmosphere. For the parallel

second set, **35i-*d*$_1$** was used (instead of **35i**) under standard conditions. The sealed tubes were capped and the reaction mixtures were allowed to stir at 80 ºC for 15, 30, 60, 90 and 120 mins. Reaction fractions were collected at regular time intervals, filtered and concentrated under reduced pressure. The product conversion percentage was determined by ^{1}H NMR analysis. The KIE was calculated as k_H/k_D = 1.52.

Intermolecular competitive experiment

To an oven-dried sealed tube with a screw cap (PTFE), **35b** (25.23 mg, 0.1 mmol), (**35b-*d*$_2$**) (25.43 mg, 0.1 mmol), [RuCl$_2$(*p*-cymene)]$_2$ (3.06 mg, 0.005 mmol) NaOAc (4.13 mg, 0.05 mmol), phenyl isocyanate (**2a**) (17.86 mg, 0.15 mmol) and DCE (3 mL) were added under N_2 atmosphere. The sealed tube was capped and the reaction mixture was allowed to stir at 40 ºC for 2 h, the reaction was cooled to room temperature, quenched with water and extracted with DCM (2 x 15 mL). The organic layers were combined, dried over anhydrous sodium sulphate and concentrated *in vacuo*. The crude residue was purified by column chromatography using ethyl acetate/hexanes (1:9) as eluent afforded the desired product in combined yield (**36ba**:**36ba-*d*$_1$**) in 68% yield. The intermolecular P_H/P_D was found to be 3.2.

5.4 Single Crystal X-ray Diffraction Studies

In each case a suitable crystal was mounted in a nylon loop attached to a goniometer head for initial crystal evaluation and data collection were performed on a Kappa APEX II diffractometer equipped with a CCD detector (with the crystal-to-detector distance fixed at 60 mm) and sealed-tube monochromated MoKα radiation using the program APEX2.[69] Data were integrated, reflections were fitted and values of F^2 and $\sigma(F^2)$ for each reflection were obtained by using the program SAINT.[69] Data were also corrected for Lorentz and polarization effects. The subroutine XPREP[69] was used for the processing of data that included determination of space group, application of an absorption correction (SADABS),[69] merging of data, and generation of files necessary for solution and refinement. The crystal structure was solved by direct methods using the SHELXS program of the SHELXTL package and was refined using SHELXL[70,71] refinement package in Olex2.[72] All non-hydrogen atoms were refined with anisotropic displacement parameters. All hydrogen atoms were placed in ideal positions and refined as riding atoms with individual isotropic displacement parameters. Compound **37ng**, which crystallizes with a lattice water molecule in the chiral $P2_1$ space group, exists as a racemic mixture. All figures were drawn using MERCURY V 3.0[73] and DIAMOND V 4.5.0[74]

5.4.1. Crystal data for 36na (CCDC No. 2023522). $C_{17}H_{12}N_2O_3$, Mr = 292.29 g/mol, monoclinic, space group $P2_1/c$, a = 9.4454(3) Å, b = 10.6990(4) Å, c = 13.0108(5) Å, α = 90°, β = 95.422(2)°, γ = 90°, V = 1308.94(8) Å^3, Z = 4, D_{calcd} = 1.483 g/cm^3, T = 298(2) K; Full matrix least-square on F^2; R_1 = 0.0379, wR_2 = 0.1012 for 1812 observed reflections [I > 2σ(I)] and R_1 = 0.0463, wR_2 = 0.1087 for all 2303 reflections; GOF = 1.054.

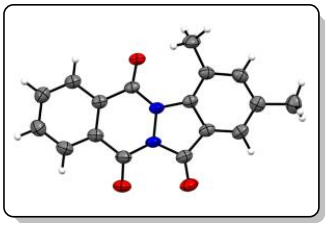

5.4.2. Crystal data for 37ng (CCDC No. 2023523). $C_{24}H_{23}N_3O_4$, Mr = 417.45 g/mol, monoclinic, space group $P2_1$, a = 9.2987(5) Å, b = 9.1501(5) Å, c = 12.3596(7) Å, α = 90°, β = 98.331(3)°, γ = 90°, V = 1040.51(9) Å^3, Z = 2, , D_{calcd} = 1.332 g/cm^3, T = 298(2) K; Full matrix least-square on F^2; R_1 = 0.0577, wR_2 = 0.1530 for 3113 observed reflections [I > 2σ(I)] and R_1 = 0.0617, wR_2 = 0.1592 for all 3432 reflections; GOF = 1.038.

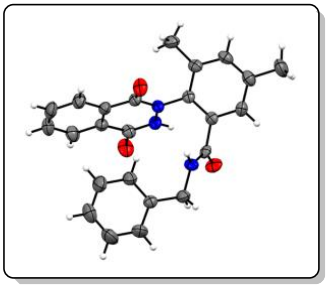

5.5 References

(1) Greenberg, A.; Breneman, C. M.; Liebman, J. F. *The Amide Linkage: Structural Significance in Chemistry, Biochemistry, and Materials Science*; John Wiley & Sons, **2000**.

(2) Roughley, S. D.; Jordan, A. M. *Journal of Medicinal Chemistry* **2011**, *54*, 3451-3479.

(3) Dunetz, J. R.; Magano, J.; Weisenburger, G. A. *Organic Process Research & Development* **2016**, *20*, 140-177.

(4) Brown, D. G.; Bostrom, J. *Journal of Medicinal Chemistry* **2016**, *59*, 4443-4458.

(5) Carey, J. S.; Laffan, D.; Thomson, C.; Williams, M. T. *Organic & Biomolecular Chemistry* **2006**, *4*, 2337-2347.

(6) Díaz, A.; Katsarava, R.; Puiggalí, J. *International Journal of Molecular Sciences* **2014**, *15*, 7064-7123.

(7) Chaudhari, M. B.; Gnanaprakasam, B. *Chemistry–An Asian Journal* **2019**, *14*, 76-93.

(8) Ackermann, L. *Chemical Reviews* **2011**, *111*, 1315-1345.

(9) Cho, S. H.; Kim, J. Y.; Kwak, J.; Chang, S. *Chemical Society Reviews* **2011**, *40*, 5068-5083.

(10) Baudoin, O. *Chemical Society Reviews* **2011**, *40*, 4902-4911.

(11) Mousseau, J. J.; Charette, A. B. *Accounts of Chemical Research* **2013**, *46*, 412-424.

(12) Ren, Y.; Liu, Y.; Gao, S.; Dong, X.; Xiao, T.; Jiang, Y. *Tetrahedron* **2020**, *76*, 130985.

(13) Guo, S.; Liu, Y.; Wang, Y.; Zhang, X.; Fan, X. *The Journal of Organic Chemistry* **2020**, *85*, 8910-8922.

(14) Zhou, Y.; Liang, H.; Sheng, Y.; Wang, S.; Gao, Y.; Zhan, L.; Zheng, Z.; Yang, M.; Liang, G.; Zhou, J. *The Journal of Organic Chemistry* **2020**, *85*, 9230-9243.

(15) Lian, Y.; Huber, T.; Hesp, K. D.; Bergman, R. G.; Ellman, J. A. *Angewandte Chemie International Edition* **2013**, *52*, 629-633.

(16) Arockiam, P. B.; Bruneau, C.; Dixneuf, P. H. *Chemical Reviews* **2012**, *112*, 5879-5918.

(17) Lyons, T. W.; Sanford, M. S. *Chemical Reviews* **2010**, *110*, 1147-1169.

(18) Wu, X.-F.; Neumann, H.; Beller, M. *Chemical Reviews* **2013**, *113*, 1-35.

(19) Beller, M.; Cornils, B.; Frohning, C. D.; Kohlpaintner, C. W. *Journal of Molecular Catalysis A: Chemical* **1995**, *104*, 17-85.

(20) Liu, Q.; Zhang, H.; Lei, A. *Angewandte Chemie International Edition* **2011**, *50*, 10788-10799.

(21) Zhang, L.; Wang, C.; Han, J.; Huang, Z.-B.; Zhao, Y. *The Journal of Organic Chemistry* **2016**, *81*, 5256-5262.

(22) Raab, V.; Merz, M.; Sundermeyer, J. *Journal of Molecular Catalysis A: Chemical* **2001**, *175*, 51-63.

(23) Casiello, M.; Monopoli, A.; Cotugno, P.; Milella, A.; Dell'Anna, M. M.; Ciminale, F.; Nacci, A. *Journal of Molecular Catalysis A: Chemical* **2014**, *381*, 99-106.

(24) Liu, J.; Zhang, R.; Wang, S.; Sun, W.; Xia, C. *Organic Letters* **2009**, *11*, 1321-1324.

(25) Kapoor, M. P.; Matsumura, Y. *Catalysis Today* **2004**, *93*, 287-291.

(26) Hasegawa, N.; Charra, V.; Inoue, S.; Fukumoto, Y.; Chatani, N. *Journal of the American Chemical Society* **2011**, *133*, 8070-8073.

(27) Hasegawa, N.; Shibata, K.; Charra, V.; Inoue, S.; Fukumoto, Y.; Chatani, N. *Tetrahedron* **2013**, *69*, 4466-4472.

(28) Du, Y.; Hyster, T. K.; Rovis, T. *Chemical Communications* **2011**, *47*, 12074-12076.

(29) Grigorjeva, L.; Daugulis, O. *Organic Letters* **2014**, *16*, 4688-4690.

(30) Williamson, P.; Galván, A.; Gaunt, M. J. *Chemical Science* **2017**, *8*, 2588-2591.

(31) Barsu, N.; Bolli, S. K.; Sundararaju, B. *Chemical Science* **2017**, *8*, 2431-2435.

(32) Wu, X.; Miao, J.; Li, Y.; Li, G.; Ge, H. *Chemical Science* **2016**, *7*, 5260-5264.

(33) Wu, X.; Zhao, Y.; Ge, H. *Journal of the American Chemical Society* **2015**, *137*, 4924-4927.

(34) Nageswar Rao, D.; Rasheed, S.; Das, P. *Organic Letters* **2016**, *18*, 3142-3145.

(35) Ling, F.; Ai, C.; Lv, Y.; Zhong, W. *Advanced Synthesis & Catalysis* **2017**, *359*, 3707-3712.

(36) Ni, J.; Li, J.; Fan, Z.; Zhang, A. *Organic Letters* **2016**, *18*, 5960-5963.

(37) Nguyen, T. T.; Grigorjeva, L.; Daugulis, O. *Chemical Communications* **2017**, *53*, 5136-5138.

(38) Fu, L.-Y.; Ying, J.; Wu, X.-F. *The Journal of Organic Chemistry* **2019**, *84*, 12648-12655.

(39) Jiang, L.-B.; Qi, X.; Wu, X.-F. *Tetrahedron Letters* **2016**, *57*, 3368-3370.

(40) Morimoto, T.; Fuji, K.; Tsutsumi, K.; Kakiuchi, K. *Journal of the American Chemical Society* **2002**, *124*, 3806-3807.

(41) Shibata, T.; Toshida, N.; Takagi, K. *The Journal of Organic Chemistry* **2002**, *67*, 7446-7450.

(42) Li, X.-F.; Shi, L.-F.; Zhang, X.-G.; Zhang, X.-H. *Organic & Biomolecular Chemistry* **2018**, *16*, 6438-6442.

(43) Muralirajan, K.; Parthasarathy, K.; Cheng, C.-H. *Organic Letters* **2012**, *14*, 4262-4265.

(44) Shakoor, S. A.; Kumari, S.; Khullar, S.; Mandal, S. K.; Kumar, A.; Sakhuja, R. *The Journal of Organic Chemistry* **2016**, *81*, 12340-12349.

(45) Geng, X.; Wang, C. *Organic & Biomolecular Chemistry* **2015**, *13*, 7619-7623.

(46) Han, S.; Mishra, N. K.; Sharma, S.; Park, J.; Choi, M.; Lee, S.-Y.; Oh, J. S.; Jung, Y. H.; Kim, I. S. *The Journal of Organic Chemistry* **2015**, *80*, 8026-8035.

(47) Jeong, T.; Han, S.; Mishra, N. K.; Sharma, S.; Lee, S.-Y.; Oh, J. S.; Kwak, J. H.; Jung, Y. H.; Kim, I. S. *The Journal of Organic Chemistry* **2015**, *80*, 7243-7250.

(48) Hummel, J. R.; Ellman, J. A. *Organic Letters* **2015**, *17*, 2400-2403.

(49) Liu, W.; Bang, J.; Zhang, Y.; Ackermann, L. *Angewandte Chemie* **2015**, *127*, 14343-14346.

(50) Ozaki, S. *Chemical Reviews* **1972**, *72*, 457-496.

(51) Villa, J.; Powell, H. *Inorganica Chimica Acta* **1979**, *32*, 199-204.

(52) Braunstein, P.; Nobel, D. *Chemical Reviews* **1989**, *89*, 1927-1945.

(53) Kuninobu, Y.; Tokunaga, Y.; Kawata, A.; Takai, K. *Journal of the American Chemical Society* **2006**, *128*, 202-209.

(54) Schleicher, K. D.; Jamison, T. F. *Organic Letters* **2007**, *9*, 875-878.

(55) Miura, T.; Mikano, Y.; Murakami, M. *Organic Letters* **2011**, *13*, 3560-3563.

(56) Hesp, K. D.; Bergman, R. G.; Ellman, J. A. *Journal of the American Chemical Society* **2011**, *133*, 11430-11433.

(57) De Sarkar, S.; Ackermann, L. *Chemistry–A European Journal* **2014**, *20*, 13932-13936.

(58) Shi, X. Y.; Renzetti, A.; Kundu, S.; Li, C. J. *Advanced Synthesis & Catalysis* **2014**, *356*, 723-728.

(59) Shi, X. Y.; Liu, K. Y.; Fan, J.; Dong, X. F.; Wei, J. F.; Li, C. J. *Chemistry–A European Journal* **2015**, *21*, 1900-1903.

(60) Fiorito, D.; Liu, Y.; Besnard, C.; Mazet, C. *Journal of the American Chemical Society* **2019**, *142*, 623-632.

(61) Han, J.; Wang, N.; Huang, Z.-B.; Zhao, Y.; Shi, D.-Q. *The Journal of Organic Chemistry* **2017**, *82*, 6831-6839.

(62) Hegab, M. I.; Taleb, N. A. A.; Hasabelnaby, S. M.; Goudah, A. *European Journal of Medicinal Chemistry* **2010**, *45*, 1267-1277.

(63) Kim, J. S.; Lee, H.-J.; Suh, M.-E.; Choo, H.-Y. P.; Lee, S. K.; Park, H. J.; Kim, C.; Park, S. W.; Lee, C.-O. *Bioorganic & Medicinal Chemistry* **2004**, *12*, 3683-3686.

(64) Chate, A. V.; Bhadke, P. K.; Khande, M. A.; Sangshetti, J. N.; Gill, C. H. *Chinese Chemical Letters* **2017**, *28*, 1577-1582.

(65) Karishma, P.; Gogia, A.; Mandal, S. K.; Sakhuja, R. *Advanced Synthesis & Catalysis* **2021**, *363*, 762-775.

(66) Shan, C.; Zhu, L.; Qu, L.-B.; Bai, R.; Lan, Y. *Chemical Society Reviews* **2018**, *47*, 7552-7576.

(67) d'Alterio, M. C.; Yuan, Y.-C.; Bruneau, C.; Talarico, G.; Gramage-Doria, R.; Poater, A. *Catalysis Science & Technology* **2020**, *10*, 180-186.

(68) Rajkumar, S.; Savarimuthu, S. A.; Kumaran, R. S.; Nagaraja, C.; Gandhi, T. *Chemical Communications* **2016**, *52*, 2509-2512.

(69) *APEX2*, *SADABS and SAINT*; Bruker AXS inc: Madison, WI, USA, **2008**.

(70) Sheldrick, G. M. *Acta Crystallographica Section A: Foundations and Advances* **2015**, *71*, 3-8.

(71) Sheldrick, G. M. *Acta Crystallographica Section C: Structural Chemistry* **2015**, *71*, 3-8.

(72) Dolomanov, O. V.; Bourhis, L. J.; Gildea, R. J.; Howard, J. A.; Puschmann, H. *Journal of Applied Crystallography* **2009**, *42*, 339-341.

(73) Macrae, C. F.; Bruno, I. J.; Chisholm, J. A.; Edgington, P. R.; McCabe, P.; Pidcock, E.; Rodriguez-Monge, L.; Taylor, R.; Streek, J.; Wood, P. A. *Journal of Applied Crystallography* **2008**, *41*, 466-470.

(74) Putz, H.; Brandenburg, K.; GbR, M. *URL: https://www. crystalimpact. de/match* **2018**.

CHAPTER 6

Conclusions of the Thesis

6.1 General Conclusions

The past few decades have witnessed impressive advancements in the area of transition metal-catalyzed C-H activation strategies, exclusively contributing towards the construction of complex heterocyclic scaffolds, centered on aza- and diazaheterocyclic molecular architectures. Among the known diazaheterocycles, phthalazines in its fused/functionalized forms have been recognized as valuable synthetic targets by organic chemists due to their wide range of applications in the field of material and medicinal chemistry. Thus, the demand of developing more efficient protocols for synthesizing funcationalized and fused phthalazines in minimum number of steps from readily available precursors *via* transition metal catalyzed C-H functionalization continues unabated. Enchanted by the interesting biological profile exhibited by phthalazine derivatives and the effective increase in the number of ongoing periodic documentation on this diazaheterocycle, the current thesis entitled "**Rhodium/Ruthenium-Catalyzed Strategies for the Synthesis of Fused and Functionalized *N*-Aryl-2,3-dihydrophthalazine-1,4-diones**" was successfully executed in due diligence of sustainable chemistry, and the thesis has been divided into six chapters (Figure 6.1.1).

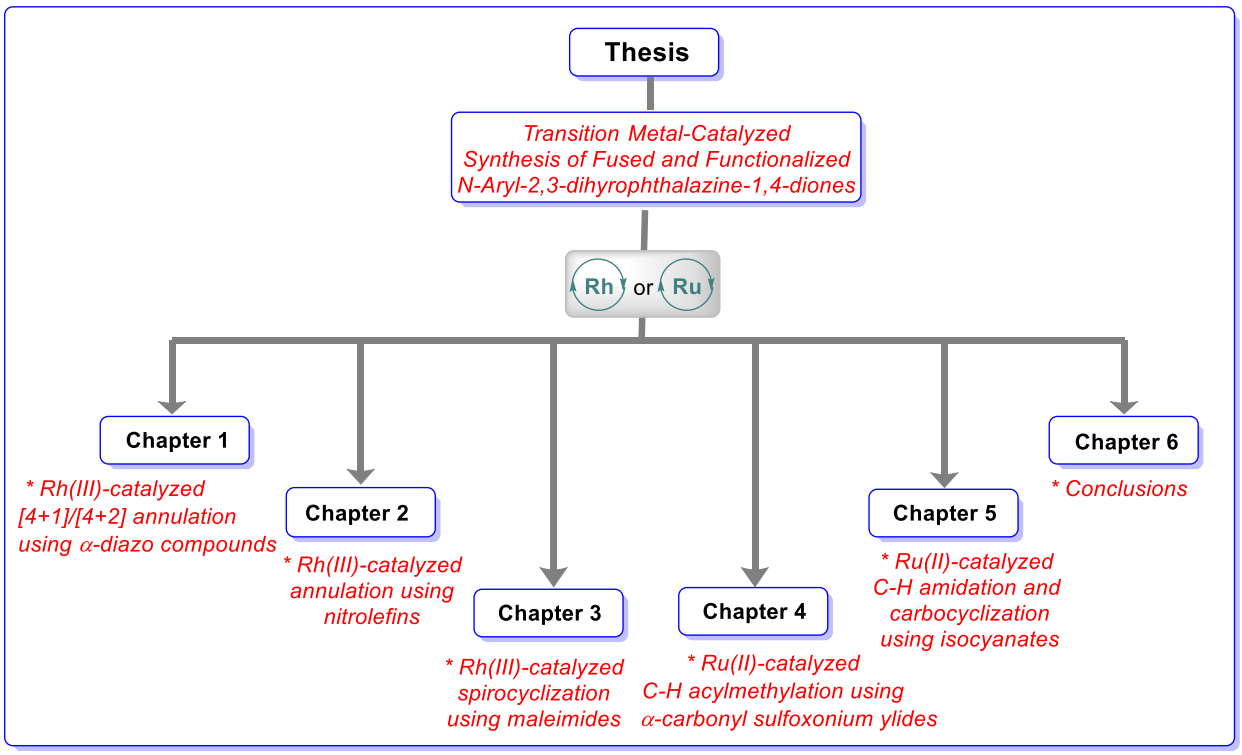

Figure 6.1.1 Systematic representation of the division of thesis

6.2 Specific Conclusions

Chapter 1: Rhodium-Catalyzed [4+1]/[4+2] Annulations of *N*-Aryl-2,3-dihydrophthalazine-1,4-diones with *α*-Diazo Carbonyl Compounds

The first chapter of the thesis commenced with a background on directing group-assisted transition metal-catalyzed C-H bond activation strategies, and the general mechanistic pathways involved in the elementary C-H bond activation step. This has been followed by an brief overview on the catalytic role of rhodium and ruthenium metals in various C-H activation proecesss. The chapter further described a significant exploration of the existing metal-catalyzed protocols successfully executed by eminent research groups towards the synthesis of new heterocyclic scaffolds, employing *α*-diazo carbonyl compounds for various alkylation, arylation and [*m*+*n*] annulations. Inspired from the literature findings, we described two efficient Rh(III)-catalyzed additive-modulated strategies for the synthesis of unprecedented hydroxy-dihydroindazolo[1,2-*b*]phthalazines and phthalazino[2,3-*a*]cinnolines in good-to-excellent yields (Scheme 6.2.1). Diversely substituted *N*-aryl-2,3-dihydrophthalazine-1,4-diones and *α*-diazo carbonyl compounds effectively coupled to afford a total of forty substituted tetra- and pentacyclic phthalazine-fused heterocycles *via* CsOAc- and $AgSbF_6$-modulated [4+1] and [4+2] annulative cyclizations. Detailed mechanistic investigations have been carried by performing a set of control experiments and *in situ* reaction monitoring by ESI-MS, while all the synthesized [4+1]/[4+2] annulated products were well characterized by ^{1}H NMR, ^{13}C NMR and HRMS analysis. Finally, the structures of [4+1]/[4+2] annulated products have been unambiguously confirmed by X-ray crystallographic studies of one of the model compounds in each series.

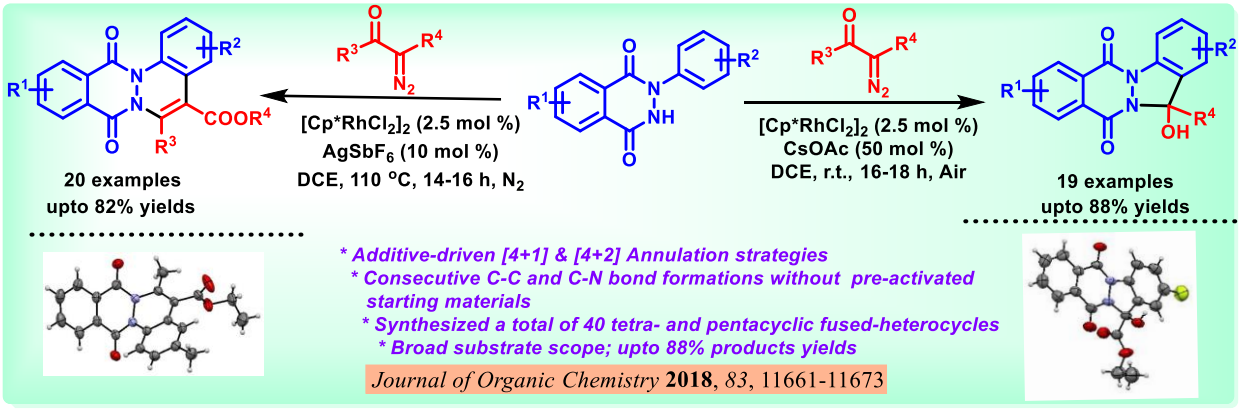

Scheme 6.2.1 Rhodium-catalyzed [4+1]/[4+2] annulations of *N*-aryl-2,3-dihydrophthalazine-1,4-diones with *α*-diazo carbonyl compounds

Chapter 2: Rhodium-Catalyzed Annulation of *N*-Aryl-2,3-dihydrophthalazine-1,4-diones with Nitroolefins

This chapter initially highlighted the importance of cinnoline and cinnolone-fused heterocycles, after which a significant exploration of nitroolefins as Michael acceptors, dienophiles in Diels-Alder reactions and efficient coupling partners in metal-catalyzed transformations, have been documented. Inspired by the profound biological importance of fused and functionalized cinnoline derivatives in medicine and material chemistry, **in this chapter,** we described a mild Rh(III)-catalyzed strategy for the synthesis of hydroxyimino functionalized phthalazino[2,3-*a*]cinnolines by reductive [4+2] annulation between *N*-aryl-2,3-dihydrophthalazine-1,4-diones with varied nitroolefins (Scheme 6.2.2). The generality of the reaction methodology was explored by taking differently substituted electron-withdrawing and electron-releasing groups on both *N*-aryl-2,3-dihyrophthalazine-diones and nitroolefins. In addition, the X-ray crystal structure of one of the synthesized compound provides a clear evidence for the formation of described products. Detailed mechanistic studies have been conducted to probe the reaction mechanism, including isotopic labelling studies and Kinetic Isotopic Effect studies. KIE experiment showcased an Inverse KIE (k_H/k_D) value of 0.75. interestingly, a key rhodacyclic intermediate has been isolated using DMSO as a stabilizing ligand. Mechanistic investigations suggested that the reaction followed an S_EAr pathway and proceeded through a sequential C-H activation/olefin insertion/reduction pathway *via* chelation-assisted directing group influence of the amide functional group.

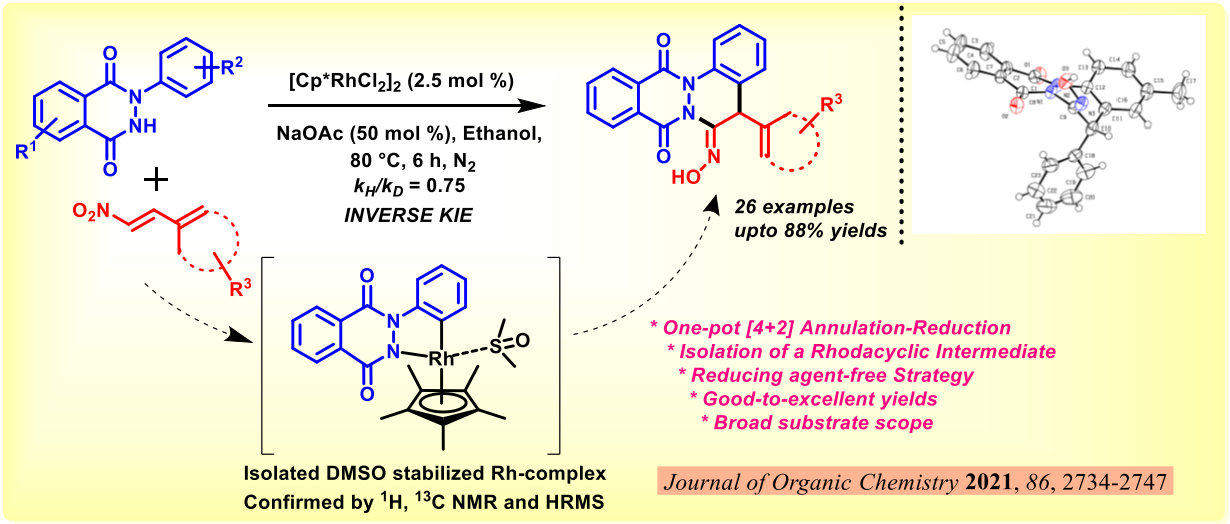

Scheme 6.2.2 Rhodium-catalyzed annulation of *N*-aryl-2,3-dihydrophthalazine-1,4-diones with nitroolefins

Chapter 3: Rhodium-Catalyzed Spirocyclization of *N*-Aryl-2,3-dihydrophthalazine-1,4-diones with Maleimides

The third chapter of the thesis focussed on the development of a one-pot Rh(III)-catalyzed oxidative coupling of *N*-aryl-2,3-dihydrophthalazine-1,4-diones with maleimides. The featured strategy furnished a series of diversely decorated spiro[indazolo[1,2-*b*]phthalazine-13,3'-pyrrolidine]-2′,5′,6,11-tetraones in high yields (Scheme 6.2.3). All the synthesized spirocyclized products have been purified by column chromatography and characterized by detailed spectroscopic analysis. Additionally, an X-ray crystal structure of one of the synthesized product provides support for the proposed to the structure of the products. Detailed mechanistic investigations, including isotopic labelling studies and Kinetic Isotopic Effect studies have been performed. Kinetic isotopic studies computed a P_H/P_D of 3.0 and k_H/k_D of 1.12 under standard conditions for the reaction, which indicated that the C–H activation step might be involved in the rate-determining step. Interestingly, the isolation and characterization of a maleimide-coordinated five-membered rhodacyclic intermediate provides a strong evidence for the proposed mechanism. Mechanistic invertigations suggested that the oxidative spirocyclization reaction proceeds through a sequential *ortho*-alkenylation followed by an intramolecular aza-Michael-type addition/protonation process.

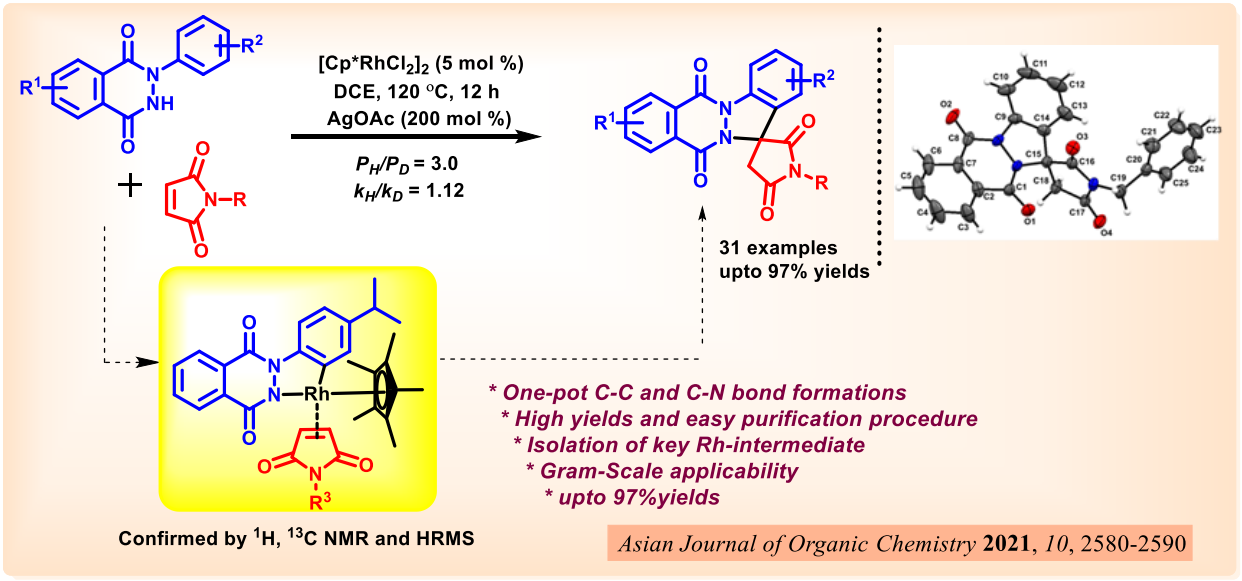

Scheme 6.2.3 Rhodium-catalyzed spirocyclization of *N*-aryl-2,3-dihydrophthalazine-1,4-diones with maleimides

Chapter 4: Ruthenium-Catalyzed C-H Acylmethylation of *N*-Aryl-2,3-dihydrophthalazine-1,4-diones with *α*-Carbonyl Sulfoxonium Ylides

The fourth chapter initially emphasized the chemical reactivity of benzoyl sulfoxonium ylides based on works conducted by synthetic chemists in the past. Thereafter, we reported a Ru(II)-catalyzed strategy for the *ortho*-Csp^2-H acylmethylation of *N*-aryl-2,3-dihydrophthalazine-1,4-diones with *α*-carbonyl sulfoxonium ylides. The protocol featured high functional group tolerance on the two substrates, including aryl, heteroaryl, and alkyl substituted *α*-carbonyl sulfoxonium ylides. The synthesized 2-(*o*-acylmethylaryl)-2,3-dihydrophthalazine-1,4-diones further underwent cyclization using Lawesson's reagent in refluxing toluene under ambient conditions to afford 6-arylphthalazino[2,3-*a*]cinnoline-8,13-diones in excellent yields. While, 5-acyl-5,6-dihydrophthalazino[2,3-*a*]cinnoline-8,13-diones have been obtained by $BF_3{\cdot}OEt_2$-mediated cyclization of 2-(*o*-acylmethylaryl)-2,3-dihydrophthalazine-1,4-diones using DMSO as a solvent and a methylene source *via* dual C-C and C-N bond formations (Scheme 6.2.4). All the synthesized *o*-acylmethylated products and cyclized products were completely characterized using ^{1}H NMR, ^{13}C NMR and HRMS. The structure of the synthesized products was further confirmed by single crystal X-ray analysis. The reaction pathway was proposed by conducting a series of control experiments and *in situ* reaction monitoring by ESI-MS, which supported the involvement of a Ru(II) speices in the C-H activation, cyclometalation and sulfoxonium ylide coordination sub-steps.

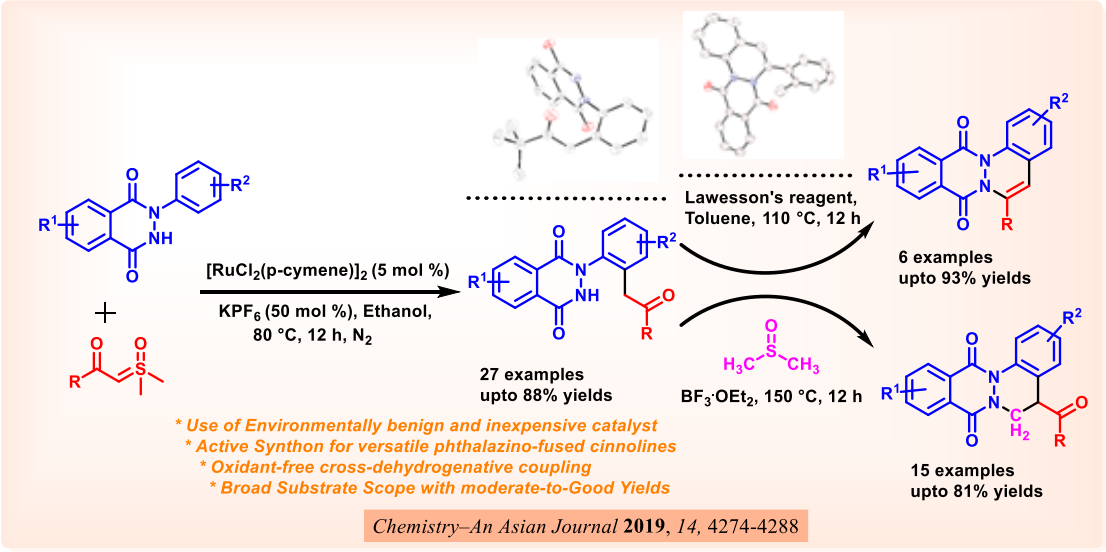

Scheme 6.2.4 Ruthenium-catalyzed C-H acylmethylation and subsequent cyclization of *N*-aryl-2,3-dihydrophthalazine-1,4-diones

Chapter 5: Ruthenium-Catalyzed C-H Amidation and Carbocyclization of *N*-aryl-2,3-dihydrophthalazine-1,4-diones with Isocyanates

In this chapter, taking a lead from the drawbacks associated with the existing carbonyl sources, we developed a feasible Ru(II)-catalyzed strategies towards a direct carbocyclization of *N*-aryl-2,3-dihydrophthalazine-1,4-diones using isocyanates as carbonyl source *via* sequential *ortho*-amidation followed by intramolecular nucleophilic substitution delivering substituted indazolo[1,2-*b*]phthalazine-triones in good-to-excellent yields (Scheme 6.2.5). The developed method underwent sequential C-C/C-N bond formations, delivering substituted indazolo[1,2-*b*]phthalazine-triones in good-to-excellent yields. Interestingly, *ortho*-substituted *N*-aryl-2,3-dihydrophthalazine-1,4-diones delivered the corresponding *ortho*-amidated *N*-aryl-2,3-dihydrophthalazine-1,4-diones in excellent yields under slightly modified the reaction parameters. Also a single crystal X-ray structure of one of the carbocyclized product as well as *o*-amidated product further confirmed the structure of the product. Isolation and characterization of a pyridine stabilized ruthenium complex proved the formation of possible five-membered ruthenacyclic complex. Successful transformations of the carbocyclized and *ortho*-amidated products resulted in chemically divergent fused and functionalized phthalazinones. Detailed mechanistic investigations have been carried out to propose the reaction mechanism including deuterium labelling studies as well as Kinetic Isotopic Effect studies. dissociation step. A P_H/P_D of 3.2 and k_H/k_D of 1.52 under standard conditions for the reaction indicated that the C–H activation step might be involved in the rate-limiting step. Easily obtainable starting materials, simple procedure, good yields are the highlights of this protocol.

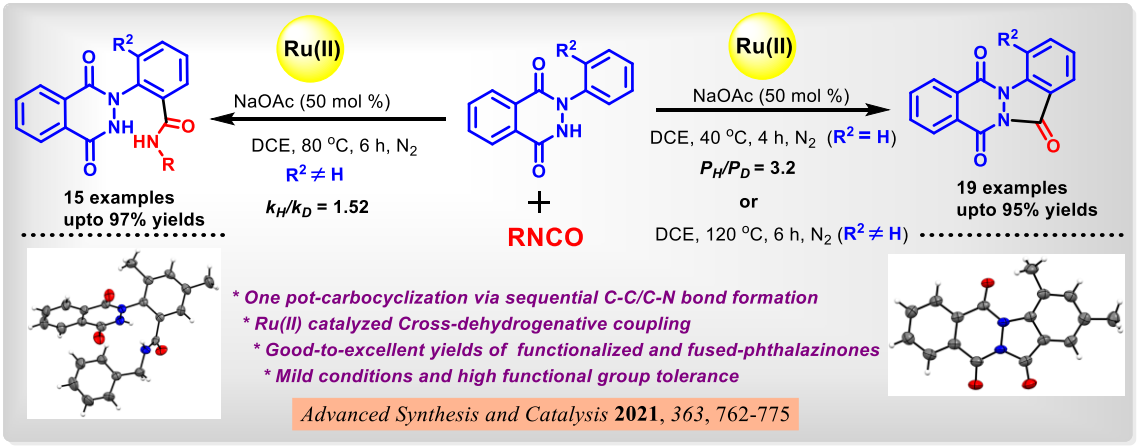

Scheme 6.2.5 Ruthenium-catalyzed C-H Amidation and Carbocyclization of *N*-aryl-2,3-dihydrophthalazine-1,4-diones

6.3 Future Scope

In recent years, a wide upsurge of activity in the metal-catalyzed preparation of fused/functionalized *N*-arylphthalazine-1,4-diones came into existence. The speed at which new contributions are brought forward is astonishing. The current thesis mainly focused on introducing new strategies for the synthesis of biologically active indazolo[1,2-*b*]phthazines and phthalazino[2,3-*a*]cinnolines under transition metal-catalyzed conditions. Expanding the scope, much more work in this area is highly desirable. In this respect, the scope of the present work could be expanded by synthesizing novel fused-phthalazine-diones (**i-iv**) given in Figure 6.3.1. Further, their biological activity and sensing ability of fluorescent molecules among these could be studied.

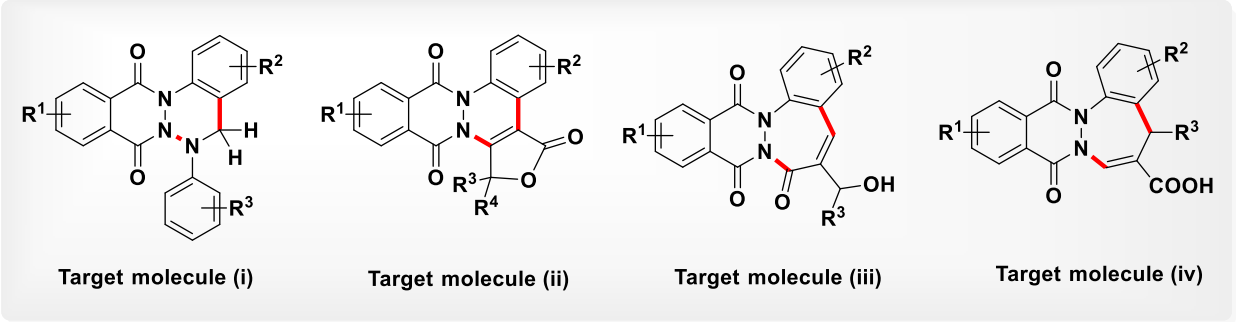

Figure 6.3.1 Structures of novel fused-phthalazine-diones for future studies

Appendices

List of Publications *[A-1]*

1. S. Naharwal, **P. Karishma,** C. K. Mahesha, K. Bajaj, S. K. Mandal, R. Sakhuja "Ruthenium-catalyzed (Spiro)Annulation of *N*-Aryl-2,3-dihydrophthalazine-1,4 diones with Quinones to Access Pentacyclic Spiro-Indazolones and Fused Cinnolines" *Organic and Biomolecular Chemistry* **2022**, 20, 4753-4764.
2. **P. Karishma,** S. K. Mandal, R. Sakhuja "Rhodium-Catalyzed Spirocyclization of Maleimide with *N*-Aryl-2,3-dihydrophthalazine-1,4-dione to Access Pentacyclic Spiro-Succinimides" *Asian Journal of Organic Chemistry* **2021**, *10*, 2580-2590.
3. K. Bajaj, **P. Karishma,** S. Khan, P. N Jha, R. Sakhuja, D. Kumar "Fluorescent Glutamine and Asparagine as Promising Probes for Chemical Biology" *Organic & Biomolecular Chemistry* **2021**, *19*, 7695-7700.
4. **P. Karishma,** C. K. Mahesha, S. K. Mandal, R. Sakhuja "Reducing-Agent-Free Convergent Synthesis of Hydroxyimino-Decorated Tetracyclic Fused Cinnolines *via* Rh^{III}-Catalyzed Annulation Using Nitroolefins" *Journal of Organic Chemistry* **2021**, *86*, 2734-2747.
5. **P. Karishma,** A. Gogia, S. K. Mandal, R. Sakhuja, "Ruthenium Catalyzed C−H Amidation and Carbocyclization using Isocyanates: An Access to Amidated 2-phenylphthalazine-1,4-diones and Indazolo [1, 2-*b*] phthalazine-triones" *Advanced Synthesis and Catalysis* **2021**, *363*, 762-775.
6. **P. Karishma,** D. S. Agarwal, B. Laha, S. K. Mandal, R. Sakhuja "Ruthenium Catalyzed C−H Acylmethylation of *N*-Arylphthalazine-1,4-diones with *α*-Carbonyl Sulfoxonium Ylides: Highway to Diversely Functionalized Phthalazino-fused Cinnolines" *Chemistry–An Asian Journal* **2019**, *14*, 4274-4288.
7. C. K. Mahesha, D. S. Agarwal, **P. Karishma,** D. Markad, S. K. Mandal, R. Sakhuja "Iridium-Catalyzed [4+2] Annulation of 1-Arylindazolones with *α*-Diazo Carbonyl Compounds: Access to Indazolone-fused Cinnolines" *Organic & Biomolecular Chemistry* **2018**, *16*, 8585-8595.
8. **P. Karishma,** C. K. Mahesha, D. S. Agarwal, S. K. Mandal, R. Sakhuja "Additive-Driven Rhodium-Catalyzed [4+1]/[4+2] Annulations of *N*-Arylphthalazine-1,4-dione with *α*-Diazo Carbonyl Compounds" *Journal of Organic Chemistry* **2018**, *83*, 11661-11673.

List of Presentations in Conferences *[A-2]*

Oral:

1. **P. Karishma,** R. Sakhuja, "Ruthenium Catalyzed C−H Acylmethylation of *N*-Arylphthalazine-1, 4-diones with *α*-Carbonyl Sulfoxonium Ylides: Highway to Diversely Functionalized Phthalazino-fused Cinnolines" at 26th ISCB International Conference jointly organized by Institute of Pharmacy, Nirma University, Ahmedabad with Indian Society of Chemists and Biologists ISCBC-NIPiCON-2020: January 22-24, 2020.

Poster:

1. **P. Karishma,** R. Sakhuja "Ruthenium Catalyzed C−H Acylmethylation of *N*-Arylphthalazine-1,4-diones with *α*-Carbonyl Sulfoxonium Ylides: Highway to Diversely Functionalized Phthalazino-fused Cinnolines" at ETC-2020, International Conference on Emerging Trends in Catalysis jointly organized by School of Advanced Science, VIT, Vellore and Royal Society of Chemistry, UK: January 6-8, 2020.
2. **P. Karishma,** R. Sakhuja "Additive-Driven Rhodium-Catalyzed [4+1]/[4+2] Annulations of *N*-Arylphthalazine-1, 4-dione with *α*-Diazo Carbonyl Compounds"at 25th ISCB International Conference (ISCBC-2019) organized by Indian Society of Chemists and Biologists at Hotel Golden Tulip, Lucknow: January 12-14, 2019.

Brief Bibliography of the Candidate *[A-3]*

Pidiyara Karishma obtained her Master's degree in Integrated Pharmaceutical Chemistry from Mahatma Gandhi University, Nalgonda, Telangana, India during 2009-14. In June 2017, she cleared the Joint TS-SET for Assistant Professor/Lectureship conducted by Osmania University on behalf of the Government of Telangana State. She joined the Department of Chemistry, BITS Pilani, Pilani Campus for a Ph.D. program in January-2017 under the guidance of Dr. Rajeev Sakhuja with the financial assistance ship from BITS Pilani. During the tenure of my Ph.D., she was actively involved in the synthesis and functionalization of the *N*-aryl-2,3-dihydrophthalazine-1,4-dione skeleton. She has published eight research articles in peer-reviewed international journals and presented papers in three international conferences.

Her main research interest lies in the development of new methods for the construction of nascent chemical bonds using novel C−H activation/functionalizations strategies under metal-catalyzed conditions.

Brief Bibliography of the Supervisor *[A-4]*

Dr. Rajeev Sakhuja obtained his M.Phil. and Ph.D. degrees from the Department of Chemistry, University of Delhi, New Delhi in the area of heterocyclic chemistry. Following this, he pursued his postdoctoral research with Prof. Alan R. Katritzky at the Center of Heterocyclic Compounds, University of Florida, Gainesville, and thereafter with Professor Raymond Booth at Department of Medicinal Chemistry, University of Florida from 2009-2012. After returning, he joined the Department of Chemistry, BITS Pilani, Pilani Campus as an Assistant Professor in March 2012. Following Ph.D., he has fourteen years of post-Ph.D. research experience in the broad field of organic synthesis. Dr. Sakhuja is presently an Associate Professor in Department of Chemistry, leading an independent research group at Birla Institute of Technology & Science, Pilani where his current area of research interests lies in the development of metal-catalyzed and metal-free strategies for the functionalization of heterocycles, synthesis of biologically important heterocyclic scaffolds, along with the development of organic materials with sensing and gelation abilities. His effective contribution in these areas has fetched him seventy one research articles, 4 reviews in peer-reviewed journals of international repute. He has successfully completely four sponsored projects funded by government agencies (DST, SERB & UGC), and private organization (BITS seed grant & additional research grant) in the past ten years.